Investigating the p53-independent responses to inhibition of RNA Polymerase I transcription by CX-5461

Jaclyn Quin

(ORCID: 0000-0001-7757-7295)

Submitted in total fulfillment of the requirements of the degree of Doctor of Philosophy

December 2017

Faculty of Medicine, Dentistry and Health Sciences
The Sir Peter MacCallum Cancer Centre
The University of Melbourne

Abstract.

Increased rates of DNA-dependent RNA Polymerase I (Pol I) transcription of the 47S pre-ribosomal RNA (rRNA) genes are observed in almost all cancer types. Cancer cells may require high rates of Pol I transcription and ribosome biogenesis to achieve their unrestrained growth and proliferative capacity, thus presenting a therapeutic window for selectively targeting cancer cells with inhibitors of Pol I transcription. Our laboratory helped develop and validate a first-in-class small molecule selective inhibitor of Pol I transcription, CX-5461 (Senhwa Biosciences). Here, we have investigated the response of cells at defined stages of malignant transformation to inhibition of Pol I transcription, utilising a panel of isogenically matched BJ fibroblast cell lines.

We compared the response of non-transformed and transformed cells of the same genetic background, and demonstrated that CX-5461 can selectively induce cell death in cancer cell lines *in vitro*. We investigated the phenotypic response of a non-transformed BJ fibroblast cell line minimally immortalized with h*TERT* (BJ-T) to CX-5461, and demonstrated that they display a proliferation defect. The proliferation defect is associated with the activation of p53 and a p53-dependent G1 cell cycle checkpoint, as well as p53-independent S-phase and G2 cell cycle checkpoints and senescence. Escape from cell cycle arrest in transformed BJ fibroblast cell lines is associated with increased rates of cell death in response to CX-5461.

To identify pathways mediating the p53-independent responses to inhibition of Pol I transcription, we have performed RNA-sequencing analysis in CX-5461 treated BJ-T cells in which p53 was silenced (BJ-T p53shRNA). The analysis identified ATM (Ataxia-telangiectasia mutated) / ATR (ATM and RAD3-related) signaling and transcriptional programs associated with senescence to be modulated following treatment with CX-5461. Further, we have demonstrated that inhibition of Pol I transcription by CX-5461 rapidly and potently activates the ATM/ATR kinase signaling pathways in the absence of global DNA damage. Combined ATM/ATR inhibition and CX-5461 treatment results in bypass of CX-5461 mediated S-phase and G2 arrest, and induced cell death in the BJ-T p53shRNA cell line.

We investigated the mechanisms by which inhibition of Pol I transcription by CX-5461 activates the ATM/ATR signaling pathways. We demonstrated that inhibition of Pol I transcription initiation by CX-5461 results in ‘exposed’ rRNA genes (rDNA) that are in

an open chromatin conformation but devoid of Pol I. Inhibition of Pol I transcription by CX-5461 also results in reorganization of nucleolar structure and translocation of proteins to and from the nucleoli. We observed increased levels of NBS1 (Nijmegen Breakage Syndrome 1) activation by ATM specifically within the nucleoli during S/G2. We propose CX-5461 treatment induces an unusual chromatin structure at the rDNA that is sufficient to activate ATM/ATR in the nucleoli. Finally, we have shown that DNA damage repair is attenuated following treatment with CX-5461. Together, our studies identify activation of ATM/ATR signaling as a key p53-independent pathway of response to inhibition of Pol I transcription, that can be targeted to improve the efficacy of CX-5461 in cancer therapy.

Declaration.

This is to certify that:

(i) the thesis comprises only my original work except where indicated in the preface;

(ii) due acknowledgement has been made in the text to all other material used;

(iii) the thesis is fewer than 100,000 words in length, exclusive of tables, maps, bibliographies and appendices

Jaclyn Quin

December 2017

Preface.

Except where indicated below, all experiments included in this thesis were designed, performed and analyzed by myself under the supervision of Dr. Elaine Sanij and Prof. Ross Hannan. I am grateful to acknowledge the assistance of my colleagues with the following experiments.

BJ human foreskin fibroblast cell lines were kindly provided by Prof. William Hahn, Harvard Medical School. U2TR and U2TR-I-*Ppo*I-dd cell lines were kindly provided by Prof. Kum Kum Khanna, QIMR Berghofer Medical Research Institute. FUCCI-labeled BJ-T p53shRNA cell line was produced by lentiviral transduction with pCSII-EF-mCherry-hCdt1 and pCSII-EF-mVenus-hGeminin (kindly provided by Dr. Atsushi Miyawaki, RIKEN, Japan), which were performed by Dr. Keefe Chan (Peter MacCallum Cancer Centre).

RNA library preparation using Illumina TruSeq RNA Sample Preparation Kits, and RNA-sequencing on Illumina HiSeq 2500 using 50bp paired-end reads, were performed by the Molecular Genomics Core Facility at Peter MacCallum Cancer Centre. Analysis of RNA-sequencing results, including alignment to the genome using Bowtie2, counting using HTSeq, and the calculating differential expression using DESeq package was performed by Dr. Jeannine Diesch (Peter MacCallum Cancer Centre).

Comet analysis of DNA damage repair in BJ-T cell lines (Figure 30 A) were performed in collaboration with Dr Amit Khot (Peter MacCallum Cancer Centre) and Dr Elaine Sanij. Immunofluoresence experiments for phos-NBS1 and γH2A.X in BJ-Tp53shRNA FUCCI cells (Figure 27 C & D), and G4 DNA following CX-5461 treatment in ovarian cancer cell lines (Supplementary Figure 31 B and C), were performed by Dr. Elaine Sanij.

Original work from this project has been included in the following publications.

Primary publications:

D. Drygin, A. Lin, J. Bliesath, C. B. Ho, S. E. O'Brien, C. Proffitt, M. Omori, M. Haddach, M. K. Schwaebe, A. Siddiqui-Jain, N. Streiner, J. E. Quin, E. Sanij, M. J. Bywater, R. D. Hannan, D. Ryckman, K. Anderes, W. G. Rice, Targeting RNA Polymerase I with an Oral Small Molecule CX-5461 Inhibits Ribosomal RNA Synthesis and Solid Tumor Growth. *Cancer Res.* **71**, 1418-1430 (2011).

J. E. Quin, K. T. Chan, J. R. Devlin, D. P. Cameron, J. Diesch, C. Cullinane, J. Ahern, A. Khot, N. Hein, A. J. George, K. M. Hannan, G. Poortinga, K. E. Sheppard, K. K. Khanna, R. W. Johnstone, D. Drygin, G. A. McArthur, R. B. Pearson, E. Sanij, R. D. Hannan, Inhibition of RNA polymerase I transcription initiation by CX-5461 activates non-canonical ATM/ATR signaling. *Oncotarget* **7**, 49800-49818 (2016)

N. Hein, D. P. Cameron, K. M. Hannan, N. N. Nguyen, C. Y. Fong, J. Sornkom, M. Wall, M. Pavy, C. Cullinane, J. Diesch, J. R. Devlin, A. J. George, E. Sanij, J. E. Quin, G. Poortinga, I. Verbrugge, A. Baker, D. Drygin, S. J. Harrison, J. D. Rozario, J. A. Powell, S. M. Pitson, J. Zuber, R. W. Johnstone, M. A. Dawson, M. A. Guthridge, A. Wei, G. A. McArthur, R. B. Pearson, R. D. Hannan, Inhibition of Pol I transcription treats murine and human AML by targeting the leukemia-initiating cell population. *Blood* **129**, 2882-2895 (2017)

Review publications:

Nadine Hein, Elaine Sanij, Jaclyn Quin, Katherine M. Hannan, Austen Ganley and Ross D. Hannan (2012). The Nucleolus and Ribosomal Genes in Aging and Senescence, Senescence, Dr. Tetsuji Nagata (Ed.), InTech, DOI: 10.5772/34581.

J. E. Quin, J. R. Devlin, D. Cameron, K. M. Hannan, R. B. Pearson, R. D. Hannan, Targeting the nucleolus for cancer intervention. *Biochim Biophys Acta* **1842**, 802-816 (2014).

No work presented in this thesis has been submitted for any other qualification or performed prior to candidature enrolment.

Jaclyn Quin was supported by an Australian Government National Health and Medical Research Council (NHMRC) postgraduate scholarship.

Acknowledgments.

The completion of my PhD would never have been possible without the teaching, guidance, support and friendship of more people than I can say. Thank you, everyone, from the bottom of my heart.

First and foremost, I would like to thank my supervisor Prof. Ross Hannan. It has been a great privilege to have been taken on by you for my research project, and to have been given the opportunity to work with someone with your vision and energy. Thank you for your honest and encouraging approach, for sharing your knowledge and ideas, for always having your door open, and for your continuous support and motivation. I am very fortunate to have had you as my supervisor. I would also like to extend my special thanks to Ross' wonderful wife Kate. Thank you for making sure I always felt part of a big research family.

To my supervisor, Dr. Elaine Sanij, thank you for the enormous amount of effort you have put in to me - you have been there every step of the way, from teaching me my first ever experiment in the lab, to proof reading my thesis in your holidays. I would never have got here without your generous instruction and support. I have been inspired by what you have achieved in the time I have known you, and I will always look up to you as an amazing role model in science. Thank you for everything.

To my fellow students and staff members at Peter MacCallum Cancer Centre, it was a pleasure to spend my PhD with people who are wonderful friends and colleagues. I have learned so much from working amongst such a talented and positive group. But most importantly, thank you for every emergency coffee trip, lunch in the park, long talk, home cooked meal, baking competition, BYO dumplings, late night in Fitzroy, camping trip, Lorne disco, outlandish Christmas party, and lab dinner. Because of you, I have amazing memories of Melbourne.

To my family, thank you for your generous and unwavering love, encouragement and support through my PhD. Even at a distance you were always there for me - from being a captive audience listening to me speak about my project for hours, to whisking me away on a holiday to not think about my project at all. Mum and Dad, thank you. I could never have achieved this moment without you.

Finally, I would like to dedicate this thesis in memory of Clint Johnson.

TABLE OF CONTENTS

CHAPTER 2: MATERIALS AND METHODS

LIST OF FIGURES AND TABLES.

CHAPTER 1: INTRODUCTION

CHAPTER 2: MATERIALS AND METHODS

CHAPTER 3: INVESTIGATING THE RESPONSE OF BJ HUMAN FIBROBLAST CELL LINES TO INHIBITION OF POL I TRANSCRIPTION WITH CX-5461.

CHAPTER 4: RNA-SEQUENCING ANALYSIS TO IDENTIFY p53-INDEPENDENT RESPONSES TO INHIBITION OF POL I TRANSCRIPTION.

CHAPTER 5: INHIBITION OF POL I TRANSCRIPTION BY CX-5461 INDUCES ACTIVATION OF ATM/ATR SIGNALING INDEPENDENTLY OF GLOBAL DNA DAMAGE.

CHAPTER 6: INHIBITION OF POL I TRANSCRIPTION INITITATION BY CX-5461 ACTIVATES ATM/ATR PATHWAY COMPONENTS WITHIN THE NUCEOLI, AND IMPAIRS DNA DAMAGE RESPONSE.

CHAPTER 7: GENERAL DISCUSSION.

LIST OF ABBREVIATIONS

47S pre-rRNA	47S pre-ribosomal RNA
53BP1	p53-binding protein 1
ActD	Actinomycin D
ALL	Acute lymphoblastic leukemia
AML	Acute myeloid leukemia
AMPK	AMP-activated protein kinase
AP-1	Activator protein 1
APC/CCdh1	Anaphase-promoting complex/cyclosome activator protein Cdh1
APE1	Apurinic/apyrimidinic endonuclease 1
ATM	Ataxia-telangiectasia mutated kinase
ATMi	ATM inhibitor KU-55933
ATMIN	ATM interacting protein
ATP	Adenosine triphosphate
ATR	Ataxia telangiectasia and Rad3-related protein
ATRi	ATR inhibitor VE-821
ATRIP	ATR interacting protein
BCL-XL	B-cell lymphoma-extra large
BER	Base excision repair
BRCA1	Breast cancer type 1
BRCA2	Breast cancer type 2
BrdU	5'-bromo-2'deoxyuridine
BSA	Bovine serum albumin
CBP	CREB binding protein
CCL2	C-C Motif Chemokine Ligand 2
CDC14B	Cell division cycle 14 B
CDC25	Cell division cycle 25
CDK	Cyclin-dependent kinase
cDNA	Complementary DNA
CHH	Cartilage hair hypoplasia
ChIP	Chromtin immunoprecipitation
CHK1	Checkpoint kinase 1
CHK1/CHK2i	CHK1 and CHK2 inhibitor AZD7762
CHK2	Checkpoint kinase 2
COX-2	Cyclooxygenase-2
CPM	Counts per minute

CSB	Cockayne syndrome protein B
CSIG	Cellular senescence inhibited gene),
CTP	Cytidine triphosphate
CYR61	Cysteine rich 61
DAPI	4',6-diamidino-2-phenylindole
DBA	Diamond–Blackfan anemia
dd	Destabilization domain
DDR	DNA damage response
DEPC	Diethylpyrocarbonate
DFC	Dense fibrillar component
DMEM	Dulbecco's Modified Eagle Medium
DMSO	Dimethyl sulphoxide
DNA	Deoxyribonucelic acid
DNA-PK	DNA-dependent protein kinase
DNA-SCARS	DNA segments with chromatin alterations reinforcing senescence
DNAse	Deoxyribonuclease
DNMT	DNA methyltransferase
dNTP	Deoxynucleotide
DSB	Double stranded DNA breaks
DTT	Dithiothreitol
DUSP1	Dual specificity phosphatase 1
EC50	Half maximal effective concentration
ECL	Enhanced chemiluminescence
ECM	Extra-cellular matrix
EDTA	Ethylenediaminetetraacetic acid
EMSA	Electromobility shift assay
EMT	Epithelial-to-mesenchymal transition
eNoSC	energy dependent nucleolar silencing
ERK	Extracellular signal-regulated kinase
ERK	Extracellular-signal-regulated kinase
ESC	Embryonic stem cell
ETM	Extent tail moment
ETS	External transcribed spacer sequence
FACS	Fluorescentactivated cell sorting
FBL	Fibrillarin
FBS	Fetal Bovine Serum
FC	Fibrillar centre

FC	Fold change
FDR	False discovery rate
FISH	Fluorescent in situ hybridization
FUCCI	Fluorescent ubiquitinylation cell cycle indicator
G4	G-quadruplex
GADD45B	Growth arrest and DNA-damage-inducible beta
GC	Granular component
γH2A.X	phospho-Ser139 Histone 2 variant A.X
GnRH	Gonadotropin-releasing hormone
GTP	Guanosine triphosphate
H1	Histone 1
H2	Histone 2
H3	Histone 3
H4	Histone 4
HBB	Hemoglobin subunit beta
HDAC	Histone deacetylase
HDM2	Human homologue of mouse double minute 2
HEPES	4-(2-hydroxyethyl)-1-piperazineethanesulfonic acid
HES1	Hairy and Enhancer of Split-1
HIF1	Hypoxia inducible factor 1
HMG	High mobility group
HR	Homolgous recombination
HSP70	Heat shock protein 70kDa
I-PpoI	Intron-encoded homing endonuclease
IC(X)	Inhibitor concentration at which rates are reduced by X
IEG	Immediate early gene
IER2	Immediate early response 2
IF	Immuofluorescence
IGF1	Insulin-like growth factor 1
IgG	Immunoglobulin G
IGS	Intergenic spacer
IL-1β	Interleukin 1 beta
IL-6	Interleukin 6
ING1	Inhibitor of growth protein 1
IP	Immunopreciptiation
IR	Ionizing radiation
ITS	Internal transcribed spacer sequences

JNK2	c-Jun NH2-terminal protein kinase 2
K	Lysine
kb	Kilobase
KDM	Lysisine specific demethylase
KMT	Lysine methyltrasferase
L	Simian virus 40 (SV40) large T antigen
M	Mitosis
MAPK	Mitogen activated protein kinase
MDC1	Mediator of DNA damage checkpoint protein 1
MDM2	Mouse double minute 2
MEK	ERK kinase
miRNA	microRNA
MLL	Mixed-linage leukemia
MMP15	Matrix metalloproteinase 15
mRNA	Messenger RNA
mTOR	Mammalian target of rapamycin
MYST1	MYST family histone acetyltransferase 1
NAD	Nucleolus-associated chromatin domain
NBS1	Nijmegen breakage syndrome 1
NCL	Nuceolin
ncRNA	Non-coding RNA
NM1	Nuclear myosin 1
NOR	Nucleolar organizing region
NoRC	Nucleolar remodeling complex
NPM1	Nucleophosmin
NTP	nucleoside triphophate
NuRD	Nucleosome remodelling and deacetylase
PAPAS	Promoter and pre-RNA antisense
PARP1	Poly(ADP-ribose) polymerase 1
PBS	Phosphate buffered saline
PCAF	p300/CBP-associated factor
PCR	Polymerase chain reaction
PEI	Polyethylenimine
phos-H3	phospho-Histone 3 (Serine 10)
PI	Propidium iodide
PI3K	Phosphoinositide 3-kinase
PIC	Pre-initiation complex

PIKK	phosphoinositide three-kinase-related kinase
PLK1	Polo-like kinase 1
PNC	Perinucleolar compartment
Pol I	DNA-dependent RNA Polymerase I
Pol II	DNA-dependent RNA Polymerase II
Pol III	DNA-dependent RNA Polymerase III
POLR1A	DNA-directed RNA polymerase I subunit RPA1
PP2A	Protein phosphatase 2A
PPIs	Protease and phophaste inhibitors
pRB	Retinoblastoma protein
pRS	pRetroSuper vector
PTEN	Phosphatase and tesin homolog
PVDF	Polyvinylidene fluoride
qRT-PCR	Quantitative reverse-trasncription polymerase chain reaction
R	H-*RASV12*
rDNA	Ribosomal DNA; 47S pre-ribosomal RNA genes
RFB	Replication fork blocking site
RNA	Ribonucleic acid
RNase	Ribonuclease
RNF8	Ring finger protein 8
RNP	Ribonucleoprotein
rNTPs	Ribonucleoside tri-phosphate
ROS	Reactive oxygen species
RP	Ribosomal protein
RPA	Replication protein A
RRN3	RNA Polymerase I-Specific Transcription Initiation Factor
rRNA	Ribosomal RNA
RSK	Ribosomal protein S6 kinase A1
RT	Room temperature
S	Simian virus 40 (SV40) small t antigen
S6K1	Ribosomal protein S6 kinase B1
SA-β-gal	Senescence associated β-galoctosidase
SAHF	Senescence-associated heterochromatin foci
SASP	Senescence –associated secretory phenotype
SDS	Sodium Dodecyl Sulphate
Ser	Serine
shRNA	Short haripin RNA

siRNA	Small interfering RNA
SIRT1	Sirtuin 1
SL1	Selective factor 1
snoRNA	Small nucleolar RNA
snoRNP	Small nucleolar ribonuclear protein
snRNA	Splicesomal RNAs
snRNP	Small nuclear ribonuclear protein
SRP	Signal recognition particle
ssDNA	Single stranded DNA
SV40	Simian virus 40
T	h*TERT*
TAF	TBP associated factor
TBP	TATA binding protein
TERC	Telomerase RNA componenent
TERT	Telomerase reverse transcriptase componenent
TGFβ	Transforming growth factor beta
Thr	Threonine
TIP5	TTF1 interacting peptide 5
TMRE	Tetramethylrhodamine ethyl
TOPBP1	DNA topoisomerase II binding protein 1
TopoI	Topoisomerase
tRNA	Transfer RNA
TTF-1	Transcription termination factor 1
TTP	Thymidine triphosphate
U2TR	U2OS cell line stably expressing tetracyclin repressor protein (TR)
UBF	Upstream binding factor
UCE	Upstream control element
UTP	Uridine triphosphate
UV	Ultraviolet
v/v	Volume/volume
VHL	Von Hippel-Lindau tumor suppressor
WRN	Werner syndrome RecQ like helicase
WSTF	William syndrome transcription factor
wt	Wild type
X-DC	X-linked dyskeratosis congenita
X-gal	5-bromo-4-chloro-3-indoyl b-D-galactopyranoside
Xi	Inactive X chromosome

CHAPTER 1. INTRODUCTION

1.1 Ribosome Biogenesis

The ribosomes are the organelles responsible for synthesizing all proteins in the cell – following the transcription of a protein coding gene, the resulting mRNA must associate with the ribosome in order for its nucleotide codon sequence to be translated into the corresponding chain of amino acids. A number of reviews describe this well characterised process, which is regulated in multiple ways to enable additional layers of control of gene expression (Reviewed in (Hershey et al., 2012; Shi and Barna, 2015; Gobet and Naef, 2017)). Due to the requirement of ribosomes for generating protein, they are absolutely necessary for cell growth (defined as an increase in cell mass), and consequently for cell proliferation (defined as undergoing mitosis) (Reviewed in (Thomas, 2000)). Unsurprisingly then, there are an enormous number of ribosomes in every cell – it is estimated that a human cell contains up to 10^7 ribosomes, and that in proliferating cells over 10,000 new ribosomes can be produced every minute, requiring up to 80% of the total energy consumption of the cell (Gorlich and Mattaj, 1996; Schmidt, 1999)(Reviewed in (Warner et al., 2001)). Therefore, ribosome biogenesis is a significant fundamental process that must be efficiently regulated.

The mature human ribosome is made up of two subunits, each composed of a catalytic core of ribosomal RNAs (rRNAs), and associated ribosomal proteins (RPs) - the large 60S subunit consists of the 5S, 5.8S, and 28S mature rRNAs assembled with 50 RPs, and the smaller 40S subunit consists of the 18S mature rRNA assembled with 33 RPs (Reviewed in (Thomson et al., 2013; Kressler et al., 2017)). Ribosome biogenesis is a complex process that requires the coordinated action of all three DNA-dependent RNA polymerases: RNA Polymerase I (Pol I), RNA Polymerase II (Pol II), and RNA Polymerase III (Pol III). The key step is the transcription of the 47S pre-rRNA, which is rapidly processed into the 18S, 5.8S and 28S mature rRNAs. There are approximately 200 copies of the 47S pre-rRNA gene in the human haploid genome, distributed in repeat arrays at five locations on the acrocentric chromosomes, collectively termed the ribosomal DNA (rDNA) (Henderson et al., 1972; Stults et al., 2008; Gibbons et al., 2015). These genes are transcribed by the specialised RNA polymerase, Pol I, which acts exclusively at the rDNA (Reviewed in (Moss et al., 2007)). The 5S rRNA is transcribed from repeated arrays at separate loci on chromosome 1 by Pol III, which is also responsible for transcription of other small non-

translated RNAs such as tRNAs (Sorensen and Frederiksen, 1991)(Reviewed in (Ciganda and Williams, 2011; Moir and Willis, 2013)). The RP genes are transcribed by RNA Pol II, then translated at existing ribosomes in the cytoplasm, before the RPs are imported back to the nucleus and incorporated with the rRNAs to form the ribosomal subunits (Reviewed in (Panse and Johnson, 2010)).

1.1.1 The nucleoli and ribosome biogenesis

The process of ribosome biogenesis occurs within the nucleoli, non-membrane bound nuclear organelles. The nucleoli are organized around nucleolar organizing regions (NORs), which refer to the tandem repeat arrays of 47S rRNA genes, visible as secondary constrictions during metaphase on the p-arms of the five acrocentric chromosomes (chromosomes 13, 14, 15, 21, and 22) (Henderson et al., 1972). Due to their highly repetitive nature, the NORs have yet to be assembled as part of the human genome sequence. However, it has been shown that rDNA clusters consist of rDNA repeats in a mostly head-to-tail orientation, and are devoid of intervening non-rDNA sequences (Caburet et al., 2005). There is significant variability in rDNA copy number, even within the same individual (Sakai et al., 1995; Stults et al., 2008). Each gene cluster on average contains approximately 80 copies of the rRNA genes, constituting approximately one third of the p-arms, with the remaining satellite regions are composed of repetitive DNA and largely devoid of transcribed sequences (Floutsakou et al., 2013)(Reviewed in (Sullivan et al., 2001)). Not all NORs are transcriptionally active - Pol I transcription machinery is associated with approximately half of the NORs at any one time, and a nucleolus can form only at these transcriptionally active locations (Roussel et al., 1996; Yuan et al., 2005; Grob et al., 2014a) (FIGURE 1).

Nucleoli have a distinct tripartite structure that is closely related to the process of ribosome biogenesis (Reviewed in (Hernandez-Verdun et al., 2010)). The fibrillar centre (FC) is positioned in the center of the nucleolus, and contains the transcribed rDNA. A single rDNA repeat is 43kb, consisting of the 13.3kb 47S pre-RNA coding region and a 30kb intergenic spacer (IGS). Pol I transcription of the 47s pre-rRNA starts at the border of the FCs, with very high density of Pol I generating abundant nascent transcripts, resulting in a Christmas tree-like structure along the length of each transcribed repeat (Puvion-Dutilleul et al., 1991; Koberna et al., 2002). Processing of the 47s pre-rRNA transcripts begins as transcription is occurring, and this takes place within the dense fibrillar component (DFC), which surrounds the FC. The major steps required to process the pre-47S rRNA into the mature rRNAs have been described in detail: extensive nucleotide modification is mediated by small nucleolar ribonuclear

protein particles (snoRNPs), in which small nucleolar RNAs (snoRNAs) guide site-specific ribose 2'-O-methylation and pseudouridine formation, catalyzed by RNP proteins fibrillarin and dyskerin, respectively (Reviewed in (Staley and Woolford, 2009)); concomitantly, endonucleolytic cleavage of the 47S pre-RNA generates the mature 18S, 5.8S and 28S rRNAs. Approximately 250 non-ribosomal nucleolar RNAs and proteins – including for example, nucleases, helicases and chaperones - act as ribosome processing and assembly factors (Reviewed in (Henras et al., 2008)). Assembly of the mature 18S, 5.8S and 28S rRNAs with the 5S rRNA and RPs into the 40S and 60S ribosome subunits begins in the DFC. The 5S rRNA are transcribed by Pol III from a chromosomal location distant from the rDNA, but which can associate with the nucleolar periphery (Matera et al., 1995)(Reviewed in (Haeusler and Engelke, 2006)). 5S RNA is imported into the nucleolus to be assembled with the 60S subunit (Reviewed in (Ciganda and Williams, 2011)). RP mRNAs are transcribed in the nucleus by Pol II, translated at cytoplasmic ribosomes, and then RPs are imported into the nucleolus from the cytoplasm in excess amounts, ensuring they are not rate limiting for ribosome biogenesis (Lam et al., 2007)(Reviewed in (Henras et al., 2008) (Robledo et al., 2008)). A single nucleolus can contain multiple FCs surrounded by DFCs, interspersed within a single peripheral granular component (GC). Immature 40S and 60S subunits, which appear as 'granules', move from the DFCs to the GC, where they undergo final processing and assembly steps prior to subunit export to the cytoplasm (FIGURE 2).

The nucleoli, therefore, are highly organized and complex organelles, dense in both RNAs and protein. However, although a nucleolus appears as a defined body, its components undergo a constant exchange with the nucleoplasm. Localisation of proteins to a nucleolus is generally transient (in the 10s of seconds), and their nucleolar occupancy relies upon their relative residence time, depending upon their affinity for complexes anchored to the nucleolus itself (Phair and Misteli, 2000). In this model the scaffold on which the nucleolus forms is the rDNA and rRNA, which recruit other nucleolar components through direct interactions, upon which a complex network is built. Many abundant nucleolar proteins (such as nucleophosmin (NPM) and nucleolin (NCL)) are proposed to act as 'hub proteins', interacting with and sequestering multiple protein partners under specific conditions (Reviewed in (Carmo-Fonseca et al., 2000) (Emmott and Hiscox, 2009)). RNAs may play a similar role, for example *alu*RNAs (non-coding RNAs transcribed from intronic Alu elements by Pol II) interact with NCL and NPM and are also required for nucleolar assembly (Caudron-Herger et al., 2015). The specific role of the rRNA in the formation of nucleolar

structure has been dissected by McStay *et al*: Pseudo-NORs - arrays of heterologous UBF binding sequences integrated into ectopic sites on human chromosomes, which are sufficient to recruit components of the Pol I transcription machinery during interphase but are transcriptionally inactive – are able to adopt some morphological characteristics of nucleoli, as they form secondary constrictions in mitotic chromosomes typical of NORs, and recruit some nucleolar factors to result in an equivalent composition to nucleolar FCs (Mais et al., 2005; Prieto and McStay, 2007); Neo-NORs – arrays of UBF binding sequence interspersed with an rDNA transcription unit, which are transcriptionally competent - are able to additionally recruit the DFC and GC components and form functionally compartmentalized nucleoli (Grob et al., 2014b). Therefore, nucleoli form only at NORs that are transcriptionally active, and the number and size of nucleoli is directly linked to rates of Pol I transcription of the 47S pre-rRNA.

1.1.2 Transcription of the rRNA genes

A single human rDNA repeat is 43kb, consisting of a 13.3kb 47S pre-RNA coding region and a 30kb intergenic spacer (IGS). The 47S pre-RNA consists of the 18S, 5,8S and 28S ribosomal RNA sequences, positioned within sequences that are removed during rRNA processing and maturation – the 5' external transcribed spacer sequence (5'ETS), the internal transcribed spacer sequences (ITS1 and ITS2) and the 3'ETS. The IGS contains the 47S rDNA promoter, which has a bipartite architecture composed of a core element and an (UCE) located 100bp upstream. In addition, the IGS harbors a number of other regulatory features, including 'spacer promoters' similar to and upstream of the 47S rDNA promoter, and terminator elements including multiple 'T' sequences 3' of the 47S rDNA coding region as well as a single 'T_0' terminator sequence 5 'of the rDNA promoter (Reviewed in (McStay and Grummt, 2008; Smirnov et al., 2016)) (FIGURE 1).

Transcription of 47S pre-rRNA genes by Pol I can occur at very high rates, accounting for >30% of the transcriptional activity of an exponentially growing cell (Reviewed in (Warner, 1999; Warner et al., 2001; Moss et al., 2007)). However, not all of the rDNA repeats are transcribed. The rDNA can exist in four distinct chromatin states: silent, pseudo-silent, poised and active. Approximately half of all rDNA repeats exhibit a silent chromatin conformation, associated with heavily CpG methylated DNA, heterochromatic histone modifications including H3K9me2/3, H4K20me3, & H3K27me/me3, and the association of heterochromatin protein HP1. The remaining rDNA repeats are associated with DNA hypomethylated at CpG sites. These repeats

can be either pseudo-silent, exhibiting a closed chromatin conformation, or transcriptionally competent, exhibiting an open chromatin conformation associated with euchromatic histone modifications, including H3 & H4 actelylation and H3K4me2. Transcriptionally competent rDNA repeats are not necessarily active, but rather can exist in a 'poised' state, as further changes in chromatin are required for initiation and elongation of Pol I transcription to occur (Reviewed in (Grummt and Pikaard, 2003; Huang et al., 2006; McStay and Grummt, 2008; Sanij and Hannan, 2009; Grummt and Langst, 2013; Hamperl et al., 2013; Östlund Farrants, 2017)) (FIGURE 3 A). While some NORs are completely silent, in others heterochromatic and euchromatic rDNA repeats are interspersed (Zillner et al., 2015).

Silent rDNA copies are maintained by NoRC (nucleolar remodeling complex; comprised of TIP5 (TTF1 interacting peptide 5) and the ISWI-ATPase SNF2h). NoRC in complex with pRNA, a noncoding RNA transcribed upstream of the rDNA promoter, recruits several silencing factors, including HDAC1 (histone deacetylase 1), DNMT1 (DNA methyltransferase 1) & DNMT3b (DNA methyltransferase 3b), and PARP1 (poly(ADP-ribose) polymerase 1) resulting in the establishment of DNA methylation and heterochromatic histone modifications such as H3K9me2/3 (Santoro et al., 2002; Zhou et al., 2002; Santoro and Grummt, 2005; Mayer et al., 2006; Schmitz et al., 2010; Cong et al., 2012; Guetg et al., 2012). In addition, KMT5C (lysine methyltransferase 5C / SUV420H2) can be recruited by *PAPAS* (promoter and pre-RNA antisense) noncoding RNAs transcribed at the rDNA promoter in the antisense direction when Pol I transcription is absent, resulting in H4K30me3 (Bierhoff et al., 2010; Bierhoff et al., 2014). Active rDNA repeats are established by chromatin remodelling factor CSB (cockayne syndrome protein B) which associates with G9a histone methyltrasferase, resulting in the establishment of euchromatic structure (Bradsher et al., 2002; Yuan et al., 2007). Both NoRC and CSB are recruited to the rDNA promoter by TTF-1 (transcription termination factor 1), which binds the T_0 terminator sequence 5' of the rDNA promoter (Nemeth et al., 2004; Li et al., 2006; Cong et al., 2012)(Reviewed in (Grummt and Langst, 2013; Östlund Farrants, 2017))(FIGURE 3 A).

At euchromatic rDNA repeats, the upstream binding factor (UBF) binds across the entire transcribed region of the gene and decondenses rDNA chromatin, establishing the transcriptionally competent state. UBF is a sequence non-specific high mobility group (HMG) protein, and its HMG boxes enable UBF dimers to loop 140bp of DNA into a single turn, inducing a nucleosome like structure termed the enhancesome (Stefanovsky et al., 2001a). UBF establishes a specialised 'open' chromatin structure

at the rDNA, which is characterised by the absence of linker histone H1 and reduced nucleosome occupancy (O'Sullivan et al., 2002; Sanij et al., 2008)(Reviewed in (Sanij and Hannan, 2009)). The open chromatin structure is necessary for Pol I transcription: euchromatic rDNA repeats with a pseudo-silent 'closed' chromatin structure can be distinguished from those with an 'open' chromatin structure associated with UBF by differential accessibility to a DNA crosslinking agent, psoralen; in the absence of UBF, euchromatic rDNA repeats form the closed structure inaccessible to psoralen, and are not associated with the Pol I transcriptional machinery (Sanij et al., 2008) (FIGURE 3 A). UBF is also associated with highly active Pol II transcribed genes, suggesting it introduces a chromatin state compatible with high levels of transcription (Diesch et al., 2015; Sanij et al., 2015). The association of UBF and open chromatin structure is stably maintained throughout the cell cycle, and confers the approximately 10-fold less compact chromatin of NORs visible as constrictions on metaphase chromosomes (Heliot et al., 1997; Chen et al., 2004; Mais et al., 2005; Sanij et al., 2008; Grob et al., 2014b).

At transcriptionally competent rDNA repeats in the poised state, the promoter exhibits H3 and H4 hypoacetylation and the bivalent histone modifications H3K4me3 and H3K27me3, and the promoter bound nucleosome occupies a position that is repressive for transcription. At transcriptionally competent rDNA repeats in the active state, the promoter exhibits H3 and H4 hyperactylation, and the promoter bound nucleosome occupies a position that is permissive for transcription (Xie et al., 2012). The active state can be established by CSB and the B-WICH complex (comprising William syndrome transcription factor (WSTF), nuclear myosin 1 (NM1), and ATPase SNF2h), which is required for the recruitment of histone acetyltransferases PCAF (p300/CBP-associated factor) and GCN5, resulting in the establishment of euchromatic structure (Bradsher et al., 2002; Yuan et al., 2007; Felle et al., 2010; Vintermist et al., 2011; Shen et al., 2013), while the poised state can be established by the chromatin remodelling complex NuRD (Nucleosome Remodelling and Deacetylase, containing class I histone deacetylases, CHD3/4 ATPases, and MDB2/3 methyl-CpG binding proteins), which co-bind with CSB to the rDNA promoter (Langst et al., 1997; Yuan et al., 2007; Xie et al., 2012) (FIGURE 3 A).

Transcription of 47S pre-RNA requires formation of a pre-initiation complex (PIC) at the promoter of active rDNA repeats. This comprises Pol I, and the regulatory factors UBF, SL1 (Selective factor 1, comprised of TATA binding protein (TBP) and TBP associated factors TAFI110/95, TAFI68, TAFI48, TAFI35, and TAFI12), and RRN3.

UBF binds the promoter as a dimer at the UCE and core elements, co-stabilising binding of the SL1 complex. This facilitates binding of initiation competent Pol I associated with RRN3, through interaction between SL1 and RRN3, and direct interaction of both UBF and SL1 with Pol I subunits (Learned et al., 1985; Learned et al., 1986) (Bell et al., 1988; Jantzen et al., 1992; Hempel et al., 1996; Tuan et al., 1999; Miller et al., 2001; Friedrich et al., 2005) (Reviewed in (Goodfellow and Zomerdijk, 2012; Diesch et al., 2014)) (FIGURE 3).

1.1.3 The regulation of 47S pre-rRNA transcription rates

Levels of 47S-preRNA are predominantly regulated by changes in rates of Pol I transcription from a fixed number of transcriptionally competent rDNA repeats, rather than changes in the proportion of open and closed rDNA repeats. The inheritance of open and closed rDNA repeats is stably transmitted throughout the cell cycle, for example with the establishment of epigenetic states occurring at rDNA repeats immediately following their replication, and with UBF associated with open rDNA repeats throughout mitosis, as described above (Scheer and Rose, 1984; Roussel et al., 1996) (Guetg et al., 2010; Guetg et al., 2012). Long-term changes in the ratio of open to closed rDNA repeats can occur: For example, the proportion of open rDNA repeats varies according to cell type, and down regulation of rDNA transcription during differentiation correlates with a decreased proportion of open repeats (Poortinga et al., 2011a; Shiao et al., 2011; Savic et al., 2014; Woolnough et al., 2016); Further, during senescence rDNA repeats are epigenetically silenced, while in contrast epigenetic activation of rDNA repeats is associated with tumor cells (Machwe et al., 2000; Powell et al., 2002; Pietrzak et al., 2011) (Reviewed in (Stefanovsky and Moss, 2006; Sanij et al., 2008; Grummt and Langst, 2013)). However, the consensus is that short-term changes in rates of Pol I transcription do not correspond with changes in active gene number, and in fact it has been shown that changes in the proportion of active genes do not result in changes in Pol I transcription rates (Stefanovsky and Moss, 2006). However, the consensus is that short-term changes in rates of Pol I transcription do not correspond with changes in active gene number, and in fact it has been shown that changes in the proportion of active genes do not result in changes in Pol I transcription rates (Stefanovsky and Moss, 2006; Sanij et al., 2008).

Rates of Pol I transcription are sensitively regulated, and respond rapidly to changes in conditions. Regulation of Pol I transcription can occur at multiple steps, including PIC assembly, initiation and promoter escape, elongation, and transcription termination and re-initiation (Hung et al., 2017)(Reviewed in (Goodfellow and Zomerdijk, 2012)).

Signaling pathways that regulate cell growth and division directly target Pol I transcription factors, including PIC components SL1, UBF, RRN3, and Pol I, as well as chromatin remodelling factors that mediate the transition between poised and active state at the rDNA promoter. This results in regulation of the rates of transcription specifically on rDNA repeats that are already in an open conformation. Broadly, pathways that upregulate rDNA transcription are those that promote cellular growth and proliferation, for example cellular energy, nutrient, and growth factor signaling pathways. While, downregulation of rDNA transcription in response to stress stimuli such as metabolic or genotoxic stress, leads to growth arrest associated with cell cycle arrest or senescence (FIGURE 3 B).

1.1.3.1. *Cell Cycle*. Pol I transcription is tightly co-ordinated with the cell cycle. 47S pre-rRNA transcription is inactivated at the start of mitosis, although Pol I transcription factors UBF and SL1 remain associated with the rDNA repeats throughout mitosis (Roussel et al., 1993; Jordan et al., 1996; Roussel et al., 1996). Reactivation of low levels of 47S pre-rRNA transcription occurs as cells enter G1, and 47S pre-rRNA transcription is increased to maximum levels during S and G2 as cells grow in preparation for cell division (Weisenberger and Scheer, 1995; Kuhn et al., 1998; Klein and Grummt, 1999; Leung et al., 2004)(Reviewed in(Russell and Zomerdijk, 2005)). This is achieved by post-transcriptional modification of Pol I transcription factors: for example, inhibitory phosphorylation of SL1 and RRN3 by the mitotic cell cycle regulatory Cyclin B/CDK1 (cyclin dependent kinase 1) complex, and deacetylation of SL1 by SIRT1, prevent formation of the active PIC during mitosis (Heix et al., 1998; Kuhn et al., 1998; Sirri et al., 1999; Voit et al., 2015); SL1 is dephosphorylated by CDC14B (cell division cycle 14B) and acetylated by PCAF upon exit from mitosis, stabilizing formation of the PIC (Muth et al., 2001; Voit et al., 2015); activating phophorylation of UBF at Ser484 by G1 cell cycle regulatory Cyclin D /CDK4 (cyclin dependent kinase 4) and at Ser388 by S phase cell cycle regulatory Cyclin E/ CDK2 (cyclin dependent kinase 2) complexes, and activating acetylation of UBF by PCAF in S phase, promotes Pol I recruitment to the PIC in G1 and S (Voit et al., 1999; Voit and Grummt, 2001; Meraner et al., 2006).

1.1.3.2 *Nutrient and energy status.* Rates of 47S pre-rRNA transcription also respond to cell energy and nutrient status, as well as growth factor signaling. For example, activation of mTOR (mammalian target of rapamycin), a key

regulator of cell growth that responds to diverse environmental cues including growth factors and energy levels, activates Pol I transcription; phosphorylation of both RRN3, and the C-terminal of UBF, by S6K1 (ribosomal protein S6 kinase B1) promotes formation of the PIC (Hannan et al., 2003; Mayer et al., 2004; Kang et al., 2016). UBF is also phosphorylated at its C-terminal by PI3K (phosphoinoside 3-kinase), for example in response to IGF1 (insulin-like growth factor 1) stimulation, promoting PIC formation (Drakas et al., 2004; Wu et al., 2005). Activation of the mitogen activated protein kinase (MAPK) pathway in the presence of growth factors results in phosphorylation of RRN3 at Ser633 and Ser649 by ERK (extracellular signal-regulated kinase) and RSK (ribosomal protein S6 kinase A1) respectively, increasing RRN3 transcriptional activity (Zhao et al., 2003). ERK can also phosphorylate UBF at Ser117 and Ser201, promoting Pol I transcription by facilitating transcriptional elongation through UBF bound rDNA (Stefanovsky et al., 2001b; Stefanovsky et al., 2006a; Stefanovsky et al., 2006b). In contrast, energy and nutrient depletion leads to downregulation of Pol I transcription. For example, AMPK (AMP-activated protein kinase) is a key regulator of cellular energy homeostasis, activated in response to changes in AMP:ATP ratio and regulating adaptive responses the reduce cellular energy consumption. AMPK reduces rDNA transcription in response to energy depletion by phosphorylating RRN3 at Ser635, impairing its interaction with SL1 and preventing PIC formation (Hoppe et al., 2009).

Complexes that change the chromatin structure state at the rDNA promoter between a poised and active are also regulated by cell energy and nutrient status. For example, SIRT1 (sirtuin 1) is activated following changes in the NAD+/NADH ratio induced by reduction in energy status. It is part of the eNoSC (energy dependent nucleolar silencing) protein complex composed of NML, SIRT1, and SUV39H1, which in response to energy deprivation driving reduction of 47S pre-rRNA transcription, is recruited to the rDNA promoter and results in deacetylation of histones by SIRT1 and dimethylation of H3K9 by SUV39H1 (Murayama et al., 2008; Kumazawa et al., 2011; Song et al., 2013; Yang et al., 2013a). SIRT1 also regulates NoRC, through TIP5 acetylation and deacetylation by MYST1 (MYST family histone acetyltransferase 1/ MOF) and SIRT1 respectively, resulting in histone deacetylation and nucleosome remodelling to a position incompatible with transcription at the rDNA promoter following reduction in intracellular energy status (Zhou et al., 2009). During

glucose starvation AMPK activates the histone demethylase KDM2A (lysisine specific demethylase 2A), which can repress 47S pre-rRNA transcription by demethylating H3K36 at the promoter of open rDNA repeats (Tanaka et al., 2010). While the binding of NuRD is to the rDNA promoter is increased during serum starvation, resulting in an increased proportion of nucleosomes in the position incompatible with transcription (Xie et al., 2012). In all of these cases the poised state is reversible, and the active state re-established upon normal growth conditions.

1.1.3.3. *Stress response.* Pol I transcription is rapidly downregulated upon conditions of cellular stress. For instance, the tumor suppressor transcription factor p53, which induces cell cycle arrest, senescence and apoptosis, directly inhibits Pol I transcription by binding to SL1 preventing its interaction with UBF and formation of the PIC (Zhai and Comai, 2000). RB (retinoblastoma protein) also negatively regulates Pol I transcription by interacting with UBF, preventing its interaction with the rDNA promoter and formation of the PIC leading to cell cycle arrest and/or senescence (Cavanaugh et al., 1995; Voit et al., 1997; Hannan et al., 2000a; Hannan et al., 2000b). p14ARF, which mediates an anti-proliferative response under conditions of oncogenic stress, inhibits Pol I transcription by both inhibiting UBF phosphorylation and hence its ability to recruit the PIC, and preventing nucleolar import of the Pol I transcription termination factor TTF-1 and other factors (Ayrault et al., 2006; Lessard et al., 2010; Saporita et al., 2011)(Reviewed in (Maggi et al., 2014)). DNA damage results in rapid inhibition of Pol I transcription, and the DNA damage response kinases ATM (ataxia-telangiectasia mutated kinase), ATR (ataxia telangiectasia and Rad3-related protein) and DNA-PK (DNA-dependent protein kinase) can each inhibit Pol I transcription by different mechanisms (Kruhlak et al., 2007; Calkins et al., 2013; Larsen et al., 2014; Sokka et al., 2015). Upon oxidative stress the stress–activated protein kinase JNK2 (c-Jun NH_2-terminal protein kinase 2) inactivates RRN3 through phosphorylation of Thr200, preventing its interaction with SL1 and Pol I and formation of the PIC (Mayer et al., 2005).

These examples illustrate that the cell exquisitely regulates rates of 47S rRNA transcription, with the many diverse cell homeostasis pathways, such as cell growth, proliferation and stress response pathways, converging upon the Pol I transcription apparatus to fine tune its activity as a key step in ribosome biogenesis. This enables a

fine balance of promoting the high rates of ribosome biogenesis necessary for cell growth and proliferation under favourable conditions, as well as restricting this most energy demanding cellular process to preserve viability under unfavourable conditions.

1.2 The multifunctional nucleolus

Rates of Pol I transcription of the 47S rRNA genes underlies the structure and function of the nucleolus (See Section 1.1.1). Importantly, in addition to its fundamental role in ribosome biogenesis, the nucleolus can perform extra-ribosomal functions. Proteomic analysis of the nucleolus illustrates its plurifunctional nature - of the 4500 proteins reported in the nucleolar protein database (NOPdb) (http:// lamondlab.com/ NOPdb3.0/), less than half have defined functions in ribosome biogenesis (Andersen et al., 2002; Scherl et al., 2002; Coute et al., 2006; Leung et al., 2006). Proteins that localize to the nucleoli are instead involved in a diverse range of functions, including cell-cycle control, DNA replication and repair, stress signaling, RNA and RNP biogenesis, and chromatin regulation. Importantly, the nucleolar proteome is not static, but dynamically altered in response to cellular signaling pathways and changes in rates of rDNA transcription, enabling regulation of protein function through nucleolar sequestration or release (Andersen et al., 2005; Boisvert et al., 2010; Kar et al., 2011; Moore et al., 2011; Yamada et al., 2013). Nucleolar regulation of these functions is in some cases well defined, while in others the role of the nucleolus has only recently begun to emerge.

1.2.1 p53 activation by the nucleolar stress pathway

The classic extra-ribosomal function of the nucleoli is activation of tumor suppressor p53 by the nucleolar stress pathway. p53 is dubbed ‘the guardian of the genome’ as it is central to the regulation of multiple cellular stress responses, such as transient cell cycle arrest, senescence and apoptosis. Under normal conditions, p53 protein is precisely maintained at basal levels, particularly by the 26S proteasome and E3 ligase HDM2 (human homologue of mouse double minute 2), which both binds p53 preventing its transcriptional activity and ubiquitinates p53 targeting it for proteasomal degradation. The activation of p53 can occur via multiple nucleolar components and signaling pathways, including for example, A) negative regulation of HDM2 by nucleolar p14ARF, B) negative regulation of HDM2 by free RPs, C) transcriptional regulation of p53 by nucleolar proteins, and D) regulation of p53 localisation and transport via the nucleoli (FIGURE 4). Further, p53 and its downstream targets can

negatively regulate rRNA transcription, conceivably resulting in a feedback loop enhancing p53 regulation by the nucleoli.

The predominantly nucleolar protein, p14ARF binds HDM2 and inhibits its activity toward p53. Under normal conditions p14ARF is maintained at low levels by ubiquitin mediated degradation. In response to a variety of signals, particularly oncogenic or genotoxic stress, p14ARF is transcriptionally upregulated and stabilized by NPM. Nucleolar localization mediates the NPM-p14ARF-p53 pathway in two ways: First, translocation of NPM from the nucleoli to the nucleoplasm promotes the interaction of p14ARF with HDM2 (Itahana et al., 2003) and disrupts HDM2 association with p53 (Kurki et al., 2004), preventing p53 ubiquitination and degradation. Second, increased nucleolar localisation of p14ARF may both result in its further stabilization, by preventing its association with nucleoplasmic ubiquitin ligases, as well as potentially sequester HDM2 from p53 (Kruse and Gu, 2009)(Reviewed in (Lee and Gu, 2010)).

Perturbations in ribosome biogenesis due to inhibition of rRNA transcription or disruption of 40S or 60S ribosomal subunit biogenesis lead to p53 activation by nucleolar stress through free RPs, L5 and L11 in particular, binding to HDM2 and inhibiting its activity towards p53 (Lohrum et al., 2003; Zhang et al., 2003; Bhat et al., 2004; Dai and Lu, 2004; Jin et al., 2004; Dai et al., 2006; Chen et al., 2007; Horn and Vousden, 2008; Zhu et al., 2009b; Zhang et al., 2010; Daftuar et al., 2013)). Upon nucleolar stress, L5 and L11 together with 5S rRNA are mutually stabilised, and as part of the RPL5/RPL11/5S rRNA complex bind HDM2 in its central zinc finger domain, inhibiting both its E3 ligase function and its association with p53 (Fumagalli et al., 2009; Bursac et al., 2012; Fumagalli et al., 2012; Sloan et al., 2013; Nishimura et al., 2015). This pathway appears to be regulated at a number of levels, for example L11 can be sequestered in the nucleoli by factors such as ribosome biogenesis factor PICT1 (protein interacting with carboxyl terminus 1) (Sasaki et al., 2011)(Reviewed in (Suzuki et al., 2012)), or through post-translation modification by NEDD8 (Neddylin) (Sundqvist et al., 2009; Mahata et al., 2012b; Ebina et al., 2013), the inhibition of which promotes association with HDM2. The requirement of RP binding to Mdm2 for p53 activation by nucleolar stress has also been confirmed an *in vivo* mouse model; mice expressing mutant Mdm2 that cannot bind RPL5 and RPL11 lack a p53 response to inhibition of ribosome biogenesis (Macias et al., 2010).

Additional factors involved in ribosome biogenesis also regulate p53 under conditions of nucleolar stress, either by stabilisation as described above, or by alternative

mechanisms. For example, p53 mRNA is stabilized by NCL and L26, which bind to the 5'UTR of p53 mRNA, resulting in increased p53 translation (Takagi et al., 2005). Interestingly under normal conditions, HDM2 targets RPL26 for proteasomal degradation by ubiquitination; thus decreased HDM2 activity following nucleolar stress would result in L26 stabilisation and further increase in p53 translation and abundance (Ofir-Rosenfeld et al., 2008). Furthermore, a number of nucleolar proteins can dissociate the interaction between p53 and HDM2, thus resulting in p53 stabilization. For example RPS3 directly interacts with p53 (Yadavilli et al., 2009), while Nucleostemin and CSIG (cellular senescence inhibited gene protein) can bind directly to HDM2 (Dai et al., 2008; Meng et al., 2008; Xie et al., 2016). Further, NCL associates with both p53 and HDM2, and depending on post-translational regulation can either antagonises their interaction or promote p53 ubiquitination (Daniely et al., 2002; Saxena et al., 2006; Bhatt et al., 2012). Also, post-translational modification and association with co-factors regulate p53 activity towards its transcriptional targets. For example, p53 transcriptional activity relies upon acetylation by its coactivator p300/CBP, which is facilitated by MYBBP1A (MYB binding protein 1A), which in turn is sequestered in the nucleolus and released upon nucleolar stress in response to nutrient starvation or DNA damage (Kumazawa et al., 2011; Kuroda et al., 2011; Mahata et al., 2012a; Ono et al., 2013; Kumazawa et al., 2015) (Kumazawa et al., 2015).

In addition to its sequestration of factors that regulate p53, the nucleolus may play direct role in p53 transport and proteasomal degradation (Boyd et al., 2011). Both HDM2 and ubiquitinated p53 traffic through the nucleolus, and this may be required for the cytoplasmic export and subsequent degradation of p53. If p53 and HDM2 are co-transported with ribosomal subunits, then disruption of ribosome biogenesis could result in p53 accumulation in part due to abrogation of this process sequestering p53 away from the proteasome (Tao and Levine, 1999b, a; Klibanov et al., 2001; Mekhail et al., 2005; Boyd et al., 2011).

It is now clear that the nucleoli integrate growth, proliferation and stress signals and coordinating cellular response through connecting ribosome biogenesis to p53 activation. The complex mechanisms by which the nucleolus and its components modulate p53 activity is indicative of its importance as central hub responsible for "fine tuning" p53 response, enabling the cell to integrate signals from multiple upstream pathways that converge on ribosome biogenesis to formulate a p53-mediated cellular response.

1.2.2 Additional functions of the nucleoli

In addition to the well characterised p53 nucleolar stress pathway, the nucleolus performs range of other extra-ribosomal functions. Some specific examples of the nucleolar regulation of components of cell cycle control, DNA replication and repair, stress signaling pathways and RNA and RNP biogenesis are presented in TABLE 1.

1.2.2.1 *Cell Cycle.* The nucleoli and ribosome biogenesis are tightly coordinated with the cell cycle. As discussed above, Pol I transcription is regulated by cell cycle specific factors to result in its activation in G1, upregulation as the cell cycle progresses, and deactivation in mitosis. Conversely, the nucleoli function in the regulation of cell cycle progression. Nucleolar control of cell cycle progression is exemplified by induction of p53-mediated cell cycle arrest following inhibition of rDNA transcription, however the nucleolus can also mediate the function of additional cell cycle regulatory proteins independent of the p53 pathway. For example, HDM2 stabilizes the E2F-1 transcription factor, and binding of free RPL11 to HDM2 can inhibit this function and thereby prevent G1-S cell cycle progression (Donati et al., 2011b). hCDC14B is sequestered in the nucleoli during interphase and its release at the onset of mitosis is required for correct mitotic progression: CDK1/cyclin B is activated by CDC25 dependent dephosphorylation, and once activated promotes entry into mitosis; upon onset of mitosis, hCDC14B dephosphorylates and inactivates CDC25, enabling efficient inactivation of CDK1 at late M phase (Tumurbaatar et al., 2011). Release of hCDC14B from the nucleoli in interphase can prevent entry into mitosis (Peddibhotla et al., 2011). These and other examples indicate that the nucleoli can mediate multiple cell cycle stages, including G1-S progression, DNA replication and mitosis (TABLE 1).

1.2.2.2 *Stress response*. While activation of p53 is the classical example of the nucleolar stress response, a number of p53-independent pathways have also been identified. For example, free RPL3 can mediate upregulation of p21 expression, and induce cell cycle arrest and apoptosis in the absence of p53 (Russo et al., 2013; Esposito et al., 2014; Russo et al., 2016). The nucleoli can sequester and release specific proteins in response to hypoxia or heat shock and mediate stress response. Under normal conditions, p14ARF can sequester hypoxia inducible factor (HIF1) alpha subunit in the nucleoli, inhibiting HIF1

transcriptional activity, and VHL (Von Hippel-Lindau tumor suppressor) ubiquitinates and targets HIF1 for proteasomal degradation. In response to hypoxia, VHL is sequestered in the nucleoli, and HIF1 can activate target gene transcription (Fatyol and Szalay, 2001; Mekhail et al., 2004). Specific long non-coding RNAs are transcribed from the IGS at the rDNA in response to stress, which can sequester and immobilize specific proteins, for example VHL under conditions of acidosis and HSP70 (heat shock protein 70kDa) following heat shock, in a distinct structure within the nucleoli termed the detention center (Audas et al., 2012; Jacob et al., 2013). (TABLE 1).

1.2.2.3 *DNA damage response.* The nucleoli may also be involved in the DNA damage response (DDR). On one hand, DNA damage results in inhibition of rDNA transcription and reorganization of nucleolar structure (Kruhlak et al., 2007; Gilder et al., 2011; Moore et al., 2011; Calkins et al., 2013; Jin et al., 2014; Larsen et al., 2014; Lin et al., 2014; Sokka et al., 2015). On the other, proteomic and fluorescent imaging analysis has shown that a number of DDR proteins localize to the nucleoli, and that in response to different genotoxic insults a distinct population of proteins translocate between the nucleoli and the nucleoplasm (Cohen et al., 2008) (Boisvert et al., 2010; Boisvert and Lamond, 2010; Moore et al., 2011). For some proteins, nucleolar regulation in DDR response has been further characterised. For example, hCDC14B is phosphorylated by CHK1 (checkpoint kinase 1) and released from the nucleoli following DNA damage, leading to hCDC14B-induced activation of APC/C^{Cdh1} (anaphase-promoting complex/cyclosome activator protein Cdh1) and the G2 DNA damage cell cycle checkpoint (Bassermann et al., 2008; Peddibhotla et al., 2011). DSB repair factor BRCA1 interacts with ribosomal protein RPSA in the nucleoli, and following irradiation it translocates to DNA-damage response foci in the nucleoplasm, then reverts to the nucleoli after several hours presumably once DNA repair is complete (Guerra-Rebollo et al., 2012). NCL relocalises from the nucleoli to the nucleoplasm upon DNA damage, where it interacts with histone H2A.X phosphorylated at Ser139 (γH2A.X) and accumulates at DNA double stranded break (DSB) sites, and NCL knockdown results in reduced DSB repair (Kobayashi et al., 2012). Finally, it has been proposed that the repetitive nature and high rates of transcription the rDNA repeats make them particularly vulnerable to genomic instability, and thus they can activate DNA damage response in a highly sensitive manner, performing a protective function for the genome as a whole (Rubbi and Milner, 2003; Stults

et al., 2008; Ganley et al., 2009; Ide et al., 2010; Kobayashi, 2011). (TABLE 1).

1.2.2.4 *Autophagy and senescence.* The nucleolus is also related to autophagy and senescence. Signaling pathways that regulate rDNA transcription can also regulate autophagy, the survival-promoting pathway that recycles intracellular proteins and organelles. Autophagy is primarily induced by nutrient stress, and thus certain stress signals can result in both inhibition of rDNA transcription and activation of autophagy (Calle et al., 1999; Hannan et al., 2003; Iadevaia et al., 2012; Chen et al., 2016a). More directly, inhibition of Pol I transcription can induce formation of autophagic vesicles (Drygin et al., 2011; Kreiner et al., 2013; Katagiri et al., 2015; Chen et al., 2016b). The mechanisms connecting nucleolar disruption to autophagy are not clear, however recent reports have implicated nucleolar proteins including NPM (Katagiri et al., 2015). Senescence is a response in which cells adopt a state of permanent cell cycle arrest. The key signaling pathways mediating senescence include p53 and p16INK4a-RB (Reviewed in (Campisi and di Fagagna, 2007)), thus the nucleolus may indirectly induce senescence through activation of p53, or through RB which transiently localizes with the nucleolus and nucleolar proteins, though the function of these associations in the regulation of the RB pathway is less well-defined (Hannan et al., 2000a; Hannan et al., 2000b; Takemura et al., 2002; Angus et al., 2003; Grinstein et al., 2006). The nucleoli may also mediate telomere stability via the regulation of the assembly and activity of both telomerase and the telomere binding complex shelterin (Reviewed in (Hein, 2012)). Therefore, the nucleoli may be involved in mediating both replicative senescence and oncogene-induced senescence, by mediating telomere stability and senescence signaling pathways. (TABLE 1).

1.2.2.5 *RNA and RNP biogenesis.* Nucleoli can also play a role in the biogenesis of non-ribosomal RNAs and protein-RNA complexes (ribonucleoproteins, or RNPs) (Reviewed in (Pederson, 1998; Gerbi et al., 2003; Pederson and Tsai, 2009)) (TABLE 1). Post-transcriptional regulation of RNAs by the nucleoli includes processing, nucleolar localisation and export, and regulation of small non-coding RNAs such as miRNAs. For example, the classic function of small nucleolar RNAs, which act as guide sequences for snoRNPs to carry out appropriate modifications to target nucleotides, is the post-transcriptional modification of rRNAs, consistent with their localization to the nucleoli. However, they are also involved in the modification of splicesomal

RNAs (snRNAs) and thus the regulation of pre-mRNA splicing; several snRNAs transiently localize to the nucleoli and can be are modified by snoRNPs prior to assembly into snRNPs (Lange and Gerbi, 2000; Yu et al., 2001; Gerbi and Lange, 2002; Huttenhofer et al., 2002). Also, specific miRNAs can be post-transcriptionally regulated by NCL (Shiohama et al., 2007; Pickering et al., 2011; Pichiorri et al., 2013), a number of miRNA are enriched in the nucleoli but can translocate to the cytoplasm upon specific stimuli (Politz et al., 2006; Politz et al., 2009) (Li et al., 2013; Bai et al., 2014). One of the first extra-ribosomal functions reported for the nucleoli was the processing of the signal recognition particle (SRP), an abundant cytosolic RNP that recognizes and binds the N-terminal hydrophobic sequence of specific newly synthesized proteins and delivers them to the endoplasmic reticulum for translocation. Both RNA and protein SRP components are localized in the nucleoli, suggesting a nuceolar phase is required for its processing and assembly (Jacobson and Pederson, 1998; Politz et al., 2000; Politz et al., 2002). This has now expanded to include the maturation and assembly of other RNPs such as telomerase, RNAse P, and snRNPs. It has been proposed that the nucleoli have evolved as a common assembly site for RNPs (Reviewed in (Pederson and Politz, 2000)). Indeed, it seems likely that, with the high density of factors involved in RNA metabolism at the nucleoli, they would be co-opted to perform extra-ribosomal RNA functions.

1.2.2.6 Differentiation. More recently, the role of the nucleoli in differentiation has been highlighted. Both rRNA transcription and active rRNA copy number are reduced during normal development processes (Poortinga et al., 2004; Poortinga et al., 2011b; Savic et al., 2014; Woolnough et al., 2016) Zhang *et al* (2014) reported in Drosophila that increasing rRNA transcription can delay differentiation (Zhang et al., 2014). In the same year, Hayashi *et al* reported that inhibition of Pol I transcription induced differentiation in human HL-60 myeloblastic and THP-1 monocytic cell lines *in vitro*, as well as mouse hematopoetic stem cells *ex vivo* (Hayashi et al., 2014). In human embryonic stem cells (ESCs), differentiation is associated with reduced rRNA transcription prior to any changes in rDNA heterochromatin, and inhibition of Pol I transcription is sufficient to induce markers of differentiation (Woolnough et al., 2016). Conversly, increased transcription of rRNA and other ncRNAs is an early hallmark of dedifferentiation of hepatocytes (Lauschke et al., 2016). It has been proposed that nucleoli may mediate pluripotency via mediating global

chromatin states (discussed further below) (Savic et al., 2014). Therefore, rRNA transcription may play a regulatory role in the control of pluripotency and differentiation.

1.2.3 The nucleoli in genome organisation and chromatin regulation.

The organization of the genome within nucleus contributes to the regulation of processes including transcription, DNA replication and establishing chromatin. Distant genomic loci can associate with each other to form both short- and long-range interactions, and changes in the positioning of genes in the nucleus can affect their regulation (Reviewed in (Gibcus and Dekker, 2013; Bonev and Cavalli, 2016)). The nucleolus is surrounded by a shell of dense heterochromatin, known as the perinucleolar heterochromatin. This region associates with the silent CpG methylated rDNA repeats (Akhmanova et al., 2000), as well as satellite DNA that surrounds the NORs (Guetg et al., 2010). Additional loci from multiple sites at different chromosomes can also be constrained at the nucleolar periphery, indicating a role for the nucleoli in higher order chromatin arrangement (Reviewed in (Guetg and Santoro, 2012)). Recent genome wide analysis classified approximately 4% of the genome, in addition to regions containing NORs, as nucleolus-associated chromatin domains (NADs) (Nemeth et al., 2010). Regions reported to associate with perinucleolar heterochromatin include satellite repeats, telomeric, and centromeric regions (Stahl et al., 1976; Leger et al., 1994; Wong et al., 2007; Nemeth et al., 2010; van Koningsbruggen et al., 2010), the Y chromosome (Comings, 1980), the inactive X chromosome (Xi) (Zhang et al., 2007b), imprinted chromatin regions (Mohammad et al., 2008; Pandey et al., 2008), and repressed gene clusters specific to different cell types (Nemeth et al., 2010; van Koningsbruggen et al., 2010). Common characteristics of NADs are repressive histone marks and reduced gene expression, including repetitive regions, regions with low gene density and regions enriched in repressed genes (Nemeth et al., 2010; van Koningsbruggen et al., 2010). Many NADs also associate with the nuclear envelope, a region known to be associated with silent heterochromatic DNA (van Koningsbruggen et al., 2010; Kind et al., 2013). Therefore, the peri-nucleolar regions are proposed to function in the maintenance of repressive epigenetic state at non-ribosomal DNA, and condensation of these regions into perinucleolar heterochromatin could be a general strategy to prevent genomic instability. In support of this, in murine cells depletion of TIP5, a component of NoRC which is required to maintain silent rDNA copies, resulted in loss of repressive histone marks and destabilization not only at the rDNA but also at associated satellite repeats (Guetg et al., 2010). Studies in Drosophila melanogaster have shown that the loss of

silent rDNA repeats result in reduced heterochromatic gene silencing across the genome (Paredes and Maggert, 2009; Paredes et al., 2011). The mechanisms that regulate the association of NADs with the nucleolar periphery and their subsequent epigenetic silencing has yet to be fully elucidated. However, non-coding RNA transcription is believed to play a key role in directing DNA sequences to the nucleolus. For example, it is proposed that the ongoing association of Xi with the perinucleolar region during S-phase is mediated by the lncRNAs Xist and Firre, and that this is required to maintain its heterochromatic silencing (Zhang et al., 2007a; Yang et al., 2015). The expression of non-coding RNA Kcnqlot1 results in relocalisation of its chromosomal domain to the perinucleolar region and its subsequent heterochromatic silencing (Mohammad et al., 2008; Pandey et al., 2008). Also, transcription of centromeric alpha-satellite RNA is required for the targeting of centromeres to the nucleoli (Wong et al., 2007). The proteins involved in mediating interactions with NADs have also begun to be elucidated, and may involve CTCF, NCL, NPM, and Ki-67, which are also involved in the regulation of rDNA transcription (Reviewed in (Matheson and Kaufman, 2016)). In contrast, actively transcribed 5S and tRNA RNA Pol III-transcribed genes can also be found at the nucleoli and enrichment for such genes has been documented in the perinucleolar region (Rawlins and Shaw, 1990; Huang et al., 1997; Bertrand et al., 1998; Thompson et al., 2003; Nemeth et al., 2010). Furthermore, a specific domain at the periphery of the nucleoli, designated the perinucleolar compartment (PNC), is highly enriched in both RNA binding proteins and Pol III transcripts (Reviewed in (Pollock and Huang, 2010)). Interestingly, in murine cells Pol III-transcribed 5S rRNA genes can induce association with the nucleoli of the genomic region in which the 5S rRNA genes are integrated, and this association can result in the repression of linked genes (Fedoriw et al., 2012). Importantly, these examples demonstrate an association between RNA expression, nucleolar localization, and the regulation of global gene expression and chromatin.

1.2.4 Summary - the nucleoli as a hub for cell homeostasis

In conclusion, the nucleolus is involved in the regulation of many key cellular processes, including cell cycle progression, stress response pathways such as p53, DDR, senescence, and apoptosis, and global regulation of gene expression through processes such as RNA and RNP biogenesis and regulation of the epigenome. Importantly, Pol I transcription is targeted by many of these same pathways (described above). As formation of a functional nucleolus depends upon active rDNA transcription, this results in changes in the nucleolar proteome and architecture (Andersen et al., 2005; Boisvert et al., 2010; Kar et al., 2011; Moore et al., 2011;

Yamada et al., 2013). It follows that changes in rates of rDNA transcription can consequently mediate multiple cellular functions. This positions the nucleolus as a central hub, which collects input from nearly all cell signaling pathways to sense the overall status of the cell and exquisitely regulate rates of ribosome biogenesis, then consequently orchestrates an appropriate response via its additional functions in cell proliferation and stress response (FIGURE 5).

1.3 The nucleolus and cancer.

Enlarged nucleoli have been associated with cancer cells since they were first described in the 19th century (Pianese, 1896). In fact, almost all cancer types display abnormal nucleoli (MacCarty, 1936) (Reviewed in (Derenzini et al., 2009)). In a broad range of tumors, nucleolar size is used as a parameter to predict clinical outcome; increased nucleolar size corresponds with worse tumor prognosis, while changes in nucleolar size have been used to measure the responsiveness of tumor cells to classical chemotherapeutic drugs (Reviewed in (Derenzini et al., 1998)). The average nucleolar size also corresponds with growth fraction, or proliferative capacity, in human tumors. As such, a higher number of cells with enlarged nucleoli indicate a higher number of proliferating cells (Derenzini et al., 2000). Similarly, as nucleolar size is closely related to rates of ribosome biogenesis, increased 47S pre-rRNA gene transcription has been widely observed in cancer, and correlated with an adverse prognosis (Williamson et al., 2006; Uemura et al., 2012). It was initially unclear whether abnormal nucleoli play a role in the cancer phenotype, or are merely an indirect effect of cell cycle-mediated regulation of Pol I transcription, which would be particularly pronounced in highly proliferative tissue (Reviewed in (Derenzini et al., 2009)). Regardless, it was hypothesised that the nucleoli are enlarged due to a requirement for enhanced ribosome biogenesis in cancer tissues, to achieve the levels of protein synthesis required for their characteristic unrestrained growth and proliferation.

1.3.1 Pol I transcription is directly regulated by tumor suppressors and oncogenes.

Support for a role of enhanced 47S pre-rRNA transcription and enlarged nucleoli in transformation comes from the fact that many tumor suppressors and proto-oncogenes directly target Pol I transcription and ribosome biogenesis. In fact, many of the components of pathways that upregulated Pol I transcription, for example MYC and the RAS/RAF/MEK/ERK and PI3K/AKT/mTOR cascades, act as oncoproteins that

drive uncontrolled proliferation; while components of pathways that downregulate Pol I transcription, for example p53, RB and p14ARF, act as tumor supressors that must be overcome for uncontrolled proliferation to occur.

A prominent example of an oncogene that upregulates ribosome biogenesis is the transcription factor MYC (product of the *C-MYC* oncogene), which drives cell growth through regulating transcription of a cohort of genes that comprise around 15% of the genome (Reviewed in (Patel et al., 2004; Dang et al., 2006; Ruggero, 2009)). MYC is overexpressed in approximately half of all cancers (Reviewed in (Nesbit et al., 1999; Dang, 2012)). MYC can directly regulate Pol I transcription by associating with SL1 to stabilize the UBF/SL1 complex, binding to the rDNA, and promoting Pol I recruitment (Arabi et al., 2005; Grandori et al., 2005; Shiue et al., 2009). Indirectly, MYC upregulates transcription of core Pol I subunits and transcription factors, including UBF and RRN3 (Poortinga et al., 2004; Grewal et al., 2005; Poortinga et al., 2011b).Further, MYC upregulates transcription of key factors required for ribosome biogenesis, such as Pol II transcription of the ribosomal protein genes, and Pol III transcription of 5S rRNA (Zeller et al., 2001; Schlosser et al., 2003; Gomez-Roman et al., 2006). Therefore MYC is a 'master regulator' of ribosome biogenesis (Reviewed in (Gomez-Roman et al., 2006; van Riggelen et al., 2010)). Other growth regulatory pathways that target Pol I transcription are also dysregulated in cancer, including the RAS/RAF/MEK/ERK and PI3K/AKT/mTOR signaling cascades (discussed above in 1.2.3). Multiple components can drive signaling down these cascades to act as oncoproteins: RAS and RAF are mutated in 30% and 6-7% of human cancers, respectively (Reviewed in (Pylayeva-Gupta et al., 2011; Osborne et al., 2012));PI3K is the most commonly overexpressed or hyperactivated in the mTOR pathway, but other molecules including AKT and S6K1 also act as oncoproteins and directly regulate Pol I transcription (Chan et al.; Samuels et al., 2004; Jastrzebski et al., 2007)(Reviewed in (Sheppard et al., 2012a)). The tumor suppressor PTEN, which is an upstream negative regulator of the P13K/AKT/mTOR pathway and also represses Pol I transcription by dissociating SL1 from the PIC complex, has reduced expression in a range of cancers (Zhang et al., 2005)(Reviewed in (Zhang and Yu, 2010)). These signaling pathways also converge in the activation of MYC (Chan et al.; Sears et al., 1999).

A prominent example of a tumor suppressor that downregulates ribosome biogenesis is p53 (discussed above in 1.2.3). As its designation as the 'guardian of the genome' implies, p53 performs numerous and diverse tumor suppressive functions, including as

a transcription factor central to the activation of cell cycle arrest, DNA damage response, senescence, and apoptosis (Reviewed in (Vousden and Lane, 2007; Sullivan et al., 2012; Mills, 2013)). It is the classic tumor suppressor – it is mutated in approximately half of all human tumors, and its function is compromised in the majority of remaining tumors expressing wild-type p53 (Petitjean et al., 2007b). p14ARF, which acts upstream of p53 and is activated in response to aberrant growth or oncogenic stress, is also a tumor suppressor commonly lost in up 40% of cancers (Zhang et al., 1998)(Reviewed in (Sharpless, 2005)). p14ARF can also act independently of p53 to induce cell cycle arrest and apoptosis, as well as directly inhibit Pol I transcription (Reviewed in (Sherr, 2006)). Downstream targets of p53 signaling also negatively regulate Pol I transcription, including repression of MYC (Ho et al., 2005), and activation of the tumor suppressor RB (Reviewed in (Sherr and McCormick, 2002)).

Consequently, dysregulated nucleoli in cancer appear to arise as a result of the normally strictly regulated control of ribosome biogenesis in cell growth and proliferation being overcome through being directly targeted by pathways that drive the process of transformation (Reviewed in (Hannan et al., 2013b)). However, the extent to which changes in the nucleoli contribute to the process of tumorigenesis remains to be answered.

1.3.2 Ribosomopathies are associated with cancer.

Further support for a role of dysregulation of the nucleoli in transformation comes from rare hereditary diseases arising from mutations in components of ribosome biogenesis, collectively termed Ribosomopathies (Reviewed in (Hannan et al., 2013a)). In many instances ribosomopathies, including Diamond–Blackfan anemia (DBA), 5q - syndrome, cartilage hair hypoplasia (CHH), Shwachman-Diamond Syndrome and X-linked dyskeratosis congenita (X-DC), are associated with cancer predisposition.

Diamond-Blackfan anemia is caused by loss of function mutations that affect ribosomal proteins, most commonly RPS19 ((Draptchinskaia et al., 1999; Gazda et al., 2006; Cmejla et al., 2007; Farrar et al., 2008) (Reviewed in (Dianzani et al., 2000)). DBA is characterised by hypoplastic anemia and a predisposition to cancer, particularly hematopoietic malignancies (Song et al., 2010; Dutt et al., 2011). 5q - myelodysplastic syndrome can be characterised by haploinsuffiency of an RP gene, as chromosome 5q deletion results in loss of one allele of *RPS14* (Ebert et al., 2008)(Reviewed in (Ebert, 2010)). Similarly to DBA, 5q-syndrome patients exhibit

impaired erythropoiesis and increased cancer susceptibility (Vlachos et al., 2012). Other ribosomopathies associated with increased cancer susceptibility affect the process of ribosome biogenesis at multiple stages, including rRNA transcription and processing and ribosome assembly. CHH results from mutations in RNase MRP (RNA component of the Mitochondrial RNA processing complex), a snoRNA that performs a number of functions, including in snRNP processing of rRNA ((Ridanpaa et al., 2001; Welting et al., 2004). Shwachman-Diamond Syndrome is due to mutations in SBDS (Shwachman-Bodian-Diamond Syndrome), a multifunctional nucleolar protein that can function in ribosomal biogenesis, particularly in assembly of ribosomal subunits (Wong et al., 2011). However, the contribution of nucleolar functions to the pathology of these diseases is not clearly defined. X-linked dyskeratosis congenita is caused by mutation in the *DKC1* gene, encoding dyskerin, a pseudouridine synthase component of snoRNPs (Heiss et al., 1998). Dyskerin mutations result in both impaired rRNA processing and decreased telomerase activity (Heiss et al., 1998; Mochizuki et al., 2004). X-DC is characterised by premature aging and increased risk of cancer. Importantly, in the case of X-DC, defects in ribosome biogenesis are reported to be responsible in part for cancer susceptibility conferred by dyskerin mutations - in mouse models of X-DC, increase in cancer incidence is observed prior to telomeric defects arising from decreased telomerase activity (Ruggero et al., 2003).

The mechanisms underlying increased cancer susceptibility in ribosomopathies are still being elucidated. Particularly, many of the mutations associated with defective ribosome biogenesis have additional, extra-ribosomal effects. However, cancer predisposition is common to ribosomopathies associated with mutations of different genes, encoding factors performing significantly dissimilar functions. In support of this, defects in ribosome biogenesis are also associated with cancer in sporadic tumors. For example, *RPL5* and *RPL11* are frequently mutated in T-cell lymphoblastic leukaemia (De Keersmaecker et al.). DKC1 expression is also reduced in a subset of human breast cancers, and pituitary adenoma (Montanaro et al., 2006; Bellodi et al.; Montanaro et al., 2010). SnoRNAs, required for post-transcriptional rRNA modification and processing, are increasingly reported to be associated with cancer (Reviewed in (Williams and Farzaneh, 2012)). For example, snoRNA U50 is reported to be mutated in breast carcinoma, prostate cancer, and B-cell lymphoma (Tanaka et al., 2000; Dong et al., 2008; Dong et al., 2009). This suggests that it is common, nucleolar related functions that play an important role in the increased risk of developing cancer.

Intriguingly, the mutations associated with ribosomopathies and increased risk of

cancer lead to defects, rather than increased rates, in ribosome biogenesis. This suggests that nucleolar dysregulation can contribute to the process of tumorigenesis independently of changes in the cells capacity for protein synthesis. Rather, the role of the nucleoli in cancer may relate to the additional functions of the nucleoli.

1.3.3 The hallmarks of cancer and functions of the nucleoli.

The fundamental 'hallmarks' of cancer are defined by Hannahan and Weinberg in their classic review as the characteristics that must be acquired during tumorigenesis - sustained proliferative signaling, evasion of growth suppressors, resistance to cell death, replicative immortality, induction of angiogenesis and activation of invasion and metastasis (Hanahan and Weinberg, 2000). The well-established association between enhanced ribosome biogenesis and cancer was traditionally proposed to be necessary for sustained cell proliferation. That is, by providing the increased rates of protein synthesis required for cell growth, it ensured cancer cells could continue to progress through the cell cycle. However, the extent to which changes in ribosome number and protein synthesis contribute to transformation has not been clearly defined. Conceptually, nucleolar dysregulation could contribute to a number of the hallmarks of cancer (FIGURE 5).

The additional functions of the nucleoli could play key roles in driving tumorigenesis. For example, increased rates of Pol I transcription and deregulation of nucleolar function may prevent p53 activation by the nucleolar stress response. In fact, Rubbi and Millner showed that irradiation of nucleoli, but no other regions in the nucleus, results in p53 activation. Thus, they proposed that targeting the nucleoli is necessary and sufficient to activate p53 (Rubbi and Milner, 2003). Activation of p53 by the nucleolar-stress pathway occurs in response to translocation of proteins to or from the nucleoli, such as RPL5/RPL11/5S. When Pol I transcription is hyperactivated, translocation of these factors may no longer be effectively regulated, resulting in the reduced activation of p53 tumor suppressor function. In support of this, the upregulation of rRNA transcription in human cancer cell lines *in vitro*, as well as a regenerating rat liver model *in vivo*, decreases the p53 response to cytotoxic stress (Donati et al., 2011a). Further, in an Eμ-Myc transgenic mouse model in which RPL5 and RPL11 are unable to bind to a MDM2 mutant, earlier onset and more frequent tumors were observed compared to MDM2 wild-type mice (Macias et al., 2010). Other p53-independent nucleolar functions could play a similar role. For example, compromised nucleolar regulation of cell cycle progression, or activation of checkpoints in response to stress such as DNA damage. In fact, many of the pathways

containing oncogenes and tumor suppressors that modulate Pol I transcription during tumorigenesis, are themselves subject to regulation by the nucleolus.

Apoptosis and senescence are closely related to the hallmarks of cancer. Programmed cell death by apoptosis is triggered by oncogenic and other cellular stresses, and must be overcome for tumorigenesis to occur (Reviewed in (Lowe et al., 2004)). Senescence limits cell proliferative capacity and results in permanent cell cycle arrest in response to oncogenic and other cellular stresses (Reviewed in (Perez-Mancera et al., 2014)). Thus, compromised nucleolar regulation of these processes could contribute to the acquisition of hallmarks such as resistance to cell death and replicative immortality, respectively. Further, the relationship between rates of rRNA transcription and pluripotency and differentiation, as discussed above (see Section 1.2.2.6), suggests that changes in rates of Pol I transcription may be involved in the various degrees of differentiation observed in tumors. This mediates numerous processes such as the self-renewal capabilites of cancer cells, or epithelial-to-mesenchymal transition, which enables invasion and metastasis by cancer cells (Reviewed in (Heerboth et al., 2015)).

Genome instability underlies the acquisition of mutations that result in the hallmarks of cancer. Nucleolar dysregulation could plausibly contribute to genome instability in a number of ways. For example, a loss of rDNA silencing could result in reduced epigenetic silencing of NADs, resulting in genomic instability particularly at repetitive regions reported to be frequently associated with nucleoli (Nemeth et al., 2010; van Koningsbruggen et al., 2010). As the rDNA repeats are particularly vulnerable to genomic instability, due to their repetitive nature and high rates of transcription, the nucleolus may protect the genome by activating DDR in a highly sensitive manner. This suggests that nucleolar dysregulation could result in both genomic instability at the rDNA repeats, as well as compromised DDR across the whole genome. In fact, upregulated rRNA synthesis in different models was responsible for both increased DNA damage at the rDNA (Wang et al., 2013), and decreased p53-mediated response to cytotoxic stress (Donati et al., 2011a). Also, nucleolar regulation of telomerase could result in telomere dysfunction when nucleoli are dysregulated. Loss of telomeric repeats or protective structures can lead to end-to-end fusions, gross chromosomal aberrations and changes in ploidy, and eventually ‘telomere healing’ – this both drives genomic instability and enables stable proliferation of resulting cells (Reviewed in (Martinez and Blasco, 2011)).

The nucleolus can regulate many cellular processes whose dysregulation drive the acquisition of the hallmarks of cancer. For example, signaling by oncogenes and tumor suppressors, apoptosis and senescence, or genomic stability. It follows that perturbations in nucleolar function and structure that lead to disruption of this regulation may drive tumorigenesis. Particularly, the nucleolus is exceptionally responsive to qualitative and quantitative changes in cellular stress signals, however in cancer activation of oncogenes (for example MYC), or loss of tumor suppressors (for example p53), result in the consistent hyperactivation of rDNA transcription. This dampens nucleolar response to upstream signaling, preventing appropriate regulation of both ribosome biogenesis and extra-ribosomal nucleolar functions. This positions the nucleolus as an interesting target for cancer therapy, as inhibition of rDNA transcription may both reduce ribosome biogenesis and the protein translation capacity of growing cancer cells, as well as restore appropriate regulation of nuclear functions that prevent acquisition of the cancer phenotype.

1.3.4 Targeting the nucleoli for cancer treatment.

Although the relationship between increased rates of Pol I transcription and cancer have been recognized for some time, the concept of targeting ribosome biogenesis as a therapeutic approach to cancer has been controversial – due to the fundamental requirement of ribosomes for cell growth and proliferation, there was not considered to be a therapeutic window to specifically target cancer cells without also affecting normal cell function. However, several lines of evidence suggest that inhibiting Pol I transcription of the 47S pre-rRNA is feasible in cancer treatment.

First, a range of therapeutic agents have retrospectively been shown to directly inhibit rates of Pol I transcription. For example, Actinomycin D, widely used as a chemotherapeutic agent since 1954, acts in part via intercalating GC-rich regions of DNA, and is thus selectively inhibits Pol I transcription at low concentrations due to preventing elongation of Pol I transcription through the GC –rich rRNA genes. Another widely used chemotherapeutic agent, cisplatin, and its platinum based derivatives, such as carboplatin and oxaliplatin, form DNA adducts that both induce DNA damage response and also inhibit transcription of the 47S pre-rRNA via sequestration of UBF (Treiber et al., 1994; Chao et al., 1996; Jordan and Carmo-Fonseca, 1998; Bruno et al., 2017). Importantly, therapeutic efficacy of oxyalypatin has recently been suggested to be predominantly though ribosome biogenesis stress (Bruno et al., 2017). Topoisomerase I inhibitors, including Camptothecin, Irinotican, and Topotecan are approved chemotherapeutic agents, that can disrupt Pol I transcription, due to

inducing DNA strand breaks in the transcribed portion of the rDNA gene where Topoisomerase I is enriched (Pondarre et al., 1997). The ellipticine family of planar alkaloids contain a number of therapeutic agents that have progressed to clinical trials, with their efficacy attributed to inhibition of Topoisomerase II; members of this family have also been shown to selectively inhibit Pol I transcription, in particular 9-hydroxyellipticine, which prevents the recruitment of SL1 to the 47pre-rRNA gene promoter (Andrews et al., 2013). In fact, when a panel of 36 common chemotherapeutic drugs were tested for activity against rRNA synthesis, 21 were found to inhibit either rRNA transcription, early rRNA processing, or late rRNA processing (Burger et al., 2010).

Second, inhibitors of oncogenic pathways that regulate ribosome biogenesis, such as those described above, are emerging as anti-cancer drugs. For example, the PI3K/AKT/mTOR pathway inhibitor rapamycin has been demonstrated to inhibit rRNA gene transcription, and novel analogs of rapamycin ('rapalogs') are undergoing clinical trials in a wide range of human tumors, with temsirolimus and everolimus approved for the treatment of breast and renal cancer (Mahajan, 1994; Meng and Zheng, 2015). Inhibitors of the RAS/RAF/MEK/ERK pathway are also undergoing clinical development, such as MEK1/2 inhibitor trametinib with is approved for treatment of $BRAF^{V600E/K}$-mutant melanoma (Reviewed in (Caunt et al., 2015)). Due to feedback and compensatory mechanisms between these pathways, pre-clinical studies have begun to address the effectiveness of combinatorial treatment with inhibitors that target the both the the PI3K/mTOR and RAS/MAPK networks (Kinross et al., 2011)(Reviewed in (Sheppard et al., 2012b; Yan et al., 2017)). Further, chemotherapeutic inhibitors of cell cycle regulatory kinases can disrupt the nucleolus - for example, treatment with CDK2 inhibitors roscovitine and olomoucine reduce levels of 47S pre-rRNA, drive nucleolar fragmentation, and result in accumulation of p53 - consistent with the co-ordination of cell cycle progression and rates of ribosome biogenesis (See section 1.1.3.1.)(Reviewed in (Asghar et al., 2015)).

These examples show that ribosome biogenesis can be safely targeted in the treatment of cancer. Further, while the impact of inhibition of Pol I transcription to therapeutic efficacy of these agents was not always a consideration during their development, it is possible that this activity significantly contributes to the clinical success of these treatments.

1.4 CX-5461 selective small molecule inhibitor of Pol I transcription.

Recent advances in our understanding of the role of the nucleolus in cancer have motivated the development of specific inhibitors of Pol I transcription and ribosome biogenesis. Despite the evidence that numerous therapeutic agents inhibit this process, until recently there were no anticancer drugs specifically designed to target ribosome biogenesis. Thus, Pol I transcription represents a novel unexploited avenue for the treatment of cancer. In collaboration with Cylene Pharmaceuticals (San Diego, California, USA), we have been involved in the development of a specific small molecule inhibitor of Pol I transcription, the benazathiozole-based 2-(4-methyl-[1,4]diazepan-1-yl)-5-oxo-5*H*-7-thia-1,11*b*-diaza-benzo[*c*]fluorene-6-carboxylic acid (5-methyl-pyrazin-2-ylmethyl)-amide (CX-5461) (Drygin et al., 2009; Drygin et al., 2011; Haddach et al., 2012) (FIGURE 6).

CX-5461 was identified in a cell-based assay designed to screen a small molecule library of new chemical entities for selective inhibition of Pol I transcription. In this screen, HCT-116 human colorectal carcinoma cells were treated with test compounds, and rates of transcription of both 47S-pre-rRNA by Pol I and *C-MYC* by Pol II were determined by qRT-PCR. Both 47S-pre-RNA and *C-MYC* transcripts have a similar, short 20-30 minute half-life, thus it is possible to use a relatively short-term treatment of 2hr that both selects for potent Pol I inhibitors and minimizes any effects due to general cellular stress, and identify agents with selectivity for inhibition of Pol I relative to Pol II transcription (Drygin et al., 2011; Haddach et al., 2012).

CX-5461 was identified as a small molecule that preferentially inhibits Pol I transcription (with an IC_{50} of 113nmol/L) compared to Pol II transcription (IC_{50} >25μmol/L), giving an over 200-fold selectivity for Pol I. The selectivity of CX-5461 for Pol I inhibition was confirmed in two additional cell lines (A365 melanoma and MIA PaCa-2 pancreatic carcinoma cell lines) (Drygin et al., 2011).

CX-5461 inhibits initiation of Pol I transcription. In 'order of addition' studies in a cell-free assay of Pol I transcription, a DNA template corresponding to -160 to +379 region of the rDNA was incubated with whole nuclear extract from HeLa S3 cells, along with the Pol II transcriptional inhibitor α-amanitin. CX-5461 was added to either a) nuclear extract prior to DNA template addition, b) nuclear extract and DNA template prior to transcription initiation by addition of rNTPs (ribonucleoside tri-phosphates), or c) nuclear extract and DNA template following transcription initiation by addition of

rNTPs. Analysis of transcription rates by qRT-PCR showed that CX-5461 most significantly inhibited Pol I transcription prior to PIC formation on the rDNA template (Drygin et al., 2011).

The mechanism by which CX-5461 inhibits Pol I transcription initiation is via disruption of the interaction of SL1 with the rDNA, preventing formation of the PIC at the rDNA promoter. ChIP analysis of the rDNA promoter following 1hr treatment with 2 μmol/L CX-5461 revealed that levels of Pol I, SL1, and UBF were reduced at the rDNA promoter. In particular, SL1 components (including TBP, TAFI110, and TAFI63) were the most depleted, suggesting that the inhibition of Pol I recruitment by CX-5461 was due to its effects on SL1. The interaction of SL1 with the rDNA promoter in the presence of CX-5461 was further examined using electromobility shift assay (EMSA). SL1 was isolated from HeLa cells and incubated with a radiolabeled DNA probe corresponding to the rDNA promoter, in the presence of either CX-5461, or a close analogue small molecule that is inactive toward Pol I transcription (CX-5447). CX-5461 disrupted the SL1-rDNA complex, while the negative control CX-5447 did not. There was no decrease in protein-protein interactions within the SL1 complex in the presence of CX-5461. Thus, we concluded CX-5461 inhibits SL1 binding at the rDNA promoter (FIGURE 6).

Another agent that inhibits Pol I transcription was also identified by Cylene Pharmaceuticals - the fluroquinine derivative CX-3543 (also known as Quarfloxin). Unlike CX-5461, CX-3543 does not directly target the Pol I transcription complex; rather, CX-3543 accumulates in the nucleoli, binds G-quadruplex (G4) DNA, disrupts the interaction of nucleolin with G4 structures at the rDNA, and inhibits Pol I transcription at the elongation stage (Drygin et al., 2009).

The specificity for CX-5461 for inhibition of Pol I transcription, rather than Pol II transcription, or DNA and protein synthesis, was confirmed. Gene expression array analysis of Pol II transcription following 1hr treatment with 300nmol/L CX-5461 (which gives over 50% reduction in rates of 47S pre-rRNA transcription) resulted in an equal number of upregulated as downregulated Pol II- transcribed genes, indicating changes in Pol II transcription are downstream of Pol I inhibition, as a general inhibition of Pol II transcription by CX-5461 would result in predominantly downregulated genes. BrdU (5'-bromo-2'deoxyuridine) or ^{35}S-methionine labeling of cells pre-incubated with 10μmol/L CX-5461 for 1hr (>100 fold IC_{50} for inhibition of Pol I transcription) showed

CX-5461 has >200-fold selectivity for inhibition of Pol I transcription over DNA replication or protein synthesis (Drygin 2011). Further characterization of CX-5461 showed that even at doses up to 50μM, CX-5461 is not a strong intercalator of DNA nor minor groove binding drug, and that it is non-mutogenic in Ames tests (Haddach et al., 2012).

CX-5461 displayed favourable pharmacokinetic properties, with good oral bioavailability (45%), moderate clearance, favorable half-life (>12hr), and volume distribution larger than total body water in Cynomolgus monkey (Haddach et al., 2012). Pre-clinical safety assays indicated that CX-5461 was unlikely to affect drug metabolism, impact cardiac function, or have off target effects on receptors, ion channels, transporters, kinases, and proteases (Haddach et al., 2012). Thus, CX-5461 had a promising pharmaceutical assessment.

Having identified CX-5461 as a first-in-class specific small molecule inhibitor of Pol I transcription, we are able to begin to investigate whether targeting ribosomal biogenesis is a viable approach for the treatment of cancer. Specifically, key questions include whether tumor cells depend upon increased rates of ribosome biogenesis to maintain their proliferative phenotype, and whether there is a therapeutic window in which inhibition of Pol I transcription can selectively target cancer cells without prohibitively detrimental effects on normal untransformed cells.

1.5 Specific Aims.

Increased rates of Pol I transcription of the 47S pre-rRNA genes is observed in almost all cancer types. It is proposed that cancer cells require high rates of Pol I transcription and ribosome biogenesis to achieve their characteristic unrestrained growth and proliferation. This may present a therapeutic window for selectively targeting cancer cells with inhibitors of Pol I transcription. However, at the commencement of this research project, it remained unclear whether targeting Pol I transcription and ribosome biogenesis is a viable strategy for the treatment of cancer.

This project seeks to utilise CX-5461, the selective small molecule inhibitor of Pol I transcription, in a panel of human isogenic cell lines at defined stages of transformation, to address the following specific aims:

1) **Investigate the response of cells at different stages of transformation to inhibition of Pol I transcription by CX-5461.**

   Does inhibition of Pol I transcription have selective anti-proliferative effects on cancer cells compared to normal cells, that enable a therapeutic window for targeting cancer cells?

2) **Investigate the phenotypic response of normal cells to the rapid and specific inhibition of inhibition of Pol I transcription by CX-5461.**

   What are the key cellular responses to inhibition of Pol I transcription and ribosome biogenesis in normal cells?

3) **Investigate the key molecular pathways that mediate the cellular responses to inhibition of Pol I transcription by CX-5461.**

   Considering the emerging knowledge about the extra-ribosomal functions of the nucleoli (for example the activation of p53 by the nucleolar stress pathway), what are the predominant pathways that mediate the response to inhibition of Pol I transcription?

We propose that advancing our understanding of the key pathways and cellular responses to inhibition of Pol I transcription, in normal and cancer cells, will inform the feasibility of this novel approach for the treatment of cancer.

FIGURE 1. The rDNA. Organisation of the 47S pre-rRNA genes. There are five nucleolar organising regions (NORs), on the acrocentric chromosomes. Together, these contain a total of ~200 canonical rDNA units in repeat arrays. Each canonical rDNA unit contains a 30kb intergenic spacer (IGS) and a 13.3kb 47S pre-rRNA gene (shown in blue) - this consists of the sequences that form the 18S, 5,8S and 28S ribosomal RNAs (light blue), positioned within the 5' external transcribed spacer sequence (5'ETS), the internal transcribed spacer sequences (ITS1 and ITS2), and the 3' external transcribed spacer sequence (3'ETS) (dark blue). 47S pre-rRNA gene promoter is bipartite, consisting a core element and an upstream control element (UCE) located 100bp upstream. Other regulatory features include the 'spacer promoters' (grey lines), and terminator elements including multiple 'T' sequences 3' of the 47S rDNA coding region as well as a single 'T_0' terminator sequence 5 'of the rDNA promoter (orange lines). The Pol I transcription start site is shown with a black arrow. Adapted from original image in Hein, Sanij, Quin *et. al.* 2012 (Hein, 2012).

FIGURE 1

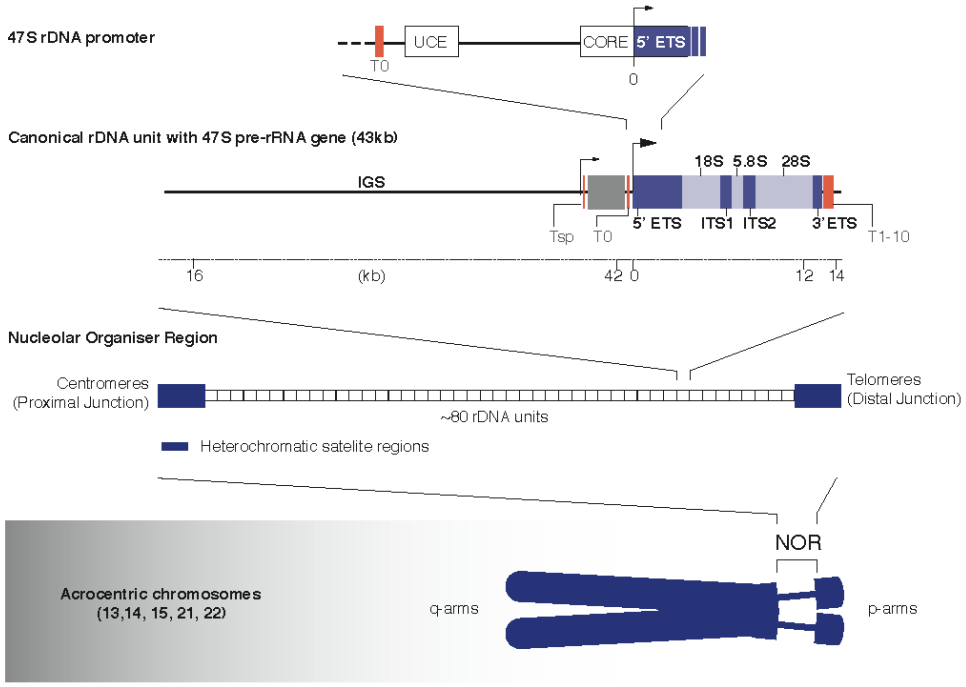
47S rDNA promoter
UCE
CORE
5' ETS
T0
0
Canonical rDNA unit with 47S pre-rRNA gene (43kb)
IGS
18S
5.8S
28S
Tsp
T0
5' ETS
ITS1
ITS2
3' ETS
T1-10
16
(kb)
42
0
12
14
Nucleolar Organiser Region
Centromeres
(Proximal Junction)
Telomeres
(Distal Junction)
~80 rDNA units
Heterochromatic satelite regions
NOR
Acrocentric chromosomes
(13,14, 15, 21, 22)
q-arms
p-arms

FIGURE 2. The nucleoli and ribosome biogenesis. A. Nucleoli observed in isolated nuclei by differential interference microscopy (HeLa cells, from Pederson 2011 (Pederson, 2011)). **B.** Electron microscopy of nucleoli showing the three nucleolar domains: the fibrillar centers (FC), dense fibrillar components (DFC), and the granular component (GC). Bar = 0.5μM (HeLa cells, from Sirri *et. al.* 2002 (Sirri et al., 2002)). **C**. Electron micrograph of a Miller spread, showing high density of active Pol I transcribing 47S pre-rRNAs (branches) on a single rDNA copy (trunk). Bar = 1μM. (HeLa cells, from Miller and Bakken, 1972 (Miller and Bakken, 1972)). **D.** Overview of ribosome biogenesis. Pol I transcription of the 47s pre-rRNA occurs at the border of the FC. In the DFC, processing of the 47S pre-rRNA transcript begins while transcription is occurring, then following cleavage and nucleotide modification, the 18S, 5.8S and 28S rRNAs are assembled with the 5S rRNA (5S gene cluster is transcribed by Pol III) and ribosomal proteins (RP genes are transcribed by Pol II, then RP mRNAs are translated at mature ribosomes in the cytoplasm). Pre-40S (18S rRNA and 'S' RPs) and pre-60S (5S, 5,8S, and 28S rRNAs and 'L' RPs) ribosomal subunits appear as granules in the GC. They continue to undergo final processing and assembly steps and are exported to the cytoplasm, where the mature 40S and 60S ribosomal subunits form the ribosome. Adapted from original image in Hein, Sanij, Quin *et. al.* 2012 (Hein, 2012).

FIGURE 2

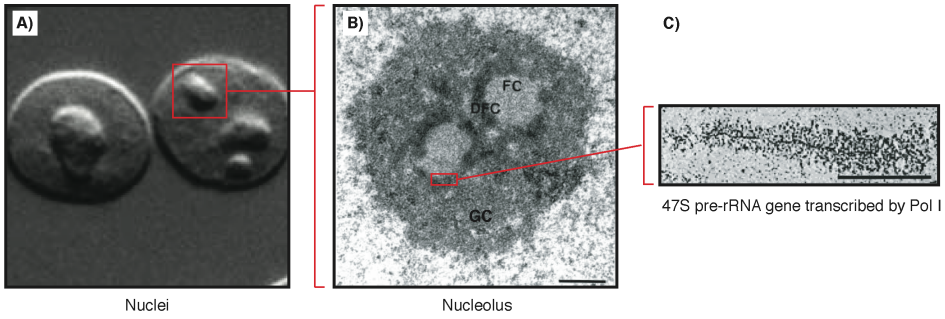
A)
B)
C)
FC
DFC
GC
47S pre-rRNA gene transcribed by Pol I
Nuclei
Nucleolus

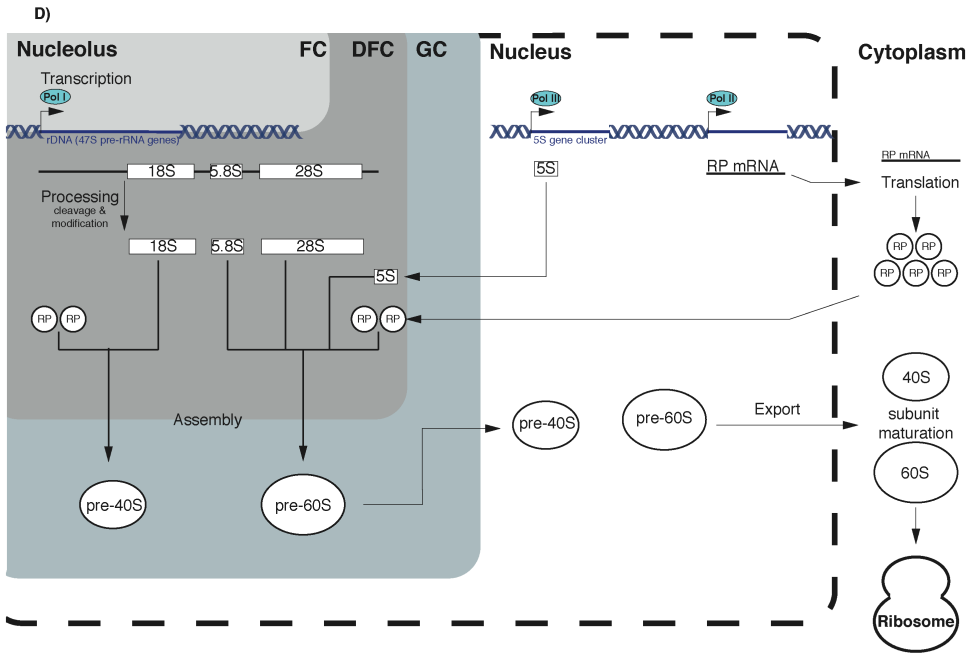
D)
Nucleolus
FC
DFC
GC
Nucleus
Cytoplasm
Transcription
Pol I
rDNA (47S pre-rRNA genes)
18S
5.8S
28S
Processing
cleavage & modification
Pol III
Pol II
5S gene cluster
5S
RP mRNA
Translation
RP
Assembly
pre-40S
pre-60S
Export
40S
subunit maturation
60S
Ribosome

FIGURE 3. Model of regulation of rDNA chromatin and Pol I transcription. A) rDNA chromatin. Approximately half of all rDNA repeats have a silent chromatin conformation, with CpG methylated DNA and heterochromatic histone modifications. The remaining rDNA repeats hypomethylated DNA and euchromatic histone modifications. These exist in different states – pseudo-silent, poised, and active. In the absence of UBF, genes are 'pseudo-silent', with a closed chromatin conformation. The binding of UBF across the entire length of the transcribed region results in an open chromatin structure characterised by the absence of linker histone H1 and reduced nucleosome occupancy. Genes associated with UBF can be either: 'poised' - with bivalent histone modifications and H3/H4 hypoacteylation at the promoter, and the promoter bound nucleosome in the 'off' position; or 'active' – with H3/H4 acetylation, and the promoter bound nucleosome in an 'on' position. Initiation of transcription requires the formation of the PIC at the promoter: UBF binds the promoter the UCE and Core elements as a dimer, and co-stabilises binding of the SL1 complex, thus recruiting initiation competent Pol I associated with RRN3, through interaction between SL1 and RRN3, and direct interaction of both UBF and SL1 with Pol I subunits. **B)** Examples of signaling pathways that regulate Pol I transcription. Signaling pathways directly target PIC components to regulate rates of Pol I transcription. For example, common cell cycle regulatory pathways, cellular energy, nutrient, and growth factor sensing signaling pathways, and stress response pathways.

FIGURE 3

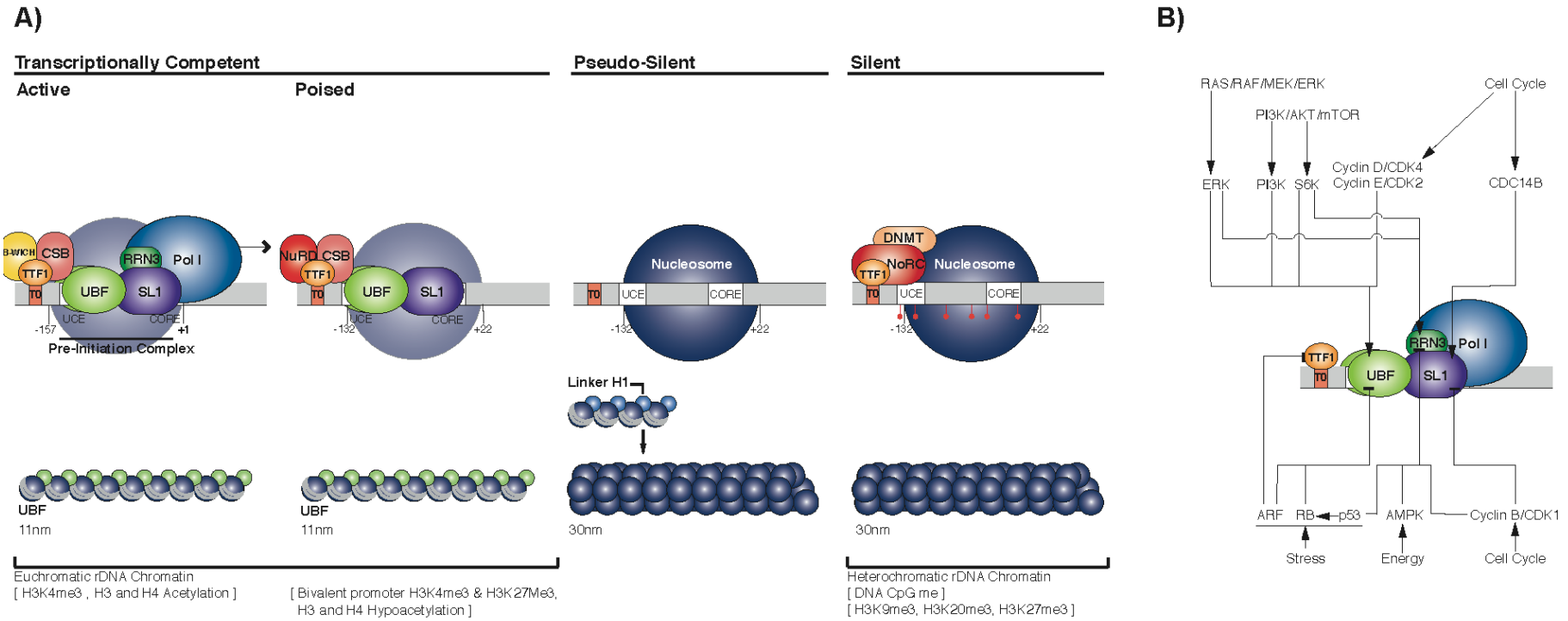
A)
Transcriptionally Competent
Active
Poised
Pseudo-Silent
Silent
B-WICH
CSB
RRN3
Pol I
TTF1
UBF
SL1
T0
UCE
CORE
-157
+1
Pre-Initiation Complex
NuRD
-132
+22
Nucleosome
DNMT
NoRC
Linker H1
UBF
11nm
30nm
Euchromatic rDNA Chromatin
[H3K4me3 , H3 and H4 Acetylation]
[Bivalent promoter H3K4me3 & H3K27Me3,
H3 and H4 Hypoacetylation]
Heterochromatic rDNA Chromatin
[DNA CpG me]
[H3K9me3, H3K20me3, H3K27me3]
B)
RAS/RAF/MEK/ERK
Cell Cycle
PI3K/AKT/mTOR
ERK
PI3K
S6K
Cyclin D/CDK4
Cyclin E/CDK2
CDC14B
ARF
RB
p53
AMPK
Cyclin B/CDK1
Stress
Energy
Cell Cycle

FIGURE 4. The p53 nucleolar stress pathway. The 'nucleolar stress pathway' activates p53. Under normal conditions, p53 is maintained at basal levels by HDM2, which both binds p53 preventing its transcriptional activity and ubiquitinates p53 targeting it for proteasomal degredation. The activation of p53 upon nucleolar stress can occur via multiple nucleolar mechanisms, with examples shown here: A) p14ARF interacts with HDM2, sequesters it in the nucleoli, and disrupts its association with p53; B) Free RPs (particularly L5 and L11 co-stabilised with 5S rRNA) bind HDM2, inhibiting its ubiquitin ligase activity and association with p53; C) p53 mRNA is stabilized by nucleolar proteins (eg NCL or L26), resulting in its increased translation; D) nucleolar proteins can dissociate the interaction between HDM2 and p53 (eg NCL, Nucelostemin) E) in the absence of co-transport of p53 and ribosome subunits, cytoplasmic export and subsequent degradation of p53 is reduced.

FIGURE 4

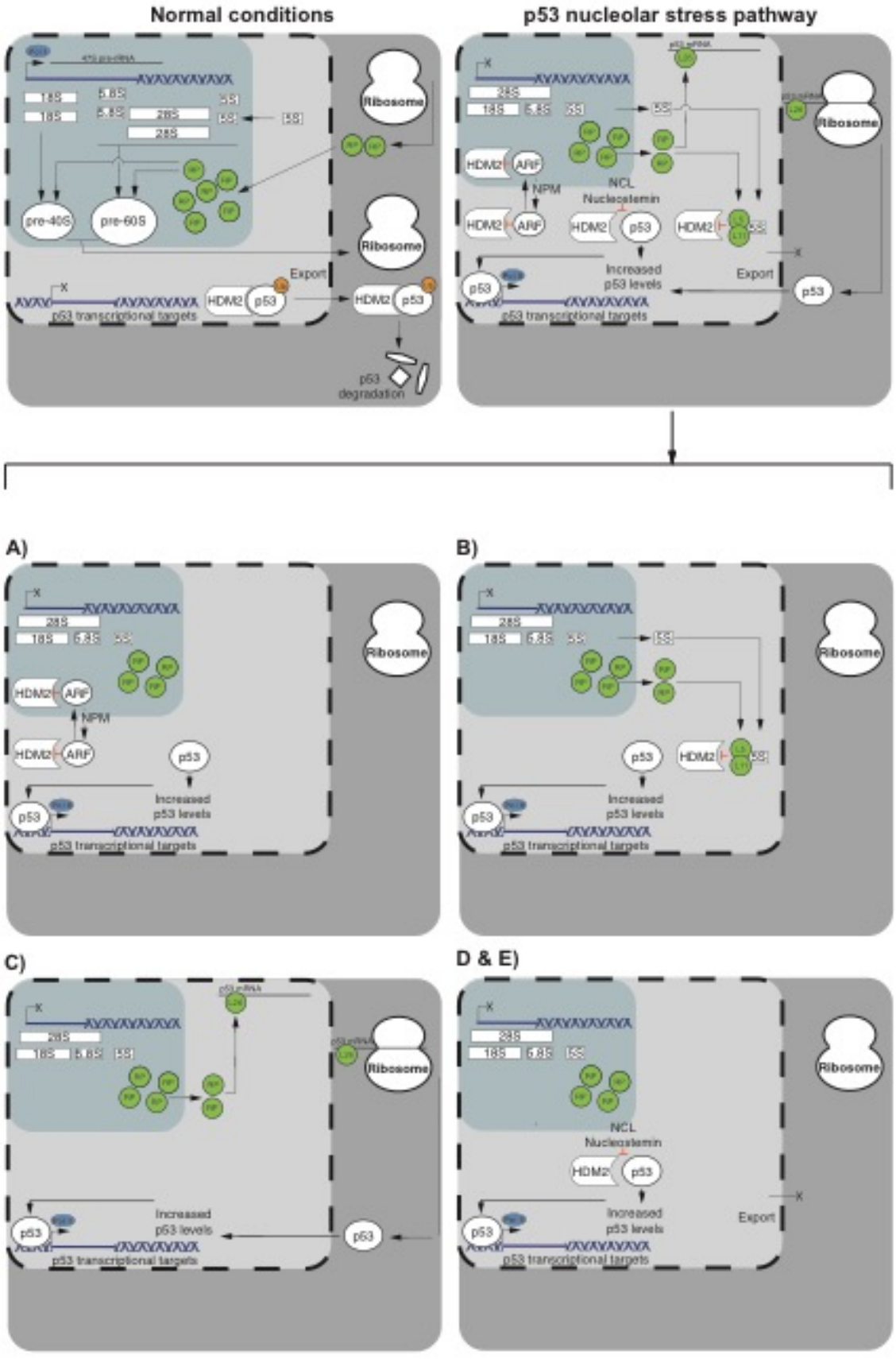
Normal conditions
p53 nucleolar stress pathway
Ribosome
pre-40S
pre-60S
Export
HDM2
p53
p53 transcriptional targets
p53 degradation
ARF
NPM
NCL
Nucleostemin
Increased p53 levels
A)
B)
C)
D & E)

TABLE 1. Examples of extra-ribosomal functions of the nucleoli.		
Cell cycle regulation		
E2F1	RPL11 inhibits HMD2 stabilization of the E2F1 transcription factor, and p14ARF binds E2F1 and inhibits its activity, preventing G1 –S cell cycle progression.	(Eymin et al., 2001; Ayrault et al., 2004; Ayrault et al., 2006; Donati et al., 2011b)
Cyclin D	Inhibition of ErbB3(80) by nucleolar sequestration prevents its activation of Cyclin D1.	(Andrique et al., 2012)
Cyclin E	SCFFbw7alpha mediated isomerization of Cyclin E results in its inactivation by nucleolar sequestration and subsequent ubiquitination by the nucleolar SCFFbw7gamma.	(Bhaskaran et al., 2013)
RPA	NCL inhibits RPA, preventing activation of DNA replication.	(Wang et al., 2001; Daniely et al., 2002)
GNL1	Translocation of GNL1 to the nucleolus during G2, from its cytoplasmic localization during G1 and S, is required for G2/M transition.	(Boddapati et al., 2012)
hCDC14B	CDC14B is sequestered in the nucleoli during interphase, and upon its release at the onset of mitosis dephosphorylates and inactivates CDC25, enabling efficient inactivation of CDK1 at late M phase.	(Tumurbaatar et al., 2011; Peddibhotla et al., 2011)
Centrosomes	NPM associates with mitotic poles during M and early G1, and its dissociation is required for centrosome duplication. NCL is also associated with mitotic poles and required for control of centrosome duplication.	(Okuda et al., 2000; Ma et al., 2007; Ugrinova et al., 2007)
Stress signaling		
p21	RPL3 upregulates p21 expression leading to in a p53-independent cell cycle arrest or apoptosis.	(Russo et al., 2013; Esposito et al., 2014; Russo et al., 2016)
HIF1	In normal conditions, p14ARF sequesters HIF1 alpha subunit in the nucleolus, inhibiting HIF1 transcriptional activity. VHL, which ubiquitinates HIF1 and targets it for proteasomal degradation under normal conditions, is sequestered in the nucleoli under hypoxic conditions.	(Fatyol and Szalay, 2001; Mekhail et al., 2004)
HSP70	HSP70 can translocate to the nucleoli under conditions of heat shock, and is immobilized by lncRNAs transcribed from the IGS in a nucleolar detention center.	(Audas et al., 2012; Jacob et al., 2013)
CSIG	Following UV induced DNA damage p33ING1 translocates to the nucleolus, where it stabilizes nucleolar protein CSIG which activates downstream effectors to promote apoptosis.	(Li et al., 2012)
CDC14B	Cdcd14B is sequestered in the nucleoli, and upon DNA damage is phosphorylated by Chk1 and released from the nucleoli leading to Cdc14B-induced activation of APC/CCdh1 and the G2 – DNA damage cell cycle checkpoint.	(Peddibhotla et al., 2011)
PARP-1	Upon DNA damage, nucleolar PARP-1 translocates to the nucleoplasm, and delocalization of PARP-1 to the nucleoplasm where it sensitizes cells to DNA damage induced apoptosis.	(Rancourt and Satoh, 2009)

DNA damage response		
BRCA1	DSB repair factors RNF8 and BRCA1 interact with ribosomal protein RPSA in the nucleoli. Following IR, they translocate to DNA-damage response foci in the nucleoplasm.	(Guerra-Rebollo et al., 2012)
Ku70/80	The 55K nucleolar isoform of CDK9 associates with Ku70, and depletion of 55K CDK9 can induce DNA damage.	(Liu et al., 2010)
Nucleolin	NCL interacts with DNA repair proteins, including TOPO1, RAD51, WRNp, and relocalises from the nucleoli to the nucleoplasm upon DNA damage, where it associates with γH2A.X at DNA DSBs.	(Edwards et al., 2000; De et al., 2006; Indig et al., 2012; Kobayashi et al., 2012)
Telomeres		
Shelterin	Shelterin component TRF1 is regulated in the nucleoplasm by the nucleolar proteins nucleostemin (NS/GNL3), which enhances TRF1 degradation, and GNL3L, which binds and stabilizes TRF1. Shelterin component TRF2 localises to the nucleoli during G1 and S phase, and diffuses to the nucleoplasm in G2.	(Zhu et al., 2006; Tsai, 2009; Zhu et al., 2009a)
Telomerase	In early S-phase, the telomerase reverse transcriptase componenent (TERT) moves to the nucleolus while the telomerase RNA componenent (TERC) accumulates in Cajal bodies at the nucleolar periphery. This nucleolar localization may be a pre-requisite for telomerase biogenesis	(Narayanan et al., 1999; Etheridge et al., 2002; Wong et al., 2002; Tomlinson et al., 2006; Her and Chung, 2012)
RNP biogenesis		
SRP	Signal recognition particle (SRP) RNA and protein components are localized in the nucleoli, suggesting a nuceolar phase is required for its processing and assembly.	(Jacobson and Pederson, 1998; Politz et al., 2000; Politz et al., 2002)
RNaseP	RNaseP catalytic RNA RNA subunit H1 RNA is found in the nucleoli, and many RNaseP Rpp protein subunits are confined to the nucleoli, which is proposed to serve as an assembly site.	(Lee et al., 1996; Jarrous et al., 1999)
Post-transcriptional regulation of RNAs		
snRNAS	U6 snRNA are modified by snoRNPs in the nucleoli prior to its assembly into snRNPs. U2, U4 and U5 snRNAs may also be modified by snoRNAs in the nucleoli.	(Lange and Gerbi, 2000; Yu et al., 2001; Gerbi and Lange, 2002; Huttenhofer et al., 2002)
miRNAs	NCL can post-transcriptionally regulate expression of certain miRNAs, snoRNAs can act as precursors to certain miRNAs, and some miRNAs are enriched in the nucleolus suggesting they are regulated via nucleolar sequestration and release. mRNAs that contain target sites for nucleolar miRNAs can also be sequestered in the nucleolus.	(Shiohama et al., 2007; Pickering et al., 2011; Politz et al., 2006; Politz et al., 2009; Williams and Farzaneh, 2012; Pichiorri et al., 2013; Li et al., 2013; Bai et al., 2014; Reyes-Gutierrez et al., 2014)

FIGURE 5. The multifunctional nucleoli. The nucleoli are sensitively regulated in response to diverse stimuli, such as cell growth, proliferation and stress response pathways, converging upon Pol I transcription to fine tune its activity and ensure appropriate rates of ribosome biogenesis. In turn, the nucleoli can perform extra-ribosomal functions including activation of p53, regulation of the cell cycle, DNA damage response, senescence and apoptosis, and genome organisation and chromatin regulation. Thus the nucleoli acts as a hub, collecting inputs from cell signaling pathways and mediating distinct responses. Dysregulation of these key cellular processes underlies the 'hallmarks' of cancer. As formation of a functional nucleolus depends upon Pol I transcription, changes in Pol I transcription regulation can conceivably contribute to the acquisition of the cancer phenotype.

FIGURE 5

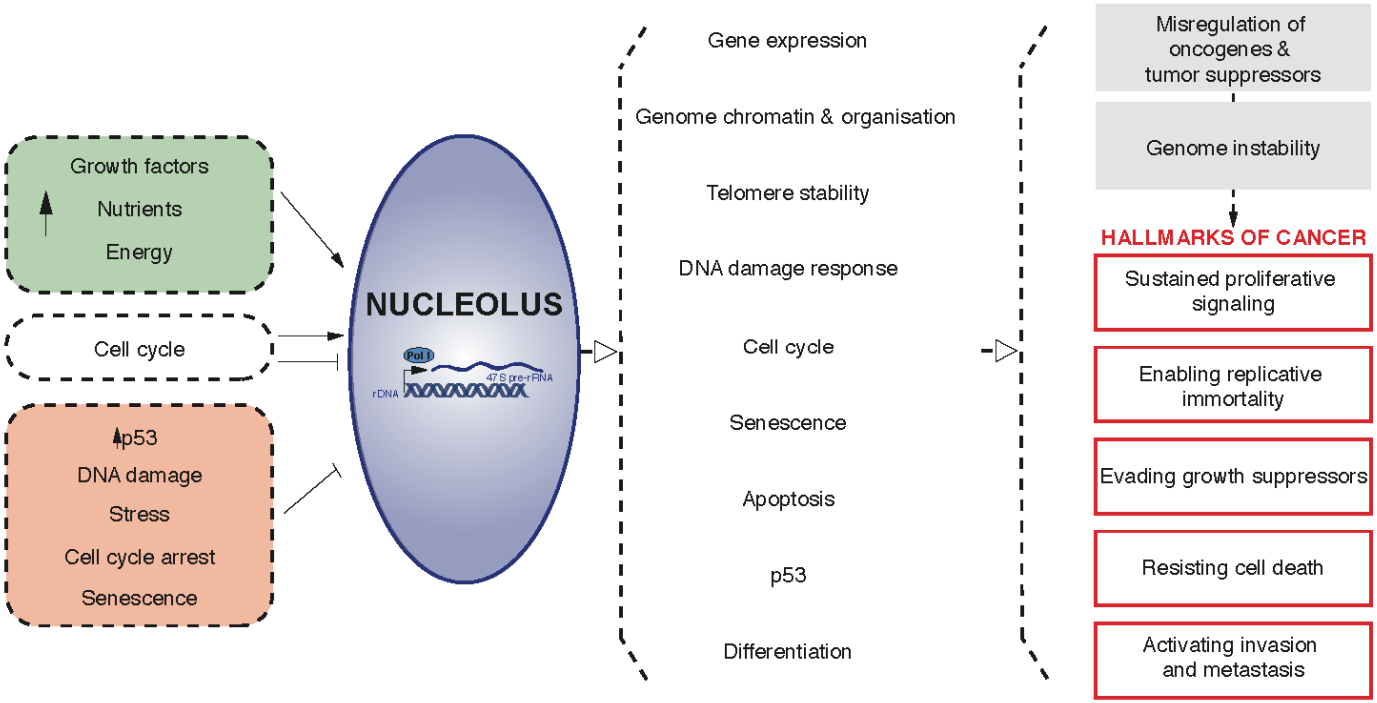
Growth factors
Nutrients
Energy
Cell cycle
p53
DNA damage
Stress
Cell cycle arrest
Senescence
NUCLEOLUS
Pol I
47S pre-rRNA
rDNA
Gene expression
Genome chromatin & organisation
Telomere stability
DNA damage response
Cell cycle
Senescence
Apoptosis
p53
Differentiation
Misregulation of oncogenes & tumor suppressors
Genome instability
HALLMARKS OF CANCER
Sustained proliferative signaling
Enabling replicative immortality
Evading growth suppressors
Resisting cell death
Activating invasion and metastasis

FIGURE 6. CX-5461. A) Structure of small molecule CX-5461. 2-(4-methyl-[1,4]diazepan-1-yl)-5-oxo-5*H*-7-thia-1,11*b*-diaza-benzo[*c*] fluorene-6-carboxylic acid (5-methyl-pyrazin-2-ylmethyl)-amide. (From Drygin *et. al*. 2011 (Drygin et al., 2011)). **B)** CX-5461 disrupts the SL1-rDNA complex, preventing formation of the PIC at the rDNA promoter, thereby specifically inhibiting Pol I transcription.

FIGURE 6.

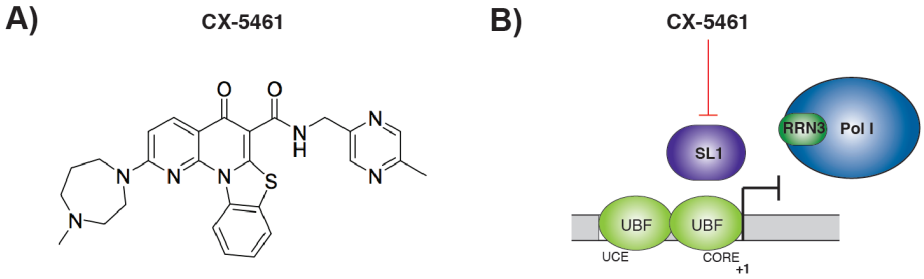
A)
CX-5461
O
O
N
H
N
N
N
N
N
S
N
B)
CX-5461
SL1
RRN3
Pol I
UBF
UBF
UCE
CORE
+1

CHAPTER 2. MATERIALS AND METHODS

2.1 Cell culture.

2.1.1 General cell culture procedures

BJ human foreskin fibroblast cell lines were kindly provided by William Hahn, Harvard Medical School. BJ cell lines were maintained in Dulbecco's Modified Eagle Medium (DMEM) plus HEPES supplemented with 10% (volume/volume(v/v)) Fetal Bovine Serum (FBS), 2mM L-glutamine and 1% (v/v) Antibiotic-Antimycotic (Gibco). U2TR and U2TR-I-*Ppo*I-dd cell lines were kindly provided by Kum Kum Khanna, QIMR Berghofer Medical Research Institute. U2TR cell lines were maintained in DMEM plus HEPES supplemented with 10% (v/v) Tetracyclin-Free FBS (Hyclone) and 2mM L-glutamine. Cell lines were passaged when cell confluency reached 80-90%, by washing with phosphate buffered saline (PBS) and detaching from tissue culture plastic using 0.25% (v/v) trypsin-EDTA (Gibco). Cell culture plasticware was manufactured by TPP (150mm &100mm cell culture plates) or Corning (multi-well cell culture plates and cell culture flasks). All cell lines were cultured under sterile conditions, incubated at 37°C in 5% CO_2 atmosphere.

2.1.2 PEI transfection and retroviral transduction.

BJ-T stable cell lines were generated using retroviral transduction with pRetroSuper (pRS) vectors ((Brummelkamp et al., 2002); provided by R. Agami and R. Bernards, The Netherlands Cancer Institute) containing genes expressing scramble- or p53-shRNA. Retrovirus expressing p53shRNA was generated by polyethylenimine (PEI) transfection of HEK-293T cells. $2x10^6$ cells were seeded in 100mm cell culture dishes in 4.5ml cell culture media 24h prior to transfection. 3μg of pRS vector and 6μg of amphotrophic packaging vector was diluted in 500μl unsupplemented DMEM and the solution was vortexed, 40.5ml 1mg/ml PEI (Bioscientific) was added and the solution was vortexed again, incubated for 15min at room temperature, vortex a final time and added dropwise to HEK-293T cells in culture. After 36hr, 48hr, and 60hr retroviral supernatant was collected, and cell culture media was replaced if required for further harvests. For transduction of BJ-T cells, $0.3x10^6$ BJ-T cells were seeded in 100mm cell culture dishes 24hr prior to transduction. The retroviral supernatant was filtered through a 0.45μM pore filter (Sartorius), made to a final volume of 7ml in cell culture media with 2μg/ml polybrine, and used to replace the BJ-T cell culture media. This was repeated 3 times over a 48hr period. Transduced cells were recovered for 2 passages in cell culture media, then selected by the addition of 1μg/ml puromycin to cell culture

media. FUCCI-labeled BJ-T p53shRNA cell line was produced by lentiviral transduction with pCSII-EF-mCherry-hCdt1 (30/120) and pCSII-EF-mVenus-hGeminin(1/110) (kindly provided by Dr. Atsushi Miyawaki, RIKEN, Japan), which were performed by Dr. Keefe Chan.

2.1.3 siRNA transfection

$0.3x10^6$ BJ-T cells were seeded in 100mm cell culture dishes 24hr prior to transfection. Separately, 13μl of Dharmafect 1 (Dharmacon) was added to 800μl unsupplemented DMEM (lipid mix), and 20.8μl of 10μM siRNA was added to 800μl of unsupplemented DMEM (siRNA mix), and both were incubated for 5min at room temperature. The lipid mix and siRNA mix were then combined and incubated for 20min at room temperature. The cell culture media on BJ-T cells was replaced with 3.6ml unsupplemented DMEM, and 1.6ml of lipid-siRNA mix was added dropwise to each plate to give a total volume of 5.6ml cell culture media, with a final concentration of 0.25% Dharmafect 1 and 40nM siRNA. After 4hr, the transfection media was replaced with cell culture media, and cells were harvested after an additional 48hr in culture. siRNAs were siPOLR1A (Dharmacon siGENOME SMARTpool # M-013983-01), siRRN3 (Dharmacon siGENOME SMARTpool # M-016947-01), or siEGFP (as described in (Sanij et al., 2008)).

2.1.4 Pharmacological inhibitors

CX-5461, CX-5447, and CX-5488 were provided by Cylene Pharmaceuticals (San Diego, CA, USA). Actinomycin D was purchased from Sigma Aldrich. AZD7726, KU-55933, and VE-821 were purchased from Selleckchem (Houston, TX, USA). 10mM CX-5461, CX-5447 and CX-5488 were prepared in 50mM NaH2PO4 (pH 4.5). 1mM Actinomycin D and 10mM AZD7726, KU-55933, and VE-821 stocks were prepared in dimethyl sulphoxide (DMSO) (Sigma Aldrich). All drug stocks were stored at -20C.

2.2 Proliferation analysis.

For cell counts proliferation analysis, $1x10^3$ cells were seeded in 24-well cell culture plates 24hr prior to treatment, with duplicate wells for each condition. Cell culture media was replaced with fresh media containing drug treatment, and cells were cultured under normal conditions. Cells were collected by washing gently with PBS, detaching with 0.25% (v/v) trypsin-EDTA, then deactivating trypsin by the addition of cell culture media. Cell counts were performed in duplicate using a Z2 AccuComp (Beckman Coulter). For cell confluency proliferation analysis, $1x10^3$ cells were seeded

in 24-well cell culture plates 24hr prior to treatment, with triplicate wells for each condition. Cell culture media was replaced with fresh media containing drug treatment, and cells were cultured under normal conditions in an IncuCyte Zoom (Essen Biosciences), which measures % confluency of live cells in culture.

2.3 Flow cytometry

2.3.1 Cell harvest

For flow cytometry analysis of cell death and cell cycle, cells were harvested by collecting supernatants from cell culture, rinsing with PBS and adding to collected supernatants, detaching cells with 0.25% Trypsin-EDTA, quenching trypsin by returning collected cell culture media to cells, and then finally collecting all cells and cell culture media from the cell culture plate.

2.3.2 Cell death analysis

For propidium iodide (PI) exclusion analysis of cell death, harvested cells and supernatant from cell culture were incubated with 1μg/ml PI for 15min at room temperature protected from light. For tetramethylrhodamine ethyl (TMRE) analysis of mitochondrial membrane potential as a measure of cell death, harvested cells and supernatant from cell culture were incubated with 100nM TMRE for 10min at room temperature. For Annexin V/PI analysis of apoptosis and cell death, harvested cells and cell culture media were centrifuged at 1200*g* for 5min at room temperature, then cells were washed in PBS, centrifuged at 1200*g* for 5min at room temperature, resuspended in 200μL of binding buffer (10mM HEPES pH7.4, 140mM NaCl, 5mM $CaCl_2$) containing 1:100 Annexin V-APC (BD Pharmingen) and 0.5μg/ml PI, and incubated for 15min at room temperature protected from light. For all cell death analysis, cells were transferred into 5ml polystyrene tubes through a cell-strainer cap (Falcon Cat. #352235), then analysed by flow cytometry on a BD FACS Canto II and % dead cells determined using FCS express analysis software.

2.3.3 Cell cycle analysis

Cells were centrifuged at 1200*g* for 5min, resuspend in 500μl PBS, then fixed with 5ml ice-cold 90% ethanol, added dropwise while gently vortexing. Cells were incubated at 4°C for 2hrs – 4 weeks. For analysis of DNA replication by 5'-bromo-2'deoxyuridine (BrdU) incorporation, live cells were treated with 10μM BrdU (Sigma Aldrich Cat. # B5002) and harvested as above. Cells were resuspended in 1ml 2N HCl + 0.5% Triton X-100 for 30min at room temperature, collected and resuspended in 1ml $Na_2B_4O_7.10H_2O$ (pH 8.5), collect and resuspended in 100μl Anti-BrdU (Becton

Dickinson Cat. #347580) (0.5µg/ml) in dilution buffer (PBS + 2% fetal calf serum) + 0.5% Tween-20 for 30min at room temperature, washed with dilution buffer, collected and resuspended in 100µl in Alexa Fluor 488 donkey anti-mouse IgG (Invitrogen Cat. #A21202) (5µg/ml) in dilution buffer + 0.5% Tween-20 for 30min on ice, then washed with dilution buffer. For analysis of mitotic cells by phospho-H3(Ser10) staining, cells were harvested as above, collected and resuspended in PBS + 0.25% Triton X-100 for 15min on ice, collected and resuspended in 100µl Anti-phospho-H3(Ser10) (Millipore Cat. #06-570) (2.5µg/ml) in dilution buffer for 3hr at room temperature, washed with dilution buffer, collected and resuspended in 100µl in Alexa Fluor 488 donkey anti-rabbit IgG (Invitrogen Cat. #A21206) (5µg/ml) in dilution buffer + 0.5% Tween-20 for 30min on ice, then washed with dilution buffer. Cells were resuspended in 10 µg/ml propidium iodide (PI) in dilution buffer at approximately $2x10^6$ cells/ml, transferred into 5ml polystyrene tubes through a cell-strainer cap, then analysed by flow cytometry on a BD FACS Canto II. Quantitation of cell cycle population was performed using FCS express and Mod Fit analysis software.

2.3.4 Isolation of G1, S, and G2 live cell populations

Cells were centrifuged at 1200*g* for 5min, resuspend at $5x10^6$ cells/ml in fresh cell culture media, and incubated with 1:40 dilution of Vybrant DyeCycle Violet Stain (Thermo Fisher Scientific) for 30min at room temperature protected from light. Cells were then transferred into 5ml polystyrene tubes through a cell-strainer cap, stored on ice, and sorted into G1, S and G2 cell cycle populations by DNA content on a BD FACSAria.

2.4 Protein Isolation and Analysis

2.4.1 Isolation of protein from cells

Cells were washed twice in 4°C PBS, then lysed in Sodium Dodecyl Sulphate (SDS) lysis buffer (0.5mM EDTA, 20mM HEPES, 2% (weight/volume (w/v)) SDS (pH 7.9)). Samples were heated at 95°C for 10min, then centrifuged at 16000*g* for 1min at room temperature. The protein concentration was determined using the detergent compatible protein assay (BioRAD 500-0112), using bovine serum albumin (BSA) to produce a standard curve for quantitation, and a Benchmark Microplate Reader (BioRAD) as per manufactures instructions.

2.4.2 SDS-PAGE and Western blot analysis

Samples were prepared with equal amounts (10-50µg) of protein in 6X sample loading buffer (62.5mM Tris-HCl pH 6.8, 2.5% (w/v) SDS, 7.5% (v/v) glycerol, 2.5% (v/v) β-

mercaptoethanol, 0.0125% (w/v) bromophenol blue), and heated at 95°C for 5 min. Protein extracts were separated using SDS-polyacrylamide gel electrophoresis (SDS-PAGE), with polyacrylamide gels made fresh according the method of Harlow and Lane (Harlow and Lane 1999), using the Mini-Protean Tetra Cell (BioRAD) with Tis-Glycine-SDS running buffer (25mM Tris,192mM Glycine, 0.1% (w/v) SDS (pH8.7)). Protein extracts were electrophoretically transferred onto Immobulin-P polyvinylidene fluoride (PVDF) membranes (Millipore Cat.#IPVH00010) using a Trans-Blot Electrophoretic Transfer Cell (BioRAD) at 4°C in Tris-Glycine-Methanol transfer buffer (0.125M Tris, 0.2M Glycine, 15% (v/v) methanol). Membranes were blocked with PBS containing 0.2% (v/v) Tween20 and 5% (w/v) skim milk powder (Diploma skim milk powder, Bonlac) for 1hr at room temperature, incubated with primary antibodies (TABLE 2) diluted in blocking solution (0.05% (v/v) Tween20 and 5% (w/v) skim milk powder in PBS), washed 3x in PBS containing 0.2% (v/v) Tween20 for 20min, incubated with horse radish peroxidase (HRP) conjugated secondary antibodies (TABLE 2) diluted in blocking solution, and washed 3x in PBS containing 0.2% (v/v) Tween20 for 20min. Antibody incubations were for 1hr at room temperature, or overnight at 4°C. Antibody binding was detected by enhanced chemiluminescence (ECL) using the Western Lighting Plus ECL kit (Perkin Elmer Cat. # NEL104001EA) and exposure of membranes to autoradiograohy film (GE Amersham Hyperfilm Cat.#28-9068-25, or Fujifilm SuperRX Cat. #47410-19284). Protein size was estimated by comparison to PageRuler plus pre-stained protein ladder (Thermoscientific Cat. # 26619).

2.5 RNA isolation and analysis

2.5.1 Isolation of RNA - Method A (RNA quantity normalised to equal cell counts)

2.5.1.1. *Cell counts and calculating RNA per cell*. Duplicate $0.3x10^6$ cells per 100mm cell culture dish were seeded and cultured overnight prior to drug treatment, with one plate used for RNA isolation and another used for cell counts. For cell counts, cells were collected by washing gently with PBS, detaching with 0.25% (v/v) trypsin-EDTA, and deactivating trypsin by the addition of cell culture media, then cell counts were performed in duplicate using a Z2 AccuComp (Beckman Coulter).

2.5.1.2. *Synthesis of α ^{32}P-uridine triphosphate riboprobe*. α ^{32}P-uridine triphosphate (UTP) riboprobe was synthesised from cDNA complementary to the 5' ETS region of the 47S rRNA gene (nucleotides 1-80) subcloned into a pGEM3Z plasmid with the addition of a HindIII restriction site at the 5' end and an EcoRI at the 3' end (Generated by Kerith Sharkey (Chan et al., 2011)). 1μg of plasmid linearised using the HindIII

restriction enzyme was incubated with T7 polymerase reaction mix for 30min at 37°C (1X T7 RNA polymerase reaction buffer, 10mM DTT, 20U T7 RNA Polymerase, 40U of RNasin ribonuclease inhibitor, 500μM each of ATP, CTP and GTP, 11μM of UTP (all Promega), and 835nM of α ^{32}P-UTP (50 μCi) (Perkin Elmer EasyTides Cat. #BLU507H250UC) in Diethylpyrocarbonate (DEPC) treated water to a final volume of 20μl), then template DNA was removed by incubation with DNAse I reaction mix for 15min at 37°C (10μg yeast tRNA, 20U RNasin, 10U DNase I (all Roche), 90μM Tris (pH8.0) and 18μM $MgCl_2$ in DEPC treated water to a final volume of 50μl). Riboprobe was isolated by phenol-cholorform extraction using 1 volume of TE-saturated phenol:chloroform:isoamyl alcohol (25:24:1), followed by column purification with an Illustra G25 Sephadex microspin column (GE Healthcare), and resuspended in 80% formamide hybridization buffer (80% deionised formamide, 40mM PIPES (pH6.7), 0.4M NaCl, 1mM EDTA) to a final volume of 200μl. To assess the specific activity of the α ^{32}P-UTP riboprobe, 1μl was spotted onto Whatman DE-81 chromatography paper (Sigma Aldrich Cat. # Z286591), placed in a scintialltion vial containing DEPC-treated water, and counts per minute (CPM) measured using a TriCarb 2910 TR quanta-counter (Perkin Elmer).

2.5.1.3 *Isolation of RNA for equal cell number.* Isolation of RNA was performed based on the method developed by Chomczynski and Sacchi (Chomczynski and Sacchi, 2006). Cells were washed twice with ice-cold PBS, lysed by the addition of 500μl GTC Solution D (4M guanidinium thiocyanate, 25mM sodium citrate, pH7.0, 0.5% (w/v) N-laurosylsarcosine and 0.1M 2-mercaptoethanol), gently scraped from the plate, passed through a pipette tip at least ten times to fragment DNA, and transferred into a 1.5 ml microcentrifuge tube. Prior to RNA purification, an equal volume of ^{32}P-UTP riboprobe (~50,000 counts per minute (cpm)) was added to each sample. RNA was precipitated by adding 1/10th volume 2M NaAc (pH4.0), 1 volume water-saturated phenol, and 1/5th volume chloroform:isoamyl alcohol (49:1), then mixing by 10x inversion, incubating on ice 15min, centrifuging at 10,000*g* for 20min at 4°C, transferring aqueous phase to fresh 1.5ml microcentrifuge tube, adding 1 volume isopropanol, incubating at -20°C for 2hr, centrifuging at 10,000*g* for 20min at 4°C, discarding the supernatant, resupending in 300μl GTC solution D, adding 1 volume isopropanol, incubating at -20°C for 1hr, centrifuging at 10,000*g* for 10min at 4°C, discarding the supernatant, washing pellet twice in 800μl of ice-cold 70% ethanol in DEPC-treated water, air drying pellet, then resuspending in 20μl of DEPC-treated water. % RNA recovery was determined by measuring cpm of 2μl of RNA using a TriCarb 2910 TR quanta-counter (Perkin Elmer).

Total RNA was determined by measuring RNA concentration using a NanoDrop ND-1000 Spectrophotometer (Thermo Fisher). RNA per cell was calculated for each sample by [Total RNA X 100] / [Cell Number x % RNA Recovery]

2.5.2 Isolation of RNA – Method B (Equal RNA)

$0.3x10^6$ cells per 100mm cell culture dish were seeded and cultured overnight prior to treatment. Cells were washed twice with ice-cold PBS, lysed by the addition of 300μl Lysis BufferR from the Bioline Isolate RNA II mini-kit (Bioline Cat. # 52073), gently scraped from the plate, transferred into a 1.5 ml microcentrifuge tube and vortexed vigorously for 10 seconds. RNA was isolated using the Bioline Isolate RNA II mini-kit according to the manufactures instructions, and resuspended in 40μl of RNAse-free water (Bioline). Total RNA was determined by measuring RNA concentration using a NanoDrop ND-1000 Spectrophotometer.

2.5.3 cDNA synthesis and qRT-PCR

Samples were prepared with either RNA equivalent to equal cell number (Method A), or equal RNA (Method B). RNA samples were treated with 1U DNAse (Promega) and 12U RNAsin (Promega) in 2x Superscript Buffer (Invitrogen) with 2mM DTT in a final volume of 20μl, with 15min incubation at 37°C, then 15min incubation at 65°C. Complementary DNA (cDNA) was synthesised by reverse transcription of RNA with Superscript III (Invitrogen) according to manufactures instructions. cDNA samples were diluted in dH_2O and stored at -20°C until required. For quantitative reverse-transcription polymerase chain reaction (qRT-PCR) analysis, cDNA was diluted in dH_2O and amplified using Fast SYBR Green Master Mix (Applied Biosystems Cat. #4385612) and 100nM primers (Forward/Reverse), using the standard protocol on a StepOne Plus Real-time PCR System (Applied Biosystems). Reactions were performed in triplicate, and a sample of untranscribed RNA included as a control for genomic DNA contamination. For Method A, changes in target gene expression were determined by $2^{-(\Delta CT)}$, and for Method B changes in target gene expression were normalized to expression of a house-keeping gene and fold change was determined by $2^{-(\Delta\Delta CT)}$.

2.6 Histochemical, Immunohistochemical, and FISH analysis of fixed cells.

2.6.1 Adherance of cells on microscope slides

Cells were seeded in 100mm cell culture dishes containing poly-l-lysine microscope slides (Polysciences Cat. # 22247), at $0.2x10^6$ cells/ plate (BJ cell lines) or $0.5x10^6$ cells/ plate (U2TR cell lines) in 10mL cell culture media, and grown for at least 2 days.

2.6.2 Sensecence-associated β-GAL analysis

Cells were measured for senescence associated β-galactosidase activity using an assay described by Debacq-Chainiaux *et al* (Debacq-Chainiaux et al., 2009). Following treatment, slides were removed and washed 2x in PBS, then cells were fixed in 2% paraformaldehyde (v/v) (Electron Microscope Sciences Cat. # 15710) and 0.2% glutaraldehyde (v/v) in PBS for 5min at room temperature, and washed twice in PBS. Slides were submerged in freshly prepared staining solution (40 mM citric acid/Na phosphate buffer (pH 6.0), 5 mM $K_4[Fe(CN)_6]$ $3H_2O$, 5 mM $K_3[Fe(CN)_6]$, 150 mM sodium chloride, 2 mM magnesium chloride) with 1mg/ml 5-bromo-4-chloro-3-indoyl β-D-galactopyranoside (X-gal) in DMSO added immediately prior to use, and incubated overnight at 37°C. Slides were washed 2x 10min in PBS, then mounted in Vectashield mounting medium + DAPI (Vector Laboratories Cat. # H-1200) and stored at 4°C protected from light.

2.6.3 Immunofluorescence analysis of protein

Following treatment, slides were removed and washed 3x in PBS, and immuofluorescence analysis was performed by Method A or Method B (See TABLE 2). For Method A, cells were fixed in 4% paraformadelyde (Electron Microscope Sciences Cat. # 15710) diluted in PBS for 10min at room temperature, washed 3x in PBS, permeabilzed with 0.05% Triton-X diluted in PBS for 15min at room temperature, then blocked in BLOTTO (5% skim milk powder (w/v) and 0.05% Triton-X diluted in PBS with 0.5% serum corresponding to secondary antibody) for 30min at room temperature. For Method B, cells were fixed in ice-cold 95% ethanol + 5% acetic acid, washed 3x in PBS, then blocked in 3% BSA diluted in PBS for 30min at room temperature. For both methods, 100µL primary antibody (TABLE 2) diluted in blocking solution was placed on slides under a coverslip for 1hr at room temperature, slides were rinsed 3x in blocking solution, 100µL secondary antibody (TABLE 2) diluted in blocking solution was placed on slides under a coverslip for 1hr at room temperature protected from light, slides were rinsed 3x in PBS, fixed in 4% paraformadelyde diluted in PBS for 10min at room temperature, and then rinsed 3x in dH_2O. Control samples of no primary antibody were included for all secondary antibodies, and single secondary

antibody were included for all dual antibody experiments. Slides were mounted in Vectashield mounting medium + DAPI (Vector Laboratories Cat. # H-1200) and stored at 4°C protected from light.

2.6.4 FISH analysis of rDNA

Fluorescent in situ hybridization (FISH) analysis was performed using a probe derived from the intergenic spacer of the human rDNA repeat, kindly provided by Brian McStay (NUI, Galway, IRL). Biotin labeled DNA probe was generated using Biotin-Nick Translation Kit (Roche Cat. #11745824910) as per manufactures instructions; briefly, 2μg DNA was incubated with Nick translation mix in a volume of 10μl at 15°C for approximately 3hr, a test sample run on a 1% agarose gel to ensure probe length of 600b-1kb, then probe was stored at a concentration of 50ng/μl at -20°C until required for use. For probe mix, 100ng of biotin-labeled probe was combined with 30μg salmon sperm DNA and 18μg Human Cot-1 DNA (Invitrogen), precipitated and resuspended in 35μl of probe solution (50% formamide and 20% dextran sulphate in 2X Saline-Sodium Citrate Buffer (SSC)), then denatured by heating at 100°C for 5min and kept on ice until required for use.

Following IF (Method A), slides were fixed in freshly made ice-cold methanol:acetic acid (3:1) for 5min, then dehydrated in a series of 70%, 75% and 80% ethanol for 2min at room temperature and air dried. Slides were then denatured in 70% deionized formamide/ 2X SSC for 10 minutes at 83 ^{0}C, and dehydrated in a series of 70%, 75% and 80% ethanol for 2min at room temperature and air dried. 100μL of probe mix was placed on slides under a coverslip and incubated at 37°C overnight, then slides were washed 3X 5min in 50% formamide in 2X SSC at 42°C, washed in 3X 5min in 0.1X SSC at 60°C, and then equilibrated in 2x SSC. 100μL of Streptavidin-Alexa Fluor 488 diluted in Boehringer block (10% BSA, 0.15M NaCl, 0.1M Tris) was placed on slides under a coverslip and incubated at 37°C for 1hr, then slides were washed 3x 5min in 0.05% Tween-20 in 4XSSC. Slides were mounted in Vectashield mounting medium + DAPI (Vector Laboratories Cat. # H-1200) and stored at 4°C protected from light.

2.6.5 Image capture and analysis

Images were captured using an Olympus BX-51 microscope with a Spot RT3 CCD Camera and Spot 5.0 Software, ensuring constant settings were used across matching control and treatment samples. Lenses were Olympus UPlanAPO 20x NA 0.7, UPlanAPO 40x NA 0.85 and UPlanAPO 60x NA 1.26; Filters were U-MWU2N (DAPI), U-MWIBA2 (Alexa Fluor 488 and SybrGreen), and U-MWIG2 (Alexa Fluor 594).

Further image adjustment was performed using Adobe Photoshop, ensuring all changes were constant across matching control and treatment samples. Quantitation was performed manually, with a minimum of 4 fields and 20 cells scored for each treatment. For quantitation of phos-NBS1 and γH2A.X in BJ-Tp53shRNA FUCCI cells, analysis was performed using the automated Definiens imaging software. The S and G2 populations were selected based on signal ratio of G1/G2 < 1.2. The mean nuclear signal or nucleolar signal (that overlapped with NPM1 staining) were normalised to the average signal intensity of the corresponding vehicle controls.

2.7 Comet Assays

Comet Assays were performed using Trevingen CometAssay Reagent Kit (Cat. # 4250-050-K), in low light. Exponentially growing BJ-T cells were transferred in cell culture plates to ice, washed in 4°C PBS, 1ml of 4°C PBS was added to plates and cells collected by gently scraping, transferred to 1.5ml tubes on ice, and diluted to 100,000 cells per 1ml PBS. 10,000 cells (100µl) were combined at a ratio of 1:10 (1ml) molten 37°C Comet LMAgarose (Cat. # 4250-050-02) in 1.5ml tubes pre-warmed to 37°C, and 50µl of cell suspension was immediately spread over the sample area of a Trevigen CometSlide. (Cat. # 4250-050-03) Slides were stored flat at 4°C protected from light for 30min. Slides were immersed in ice-cold Lysis Solution (Cat. # 4250-050-01) and at 4°C protected from light for 45min, then immersed in RT Alkaline Unwinding Solution (300mM NaOH, 1mM EDTA, (pH>13)) and stored at RT protected from light for 60min. Slides were placed equidistant from each electrode in a BIO-RAD Sub-Cell GT Basic electrophoresis apparatus, containing 4°C Alkaline Electrophoresis Solution (300mM NaOH, 1mM EDTA, (pH >13)) at a level that resulted in a current of 300mA when the Voltage was set to 31V (~1 volt/cm in 30cm electrophoresis apparatus), and electrophoresis performed under these conditions for 30min at 4°C protected from light (volume of Alkaline Electrophoresis Solution was adjusted as necessary during electrophoresis). Slides were rinsed briefly several times in RT dH_2O, washed in RT 70% ethanol for 5min, and air-dried at RT overnight protected from light. 50µl of Sybr Green I nucleic acid gel stain (Cat. # 4250-050-05) diluted 1:10,000 (v/v) in TE Buffer (10mM Tris-HCl (pH 7.5), 1mM EDTA) was placed onto each sample on CometSlides for 5min at 4°C protected from light, then slides were air-dried at RT protected from light. 50µl of Vectashield mounting medium (Vector Laboratories, Cat. # H-1000) under a glass coverslip was placed on each slide. Images were captured on an Olympus BX-51 microcope as described above. Tail Length and Tail % DNA was calculated using Metamorph MetaImaging Series 7.7; Extent tail moment = Tail Length x Tail % DNA.

Image adjustment was performed using Adobe Photoshop, ensuring all changes in colour and levels were constant across matching control and treatment samples.

2.8 ChIP analysis

2.8.1 ChIP analysis in BJ cells (Method A)

For chromatin immunoprecipitation (ChIP) analysis in BJ cells $2x10^6$ cells per IP were crosslinked in 0.6% formaldehyde at 37°C for 10min, then quenched in 0.125M glycine at room temperature for 10min. Cells were harvested on ice by rinsing with PBS, treating with 0.025% Trypsin-EDTA in PBS for 5min, quenching in cell culture media, gently scraping to collect, transferring to 50ml falcon tube, centrifuging at 1200*g* at 4°C for 10min and rinsing with PBS. Cells were lysed in NP-40 cell lysis buffer (10mM Tris-HCl (pH 7.4), 10mM NaCl, 10mM $MgCl_2$, 0.5% NP-40, 1x Complete protease inhibitor cocktail tablets (Roche Cat. #04693132001)) at 1.5 $x10^6$ cells per 1ml on ice for 10min, centrifuged at 1200*g* at 4°C for 10min, then nuclei resuspended in SDS lysis buffer (50mM Tris HCl (pH 8.1), 10mM EDTA, 1% SDS, 1mM DTT, 1x Complete protease inhibitor cocktail tablets (Roche Cat. #04693132001)) at 300μl volume per sample for sonication, and incubated on ice for 10min. Chromatin was sheared to approximately 0.2kb fragments using Covaris S2 sonicator, according to manufactures instructions, an aliquot of each sample was retained to check shearing quality on a 1% agarose gel. Samples were centrifuged at 13,000*g* at 4°C for 10min, the supernatant divided into equal volumes equivalent to $2x10^6$ cells, and diluted in ChIP dilution buffer to final volume 1.5ml per IP. An equal volume (20-60μl) was removed from each aliquot and set aside to use as Input. Samples were pre-cleared with 35μl 50% Protein A agarose / salmon sperm DNA (Upstate) in PBS at 4°C on a rotating platform for 1hr, centrifuged at 700*g* at 4°C for 1min, the supernantant transferred to new 1.5ml microfuge tubes, incubated with 4μg of purified antibody (TABLE 2) or 8μl of pre-immune sera at 4°C on a rotating platform overnight, incubated with 50μl 50% Protein A agarose / salmon sperm DNA (Upstate) in PBS at 4°C on a rotating platform for 1hr, centrifuged at 700*g* at 4°C for 1min and supernatant discarded. Beads were washed at 4°C on a rotating platform for 5min, then centrifuged at 700*g* at 4°C for 1min, with the following solutions: one wash with low salt immune complex wash (20mM Tris-HCl (pH 8.1), 2mM EDTA, 1% Triton X-100, 0.1% SDS, 150mM NaCl), high salt immune complex wash (20mM Tris-HCl (pH 8.1), 2mM EDTA, 1% Triton X-100, 0.1% SDS, 500mM NaCl), LiCl immune complex wash (10mM Tris-HCl (pH 8.0), 1mM EDTA, 0.25M LiCl, 0.5% NP-40, 0.5% Deoxycholate), and two washes with TE Buffer (10mM Tris, 1mM EDTA). Immune complex was eluted from beads by incubating with 250μl

elution buffer (1%SDS, 0.1M $NaHCO_3$) at room temperature on a rotating platform for 15min, centrifuging at 700*g* at 4°C, collecting supernatant, and repeating elution to give final volume of 500μl eluate. Input samples were also made up to final volume of 500μl with elution buffer. 20μl of 5M NaCl was added to all samples and incubated at 65°C for 4hrs to reverse crosslinks, then 10μl of 0.5M EDTA, 20μl of 1M Tris-HCl (pH 6.5) and 1μl of 20mg/ml proteinase K was added to samples incubated at 45°C for 1hr, then DNA was precipitated by standard phenol/chloroform extraction, and resuspend in dH_2O.

2.8.2 ChIP analysis in U2TR cells (Method B)

For ChIP analysis in U2TR cells (adapted from (Berkovich et al., 2008)), $5x10^6$ cells per IP were crosslinked in 1% formaldehyde at room temperature for 10min, then quenched in 0.125M glycine at room temperature for 5min. Cells were harvested on ice by rinsing twice with PBS, gently scraping to collect in PBS, transferring to a 50ml falcon tube, centrifuging at 750*g* at 4°C for 5min, rinsing with PBS containing 1x cOmplete Protease Inhibitor Cocktail (Roche Cat.# 04693116001), and 1x PhosSTOP (Roche Cat.# 04906845001) (PPIs) then centrifuging at 750*g* at 4°C for 5min. Cells were lysed by resuspending in 1ml cell lysis buffer 1 (10mM HEPES (pH6.5), 10mM EDTA, 0.5mM EGTA, 0.25% Triton X-100 (v/v), 1x PPIs), incubating on ice 10min, centrifuging at 1700*g* at 4°C for 5min, resupending in cell lysis buffer 2 (10mM HEPES (pH6.5), 1mM EDTA, 0.5mM EGTA, 200mM NaCl, 1x PPIs), centrifuging at 1700*g* at 4°C for 5min, resuspending in nuclei lysis buffer at 300μl volume per $20x10^6$ cells (50mM Tris-Cl (pH8.1), 10mM EDTA, 0.5% SDS (v/v), 1x PPIs), and incubating on ice for at least 10min prior to sonication. Chromatin was sheared to approximately 1000bp fragments using Covaris S2 sonicator, according to manufactures instructions, and an aliquot of each sample was retained to check shearing quality on a 1% agarose gel. Samples were centrifuged at 20,000*g* at 4°C for 10min, and the supernatant diluted 1:5 in IP dilution buffer (20mM Tris-Cl (pH8.1), 2mM EDTA, 150mM NaCl, 1% Triton X-100 (v/v), 1x PPIs). For each treatment, 1% (150μl) Input sample was removed and incubated with 10μg Proteinase K at 65°C for 4hr, then Input DNA was isolated using QIAquick PCR purification kit (Qiagen Cat.# 28104) and resuspended in 30μl dH_2O. The concentration of Input DNA was measured using a NanoDrop ND-1000 Spectrophotometer, and used to calculate the volume of IP sample that gives 50μg of DNA. For each IP, chromatin equivalent to 50μg of DNA was prepared in 1ml IP dilution buffer, precleared with 30μl Protein A bead suspension (50% Protein A agarose beads (v/v) (Roche Cat.#11719408001), 100μg/ml tRNA (Sigma Cat.#

R8505), 100mg/ml BSA (Sigma Cat.# A4378) washed and resuspended in IP dilution buffer) at 4°C on a rotating platform for 2hr, centrifuged at 20,000*g* at 4°C for 5min, supernatant transferred to fresh 1.5ml microcentrifuge tube and again precleared with 30μl Protein A bead suspension at 4°C on a rotating platform for 2hr, centrifuged at 20,000*g* at 4°C for 10min, and supernatant transferred to fresh 1.5ml microcentrifuge tube. 2μg of primary antibody (TABLE 2) or IgG was added to each sample, and incubated at 4°C on a rotating platform overnight. 30μl Protein A bead suspension was added to each sample, and incubated at 4°C on a rotating platform for 3hr. Beads were washed at 4°C on a rotating platform for 3min and centrifuged at 950*g* at 4°C for 1min, seven times with IP wash buffer (20mM Tris-Cl (pH8.0), 0.5M NaCl, 2mM EDTA, 0.1% (v/v) SDS, 1% NP-40 (v/v), 1x PPIs), and twice with TE (10mM Tris-Cl (pH 8.0), 1mM EDTA). Chromatin was eluted from beads in 100μl elution buffer (1% SDS (v/v) in 0.1M $NaHCO_3$) at 65°C on a shaking platform for 15min. Beads were centrifuged at 950*g* at room temperature for 1min, and supernatant transferred to a fresh 1.5ml microcentrifuge tube, then elution step was repeated and supernatant transferred to same tube to give a 200μl volume. Sample DNA was purified by adding 1μg of RNAse A to samples, incubating at 37°C for 1hr, adding 1/100th volume 1M Tris-CL (pH 8.0), 1/50th volume 0.5M EDTA, and 20μg Proteinase K, incubating at 65°C overnight, then DNA was isolated using QIAquick PCR purification kit and resuspended in 30μl dH_2O.

2.8.3 Analysis of ChIP experiments

For both Method A and Method B, quantitation of immunoprecipitated DNA was performed by qRT-PCR analysis using Fast SYBR Green Master Mix and 100nM primers (Forward/Reverse; TABLE 3), with triplicate reactions for each sample, using the standard protocol on a StepOne Plus Real-time PCR System. The percentage of immunoprecipitated DNA was calculated by $2^{(\Delta CTx\ I)}$, where ΔCT is determined by CT(Input) – CT(IP), and I represents the percentage of DNA of the input reference.

2.9 BrdU Immunoprecipitation

For BrdU Immunoprecipitation (BrdU-IP, protocol adapted from (Ryba et al., 2011)), exponentially growing BJ-T cells were treated with 50μM BrdU for 2hr in culture. Cells were fixed in 75% ethanol as described above, and stored at -20°C protected from light. Immediately prior to FACS sorting, fixed cells were washed twice in PBS + 1% FBS, resuspended at 5x10^6 cells/ml in PBS+1% FBS containing 50μg/ml PI and 250μg/ml RNase A, incubated at RT for 30min protected from light, and transferred into 5ml polystyrene tubes through a cell-strainer cap on ice. Cells were sorted using a

BD FACSAria into G1, early S and late S cell cycle populations, where phase of cell cycle was determined by PI staining for DNA content. Mock sorted populations were treated in the same manner, but all cells were collected. Sorted populations were transferred into 1.5ml tubes, centrifuged at 400*g* for 10min at 4°C, then resuspended at 100,000 cells per 1ml SDS-PK buffer (50mM Tris-HCl (pH8.0), 10mM EDTA, 1M NaCl, 0.5% SDS) containing 0.2mg/ml Proteinase K and 0.05mg/ml glycogen, and incubated at 56°C for 2h. Cell lysates were aliquoted into 200µl (20,000 cell equivalent) volumes, and diluted with 200µl SDS-PK buffer containing 0.05mg/ml glycogen to give 400µl total volume. DNA was extracted using phenol:chloroform precipitation method, resuspended in 100ul of TE (pH 8.0), and transferred into Covaris microTUBEs (Covaris Cat. # 520045). DNA was sheared to approximately 0.8kb fragments by sonication on a Covaris S2 sonicator, according to manufactures instructions. 2µl of each sample was removed to check DNA size and quality (on Agilent 2100 Bioanalyzer, using Agilent High Sensitivity DNA Kit (Cat. #5067-4626) according to manufactures instructions), and remaining sample was diluted to 500µl final volume in TE (pH 8.0). Prior to BrdU IP, 20µl of each sample was removed and stored at -20°C to use as Input (4%). Samples were then incubated at 95°C to heat denature DNA, and transferred to ice for 2min. For BrdU IP, 480µl of each sample, 58µl of 10x IP buffer (100mM Sodium Phosphate (pH 7.0), 1.4M NaCl, 0.5% Triton X-100), and 40µl of BrdU antibody (BD Cat. # 555627) diluted to 12.5µg/ml in PBS were added to a new 1.5ml tube, and incubated for 20min at 4°C with constant agitation. 20µg of rabbit anti-mouse IgG (Sigma Cat. # M7023, Lot # 091M4788 5.1mg/ml) was added, and samples incubated for a further 20min at 4°C with constant agitation. To precipitate antibody-DNA complexes, samples were centrifuged at 16,000*g* for 5min at 4°C, resuspended in 750µL ice-cold 1X IP buffer, centrifuged again at 16,000*g* for 5min at 4°C, and supernatant removed completely from pellets. To purify DNA, samples (including Input samples) were resuspended in 200µl digestion buffer (50mM Tris-HCl (pH 8.0), 10mM EDTA, 0.5% SDS) containing 0.25mg/ml Proteinase K and incubated overnight at 37°C, then a further 100µl of digestion buffer containing 0.25mg/ml Proteinase K was added and samples incubated for 1hr at 56°C. Equal volume of phenol/chloroform/isoamyl alchohol (25:24:1) was added to sample, then centrifuged at 10,000*g* for 10min at 4°C. Aqueous phase was transferred to a fresh 1.5ml tube, equal volume of chloroform/isoamyl alchohol (24:1) was added, then centrifuged at 10,000*g* for 10min at 4°C. 250ul of aqueous phase was transferred to fresh 1.5ml tube, then 0.625µl of 20mg/ml glycogen, 85µl of 10M ammonium acetate, and 670µl of ethanol was added, vortexed briefly, and stored at -20C for 1hr. Samples were centrifuged at 16,000*g* for 30min at 4°C, resuspended in 70% ethanol,

centrifuged at 16,000*g* for 5min at 4°C, supernatants removed, and DNA pellets air dried, then resuspended in TE. Quantitation of immunoprecipitated DNA was performed by qRT-PCR using Fast SYBR Green Master Mix and 100nM primers (Forward/Reverse; TABLE 3), with triplicate reactions for each sample, using the standard protocol on a StepOne Plus Real-time PCR System. Changes in target gene enrichment were normalized to Mitochondrial DNA and fold change was determined by $2^{-(\Delta\Delta CT)}$.

2.10 Psoralen Crosslinking Southern Analysis

2.10.1 Nuclei harvesting and rDNA resolution by psoralen crosslinking

For psoralen crosslinking southern analysis, 6x 100mm cell culture plates were seeded with $0.5x10^6$ cells and grown overnight to give ~$6x10^6$ cells for each treatment condition. An extra plate was seeded for each treatment condition and used for cell counts. Following treatment, cells were rinsed in ice cold PBS, collected in 2ml ice cold PBS by gentle scraping, centrifuged at 500*g* for 10min at 4°C, resuspended in ice cold NP-40 lysis buffer (10mM Tris-HCl (pH 7.4) 10mM NaCl, 3mM $MgCl_2$, 0.5% (v/v) NP-40 added fresh) at a concentration of $1.5x10^6$ cell/ml, briefly vortexed, and incubated 10min on ice. Samples were then transferred into fresh tubes in 4ml aliquots (equivalent to $6x10^6$ cells), centrifuged at 500*g* for 10 min a 4°C, and resuspended in 700μl nuclear freezing buffer (50mM Tris- HCl (pH 8.3) 40% glycerol, 5mM $MgCl_2$, and 0.1mM EDTA), snap frozen in liquid nitrogen and stored at -80°C. Nuclei were thawed on ice immediately prior to crosslinking, then irradiated in the presence of 4,5,8 - trimethylpsoralen (Psoralen, Sigma Aldrich) using a 366-nm UV light box at a distance of 6cm, with 200μg/ml psoralen added at 1:20 dilution every 4 min for a total irradiation time of 20 min. Genomic DNA was isolated using Qiagen genomic DNA purification kit (20/G tips) as per the manufacturers instructions. DNA concentration was measured using a NanoDrop ND-1000 Spectrophotometer, and for each treatment condition equal DNA (4-12μg) was digested with 30U SalI (Promega) overnight at 37°C. Digested DNA was phenol:chloroform extracted, isopropanol precipitated, resuspended in 20ul dH_2O with 2x orangeG DNA loading dye, heat denatured by incubation at 65°C for 5min, then cooled directly on ice. Samples were run overnight at 60V on a 0.9% agarose gel of 24cm length until samples had run approximately 14cm from wells, then the gel was stained with ethidium bromide (1μg/ml) for 20min at room temperature, visualized under UV light and trimmed in order to retain the region between the 2 and 4kb markers that contain the 3.5kb bands of interest.

2.10.2 Southern blotting

The retained gel was soaked in depurination solution (0.25N HCl) for 10min, rinsed 3x in dH_2O, soaked 2x in denaturation solution (0.5N NaOH, 1.5M NaCl), rinsed 3x in dH_2O, and soaked 2x in neutralization solution (0.5M Tris-Cl (pH7.5), 3M NaCl). The DNA was then transferred onto Hybond-N+ nylon membrane (Amersham) by Southern blot hybridsation in 20x SSC solution (0.3M Tri Sodium Citrate, 3M NaCl) overnight. DNA was crosslinked to the wet membrane by exposure to 1200 x 100μJ/cm^2, using the Stratalinker UV Crosslinker 2400 (Stratagene, La Jolla, CA), the membrane was dried between Whatman paper, and then exposed to 1875 x 100μJ/cm^2 Stratalinker UV Crosslinker 2400 to reverse the crosslinking of psoralen and DNA.

2.10.3 Synthesis of rDNA probe

^{32}P isotope-labelled rDNA probe corresponding to +1.593 to +2.087 Kb 5'ETS region of the rDNA was freshly made. Template DNA was generated from BJ-T total genomic DNA, using KOD Hot Start DNA Polymerase Kit (Roche) following manufactures instructions, in the presence of 0.3μM forward and reverse primers. PCR product was separated on 1% agarose gel, the amplified 0.49kb fragment purified using QIAquick Gel Extraction Kit (Qiagen) following manufactures instructions, and template DNA stored at -20°C until required for use. ^{32}P isotope-labelled probe was generated using Nick Translation Kit (Roche): 0.1μg of template DNA and 100μCi α-^{32}P dATP (Perkin Elmer EasyTides Cat.# NEG502A100UC) were added to reaction mixture (0.4mM dCTP, 0.4mM dTTP, 0.4mM dGTP, 1x Nick Translation Buffer, 1x Enzyme Mix), the total volume adjusted to 20μL with ddH_20, then incubated at 15°C for 70min, followed by 65°C for 10min. The probe was purified using an Illustra G25 Sephadex microspin column, as per the manufacturers instructions. To assess the $\alpha^{32}P$-ATP DNA probe, 1ml was spotted onto separate pieces of Whatman DE-81 chromatography paper both before and after column purification, then placed in scintillation vials containing DEPC-treated water, and counts per minute (CPM) measured using a TriCarb 2910 TR quanta-counter, and specific activity of the probe was calculated from total and incorporated radioactivity using DNA specific activity calculator software (Ambion).

2.10.4 Hybridisation of probe to rDNA

The membrane was incubated with prehybridisation solution (5x SSC, 0.1% N-lauroylsarcosine (v/v), 0.02% SDS (v/v), 5% skim milk powder (w/v)) for 2hr on a rotating wheel at 65°C. The probe was denatured by incubation at 95°C for 10min then cooled directly on ice. To make hybridization solution, the probe was diluted to 2-10ng/ml (for specific activity of 10^9dpm/μg - 10^8dpm/μg) in prehybridisation solution

prewarmed to 65°C. The membrane was incubated with the hybridization solution overnight on a rotating wheel at 65°C, washed twice in 2x wash solution (2x SSC, 0.1% SDS (v/v)) for 5min at room temperature, then washed twice in 0.5x wash solution (0.5x SSC, 0.1% SDS (v/v)) for 15min at 68°C. The membrane was then sealed in plastic, and exposed to a phospho-imaging screen for 2-48hr. The radioactivity of each band was measured using the Typhoon Trio variable mode imager (GE Healthcare) and analysed using Image Quant (GE Healthcare).

2.11 RNA Sequencing sample preparation and analysis

BJ-T p53shRNA cells were plated at $0.3x10^6$ cells per 10cm plate in cell culture media and grown overnight. Duplicate plates of approximately $0.5\ x10^6$ exponentially growing cells were treated with 5nM NaH_2PO_4 (vehicle control), 5nM Actinomycin D, or 1μM CX-5461 in fresh cell culture media. For each treatment, one plate was used to isolate RNA, the other was used to perform cell counts, cell cycle analysis, and Western blot analysis (as described above).

RNA was isolated using Qiagen RNeasy (Cat. # 74104 Qiagen, Valencia, CA) following manufacturer's instructions. Briefly, 600μl of Buffer RLT was added dropwise to plates rinsed with PBS, lysate was collected with a rubber scraper, pipetted several times until no clumps were visible, transferred to QIAshredder spin colum (Cat. # 79654 Qiagen, Valencia, CA) and centrifuged for 2min and 13,500 rpm to homogenize sample, diluted with 1 volume 70% ethanol (in DEPC treated ddH_20), transferred to RNeasy Mini spin column and centrifuged for 15s at 9,200rpm to bind RNA to membrane. The RNeasy Mini spin column was then washed with 500μl Buffer RPE centrifuged for 15s at 9,200rpm, washed again with 500μl Buffer RPE centrifuged for 2min at 9,200rpm, transferred to a new collection tube and centrifuged for 1 min at 13,500 rpm, transferred to a new collection tube, then 50ul of RNAse free H_20 was added directly to the membrane and centrifuged for 1min at 9,200rpm to elute RNA. Isolated RNA was aliquoted into duplicate 20μl volumes and stored at -20°C. 1μl of remaining RNA was analysed on an Agilent 2100 Bioanalyzer, using Agilent RNA 6000 Nano Kit Eukaryote Total RNA Assay (Cat. # 5067-1512 Agilent Technologies, Santa Clara, CA) according to manufacturer's instructions, to determine RNA concentration and quality. One of each of the duplicate RNA samples was used to generate cDNA and determine levels of inhibition of 47S pre-rRNA transcription by qRT-PCR (as described above). The second duplicate RNA samples were used to generate a library for sequencing.

For triplicate sample sets, 1µg of total RNA was provided to the Molecular Genomics Core Facility at Peter MacCallum Cancer Centre, where poly-A containing RNA was purified and converted into a library of template molecules using Illumina TruSeq RNA Sample Preparation Kits (Illumina, San Diego, CA). Libraries were quantified by qPCR, normalised and pooled to 2nM, then sequenced on an Illumina HiSeq 2500 (Illumina, San Diego, CA) using 50bp paired-end reads (6 samples per lane). The sequencing results were aligned to the genome using Bowtie2 (Langmead et al., 2009) and the counted using HTSeq (Anders et al., 2015) and the differential expression was calculated utilising the DESeq package (Anders and Huber, 2010) in R (version 3.0.0).

TABLE 2. Antibodies for Western blotting, IP, flow cytometry, and microscopy.							
Protein	**Origin**	**Application**				**Source**	**Product Code**
		WB	IP	FCS	IF		
ATM	Rabbit		2μg (B)			Callbiochem	PC116
ATM	Mouse		2μg (A)			GeneTex	GTX70103
pATM-S1981	Mouse				1:400 (A)	Millipore	05-740
BrdU	Mouse			1:50		BD Biosciences	347580
BrdU	Mouse		0.5μg			BD Pharmingen	555627
pCDK1-Y15	Rabbit	1:400				Cell Signalling	CS9111
CHK1	Mouse	1:400				Cell Signalling	CS2360
pCHK1-S345	Rabbit	1:400				Cell Signalling	CS2348
CHK2	Rabbit	1:400				Cell Signalling	CS2662
pCHK2-T68	Rabbit	1:400				Cell Signalling	CS2661
Cyclin B	Rabbit	1:1000				Santa Cruz	sc-752
Fibrillarin	Rabbit				1:400 (A)	AbCam	ab5821
γH2A.X	Mouse		2μg (B)		1:500 (B)	Millipore	05-636
γH2A.X	Mouse	1:1000				AbCam	ab22551
pH3-S10	Rabbit			1:400		Millipore	06-570
pNBS1-S343	Rabbit		2μg (B)		1:400(A)	Cell Signalling	CS3001
NPM	Mouse	1:400			1:400(A)	AbCam	ab10530
p21	Rabbit	1:800				Santa Cruz	sc-397
p53	Mouse	1:2000				Santa Cruz	sc-126
pp53-S15	Rabbit	1:1000				Cell Signalling	CS9284
Pol I (E31)	Rabbit		8μl (A)			Larry Rothblum	-
Rabbit IgG	Rabbit		2μg (B)			Santa Cruz	sc-2027
RB	Rabbit	1:1000				Santa Cruz	sc-50
hypo-pRB	Rabbit	1:1000				BD Pharmingen	554136
RPA	Mouse				1:40 (A)	Millipore	NA13-100G
RPA	Rabbit		2μg (A)			Bethyl	A300-245A
Tubulin	Mouse	1:20,000				Sigma	T5168
UBF	Rabbit				1:400 (B)	In house	-
WRN	Rabbit	1:200				Santa Cruz	sc-468
Anti-Mouse IgG	Rabbit		20μg			Sigma	M-7023
Alexa Fluor 488 anti-mouse IgG	Donkey			1:400	1:2000	Invitrogen	A21202
Alexa Fluor 488 anti-rabbit IgG	Donkey			1:400	1:2000	Invitrogen	A11008
Alexa Fluor 596 anti-mouse IgG	Donkey				1:2000	Invitrogen	A21203
Alexa Fluor 596 anti-rabbit IgG	Donkey				1:2000	Invitrogen	A11012
Streptavidin - Alexa-Fluor 488	-				1:2000	Invitrogen	S11223

TABLE 3 Oligonucleotide sequences			
Target	**Application**	**Direction**	**Sequence (5'-3')**
47S 5'ETS	pre-rRNA	F	GCT CTT CGA TCG ATG TGG TGA CG
		R	CGG GCG GAG CGA GAA GGA C
MYC	mRNA	F	GGA CGA CGA GAC CTT CAT CAA
		R	CCA GCT TCT CTG AGA CGA GCT T
POLR1A	mRNA	F	AAG GAT GTG TTT GCC GTG TA
		R	GCG ATT CAG TGG CTT GTA AA
RRN3	mRNA	F	ACC AGA TGG TGC ATC CTG TA
		R	TGC CGT TAT CAA CCT TAC CA
Vimentin	mRNA	F	AGA GAA CTT TGC CGT TGA AGC T
		R	GAA GGT GAC GAG CCA TTT CC
rDNA Enhancer	ChIP	F	AGA GGG GCT GCG TTT TCG GCC
		R	CGA GAC AGA TCC GGC TGG CAG
rDNA Promoter	ChIP	F	CCC GGG GGA GGT ATA TCT TT
		R	CCA ACC TCT CCG ACG ACA
rDNA ETS1	ChIP DNA BrdU-IP	F	GCT CTT CGA TCG ATG TGG TGA CG
		R	CGG GCG GAG CGA GAA GGA C
rDNA ETS2	ChIP	F	GGC GGT TTG AGT GAG ACG AGA
		R	ACG TGC GCT CAC CGA GAG CAG
rDNA 18S	ChIP	F	CGA CGA CCC ATT CGA ACG TCT
		R	CTC TCC GGA ATC GAA CCC TGA
rDNA ITS1	ChIP	F	GAG AAC TCG GGA GGG AGA C
		R	GAC ACG CCC TTC TTT CTC TC
rDNA ITS2	ChIP	F	GAG AGA GAC GGG GAG GGC GG
		R	CCG AGG GAG GAA CCC GGA CC
rDNA 28S	ChIP	F	AGT CGG GTT GCT TGG GAA TGC
		R	CCC TTA CGG TAC TTG TTG ACT
rDNA Terminator	ChIP	F	ACC TGG CGC TAA ACC ATT CGT
		R	GGA CAA ACC CTT GTG TCG AGG
rDNA RFB	ChIP	F	GTGTAGGAGTGCCCGTCG
		R	AAATGTGGGAGAGGGAGTTC
rDNA IGS	ChIP	F	GTT GAC GTA CAG GGT GGA CTG
		R	GGA AGT TGT CTT CAC GCC TGA
Mitochondria DNA	DNA BrdU-IP	F	CCT AGG AAT CAC CTC CCA TTC C
		R	GTG TTT AAG GGG TTG GCT AGG G
HBB	DNA BrdU-IP	F	CCT GAG GAG AAG TCT GCC GTT A
		R	GAA CCT CTG GGT CCA AGG GTA G
MMP15	DNA BrdU-IP	F	CAG GCC TCT GGT CTC TGT CAT T
		R	AGA GCT GAG AAA CCA CCA CCA G
I-*Ppo*I target site 28S rDNA	DNA repair	F	ACG CGA TGT GAT TTC TGC CC
		R	TCT TCT TTC CCC GCT GAT TCC
I-*Ppo*I target site 28S rDNA (3')	ChIP	F	TGG AGC AGA AGG GCA AAA GC
		R	TAG GAA GAG CCG ACA TCG AAG G
rDNA +1.593 - 2.087 Kb	Psoralen probe	F	GAG TGC GGC TCG TCG CCT AC
		R	TCC CAC CGC CAC AGA CAC GA

CHAPTER 3. INVESTIGATING THE RESPONSE OF BJ HUMAN FIBROBLAST CELL LINES TO INHIBITION OF POL I TRANSCRIPTION WITH CX-5461

3.1 Introduction.

To investigate the efficacy of CX-5461 in cells at different stages of transformation, and identify the pathways involved in driving the response to inhibition of Pol I transcription by CX-5461, we utilised a panel of BJ isogenic cell lines developed by Hahn *et al* (Hahn et al., 1999).These lines comprise normal human BJ fibroblast cells immortalised by expression of the gene encoding the telomerase catalytic subunit (*hTERT*) and additional expression of genes encoding transforming proteins including the simian virus 40 (SV40) large T antigen, SV40 small t antigen, and an oncogenic allele of the *RAS* gene (H-*RAS*V12). Together these elements contribute to the tumorigenic transformation of these cells.

The large T antigen (L) and small t antigen (S) encoded by the oncogenic virus SV40 early region bind to and modulate the actions of many host cell proteins. L performs its role in transformation through the inactivation of retinoblastoma (RB) and p53 tumor suppressor pathways, while S alters the activity of protein phosphatase 2A (PP2A). RAS activates several signaling pathways implicated in cancer; oncogenic H-*RAS*V12 is constitutively active resulting in a sustained mitogenic signaling. Thus, the stepwise addition of each of these elements results in human BJ fibroblast cell lines that range from minimally immortalised (BJ-T), through different stages of transformation (BJ-LT, LST, LTR), to tumorigenic (BJ-LSTR) (Reviewed in (Zhao et al., 2004)) (FIGURE 7).

This model enabled us, first, to investigate the biological responses of cells at different stages of transformation to inhibition of Pol I transcription by CX-5461. As cells are isogenically matched, this makes them suitable for determining whether differences in response are specifically due to characteristics associated with transformation, rather than differences in for example unknown genetic changes or cell type. Second, this model enabled us to investigate the pathways mediating the response to inhibition of Pol I transcription by CX-5461 in 'normal' human cells which are minimally immortalized with hTERT (BJ-T). Untransformed cells are expected to have an intact genetic background, which has not been compromised by the numerous unknown genetic lesions associated with the cancer phenotype (Reviewed in (Hanahan and Weinberg, 2011b)). Therefore, these cells are suitable for the identification of

mechanisms mediating the response to CX-5461, as the integrity of specific molecules and pathways should be conserved.

3.2 CX-5461 small molecule inhibitor rapidly inhibits rates of Pol I transcription of 47S pre-rRNA genes in human BJ fibroblasts.

First, we examined the activity of CX-5461 in these BJ cell lines. The levels of inhibition of Pol I transcription can measured by quantitative reverse transcription PCR (qRT-PCR) with primers directed to the 5'ETS region of the 47S pre-rRNA. This 5'ETS sequence is rapidly removed and degraded during the processing of the 47S pre-rRNA into the mature 5.8S, 18S, and 28S rRNA, therefore qRT-PCR of this region gives an indirect measure of rates of transcription of the 47S pre-rRNA genes (rDNA).

Analysis of rates of Pol I transcription of the rDNA in BJ-T cells following treatment with CX-5461 for 3hr demonstrated that the inhibitor concentration at which rates of transcription were reduced by half (IC50) is approximately 25nM. Rates of transcription could be reduced by over 80% at higher doses, with an IC80 of approximately 2μM. In contrast, rates of Pol II transcription of a control 'housekeeping' gene (*VIM*, encoding the cytoskeletal protein Vimentin) were not significantly reduced at any dose used (FIGURE 8 A and B). We chose to use the dose at which maximal inhibition of Pol I transcription was observed for further experiments (1μM CX-5461). Analysis of rates of Pol I transcription in BJ-T cells following treatment with 1μM CX-5461 over a time course of 30min – 24hr demonstrated that at this dose, Pol I transcription was significantly inhibited within 30min following treatment (by 72%, ***p=0.0002), and that maximal inhibition of Pol I transcription was reached within 1hr (by 85%, ***p=0.0006) and sustained for at least 24hr following treatment (**p=0.0012) (FIGURE 8 C). These results demonstrate that in BJ cell lines, CX-5461 rapidly and selectively inhibits rates of Pol I transcription.

As rates of Pol I transcription can account for up to 60% of the transcriptional capacity of exponentially growing cells (Warner et al., 2001), we initially performed qRT-PCR analysis on RNA extracted from equal cell number, rather than analysing equal RNA for each sample, to ensure that changes in total cellular RNA did not affect our results. However, analysis of total RNA per cell following treatment with 1μM CX-5461 showed that there was no significant change in total RNA levels even after 24hr (FIGURE 8 D). Further, qRT-PCR analysis of rates of Pol I transcription performed for equal RNA for

each sample, corresponded to qRT-PCR analysis of rates of Pol I transcription performed for equal cells for each sample. Therefore, we chose to use this later method for further experiments (FIGURE 2 E). Together, these results show that at early time points there are no significant changes in total cellular RNA following inhibition of Pol I transcription by CX-5461.

3.3 Inhibition of Pol I transcription by CX-5461 induces an anti-proliferative response across a panel of human BJ fibroblast cell lines.

Next, we examine the biological response of the panel of BJ cell lines following inhibition of Pol I transcription with CX-5461. Dose-response experiments of BJ cell lines were performed following treatment with CX-5461 for 96hr. Cell viability was determined by the proportion of live cells following 96hr treatment relative to vehicle treated control. For all BJ cell lines, the dose curves were biphasic: CX-5461 had an anti-proliferative effect at doses of 10-100nM and above; while there was complete cell death at doses of 10μM and above (FIGURE 9 A). The half maximal effective concentration (EC_{50}) of CX-5461 was significantly lower for minimally immortalised BJ-T cells (EC_{50} =3.47nM, ****p<0.0001) than for all other cell lines, partially transformed BJ-LT (EC_{50} =15.06nM), -LST (EC_{50} =21.52nM), and –LTR (EC_{50} =30.54nM) had higher EC_{50}, and tumorigenic BJ-LSTR cells had the highest EC_{50} of all of the panel of BJ cell lines (EC_{50} =36.14nM) (FIGURE 9 B). Proliferation analysis of BJ cell lines treated with CX-5461 over 96hr showed that the BJ panel of cell lines had distinctly different responses to the inhibitor (FIGURE 9 C). BJ-T cells display reduced rates of proliferation from 10nM CX-5461, with a complete absence of proliferation at 1μM CX-5461. BJ-LT cells also display reduced rates of proliferation from 10nM CX-5461, and at doses of 300nM CX-5461 and above they undergo cell death. BJ-LST and -LTR cells have the most similar responses, with reduced rates of proliferation at doses from 30nM CX-5461, with a complete absence of proliferation at doses of 300nM CX-5461 and above. BJ-LSTR cells initially maintain rates of proliferation, but by 24hr following CX-5461 treatment they displayed reduced rates of proliferation associated with cell death (FIGURE 9 C). For all BJ cell lines, we once again observed complete cell death at 10μM CX-5461 and above, and we predict that this is due to off target effects of CX-5461 at these high doses. These results suggest that while the EC_{50} of CX-5461 is lower in the non-tumorigenic BJ-T cell line than the tumorigenic BJ-LSTR cell line, the phenotypic responses of transformed cell lines following CX-5461 treatment may be markedly different and depend upon the pathways that confer the transformed phenotype rather than the stage of transformation *per se*.

3.4 Inhibition of Pol I transcription by CX-5461 can induce different phenotypic responses in BJ isogenic cell lines transformed by defined genetic elements.

To determine whether the phenotypic responses to inhibition of Pol I transcription by CX-5461 were in fact different between these isogenic cell lines, we selected three of the BJ cell lines for further characterisation. These were the minimally immortalised BJ-T cell line, the partially transformed BJ-LT cell line (in which the p53 and RB pathways are inactivated by SV40 large T antigen), and the tumorigenic BJ-LSTR cell line.

First, we determined whether these cell lines undergo cell death following treatment with CX-5461. Analysis of live cells by propidium iodide (PI) exclusion assay showed that following 24hr treatment, there was no significant increase in cell death in BJ-T, BJ-LT or BJ-LSTR cell lines at any doses less than 10μM CX-5461. However, following 48hr and 96hr treatment with 1μM CX-5461, there was a slight increase in cell death in BJ-LT and BJ-LSTR cell lines (approximately 10% in BJ-LT and 20% in BJ-LSTR by 96hr, n.s.) (FIGURE 10 B and C). These results were supported by two additional cell death assays in the BJ-LT and BJ-LSTR cell lines – sub-G1 DNA content analysis of DNA fragmentation, and TMRE uptake analysis of mitochondrial membrane potential – which also showed a moderate increase in cell death following 48hr and 96hr treatment with 1μM CX-5461 (FIGURE 10 C). Together with the proliferation assays described above, these results indicate that BJ-LT and BJ-LSTR cell lines have sustained low levels of cell death after long term treatment with 1μM CX-5461.

Next, we determined whether any of these cell lines undergo cell cycle arrest following treatment with CX-5461. We performed FACS analysis of cells with PI staining for DNA content and BrdU staining to identify cells in S phase. BrdU is a synthetic nucleoside that can be incorporated into newly synthesised DNA in place of thymidine during DNA replication. In these experiments, cells were treated with BrdU directly prior to analysis. We also performed FACS analysis of cells with staining for phos-H3 to identify mitotic cells. Histone H3 phosphorylation at Ser10 by Aurora B kinase occurs during chromosome condensation during mitosis (prophase -anaphase) (Hendzel et al., 1997; Hirota et al., 2005). Following treatment with 1μM CX-5461, BJ-

T cells underwent both a G1 and G2 cell cycle arrest: the absence of BrdU positive cells indicated that the population of G1 cells were arrested and not entering S-phase; the absence of phos-H3 positive cells indicated that the significantly increased population of cells with a G2/M DNA content (from 14% to 62%, ***$p<0.0005$) were arrested in G2 and not M (FIGURE 10 D). BJ-LT cells do not undergo cell cycle arrest: the presence of BrdU positive cells indicated that cells were not arrested in G1 and entered S-phase; there was no significant increase in cells with a G2/M DNA content, which indicated that cells were not arrested in G2 or M (FIGURE 10 E). BJ-LSTR cells displayed a mitotic defect: the presence of both BrdU positive and phos-H3 positive cells indicated that cells were not arrested in G1 or G2; the significant increase in cells with an N=4 and N=8 DNA content (from 4% to 32% by 144hr for n=8, *$p<0.05$) indicated that cells were failing to correctly complete mitosis and undergo cytokinesis to produce two N=2 DNA content daughter cells (FIGURE 10 F).

These results show that isogenic cell lines, which have been transformed by a limited number of defined genetic elements, can undergo strikingly different phenotypic responses to inhibition of Pol I transcription by CX-5461: BJ-T cells undergo G1 and G2 cell cycle arrest; BJ-LT cells undergo cell death at sustained low levels over long term treatment; BJ-LSTR cells continue to proliferate with both a mitotic defect and increased levels of cell death. Collectively, this supports a model in which the cellular response to inhibition of Pol I transcription is mediated by distinct pathways, rather than a single response that is amplified according to the stage of transformation of the cell.

3.5 Inhibition of Pol I transcription by CX-5461 induces multiple cell cycle defects and senescence in BJ-T cells.

In order to begin to investigate the specific pathways that mediate the cellular response to inhibition of Pol I transcription by CX-5461, we selected the minimally immortalised BJ-T cells for more detailed characterisation. We hypothesised that identifying the key phenotypic responses would enable us to then examine the pathways that are responsible for their activation, such as cell cycle and stress response signaling pathways. This would then provide a framework from which we could begin to understand how the changes associated with transformation might alter the cellular response to CX-5461 in cancer. We had previously shown that BJ-T cells display a proliferation defect associated with cell cycle arrest, but not cell death, following inhibition of Pol I transcription by CX-5461 (See FIGURE 9 and 10).

Therefore, we performed analysis of cell cycle checkpoints, as well as analysis of irreversible cell cycle arrest due to cellular senescence, in BJ-T cell lines.

First, to extend the BJ-T cell cycle analysis performed for 48hr and 96hr above, we performed cell cycle analysis over a time course of 0-48hr following treatment with CX-5461 (FIGURE 11 A). These results demonstrate that BJ-T cells in G1-phase of the cell cycle remain arrested in G1 following CX-5461 treatment, as the G1 population was maintained from 0-48hr; cells in S-phase of the cell cycle appear to be delayed following CX-5461 treatment, as the S-phase population was maintained even after 12hr; S-phase cells then eventually arrest in G2-phase of the cell cycle, as the G2/M population was significantly increased after 24hr-48hr. We therefore performed further experiments to establish whether inhibition of Pol I transcription can induce all of these cells cycle defects.

To determine whether cells arrest in G1 following CX-5461 treatment, we performed cell cycle analysis following CX-5461 treatment in the constant presence of BrdU over a timecourse of 0-24hr (FIGURE 11 B). Under these conditions, any cell that exits G1 to replicate DNA in S-phase would incorporate BrdU. The proportion of BrdU negative cells remained constant from 0-24hr following CX-5461 treatment, indicating that cells did not exit G1 (49% BrdU +, compared to 36% BrdU + at 0hr. n.s.). In contrast, the majority of control cells progressed through the cell cycle and were BrdU positive by 24hr (91% BrdU +, compared to 36% BrdU+ at 0hr. **$p<0.005$). Therefore, inhibition of Pol I transcription in BJ-T cells induces a G1 cell cycle arrest.

To determine whether cells were delayed in S-phase following CX-5461 treatment, we performed cell cycle analysis with a short pulse of BrdU treatment, prior to CX-5461 treatment over a time course of 0 – 24hr (BrdU pulse-chase) (FIGURE 11 C). Under these conditions, only cells that were in S-phase at 0hr would be BrdU positive. The progression of this specific population of cells through the cell cycle could then be determined by DNA content. In control cells, the BrdU positive population progressed through S-phase to G2 within 6hr, and progressed through M to G1 within 12hr. Following CX-5461 treatment, the BrdU positive population remained in S-phase after 6hr, and remained largely in G2 after 12-24hr. Therefore, inhibition of Pol I transcription in BJ-T cells induces a S-phase delay.

To determine whether cells were arrested in G2 following CX-5461 treatment, we performed phos-H3 analysis to identify mitotic cells following 24hr and 48hr CX-5461

treatment (FIGURE 11 D). In control cells, only approximately 1% of cells were detected in M. Following 48hr CX-5461 treatment, this was significantly reduced, with almost no cells detected in M (less than 0.05%, *p<0.05). This indicated that the significantly increased proportion of cells with a G2 DNA content were arrested in G2, and not entering M. As the proportion of cells detected in M was very low, we also performed phos-H3 analysis following treatment in the presence of nocodazole. Nocodazole is commonly used to arrest cells in mitosis as it interferes with the polymerization of microtubules and prevents microtubule attachment to kinetochores, causing activation of the spindle assembly checkpoint and arrest in prometaphase (Zieve et al., 1980)(Reviewed in (Harper, 2005)). Following 24hr, approximately 20% of control cells treated with nocodazole alone were detected in M, while less than 5% of cells treated with both nocodazole and CX-5461 were detected in M. This indicated that following CX-5461 treatment, a reduced number of cells enter M. Therefore, inhibition of Pol I transcription in BJ-T cells induces a G2 cell cycle arrest.

To further illustrate that BJ-T cells arrest in both G1 and G2 following CX-5461 treatment, we performed cell cycle analysis on BJ-T cell populations that had been either enriched in G0/G1 by serum starvation, or enriched in S phase by thymidine treatment (FIGURE 11 E). Withdrawing serum from cells in culture causes them to be enriched in cell at G0/G1 phase of the cell cycle (Reviewed in (Jackman and O'Connor, 2001)). BJ-T cells grown cultured in serum-free media for 24hr were enriched in cells with G0/G1. When cells were restored to normal culture conditions, CX-5461 treated cells maintained their G1 population. Treatment with excess thymidine enriches cells in S-phase via feedback inhibition of nucleoside synthesis (Bootsma et al., 1964; Thomas and Lingwood, 1975). BJ-T cells treated with thymidine for 24hr were enriched in cells in S-phase. When cells were restored to normal culture conditions, control cells were able to proceed through the cell cycle and re-enter G1, while CX-5461 treated cells became arrested in G2. Collectively, these results show that inhibition of Pol I transcription by CX-5461 induces multiple cell cycle defects, including G1 arrest, S-phase delay and G2 arrest, in non-tumorigenic minimally immortalised BJ-T cells.

Finally, to establish whether inhibition of Pol I transcription by another method also results in similar cell cycle defects in BJ-T cells, we performed siRNA knock-down of Pol I transcription. We transfected BJ-T cells with siRNAs targeting both *POLR1A* (encoding the catalytic subunit of Pol I, DNA-directed RNA polymerase I subunit RPA1) and *RRN3* (encoding a Pol I transcription factors required for PIC formation,

RNA Polymerase I-Specific Transcription Initiation Factor RRN3) for 48hr. We were able to achieve over 80% reduction in *POLR1A* and *RRN3* transcripts (20% *POLR1A* and 12% *RRN3* compared to levels in control cells, ****p<0.0001), and this resulted in an approximately 50% reduction in rates of Pol I transcription of the rDNA (44% 47S-pre-rRNA compared to levels in control cells, ****p<0.0001) (FIGURE 11 F). Following inhibition of Pol I transcription by this method, BJ-T cells appeared to have reduced rates of proliferation (with approximately half as many total cells following 48hr knock-down, **p<0.005), associated with both G1 and G2 cell cycle defects. However, the phenotype was less clear than for 48hr 1μM CX-5461 treatment (with an increase in G2 cells from 6% to 18% following 48hr knock-down. n.s.) (FIGURE 11 F). One possibility for this discordance with CX-5461 data is the different levels of inhibition of Pol I transcription achieved by these two methods, and this was supported by the observation that when BJ-T cells were treated with a 30nM dose of CX-5461 that results in similar levels of inhibition, there are no significant differences in cell cycle populations (results not shown). Together, these results suggest that inhibition of Pol I transcription by a number of mechanisms can result in reduced proliferation associated with G1 and G2 cell cycle arrest.

Next, we investigated whether BJ-T cells undergo senescence following inhibition of Pol I transcription by CX-5461. Senescence is defined as a state of irreversible cell cycle arrest, which can be induced by diverse stimuli (Reviewed in (Campisi and di Fagagna, 2007)). Typically senescent cells remain metabolically active and viable for many weeks, but display a number of different phenotypes, some of which develop early and others which take many days to become apparent (Reviewed in (Rodier and Campisi, 2011)). These can include increased size (up to two-fold), expression of senescence-associated β-galactosidase (also associated with an increase in lysomal mass), expression of $p16^{INK4A}$, formation of senescence-associated heterochromatin foci (SAHFs), persistent nuclear foci of activated DNA damage proteins (also termed 'DNA segments with chromatin alterations reinforcing senescence' or DNA-SCARS), and secretion of factors including growth factors, proteases and cytokines (also termed the 'senescence –associated secretory phenotype' or SASP) (Reviewed in (Rodier and Campisi, 2011)).

We had previously observed while performing proliferation assays that BJ-T cells treated with 1μM CX-5461 were viable for over a week (FIGURE 9). Therefore, we performed histochemical analysis of senescence associated β-galactosidase activity

(SA-β-gal), a commonly used marker of senescence (Dimri et al., 1995). Following 96hr treatment with CX-5461, over 90% of BJ-T cells were positive for SA-β-gal (compared to only 20% of control treated cells, ****p<0.0001) (FIGURE 12 A). Therefore, CX-5461 treatment may induce senescence in BJ-T cells. Not all senescent cells express all documented markers of senescence, and no individual phenotype typical of senescence is sufficient to define a senescent state. Therefore, we examined a number of other markers of senescence. Following 24hr treatment with CX-5461, BJ-T cells displayed a significant increase in cell volume (approximately 1.5X, *p<0.05) (FIGURE 12 C). We also performed immunofluorescence (IF) analysis of γH2A.X. Histone variant H2A.X is incorporated into 5-25% of histone octamers, and it is phosphorylated at Ser139 over regions that can spread up to several megabases as part of the DNA damage response. Therefore, it is associated with senescence as part of nuclear foci of activated DNA damage proteins (Rodier et al., 2011). Following 96hr treatment with CX-5461, the number of cells displaying γH2A.X foci was significantly increased (from 8% of control treated cells to 47% of CX-5461 treated cells, **p<0.005) (FIGURE 12 B). Finally, we performed Western blot analysis of the p53/p21 and $p16^{INK4A}$/RB signaling pathways, which are commonly activated in order to induce senescence. Following 24hr treatment with CX-5461, we observed increased levels of p53, as well as increased levels of its transcriptional target p21, indicating that p53 is activated following CX-5461 treatment. We did not observe any increase in levels of $p16^{INK4A}$. However, we did observe increased levels of hypo-phosphorylated active RB (FIGURE 12 D). Collectively, these results show that inhibition of Pol I transcription by CX-5461 can induce a novel form of senescence in BJ-T cells characterised by a lack of $p16^{INK4A}$ activation.

3.6 Inhibition of Pol I transcription by CX-5461 induces p53-independent cell cycle defects and senescence in BJ-T cell lines.

The transcription factor p53 plays critical roles in the control of both cell cycle arrest and senescence, through multiple transcriptional targets and complex pathways (Reviewed in (Giono and Manfredi, 2006; Campisi and di Fagagna, 2007)). In one of its best characterised pathways, p53 induces the expression of p21 (cyclin-dependent kinase inhibitor 1), resulting in inhibition of cyclin/CDK complexes and the induction of cell cycle arrest. Inhibition of cyclin/CDK complexes in G1, for example by p21 or $p16^{INK4A}$, prevents the phosphorylation and inactivation of RB, resulting in repression of E2F family transcription factors and their target genes involved in cell proliferation.

These p53 and $p16^{INK4A}$/RB pathways are also considered to be the master regulators of senescence. The activation of p53 by the nucleolar stress pathway following inhibition of Pol I transcription is a well described phenomenon (See Section 1.2.1). Consistent with this, we observed the activation of p53 following 24h inhibition of Pol I transcription by CX-5461 in BJ-T cells. Therefore, we hypothesised that the cell cycle arrest and senescence phenotypes we observed following CX-5461 treatment in BJ-T cells were mediated by activation of the p53 nucleolar stress pathway.

First, we examined whether p53 was activated immediately following inhibition of Pol I transcription with CX-5461. Western analysis of p53 activation following 1hr-24hr treatment with CX-5461 revealed that levels of p53 and its transcriptional target p21 were increased by 1hr, and that after this time levels of both proteins continued to rise. Western analysis of p53 activation at earlier time points showed p53 levels were increased as early as 30 minutes following CX-5461 treatment (FIGURE 13 A). This acute activation of p53 is consistent with a role for the p53 nucleolar stress pathway in mediating the onset of proliferation and cell cycle defects in BJ-T cells in response to CX-5461.

To interrogate the requirement for p53 in mediating these responses, we established BJ-T cells stably expressing a short hairpin RNA (shRNA) targeting p53 (BJ-T p53shRNA cell lines). Western analysis of p53 protein levels showed that in these cells lines, p53 was not active; neither p53 nor p21 could not be detected at levels above those in untreated BJ-T cell lines, even following p53 induction by 24hr CX-5461 treatment (FIGURE 13 B).

Using this BJ-T p53shRNA cell line, we investigated whether knock down of p53 could rescue the phenotypic response of BJ-T cells to inhibition of Pol I transcription by CX-5461. Strikingly, BJ-T and BJ-T p53shRNA cell lines displayed an equivalent proliferation defect following treatment with CX-5461 (FIGURE 13 C). Therefore, while p53 is acutely activated in BJ-T cells following CX-5461 treatment, it appears that p53-independent pathways mediate the phenotypic response to inhibition of Pol I transcription.

To further characterise the p53-independent proliferation defect in BJ-T cells, we performed analysis of the G1, S, and G2 cell cycle defects induced by inhibition of Pol I transcription in these cell lines. Cell cycle analysis over a time course of 0-48hr following treatment with CX-5461 suggested that BJ-T p53shRNA cells are delayed in

S-phase and arrest in G2 following CX-5461 treatment; there is a significant increase in the S-phase population following CX-5461 treatment (from 28% in control treated cells to 46% in CX-5461 treated cells, ****p<0.0001), then cells eventually accumulate in G2-phase of the cell cycle (with 15% in control treated cells and 51% in CX-5461 treated cells at 48hr, n.s). However, unlike BJ-T cells wild type for p53, BJ-T p53shRNA cells do not appear to arrest in G1; the G1 population is significantly reduced following CX-5461 treatment (from 70% in control treated cells to 28% in CX-5461 treated cells, **p<0.005), and cells continue to enter S-phase (FIGURE 14 A). Therefore, p53 knock down appears to rescue the G1, but not S or G2 cell cycle defects induced by CX-5461 treatment in BJ-T cells.

We performed more detailed cell cycle experiments to further investigate the role of p53 in mediating each of these cell cycle defects following inhibition of Pol I transcription. To determine whether BJ-T p53shRNA cells arrest in G1 following CX-5461 treatment, we performed cell cycle in the constant presence of BrdU over a timecourse of 0-24hr. The proportion of BrdU negative cells was gradually depleted over 0-24hr following CX-5461 treatment (89% BrdU + in control treated cells and 73% BrdU + in CX-5461 treated cells, compared to 40% BrdU + at 0hr), indicating that cells continued exiting G1. Therefore, inhibition of Pol I transcription in BJ-T p53shRNA cells did not induce G1 cell cycle arrest. (FIGURE 14 B). Interestingly, control and CX-5461 treated populations displayed a similar proportion of BrdU positive cells following 24hr CX-5461 treatment, and in both control and CX-5461 treated populations the population of BrdU negative cells in G2 phase of the cell cycle was not maintained. This suggests that in the absence of p53, BJ-T cells arrest in G2 only once they have passed through S-phase. To determine whether BJ-T p53shRNA cells were delayed in S-phase following CX-5461 treatment, we performed BrdU pulse-chase cell cycle analysis over a time course of 0 – 24hr. In control cells, the BrdU positive population progressed through S-phase to G2 within 6hr, and progressed through M to G1 within 12hr. Following CX-5461 treatment, the BrdU positive population remained in S-phase after 12hr. Therefore, inhibition of Pol I transcription in BJ-T p53shRNA cells induces a S-phase delay (FIGURE 14 C). To determine whether cells were arrested in G2 following CX-5461 treatment, we performed phos-H3 analysis to identify mitotic cells following 24hr CX-5461 treatment. In control cells, less than 5% of cells were detected in M. Following 24hr CX-5461 treatment the proportion of cells in M was reduced (to 2%, n.s.), indicating that cells were arrested in G2, and not M. As the proportion of cells detected in M was very low, we once again performed phos-H3 analysis following treatment in the presence of nocodazole. Following 24hr, approximately 20% of control

cells treated with nocodazole alone were detected in M, while less than 5% of cells treated with both nocodazole and CX-5461 were detected in M. This indicated that following CX-5461 treatment, a reduced number of cells enter M. Therefore, inhibition of Pol I transcription in BJ-T p53shRNA cells induces a G2 cell cycle arrest (FIGURE 14 D). Collectively, these results show that inhibition of Pol I transcription by CX-5461 induces a p53-dependent G1 arrest, and a p53-independent S-phase delay and G2 arrest to in BJ-T cells.

Finally, we examined whether inhibition of Pol I transcription could also induce senescence in BJ-T p53shRNA cells. Following 96hr treatment with CX-5461 the proportion of cells positive for SA-β-gal was significantly increased (from 14% in control treated cells to 50% in CX-5461 treated cells, *$p<0.05$) (FIGURE 15). However, this was less that for BJ-T cells wild type for p53, with approximately 50% of BJ-T p53shRNA positive for SA-β-gal, compared to over 90% of parental BJ-T cells positive for SA-β-gal. This indicated that knock down of p53 can partially rescue the senescence phenotype induced by CX-5461 treatment.

Therefore, our results suggest that p53 is activated following inhibition of Pol I transcription by CX-5461, most likely by the nucleolar stress pathway. The G1 arrest, G2 arrest, and senescence phenotype induced by CX-5461 treatment are partially rescued in BJ-T p53shRNA cells, suggesting that the p53 pathway is involved in mediating these responses to inhibition of Pol I transcription. However, predominantly, the proliferation and cell cycle defects induced by CX-5461 in BJ-T cell lines appear to be mediated by p53-independent pathways.

3.7 Discussion

In collaboration with Cylene Pharamceuticals (San Diego, Calafornia), our laboratory helped develop and test a first in class small-molecule inhibitor of Pol I transcription. As part of the primary publication describing the drug, its efficacy and antitumor activity was tested in non-transformed cell lines, a panel of human cancer cell lines, and murine Xenograft models (Drygin et al., 2011). Here, we characterised the cellular response of a panel of isogenic BJ human fibroblast cell lines to CX-5461, which enabled us to compare how non-transformed and transformed cells of the same genetic background respond to inhibition of Pol I transcription.

The panel of BJ cell lines range from non-tumorigenic to tumorigenic, through the sequential addition of known genes encoding transforming proteins (Reviewed in (Zhao et al., 2004)). In contrast, established patient derived cancer cell lines are of different cell types and genetic backgrounds, and are expected to have a multitude of genetic lesions associated with the cancer phenotype (Reviewed in (Hanahan and Weinberg, 2011b)). Therefore, using the BJ cell lines as a model system to investigate the response to inhibition of Pol I transcription by CX-5461 has a number of advantages. For example, we were able to investigate the response to inhibition of Pol I transcription in 'normal' untransformed human cells, as well as determining whether tumorigenic cells have increased sensitivity to the drug.

We first examined the activity of CX-5461 in BJ cells by determining the inhibition of Pol I transcription following treatment with the drug. In BJ-T cells, CX-5461 rapidly and significantly inhibits rates of Pol I transcription of 47S pre-rRNA genes, with an IC50 of approximately 25nM and maximal inhibition achieved within 1hr of treatment with the drug. The dose of 1μM CX-5461 was selected for future experiments to characterise the cellular response to CX-5461 in these cell lines, as maximal inhibition of Pol I transcription was achieved at this dose (with levels of 47S pre-rRNA approximately 20% of those in vehicle treated cells) (FIGURE 8). These results correlated closely with those for other cell lines treated with CX-5461, with similar IC50s for Pol I transcription of the rDNA reported in all solid tumor cell lines tested (Drygin et al., 2011).

The activity of CX-5461 was also selective for inhibition of Pol I, rather than Pol II transcription. Specifically, in BJ-T cells, there was no reduction in the rates of transcription of a Pol II transcribed housekeeping gene at doses up to 10μM (FIGURE 8). This was supported by gene expression arrays in two additional cell lines (MIA PaCa-2 and A375). Following inhibition of Pol I transcription with CX-5461 for 1hr, an equal number of Pol-II transcribed genes are up-regulated as down-regulated, indicating changes in rates of transcription of Pol-II transcribed genes are likely due to indirect effects of inhibition of Pol I transcription, rather than general inhibition of Pol II transcription by CX-5461 (Drygin et al., 2011).

The very high rates of Pol I transcription mean that 47S pre-rRNA can account for a significant proportion of newly synthesised RNA (over 30% in exponentially growing cells), while mature rRNA accounts for the majority of total RNA in the cell as part of

ribosomes in the cytoplasm (Warner et al., 2001) (Reviewed in (Moss, 2004)). Therefore, we examined whether inhibition of Pol I transcription results in a reduction in total cellular RNA. After 24hr treatment with CX-5461 no reduction in total cellular RNA was observed (FIGURE 8 D). This suggests there is no change in the total level of ribosomes of the cells at this time, which is consistent with reports indicating that ribosome are very stable in growing mammalian cells, with half lives of days to weeks (Reviewed in (White, 2005)). Further, other work from our laboratory has shown that following Rrn3 knockdown in Eu-*Myc*-Bcl2+ cells, which resulted in a 35% reduction in rDNA transcription, cells displayed no proliferative disadvantage for up to 4 days when Bcl2 was overexpressed to prevent apoptosis (Bywater et al., 2012). This suggests that rRNA is produced at levels in excess of that which is required for efficient proliferation. Collectively these results indicate that early phenotypic responses observed following inhibition of Pol I transcription, such as cell cycle arrest, do not arise as a result of changes in ribosome insufficiency and thus reduced translation capacity of the cell, but rather directly as a consequence of changes in the rates of transcription of the 47S rRNA genes. This is consistent with a model where inhibition of Pol I transcription induces p53 activation and checkpoint responses via the nucleolar stress pathway.

Next we compared the sensitivity of the panel of BJ cell lines to CX-5461 at defined stages of transformation, from non-tumorigenic BJ-T cells, through the addition of transforming genetic elements in BJ-LT, -LST, and -LTR cells, to tumorigenic BJ-LSTR cells. As increased rates of rRNA synthesis and proliferation are associated with cancer, we had initially hypothesised that that as cells progressed towards a tumorigenic phenotype, they would become reliant upon high rates of Pol I transcription, and consequently more sensitive to CX-5461 treatment (See Section 1.3). Consistent with this idea, across the panel of 5 nontransformed and 50 tumor cell lines in which we tested CX-5461 anti-proliferative activity, the average EC_{50} of normal cell lines was markedly higher than that of cancer cell lines (Drygin et al., 2011). CX-5461 exhibited a broad range of anti-proliferative activity against cancer cell lines, with EC_{50} values ranging from 3nM to 5.5μM, and a median EC_{50} of 147nM in the 50 cell lines tested. The 5 non-tumorigenic cell lines were relatively resistant to CX-5461, with EC_{50} values of approximately 5μM. However, we found that BJ cell lines became less sensitive to inhibition of Pol I transcription by CX-5461 as they progressed toward the tumorigenic phenotype. BJ-T cells had a significantly lower EC_{50} than other BJ cells lines, while BJ-LSTR cells had a higher EC_{50} than the other BJ cell lines (FIGURE 9 A). These data indicated that sensitivity to CX-5461, when

defined by anti-proliferative EC_{50}, does not simply correlate with the process of transformation in BJ fibroblasts.

A more in depth analysis of the anti-proliferative effect of CX-5461 in BJ cell lines indicated that there were distinctly different phenotypic responses between the different isogenic BJ cell lines, which could translate to a therapeutic window in *in vivo* models. We compared the response of minimally immortalised BJ-T, BJ-LT (inactive for p53), and tumorigenic BJ-LSTR cells to inhibition of Pol I transcription by CX-5461: BJ-T populations undergo cell cycle arrest, BJ-LT cells undergo sustained low levels of cell death over long term treatment, while BJ-LSTR cells continue to proliferate but undergo increased levels of cell death that appear to coincide with progression through defective mitosis (FIGURE 10). Therefore, tumorigenic BJ-LSTR cells are in fact more prone to undergo cell death than BJ-T cells following inhibition of Pol I transcription by CX-5461. We speculate that BJ-LT and BJ-LSTR cells are able to escape cell cycle arrest upon inhibition of Pol I transcription due to the inactivation of cell cycle regulatory proteins by SV40 large-T antigen, and that inappropriate progression through the cell cycle (particularly M phase) may drive cell death in these lines. However, each of the defined transforming genetic elements in the BJ panel of cell lines can affect multiple complex pathways. For instance, the targets of large-T and small-t antigens of the tumor virus SV-40 are numerous, including p53, RB, p300/CBP, BUB1, the IGF1 (insulin-like growth factor 1) pathway, and PP2A, but they also have additional targets that have not been comprehensively defined (Reviewed in (Ahuja et al., 2005)). Similarly, RAS performs its role as a key regulator of cell growth and proliferation via signaling through multiple downstream pathways (Reviewed in (Zhao et al., 2004)). Therefore, it is difficult to draw conclusions regarding the predominant signaling pathways mediating the phenotypic response to inhibition of Pol I transcription in these cell lines. Collectively, these results suggest that the cellular phenotypic response to CX-5461 (for example, cell cycle arrest, senescence or cell death) is dependent upon the integrity of specific signaling pathways and checkpoints. Identifying these specific signaling pathways, and the mechanisms by which they mediate the phenotypic response to CX-5461, will therefore be vital to understanding the potential efficacy of CX-5461 in the treatment of different cancers.

To begin to investigate the molecular responses to inhibition of Pol I transcription by CX-5461, we chose to further characterise the cellular and molecular responses to CX-5461 in minimally immortalised BJ-T cells, as their pathways are not compromised by the process of transformation. In response to inhibition of Pol I transcription by CX-

5461, BJ-T cells displayed activation of multiple cell cycle checkpoints, including G1 cell cycle arrest, S-phase delay, and G2 cell cycle arrest, and also underwent senescence (FIGURE 11 and 12). Activation of p53 is known to induce both cell cycle arrest and senescence. Consistent with this, p53 was rapidly activated in BJ-T cells following inhibition of Pol I transcription by CX-5461 (FIGURE 13). However, BJ-T p53 knock-down cells displayed an equivalent proliferation defect in response to inhibition of Pol I transcription. In BJ-T cells, p53 knock down rescued the G1 cell cycle arrest, but did not rescue the S-phase delay, or G2 cell cycle arrest (FIGURE 14). This indicates that other, p53-independent pathways can mediate BJ-T response to inhibition of Pol I transcription by CX-5461. In fact, across the panel of solid tumor cell lines in which the anti-proliferative activity of CX-5461 was tested in Drygin *et al* (Drygin et al., 2011), we observed no correlation between p53 status and sensitivity to CX-5461, with p53 mutant cells having a similar median EC_{50} as p53 wild-type cells. In these cells lines (A375 and MIA PaCa-2c), CX-5461 induced senescence and autophagy, but not apoptosis, consistent with the phenotype observed in BJ-T cells. Collectively this suggests that inhibition of Pol I transcription can confer a therapeutic response in cancer cells independently of p53, via additional pathways.

A key study from our research group by Bywater *et. al.* (Bywater et al., 2012) examined the ability of CX-5461 to selectively target malignant cells *in vivo*, using a murine model of lymphoma driven by MYC (Eμ-*Myc)* (Adams et al., 1985). MYC is a prominent oncogene dysregulated in almost half of all human cancers, that directly upregulates Pol I transcription and ribosome biogenesis (See Section 1.4.1). Eμ-*Myc* lymphoma cells isolated from tumor bearing mice displayed sensitivity to CX-5461 when cultured *in vitro*, with an EC_{50} for cell death of 5.4nM after 16hr (compared to the average anti-proliferative EC_{50} of 147nM in solid tumor cell lines after 48hr (Drygin et al., 2011)) These cells were also sensitive to inhibition of Pol I transcription by RNAi mediated knockdown of UBF or RRN3; knockdown of Pol I transcription by 35% resulted in increased cell death and a strong disadvantage in competition assays. Importantly, in mice with established disease from transplanted Eμ-*Myc* lymphoma, CX-5461 treatment *in vivo* selectively induced cell death in malignant B-cells, but not normal B-cells, and prolonged their survival. The induction of cell death occurred immediately (by 6hr following treatment) and prior to any changes in total RNA levels, consistent with a direct effect of inhibition of Pol I transcription and not an indirect effect due to ribosome insufficiency. Therefore, inhibition of Pol I transcription by CX-5461 can selectively target tumor cells *in vivo.*

Interestingly, in contrast to the results above, the sensitivity of Eμ-*Myc* lymphomas to CX-5461 was dependent upon p53. Treatment of Eμ-*Myc* lymphoma cells with CX-5461 *in vitro* resulted in nucleolar disruption, increased amount of RPL5 and RPL11 associated with MDM2, increased p53 levels, transactivation of p53 target genes by 1hr, and induction of apoptosis by 2hr following treatment. This is consistent with acute activation of p53 by the nucleolar stress pathway. In a panel of Eμ-*Myc* lymphomas, cells mutant or null for p53 displayed over 100-fold decreased sensitivity to CX-5461 (Bywater et al., 2012). In fact, in the original publication describing the drug, the sensitivity of cell lines derived from hematologic malignancies did correlate with p53 status, and those that were p53 wild type included the 3 cell lines most sensitive to CX-5461 (Drygin et al., 2011). Therefore, inhibition of Pol I transcription by CX-5461 can specifically activate p53 via the nucleolar stress pathway to induce apoptosis and confer a therapeutic response in cancer cell lines *in vivo*. However, p53-dependent sensitivity appears to be specific to certain cancer types.

In conclusion, our studies demonstrate that inhibition of Pol I transcription by CX-5461 has potential as a novel therapeutic strategy for the treatment of cancer. CX-5461 can selectively induce cell death in cancer cell lines *in vitro*, as shown here for isogenic BJ-T and BJ-LSTR cell lines. The therapeutic efficacy of CX-5461 is not simply an indirect consequence of changes in the number of cellular ribosomes, but instead a result of acute activation of pathways that mediate stress response, such as cell cycle arrest, senescence and apoptosis. Consistent with previous reports, inhibition of Pol I transcription by CX-5461 can activate p53 via the nuclear stress response pathway. However, the data presented here show that additional, p53-independent pathways, resulting in S-phase and G2 cell cycles defects and senescence, can mediate the response to inhibition of Pol I transcription by CX-5461. Identifying the key p53-independent pathways that underlie the therapeutic response to CX-5461 will enable us to better understand its potential to target different cancers.

FIGURE 7. Characteristics of the BJ fibroblast isogenic cell lines at defined stages of transformation. A) Expression the telomerase catalytic subunit (*hTERT; T*), the oncogenic simian virus 40 (SV40) early region (encoding SV40 Large T antigen (L), and SV40 small t antigen (S)), and the H-*RAS*V12 oncogenic allele of the *RAS* gene (R) in BJ fibroblasts contribute to the tumorigenic transformation of these cell lines (shown in red). Key pathways contributing to acquisition of the transformed phenotype are also shown (in white). **B)** Stepwise addition of these elements results in human BJ fibroblast cell lines that range from minimally immortalised (BJ-T), through different stages of transformation (BJ-LT, LST, LTR), to tumorigenic (BJ-LSTR). **C)** Western blot analysis of exponentially growing BJ isogenic cell lines was used for cell line identity confirmation. Expression of large T, small t, and RAS, and their downstream targets p53 (inhibition of p53 activity results in feedback upregulation of total p53 levels) and phos-ERK (indicative of MAPK pathway activity).

FIGURE 7

A)

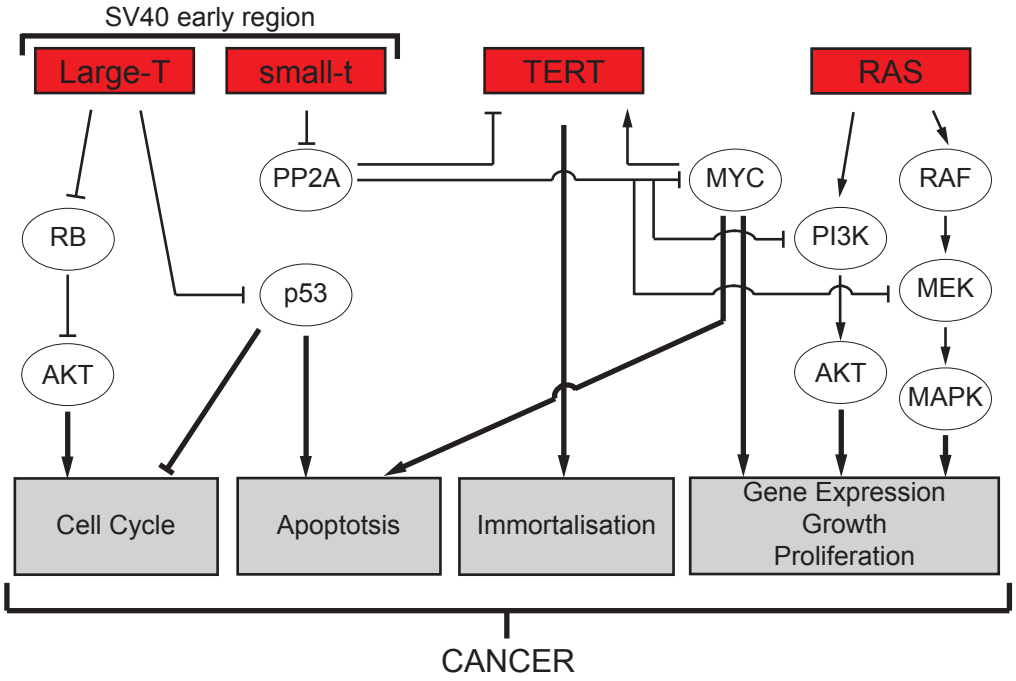

B)

Minimally Immortalised

Tumorigenic Transformation

Tumorigenic

BJ-T
BJ-LT
BJ-LST
BJ-LTR
BJ-LSTR

BJ-T	hTERT
BJ-LT	Large-T, hTERT
BJ-LST	Large-T, small-t, hTERT
BJ-LTR	Large-T, hRASV12, hTERT
BJ-LSTR	Large-T, small-t, hRASV12, hTERT

C)

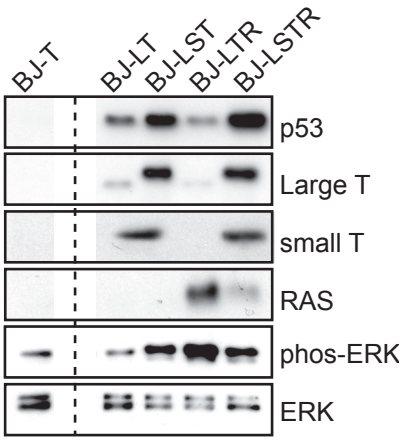

FIGURE 8. CX-5461 small molecule inhibitor rapidly inhibits rates of Pol I transcription of 47S pre-rRNA in human BJ-T fibroblasts. A) qRT-PCR analysis of expression of 47S pre-rRNA in BJ-T cells treated with CX-5461 for 3hr. RNA quantity is normalised to equal cell counts. Relative fold change to vehicle control samples (n=3, mean±sem). **B)** qRT-PCR analysis of expression of *VIM* in BJ-T cells treated with CX-5461 for 3hr. RNA quantity is normalised to equal cell counts. Relative fold change to vehicle control samples (n=3, mean±sem). **C)** qRT-PCR analysis of expression of 47S pre-rRNA in BJ-T cells treated with 1μM CX-5461 for 30min, 1hr, 3hr, 6hr, 12hr and 24hr). RNA quantity is normalised to equal cell counts. Relative fold change to vehicle control sample (t=0). (n=3, mean±sem **p<0.05, ***p<0.005 compared to vehicle control sample). **D)** Total RNA per cell following 3hr and 24hr treatment with 1μM CX-5461. RNA purification was performed for a known number of cells in the presence of α^{32}P-UTP riboprobe. (RNA per cell = [Total RNA X 100] / [Cell Number x % RNA Recovery]). (n=3-6, mean±SD). **E)** qRT-PCR analysis of expression of 47S pre-rRNA in BJ-T cells treated with CX-5461 for 3hr. Equal RNA quantity is calculated for each sample (shown in solid line). For comparison, qRT-PCR analysis of expression when RNA quantity normalised to equal cell counts (from (A)) is shown in dotted line. Relative fold change to vehicle treated samples (n=4, mean±sem).

FIGURE 8

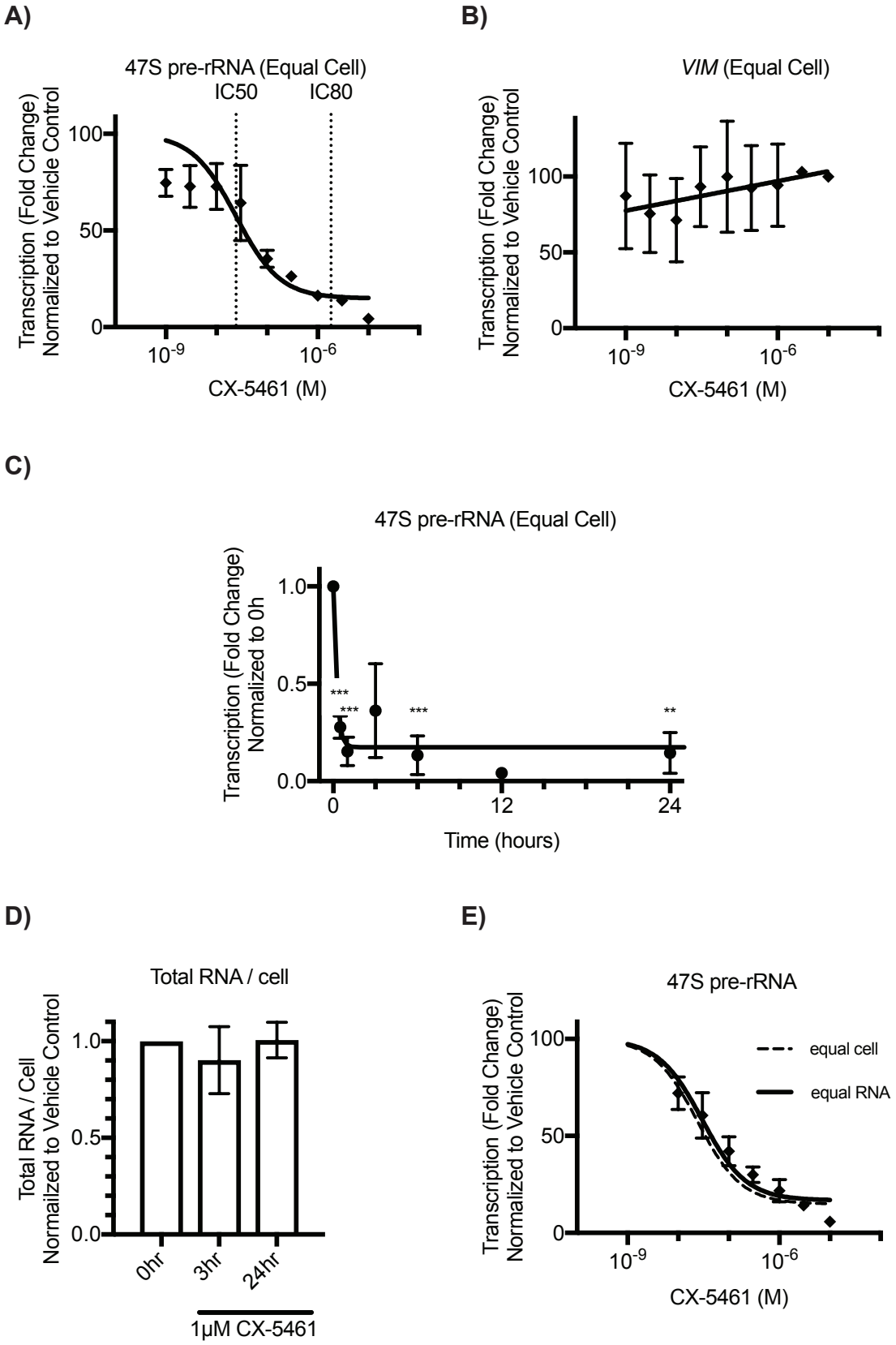
A)
47S pre-rRNA (Equal Cell)
IC50
IC80
Transcription (Fold Change) Normalized to Vehicle Control
100
50
0
10^{-9}
10^{-6}
CX-5461 (M)
B)
VIM (Equal Cell)
Transcription (Fold Change) Normalized to Vehicle Control
100
50
0
10^{-9}
10^{-6}
CX-5461 (M)
C)
47S pre-rRNA (Equal Cell)
Transcription (Fold Change) Normalized to 0h
1.0
0.5
0.0
***
***
***
**
0
12
24
Time (hours)
D)
Total RNA / cell
Total RNA / Cell Normalized to Vehicle Control
1.0
0.5
0.0
0hr
3hr
24hr
1μM CX-5461
E)
47S pre-rRNA
Transcription (Fold Change) Normalized to Vehicle Control
100
50
0
equal cell
equal RNA
10^{-9}
10^{-6}
CX-5461 (M)

FIGURE 9. Inhibition of Pol I transcription by CX-5461 induces an anti-proliferative response across a panel of human BJ fibroblast cell lines. A) Dose-response cell viability assays for BJ cell lines following treatment with 0.1nM to 30μM CX-5461 for 96hr. Cell viability is determined by total live cells relative to vehicle control (=100%) (n=6, mean±SD). EC50 values are shown (dashed line) with 95% confidence interval (dotted lines). **B)** EC50 values for dose-response cell viability assays for BJ cell lines treated with CX-5461 (from (A)) (n=6, mean±sem. **p<0.005, ****p<0.0001). **C)** Dose-response cell proliferation assays for BJ cell lines following treatment with 10nM to 10μM CX-5461 from 0hr to 96hr. Cell proliferation is determined by % confluency of live cells in culture measured using an IncuCyte Zoom (Essen Biosciences). (representative experiment of n=4-6, mean±SD of technical replicates).

FIGURE 9
A)

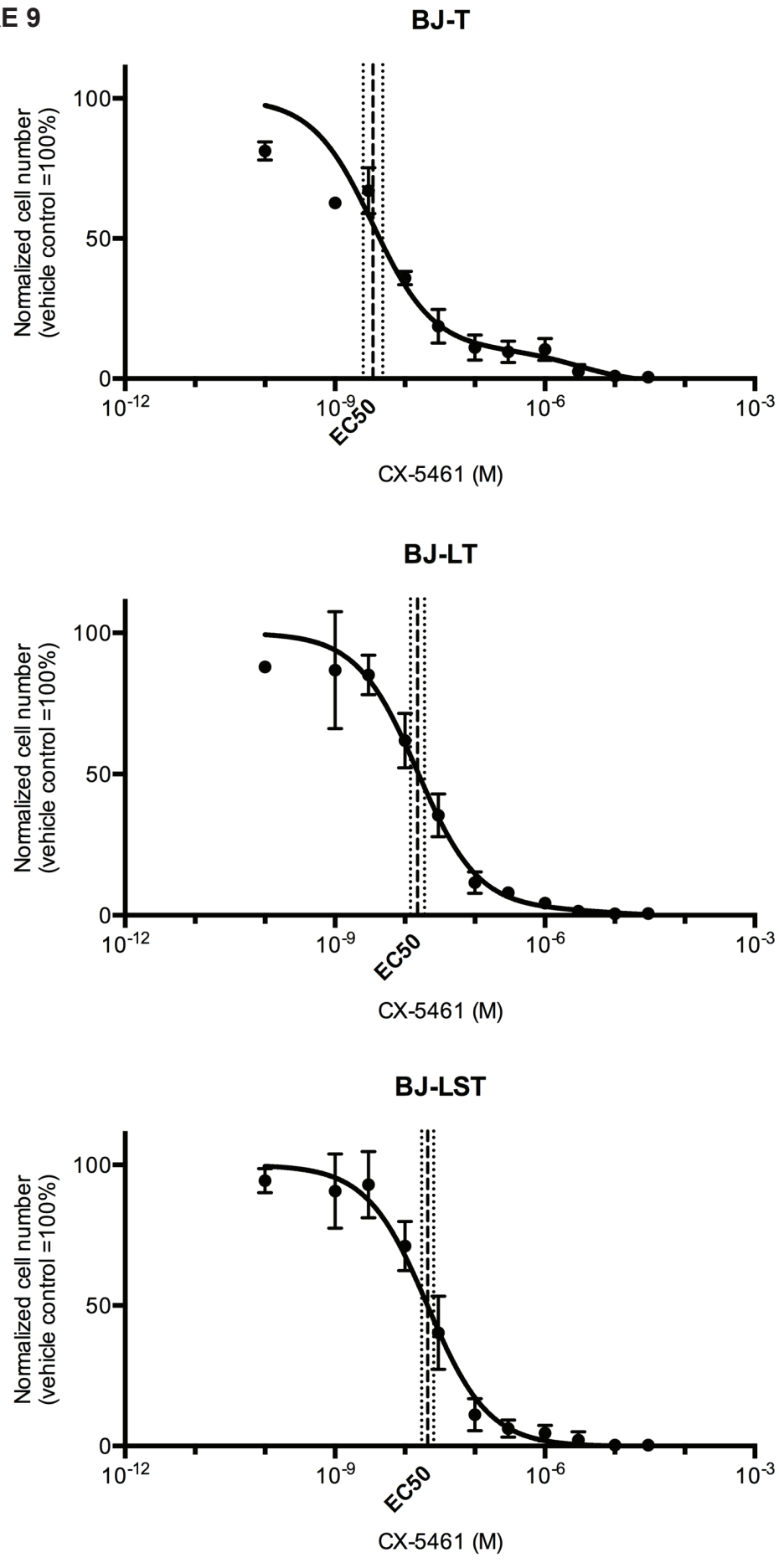
BJ-T
Normalized cell number
(vehicle control =100%)
100
50
0
10^{-12}
10^{-9}
EC50
10^{-6}
10^{-3}
CX-5461 (M)
BJ-LT
Normalized cell number
(vehicle control =100%)
100
50
0
10^{-12}
10^{-9}
EC50
10^{-6}
10^{-3}
CX-5461 (M)
BJ-LST
Normalized cell number
(vehicle control =100%)
100
50
0
10^{-12}
10^{-9}
EC50
10^{-6}
10^{-3}
CX-5461 (M)

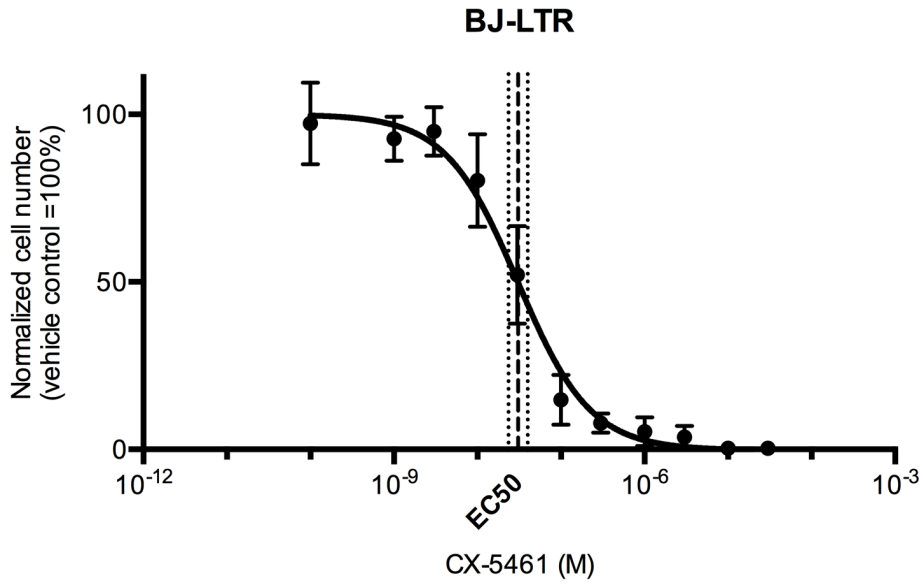
BJ-LTR
Normalized cell number
(vehicle control =100%)
100
50
0
10^{-12}
10^{-9}
EC50
10^{-6}
10^{-3}
CX-5461 (M)

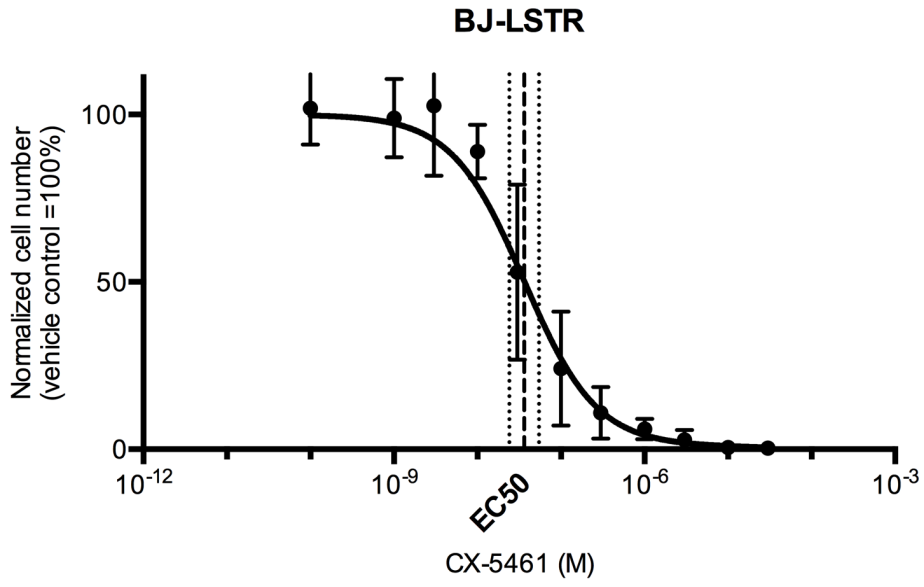
BJ-LSTR
Normalized cell number
(vehicle control =100%)
100
50
0
10^{-12}
10^{-9}
EC50
10^{-6}
10^{-3}
CX-5461 (M)

B)

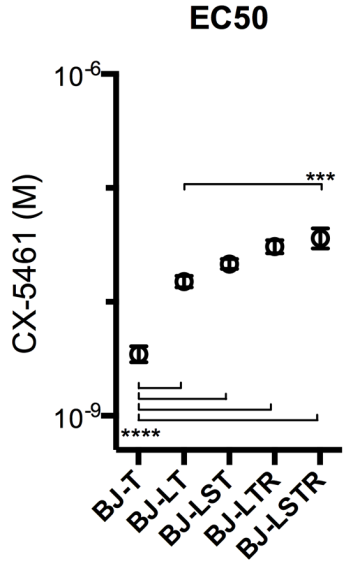
EC50
10^{-6}
10^{-9}
CX-5461 (M)
***
****
BJ-T
BJ-LT
BJ-LST
BJ-LTR
BJ-LSTR

C)

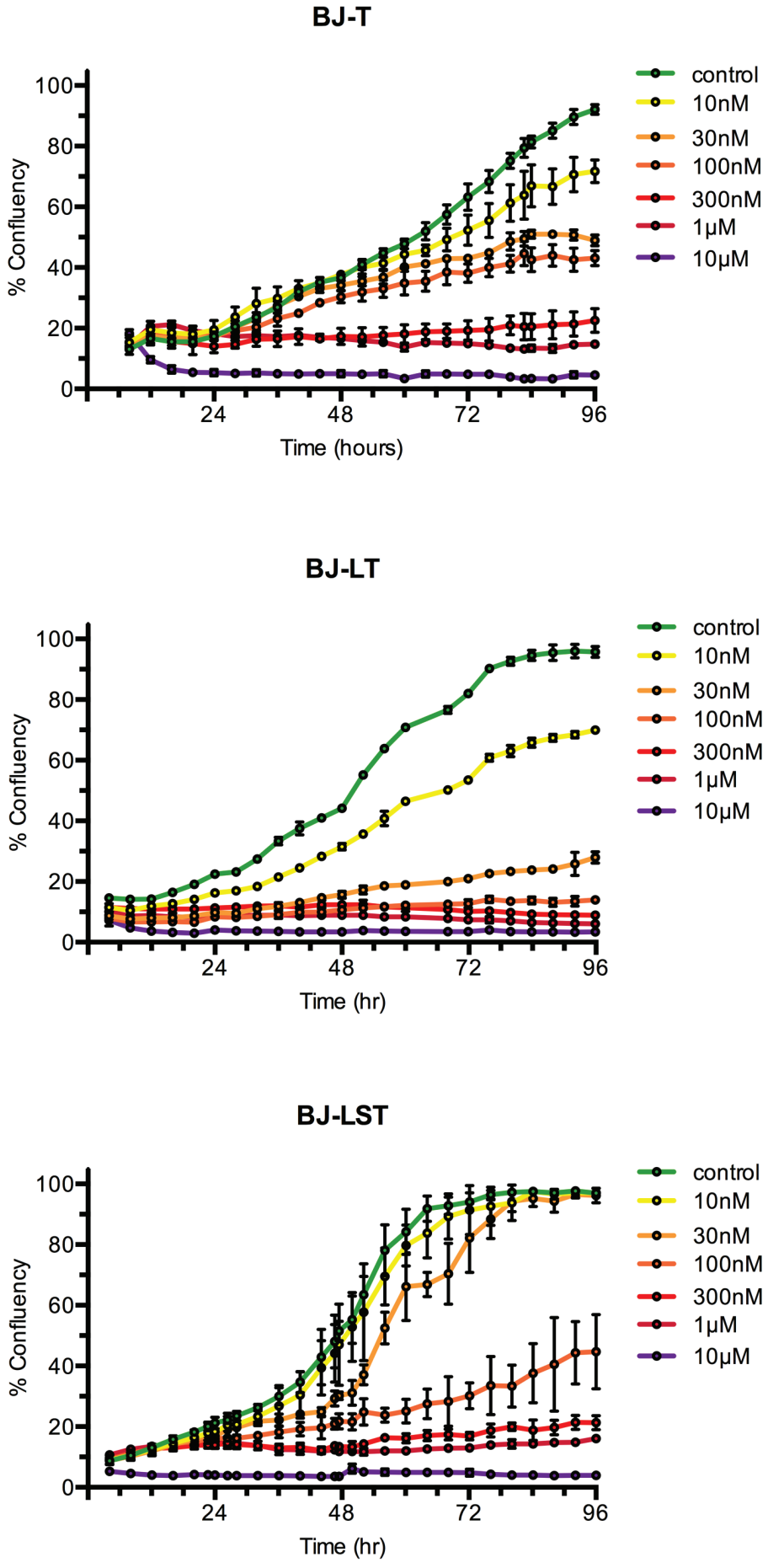
BJ-T
% Confluency
Time (hours)
control
10nM
30nM
100nM
300nM
1μM
10μM
BJ-LT
% Confluency
Time (hr)
control
10nM
30nM
100nM
300nM
1μM
10μM
BJ-LST
% Confluency
Time (hr)
control
10nM
30nM
100nM
300nM
1μM
10μM

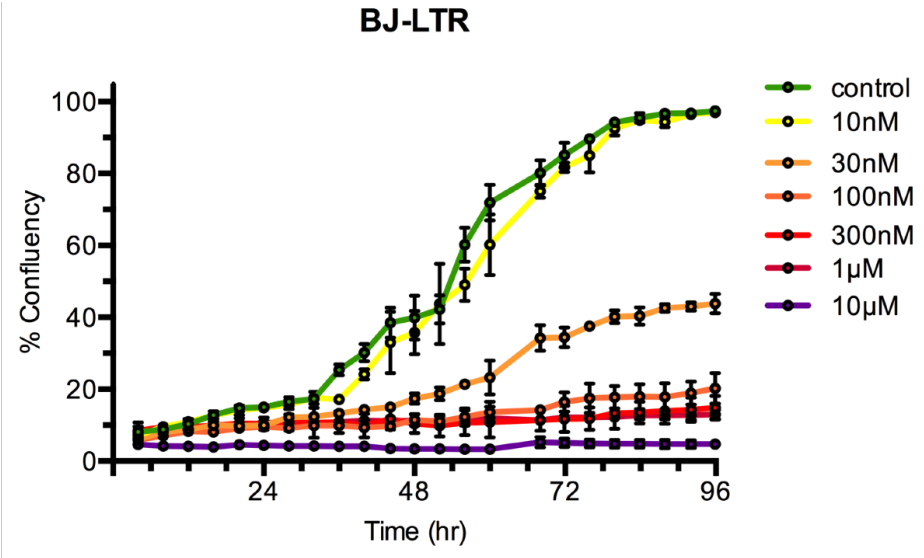
BJ-LTR
% Confluency
100
80
60
40
20
0
24
48
72
96
Time (hr)
control
10nM
30nM
100nM
300nM
1μM
10μM

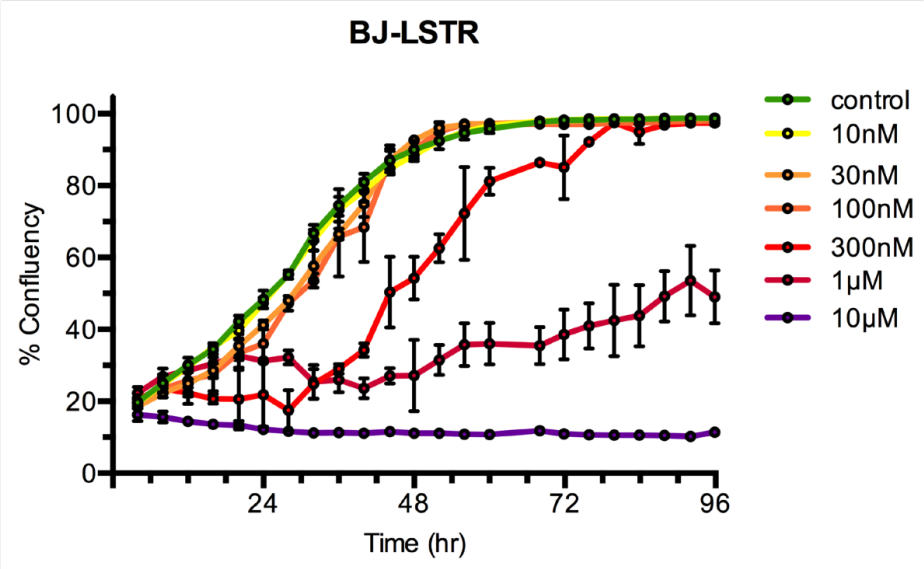
BJ-LSTR
% Confluency
100
80
60
40
20
0
24
48
72
96
Time (hr)
control
10nM
30nM
100nM
300nM
1μM
10μM

FIGURE 10. Inhibition of Pol I transcription by CX-5461 can induce different phenotypic responses in BJ isogenic cell lines. A) Analysis of % live cells by PI exclusion assay for BJ-T, BJ-LT, and BJ-LSTR cells treated with 10nM-10μM CX-5461 for 24hr (n=3, mean±SD). **B)** Analysis of % cell death PI uptake analysis for BJ-T, BJ-LT, and BJ-LSTR cells treated with vehicle control for 48hr or 1μM CX-5461 for 24hr, 48hr, and 72hr. (n=3-5, mean±SD). **C)** Analysis of % cell death by sub-G1 DNA content analysis of DNA fragmentation (left panel: n=3-5, mean±SD, *p<0.05 relative to vehicle control), and TMRE uptake analysis of mitochondrial membrane potential (right panel: n=2-3, mean±SD). **D-F)** Cell cycle analysis of BJ cell lines following treatment with vehicle control or 1μM CX-5461. Cells were incubated with BrdU for 30min in culture immediately prior to collection. Cells were stained for PI for DNA content (G1 and G2/M), and either BrdU incorporation for DNA replication (S-phase) or phos-H3 for mitotic cells (M). Upper panel: Representative cell cycle profiles of n=3 experiments. Lower panel: Quantitation of cell cycle populations in live cells using FCS express software. D) BJ-T cells (n=3, mean ± SD, ***p<0.0001, **p<0.005, and *p<0.05 relative to vehicle treated population). E) BJ-LT cells (n=3, mean ± SD). F) BJ-LSTR cells (n=3-5, mean ± SD, *p<0.05 relative to vehicle treated population).

FIGURE 10

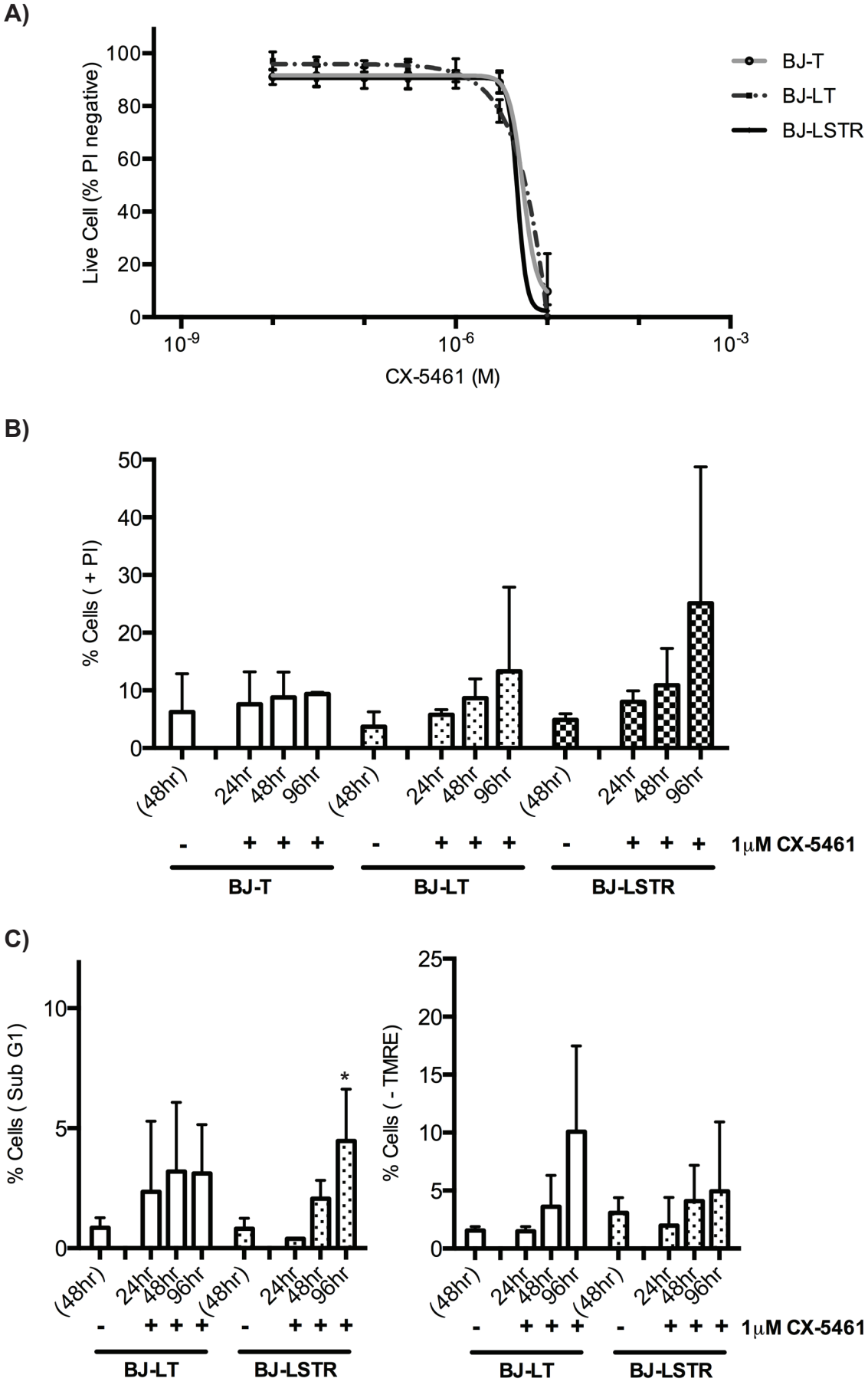
A)
Live Cell (% PI negative)
100
80
60
40
20
0
10^{-9}
10^{-6}
10^{-3}
CX-5461 (M)
BJ-T
BJ-LT
BJ-LSTR
B)
% Cells (+ PI)
50
40
30
20
10
0
(48hr)
24hr
48hr
96hr
- + + +
1μM CX-5461
BJ-T
BJ-LT
BJ-LSTR
C)
% Cells (Sub G1)
10
5
0
*
% Cells (- TMRE)
25
20
15
10
5
0
BJ-LT
BJ-LSTR

D)

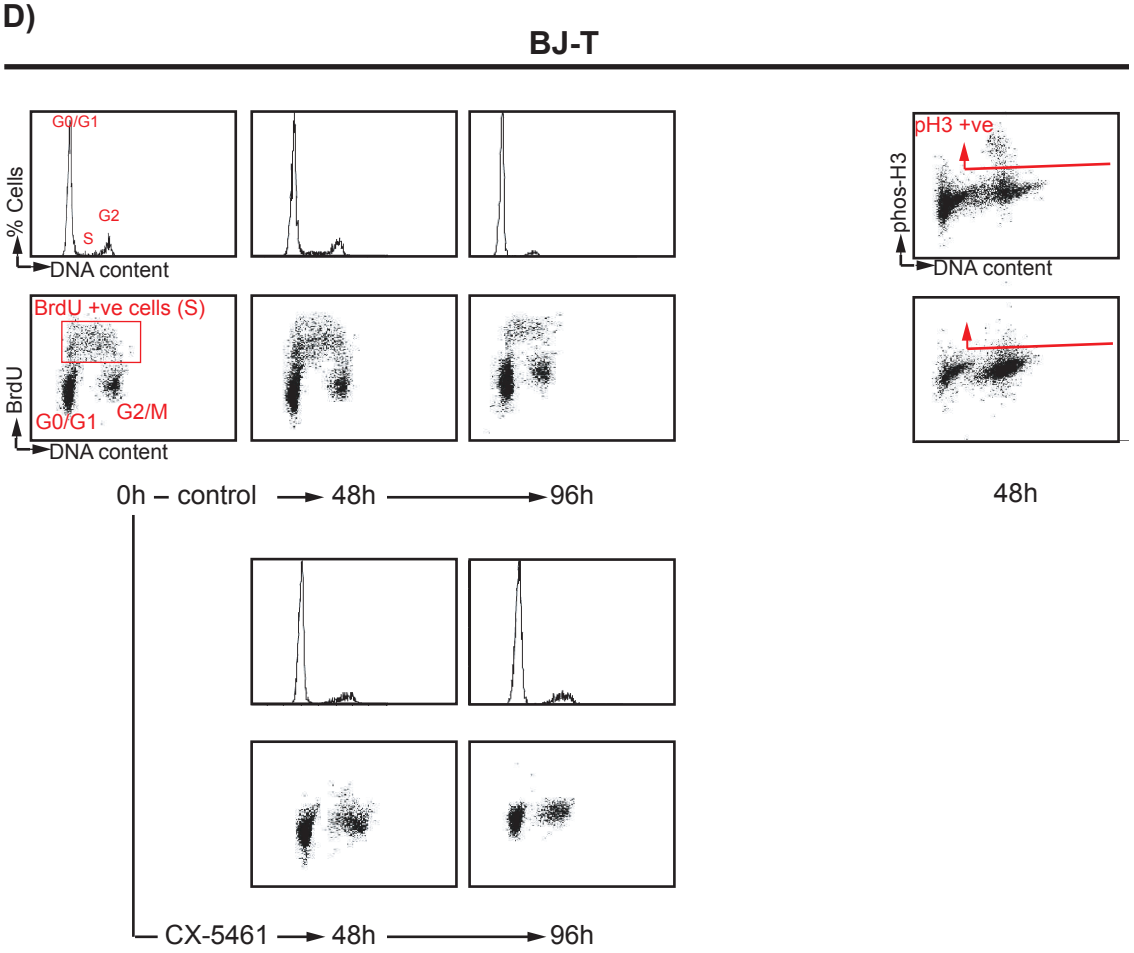
BJ-T
G0/G1
S
G2
% Cells
DNA content
BrdU +ve cells (S)
BrdU
G0/G1
G2/M
DNA content
pH3 +ve
phos-H3
DNA content
0h – control
48h
96h
48h
CX-5461
48h
96h

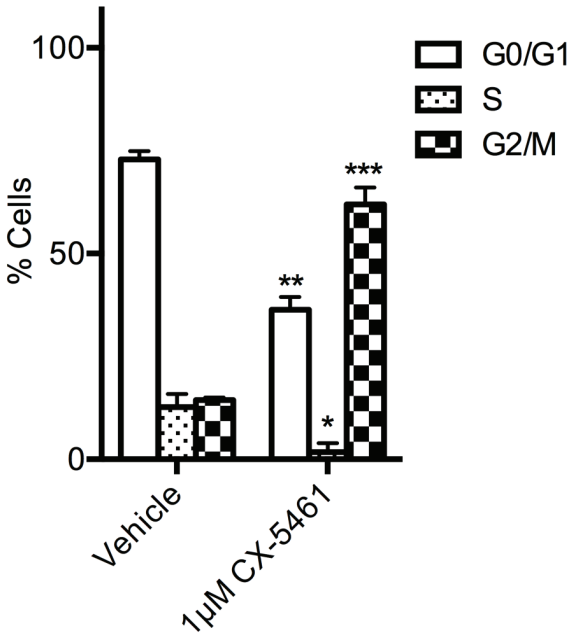
100
50
0
% Cells
G0/G1
S
G2/M
**
*
***
Vehicle
1μM CX-5461

E)

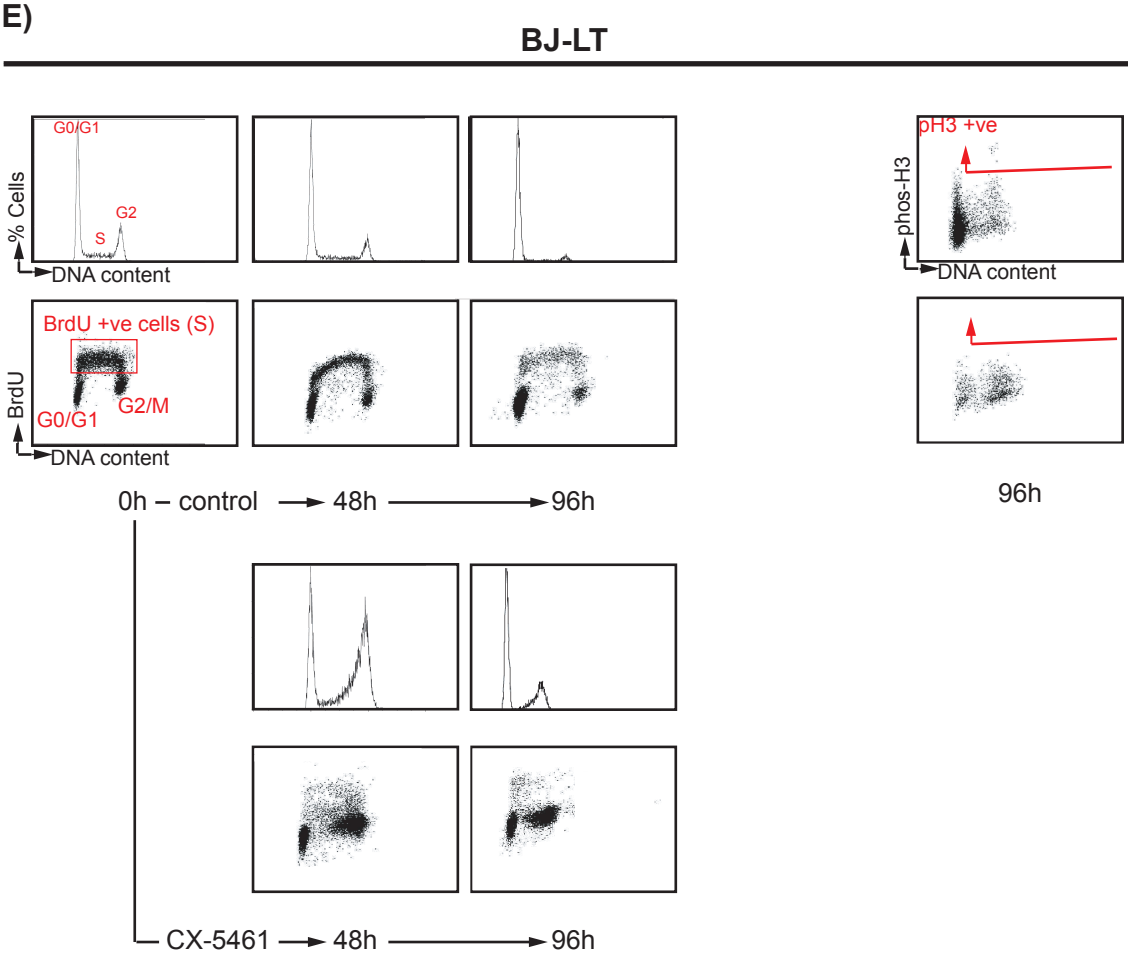
BJ-LT
G0/G1
G2
S
% Cells
DNA content
pH3 +ve
phos-H3
DNA content
BrdU +ve cells (S)
G0/G1
G2/M
BrdU
DNA content
96h
0h – control
48h
96h
CX-5461
48h
96h

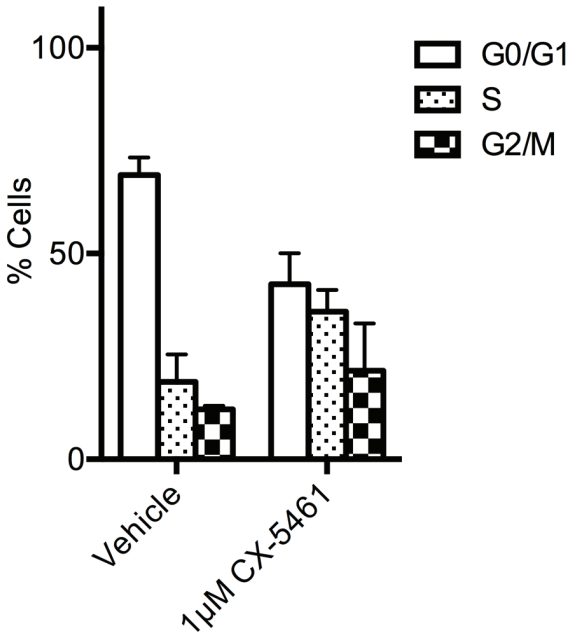
100
50
0
% Cells
G0/G1
S
G2/M
Vehicle
1μM CX-5461

F)

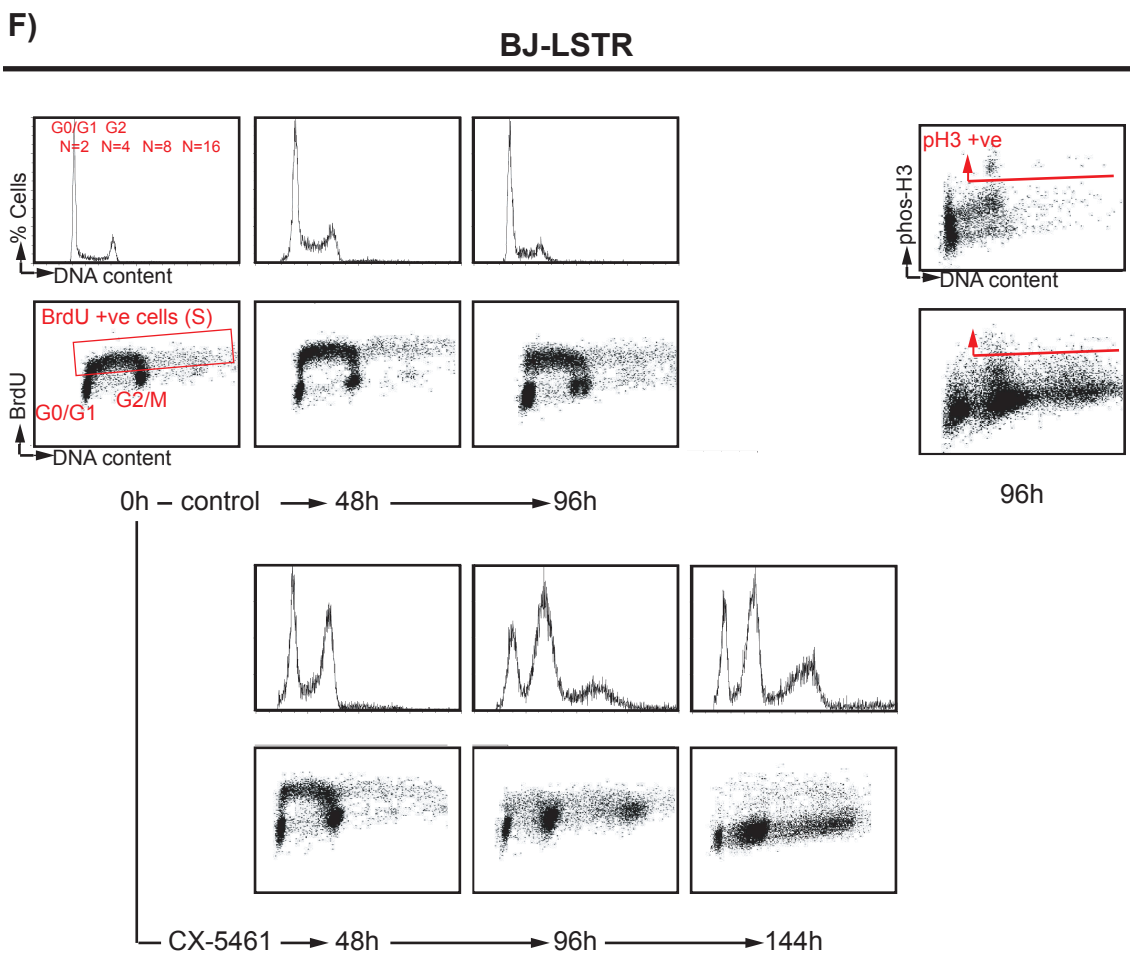
BJ-LSTR
G0/G1 G2
N=2 N=4 N=8 N=16
% Cells
DNA content
pH3 +ve
phos-H3
DNA content
BrdU +ve cells (S)
BrdU
G0/G1
G2/M
DNA content
0h – control
48h
96h
96h
CX-5461
48h
96h
144h

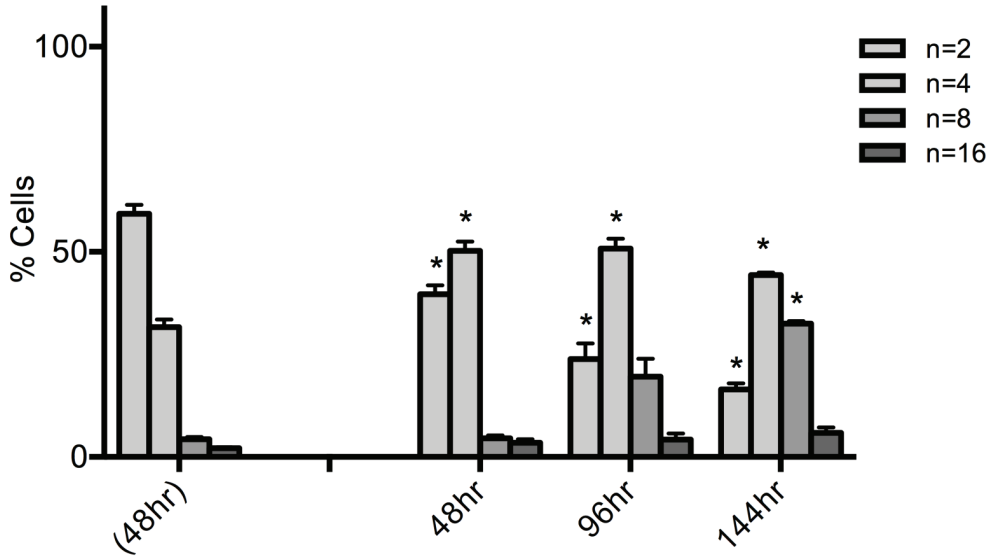
100
50
0
% Cells
n=2
n=4
n=8
n=16
(48hr)
48hr
96hr
144hr

FIGURE 11. Inhibition of Pol I transcription by CX-5461 induces multiple cell cycle defects in BJ-T cells. A) Cell cycle analysis of BJ-T cells following 0-24hr treatment with vehicle control or 1μM CX-5461. Cells were incubated with BrdU for 30min in culture immediately prior to collection. Cells were stained for BrdU incorporation for DNA replication (S-phase), and PI for DNA content (G1 and G2/M). Upper page: Representative cell cycle profiles of n=3 experiments. Lower page: Quantitation of cell cycle populations in live cells using FCS express software. (Left) all 6,12, 24 and 48hr populations (n=3, mean±sem). (Right) statistical analysis of 24hr and 48hr populations (n=3, mean ± SD, ***p<0.0005, **p<0.005, and *p<0.05 relative to vehicle treated population). **B)** Cell cycle analysis of BJ-T cells following 0-24hr treatment with vehicle control or 1μM CX-5461 in the constant presence of BrdU. Cells were stained for BrdU incorporation (for exit from G1 and progression through the cell cycle) and PI (for DNA content in G1 and G2/M). Upper panel: Representative cell cycle profiles of n=3 experiments. Lower panel: Quantitation of BrdU positive populations in live cells using FCS express software. (Left) BrdU positive populations from a n=1 representative experiment. (Right) BrdU positive populations following 24hr treatment with vehicle control or 1μM CX-5461 (n=3. mean±SD. **p<0.005 relative to 24hr vehicle control). **C)** Cell cycle analysis of BJ-T cells following 0-24hr treatment with vehicle control or 1μM CX-5461. Cells were incubated with BrdU for 30min in culture prior to treatment at t=0hr. Cells were stained for BrdU incorporation (for t=0hr S-phase population), and PI (for DNA content in G1 and G2/M). Representative cell cycle profiles of n=2 experiments. Upper panels show all cell populations (black). Lower panels show BrdU positive cell populations only (red boxes). **D)** Phos-H3 staining analysis of mitotic cells. Left panel: Cell cycle profiles showing phos-H3 positive populations in BJ-T cells treated with vehicle or 1μM CX-5461 for 24hr in the presence or absence of 50 μM nocodazole. Right panel: Quantitation of phos-H3 positive cells using FCS express software. (Top) n=1 experiment of BJ-T cells treated with vehicle or 1μM CX-5461 for 24hr in the presence or absence of 50 μM nocodazole. (Bottom). BJ-T cells treated with vehicle control or 1μM CX-5461 for 24hr and 48hr (n=4, mean±SD. *p<0.005 relative to 48hr vehicle control). **E)** Cell cycle profiles showing PI staining for DNA content (G1 and G2/M) in BJ-T cells treated with vehicle or 1μM CX-5461 for 48hr following synchronization in either G1 by 24hr culture in serum-free media (upper panel), or S-phase by 24hr culture in the presence of 2.5mM thymidine (lower panel) (n=1). **F)** Cell cycle analysis of BJ-T cells following inhibition of Pol I transcription by siRNA knock-down of POLR1A and RRN3. i) qRT-PCR analysis of expression of *POLR1A* and *RRN3* 48hr following transfection with siPOLR1A/siRRN3. Expression levels were normalized to *VIM* and expressed as fold

change relative to siEGFP transfected control (n=4, mean±sem ****p<0.0001 relative to siEGFP transfected control). ii) qRT-PCR analysis of transcription of 47S pre-RNA 48hr following transfection with siPOLR1A/siRRN3. Expression levels were normalized to *VIM* and expressed as fold change relative to siEGFP transfected control (n=4, mean±sem ****p<0.0001 relative to siEGFP transfected control). iii) Cell counts 48hr following transfection with siEGFP or siPOLR1A/siRRN3 (n=4, mean±sem, **p<0.005). iv) Quantitation of cell cycle analysis by PI staining for DNA content of BJ-T cells 48hr following transfection with siEGFP or siPOLR1A/siRRN3 (n=4, mean±sem).

FIGURE 11
A)

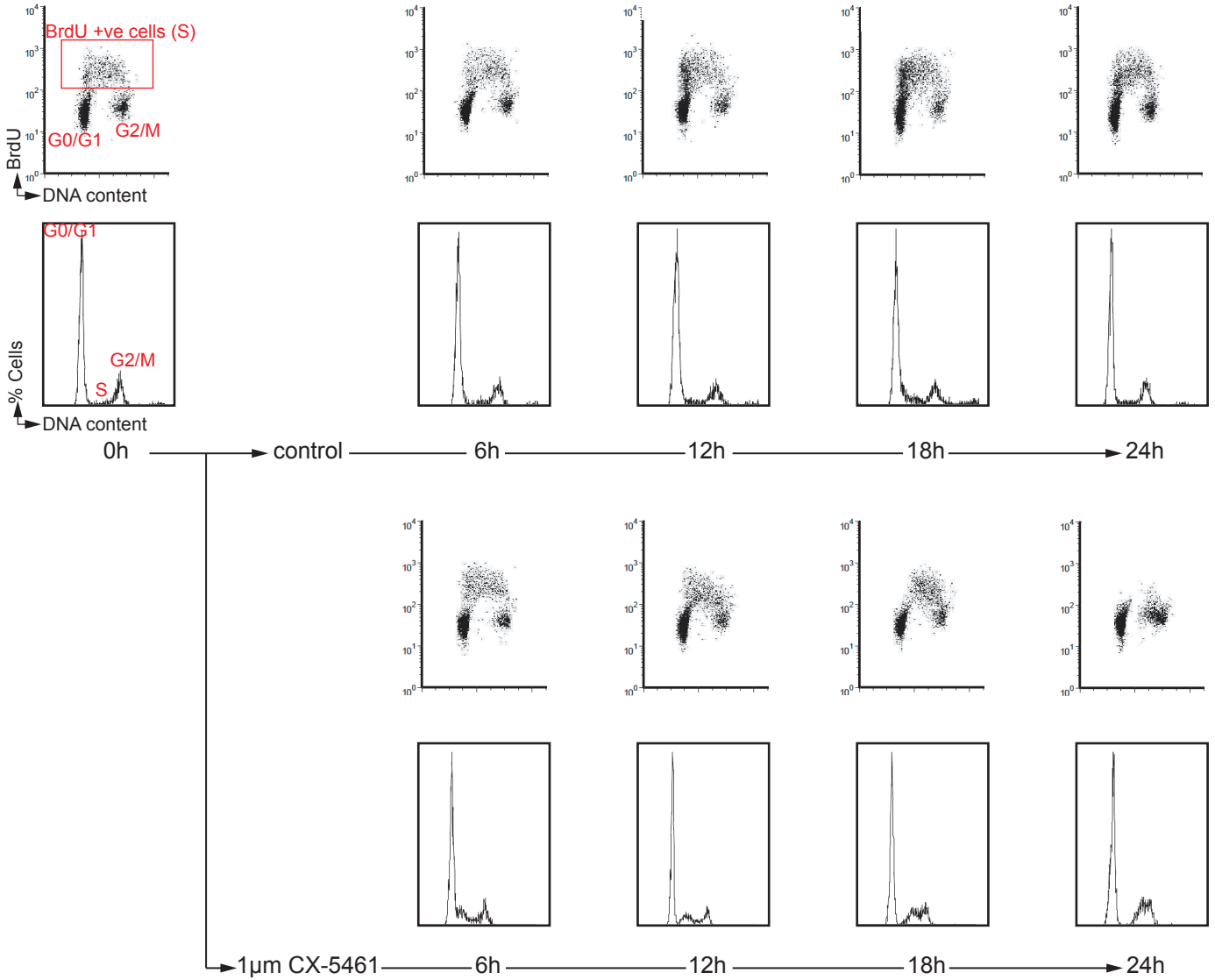
BrdU +ve cells (S)
G0/G1
G2/M
BrdU
DNA content
G0/G1
G2/M
S
% Cells
DNA content
0h
control
6h
12h
18h
24h
1µm CX-5461
6h
12h
18h
24h

B)

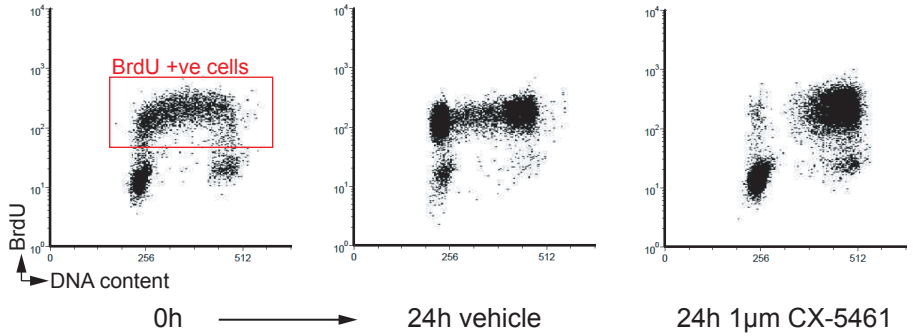
BrdU +ve cells
BrdU
DNA content
0h
24h vehicle
24h 1µm CX-5461

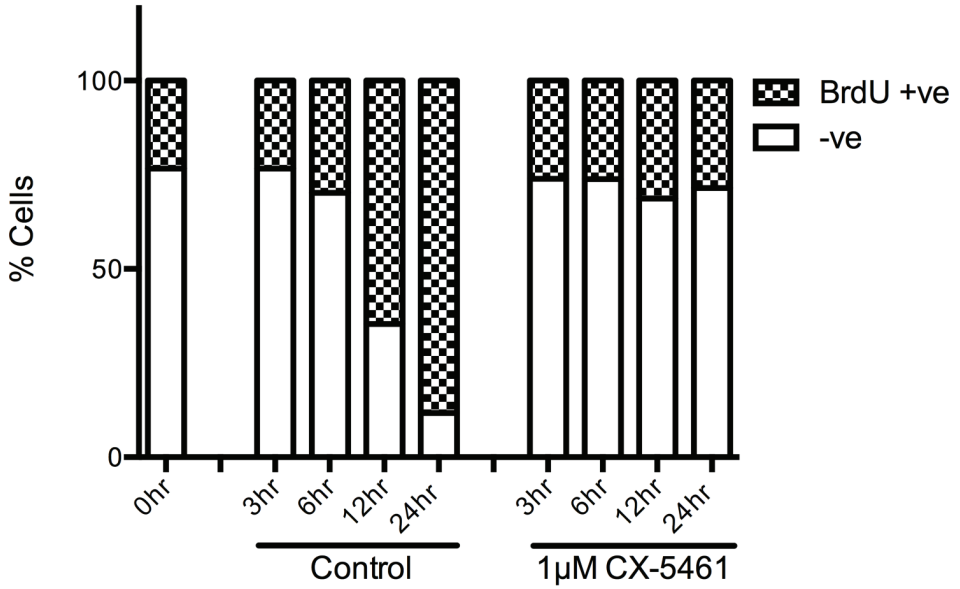
% Cells
100
50
0
BrdU +ve
-ve
0hr
3hr
6hr
12hr
24hr
3hr
6hr
12hr
24hr
Control
1µM CX-5461

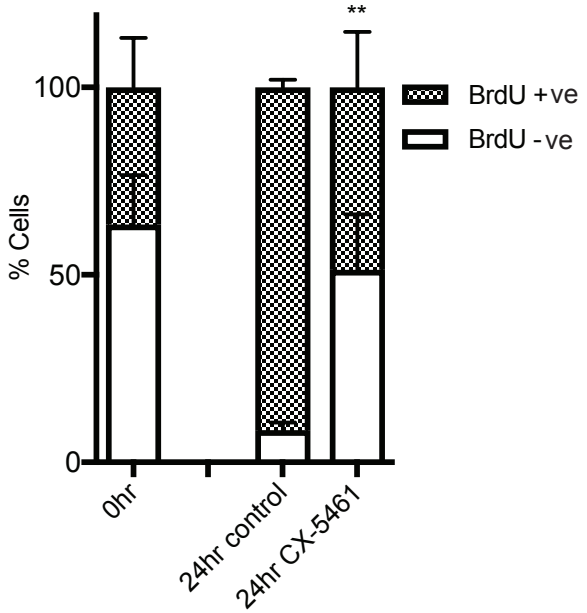
**
% Cells
100
50
0
BrdU +ve
BrdU -ve
0hr
24hr control
24hr CX-5461

C)

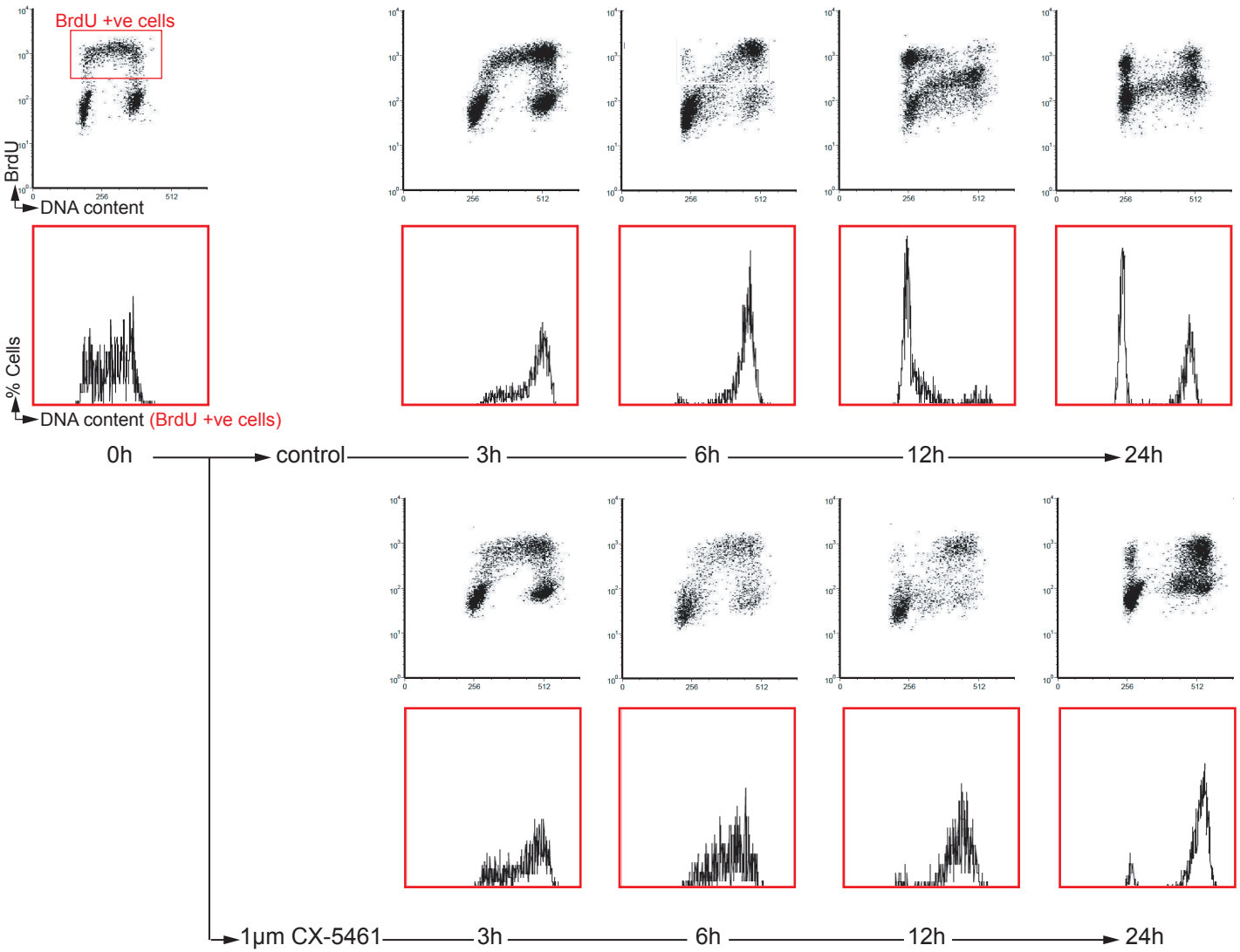
BrdU +ve cells
BrdU
DNA content
% Cells
DNA content (BrdU +ve cells)
0h
control
3h
6h
12h
24h
1µm CX-5461
3h
6h
12h
24h

D)

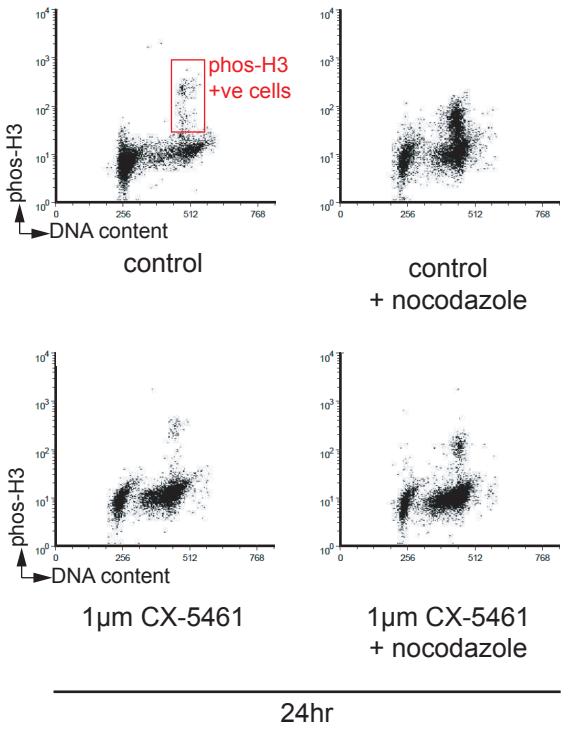
phos-H3
+ve cells
phos-H3
DNA content
control
control
+ nocodazole
phos-H3
DNA content
1µm CX-5461
1µm CX-5461
+ nocodazole
24hr

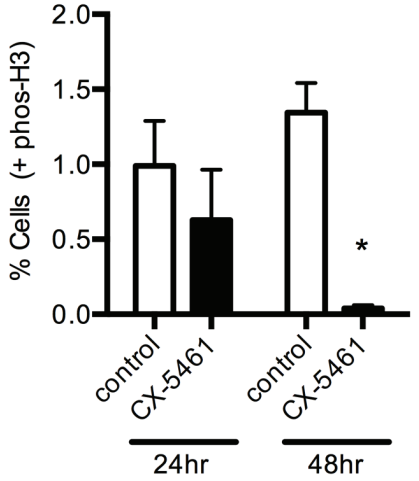
% Cells (+ phos-H3)
2.0
1.5
1.0
0.5
0.0
*
control
CX-5461
control
CX-5461
24hr
48hr

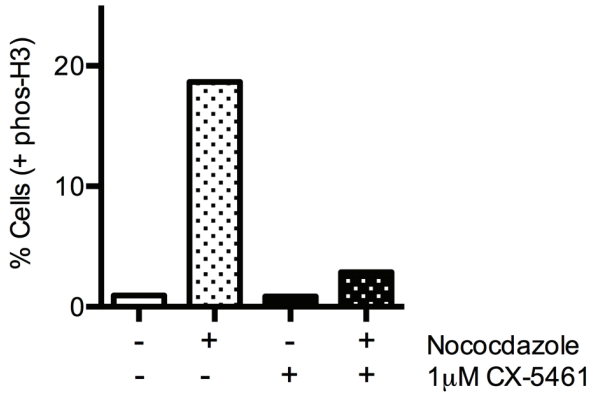
% Cells (+ phos-H3)
20
10
0
- + - +
- - + +
Nococdazole
1µM CX-5461

E)

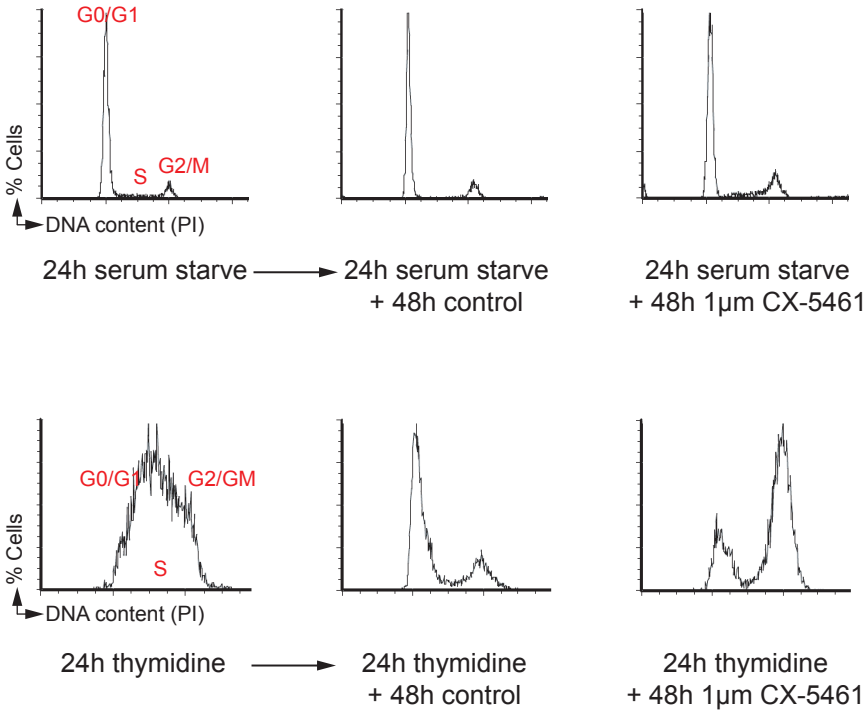
G0/G1
S
G2/M
% Cells
DNA content (PI)
24h serum starve
24h serum starve
+ 48h control
24h serum starve
+ 48h 1µm CX-5461
G0/G1
G2/GM
S
% Cells
DNA content (PI)
24h thymidine
24h thymidine
+ 48h control
24h thymidine
+ 48h 1µm CX-5461

F)

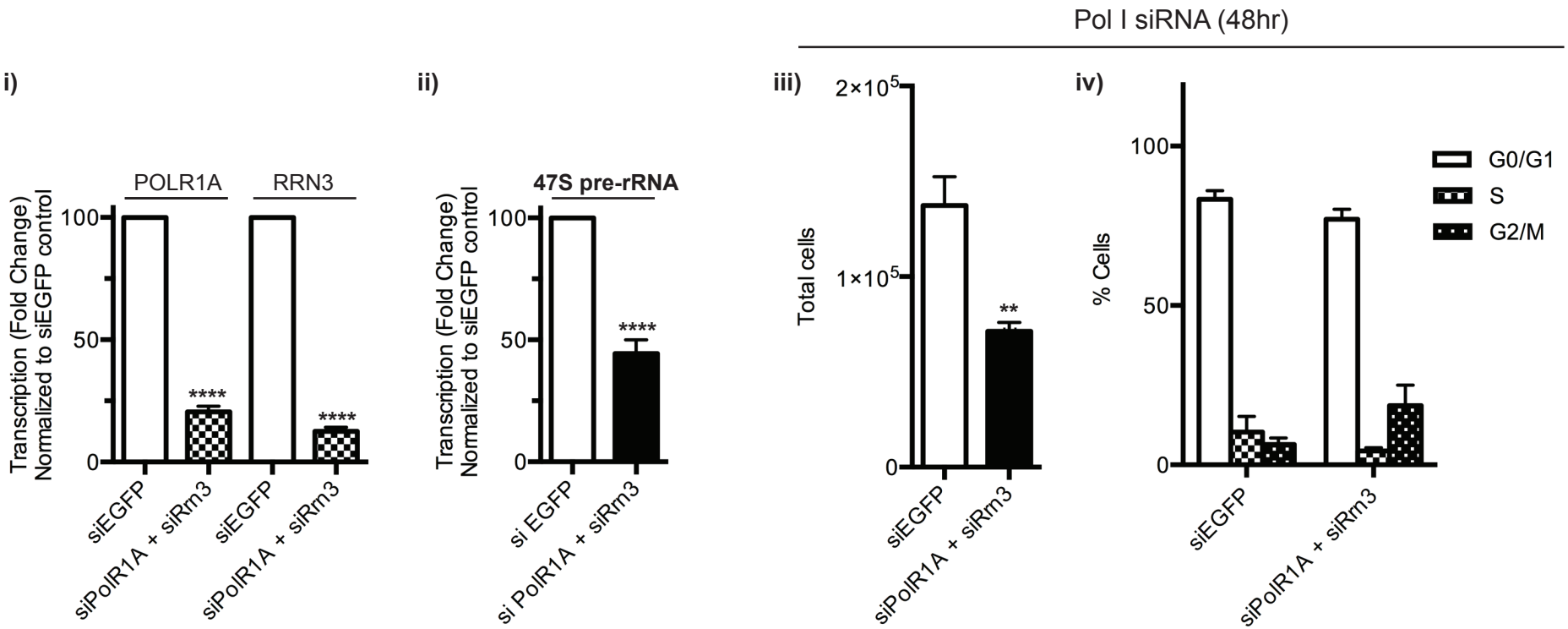
Pol I siRNA (48hr)
i)
POLR1A
RRN3
Transcription (Fold Change)
Normalized to siEGFP control
100
50
0
****
****
siEGFP
siPolR1A + siRrn3
siEGFP
siPolR1A + siRrn3
ii)
47S pre-rRNA
Transcription (Fold Change)
Normalized to siEGFP control
100
50
0
****
si EGFP
si PolR1A + siRrn3
iii)
Total cells
2×10^5
1×10^5
0
**
siEGFP
siPolR1A + siRrn3
iv)
% Cells
100
50
0
G0/G1
S
G2/M
siEGFP
siPolR1A + siRrn3

FIGURE 12. Inhibition of Pol I transcription by CX-5461 induces senescence in BJ-T cells. A) Histochemical analysis of SA-β-gal activity in BJ-T cells following 96hr treatment with 1μM CX-5461. Upper panel: Quantitation of SA-β-gal positive cells for n=4 experiments (mean±sem. ****p<0.0001 relative to vehicle control). Lower panel: representative images of histochemical staining for SA-β-gal positive cells (X-gal cytochemical staining for SA-β-gal activity, and DAPI staining for DNA to identify single cell nuclei). **B)** Immunofluorescence analysis of γH2A.X in BJ-T cells following 96hr treatment with 1μM CX-5461. Upper panel: Quantitation of γH2A.X positive cells for n=4 experiments (n=3, mean±sem. **p<0.005 relative to vehicle control). Lower panel: representative images of immunofluorescent staining for γH2A.X (green), with DAPI staining for DNA to identify single cell nuclei (blue). **C)** Cell volume analysis of BJ-T cells following 24hr treatment with 1μM CX-5461. Cell volume was measured on a Z2 AccuComp. (n=4, mean±sem. *p<0.05 relative to 24hr vehicle control). **D)** Western blot analysis of p53, p21, RB (hypo-phosphorylated active pRB and hyper-phosphorylated inactive ppRB), $p16^{INK4A}$ and tubulin levels in BJ-T cells treated with 1μM CX-5461 for 24hr (representative blots of n=4 experiments).

FIGURE 12
A)

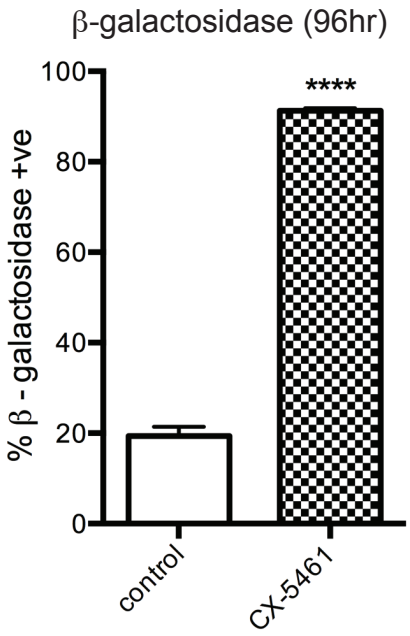
β-galactosidase (96hr)
% β - galactosidase +ve
100
80
60
40
20
0
****
control
CX-5461

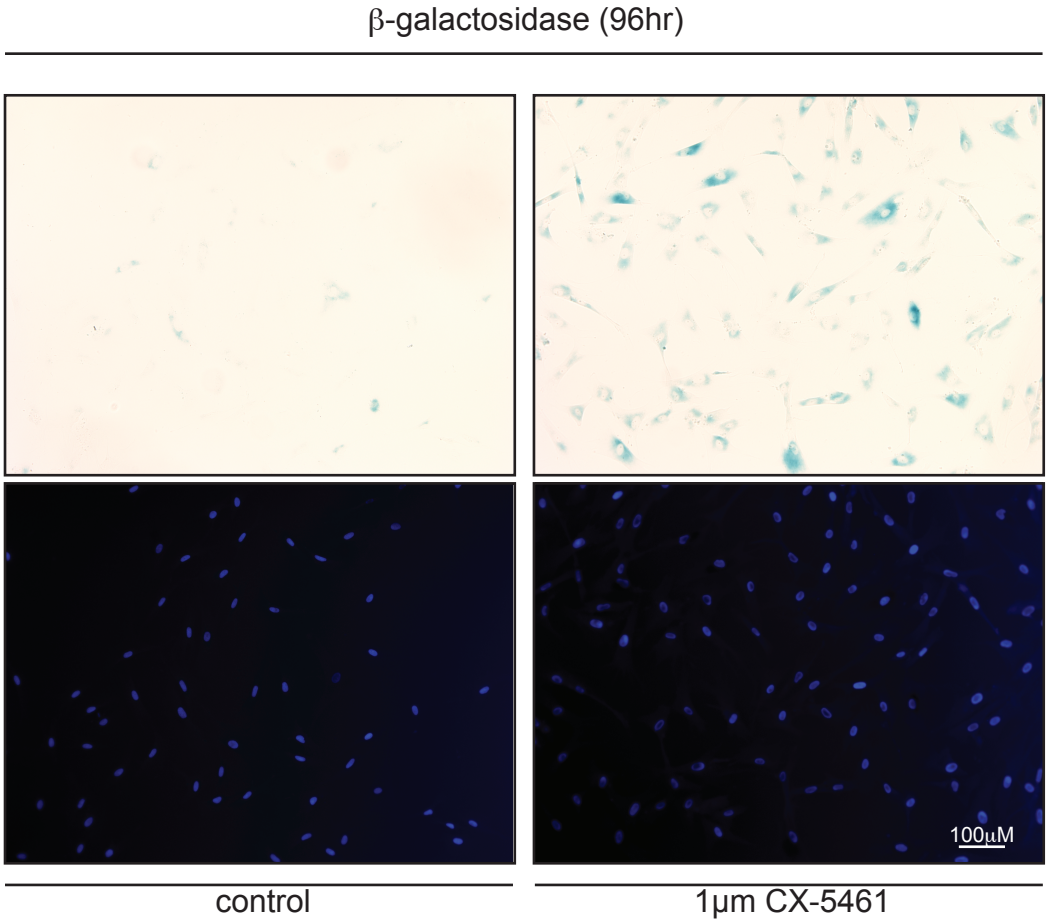
β-galactosidase (96hr)
100μM
control
1μm CX-5461

B)

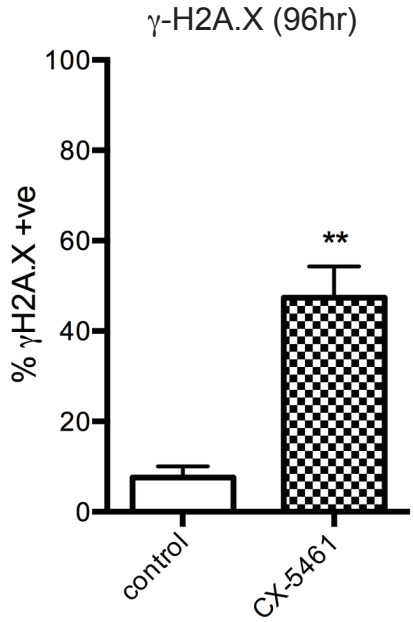
γ-H2A.X (96hr)
% γH2A.X +ve
100
80
60
40
20
0
**
control
CX-5461

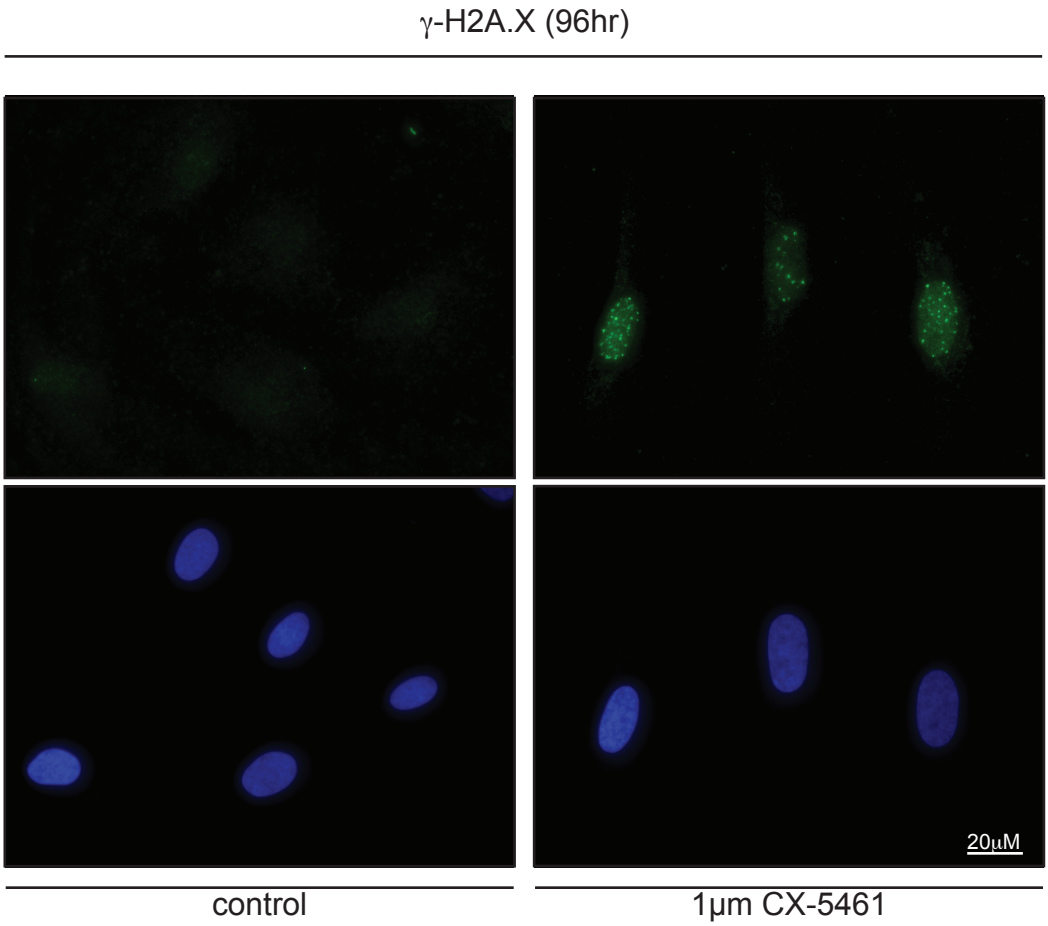
γ-H2A.X (96hr)
20μM
control
1μm CX-5461

C)

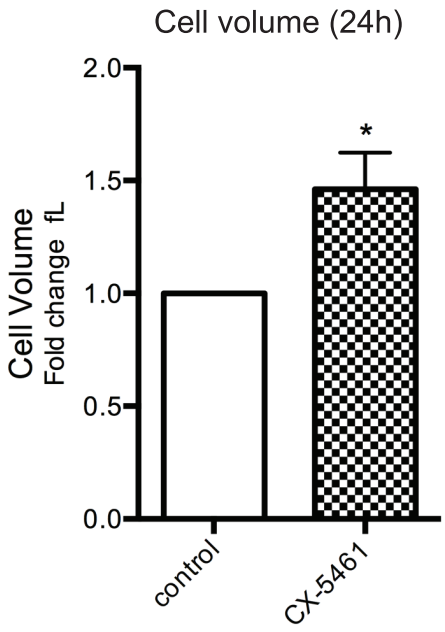
Cell volume (24h)
Cell Volume
Fold change fL
2.0
1.5
1.0
0.5
0.0
*
control
CX-5461

D)

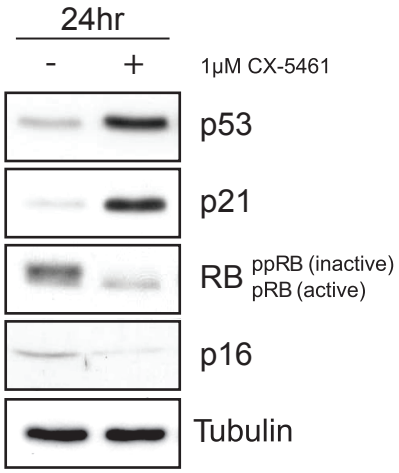
24hr
-
+
1μM CX-5461
p53
p21
RB
ppRB (inactive)
pRB (active)
p16
Tubulin

FIGURE 13. Inhibition of Pol I transcription by CX-5461 induces a p53-independent proliferation defect in BJ-T cells. A) Western blot analysis of total p53, p21 and tubulin levels in BJ-T cells treated with 1μM CX-5461 for a time course of 1hr-24hr (top) and 10min-3hr (bottom) (representative of n=3). **B)** Western blot analysis of total p53, p21 and tubulin levels in BJ-T cells stably transfected with pRS vectors expressing scramble- or p53-shRNA, following 24hr treatment with vehicle control or 1μM CX-5461. **C)** Dose-response cell proliferation assays for BJ-T (green) and BJ-T p53shRNA (red) cells treated with vehicle control or 1μM CX-5461 from 0hr to 96hr. Cell proliferation is determined by % confluency of live cells in culture measured using an IncuCyte Zoom (Essen Biosciences). (representative experiment of n=6, mean±SD of technical replicates).

FIGURE 13
A)

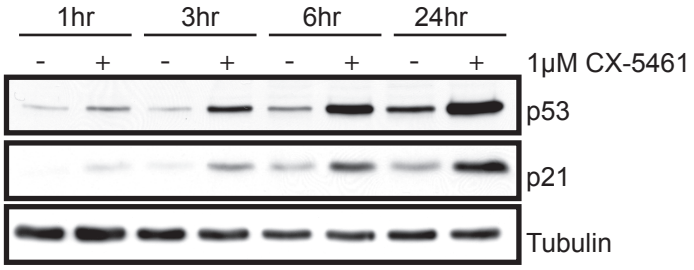
1hr
3hr
6hr
24hr
- + - + - + - +
1μM CX-5461
p53
p21
Tubulin

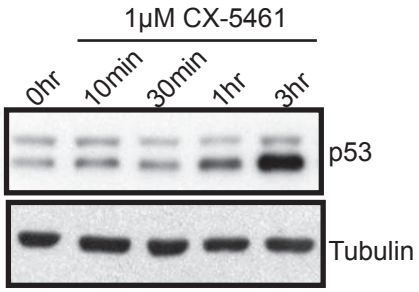
1μM CX-5461
0hr
10min
30min
1hr
3hr
p53
Tubulin

B)

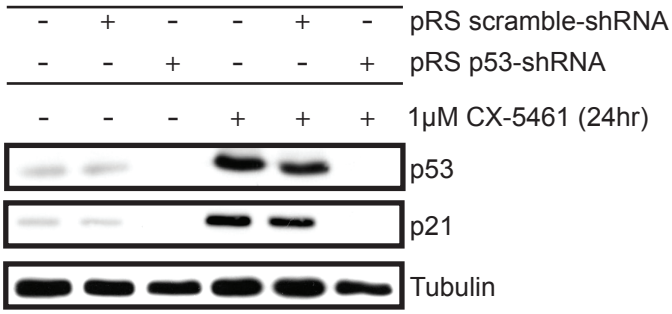
- + - - + - pRS scramble-shRNA
- - + - - + pRS p53-shRNA
- - - + + + 1μM CX-5461 (24hr)
p53
p21
Tubulin

C)

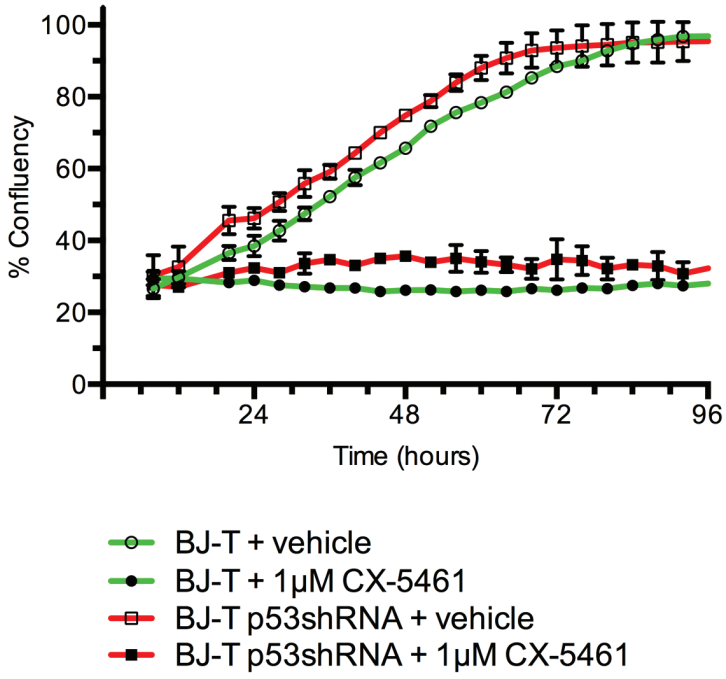
100
80
60
40
20
0
% Confluency
24
48
72
96
Time (hours)
BJ-T + vehicle
BJ-T + 1μM CX-5461
BJ-T p53shRNA + vehicle
BJ-T p53shRNA + 1μM CX-5461

FIGURE 14. Inhibition of Pol I transcription by CX-5461 induces p53-independent cell cycle defects in BJ-T p53shRNA cells. A) Cell cycle analysis of BJ-T p53shRNA cells following 0-24hr treatment with vehicle control or 1μM CX-5461. Cells were incubated with BrdU for 30min in culture immediately prior to collection. Cells were stained for BrdU incorporation for DNA replication (S-phase), and PI for DNA content (G1 and G2/M). Upper page: Representative cell cycle profiles of n=3 experiments. Lower page: Quantitation of cell cycle populations in live cells using FCS express software. (Left) all 6, 12, 24, and 48hr populations (n=3, mean±sem). (Right) statistical analysis of 24hr and 48hr populations (n=3, mean ± SD, ****$p<0.0001$, **$p<0.005$, and *$p<0.05$ relative to vehicle control population). **B)** Cell cycle analysis of BJ-T p53shRNA cells following 0-24hr treatment with vehicle control or 1μM CX-5461 in the constant presence of BrdU. Cells were stained for BrdU incorporation (for exit from G1 and progression through the cell cycle) and PI (for DNA content in G1 and G2/M). Upper panel: Representative cell cycle profiles of n=2 experiments. Lower panel: Quantitation of BrdU positive populations in live cells using FCS express software. (Left) BrdU positive populations from a n=1 representative experiment. (Right) BrdU positive populations following 24hr treatment with vehicle control or 1μM CX-5461 (n=2. mean±sem). **C)** Cell cycle analysis of BJ-T p53shRNA cells following 0-24hr treatment with vehicle control or 1μM CX-5461. Cells were incubated with BrdU for 30min in culture prior to treatment at t=0hr. Cells were stained for BrdU incorporation (for t=0hr S-phase population), and PI (for DNA content in G1 and G2/M). Representative cell cycle profiles of n=3 experiments. Upper panels show all cell populations (black). Lower panels show BrdU positive cell populations only (red boxes). **D)** Phos-H3 staining analysis of mitotic cells. Left panel: Cell cycle profiles showing phos-H3 positive populations in p53shRNA cells treated with vehicle or 1μM CX-5461 for 24hr in the presence or absence of 50 μM nocodazole (representative of n=2). Right panel: Quantitation of phos-H3 positive cells using FCS express software. (Top) BJ-T cells treated with vehicle control or 1μM CX-5461 for 24hr and 48hr (n=5, mean±SD). (Bottom). BJ-T cells treated with vehicle or 1μM CX-5461 for 24hr in the presence or absence of 50μM nocodazole (n=2 mean±sem).

FIGURE 14
A)

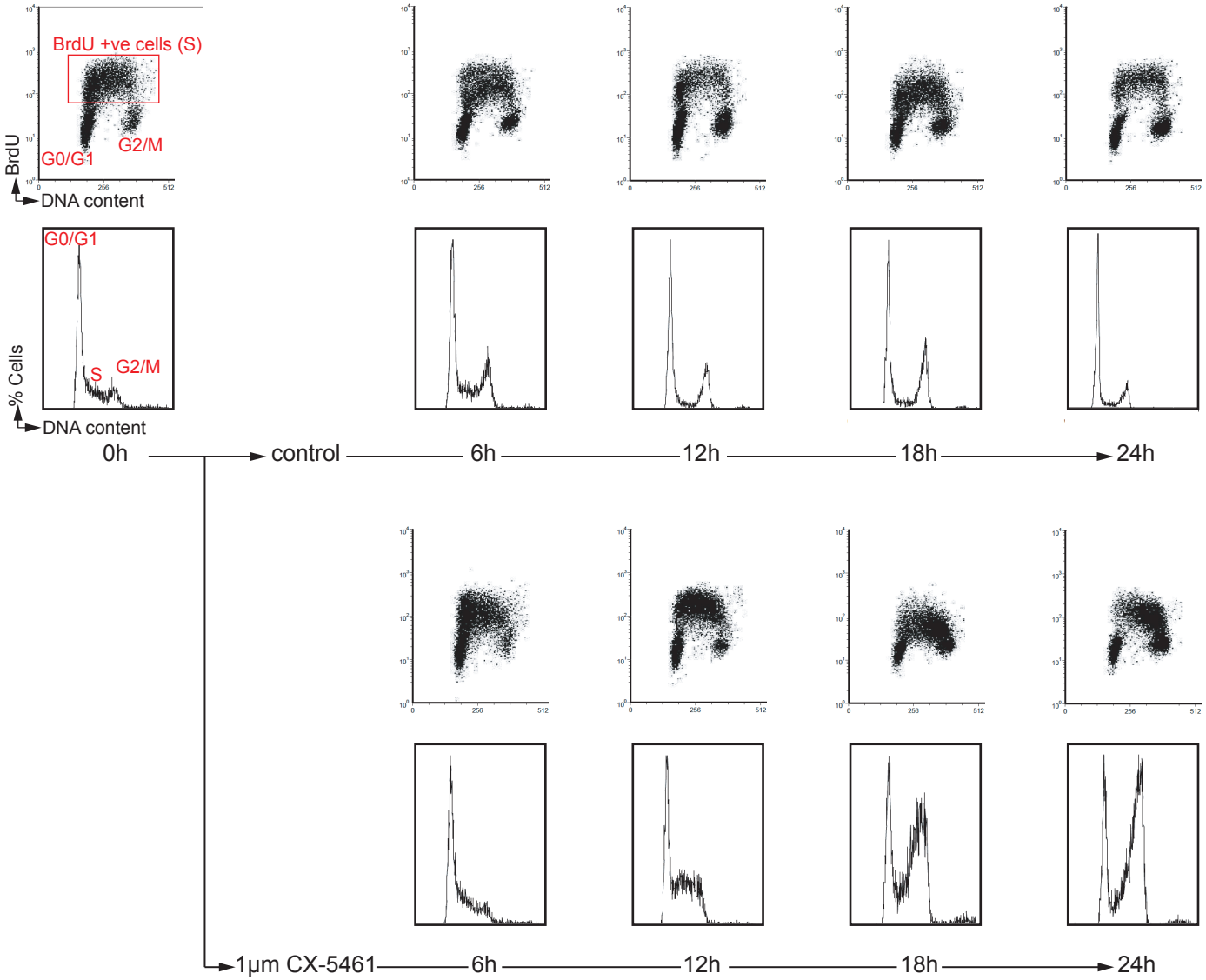
BrdU +ve cells (S)
G0/G1
G2/M
BrdU
DNA content
G0/G1
S
G2/M
% Cells
DNA content
0h
control
6h
12h
18h
24h
1µm CX-5461
6h
12h
18h
24h

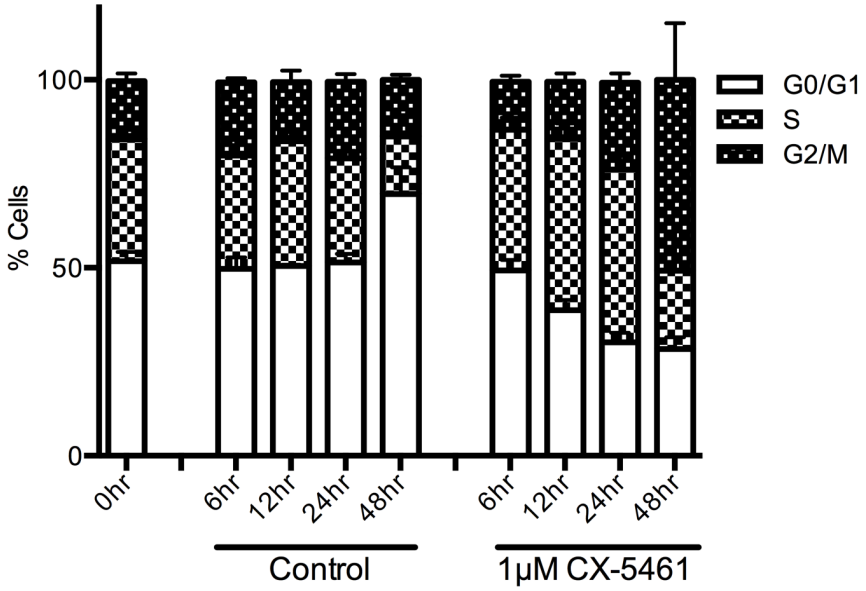
100
50
0
% Cells
G0/G1
S
G2/M
0hr
6hr
12hr
24hr
48hr
6hr
12hr
24hr
48hr
Control
1μM CX-5461

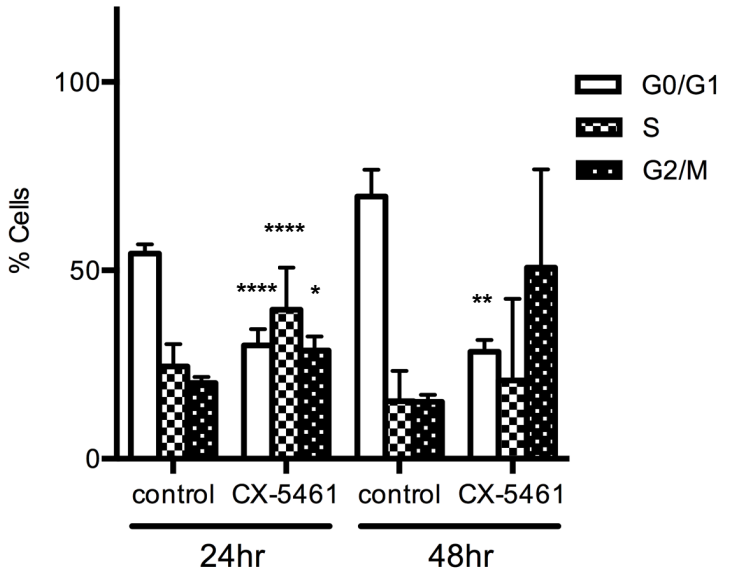
100
50
0
% Cells
G0/G1
S
G2/M
****
****
*
**
control
CX-5461
control
CX-5461
24hr
48hr

B)

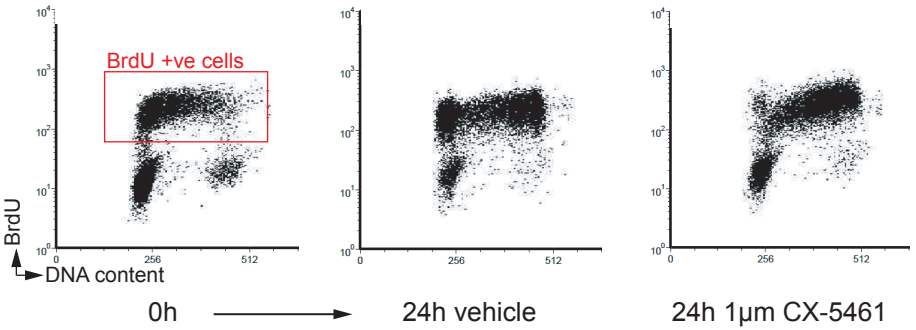
BrdU +ve cells
BrdU
DNA content
0h
24h vehicle
24h 1µm CX-5461

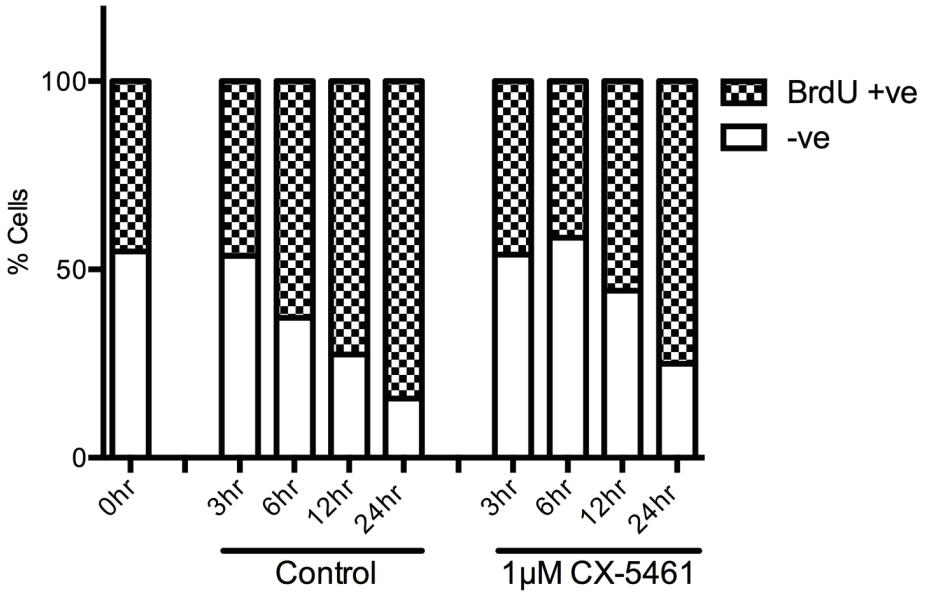
% Cells
100
50
0
BrdU +ve
-ve
0hr
3hr
6hr
12hr
24hr
3hr
6hr
12hr
24hr
Control
1µM CX-5461

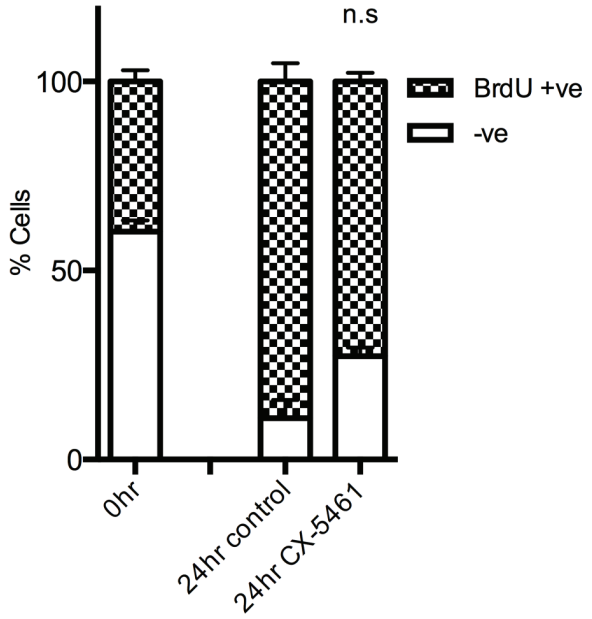
n.s
% Cells
100
50
0
BrdU +ve
-ve
0hr
24hr control
24hr CX-5461

C)

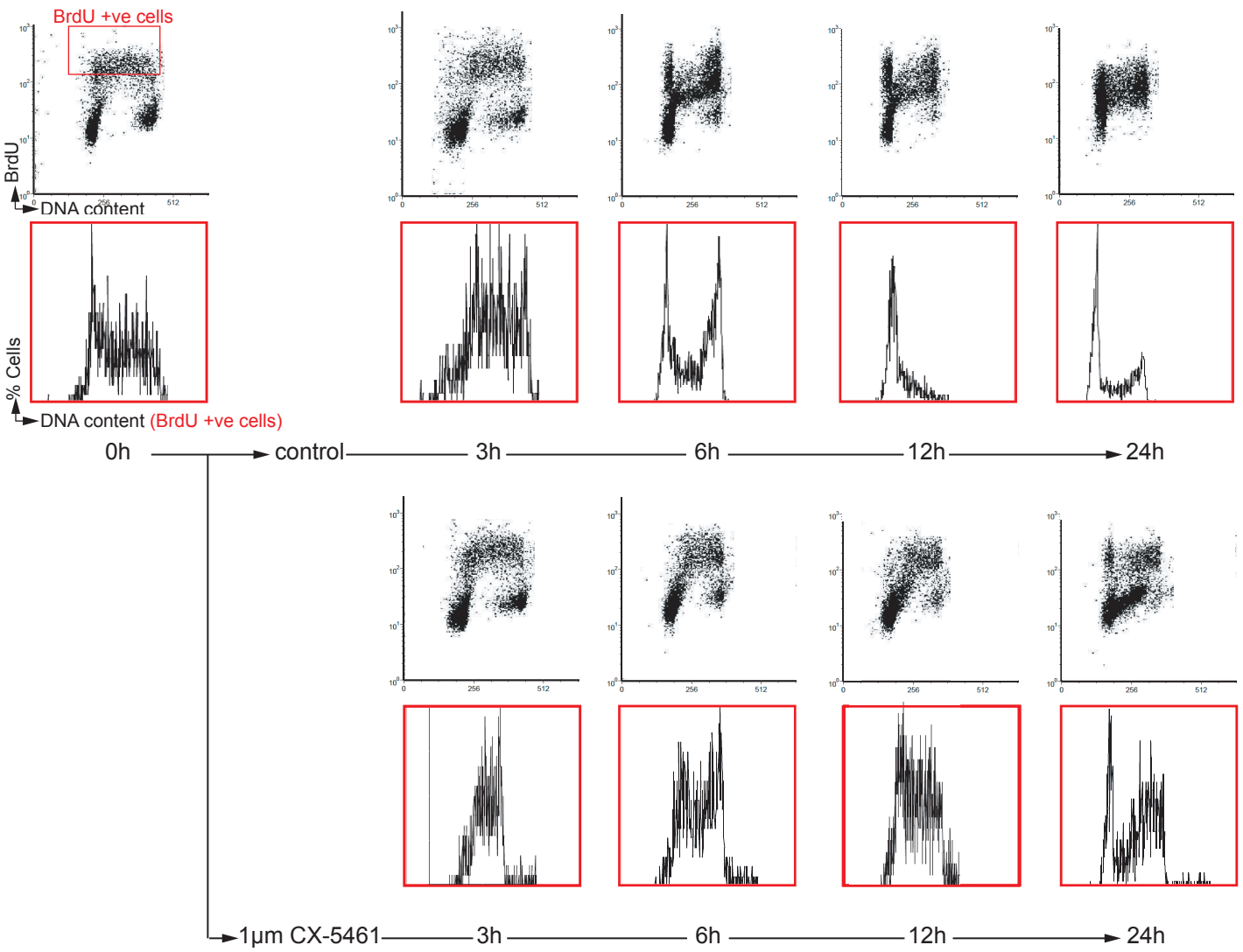
BrdU +ve cells
BrdU
DNA content
% Cells
DNA content (BrdU +ve cells)
0h
control
3h
6h
12h
24h
1µm CX-5461
3h
6h
12h
24h

D)

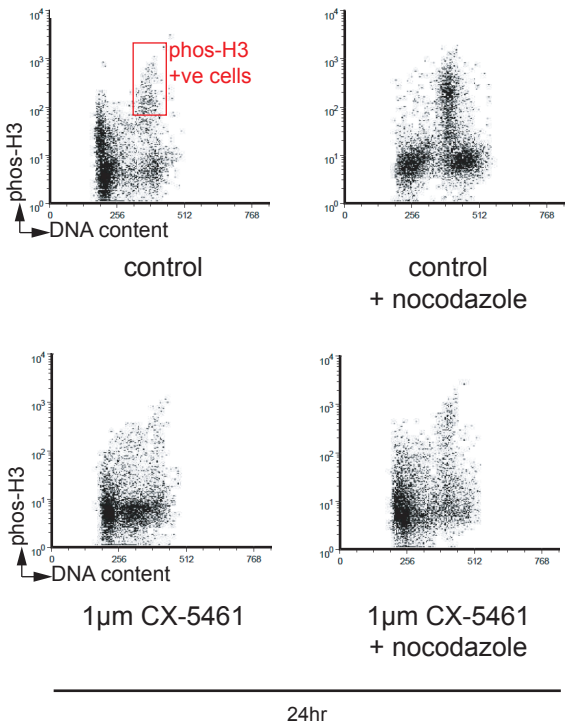
phos-H3
+ve cells
phos-H3
DNA content
control
control
+ nocodazole
phos-H3
DNA content
1µm CX-5461
1µm CX-5461
+ nocodazole
24hr

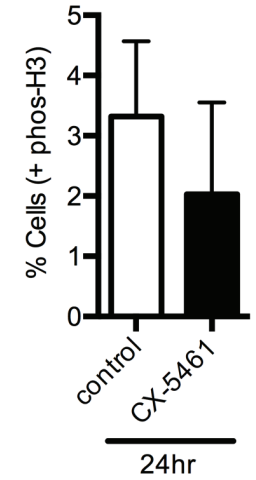
% Cells (+ phos-H3)
control
CX-5461
24hr

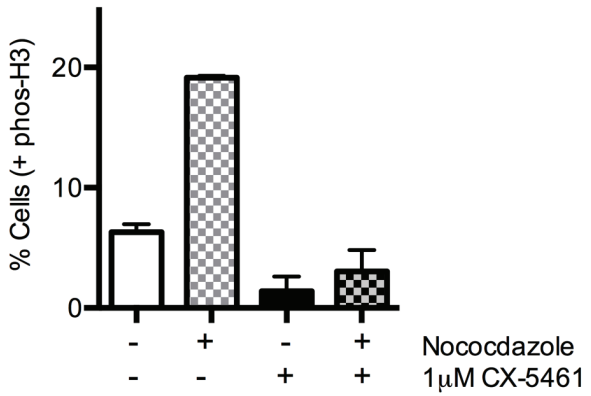
% Cells (+ phos-H3)
Nococdazole
1µM CX-5461

FIGURE 15. Inhibition of Pol I transcription by CX-5461 induces senescence in BJ-T p53shRNA cells. Histochemical analysis of SA-β-gal activity in BJ-T p53shRNA cells following 96hr treatment with 1μM CX-5461. Upper panel: Quantitation of SA-β-gal positive cells for n=3 experiments (mean±sem. *$p<0.05$ relative to vehicle control). Lower panel: representative images of histochemical staining for SA-β-gal positive cells (X-gal cytochemical staining for SA-β-gal activity, and DAPI staining for DNA to identify single cell nuclei).

FIGURE 15

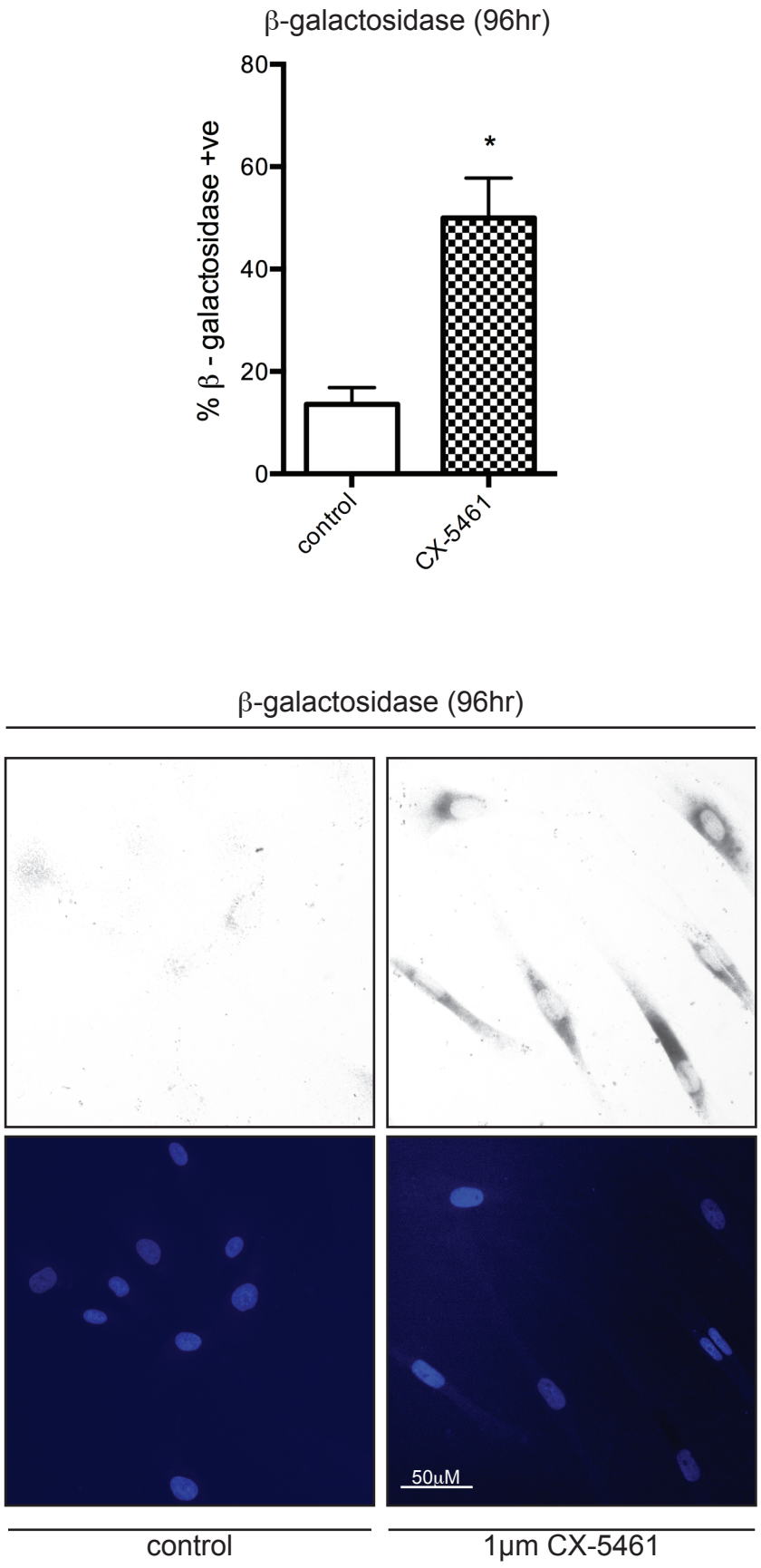
β-galactosidase (96hr)
% β - galactosidase +ve
80
60
40
20
0
*
control
CX-5461
β-galactosidase (96hr)
50μM
control
1μm CX-5461

CHAPTER 4. RNA-SEQUENCING ANALYSIS TO IDENTIFY p53-INDEPENDENT RESPONSES TO INHIBITION OF POL I TRANSCRIPTION.

4.1 Introduction.

While the best characterised nucleolar stress signaling pathway involves activation of p53 (See Section 1.2.1), numerous reports have shown that the nucleoli can mediate cell growth and stress signaling by additional mechanisms (See Section 1.2.2). In cells where p53 is not active, inhibition of Pol I transcription can result in diverse phenotypes, from undisturbed proliferation, to cell cycle arrest, or cell death (Reviewed in (Holmberg Olausson et al., 2012; Donati et al., 2011c)). However, these studies have largely been performed in diverse, tumorigenic human cell lines. This makes it difficult to determine the key pathways that drive cellular response to inhibition of Pol I transcription independently of p53.

Importantly, p53-independent pathways can mediate therapeutic response to inhibition of Pol I transcription. In a panel of transformed human cell lines tested for sensitivity to CX-5461, CX-5461 exhibited a broad range of anti-proliferative activity against cancer cell lines, with a median EC_{50} of 147nM in the 50 cell lines tested (compared to a median EC_{50} of approximately 5μM in 5 non-tumorigenic cell lines). There was no correlation between p53 status and sensitivity to CX-5461 across the panel, with p53 mutant cells having a similar median EC_{50} as p53 wild-type cells (Drygin et al., 2011). This indicates that inhibition of Pol I transcription has anti-proliferative effects on cancer cells independently of p53, and that additional pathways must confer the therapeutic response.

At the time my thesis was undertaken, genome-wide analysis had not previously been performed to identify p53-independent pathways activated in response to inhibition of Pol I transcription. We have previously reported gene expression data in both A375 p53-wild type melanoma and MIA PaCa-2 p53-mutant pancreatic cancer cell lines following 1hr 300nM CX-5461 treatment, which showed broad differential gene expression profiles, with an equal number of Pol II transcribed genes significantly upregulated as down regulated. However, we have not further characterised these observations (Drygin et al., 2011). As transformed cell lines exhibit dysregulation of multiple key cell growth and stress signaling pathways (Reviewed in (Hanahan and Weinberg, 2011a)), global gene expression analysis in untransformed cell lines may better enable identification of novel pathways and assessment of the relative

importance of pathway activation.

Therefore, we decided to take an unbiased approach to identify p53-independent pathways that mediate the response to inhibition of Pol I transcription, by performing RNA-Sequencing analysis in BJ-T p53shRNA cells following CX-5461 treatment. We chose to perform analysis in p53 knock-down cell lines, as in p53 wild-type cells activation of the p53 nucleolar stress response pathway may override or mask the activation of alternative pathways. Further, inhibition of Pol I transcription may activate alternative pathways in the presence or absence of p53. For example, Boisvert and Lamond have reported that changes in the nucleolar proteome upon stress are markedly different between p53 wild type and p53 mutant cell lines (Boisvert and Lamond, 2010). RNA-sequencing has a number of advantages as a method to investigate the pathways that mediate response to CX-5461. As CX-5461 is a small molecule inhibitor of transcription, RNA-sequencing can provide additional information regarding the specificity of the drug to Pol I transcription, compared to Pol II transcription. Further, while the sequestration and release of numerous proteins from the nucleoli has been described following inhibition of Pol I transcription, the consequences of their translocation have not been characterised, except in the case of a small number of specific pathways. Therefore, we expected that RNA-sequencing would allow interrogation of early downstream responses to inhibition of Pol I transcription to identify these signaling events.

4.2 RNA-Sequencing analysis following Pol I inhibition in BJ-T p53shRNA cells.

4.2.1 Characterisation of RNA sequencing samples.

We performed RNA sequencing analysis across a time course of 1μM CX-5461 treatment, from 30 minutes to 1hr, 3hr, 6hr, 12hr and 24hr (See FIGURE 16 A). This was in order to investigate acute pathways that are activated at early time points to drive the response to inhibition of Pol I transcription, and also to determine the resulting phenotype that is established in cells after treatment with the drug.

We also included a commonly utilized inhibitor of Pol I transcription, 5nM Actinomycin D (ActD), for 30min, 3hr and 24hr time points (See FIGURE 16 A). ActD is a cyclic polypeptide-containing antibiotic that can bind dsDNA with high affinity, preferentially intercalating between GpC base pair sequences and binding the minor groove of the DNA helix above and below this site via adjacent guanosine residues (Reviewed in

(Koba and Konopa, 2005)). ActD non-specifically inhibits RNA synthesis, by preventing the progression of RNA polymerase through the DNA to which it is bound (Reviewed in (Sobell, 1985)). Pol I transcription is particularly sensitive to ActD, with over 10-fold selectivity for rRNA compared to total mRNAs in mammalian cells (Perry, 1963; Perry and Kelley, 1970)(Reviewed in (Sartorelli et al., 1975)). ActD does not interfere with the Pol I transcriptional complex or initiation of Pol I transcription (Fetherston et al., 1984) (Sollnerwebb and Tower, 1986); rather, ActD intercalates in GC rich regions of the rDNA and inhibits Pol I transcription elongation. However ActD has additional mechanisms of action, including: inhibition of DNA replication (Lian et al., 1996; Rill and Hecker, 1996); stabilization of cleavable complexes of topoisomerase I and II with the DNA (Trask and Muller, 1988); and inhibition of transcription from promoters containing G-quadruplexes (Kang and Park, 2009). Therefore, while at low concentrations of ActD rRNA is the primarily inhibited transcript, ActD may also have additional biological activities.

The levels of inhibition of Pol I transcription for each of the 1μM CX-5461 and 5nM ActD samples, relative to the 30min NaH_2PO_4 vehicle control, are shown in FIGURE 16 B. Consistent with earlier results in BJ-T p53 wild-type cells (See FIGURE 8), CX-5461 treated cells demonstrate a rapid reduction in Pol I transcription, with levels reduced by approximately 74% compared to untreated cells by 30 minutes, and approximately 85% by 1hr. This level of inhibition is maintained to 24hr CX-5461 treatment. ActD treated cells demonstrate a comparatively delayed reduction in Pol I transcription, with no significant reduction by 30 minutes, and an approximately 63% reduction compared to untreated cells by 3hr. Following 24hr ActD treatment, levels of Pol I transcription are reduced by approximately 75% compared to untreated cells. *MYC* mRNA was chosen as a control of Pol II mediated transcription, due to a) the similar half-life of its mRNA to pre-rRNA (Drygin et al., 2011), and b) the presence of G-quadruplexes in its promoter, which are reported to result in inhibition of its transcription by ActD at high doses (Kang and Park, 2009). Pol II transcription of *MYC* was not inhibited by treatment with either 1μM CX-5461 or 5nM ActD (results for 24hr shown in FIGURE 16 B). Therefore, both CX-5461 and ActD selectively inhibit Pol I transcription at these doses. Western analysis was also performed, to confirm knockdown of p53. The abundance of p53 in BJ-T p53shRNA cells treated with either CX-5461 or ActD remained below those in untreated control BJ-T cells for all demonstrating that these cells have a robust attenuation of the p53 response (FIGURE 16 D).

Cell cycle analysis was performed to characterize the phenotype of the treated BJ-T p53shRNA populations at each time point. As previously described (See FIGURE 14), CX-5461 treated BJ-T p53shRNA cells had an S-phase delay, and appeared to arrest in G2 (FIGURE 16 D). Interestingly, treatment with ActD was not sufficient to activate G2 cell cycle arrest, which had previously been observed upon Pol I inhibition in BJ-T cells by other mechanisms, including both CX-5461 and siPOLR1A/siRRN3 (See FIGURE 11). It is unlikely that this was due to the degree of inhibition of Pol I transcription by ActD: G2 cell cycle arrest was observed in BJ-T cells under conditions where Pol I transcription was inhibited to a lesser degree, both by 100nM CX-5461 and by siPOLR1A/siRRN3 (See FIGURE 8 and 11). Therefore, we propose that different mechanisms of Pol I inhibition, at either initiation or elongation stages, trigger different phenotypic responses.

4.2.2 General analysis of RNA-sequencing results.

Sequencing of the RNA samples described above was performed at the Victorian Centre for Functional Genomics (Peter MacCallum Cancer Centre, Victoria, Australia). The facility used 50bp paired-end reads on an Illumina HiSeq 2000 (6 samples per lane). To analyse the sequencing data, reads were aligned to the genome using Bowtie2 (Langmead et al., 2009) and counted using HTSeq (Anders and Huber, 2010). The differential expression was then calculated utilising the Bioconductor DESeq package (Anders and Huber, 2010) in R (version 3.0.0), and genes with significantly different expression were determined using adjusted p-values that control for false discovery rate (FDR) using the Benjamini-Hochberg procedure. The RNA sequencing results are shown in FIGURE 17 A and B, with differentially expressed genes indicated in red (adjusted p-value <0.1). We used more stringent criteria to define differentially expressed genes for further analysis, with adjusted p-value <0.05, and $\log_2$ fold change of expression either $-0.5<\log_2 FC>0.5$ or $-1.0<\log_2 FC>1.0$ as specified below (FIGURE 17 TABLE C). The number of differentially expressed genes for each treatment using the most stringent criteria ($-1.0<\log_2 FC>1.0$) is displayed in FIGURE 17 D.

Following CX-5461 treatment, 429 genes were significantly differentially expressed by 1hr, and over 3000 genes were significantly differentially expressed from 3hr to 24hr time points (adjusted p-value <0.05). At all time points following CX-5461 treatment, a higher proportion of genes had increased levels of expression than decreased levels of expression, indicating that CX-5461 does not act as a general inhibitor of Pol II transcription at this dose. Following ActD treatment, 1718 genes were differentially

expressed by 3hr, and 4624 genes were differentially expressed by 24hr (adjusted p-value <0.05). There were no differentially expressed genes following 30min ActD treatment, consistent with our observation that at this time point levels of Pol I transcription were not significantly reduced. The overlap between differentially expressed genes following CX-5461 and ActD treatment is shown in FIGURE 17 E. Approximately 80% of genes differentially expressed following 3hr ActD treatment are also differentially expressed following 3hr CX-5461 treatment. This suggests that changes in expression following treatment with these inhibitors are a result of inhibition of Pol I transcription specifically. However, CX-5461 has a larger set of differentially expressed genes at this time point, possibly because the repression of Pol I transcription following 1μM CX-5461 was greater than following inhibition with 5nM ActD, or alternatively because additional pathways are activated in response to inhibition of Pol I transcription initiation by CX-5461 than by inhibition of Pol I transcriptional elongation by ActD.

We then examined the time course of changes in genes expression following CX-5461, using the most stringent criteria of differentially expressed genes to reduce the data set for analysis ($-1.0<\log_2 FC>1.0$). The overlap between differentially expressed genes at each time point following CX-5461 treatment is shown in FIGURE 17 F, and the fold change in expression of each individual gene that is differentially expressed is shown in FIGURE 17 G. This analysis shows that while a large proportion of genes remain differentially expressed across the time course of CX-5461 treatment, in addition a new set of genes becomes differentially expressed at each time point. This may represent the transition from acute to chronic signaling pathways in response to inhibition of Pol I signaling by CX-5461.

4.2.3 Analysis of pathways acutely activated in response to CX-5461.

We focused on early time points (30min to 3hr) to identify signaling pathways that mediate the response to CX-5461. Following 30min treatment with CX-5461, only 4 genes were differentially expressed (FIGURE 18 TABLE A and BOX 18 A). Levels of *HES1* (Hairy and Enhancer of Split-1), a member of the HES family of transcription factors that functions as a transcriptional repressor to influence cell proliferation and differentiation, were increased at this time point (FC=1.6). Three other genes had decreased levels of expression: *DUSP1* (Dual specificity phosphatase 1 / MKP-1; FC=0.6), which inactivates MAPK in response to stress signals or growth factors; *IER2* (Immediate early response 2; FC=0.6); and *CYR61* (cysteine rich 61/ CCN1; FC=0.7), an excreted extra-cellular matrix signaling protein that is capable of regulating a range

of cellular activities, such as cell adhesion, migration, proliferation, apoptosis and senescence in different cell types. *CYR61*, *IER2,* and *DUSP1* are immediate early genes (IEGs) - a group of a broad range of genes that can be rapidly activated and expressed, without requiring an initial round of protein synthesis for their transcription (Lau and Nathans, 1987) (See BOX 18 A for more details). Therefore, the identification of changes in expression of predominantly IEGs at the early time 30min time point is likely a consequence of the unique mechanisms regulating their expression, which enable more rapid changes in mRNA levels than for other genes. The small number of genes differentially expressed at this time point, where qRT-PCR of 47S pre-RNA indicated an approximately 75% reduction in levels of Pol I transcription (see FIGURE 16 B), further supports the selectivity of CX-5461 toward inhibition of Pol I, but not Pol II transcribed genes.

Following 1hr treatment with CX-5461, 429 genes were differentially expressed ($-0.5<\log_2FC>0.5$, adjusted p-value <0.05). To identify pathways involved in the response to inhibition of Pol I transcription, a more stringent data set of 71 differentially expressed genes was used (59 genes $\log_2FC>1$, 12 genes $\log_2FC<-1$; FIGURE 18 TABLE B). Analysis of these genes indicates that CX-5461 treatment rapidly initiates a broad anti-proliferative response (See BOX 18 B for more details). For example, the MYC, NF-κB, and AP-1 (Activator protein 1) signaling pathways are immediate early response networks that can each control a broad transcriptional response, and following 1hr CX-5461 treatment changes in gene expression indicate these pathways are being regulated in a manner that prevents proliferation (eg. Increased expression of MYC antagonist MAD1, increased expression of NF-κB transcriptional targets, and increased expression of anti-proliferative AP-1 complex component JUNB). More directly, there is increased expression of cell cycle regulatory proteins p21 and GADD45B which directly inhibit CDKs to lead to cell cycle arrest. Therefore, it appears that by 1hr following CX-5461 treatment the acute pathways that drive the p53-independent response to inhibition of Pol I transcription have already been activated.

To further examine which signaling pathways were activated in response to CX-5461 treatment, we performed pathway enrichment analysis for only the early time points, for differentially expressed genes following 1hr CX-5461 ($-0.5<\log_2FC>0.5$) and 3hr CX-5461 ($-0.5<\log_2FC>0.5$) treatment combined, using Metacore GeneGo functional ontology enrichment analysis. The ten pathway maps most significantly enriched for differentially expressed genes are shown in FIGURE 18 TABLE C. A number of pathways identified, including GnRH (gonadotropin-releasing hormone) signaling,

immune response, and NF-κB activation pathways, have significant overlap of differentially expressed genes, with pathway enrichment largely being a result of common signaling to NF-κB and AP-1 transcription factors, consistent with the results described above. The relationships between the differentially expressed genes in these pathways is shown in FIGURE 18 D. Additional pathways that were identified by this analysis include the WNT, TGFβ (transforming growth factor β) receptor, and DNA damage signaling pathways (See BOX 18 C for more details). The relationships between the differentially expressed genes in these pathways are shown for each in FIGURE 18 E-G. A common feature is enrichment of differentially expressed genes in pathways associated with senescence. These include cell cycle, DNA damage, immune response, extra-cellular matrix (ECM) remodeling, and epithelial-to-mesenchymal transition (EMT) pathways.

The defining characteristic of senescent cells is irreversible cell cycle arrest, as discussed above in Section 3.5. In addition to this, senescent cells undergo widespread changes in expression of a set of secreted proteins - a phenotype termed the senescence associated secretory phenotype (SASP) (Reviewed in (Campisi and di Fagagna, 2007)). The SASP includes signaling factors (cytokines, chemokines and growth factors), secreted proteases, and ECM components (Reviewed in (Coppe et al., 2010)). Through these components SASP can mediate diverse processes, including modulating tissue architecture through changes in the ECM (Shelton et al., 1999), promoting EMT (Parrinello et al., 2005), stimulating angiogenesis (Coppe et al., 2006), and inducing inflammatory and immune response (Freund et al., 2010). SASP factors can also reinforce senescence growth arrest, for example through the most prominent SASP cytokine IL-6 (which has increased expression from 1-24hr following CX-5461 treatment), as well as through IL-1β and TGFβ family ligands (which have increased expression from 3-24hr following CX-5461 treatment) (Reviewed in (Acosta et al., 2013; Salama et al., 2014)). Following CX-5461 treatment, the increased expression of *CDKN1A* (p21) is consistent with cell cycle arrest associated with senescence. The activation of immune response signaling pathways is consistent with the expression of SASP components, including COX-2, CCL2, IL-6, and IL-1β (Coppe et al., 2010; Acosta et al., 2013; Salama et al., 2014), through NF-κB activation. Increased expression of NF-κB targets, such as IL-6 and IL-1β can also result in feedback activation of both the canonical and non-canonical NF-κB pathways. The TGFβ signaling pathway is involved in many cellular processes, including growth inhibition, cell migration, EMT, ECM remodeling and immune suppression (Reviewed

in (Akhurst and Hata, 2012)). The TGFβ family ligands are also components of SASP, which provide positive feedback by regulating p15 and p21, and mediating multiple senescence responses such as DNA damage signaling and EMT (Reviewed in (Hubackova et al., 2012; Acosta et al., 2013)) The downregulation of WNT is also consistent with senescence. WNT signaling pathway is fundamental to tissue homeostasis, with target genes involved in cell cycle progression, ECM, cell adhesion and differentiation (Reviewed in (MacDonald et al., 2009b)), and WNT signaling is reported to be downregulated early in senescence (Ye et al., 2007). Therefore, our RNA sequencing results suggest that following CX-5461 treatment there is early activation of pathways associated with the onset of senescence.

To examine if senescence associated pathways were also enriched for later time points, we performed pathway enrichment analysis for differentially expressed genes following 1hr – 24hr CX-5461 combined ($0.5<\log_2 FC>0.5$) (FIGURE 18 TABLE H). Similar to early time points, there is increased expression of NF-κB and its transcriptional targets, including anti-apoptotic proteins (eg BCL-XL) and SASP components. DNA damage, immune response, TGFβ, EMT, and angiotensin signaling pathways associated with senescence are also enriched. Therefore, collectively these results suggest that following CX-5461 treatment in BJ-T p53shRNA cells, early signaling events drive the onset of a sustained senescent phenotype. This is consistent with our results that show BJ-T p53shRNA cells undergo cell cycle arrest and eventually senescence following treatment with CX-5461 (FIGURE 15).

In order to determine which is the primary signaling event driving these responses, we focused on pathways enriched in differentially expressed genes at early time points, and selected the DNA damage response (DDR) pathway for further investigation. While the hallmark of senescent cells is activation of the p53 and $p16^{INK4A}$ /RB and irreversible cell cycle arrest, the onset of senescence is also associated with persistent DDR (Reviewed in (Burton and Krizhanovsky, 2014)). Particularly, SASP activation requires DDR signaling, but does not require p53 signaling (Reviewed in (Coppe et al., 2010)). In addition, DDR rapidly activates cell cycle checkpoint pathways (Reviewed in (Giglia-Mari et al., 2011b)). In our RNA-sequencing results, DDR pathway components including p21 are upregulated by 1hr, as are targets of NF-κB, which is known to be activated as part of the DDR (Reviewed in (Salminen et al., 2012)). Therefore, we predicted that DDR could be a primary signaling event activated in response to inhibition of Pol I transcription by CX-5461, driving the cell cycle arrest and senescent phenotypes observed in BJ-T p53shRNA cells.

4.3 Discussion

Our earlier results established that inhibition of Pol I transcription by CX-5461 can acutely induce phenotypic responses independently of the previously described p53 nucleolar stress pathway. Specifically, minimally immortalized cell BJ-T cells undergo a p53-independent proliferation defect associated with S-phase delay and G2 cell cycle arrest, and senescence. Further, tumorigenic BJ-LSTR cells, which are functionally inactive for p53, have defective progression through the cell cycle and increased levels of cell death. The majority of human cancers are inactive for p53 (Petitjean et al., 2007b). In addition, p53 pathway mutations are associated with resistance to many common cancer therapeutics. Treatment approaches are typically genotoxic, as they exploit the sensitization of p53-deficient tumors to DNA-damaging agents (Reviewed in (Hientz et al., 2017)). Therefore, the identification of new non-genotoxic therapeutic strategies for cancers inactive for p53 is a potentially valuable application of inhibition of Pol I transcription. The characteristics of the newly developed CX-5461 as a rapid and specific inhibitor of Pol I transcription provided a unique opportunity to perform an unbiased analysis to identify the key pathways that mediate the acute responses to inhibition of Pol I transcription. Therefore, we performed RNA-sequencing analysis in minimally immortalized cells inactive for p53 (BJ-T p53shRNA cells) across a time course of CX-5461 treatment to interrogate the p53-independent responses to inhibition of Pol I transcription.

Our RNA-sequencing results confirmed the specificity of CX-5461 for inhibition of Pol I transcription. After 30min CX-5461 treatment, at which time we observed an approximately 75% reduction in Pol I transcription, only 4 other genes were significantly differentially expressed (See FIGURE 18 TABLE A). Those that were downregulated are immediate early response genes (IEGs), which can rapidly respond to stress stimuli (See BOX 18 A), suggesting that changes in expression of these genes is an indirect response to inhibition of Pol I transcription rather than due to their being directly target by CX-5461. Further, consistent with the results of gene expression arrays following CX-5461 treatment in MIA PaCa-2 and A375 cells (Drygin et al., 2011), a larger number of genes were significantly upregulated than downregulated at all time points (1hr- 24hr) following CX-5461 treatment (FIGURE 17 C). This indicates that CX-5461 does not act as a general inhibitor of Pol II transcription. In contrast, ActD inhibited Pol I transcription less rapidly than CX-5461, with no significant reduction in Pol I transcription after 30min treatment, and after 24hr ActD treatment almost twice as many genes were significantly downregulated as

upregulated (FIGURE 17 C). Although fewer genes were differentially expressed following 3hr ActD than 3hr CX-5461 treatment, there was significant overlap between the two data sets (approximately 80%), further reinforcing the specificity of CX-5461 for inhibition of Pol I transcription.

One interesting observation is that in BJ-T p53shRNA cells, in contrast to inhibition of Pol I transcription by CX-5461, inhibition of Pol I transcription by ActD does not induce G2 cell cycle arrest. Further, following 24hr ActD treatment compared to 24hr CX-5461 treatment, there is reduced overlap of differentially expressed genes between the two data sets (approximately 60%), supporting that there are some differences in the phenotype established by the two treatments. This difference might be due to the activation of different downstream signaling pathways by the different mechanisms of inhibition of Pol I transcription by these drugs: CX-5461 inhibits Pol I transcription initiation, while ActD results in stalled Pol I at the elongation phase. Alternatively, the distinctive responses might reflect the different dynamics of inhibition of Pol I transcription, as CX-5461 acts significantly more rapidly than ActD (with ActD taking over 3hr to reach levels of inhibition that are achieved by CX-5461 by 30min, FIGURE 16 B).

The response to inhibition of rRNA gene transcription is strikingly immediate, with over 400 genes significantly differentially expressed by 1hr following treatment with CX-5461 (FIGURE 17 C and D). This reflects the rapid pathway activation and phenotypic responses we have observed following CX-5461 treatment. For example, in BJ-T p53 wild-type cells, activation of both p53 and its transcriptional target p21 occur by 1hr following treatment (See FIGURE 13). Or, for example, in the murine model of Eμ-Myc lymphoma, transactivation of p53 target genes is observed by 1hr and apoptosis by 2hr following treatment of cells in vitro, and induction of cell death occurs by just 6hrs following treatment in vivo (Bywater et al., 2012). The RNA –seq data indicates that by 1hr following CX-5461 treatment BJ-T p53shRNA cells have already activated anti-proliferative and stress response programs, including immediate early genes (IEGs) that rapidly respond to stress stimuli, antiproliferative AP-1 and NF-κB transcriptional response networks, cell cycle regulatory proteins, DNA damage response signaling, and senescence pathways (notably SASP components such as inflammatory cytokines) (FIGURE 18). This suggests that the cell takes advantage of specialised mechanisms to acutely regulate gene expression and pathway activation, to enable it to vigilantly respond to changes in rRNA gene transcription and nucleolar function. As

the RNA-seq analysis here is based on steady-state levels of mRNA, it does not distinguish between mechanisms that regulate gene expression via rates of gene transcription (such as epigenetic mechanisms and transcription factors), RNA stability (such as miRNAs and RNA binding proteins), and/or rates of translation into protein. However, any of these stages may contribute to the observed changes in gene expression. For example, IEGs which are prevalent in differentially expressed genes following 30min and 1hr CX-5461 treatment, can be rapidly activated within minutes of stimulation as they do not require an initial round of protein synthesis for their transcription, as necessary transcription factors and other proteins are already present in the cell (Reviewed in (Bahrami and Drablos, 2016)). Or, for example, new techniques that enable sequencing analysis specifically of nascent RNA and RNA stability have shown that exposure of human fibroblasts to inflammatory cytokines, which results in similarly rapid and dramatic changes in gene expression, regulates both gene transcription, with many transcripts having low intrinsic stability, as well as stabilizing or destabilizing transcripts (Paulsen et al., 2013). Similarly, following DNA damage from a clinically relevant dose of IR, genes in the p53-signaling pathway can be coordinately up-regulated by both increased synthesis and RNA stability (Venkata Narayanan et al., 2017). As the nucleoli are enriched in diverse and abundant proteins (such as those involved in chromatin regulation, cell-cycle control and stress signaling, and RNA and RNP biogenesis) as well as RNA species, it is tempting to speculate that it can utilize these to efficiently exert control of gene expression at multiple levels following nucleolar stress.

Analysis of significantly differentially expressed genes following inhibition of Pol I transcription by CX-5461 identified over 400 differentially expressed genes by 1hr treatment, and over 3000 differentially expressed genes by 3hr treatment. To identify primary signaling pathways that underlie the phenotypic responses, we focused on the early time points. One of the pathways that was identified by functional gene ontology enrichment analysis of differentially expressed genes was DNA damage (ATM/ATR regulation). We have selected this pathway for further validation as it is consistent with the phenotype we observe following inhibition of Pol I transcription by CX-5461 in BJ-T p53shRNA cells. Specifically, DDR rapidly activates cell cycle checkpoint pathways, consistent with the S-phase delay and G2 cell cycle arrest observed in response to CX-5461. Moreover, persistent DDR is associated with the onset of senescence, which was also observed in response to CX-5461 (Reviewed in (Giglia-Mari et al., 2011a; Burton and Krizhanovsky, 2014)).

FIGURE 16. Characterisation of 5nM ActD and 1μM CX-5461 treated BJ-T p53shRNA cell samples used for RNA-Sequencing analysis. A) Schematic of BJ-T p53shRNA cell samples included in RNA-Sequencing analysis. **B)** qRT-PCR analysis of expression of 47S pre-rRNA (left panel) and *MYC* mRNA (right panel) normalised to *VIM* mRNA, following 5nM ActD (30min, 3hr, 24hr) or 1μM CX-5461 (30min, 1hr, 3hr, 6hr, 12hr, 24hr) treatment relative to 30min NaH_2PO_4 vehicle control (t=0) (n=3, mean ± SD). **C)** Western blot analysis of total p53 levels in in BJ-T p53shRNA cells following treatment with NaH_2PO_4 vehicle control (30min), 5nM ActD (30min, 3hr) or 1μM CX-5461 (30min, 1hr, 3hr, 6hr, 12hr, 24hr), compared to parental BJ-T cells following treatment with NaH_2PO_4 vehicle control (representative of n=6). **D)** Cell cycle analysis by fixed cell PI staining for DNA content following treatment with 5nM ActD (3hr, 24hr), 1μM CX-5461 (3hr, 6hr, 12hr, 24hr), or NaH_2PO_4 vehicle control (30min, 24hr). Upper panel: representative experiment of n=3-5. Lower panel: quantitation of G1, S and G2/M cell cycle populations (n=3-5, mean ± SD).

FIGURE 16

A)

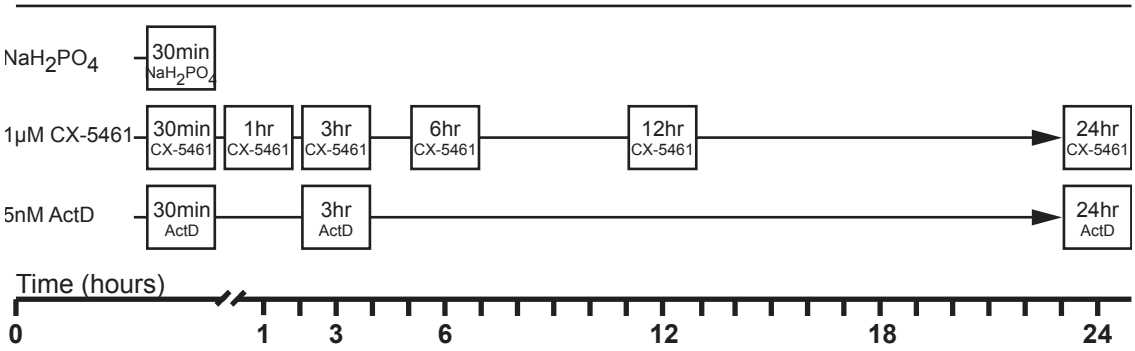

B)

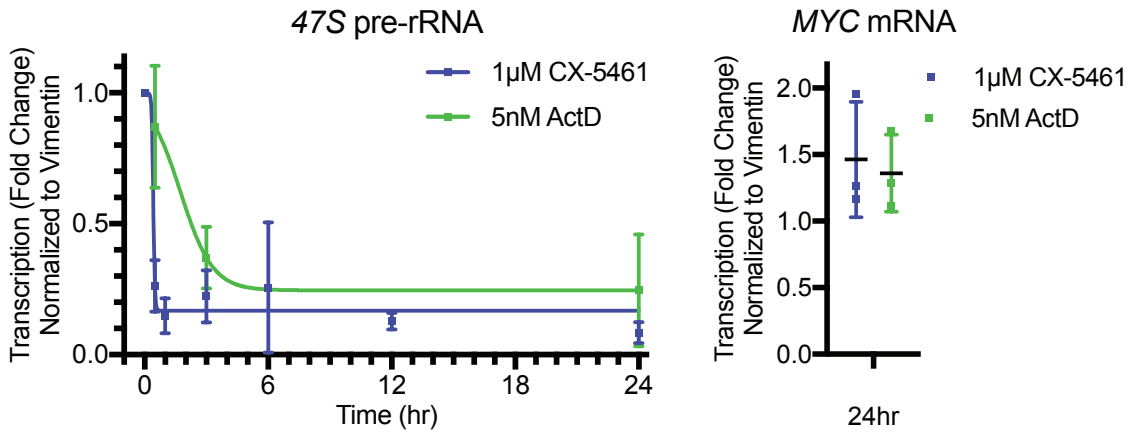

C)

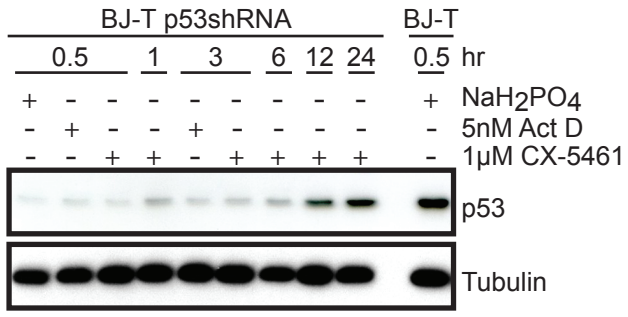

D)

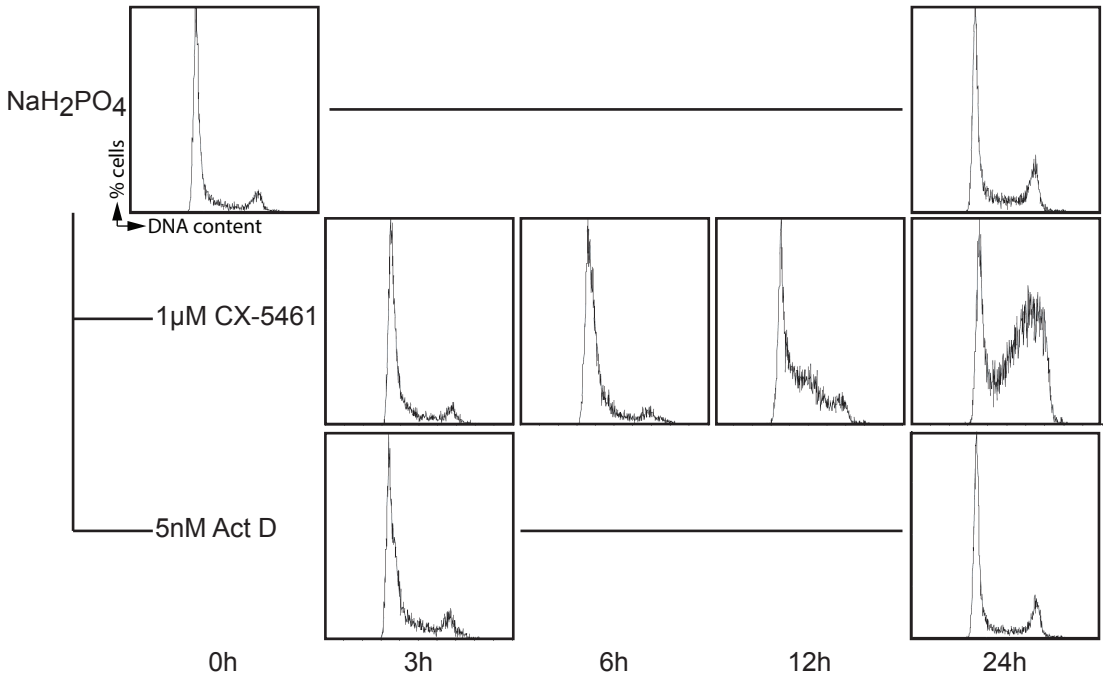
NaH2PO4
% cells
DNA content
1μM CX-5461
5nM Act D
0h
3h
6h
12h
24h

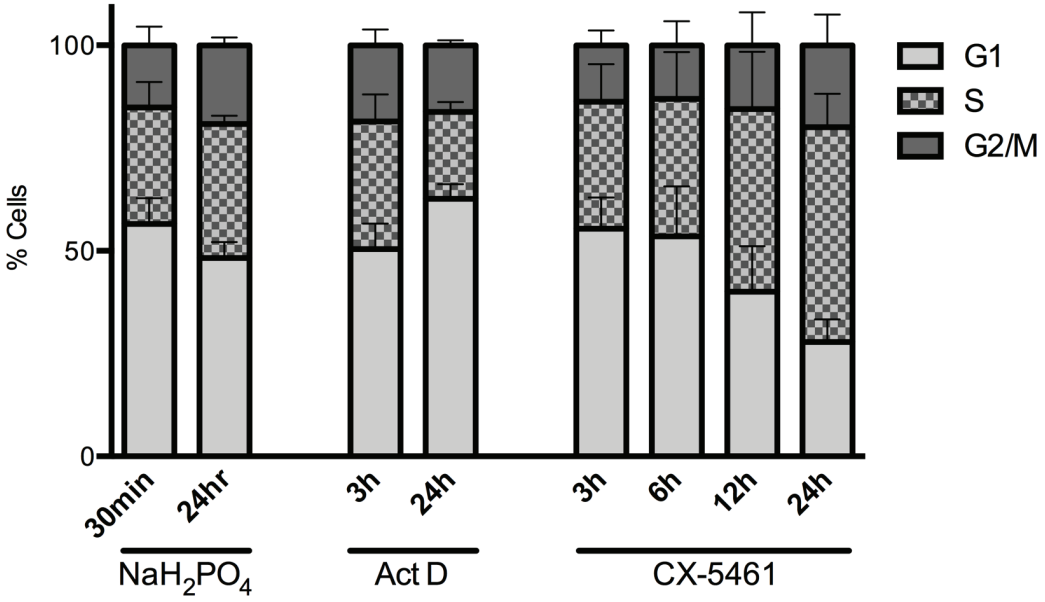
100
50
0
% Cells
G1
S
G2/M
30min
24hr
3h
24h
3h
6h
12h
24h
NaH2PO4
Act D
CX-5461

FIGURE 17. Results of RNA-sequencing analysis of 5nM ActD and 1μM CX-5461 treated BJ-T p53shRNA cell samples. A&B) Differential gene expression relative to 30min NaH_2PO_4 vehicle control. MA plot where M is Log_2FC and A is mean of normalized counts, for A) 1μM CX-5461 (30min, 1hr, 3hr, 6hr, 12hr, 24hr) treatment, and B) 5nM ActD (30min, 3hr, 24hr) treatment. Significantly differentially expressed genes are indicated in red (adjusted p value <0.1). **C)** Table of the number of significantly differentially expressed genes, for adjusted p-value <0.1 or <0.05, and log_2 fold change of expression -0.5<log_2FC>0.5 or -1.0<log_2FC>1.0, for each treatment relative to 30min NaH_2PO_4 vehicle control. **D)** Graphical representation of the number of significantly differentially expressed genes, defined as adjusted p-value <0.05, and -1.0<log_2FC>1.0. The number of upregulated genes (red) and down regulated genes (blue) relative to 30min NaH_2PO_4 vehicle control is shown for each treatment. **E)** Venn diagrams showing common significantly differentially expressed genes for ActD (red) and CX-5461 (green), following 3hr (left panel) and 24hr (right panel) treatments (adjusted p-value <0.05). % common genes shown for ActD in both comparisons. **F)** Venn diagrams showing common significantly differentially expressed genes for consecutive time points following 1μM CX-5461 treatment (adjusted p-value <0.05, -1.0<log_2FC>1.0). % common genes shown for earlier time point in all comparisons. **G)** Change in expression of individual significantly differentially expressed genes for 1-24hr 1μM CX-5461 treatments (adjusted p-value <0.05, -1.0<log_2FC>1.0). Each position on the X axis represents the same single significantly differentially expressed gene (vertical line) across all time points.

FIGURE 17
A)

1μM CX-5461

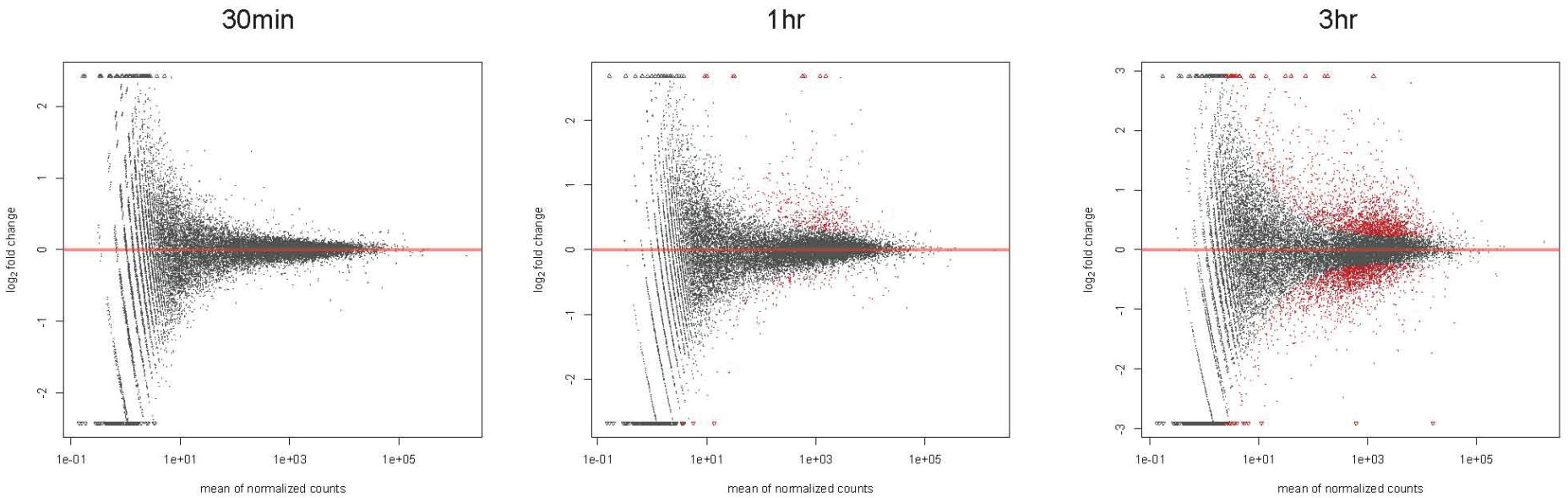

1μM CX-5461

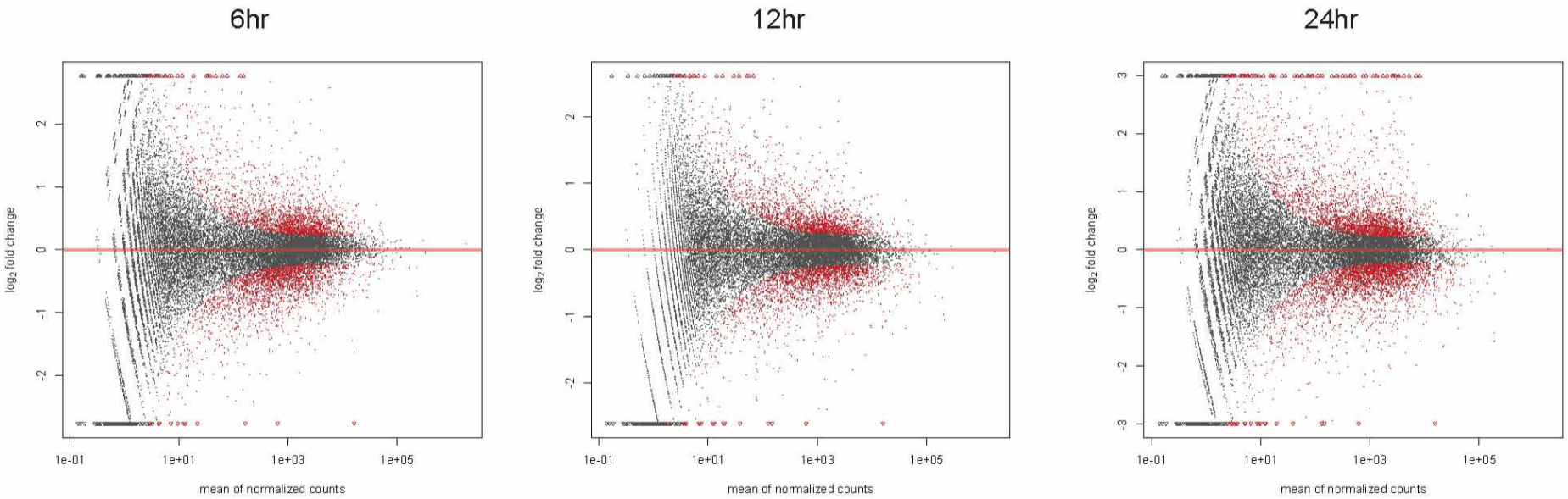
6hr
12hr
24hr
log2 fold change
mean of normalized counts
1e-01
1e+01
1e+03
1e+05

B)

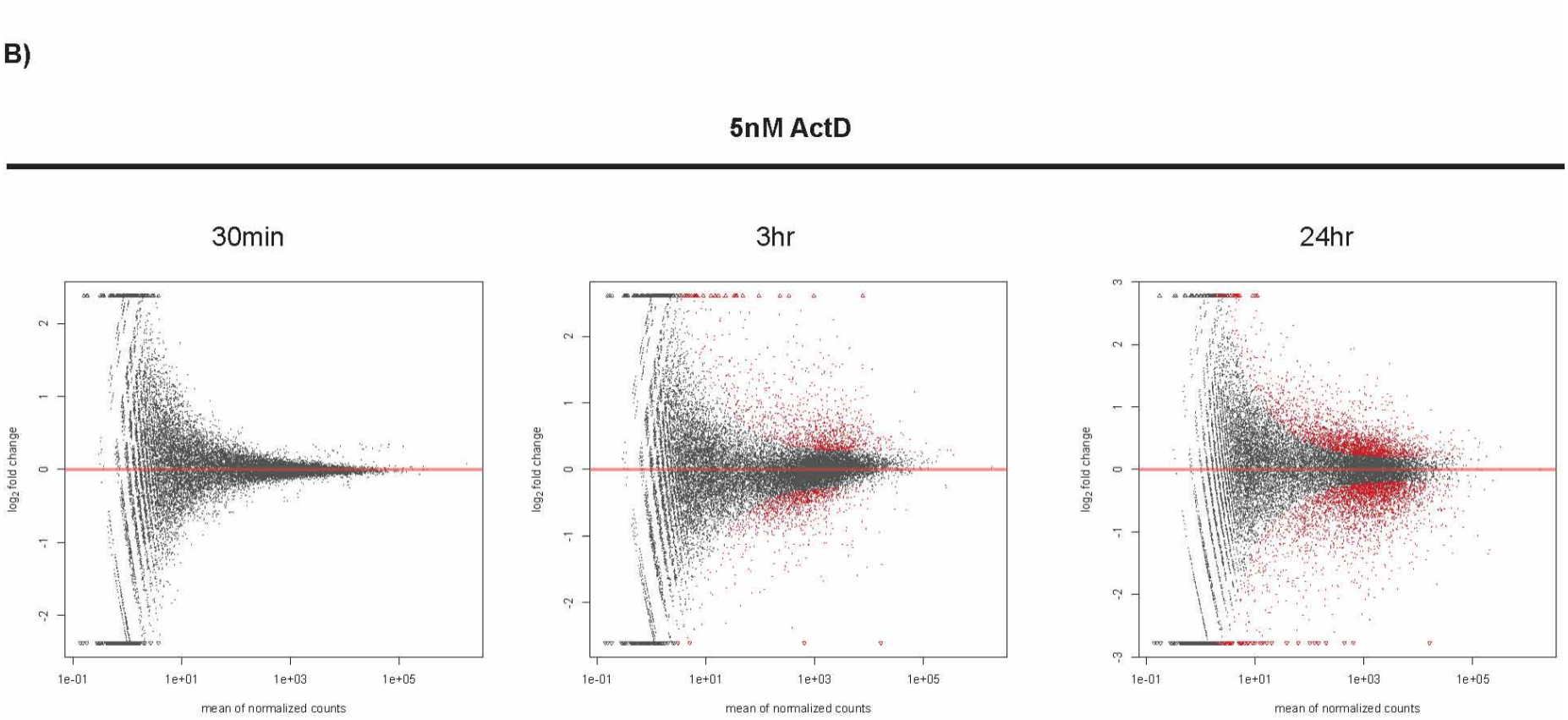
5nM ActD
30min
3hr
24hr
log2 fold change
mean of normalized counts
1e-01
1e+01
1e+03
1e+05

C)

Table of number of signicantly differentially expressed genes relative to 30min NaH2PO4 vehicle control.

	Adj p-value <0.1 -	Adj p-value <0.05 -	Adj p-value <0.05 -0.5< Log_2FC >0.5	Adj p-value <0.05 -1.0< Log_2FC >1.0
30min CX-5461	4	4	4	-
1hr CX-5461	520	429	254	72
3hr CX-5461	3797	3180	1654	441
6hr CX-5461	4297	3604	1844	523
12hr CX-5461	3757	2966	1362	379
24hr CX-5461	5628	4816	2636	861
30min ActD	-	-	-	-
3hr ActD	2068	1718	1008	262
24hr ActD	5452	4624	2135	599

D)

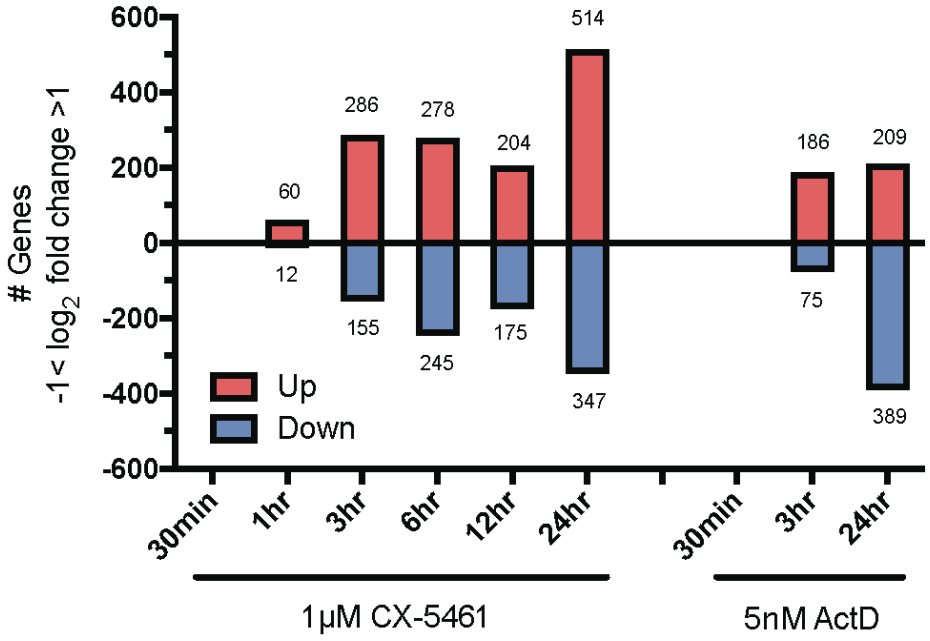
600
400
200
0
-200
-400
-600
Genes
-1< log2 fold change >1
60
12
286
155
278
245
204
175
514
347
186
75
209
389
Up
Down
30min
1hr
3hr
6hr
12hr
24hr
30min
3hr
24hr
1μM CX-5461
5nM ActD

E)

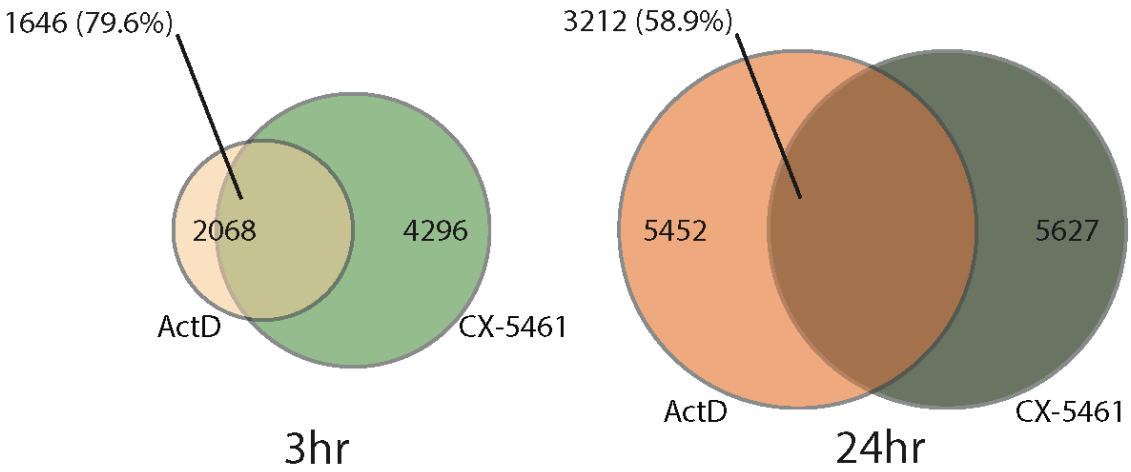
1646 (79.6%)
2068
4296
ActD
CX-5461
3hr
3212 (58.9%)
5452
5627
ActD
CX-5461
24hr

F)

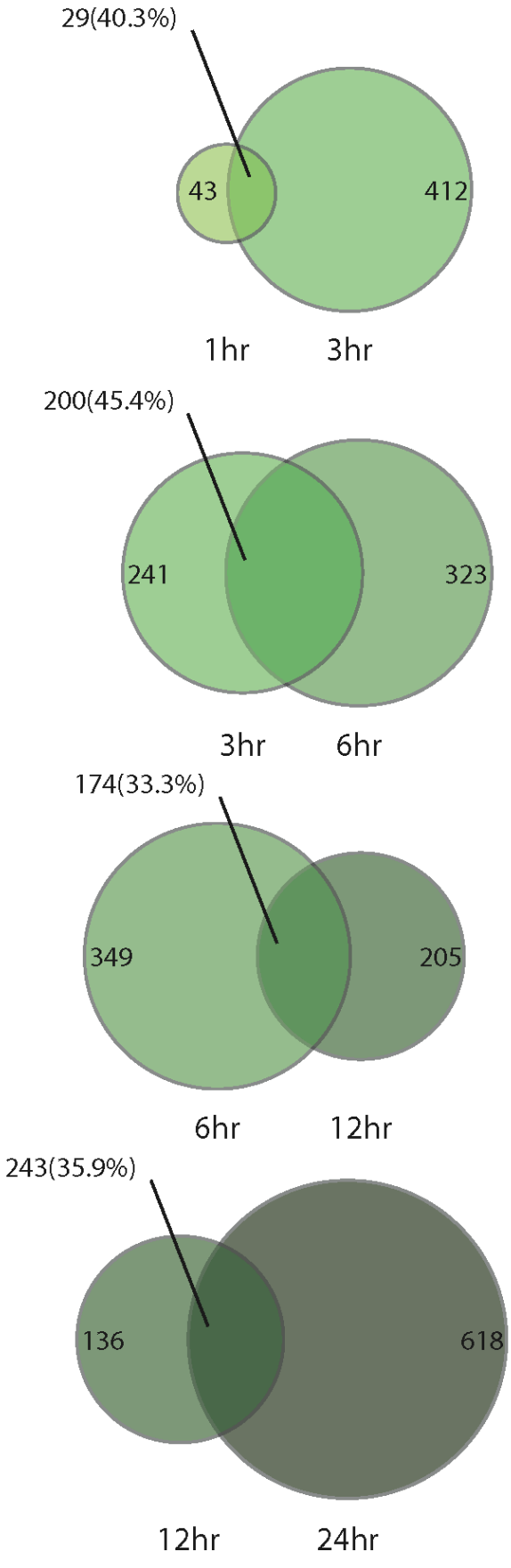
29(40.3%)
43
412
1hr
3hr
200(45.4%)
241
323
3hr
6hr
174(33.3%)
349
205
6hr
12hr
243(35.9%)
136
618
12hr
24hr

G)

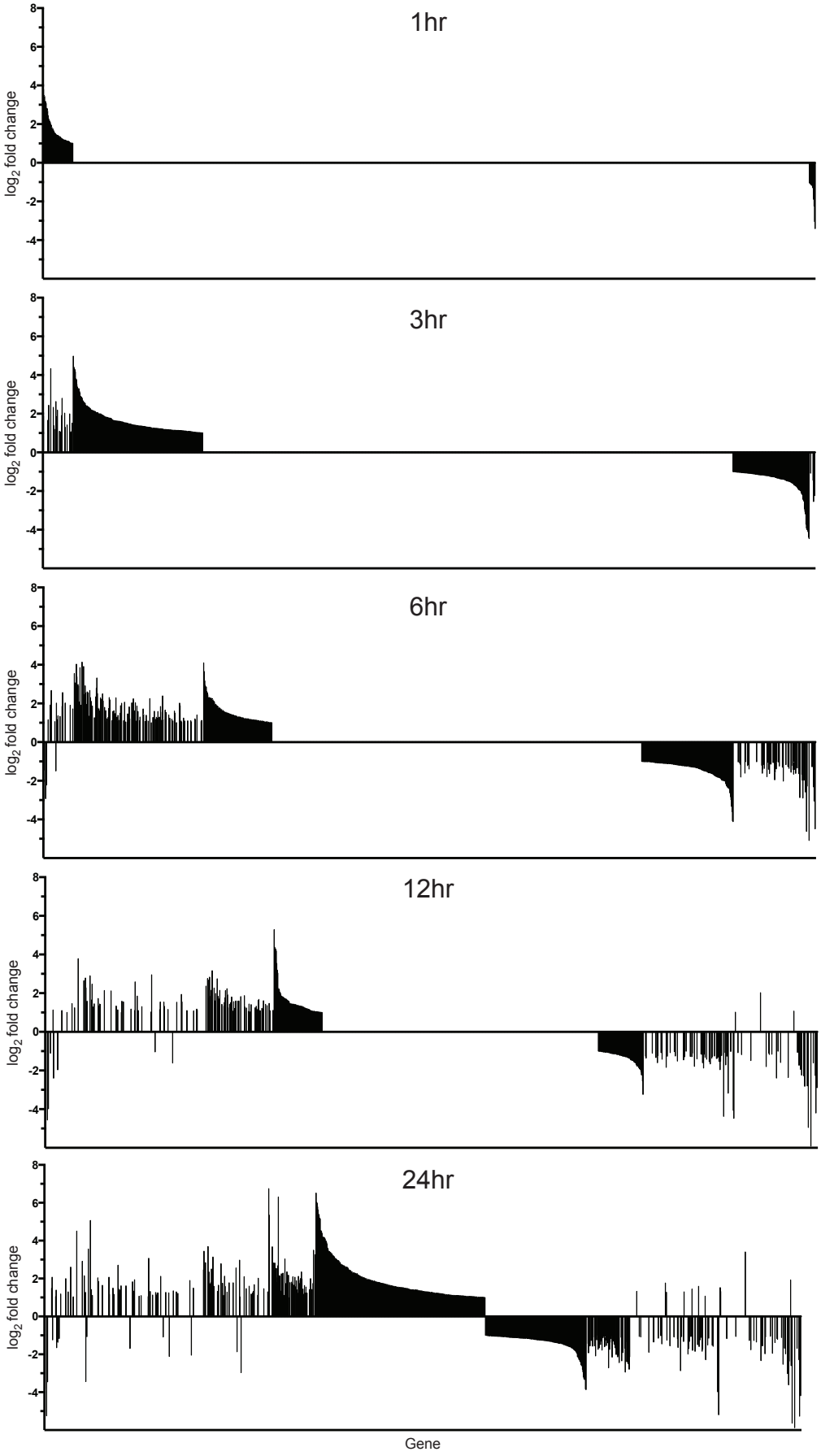

FIGURE 18. Significantly differentially expressed genes following treatment with 1μM CX-5461. A) Table of significantly differentially expressed genes following 30min 1μM CX-5461 treatment relative to 30min NaH_2PO_4 vehicle control (adjusted p-value <0.05, -1.0<log_2FC>1.0). **B)** Table of significantly differentially expressed genes following 1hr 1μM CX-5461 treatment relative to 30min NaH_2PO_4 vehicle control (adjusted p-value <0.05, -1<log_2FC>1). 59 genes have increased expression, log_2FC>1, and 12 genes have decreased expression, log_2FC<-1. Genes highlighted in grey are discussed further in the text and Box A (HES1) & Box B (GADD45B, CDKN1A, SERTAD1, MXD1, NFKB1A, BCL3, JUNB, FOSB, MIR221). **C)** Table of 10 pathways most significantly enriched for differentially expressed genes (using Metacore GeneGo functional ontology enrichment analysis) following 1hr-3hr CX-5461 (adjusted p-value <0.05, -0.5<log_2FC>0.5). **D-G)** Schematic of the relationship between significantly differentially expressed genes, shown in red (upregulated) and blue (downregulated), in pathways identified by functional ontology enrichment analysis, including D) GnRH signaling, immune response, and NF-κB activation pathways, E) TGF-β receptor signaling, F) WNT signaling pathway, and G) DNA damage pathways. **H)** Table of 20 pathways most significantly enriched for differentially expressed genes (using Metacore GeneGo functional ontology enrichment analysis) following 1hr-24hr CX-5461 (adjusted p-value <0.05, -0.5<log_2FC>0.5).

FIGURE 18

A)

Table of significantly differentially expressed genes following 30min 1μM CX-5461

Gene Name	Fold Change	Log_2 Fold Change	p-value	Adj p-value
HES1	1.6136	0.6903	5.34E-07	0.0063
CYR61	0.6922	-0.5306	6.71E-07	0.0063
IER2	0.6143	-0.7030	1.13E-10	3.21E-06
DUSP1	0.5591	-0.8389	1.63E-06	0.0116

BOX 18 A. Significantly differentially expressed genes following 30min 1μM CX-5461.

HES1. *HES1* (Hairy and Enhancer of Split-1) is one of seven members of the HES gene family (*HES1-HES7*) of basic helix-loop-helix transcription factors. HES proteins are primary targets of the Notch singling pathway, and HES1, in conjunction with binding partners from the transducin-like enhancer (TLE) family, acts as a transcriptional repressor that is a key regulator of cell proliferation and differentiation during embryogenesis (Reviewed in (Fischer and Gessler, 2007)). However, less is known about the role of HES1 after birth. Recent publications have shown that HES1 is rapidly upregulated by quiescent signals and can protect cells from differentiation or senescence (Reviewed in (Sang et al., 2010)). Transcriptional targets of HES1 include proteins involved in proliferation, such as E2F1, p21, and p27 (Reviewed in (Fischer and Gessler, 2007)). HES1 may also play a role in response to DNA damage and stress, such as by interacting with FA core complex (Tremblay et al., 2008) (Tremblay et al., 2009) and PARP1 (Kannan et al., 2011), or regulating the expression of GADD45α (Chiou et al., 2014). The canonical signaling pathway that regulates HES1 is the Notch pathway. Following activation of Notch receptors, the Notch intracellular domain (NICD) translocates to the nucleus and associates with the RBP-Jκ transcription factor, which allows the recruitment of coactivators and the transcription of target genes, including *HES1* (Ohtsuka et al., 1999). However, numerous other pathways have been reported to regulate *HES1* expression, including Hedgehog signaling (Ingram et al., 2008; Wall et al., 2009), TGFα/Ras/MAPK (Stockhausen et al., 2005), JNK (Curry et al., 2006), or NF-κB (Revollo et al., 2013). Further, post-translation modification of HES1 has recently been shown to mediate its activity (Lin and Lee, 2012; Chiou et al., 2014). HES1 regulates its own expression via a negative feedback loop.

Immediate Early Genes. *CYR61, IER2* and *DUSP1* are immediate early genes (IEGs). IEGs are a group of genes that were initially described as rapidly induced in quiescent cells upon treatment with growth factors. This group has now expanded to include a broad range of genes, including those encoding transcription factors, cytoplasmic enzymes and secreted proteins, that can be induced in interphasic cells in response to diverse extracellular signals, such as growth factors, mitogens, or stress. The common defining characteristic of IEGs is that they are rapidly activated and expressed, without requiring an initial round of protein synthesis for their transcription (Lau and Nathans, 1987), and then normally return to undetectable levels shortly following induction. Hence, these genes are considered a primary cellular response. The mechanisms underlying the rapid response of IEGs to diverse stimuli include pre-assembly and pre-initiation of RNA Pol II at IEG promoters, and GC rich promoters with CpG islands that act as nucleosome destabilisers, enabling transcriptional activators to access the promoter. IEG expression can be induced by RAS-MAPK and p38-MAPK pathways (Reviewed in (McKay and Morrison, 2007)). These lead to activation of proteins involved in IEG expression, including MSK1/2, which modify the IEG promoter to enable chromatin remodelling required for transcription, and also activate multiple transcription factors responsible for IEG expression, including NF-κB and CREB. RAS-MAPK and p38-MAPK pathways also activate transcription factors ELK and ETS1/2, and regulatory factors SRF and Mediator complex, which are required for IEG induction (Fowler et al., 2011; Galbraith and Espinosa, 2011). IEG transcripts are targeted by a family of microRNAs (Avraham et al., 2010), which leads to mRNA degradation under basal conditions. Following IEG activation, the production of these microRNAs is blocked, enabling IEG expression, but then rapidly returned to normal levels. Further, IEG protein products are typically unstable, and can even be targeted for proteasomal degradation without prior ubiquitination (Gomard et al., 2008).Collectively these mediate the rapid and transient expression of IEGs.

IER2. *IER2* (Immediate early response 2), originally identified in mouse fibroblasts where it is upregulated upon serum stimulation, was one of the first described members of the immediate early genes (Lau and Nathans, 1985). However, the function of IER2 remains largely unknown. *IER2* is located in the same region of chromosome 19 as *junB* and *junD*, and their proteins have limited homology (Coleclough et al., 1990; Scott et al., 1994). IER2 contains two putative nuclear localization signals (Shimizu et al., 1991), and may translocate from the cytoplasm to the nucleus in order to regulate transcription (Takaya et al., 2009; Neeb et al., 2012). Consistent with other IEGs, its expression can be induced under a wide variety of conditions, such as stimulation with serum or growth factors (Reviewed in (Neeb et al., 2012)), during differentiation (Charles et al., 1990; Chung et al., 1998; Eschelbach et al., 1998), or during the induction of apoptosis (Chung et al., 2000a; Chung et al., 2000b; Schneider et al., 2004). IER2 is upregulated in a variety of human tumors (Reviewed in (Neeb et al., 2012)). In fact, HTLV-1 (human t-cell leukemia virus type 1) Tax directly induces *IER2* transcription (Chen et al., 2003). IER2 can also promote tumor cell motility and metastasis (Neeb et al., 2012). Therefore it has been suggested that IER2 promotes transformation.

CYR61. CYR61 (cysteine rich 61/ CCN1) is a secreted extracellular matrix (ECM) associated protein of the CCN family. The six members of the CCN family are 'matricellular proteins' - ECM proteins which, rather than playing a structural role, are dynamically expressed and serve as signaling proteins that regulate a number of cellular responses (Reviewed in (Jun and Lau, 2011)). *CYR61* is expressed at very low levels in quiescent fibroblasts, but is transcriptionally activated in response to a wide range of stimuli, including mitogenic growth factors, bacterial and viral infection, inflammatory cytokines, GPCR agonists, hypoxia, UV, or mechanical stretch (Reviewed in (Lau, 2011)). The *CYR61* promoter contains a serum response element (SRE) to which serum response factor (SRF) binds to mediate transcriptional activation. *CYR61* transcription can be regulated by a number of co-activators, for example: RhoA GTPase promotes recruitment of MRTF-A, a SRF co-activator, to the SRE; p38 MAPK enhances the histone acetyltransferase activity of CBP and its recruitment to the SRF–MRTF-A complex, enhancing *CYR61* expression; YAP/TAZ transcriptional co-activators interact with TEAD transcription factors to regulate expression of genes related to proliferation and survival, including *CYR61*. *CYR61* is also regulated post-transcriptionally, for example down regulation by microRNAs, or preferential translation under conditions of stress through its IRES. CYR61 is essential for cardiovascular development during embryogenesis. In adult tissue CYR61 regulates a range of sometimes conflicting activities, mediated by its binding to distinct cell surface integrins and heparen sulphate proteoglycans (HSPGs) in different cell types and contexts. CYR61 supports cell adhesion, resulting in adhesive signaling events including cytoskeleton reorganization and formation of structures for cell motility. The process of cell adhesion may drive other cellular responses, for example CYR61 can stimulate migration, and can enhance proliferation induced by other mitogens. Conversly, CYR61 can induce both senescence and cell death. CYR61 can activate NOX1 to produce reactive oxygen species (ROS), which leads to the activation of DDR (including ATM, CHK1, CHK2 and p53), p38 MAPK and ERK, and consequently pRB. Activation of p53 and pRB result in senescence. CYR61 can also induce ROS through other pathways, for example via 5-lipoxygenase and mitochondria, and enhances the activity of the TNF family of apoptotic factors TNF-α, FasL and TRAIL. The ability of CYR61 to modulate the activity of inflammatory cytokines such as TNF-α is consistent with its proposed role in inflammation.

DUSP1. DUSP1 (Dual specificity phosphatase 1), or MKP-1 (Mitogen activated protein kinase phosphatase 1), is the archetypical member of the DUSP family, which can dephosphorylate both tyrosine

and serine/threonine residues of their substrates. DUSP1/MKP-1 regulates the activities of MAP kinases (MAPKs), including p38, JNK and ERK, by dephosphorylating the TXY motif in the kinase domain leading to their inactivation. It has the highest affinity for p38 and JNK, however substrate specificity varies depending on cell type and mechanisms of activation (Reviewed in (Korhonen and Moilanen, 2014)). Through its mediation of these MAPK pathways, it has been shown that DUSP1/MKP-1 can negatively regulate cell cycle transition and proliferation, facilitate differentiation, negatively regulate inflammation and immune response, and increase survival through the negative regulation of apoptosis (Reviewed in (Boutros et al., 2008)) DUSP1/MKP-1 is regulated at multiple levels, including transcription, mRNA stability, protein stability and post-translational modification (Reviewed in (Boutros et al., 2008)). Signaling pathways that are reported to mediate DUSP1/MKP-1 include ERK1/2, p38 MAPK, JNK, protein kinase C (PKC)ε, cAMP/protein kinase A (PKA); thus, DUSP1/MKP-1 is a negative feedback regulator of MAPKs. Typically DUSP1/MKP-1 protein is returned to basal level only a few hours after stimulation. Consistent with other IEGs, it is activated in response to numerous stimuli in different cell types, for example growth factors, cytokines, or stresses such as heat shock, hypoxia or DNA damage (Reviewed in (Boutros et al., 2008)). Accordingly, *DUSP1* transcription is regulated by numerous factors, including AP-1, CREB, GR, NF-κB, and p53. *DUSP1* mRNA is also stabilized, such as by binding proteins ELAV (or HuR) and NF90 in response to certain stresses (Reviewed in (Korhonen and Moilanen, 2014)). Conversely, *DUSP1* mRNA is also targeted my miR-101 to reduce DUSP1/MKP-1 levels and allow effective p38 MAPK and JNK signaling (Zhu et al., 2010).

B)

Table of significantly differentially expressed genes following 1hr 1μM CX-5461.

Gene Name	Fold Change	Log_2FC	p-value	Adj p-value
RGS16	31.6509	4.9842	1.09E-27	2.78E-24
FOSB	13.9362	3.8008	5.88E-18	7.16E-15
HES1	11.2021	3.4857	2.87E-09	9.57E-07
EGR4	10.8062	3.4338	3.55E-07	7.11E-05
EGR3	9.0163	3.1725	4.03E-196	1.13E-191
TMEM88	9.0016	3.1702	2.08E-05	2.42E-03
EGR2	8.4245	3.0746	1.13E-10	5.74E-08
GPR62	7.0781	2.8234	1.11E-04	9.82E-03
hsa-mir-3187	7.0078	2.8090	2.57E-05	2.82E-03
BHLHE40	6.3736	2.6721	3.31E-06	4.73E-04
NR4A3	5.4380	2.4431	1.26E-10	6.17E-08
AC012360.6	4.8428	2.2758	8.67E-06	1.11E-03
KLF10	4.5211	2.1767	1.70E-09	6.19E-07
RP11-405L18.4	4.4771	2.1626	5.28E-04	3.66E-02
ATF3	4.2675	2.0934	3.89E-48	2.18E-44
LIF	3.9746	1.9908	1.29E-12	8.83E-10
NR4A1	3.8623	1.9495	1.17E-09	4.61E-07
ZC3H12A	3.5721	1.8368	7.19E-16	7.75E-13
CSRNP1	3.4285	1.7776	5.57E-78	7.80E-74
ARC	3.3886	1.7607	5.71E-07	1.04E-04
DACT1	3.1479	1.6544	3.32E-04	2.49E-02
KDM6B	3.1419	1.6516	4.11E-06	5.82E-04
SIK1	2.9524	1.5619	7.77E-20	1.15E-16
NUAK2	2.9365	1.5541	1.19E-49	8.33E-46
JUNB	2.8433	1.5076	6.02E-31	1.87E-27
AC016999.2	2.7599	1.4646	7.14E-04	4.72E-02
ERRFI1	2.7316	1.4498	3.74E-57	3.50E-53
KBTBD8	2.7005	1.4332	3.59E-27	8.10E-24
SLC19A2	2.6767	1.4205	8.09E-07	1.39E-04
DLX2	2.6733	1.4186	3.41E-05	3.60E-03
GADD45B	2.6104	1.3843	5.14E-07	9.69E-05
PER1	2.6076	1.3827	1.71E-08	4.79E-06
CLK1	2.5674	1.3603	2.47E-05	2.76E-03
MXD1	2.5246	1.3360	3.69E-13	3.14E-10
SPRY4	2.5217	1.3344	1.57E-39	6.27E-36
TRIB1	2.4431	1.2887	5.28E-12	3.43E-09
SLFNL1	2.3861	1.2547	7.12E-06	9.45E-04
IL11	2.3586	1.2380	1.09E-40	5.10E-37
ID4	2.3511	1.2333	1.98E-05	2.33E-03
SERTAD1	2.3088	1.2072	1.13E-36	3.97E-33
ZNF597	2.2780	1.1877	7.58E-13	5.59E-10
FAM46C	2.2762	1.1866	6.87E-06	9.21E-04
IL6	2.2569	1.1743	1.95E-20	3.21E-17
RGS2	2.2555	1.1735	2.91E-06	4.23E-04
MYLIP	2.2526	1.1716	1.40E-06	2.25E-04
CCRN4L	2.1921	1.1323	7.97E-13	5.72E-10

NPAS4	2.1918	1.1321	9.37E-05	8.69E-03
BCL2L11	2.1802	1.1245	2.72E-04	2.13E-02
ARL5B	2.1693	1.1172	8.24E-31	2.31E-27
DUSP8	2.1626	1.1127	7.08E-11	3.82E-08
TNFSF9	2.1610	1.1117	2.51E-06	3.76E-04
MIDN	2.1361	1.0950	2.22E-15	2.31E-12
CDKN1A	2.0758	1.0537	2.59E-08	6.92E-06
ZNF124	2.0570	1.0406	1.11E-08	3.33E-06
C21orf91	2.0295	1.0211	1.96E-09	6.96E-07
NFKBIA	2.0294	1.0210	1.98E-19	2.64E-16
MAFF	2.0235	1.0169	3.76E-27	8.10E-24
FOXD1	2.0209	1.0150	3.71E-05	3.85E-03
BCL3	2.0197	1.0141	2.89E-04	2.25E-02

IQCC	0.4823	-1.0520	1.49E-07	3.28E-05
ZNF658	0.4761	-1.0708	3.14E-04	2.39E-02
ZNF624	0.4588	-1.1241	6.87E-10	2.91E-07
MIR221	0.4579	-1.1270	3.80E-08	9.69E-06
SNORD104	0.4453	-1.1672	3.50E-04	2.61E-02
RP11-181K3.4	0.4444	-1.1701	1.97E-04	1.62E-02
ZNF572	0.4115	-1.2810	6.03E-04	4.10E-02
RN5-8S1	0.4049	-1.3044	2.68E-04	2.10E-02
RP3-410C9.1	0.2687	-1.8961	5.75E-07	1.04E-04
SNORD78	0.2112	-2.2432	1.16E-04	1.01E-02
AL592188.2	0.1210	-3.0470	2.37E-04	1.89E-02
RP11-305P14.1	0.0943	-3.4069	1.92E-04	1.60E-02

BOX 18 B. Significantly differentially expressed genes following 1hr 1μM CX-5461.

GADD45B. *GADD45B* is a member of the Gadd45 (Growth arrest and DNA damage-inducible protein) group of genes, which encode GADD45α, GADD45β, and GADD45γ. Expression of these proteins is induced in response to stress, such as DNA damage, resulting in cell cycle arrest, DNA repair, senescence or apoptosis (Reviewed in (Tamura et al., 2012)). GADD45β participates in DNA repair, interacting with PCNA to promote nucleotide excision repair (NER) (Vairapandi et al., 1996). It both augments p21 activity and disrupts the CDK1/cyclinB complex, leading to cell cycle arrest at G1/S and G2/M (Vairapandi et al., 1996; Vairapandi et al., 2002). GADD45β can also activate p38 and JNK MAPK pathways, promoting senescence or apoptosis, by interacting with the upstream kinase MKK4 (Takekawa and Saito, 1998; Mita et al., 2002; Takekawa et al., 2002; Yoo et al., 2003; Lu et al., 2004; Cho et al.). Conversely, it can prevent activation of the JNK pathway, resulting in resistance to apoptosis, by interacting with MKK7 (De Smaele et al., 2001; Papa et al., 2004; Papa et al., 2007). *GADD45B* transcription is induced by NF-κB, directly through NF-κB binding sites at its promoter (Jin et al., 2002). NFY, SP1, EGR1 and SMAD transcription factors are also reported to induce *GADD45B* expression (Yoo et al., 2003; Zumbrun et al., 2009). *GADD45B* can also be induced by mRNA stabilization (Zumbrun et al., 2009).

CDKN1A. Cyclin-dependent kinase inhibitor 1A (*CDKN1A*) encodes the p21 protein (Reviewed in (Abbas and Dutta, 2009b; Jung et al., 2010)). p21 is a predominant member of the Cip/Kip family of cyclin-dependent kinase inhibitors (CDKIs). Following cell stress, such as DNA damage or oncogene activation, p21 associates with several CDK complexes to regulate progression of the cell cycle. Particularly, p21 inhibits CDK1 and CDK2, which is required for both the activation of RB and the consequent inhibition of E2F-dependent gene expression, and also the firing of replication origins and activation of proteins involved directly in DNA synthesis. In addition, p21 has roles in stress responses such as cell death, DNA repair, and senescence that are independent of its CDKI activity. For example, p21 interacts with PCNA (proliferating nuclear antigen), a subunit of DNA polymerase δ, inhibiting DNA replication and PCNA-dependent DNA repair processes. p21 also associates with transcription factors, including E2F1, STAT3, and MYC, and represses their transcriptional activity, thereby further inhibiting both cell growth and apoptosis. The anti-apoptotic activity of p21 can also occur in the cytoplasm, where it binds and inhibits proteins directly involved in the induction of apoptosis. *CDKN1A* is one of the key transcriptional targets of p53 (el-Deiry et al., 1993), in fact p21 is required for p53 mediated G1 and G2 cell cycle arrest (Waldman et al., 1995; Bunz et al., 1998). In addition to its regulation by p53, p21 is also induced in response to diverse stimuli in a p53-independent manner, including DNA damage, TGF-β, $p16^{INK4a}$ -RB, or RAS-RAF-MAPK signalling. Several transcription factors activate p21 independently of p53 (Reviewed in (Abbas and Dutta, 2009a)) : SP1/SP3 have six binding sites in the *CDKN1A* promoter, and regulate p21 induction in response to various stimuli and stress signals; E2F1 and E2F3 strongly activate *CDKN1A*; a number of members of the Kruppel-like transcription factor (KLF) family, which are key transcriptional regulators of proliferation and differentiation, also upregulate *CDKN1A* transcription; others include AP2, STATs, C/EBPα and β, NEUROD1, GAX, HOXA10, CDX2 and MYOD1. p300/CBP can cooperate with several of these transcription factors to induce p21. *CDKN1A* transcription is also activated by several nuclear receptors, though binding to their responses elements in the *CDKN1A* promoter. Alternatively, c-MYC can repress the transcription of p21, through interacting with SP1 and other transcription factors. *CDKN1A* transcription is also regulated at the level of transcriptional elongation. p53-dependent activation of *CDKN1A* involves Pol II phosphorylation and recruitment of transcription

elongation factors, and this is ablated when cells are blocked in S-phase. CHK1 can inhibit *CDKN1A* transcriptional elongation by disassembling elongation factors (Beckerman et al., 2009). SP3 can inhibit *CDKN1A* transcription by promoter bound Pol II (Valin et al., 2013). *CDKN1A* mRNA stability and translation is mediated by micro RNAs, including the miR-17-92, miR-106a-363, and miR-106b-25 clusters which have been shown to down-regulate *CDKN1A* expression, as well as RNA binding proteins that can stabilise or destabilise *CDKN1A* mRNA (Reviewed in (Freeman and Espinosa, 2013; Khuu et al., 2016)).

SERTAD1. *SERTAD1* is a recently identified oncogene, that encodes the p34/SEI-1 protein. p34 promotes cycle progression by binding to CDK4 and antagonising the regulatory effect of $p16^{INK4a}$ on the CDK4/Cyclin D complex (Sugimoto et al., 1999; Li et al., 2004). p34 contains two transactivation domains and has intrinsic activation activity, but it does not directly interact with DNA; it is reported to interact with PHD- and/or bromodomain-containing transcription factors to co-activate its target genes, such as at E2F, p53, and SMAD1 responsive promoters (Hsu et al., 2001; Watanabe-Fukunaga et al., 2005; Peng et al., 2013). p34 directly interacts with XIAP (X-linked inhibitor of apoptosis protein), protecting it from ubiquitination and degradation, thereby enhancing XIAP antiapoptotic activity (Hong et al., 2009). It has also been shown to inhibit ROS-induced cell death and/or senescence, which involve indirectly inducing ubiquitination of PKC-δ and/or ASK1, respectively (Lee et al., 2009; Hong et al., 2011). Finally, p34 can downregulate the tumor suppressor PTEN, by interacting with NEDD4-1 E3 ubiquitin ligase and enhancing its stability, resulting in PTEN degradation and activation of the PI3K/AKT pathway (Jung et al., 2013; Hong et al., 2014). Therefore, p34 may act as an oncoprotein through control of cell-cycle progression and apoptosis, by both transcriptional regulation and direct interaction with regulatory complexes.

NF-κB (NFKB1A, BCL3). The NF-κB signaling pathway is an immediate early response network that transduces signals from diverse stimuli to the NF-κB transcription factor. NF-κB denotes a family of proteins that associate as homo- or heterodimers, including NFKB1 (p50), NFKB2 (p52), REL, RELA (p65), or RELB. Under normal conditions, the majority of NF-κB dimers are bound by IκBs (inhibitors of κB) in the cytoplasm, preventing their nuclear localization and transcriptional activity. IκBs are characterized by ankyrin repeat domains capable of interacting with the Rel homology domains present in NF-κB transcription factors (Nolan et al., 1993), and include the typical family members IκBα, IκBβ, IκBε, and IκBδ, as well as two atypical family members Bcl-3 and IκBζ. The canonical and non-canonical NF-κB pathways are well characterized. In the canonical pathway, an extracellular signal initiates the assembly of the IκB kinase (IKK), which phosphorylates NF-κB bound IκB, leading to its ubiquitination and degradation by the proteasome, and to the translocation of NF-κB dimers to the nucleus where they regulate the transcription of target genes. In the noncanonical pathway, IKK phosphorylates the precursor protein p100 (NFKB1), which exists in inactive NF- κB dimers, resulting in its processing to p50. The resulting population of active NF- κB dimers is different from that in the canonical pathway, and drive transcription of a different set of genes. The most significant role of NF-κB is in the immune system, regulating the expression numerous genes in response to pathogens (Reviewed in (Bonizzi and Karin, 2004)). However, NF-κB also regulates genes with diverse cellular functions such as cell growth, proliferation, differentiation, apoptosis and stress response. The set of genes that are activated by NF-κB are unique for different stimuli, and display varying rates of induction, transcription, and repression. The mechanisms that drive this diversity include the selective regulation of IκBs, which display selectivity for certain NF-κB family members, and the different activities of the NF- κB hetero- and homo-dimers. NF- κB

dimers have varied binding preference for NF-κB consensus sequences, which show considerable sequence variability. Only p65, c-Rel and Rel-B contain the transcription activation domain (TAD) necessary for positive regulation of gene expression; p50 and p52 lack TADs, and may therefore repress transcription. NF- κB dimers also undergo posttranslational modifications that affect their ability to recruit transcriptional coactivators, which include p300/CBP, p/CAF, and p160 proteins (SRC-1, SRC-2, and SRC-3). ***NFKB1A***. IκBα is the prototypical member of the IκB family. Its rapid degradation following activation of NF-κB signaling pathways leads to the release of multiple NF-κB dimers, although p65:p50 heterodimers are reported to be the its primary target. *NFKBIA,* encoding IκBα, is strongly activated by NF-κB (Brown et al., 1993; Scott et al., 1993; Sun et al., 1993). The newly synthesized IκBα then binds to NF-κB, resulting in a negative feedback loop (Arenzana-Seisdedos et al., 1997). Hence, levels of IκBα are central to the control of NF-κB signaling. ***BCL3***. BCL3 is an atypical member of the inhibitor of IκB family of proteins. In contrast to the typical members of this family, BCL3 associates with nuclear p50 or p52 homodimers, and can both promote or repress transcription of NF-κB target genes (Reviewed in (Maldonado and Melendez-Zajgla, 2011)). BCL3 was identified by translocation into the immunoglobulin alpha-locus in some cases of B-cell leukemia, and has since been found overexpressed in a number of cancers (Cogswell et al., 2000; Thornburg et al., 2003; Pallares et al., 2004; Liu et al., 2013; Tu et al., 2016). Its oncogenic properties are proposed to arise from dysregulation of genes targeted by these NF-κB dimers. BCL3 has been shown upregulate cyclin D expression (Park et al., 2006), inhibit p53 through upregulation of HDM2 (Kashatus et al., 2006), and play a role in stabilizing c-MYC (Liu et al., 2013). Like IκBα, the transcription of *BCL3* is induced by NF-κB. It can also be induced by AP-1 (Rebollo et al., 2000) and the Jak/STAT pathway (Richard et al., 1999). BCL3 also negatively regulates its own transcription(Brocke-Heidrich et al., 2006).

MXD1. Max dimerisation protein 1 (*MXD1, MAD1*) encodes a member of a sub-family of MAX interacting proteins that form part of the basic helix-loop-helix leucine zipper protein MYC/MAX/MAD network of transcription factors (Ayer et al., 1993)(Reviewed in (Luscher, 2012)). The bHLH-Zip motif functions as a DNA binding and dimerisation module, and homo- or heterodimerization of this class of transcription factor is required for specific DNA binding. MAX serves as a cofactor for DNA binding by both the MYC family of transcription factors as well as MXD1-4. Enhanced or deregulated expression of MYC is one of the most frequent events associated with human cancer (Reviewed in (Grandori et al., 2000)). MYC directly regulates a considerable number of genes; its transcriptome includes proteins with roles in cell cycle control, protein translation and metabolism, ribosome biogenesis, differentiation and apoptosis. Consequently, MYC is capable of driving cell cycle progression and blocking terminal differentiation of many cell types (Reviewed in (Hurlin and Huang, 2006)). MYC family proteins heterodimerize with MAX, which is essential for most of the activities of MYC, and generally activate transcription. MXD1-4 also heterodimerise with MAX, acting as MYC antagonists but also performing functions in their own right. MXD1 antagonises MYC-mediated transcriptional activation by competing for binding to MAX, as well as recruiting repressor complexes to common target genes, and can block MYC-dependent cell transformation (Reviewed in(Luscher, 2012)). MXD1 acts as a transcriptional repressor at its target genes, which have roles in cell proliferation and apoptosis, and acts as an inhibitor of cell proliferation. Target genes identified for MXD1 include *CCND2* (Cyclin D2), *TERT*, *FOXM1*, *BCL6*, *PTEN*, and those encoding eIF4F subunits. MXD1 also heterodimerises with the bHLH-Zip protein MLX, a common dimerisation partner of MXD1, MXD4, MONDOA and MONDOB. Thus MXD1 acts in different transcriptional networks, though less is known about the function of MXD1/MLX complexes (Billin et al., 1999; Meroni et al., 2000). Key to the regulation of *MXD1* is that Pol II is paused at the *MXD1* promoter prior to stimulation, and

C/EPB and SP transcriptional regulators also bind constitutively to the promoter where they cooperate in activating *MXD1(Jiang et al., 2008; Hein et al., 2011)*. Thus pathways that target these factors are central to *MXD1* transcriptional activity, including STAT3 and RAS/RAF/ERK pathways, for example G-CSF and TGFβ cytokines activate *MXD1* via these pathways.

AP-1 (*JUNB and FOSB*). The AP-1 (Activator Protein 1) transcription factor regulates a wide range of cellular processes, including proliferation, differentiation, survival, inflammation, migration and wound healing (Reviewed in (Shaulian, 2010)). The ability of this transcription factor to control a diverse range of target genes and processes arises from its structural complexity: AP-1 is a dimeric complex comprised of JUN (JUN, JUNB, JUND), FOS (c-FOS, FOSB, FRA1 and FRA2), MAF, and ATF protein sub-families. The composition of AP-1 complexes and the targeting of specific AP-1 components by multiple signal transduction events underlie the complexity transcriptional regulation by AP-1. JUN is the most potent transcriptional activator in its group, while its transcriptional activity is attenuated or antagonized by JUNB. Broadly, JUN is considered to positively regulate cell proliferation, while JUNB and JUND negatively regulate proliferation. Consistent with this, JUNB competitively inhibits the JUN mediated induction of cell cycle regulatory proteins such as cyclin D1. In addition, JUNB containing AP-1 complexes also directly regulate the expression of cell cycle regulatory proteins, including cyclin A and $p16^{INK4A}$, preventing G1/S transition. FOS proteins cannot homodimerise, but form stable heterodimers with JUN family proteins and enhance their DNA binding activity. c-FOS and FOSB contain transcriptional activation domains, while FRA1 and FRA2 do not. FOS family members exhibit different expression patterns during the cell cycle: while c-FOS and FOSB are only found during G0/G1 transition, FRA1 and FRA2 are also present in exponentially growing cells. AP-1 is regulated by MAPK signaling cascades, including the ERK (for example, in response to serum and growth factors), JNK and p38 families (for example, in response to pro-inflammatory cytokines and genotoxic stress) (Reviewed in (Karin, 1995)). MAPKs activate various transcription factors that induce specific *JUN* and *FOS* family genes, resulting in increased AP-1 complexes. MAPKs also mediate post-translational phosphorylation of AP-1 components directly, regulating their activity, including transactivation potential, DNA binding, and protein stability.

microRNA-221 microRNA-221 (*miR-221*) is encoded in a cluster with the closely related *miR-222* on the X chromosome. It is one of the most frequently upregulated mRNAs in human cancer, and its expression correlates with aggressive tumor features and poor overall survival (Reviewed in (Garofalo et al., 2012; Chen et al., 2013; Wang et al., 2014)). The role of miR-221 as an oncomiR reflects its biological functions; it downregulates several tumor suppressors and promotes cell proliferation, invasive capabilites, resistance to apotosis, and maintenance of an undifferentiated state. Some of its well characterised gene targets include: cyclin dependent kinase inhibitors *CDNK1B* (p27) and *CDKN1C* (p57), supporting progression through the cell cycle; the pro-apoptotic factors BMF and PUMA, consistent with role in protecting cells from apoptosis; MyoD and KIT, preventing differentiation (Yang et al., 2013b; Tan et al., 2014); PTPμ, a tyrosine phosphatase that participates in cell adhesion regulation, therefore promoting migration; TRPS1 transcription factor, resulting in increased levels of EMT-promoting ZEB2; TIMP3, a metallopeptidase inhibitor, resulting in activation of MMPs; ER-α and FOXO3 transcription factors; and PTEN, resulting in activation of the pro-survival PI3K/AKT pathway. miR-221 activation of AKT can also modulate DNA damage repair and confer protection from cell death by PTEN independent mechanisms (Li et al., 2014). Recently, gene expression profiling identified 602 mRNAs - including RB and Wee1 cell cycle inhibitors, pro-apoptotic factor APAF1, and transcriptional repressors ANXA1 and CTCF - as new miR-221 targets. The same study found that MYC/MAX, NF-κB, Wnt/β-catenin, and RB-E2F pathways

are induced in miR-221 expressing cells (Lupini et al., 2013). Finally, MDM2 is a direct target of miR-221, resulting in activation of p53 (Fornari et al., 2014). While research into mir-221 has largely focused on its targets, rather than its transcriptional regulation, recent publications have reported that p53 (Fornari et al., 2014), NF-κB and c-Jun (Galardi et al., 2011) can induce miR-221/222 transcription. The ERK1/2 pathway also promotes miR-221/222 expression (Terasawa et al., 2009). Conversly, mir-221 has also been reported to activate NF-κB by binding directly to the coding region of RelA mRNA and increasing its stability. It can also reduce the degradation of RelA and STAT3 protein by downregulating the ubiquitin E3 ligase PDLIM2 (Liu et al., 2014). Therefore mir-221/222 act in a positive feedback loop with both NF-κB, through RelA, and p53, through MDM2. ER-α is able to repress miR-221/222 transcription, in this case forming a negative feedback loop, as it is target itself by miR-221 (Di Leva et al., 2010). miR-221/222 is also reported to be down regulated in response to inflammatory stimuli (Dentelli et al., 2010). Interestingly, while miR-221 and miR-222 are reportedly co-expressed, miR-222 levels were not significant in our data set.

C)

Table of pathways significantly enriched in differentially expressed genes expressed genes following 1-3hr 1μM CX-5461.

			1hr CX-5461		3hr CX-5461	
		minimum adjusted p-value	adjusted p-value	Differentially expressed genes	adjusted p-value	Differentially expressed genes
1	WNT signaling pathway	1.149E-06	2.115E-01	SNAIL1 DKK1	1.149E-06	CSNK2A2, NLK, VEGF-A, ENC1, TCF7, REST, CLDN1, AXIN1, LEF1, FZD8, FZD9 FRAT1, WNT16, BMP4, AXIN2, FZD2, JUN, DKK1, TAB1
2	GnRH signaling	5.560E-06	5.560E-06	JUNB, FOSB, PER1, ATF-3, MEF2D, NUR77 DUSP1	2.721E-03	DUSP4, MEF2D, SRC, MAP2K3 EGR1, FOS, JUN, PLCB2, PLCB4, DUSP1
3	Immune response (HSP60 and HSP70/ TLR signaling pathway)	6.677E-06	8.278E-02	JUNB, FOSB, IL6, NFKBIA, NFKBIE 	6.677E-06	IL1B, IL6, NFKBIE, IRAK2, FOSB, NFKB1, RELB, ICAM1, HSPA14, IL12A, TLR4, MAP2K3 JUN, FOS, TAB1
4	Immune response (TLR2 and TLR4 signaling pathways)	7.223E-05	3.112E-02	JUNB, FOSB, IL6, NFKBIA, NFKBIE, PEL1 	7.223E-05	IRAK2, PTGS2, IL1B, IL6, NFKBIE, FOSB, PEL1, NFKB1, RELB, TLR4, MAP2K3 JUN, FOS, TAB1
5	Immune response (IL-18 signaling)	1.071E-04	9.741E-02	JUNB, FOSB, IL6, NFKBIA, NFKBIE 	1.071E-04	PTGS2, IL1B, IL6, NFKBIE, FOSB, NFKB1, RELB, ICAM1, CCL2, SRC, MAP2K3 JUN, FOS, TAB1

6	Immune response (TLR5, TLR7, TLR8, and TLR9 signaling pathways)	2.154E-04	6.284E-03	JUNB, FOSB, IRF1, IRF7, IL6, NFKBIA, NFKBIE	2.154E-04	IRAK2, IRF7, IL1B, IL6, NFKBIE, FOSB, NFKB1, RELB MAP2K3 JUN, FOS, TAB1
7	DNA Damage (ATM/ATR regulation of G2/M checkpoint)	2.154E-04	3.021E-02	CDKN1A, PLK3, GADD45B	2.154E-04	PLK3, CDKN1A,GADD45B CHEK2, CCNA2, WEE1, CDC25C, ATRIP, CDC25B
8	TGF-β receptor signaling	2.510E-04	2.382E-02	CDKN1A, NFKBIA, KLF10, GADD45B	2.510E-04	CDKN2B, TNPO1, NFKB1, RELB, CDKN1A, SMURF1, SKI, MAP2K3, SKIL, TSC22D1, GADD45B ER81, TAB1
9	Immune response (C5a signaling)	2.510E-04	2.039E-01	JUNB, FOSB, NFKBIA, NFKBIE	2.510E-04	SPHK1, C5AR1, IL1B, NFKBIE, NFKB1, RELB, FOSB JUN, FOS, PLCB2, PLCB4,GNAZ, C5
10	NF-κB activation pathways	2.657E-04	2.039E-01	PELI1, NFKBIA, NFKBIE	2.657E-04	IRAK2, IL1B, NFKBIE, PEL1, NFKB1, RELB, MALT1, TLR4 TNFRSF13C, TAB1

Box 18 C. Selected pathways enriched in significantly differentially expressed genes following 1-3hr 1μM CX-5461.

WNT signaling pathway. The Wnt signaling pathway is fundamental in development and tissue homeostasis, regulating cell proliferation, polarity, migration, and fate determination (Reviewed in (MacDonald et al., 2009a)). The canonical Wnt signaling pathway functions by regulating levels of the β-catenin transcriptional co-activator. In the absense of Wnt, β-catenin is targeted for proteasomal degredation as a result of modification by a complex consisting of Axin, APC, CK1α, and GSK3β, and Wnt target genes are repressed by the TCF/LEF family of HMG box proteins. Binding of a member of the Wnt family ligands to a Fzd family receptor and its co-receptor LRP5/6 results in the recruitment of DSH and inhibition of Axin-APC-CK1α-GSK3β modification of β-catenin. Stabilized β-catenin associates with TCF/LEF, resulting in the activation of Wnt target genes. Wnt also activates a number of non-canonical signaling pathways that are independent of β-catenin. In mammals, there are 19 Wnt ligands and 10 Fzd receptors, which in combination have variable capacities to activate β-catenin. Cell context dependent expression of TCF/LEF HMG box family members (LEF1, TCF7, TCF7L1, TCF7L2) confers further diversity, with LEF1 generally behaving as an activator, TCF7L1 as a repressor, and TCF7 and TCF7L2 as both. TCF/ β-catenin transcription is regulated at a number of different levels, including alternative promoter transcription of dominant negative TCF7 and LEF1 genes, antagonists that disrupt TCF/ β-catenin complexes or transcriptional activity, and post-translational modification of specific TCF/LEF proteins. This enables the diverse, context specific activation of Wnt target genes, including genes involved in cell cycle progression, extracellular matrix remodeling, cell adhesion, and cell differentiation. A number of Wnt signaling proteins are regulated by TCF/ β-catenin, including upregulation of DKK1, Axin2, LEF1, TCF7, and some members of the FZD family, resulting in a complicated feedback loop.

TGFβ signaling pathway. TGFβ signaling is involved in many cellular processes, including growth inhibition, cell migration, EMT, ECM remodeling and immune suppression (Reviewed in (Akhurst and Hata, 2012)). The canonical TGFβ signaling pathway is relatively straightforward, however the action of TGFβ is highly cell type and context dependent. TGFβ superfamily ligands are synthesized as a precursor which form homodimers and associate in large latent complex with latency-associated peptid (LAP) and latent TGFβ binding protein (LTBP) at the ECM. Release of this complex from the ECM and proteolysis of LAP makes TGFβ available for signaling via a heteromeric complex of two related type I and type II receptors. Binding of the ligand induces phosphorylation and activation of the type I receptor by the type II receptor, and subsequent phosphoryltaion and activation of TGFβ receptor-specific SMADs (R-SMADs: SMAD2 or SMAD3). R-SMADs then form complexes with the common mediator SMAD (co-SMAD: SMAD4) and translocate to the nucleus, where they bind SMAD-binding element (SBE), usually in concert with other transcription factors that mediate the TGFβ signaling transcriptional response. Binding of TGFβ ligands to their receptor complex also results in activation of non-cononical SMAD independent signaling pathways, including the MAPK, PI3K/AKT, and NF-κB pathways. Further, crosstalk with these and other pathways, particularly WNT, Hedgehog, Notch and Interferon pathways, significantly influences TGFβ signaling. This generates the complex responses that enable TGFβ to be involved in diverse biological processes during both development and in adult tissue homeostasis.

D)

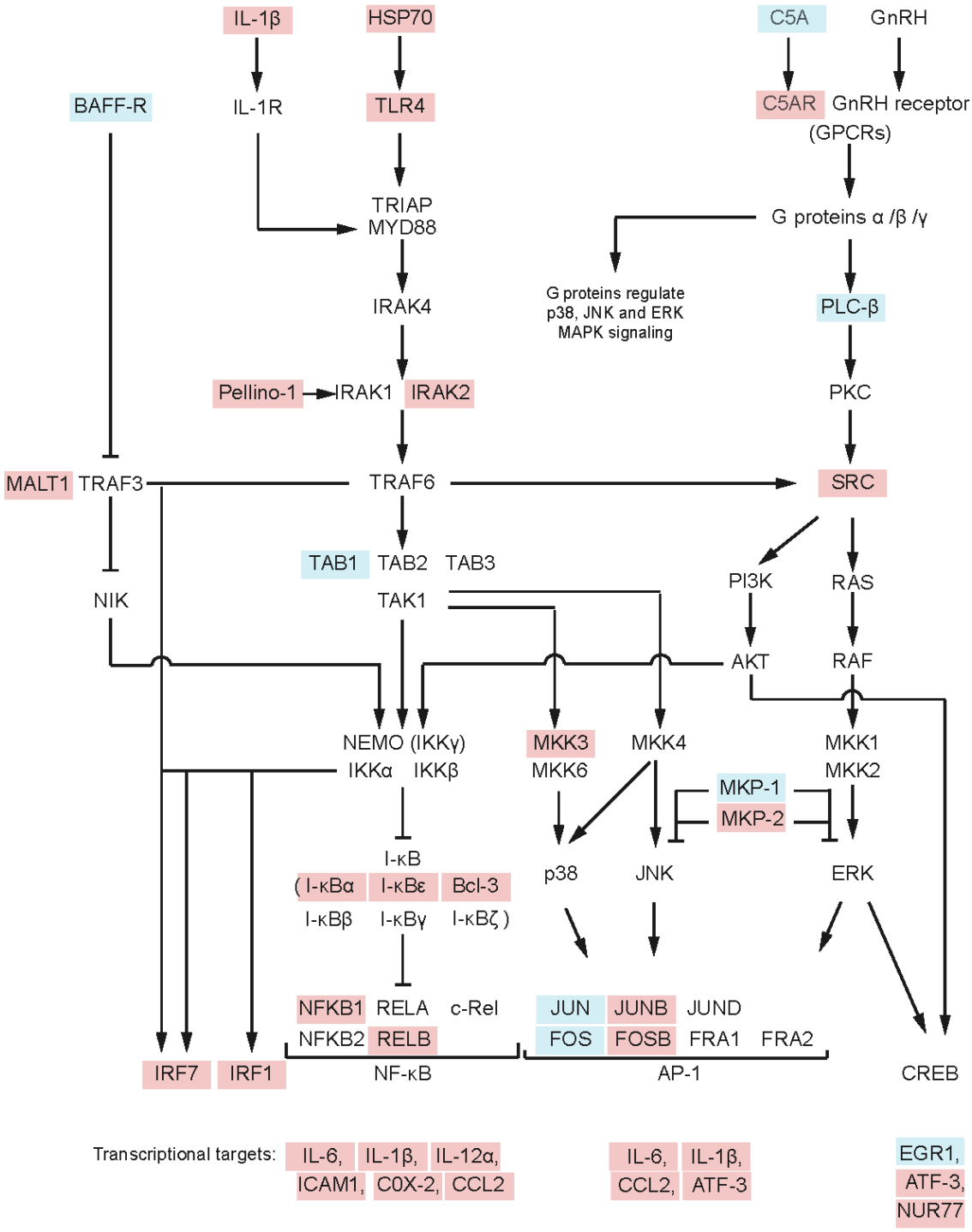
IL-1β
HSP70
C5A
GnRH
BAFF-R
IL-1R
TLR4
C5AR
GnRH receptor
(GPCRs)
TRIAP
MYD88
G proteins α /β /γ
G proteins regulate
p38, JNK and ERK
MAPK signaling
IRAK4
PLC-β
Pellino-1
IRAK1
IRAK2
PKC
MALT1
TRAF3
TRAF6
SRC
TAB1
TAB2
TAB3
PI3K
RAS
NIK
TAK1
AKT
RAF
NEMO (IKKγ)
IKKα
IKKβ
MKK3
MKK6
MKK4
MKK1
MKK2
MKP-1
MKP-2
I-κB
(I-κBα
I-κBε
Bcl-3
I-κBβ
I-κBγ
I-κBζ)
p38
JNK
ERK
NFKB1
RELA
c-Rel
NFKB2
RELB
JUN
JUNB
JUND
FOS
FOSB
FRA1
FRA2
IRF7
IRF1
NF-κB
AP-1
CREB
Transcriptional targets:
IL-6,
IL-1β,
IL-12α,
ICAM1,
C0X-2,
CCL2
IL-6,
IL-1β,
CCL2,
ATF-3
EGR1,
ATF-3,
NUR77

E)

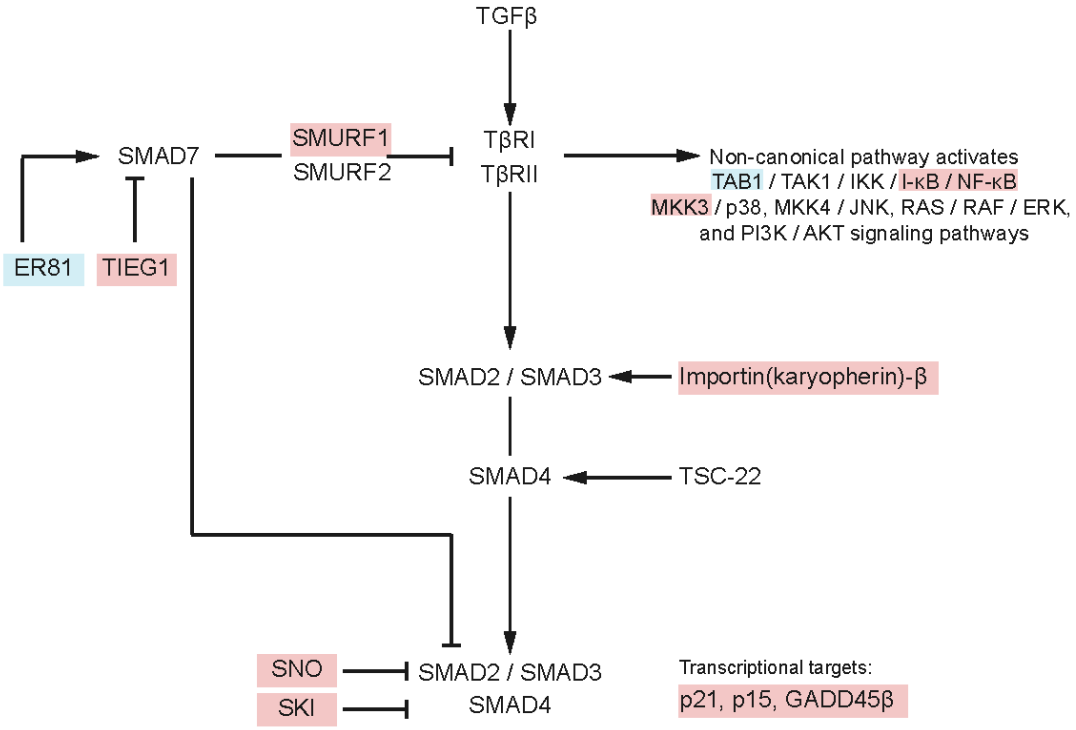
TGFβ
TβRI
TβRII
SMURF1
SMURF2
SMAD7
ER81
TIEG1
Non-canonical pathway activates
TAB1 / TAK1 / IKK / I-κB / NF-κB
MKK3 / p38, MKK4 / JNK, RAS / RAF / ERK,
and PI3K / AKT signaling pathways
SMAD2 / SMAD3
Importin(karyopherin)-β
SMAD4
TSC-22
SNO
SKI
SMAD2 / SMAD3
SMAD4
Transcriptional targets:
p21, p15, GADD45β

F)

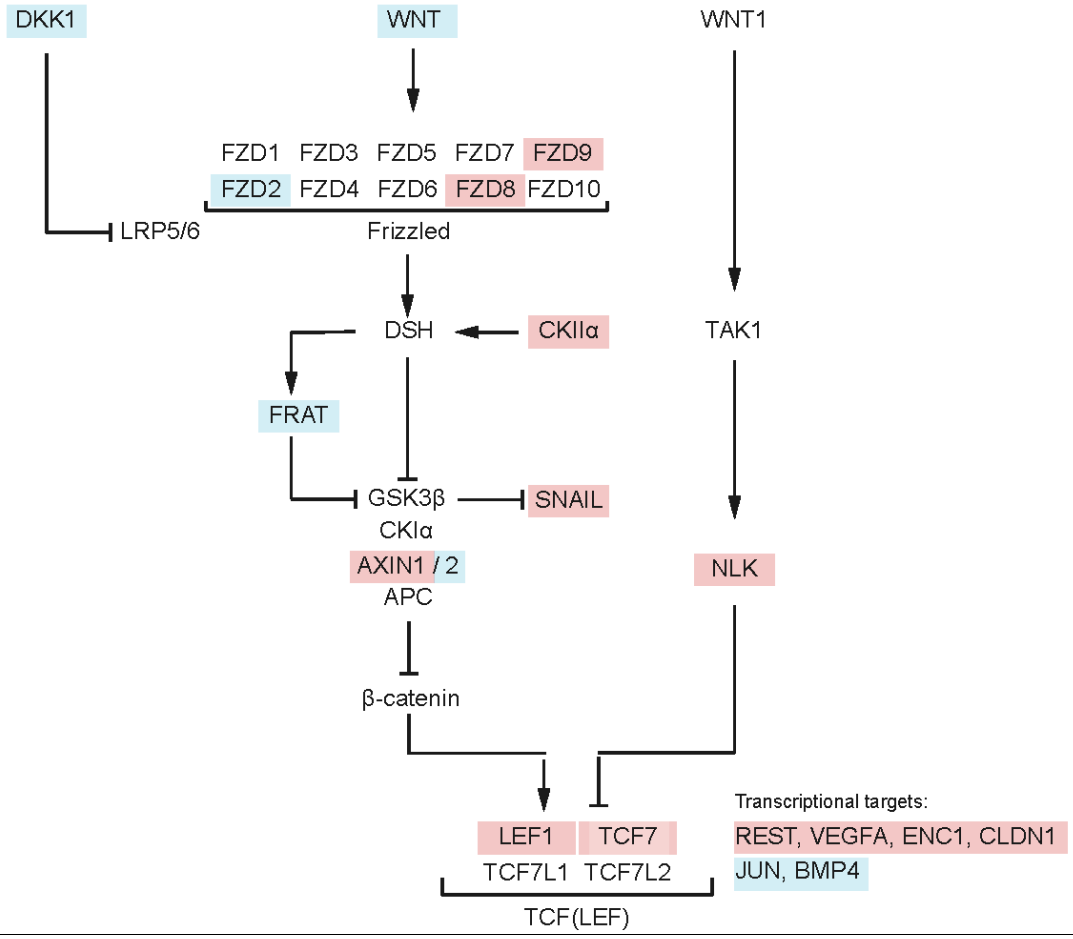
DKK1
WNT
WNT1
FZD1 FZD3 FZD5 FZD7 FZD9
FZD2 FZD4 FZD6 FZD8 FZD10
LRP5/6
Frizzled
DSH
CKIIα
TAK1
FRAT
GSK3β
CKIα
SNAIL
AXIN1 / 2
APC
NLK
β-catenin
LEF1 TCF7
TCF7L1 TCF7L2
TCF(LEF)
Transcriptional targets:
REST, VEGFA, ENC1, CLDN1
JUN, BMP4

G)

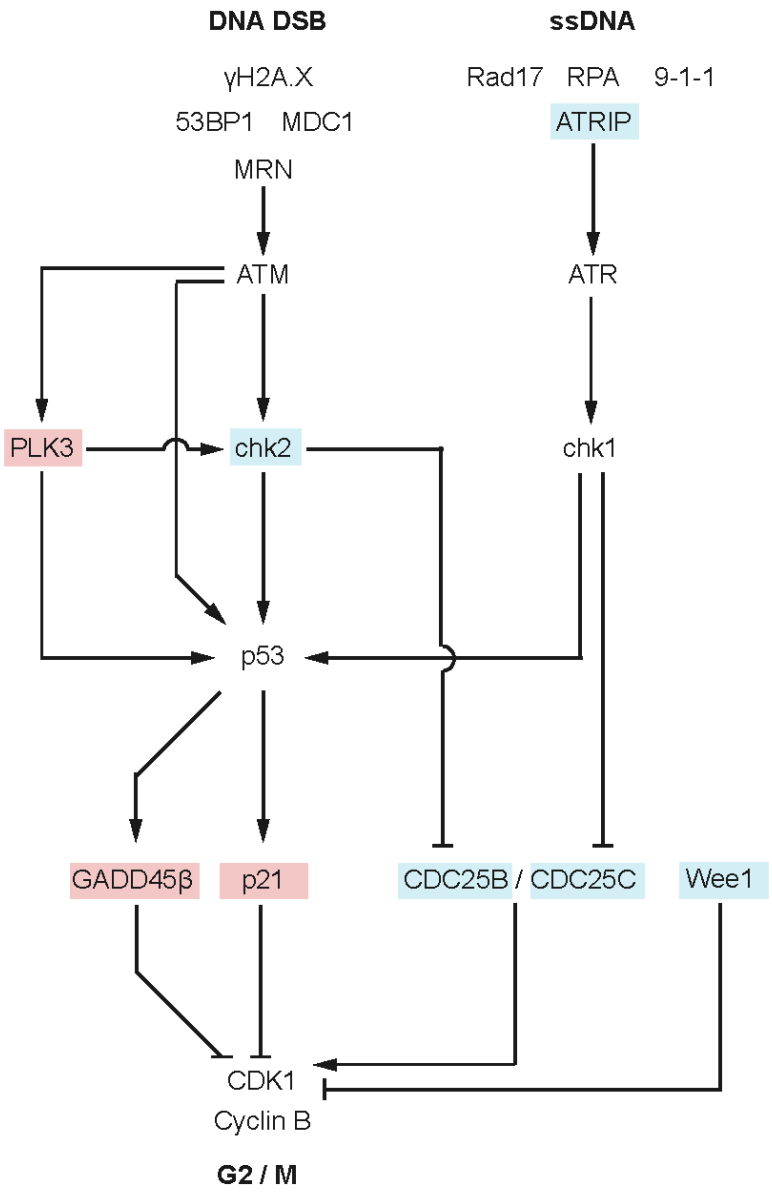
DNA DSB
ssDNA
γH2A.X
53BP1 MDC1
MRN
Rad17 RPA 9-1-1
ATRIP
ATM
ATR
PLK3
chk2
chk1
p53
GADD45β
p21
CDC25B / CDC25C
Wee1
CDK1
Cyclin B
G2 / M

H) Table of pathways significantly enriched in differentially expressed genes expressed genes following 1-24hr 1μM CX-5461.

		1hr CX-5461	3hr CX-5461	6hr CX-5461	12hr CX-5461	24hr CX-5461
		adjusted p-value	adjusted p-value	adjusted p-value	adjusted p-value	adjusted p-value
1	Development (WNT signaling pathway. Part 2)	9.446E-02	1.851E-09	1.211E-05	3.391E-03	5.129E-04
2	Reproduction (GnRH signaling)	2.774E-08	1.489E-04	5.553E-09	1.943E-07	3.485E-05
3	Development (PEDF signaling)	1.290E-03	2.157E-03	1.475E-08	2.820E-02	8.479E-04
4	Immune response (HSP60 and HSP70/ TLR signaling pathway)	1.562E-02	2.124E-08	2.755E-06	9.313E-04	6.412E-03
5	Colorectal cancer (general schema)	3.439E-02	7.477E-06	4.863E-05	6.240E-08	2.567E-05
6	Immune response (C5a signaling)	8.553E-02	3.086E-06	1.498E-07	1.024E-04	3.057E-06
7	Immune response (TLR2 and TLR4 signaling pathways)	2.267E-03	3.399E-07	5.513E-06	3.189E-04	3.390E-03
8	Development (Role of HDAC and calcium/calmodulin-dependent kinase (CaMK) in control of skeletal myogenesis)	1.562E-02	4.034E-03	4.588E-07	1.372E-02	6.412E-03
9	Immune response (IL-18 signaling)	2.067E-02	6.708E-07	2.005E-06	7.323E-03	1.546E-04
10	NF-AT signaling in cardiac hypertrophy	2.548E-02	1.007E-03	1.146E-06	3.523E-03	1.011E-02

11	Development (Angiotensin signaling via STATs)	2.700E-01	1.744E-02	5.134E-04	1.683E-02	1.202E-06
12	Development (TGF-beta-dependent induction of EMT via MAPK)	7.689E-02	6.333E-05	4.313E-04	1.378E-06	1.405E-04
13	Development (Regulation of epithelial-to-mesenchymal transition (EMT))	1.292E-01	8.898E-04	1.503E-03	1.392E-06	2.455E-05
14	DNA damage (ATM / ATR regulation of G2 / M checkpoint)	1.992E-03	1.941E-06	1.413E-06	6.949E-03	2.254E-02
15	Immune response (TNF-R2 signaling pathways)	9.515E-03	1.220E-03	1.650E-06	5.074E-03	8.603E-05
16	Transcription (Role of AP-1 in regulation of cellular metabolism)	4.877E-04	1.981E-03	6.467E-05	7.886E-06	1.892E-06
17	Immune response (TLR5, TLR7, TLR8 and TLR9 signaling pathways)	9.781E-05	1.934E-06	2.129E-05	7.283E-03	2.454E-03
18	Immune response (IL-17 signaling pathways)	2.067E-02	4.112E-06	2.005E-06	2.010E-03	4.021E-05
19	Breast cancer (general schema)	3.319E-01	6.403E-04	1.300E-04	2.239E-06	6.050E-04
20	Development (TGF-beta receptor signaling)	1.392E-03	3.086E-06	9.995E-03	2.327E-03	2.823E-02

CHAPTER 5. INHIBITION OF POL I TRANSCRIPTION BY CX-5461 INDUCES ACTIVATION OF ATM/ATR SIGNALING INDEPENDENTLY OF GLOBAL DNA DAMAGE

5.1 Introduction

RNA-sequencing analysis in BJ-T p53shRNA cells indicated that the DNA damage response (DDR) pathway is acutely regulated in response to CX-5461 treatment. Activation of these pathways results in multiple checkpoint responses, including G1 arrest, delayed replication of DNA (intra-S checkpoint), and G2 arrest (Reviewed in (Smith et al., 2010)). Further, sustained DDR pathway activation results in senescence or apoptosis (Rodier et al., 2009)(Reviewed in (Salama et al., 2014)). Therefore, activation of DDR is consistent with the phenotype observed in BJ-T and BJ-T p53shRNA cells after inhibition of Pol I transcription, and we have selected this pathway for validation.

DNA damage response (DDR) refers to the interwoven network of processes, including DNA damage recognition processes, repair pathways, and cell cycle checkpoints, which safeguard genomic integrity following structural changes to DNA. Genomic insults can create a huge variety of structurally diverse DNA lesions, and it is estimated a cell can experience 10^4-10^5 lesions each day. The vast majority of these arise as a result of direct damage by environmental agents (such as UV, IR, or genotoxic chemicals), reactive oxygen species (ROS), or spontaneous hydrolysis of nucleotide residues. Some however can also arise as a result of DNA metabolism processes, such as replication errors or uncontrolled recombination. A diverse array of specific recognition proteins and processes is required for the detection and resolution of each of these DNA alterations (Reviewed in (Giglia-Mari et al., 2011b)). However, the activation of DDR checkpoints generally involves common DNA-protein complexes that localise to either single stranded DNA (ssDNA) or double stranded breaks (DSBs), and initiate signaling cascades under the control of ATR (ATM and RAD3-related) and ATM (Ataxia-telangiectasia mutated), respectively (Reviewed in (Warmerdam and Kanaar, 2010)). ATR and ATM are phosphoinositide three-kinase-related kinases (PIKK) family kinases, which preferentially phosphorylate target proteins on serine (Ser) or threonine (Thr) residues. The mechanisms of activation and relationship between the ATM and ATR pathways are complex (Reviewed in (Smith et al., 2010)), however some characteristics of this DNA damage response are well established (FIGURE 19). ATM is activated as a result of DSBs, which can arise as a result of DNA damaging agents, collapse of replication forks, or uncapped telomeres. In

undamaged cells, ATM exists as homodimers; upon DNA damage ATM dissociate into active monomers, undergoes post-translational modification at number of sites (including autophosphorylation at Ser1981 and three other residues), and is recruited to DSB sites (Bakkenist and Kastan, 2003). The MRE11–RAD50–NBS1 (MRN) complex is also recruited to DSB sites, where it acts as a damage sensor and is required for timely DNA repair. The interaction between ATM and NBS1 (Nijmegen breakage syndrome 1) is central to ATM recruitment to DSB sites. Two major sensor proteins, 53BP1 (p53-binding protein 1) and BRCA1 (breast cancer type 1), mediate this interaction, and post-translational modification of NBS1 is also required. ATM phosphorylates MRN complex components, which in turn activate DDR processes, and maintain ATM activity at the DSB. ATM also interacts with MDC1 (mediator of DNA damage checkpoint protein 1), which is anchored to DSB sites via its interaction with histone H2A.X that is phosphorylated at Ser319 (γH2A.X). ATM phosphorylates both MDC1, enhancing its oligomerization at the DSB, and H2A.X. This results in the repeated binding of additional MDC1 molecules and the expansion of γH2A.X and the DSB foci. ATR is activated as a result of ssDNA, which can arise as a result of UV or bulky lesions that result in replication fork stalling, or resection of DSBs. RPA (Replication protein A) binds to ssDNA and recruits ATR, via both its association with ATRIP (ATR interacting protein), and its association with 9-1-1 (RAD9-HUS1-RAD1) which is recruited through RAD17. TOPBP1 (DNA topoisomerase II binding protein 1) is also localized to sites of damage, and further activates ATR. ATR phophorylates RPA, ATRIP, Rad17, 9-1-1 and TOPBP1, acting as a feedback loop to amplify checkpoint activation. The phosphorylation of a wealth of transducers by ATM and ATR, many of which are also protein kinases, relays a wide-spread signal to numerous downstream effectors of DDR, thereby activating cell cycle checkpoints and DNA repair, and mediating either checkpoint recovery or alternatively senescence or apoptosis (Matsuoka et al., 2007).

A well characterised example of ATM and ATR signaling is the activation of cell cycle checkpoints, via targeting of the CHK1 (checkpoint kinase 1) and CHK2 (checkpoint kinase 2) effector kinases (FIGURE 19). Following DNA damage, ATM-CHK2 and ATR-CHK1 pathways are activated in response to DNA double-strand breaks (DSBs) and single-stranded DNA (ssDNA) respectively. Phosphorylation of CHK1 and CHK2 occur at distinct sites, including CHK1-S317 and -S345 phosphorylation by ATR, and CHK2-T68 phosphorylation by ATM, which are commonly utilized to establish pathway activation. Progression through the cell cycle is mediated by Cyclin-CDK complexes - phosphorylation of CDK reduces the activity of these complexes to prevent cell cycle

progression, while CDC25 (cell division cycle 25) phosphatases remove inhibitory phosphate groups from CDK to enable cell cycle progression. Inhibitory phosphorylation of the CDC25A phosphatase during G1/S, and CDC25C during G2/M, by CHK1 and/or CHK2 prevents CDC25 dephosphorylation of CDKs, resulting in cell cycle arrest. Further, p53 is targeted by ATM and/or ATR (via phosphorylation at S15), or by CHK1 and/or CHK2 (via phosphorylation at S20), resulting in p53 stabilization and activation of p53-dependent cell cycle checkpoints or programmed cell death. As DDR is primarily regulated by post-translational signaling cascades, we chose to perform Western analysis of these well characterised ATM and ATR target sites to interrogate DDR pathway activation following inhibition of Pol I transcription.

5.2 ATM and ATR signaling pathways are acutely activated following inhibition of Pol I transcription by CX-5461.

Initially we examined CHK1 and CHK2 activation over a 24hr time course (FIGURE 20 A). BJ-T cells with wild-type p53 levels were used, as both ATM-CHK2 and ATR-CHK1 pathways converge at p53, and thus activation of this protein was used as a measure of pathway activity. Following 1μM CX-5461 treatment, levels of CHK2-T68 phosphorylation were increased for at early time points up to 12hrs, consistent with CHK2 activation by ATM. Levels of levels of CHK1-S345 phosphorylation were also increased for at early time points up to 6hrs, consistent with CHK1 activation by ATR. Further, levels of p53-S15 phosphorylation were increased prior to total levels of p53, consistent with p53 activation by ATM and/or ATR. Downstream cell cycle checkpoint proteins CDC25A and CDK1 were also examined. CDC25A phosphatase showed reduced levels after 24h CX-5461 treatment, consistent with its phosphorylation by CHK2, resulting in its nuclear exclusion and subsequent proteasomal degradation (Reviewed in (Donzelli and Draetta, 2003)). CDK1-Y15 phosphorylation is increased following 3h CX-5461 treatment, consistent with CDC25 inactivation. Sustained inhibitory phosphoryation of CDK1 prevents CDK1-cyclin B mediated cell cycle progression, and thus G2 cell cycle arrest (Reviewed in (Donzelli and Draetta, 2003)). Together, the data indicate that the DDR pathway is acutely activated in response to CX-5461 treatment, consistent with the RNA-Sequencing results in BJ-T p53shRNA cell lines.

To further investigate the dynamics of pathway activation, we performed Western analysis in both BJ-T and BJ-T p53shRNA cell lines at acute time points (30min to 3hr) following 1μM CX-5461 treatment (FIGURE 20 B). Increased levels of CHK2-T68,

CHK1-S345, and p53-S15 phosphorylation were observed within 30min, while increased total levels of p53 were not observed until 1hr following CX-5461 treatment. This is consistent with early p53 activation by DDR pathways. Phosphorylation of p53-S20 was not consistently observed, however phosphorylation at this site is reported to occur transiently. We were not reliably able to detect p53-S20 phosphorylation following 10Gy γIR as a positive control, and therefore we cannot conclude whether p53 is phosphorylated at this CHK1 and CHK2 target site (results not shown). Increased levels of CDK1-Y15 phosphorylation were observed at later time points, 3hr following CX-5461 treatment. Together the data indicate that both ATM and ATR targets are acutely activated following CX-5461 treatment, preceding changes in p53 and cell cycle regulatory proteins.

To investigate ATM and ATR pathway activation at different phases of the cell cycle, we performed Western analysis on live cell sorted G1, S and G2 populations of BJ-T and BJ-T p53shRNA cells (FIGURE 20 C). Following 2hr CX-5461 treatment, CHK1-S345, CHK2-T68 and p53-S15 phosphorylation occurred predominantly during S and to a lesser degree G2, but not G1 phases of the cell cycle. In contrast, total levels of p53 were increased equally across all phases of the cell cycle. To control for accuracy of sorting, RB (active in G1) and Cyclin B (expressed in G2) were used as cell cycle marker proteins. This data supports a model where ATR- and ATM- dependent signaling pathways are activated during S and G2 phases of the cell cycle in response to inhibition of Pol I transcription, by a mechanism that is independent of the well-established p53 activation by nucleolar stress (FIGURE 20 C).

To confirm that CHK1/CHK2 pathway activation was by ATM and ATR, we performed CX-5461 treatment in the presence of the ATM inhibitor KU-55933 (ATMi) (Hickson et al., 2004) and ATR inhibitor VE-821 (ATRi) (Reaper et al., 2011) (FIGURE 20 D). BJ-T cells were pre-treated with either ATMi or ATRi for 30min, prior to the addition of 1μM CX-5461 for 2hr. Phosphorylation of CHK1-S345 was inhibited in the presence of ATRi, while phosphorylation of CHK2-T68 was inhibited in the presence of ATMi. Levels of total p53 and p53-S15 phosphorylation were not reduced by either ATMi or ATRi alone, but in the presence of combined ATMi/ATRi p53-S15 phosphorylation was inhibited and levels of total p53 were reduced. This suggests that increased levels of total p53 following CX-5461 treatment were caused in part by DDR pathway activation. To confirm that the ATM and ATR signaling pathways were activated independently of p53, we also performed Western analysis of BJ-T p53shRNA cells following CX-5461 treatment in the presence of ATMi and ATRi (FIGURE 20 E). Following 2h 1μM CX-

5461 treatment, phosphorylation of CHK1-S345 and CHK2-T68 occurred at similar levels in BJ-T and BJ-T p53shRNA cells, and were dependent upon the activity of ATR and ATM respectively. Therefore, these data demonstrate that CX-5461 induces p53-independent activation of the ATM/ATR signaling pathways.

The above data demonstrates that key DDR ATM/ATR signaling pathways are activated at early time points following CX-5461 treatment, prior to the activation of p53. We have shown that ATM/ATR signaling induced by p53 activates both p53 and CHK1/CHK2 during S and G2 cell cycle phases. This is consistent with our observations that BJ-T cells treated with CX-5461 undergo p53-dependent G1 cell cycle arrest, and p53-independent S-phase delay and G2 cell cycle arrest (FIGURE 11). Therefore, the data support a model in which ATM/ATR signaling pathways mediate the p53-independent proliferation defect following inhibition of Pol I transcription by CX-5461.

5.3 ATM and ATR signaling pathways are activated in the absence of global DNA damage following inhibition of Pol I transcription by CX-5461.

As the canonical ATM and ATR signaling pathways are activated in response to DNA damage, we examined whether inhibition of Pol I transcription by CX-5461 was associated with induction of DNA damage. BJ-T cells wild-type for p53 were utilized for these assays: the ATM and ATR signaling pathways are activated in both BJ-T p53 wild type and p53shRNA cells following CX-5461 treatment (see FIGURE 20), however since p53 has established functions following DNA damage, BJ-T p53 wild type cells were expected to have greater integrity of DDR for pathway detection.

First, we examined the commonly used marker of DNA damage, γH2A.X. Depending upon the type of DNA damage, γH2A.X can spread over several megabases around DNA damage sites forming condensed foci (for example at DSBs), or can be homogenously distributed throughout the nucleus (for example at UV lesions) (Reviewed in (Giglia-Mari et al., 2011b)). Western analysis of γH2A.X was performed following treatment of BJ-T cells with 1μM CX-5461 over a time course of 10min to 3hr. No accumulation in γH2A.X levels was observed compared to untreated controls (FIGURE 21 A). In contrast, ATM/ATR signaling pathway activation was observed following just 10min of CX-5461 treatment, with maximal response by 30min (FIGURE 21 A). Therefore, we expected DNA damage to have arisen by these time points if it

was in fact driving the observed ATM/ATR signaling response. As a positive control, BJ-T cells were exposed to 10Gy γIR to induce DSBs. These cells showed increased γH2A.X levels, which were highest 30min following IR (FIGURE 21 A), consistent with reports that DSB foci are maximal approximately 30min following the induction of DSBs. Therefore, CX-5461 treatment did not induce γH2A.X levels at early time points at which ATM/ATR signaling pathway activation was detected.

We also performed immunofluorescence (IF) analysis of both γH2A.X and ATM auto-phosphorylation at Ser1981. DNA damage sites can be identified by the local concentration of DDR signaling proteins activated at the chromatin surrounding the break site, including γH2A.X and active ATM at DNA DSBs. Following 30min treatment with 1μM CX-5461, no increase was observed in DNA damage foci, using either marker. For ATM phos-S1981 foci, most cells (approximately 70-80%) displayed background foci, with an average of <5 foci per cell; no significant difference was observed in either measure between control and CX-5461 treated populations (difference between means foci per cell 0.93±2.71) (FIGURE 21 B). Positive control cells exposed to 5Gy γIR displayed an increase in ATM phos-S1981 foci (approximately 20 foci per cell. n.s.), while cells treated with 10μM KU-55933, which inhibits ATM auto-phosphoryation at S1981 and therefore acts as a negative control, did not display any detectable foci (FIGURE 21 B). For γH2A.X foci, approximately 10-15% of cells displayed foci, with an average of less than one foci per cell; no significant difference was observed in either measure between control and CX-5461 treated populations (difference between means foci per cell -0.27±0.29) (FIGURE 21 C). All positive control cells exposed to 5Gy γIR displayed abundant γH2A.X foci (approximately 35 foci per cell. **p<0.005 compared to control and CX-5461 treated cells) (FIGURE 21 C). These results are consistent with earlier experiments establishing the senescence phenotype, which showed γH2A.X foci did not increase until 48-96hr following CX-5461 treatment (See FIGURE 12). Thus to summarise, DNA damage foci were not detected at early time points following CX-5461 treatment, indicating that the ATM/ATR signaling pathway was not activated as a result of DNA damage.

We considered that ATM/ATR signaling pathway activation might occur as a result of DNA damage specifically at the rDNA, and that our assays might not have been sensitive enough to detect the induction of DNA damage at these sites. Therefore, as a positive control we utilised an established U2TR I-*Ppo*I-dd cell line in which DNA

damage can be induced at a defined site in the rDNA. I-*Ppo*I is an intron-encoded homing endonuclease from the myxomycete *Physarum polycephalum* that cuts with high specificity at an endogenous 15bp recognition sequence. This recognition sequence exists in the 28S transcribed region of rDNA. In human cells, it has been reported that approximately 10% of the rDNA copies are cut in presence of the I-*Ppo*I enzyme. A few other single copy cut sites can also be found outside the rDNA repeats, due to the degeneracy of the I-*Ppo*I restriction sequence (Muscarella et al., 1990; Flick et al., 1998; Monnat Jr et al., 1999). The human osteosarcoma U2OS cell line was derived from a moderately differentiated sarcoma in a 15 year old female, in 1964 (Ponten and Saksela, 1967). It contains functional p53 and RB, but does not express endogenous p16 (Diller et al., 1990; Stott et al., 1998). Importantly, it expresses ATM, ATR and other DDR pathway proteins at high levels, and is commonly utilised for interrogation of these pathways (Gately et al., 1998). The U2TR I-*Ppo*I-dd system has two levels of control of endonuclease activity. First, U2OS-TR (U2TR) cells stably express tetracyclin repressor protein, enabling levels of expression of the I-*Ppo*I-dd protein to be regulated through a tetracycline inducible promoter. Second, the addition of a destabilization domain (dd) to I-*Ppo*I targets the endonuclease for proteasomal degradation. Shield-1 ligand binds to this domain and stabilizes the I-*Ppo*I-dd protein, enabling rapid induction of its levels in the cell (Banaszynski et al., 2006). Together these provide tight control of onset of DSBs at the rDNA.

We induced I-*Ppo*I endonuclease activity for 3hr in U2TR I-*Ppo*I-dd in order to generate DSBs at 28S rDNA. The level of DNA damage at the 28S target site can be determined by qRT-PCR using primers that flank the I-*Ppo*I target site, as DSBs within the amplified region result in a loss of PCR product compared to undamaged sites in the human genome (Berkovich et al., 2007, 2008). Following 3hr I-*Ppo*I induction, amplification of the 28S rDNA cut site was significantly reduced (FC=0.65, *$p<0.05$ compared to uninduced vehicle control), indicating that there are sufficient levels of endonuclease activity and DNA damage at the rDNA (FIGURE 21 D). We also performed Western analysis to determine whether the ATM/ATR signaling pathways were activated. Following 2hr 1μM CX-5461 treatment, increased levels of p53-S15 phosphorylation and CHK2-T68 phosphorylation were detected, consistent with the results in BJ-T cells. Following 3hr I-*Ppo*I induction, increased levels of p53-S15 phosphorylation and CHK2-T68 phosphorylation were also detected, and I-*Ppo*I induced cells also displayed increased levels of γH2A.X (FIGURE 21 E). This indicates that following I-*Ppo*I induction, DNA damage is induced at the 28S endonuclease

target site in the rDNA, and activation of ATM/ATR signaling pathway can be robustly detected.

To determine whether the induction of DNA damage could be detected when it occurs specifically at the rDNA, we performed co-immunofluorescence analysis of DNA damage foci at the nucleoli (FIGURE 21 F and G). UBF was selected to be the nucleolar marker, as it binds across the entire transcribed region of transcriptionally competent rDNA, and therefore is expected to associate closely with the 28S cleavage site. ATM phos-S1981 and γH2A.X were used as markers of DSB foci. IF analysis showed that in the absence of I-*Ppo*I induction, cells have low levels of DNA damage at sites outside of the rDNA repeats. For both ATM phos-S1981 and γH2A.X, the majority of cells displayed less than ten DSB foci. Some cells displayed DSB foci that co-localised with the nucleolar marker UBF (in approximately 28% of cells for ATM phos-S1981 and 13% of cells for γH2A.X), which could be due to background I-*Ppo*I activity. However, very few cells displayed multiple DSB foci at the rDNA or altered nucleolar morphology, indicating background I-*Ppo*I activity is low relative to that in I-*Ppo*I induced cells. In cells in which I-*Ppo*I was induced, multiple DSB foci co-localised with the nucleolar marker UBF (in approximately 55% of cells for ATM phos-S1981 and 74% of cells for γH2A.X). These cells, in which DSB foci are detected at the rDNA, also displayed strikingly altered nucleolar morphology. Specifically, UBF relocalised to one or two foci at the periphery of a condensed nucleoli, which could be identified by the absence of DAPI staining of DNA. This is consistent with the direct inhibition of Pol I transcription by DDR pathways, as has been previously reported, and the well-described reorganisation of the nucleoli following DNA damage that results in altered nucleolar proteome and the formation of nucleolar caps around a nucleolar remnant (Shav-Tal et al., 2005; Kruhlak et al., 2007; Boisvert et al., 2010; Calkins et al., 2013) (Reviewed in (Boulon et al., 2010a)). Therefore, our assays are clearly able to detect DNA damage when it is present specifically at the rDNA. To further confirm that DNA damage was not induced at the rDNA following inhibition of Pol I transcription by CX-5461, we performed IF analysis for ATM phos-S1981 and γH2A.X in U2TR I-*Ppo*I-dd cell lines following 2hr 1μM CX-5461 treatment (FIGURE 21 F&G). Consistent with our results in BJ-T cells, no increase in DNA damage foci could be detected following CX-5461 treatment (with DSB foci co-localised with UBF in approximately 10% of cells for both ATM phos-S1981 and γH2A.X).

Finally, we extended our analysis of DNA damage following CX-5461 treatment in BJ-T cells to include additional types of DNA lesions. Comet assays are commonly used to determine levels of DNA damage; they can be performed under neutral conditions, which detect DSBs, or alkaline conditions, which detect DSBs, SSBs, and the majority of abasic sites and DNA adducts (Collins, 2002). In cells that have DNA damage, fragments migrate out of the nucleus under the influence of an electric current, forming a 'tail'. Increased extent tail moment (ETM), a measure of the length and proportion of DNA in the tail, reflects increased levels of DNA damage. Following 30min treatment with 1μM CX-5461, no difference was observed in comet tails under neutral conditions, between control and treated cells (results not shown). Subsequently, more sensitive alkali conditions were used for analysis. Following 30min treatment with 1μM CX-5461, comet tails under alkali conditions also had no significant difference in ETM between control and CX-5461 treated populations (difference between means 0.24±45.6, n.s. for n=4 experiments) (FIGURE 21 H). In contrast, significantly increased ETM was observed for positive control cells exposed to 500μJ UV (from 140 ETM in control and CX-5461 treated cells, to 290 ETM in UV treated cells **$p<0.005$). Therefore, CX-5461 treatment does not increase general DNA damage in the cell at this early time point.

Therefore, we have shown 30min 1μM CX-5461 treatment did not induce detectable DNA damage, either genome wide or specifically at the rDNA, as determined by Western analysis of γH2A.X, IF analysis of DNA damage foci, and comet analysis. As activation of the ATM/ATR signaling pathways is observed following 30min 1μM CX-5461 treatment, we conclude that this pathway is likely being activated by a mechanism other than the induction of DNA damage typically associated with ATM/ATR activation.

5.4 ATM and ATR signaling pathways mediate the p53-independent cell cycle checkpoints following inhibition of Pol I transcription with CX-5461.

We have shown that following CX-5461 treatment of BJ-T cells, the ATM and ATR signaling pathways are activated predominantly in S and G2 phases of the cell cycle, and cells undergo p53-independent S-phase delay and G2 cell cycle arrest. This led us to propose that the p53-independent proliferation defect is mediated by ATM/ATR signaling pathway. Therefore, we investigated the relative contribution of ATM and ATR signaling to the regulation of cell cycle checkpoints following inhibition of Pol I transcription with CX-5461.

First, we examined cell cycle profiles in BJ-T and BJ-T p53shRNA cells treated with CX-5461 in the presence of the ATM and/or ATR inhibitors (FIGURE 22 A and B). BJ-T and BJ-T p53shRNA cells treated with either 5μM KU-55933 (ATMi) and/or 1μM VE-821 (ATRi) alone did not display any changes in BrdU/PI cell cycle profiles following 24hr treatment. BJ-T cells treated with CX-5461 displayed similar proportions of G1 and G2/M cell cycle arrest in the presence of ATMi and ATRi, though the S-phase delay appeared to be partially rescued in the presence of both inhibitors (FIGURE 22 A). In contrast, BJ-T p53shRNA cells treated with CX-5461 displayed markedly different proportions of G1, S, and G2/M cell cycle populations following 24hr treatment in the presence of ATMi and ATRi (FIGURE 22 B). Cells treated with CX-5461 in the presence of ATMi or ATRi alone exhibited a relatively reduced proportion of cells in S phase, compared to cells treated with CX-5461 alone (50% in CX-5461 only treated cells, compared to 42% in ATMi (*$p<0.05$) and 37% in ATRi combination treated cells). Cells treated with CX-5461 in the presence of ATMi/ATRi combined displayed a relatively reduced proportion of cells in S-phase, and also an increased proportion of cells in both G1 and G2/M phase (33% G1 / 15% S / 17% G2/M in CX-5461 only, compared to 38% G1 / 32% S / 29% G2/M in ATMi/ATRi combination treated cells). This suggests that inhibition of ATM and ATR activity can partially rescue the p53-independent S-phase delay and G2 cell cycle arrest following treatment with CX-5461.

Escape from the G2 cell cycle arrest appeared to be associated with increased cell death. BJ-T cells treated with CX-5461 displayed similar levels of cell death in the presence of ATMi and ATRi, with no increase in either Sub-G1 populations after 24hr (3-5% of cells), or Annexin V positive populations after 72hr (10-15% of cells), compared to cells treated with CX-5461 alone (FIGURE 22 A). In contrast, BJ-T p53shRNA cells treated with CX-5461 displayed increased levels of cell death in the presence of ATMi /ATRi combined, with slightly increased proportions of Sub-G1 populations after 24hr (from 2% to 12%, *$p<0.05$), and Annexin V positive populations after 72hr (from 14% to 29%), compared to cells treated with CX-5461 alone (FIGURE 22 B).

To further establish the role of ATM and ATR signaling in the activation of p53-independent cell cycle checkpoints following CX-5461 treatment, we performed time-course cell cycle experiments of BJ-T p53shRNA cells treated with CX-5461 in the presence of high dose ATM and ATR inhibitors (FIGURE 22 C). BrdU/PI cell cycle

analysis was performed at 3hr, 6hr, 12hr, 24hr, and 96hr. Cells treated with CX-5461 in the presence of 10μM KU-55933 (ATMi) displayed partial rescue of the S-phase delay, but a similar proportion of cells arrested in G2, compared to cells treated with CX-5461 alone. Cells treated with CX-5461 in the presence of 10μM VE-821 (ATRi) displayed a decreased proportion of cells in G2, compared to cells treated with CX-5461 alone. Cells treated with CX-5461 in the presence of ATMi/ATRi combined display a markedly decreased proportion of cells in G2. To determine if the decreased proportion of cells in G2 was associated with an increased proportion of cells entering M, we performed phos-H3 analysis of cells following 12hr treatment. Cells treated with CX-5461 in the presence of ATRi, or ATMi/ATRi combined, appeared to have an increased proportion of cells in M (with levels restored to those observed in vehicle control cells, approximately 1-1.5%) (FIGURE 22 D). This supported our earlier results, indicating that inhibition of ATM and ATR activity can partially rescue the p53-independent S-phase delay and G2 cell cycle arrest following treatment with CX-5461.

We had observed both rescue of the S-phase and G2 cell cycle defects, as well as increased levels of cell death, in BJ-T p53shRNA cells treated with CX-5461 when ATM and ATR activity are inhibited. Therefore, we next examined whether rates of cell proliferation following CX-5461 treatment are increased or decreased in the presence of ATMi and/or ATRi. BJ-T and BJ-T p53shRNA cells were treated with 5μM KU-55933 (ATMi) and/or 1μM VE-821 (ATRi), at which doses we did not observe changes in rates of proliferation following treatment alone (FIGURE 23 A and B); and 100nM CX-5461, at which dose we had previously observed reduced levels of proliferation but no increase in cell death (BJ-T approximate doubling times: control=40hr, CX-5461=183hr ****$p<0.0001$ for n=3 experiments. BJ-T p53shRNA approximate doubling times: control=37hr, CX-5461=112hr **$p<0.005$ for n=3 experiments) (See FIGURE 9). In BJ-T cells treated with CX-5461, we did not observe a change in the rates of proliferation in the presence of ATMi, we observed slightly reduced rates of proliferation in the presence of ATRi (approximate doubling times: CX-5461=183hr, CX-5461/ATRi=506hr **$p<0.005$ for n=3 experiments), and cells were arrested completely in the presence of ATMi/ATRi combined (approximate doubling times: CX-5461=183hr, CX-5461/ATMi/ATRi=∞ **$p<0.005$ for n=3 experiments) (FIGURE 23 A). As we did not observe increase in cell death in BJ-T cells treated with CX-5461 and ATMi/ATRi combined (FIGURE 22 A), these results suggest treatment with ATMi and ATRi promotes activation of p53-dependent cell cycle checkpoints following CX-5461 treatment. In BJ-T p53shRNA cells treated with CX-5461, we did not observe a

change in rates of proliferation in the presence of ATMi, but we observed reduced rates of proliferation at levels indicative of cell death in the presence of ATRi (approximate doubling times: CX-5461=112hr, CX-5461/ATRi=∞ *p<0.05 for n=3 experiments), and to a greater degree in the presence of ATMi/ATRi combined (approximate doubling times: CX-5461=112hr, CX-5461/ATMi/ATRi=∞ *p<0.05 for n=3 experiments) (FIGURE 23 B). As rescue of the G2 cell cycle defect was also observed in BJ-T p53shRNA cells treated with ATRi and combined ATMi/ATRi (FIGURE 22 B), these results suggest that escape from ATM and ATR mediated cell cycle checkpoints following CX-5461 treatment does not result in increased rates of proliferation, but instead results in cell death.

We also examined rate of cell proliferation following CX-5461 treatment in the presence of combined CHK1/CHK2 inhibitor AZD7762 (CHK1/CHK2i) (Zabludoff et al., 2008). In BJ-T cells, slightly reduced rates of proliferation were observed in both cells treated with CHK1/CHK2i alone, and cells treated with CX-5461 and CHK1/CHK2i (FIGURE 23 A). This suggests that when ATM and ATR are active, inhibition of CHK1 and CHK2 can result in activation of p53-dependent cell cycle checkpoints, consistent with previously published results. In BJ-T p53shRNA cells and BJ-LSTR cells, we did not observe changes in rates of proliferation following treatment with CHK1/CHK2i alone. In cells treated with CX-5461, only a slight reduction of proliferation was observed in the presence of CHK1/CHK2i (n.s. for n=3 experiments) (FIGURE 23 B and C). This suggests that the ATM and ATR kinases can mediate the response to CX-5461 through their targets in addition to CHK1 and CHK2.

Finally, we examined whether inhibition of the ATM and ATR signaling pathway can also promote the anti-proliferative effect of CX-5461 in transformed BJ-LSTR cell lines. In BJ-LSTR cells, slightly reduced rates of proliferation were observed in both cells treated with ATMi alone (*p<0.05 for n=3 experiments), and cells treated with combined ATMi/ATRi alone (**p<0.005 for n=3 experiments). This suggests ATMi has an anti-proliferative effect in this transformed cell line, consistent with previously published results (Li and Yang, 2010). However, BJ-LSTR cells treated with ATRi alone did not display a change in rates of proliferation, while BJ-LSTR cells treated with CX-5461 displayed reduced rates of proliferation indicative of cell death in the presence of ATRi, and to a greater degree in the presence of ATMi/ATRi combined (approximate doubling times: control=34hr, CX-5461=81hr ****p<0.0001 for n=3 experiments, CX-5461=81hr, CX-5461/ATRi=∞ ****p<0.0001 for n=3 experiments,

CX-5461=81hr, CX-5461/ATMi/ATRi=∞ ***p<0.0005 for n=3 experiments) (FIGURE 23 C). These results suggest that the combination of ATM and ATR inhibitors with CX-5461 treatment can moderately increase the anti-proliferative effect of these inhibitors in transformed cell lines.

Collectively, these results show that the ATM and ATR signaling pathways mediate, at least in part, the p53-independent cell cycle checkpoints following inhibition of Pol I transcription by CX-5461. Inhibition of ATR and ATM activity in BJ-T p53shRNA cells can rescue the cell cycle defects, with cells partially escaping S-phase delay and G2 arrest induced by CX-5461 treatment. In contrast, inhibition of ATM and ATR activity in BJ-T p53 wild-type cells does not rescue the G2 cell cycle arrest, indicating that p53 can mediate both G1 and G2 cell cycle arrest following CX-5461 treatment, consistent with the known functions of p53 in cell cycle checkpoint regulation. BJ-T p53shRNA cells also display reduced rates of proliferation associated with increased levels of cell death following CX-5461 treatments in the presence of ATR and ATM inhibitors, suggesting that escape from cell cycle checkpoints following CX-5461 treatment drives cells to undergo cell death.

5.5 Discussion

To identify primary signaling pathways that underlie the p53-independent phenotypic responses to inhibition of Pol I transcription by CX-5461, we had performed RNA-sequencing analysis in BJ-T p53shRNA cells at acute time points following CX-5461 treatment. The DNA damage (ATM/ATR regulation) pathway was identified by functional gene ontology enrichment analysis of differentially expressed genes, and we selected this pathway for further validation. Western analysis of ATM/ATR kinase substrates CHK1 and CHK2 demonstrated that they were activated by phosphorylation at their ATM and ATR target sites, CHK2 phos-T68 and CHK1 phos-S345 respectively, by 30min following CX-5461 treatment (FIGURE 20 B). In addition, co-treatment with ATM inhibitor prevented activation of CHK2 phos-T68, and ATR inhibitor prevented activation of CHK1 phos-S345. This confirms that ATM and ATR are required for the activation of this pathway following CX-5461 treatment (FIGURE 20 B). Further work from our laboratory has also directly detected activation of ATM by western analysis of its auto-phosphorylation site ATM phos-S1987 following 2hr treatment with 1μM CX-5461 in BJ-T cells (Quin et al., 2016). Therefore, we were able

to validate our RNA-sequencing data and demonstrate that ATM/ATR signaling pathway is rapidly activated in response to inhibition of Pol I transcription by CX-5461.

One surprising result is that the ATM/ATR signaling pathway is activated in the apparent absence of DNA damage. The canonical ATM and ATR signaling pathways are activated in response to DSBs and ssDNA, respectively (Reviewed in (Giglia-Mari et al., 2011a)). However, at early time points following CX-5461 treatment, at which we could detect ATM/ATR dependent activation of CHK1 phos-S345 and CHK2 phos-T68, we did not detect any increase in DNA damage. We utilized a number of assays for DNA damage. These included western analysis of levels of the commonly used marker of DNA damage γH2A.X, IF analysis for specific DNA damage foci using both γH2A.X and ATM autophosphorylation site ATM phos-S1981, and alkaline comet assays which detect DSBs, SSBs, as well as other DNA lesions. However, no DNA damage above background was detected by any of these assays 30min following CX-5461 treatment (FIGURE 21), at which time increased levels of CHK1 phos-S345 and CHK2 phos-T68 could already be observed. Further, no increase in γH2A.X levels could be detected by western analysis for up to 3hr following CX-5461 treatment, at which time robustly increased levels of CHK1 phos-S345 and CHK2 phos-T68 had been observed for over 2hrs (FIGURE 21 A). We also utilized an rDNA targeting endonuclease (I-*Ppo*I) as a positive control for detection of DNA damage at the rDNA, in an inducible expression system in U2OS cell lines. In this U2TR I-*Ppo*I-dd system, we could detect DNA damage by both western analysis of γH2A.X levels (FIGURE 21 E), and IF analysis of DNA damage foci at the rDNA using IF for both γH2A.X and ATM phos-S1981 (FIGURE 21 F and G), giving us confidence our assays were of sufficient sensitivity to detect DNA damage specifically at these sites. The activation of ATM and ATR by non-canonical mechanisms independent of DNA damage has previously been reported (See Section 5.1 for examples). However, a mechanism accounting for the activation of ATM/ATR by inhibition of Pol I transcription and/or nucleolar disruption had not previously been described. Thus, ATM/ATR signaling is activated independently of DNA damage by a novel non-canonical pathway following inhibition of Pol I transcription by CX-5461.

To better understand the roles of the p53 and ATM/ATR signaling pathways in mediating the cell cycle checkpoint responses to inhibition of Pol I transcription by CX-5461, we performed western analysis of pathway activation in G1, S and G2 population, as well as western and cell cycle analysis in the presence of ATM and ATR

inhibitors. These results lead us to propose the following model, which is presented in FIGURE 24. First, activation of p53 by the nucleolar stress pathway mediates G1 cell cycle arrest. In support of this, knock-down of p53 is sufficient to rescue the G1 arrest phenotype (FIGURE 22 A and B), and in G1 only increased levels of total p53, and not increased levels of ATM/ATR signaling targets p53 phos-S15, CHK1 phos-S345 and CHK2 phos-T68, are observed (FIGURE 20 C). Second, activation of p53 by the nucleolar stress pathway may mediate S-phase delay and G2 cell cycle arrest independently of ATM/ATR. In support of this, p53 wild type cells maintain G2 cell cycle arrest in the presence of combined ATM/ATR inhibition (FIGURE 22 A), and levels of total p53 are increased in G1, S and G2 (FIGURE 20 C). Levels of total p53 are also increased in in the presence of combined ATM/ATR inhibition, though at a reduced amount (FIGURE 20 C). Third, ATM/ATR signaling is specifically activated in S and G2. In support of this, levels of ATM/ATR signaling targets p53 phos-S15, CHK1 phos-S345 and CHK2 phos-T68 are not increased in G1, but are increased predominantly in S-phase, and also to a lesser extent in G2 (FIGURE 20 C). Fourth, ATM/ATR signaling can also activate p53. In support of this, levels of ATM/ATR signaling target p53 phos-S15 are increased concomitantly with ATM/ATR signaling targets CHK1 phos-S345 and CHK2 phos-T68 (FIGURE 20 B and C), and inhibition of both ATM and ATR results in the absence of p53 phos-S15, and reduced levels of total p53 (FIGURE 20 D). Fifth and finally, ATM/ATR signaling mediates p53-independent S-phase delay and G2 cell cycle arrest. In support of this, in the absence of p53, inhibition of ATM or ATR partially rescue the cell cycle defects, particularly the S-phase delay, and combined inhibition of ATM and ATR rescues the cell cycle defects to enable cells to progress to mitosis at rates equivalent to that in untreated cells (FIGURE 22 C and D). Therefore, according to our model, inhibition of both p53 and ATM/ATR signaling pathways is required for cells to escape the cell cycle checkpoint responses to inhibition of Pol I transcription by CX-5461 (FIGURE 24). Cells that escape cell cycle checkpoint responses to CX-5461 remain unable to execute normal proliferation, and instead progression through G2 and into mitosis is associated with increased levels of cell death (FIGURE 22 B).

The identification of this pathway has important implications for the therapeutic use of CX-5461. We have shown that in tumorigenic BJ-LSTR cell lines, combined ATM/ATR inhibition and CX- 5461 treatment resulted in an increased anti-proliferative effect of CX-5461 (FIGURE 23 C). Therefore, we extended our analysis to determine whether combination therapy with ATM/ATR inhibitors increased the therapeutic efficacy of CX-5461, using the murine model of Eμ-*Myc* lymphoma. Our research group had

previously shown that CX-5461 selectively induces cell death in malignant B-cells *in vivo* in this model, and that sensitivity of this tumor type to CX-5461 is dependent upon p53 (Bywater et al., 2012) (See Section 3.7). In experiments performed by Jennifer Devlin, we first examined whether CX-5461 activates ATM/ATR signaling in p53 wild-type and p53 -/- Eμ-*Myc* lymphoma cell lines. Following 30min treatment with CX-5461, activation of p53 phos-S15 was observed in p53 wt cells, and activation of chk1 phos-S345 was observed in both p53 wt and p53 -/- cells, at doses of 300nM and above. We could not examine activation of chk2 phos-T68 due to a lack of mouse specific antibodies. Therefore, inhibition of Pol I transcription by CX-5461 also acutely activates the ATM/ATR singling pathway in this model. Cell cycle analysis of these p53 wt and p53 -/- Eμ-*Myc* lymphoma cell lines following 24hr treatment with 100nM CX-5461 indicated that while p53 wt cells are more sensitive to CX-5461 (~10% Sub-G1 in vehicle, and ~70% Sub-G1 in CX-5461 treated cells), inhibition of Pol I transcription by CX-5461 induces a G2 cell cycle defect and cell death in p53 -/- cells (~ 5% Sub-G1 in vehicle, and ~60% Sub-G1 in CX-5461 treated cells). Importantly, combined treatment of p53-/- Eμ-*Myc* lymphoma cells with CX-5461 and the dual Chk1/Chk2 inhibitor AZD7726 abrogates the G2 arrest, and results in significantly increased levels of cell death compared to treatment with CX-5461 alone (Quin et al., 2016). Finally, *in vivo* analysis in mice with established disease from transplanted p53 -/- Eμ-*Myc* lymphoma showed that treatment with CX-5461 can provide a modest survival benefit in p53 -/- Eμ-*Myc* lymphoma, and that combination therapy with CX-5461 and AZD7726 resulted in significantly increased survival benefit compared to single agent treatment (Quin et al., 2016). Therefore, we have shown that targeted inhibition of the ATM/ATR signaling pathway can lead to improved therapeutic benefit in the treatment of cancers lacking functional p53 with CX-5461.

Two recently published papers report similar activation of ATM/ATR signaling. Ma and Pederson (Ma and Pederson, 2013) reported that inhibition of Pol I transcription by ActD treatment in the HeLa cervical adenocarcinoma cell line induces activation of an ATR-CHK1 meditated G2 checkpoint in the absence of DNA damage, but that activation of this pathway requires that cells be treated with the inhibitor for sufficient time (>2hr) to prevent rRNA synthesis recovering to normal levels following withdrawal of treatment. Negi and Brown (Negi and Brown, 2015a) reported that inhibition of Pol I transcription by CX-5461 treatment in the NALM-6 p53 wild type and SEM p53 mutant acute lymphoblastic leukemia (ALL) cell lines results in activation of ATM/ATR mediated G2 cell cycle arrest and induces apoptosis. In the SEM cell line, treatment

with ATR inhibitor VE-821 or CHK1/CHK2 inhibitor UCN-01 was sufficient to rescue the G2 cell cycle arrest and enhance apoptosis in combination with CX-5461. In ALL cells, transient inhibition of Pol I transcription by CX-5461 was sufficient to induce G2 arrest and commit cells to cell death, despite reactivation of rRNA synthesis within 24hr (Negi and Brown, 2015b). These findings support our results identifying ATM/ATR signaling as a key pathway mediating the response to inhibition of Pol I transcription, that can be exploited for improved therapeutic applications.

Other research groups have also reported alternative p53-independent mechanisms of cell cycle regulation following inhibition of Pol I transcription (Reviewed in (James et al., 2014)). For example, RP11 inhibition of HDM2 results in the destabilization of E2F-1 transcription factor following siRNA knock-down of *POLR1A,* encoding the catalytic subunit of RNA polymerase I (Donati et al., 2011b); or increased proteasomal degradation of PIM1 results in increased levels of its target $p27^{Kip1}$ cell cycle inhibitor, following ActD treatment (Iadevaia et al., 2010). While we have identified and validated one pathway by which inhibition of Pol I transcription can mediate phenotypic responses in BJ-T cells, we believe it is likely that other pathways are also involved. This is supported by our observation that while inhibition of the ATM/ATR signaling pathways rescues BJ-T cells from p53-independent S and G2 phase cell cycle arrest, these cells still display additional phenotypes including a mitotic cell cycle defect and increased rates of cell death, suggesting undefined nucleolar functions mediate additional responses to inhibition of Pol I transcription. The RNA-sequencing data we present here may be a valuable tool for the identification and validation of additional pathways involved in mediating the response to both acute and long-term inhibition of Pol I transcription.

FIGURE 19. Schematic of the ATM and ATR DNA damage response signaling pathways. ATM is activated in response to DNA double stranded breaks (DSBs). ATM dissociates from homodimers into active monomers, undergoes post-translational modification at number of sites (including autophosphorylation at Ser1981) and is recruited to DSB sites. The MRE11–RAD50–NBS1 (MRN) complex is also recruited to DSB sites. The interaction between ATM and NBS1 is central to ATM recruitment to DSB sites, and this interaction is mediated by 53BP1 and BRCA1. ATM phosphorylates MRN complex components, which in turn activate DDR processes, and maintain ATM activity at the DSB. MDC1 is anchored to DSB sites by γH2A.X. ATM phosphorylates both MDC1, enhancing its oligomerization at the DSB, and H2A.X, resulting in expansion of MDC1 molecules and γH2A.X and the DSB foci. ATR is activated in response to single stranded DNA (ssDNA). RPA binds to ssDNA and recruits ATR, via its association with both ATRIP and RAD9-HUS1-RAD1 (9-1-1) complex which is recruited through RAD17. TOPBP1 is also localized to sites of damage, and further activates ATR. ATR phophorylates RPA, ATRIP, RAD17, 9-1-1 and TOPBP1 amplifying checkpoint activation. The phosphorylation of downstream transducers by ATM and ATR relays a wide-spread signal to numerous effectors of DDR. The activation of cell cycle checkpoints is one example. ATM activates CHK2 (including Thr68 phosphorylation), while ATR activates CHK1 (including Ser317 and Ser345 phosphorylation). Inhibitory phosphorylation of the CDC25A (G1/S), and CDC25C (G2/M), by CHK1 and/or CHK2 prevents CDC25 activating dephosphorylation of CDKs, resulting in cell cycle arrest. p53 is targeted by ATM and/or ATR (via phosphorylation at S15), or by CHK1 and/or CHK2 (via phosphorylation at S20), resulting in p53 stabilization and activation.

FIGURE 19

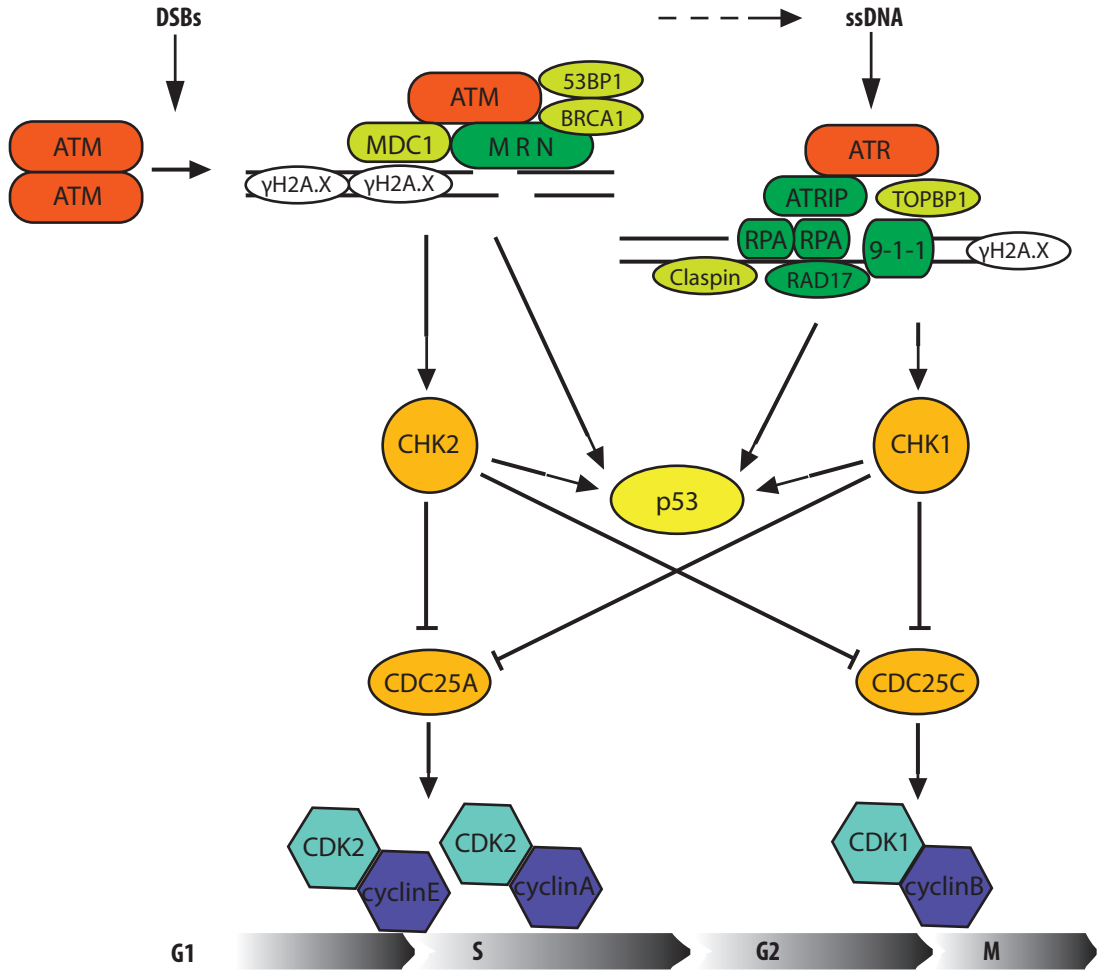
DSBs
ssDNA
ATM
ATM
ATM
53BP1
BRCA1
MDC1
M R N
γH2A.X
γH2A.X
ATR
ATRIP
TOPBP1
RPA
RPA
9-1-1
γH2A.X
Claspin
RAD17
CHK2
CHK1
p53
CDC25A
CDC25C
CDK2
cyclinE
CDK2
cyclinA
CDK1
cyclinB
G1
S
G2
M

FIGURE 20. Inhibition of Pol I transcription by 1μM CX-5461 treatment acutely activates ATM and ATR signaling pathways in BJ-T cells. A) Western blot of analysis of BJ-T cells treated with 1μM CX-5461 for 3hr, 6hr, 12hr, and 24hr compared to untreated control (representative of n=2 experiments). **B)** Western blot of analysis of BJ-T (left panel) and BJ-T p53shRNA (right panel) cells treated with 1μM CX-5461 for 30min, 1hr, 2hr, and 3hr compared to 30min NaH_2PO_4 vehicle control (0hr) (representative of n=5 experiments). **C)** Western blot of analysis of BJ-T (left panel) and BJ-T p53shRNA (right panel) cells treated with 1μM CX-5461 for 2hr, then sorted into G1, S and G2/M phase populations based on live cell DNA stain using FACS. Active RB and Cyclin B levels were used to control for G1 and G2 phase populations, respectively (representative of n=3 experiments). **D)** Western blot of analysis of BJ-T cells +/- pre-treated with ATMi KU55933 or ATRi VE-821 for 30min, then +/- treated with 1μM CX-5461 in the presence of the inhibitors for an additional 2hr (representative of n=5) **E)** Western blot of analysis of BJ-T p53shRNA cells +/- pre-treated with ATMi KU55933 or ATRi VE-821 for 30min, then +/- treated with 1μM CX-5461 in the presence of the inhibitors for an additional 2hr, compared to BJ-T cells treated with CX-5461 for 2hrs (representative of n=3).

FIGURE 20
A)

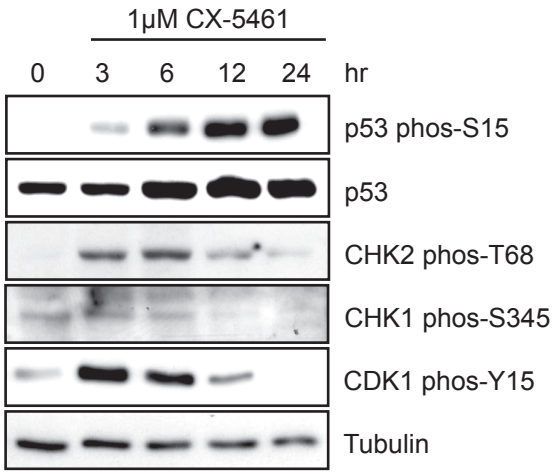
1μM CX-5461
0
3
6
12
24
hr
p53 phos-S15
p53
CHK2 phos-T68
CHK1 phos-S345
CDK1 phos-Y15
Tubulin

B)

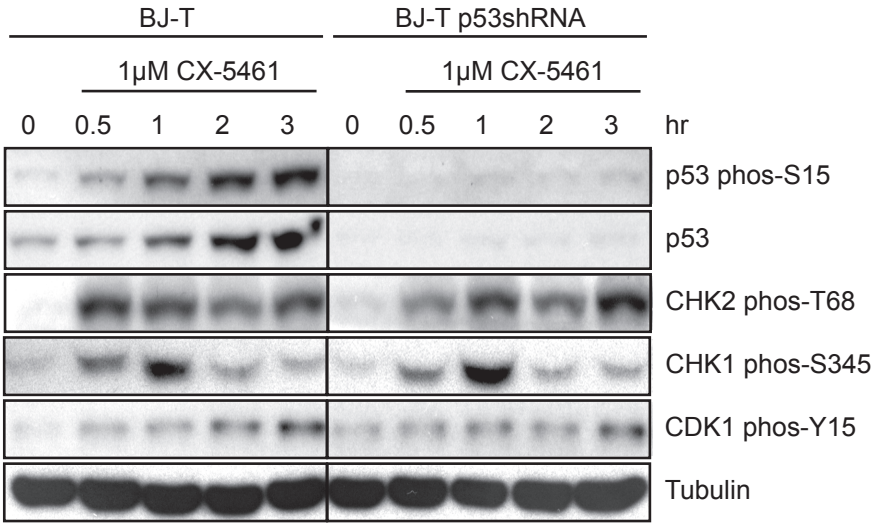
BJ-T
BJ-T p53shRNA
1μM CX-5461
1μM CX-5461
0
0.5
1
2
3
0
0.5
1
2
3
hr
p53 phos-S15
p53
CHK2 phos-T68
CHK1 phos-S345
CDK1 phos-Y15
Tubulin

C)

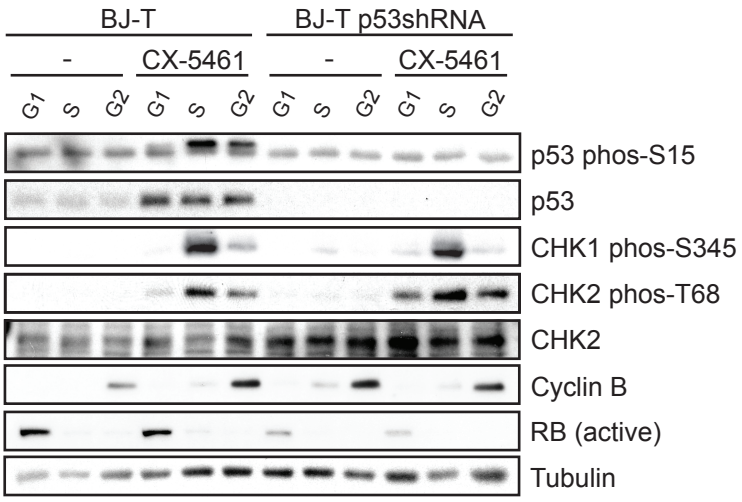
BJ-T
BJ-T p53shRNA
-
CX-5461
-
CX-5461
G1
S
G2
G1
S
G2
G1
S
G2
G1
S
G2
p53 phos-S15
p53
CHK1 phos-S345
CHK2 phos-T68
CHK2
Cyclin B
RB (active)
Tubulin

D)

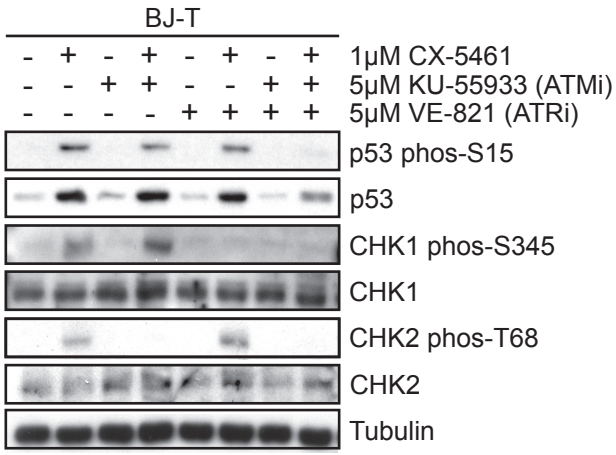
BJ-T
- + - + - + - + 1μM CX-5461
- - + + - - + + 5μM KU-55933 (ATMi)
- - - - + + + + 5μM VE-821 (ATRi)
p53 phos-S15
p53
CHK1 phos-S345
CHK1
CHK2 phos-T68
CHK2
Tubulin

E)

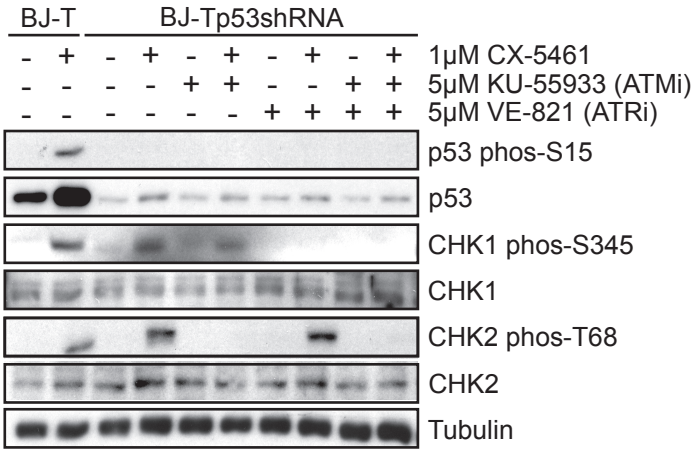
BJ-T
BJ-Tp53shRNA
- + - + - + - + - + 1μM CX-5461
- - - - + + - - + + 5μM KU-55933 (ATMi)
- - - - - - + + + + 5μM VE-821 (ATRi)
p53 phos-S15
p53
CHK1 phos-S345
CHK1
CHK2 phos-T68
CHK2
Tubulin

FIGURE 21. Inhibition of Pol I transcription by 1μM CX-5461 treatment activates ATM and ATR signaling pathways in BJ-T cells independently of global DNA damage. A) Western blot of analysis of BJ-T cells treated for 10min, 30min, 1hr and 3hr with 1μM CX-5461, or 10min, 1hr and 3hr following 10Gy ionizing radiation (IR) (representative of n=3). IR was used as a positive control for induction of γH2A.X following DNA damage. **B)** Immunofluorescence analysis of ATM phos-S1981 for 30min treatment with 1μM CX-5461, or 30min following 5Gy IR. Upper panel: quantitation of number of foci per cell nucleus for n=3 experiments (mean ± sem. All values n.s.) Lower panel: representative cells for n=3 experiments. 30min treatment with ATMi KU-55933 was included to demonstrate specificity of staining for ATM activity (n=1). **C)** Immunofluorescence analysis of γH2A.X for 30min treatment with 1μM CX-5461, or 30min following 5Gy IR (mean ± sem. **p<0.005) Upper panel: quantitation of number of foci per cell nucleus for n=3 experiments. Lower panel: representative cells for n=3 experiments. **D)** qRT-PCR analysis of DNA damage induced at the I-*Ppo*I restriction sequence in 28S rDNA following 3hr stabilization of I-*Ppo*I endonuclease in U2TR I-*Ppo*I-dd cells. Relative amplification across the 28S rDNA cut site in I-*Ppo*I induced compared to vehicle treated cells, normalized to amplification of the rDNA promoter to control for rDNA copy number (n=3, mean ±sem. *p<0.05). **E)** Western blot of analysis of U2TR I-*Ppo*I-dd cells following 2hr treatment with 1μM CX-5461, 3hr stabilization of I-*Ppo*I endonuclease in U2TR I-*Ppo*I-dd cells, and 2hr following 5Gy IR (representative of n=2). **F)** Co-immunofluorescence analysis of rDNA binding protein UBF (red) and ATM phos-S1981 (green) following 3hr stabilization of I-*Ppo*I endonuclease in U2TR I-*Ppo*I-dd cells, or 2hr treatment with 1μM CX-5461. Upper panel: quantitation of number of cells displaying ATM phos-S1981 foci that colocalise with rDNA (n=2 experiments, mean ± SD). Lower panel: representative cell for each treatment. **G)** Co-immunofluorescence analysis of rDNA binding protein UBF (red) and γH2A.X (green) following 3hr stabilization of I-*Ppo*I endonuclease in U2TR I-*Ppo*I-dd cells, or 2hr treatment with 1μM CX-5461. Upper panel: quantitation of number of cells displaying γH2A.X foci that colocalise with rDNA (n=2 experiments, mean ± SD). Lower panel: representative cell for each treatment. **H)** Alkaline comet assay for DNA damage following 30min treatment with NaH_2PO_4 vehicle control or 1μM CX-5461 (n=4), and positive controls for DNA damage 30min treatment with 10μM etoposide (n=1) or 30min following 500μJ UV irradiation (n=2). Upper panel: quantitation of extent tail moment (Extent tail moment = Tail Length x Tail % DNA, calculated using MetaMorph MetaImaging Software. mean±SD). Lower panel:

representative images for 60x magnification (single nuclei) and 20x magnification (whole field).

FIGURE 21
A)

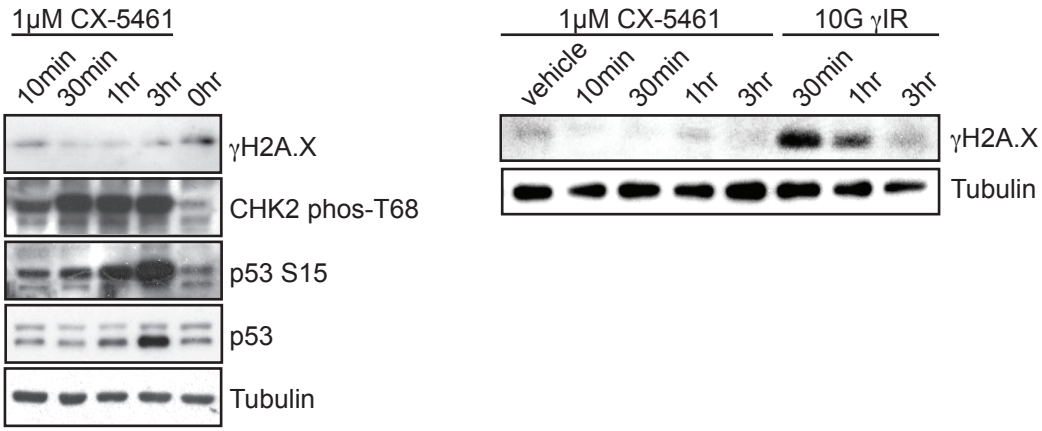
1μM CX-5461
10min
30min
1hr
3hr
0hr
γH2A.X
CHK2 phos-T68
p53 S15
p53
Tubulin
1μM CX-5461
10G γIR
vehicle
10min
30min
1hr
3hr
30min
1hr
3hr
γH2A.X
Tubulin

B)

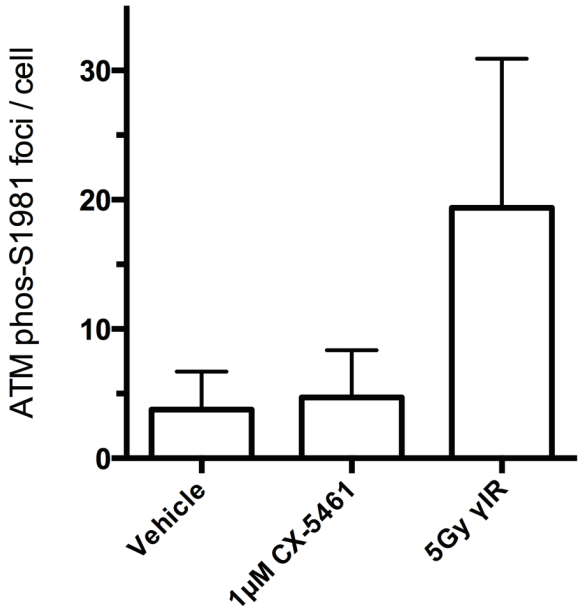

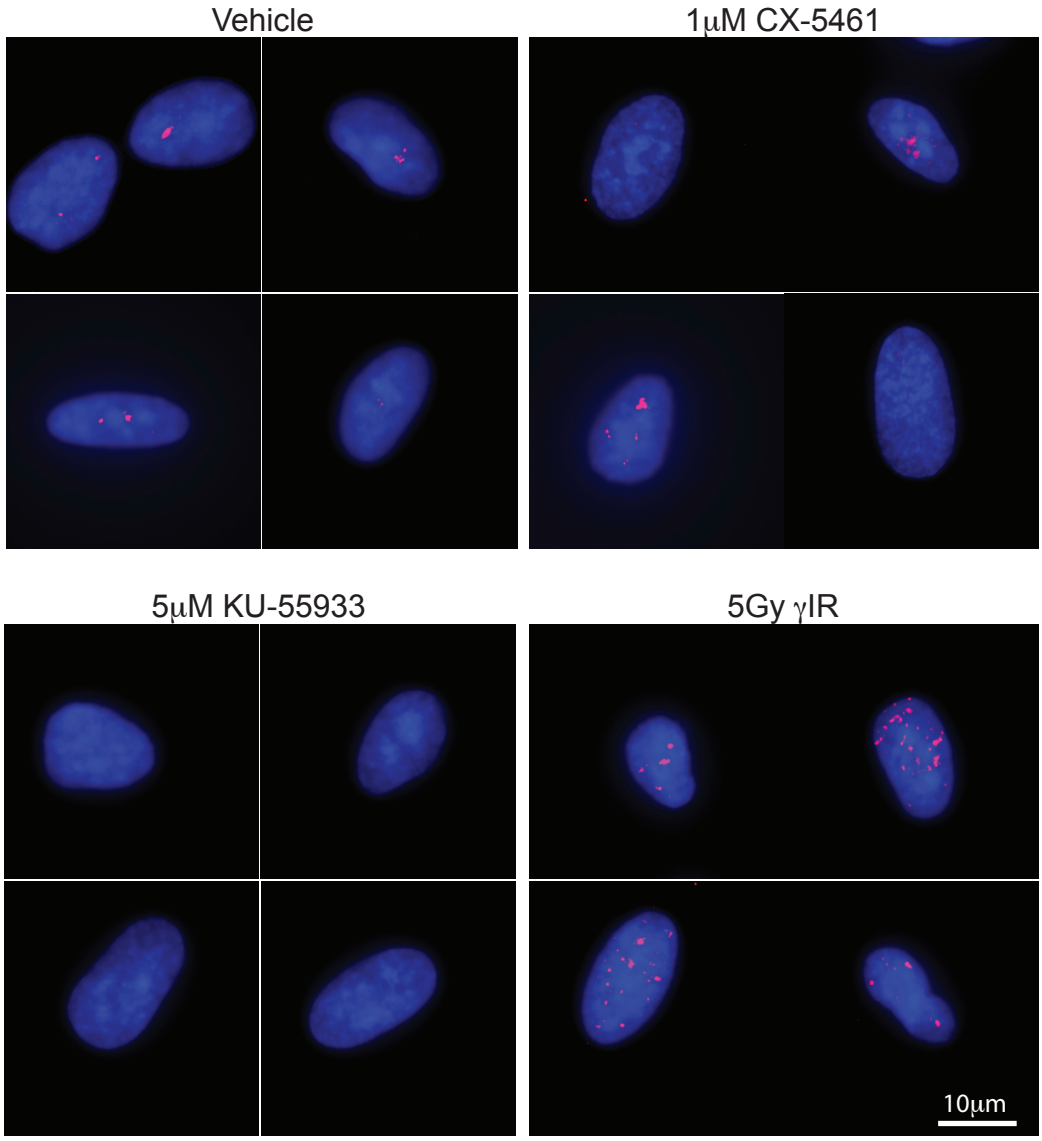

DAPI / ATM phos-S1981

C)

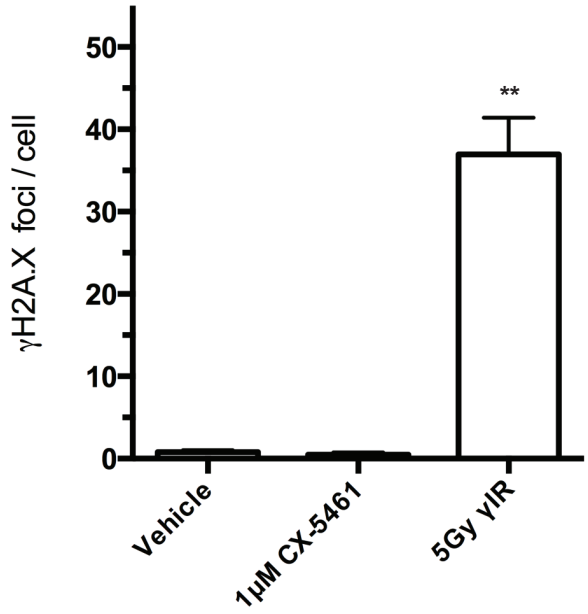
γH2A.X foci / cell
50
40
30
20
10
0
**
Vehicle
1μM CX-5461
5Gy γIR

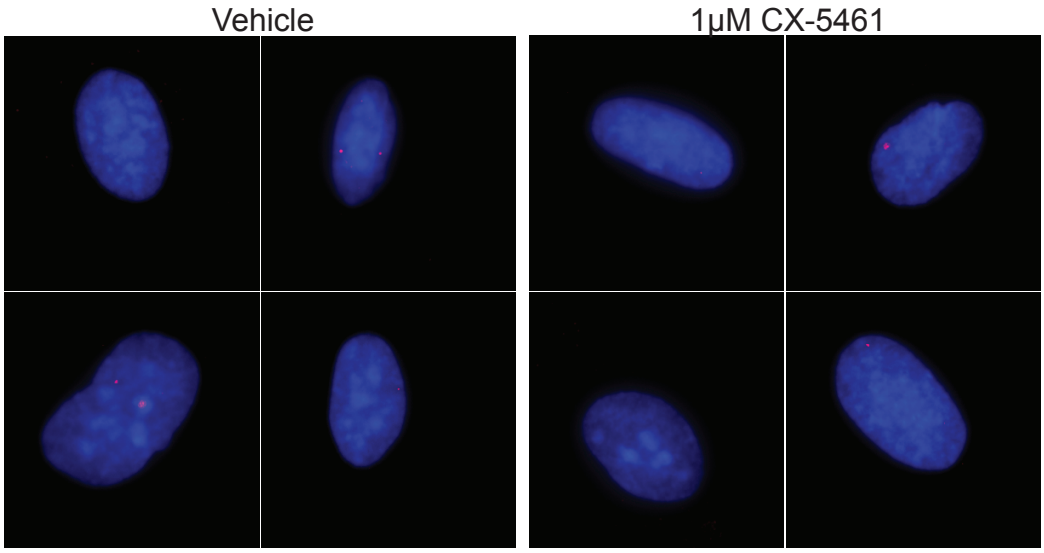
Vehicle
1μM CX-5461

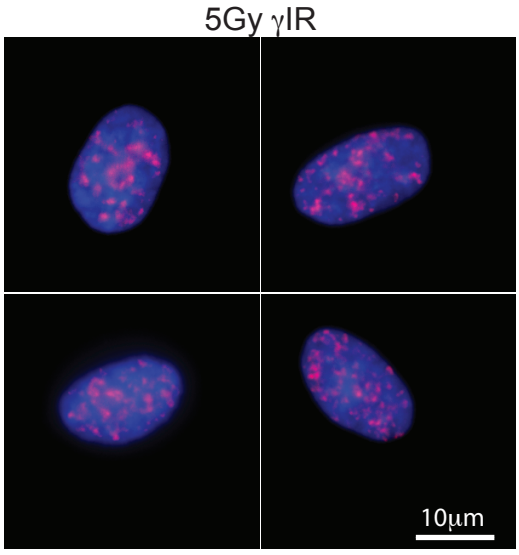
5Gy γIR
10μm

DAPI / γH2A.X

D)

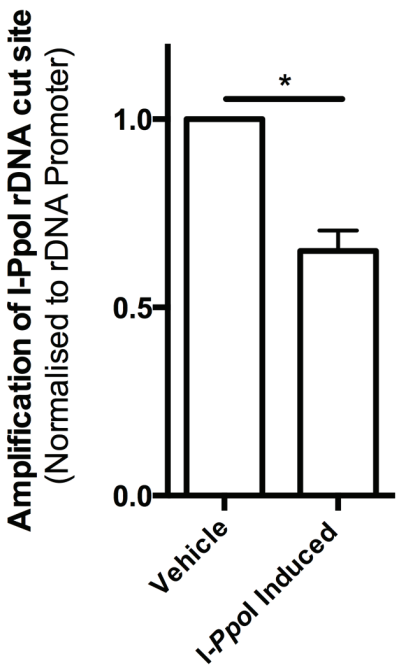
Amplification of I-Ppol rDNA cut site
(Normalised to rDNA Promoter)
1.0
0.5
0.0
*
Vehicle
I-Ppol Induced

E)

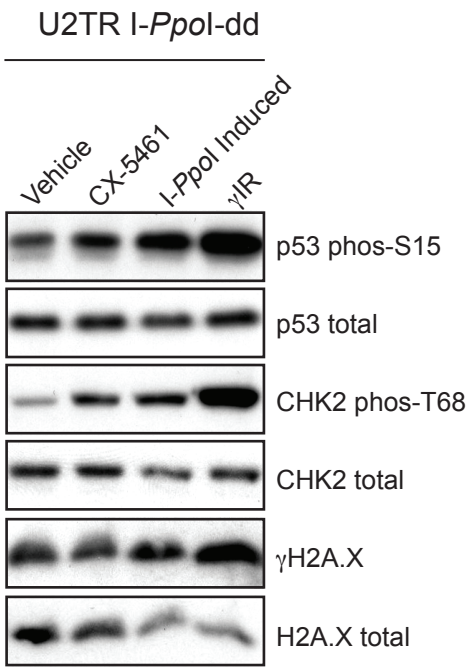
U2TR I-Ppol-dd
Vehicle
CX-5461
I-Ppol Induced
γIR
p53 phos-S15
p53 total
CHK2 phos-T68
CHK2 total
γH2A.X
H2A.X total

F)

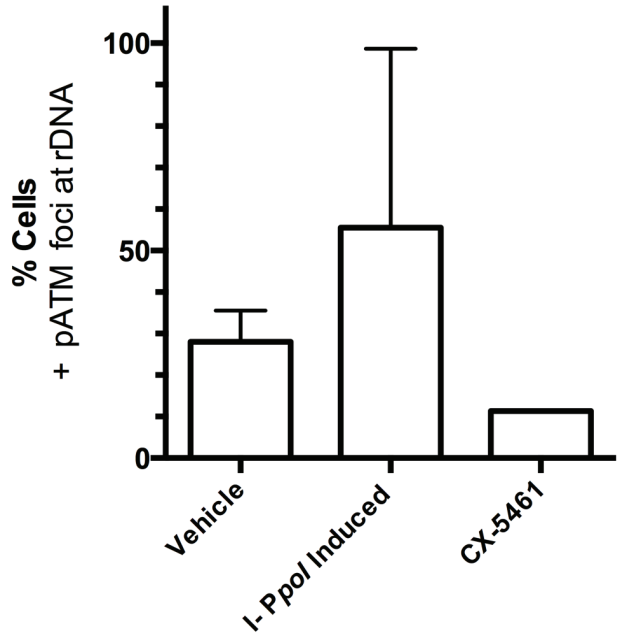
% Cells
+ pATM foci at rDNA
100
50
0
Vehicle
I-PpoI Induced
CX-5461

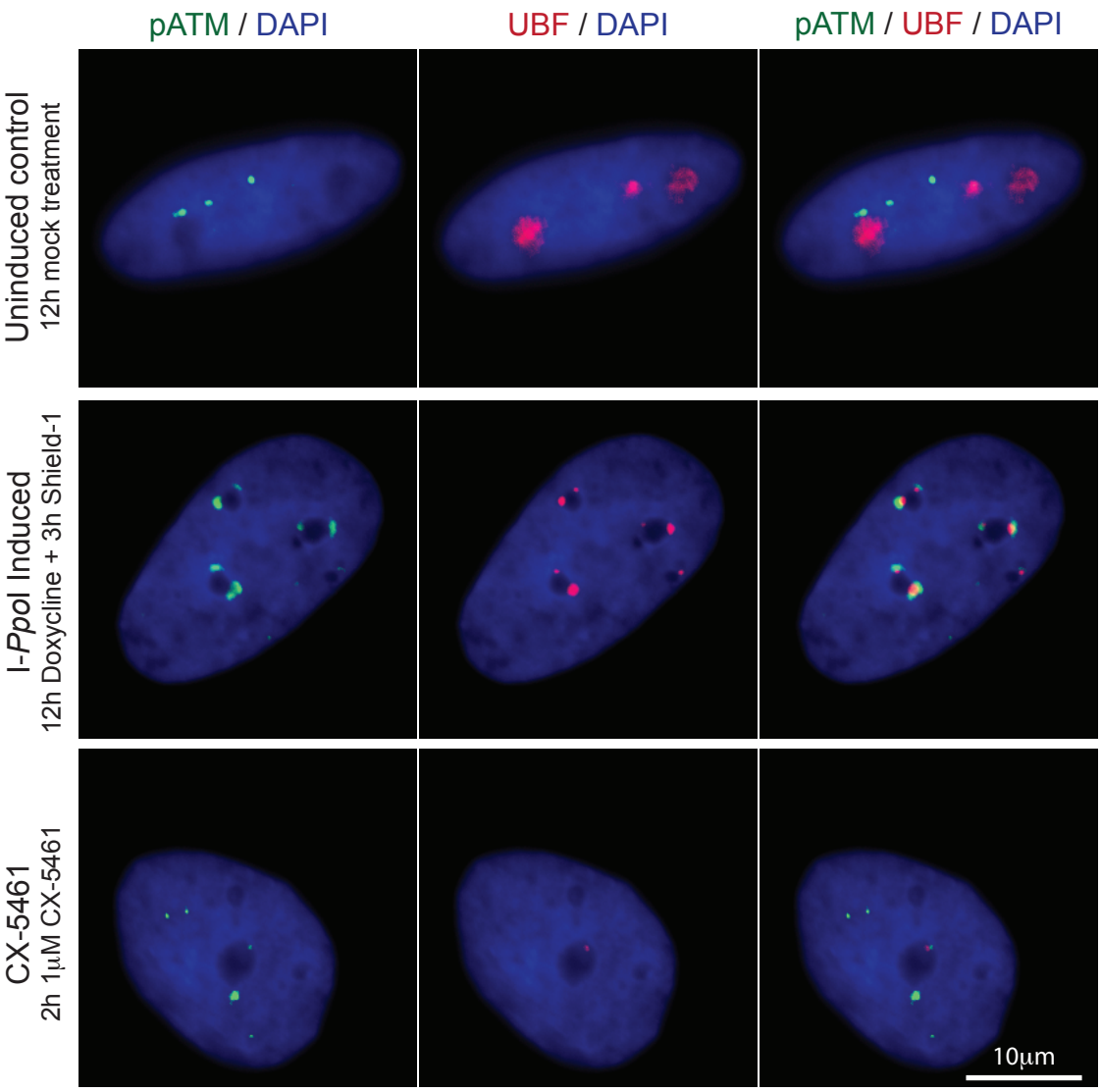
pATM / DAPI
UBF / DAPI
pATM / UBF / DAPI
Uninduced control
12h mock treatment
I-PpoI Induced
12h Doxycline + 3h Shield-1
CX-5461
2h 1μM CX-5461
10μm

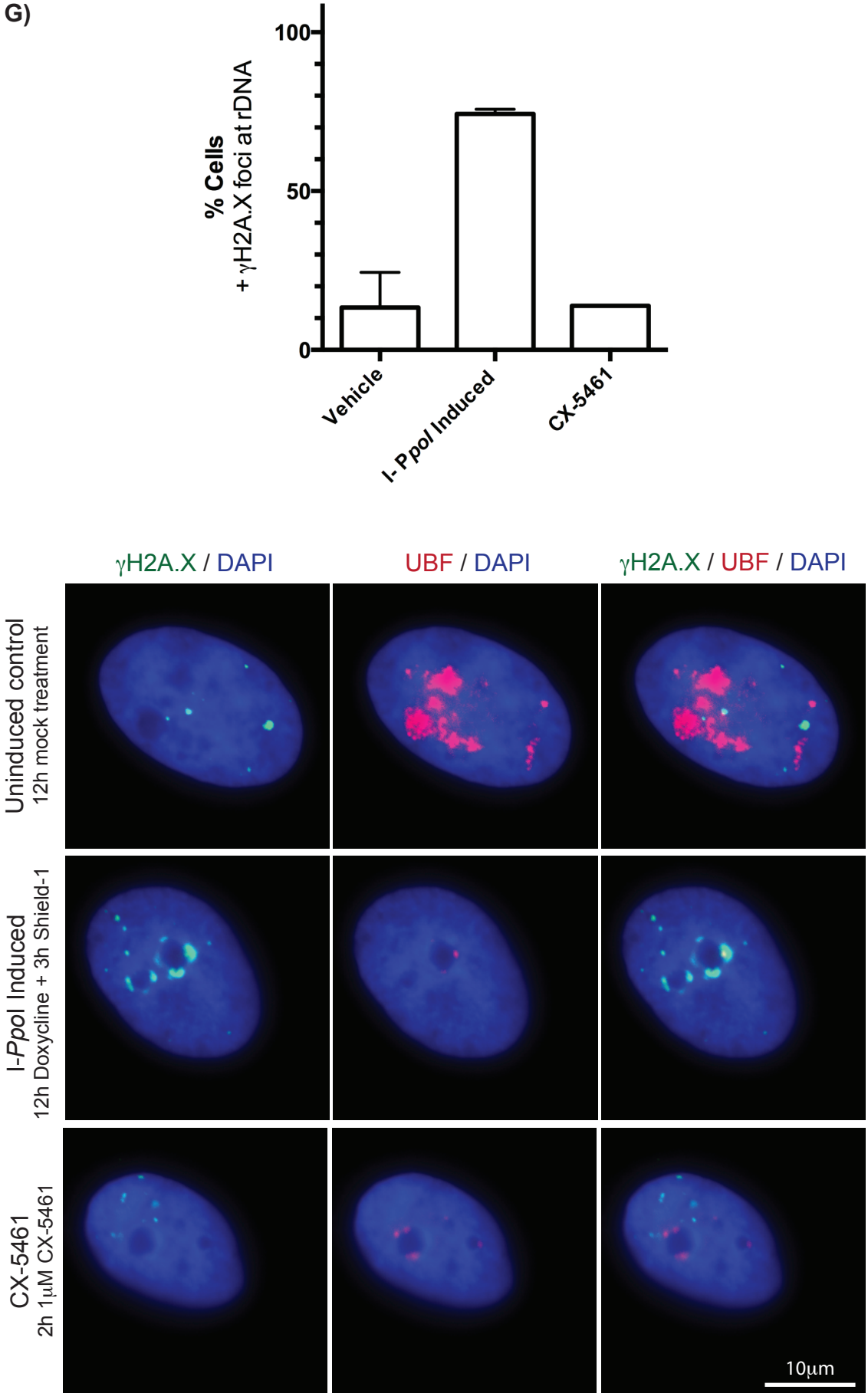
G)
% Cells
+ γH2A.X foci at rDNA
100
50
0
Vehicle
I-PpoI Induced
CX-5461
γH2A.X / DAPI
UBF / DAPI
γH2A.X / UBF / DAPI
Uninduced control
12h mock treatment
I-PpoI Induced
12h Doxycline + 3h Shield-1
CX-5461
2h 1μM CX-5461
10μm

H)

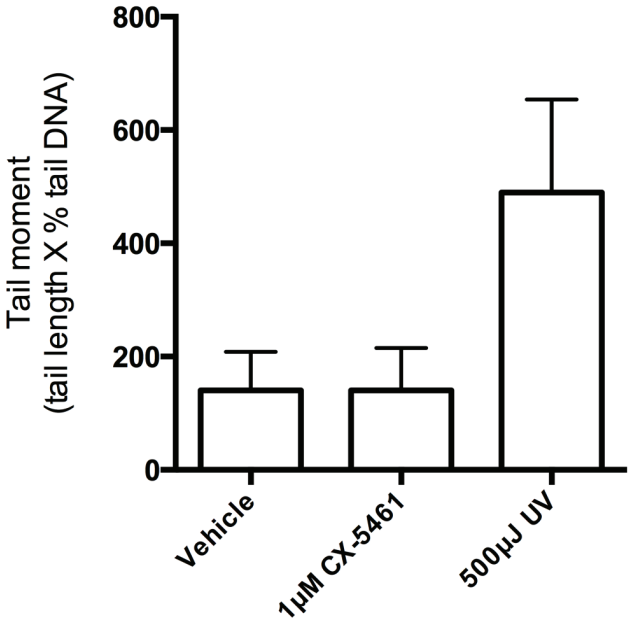
800
600
400
200
0
Tail moment
(tail length X % tail DNA)
Vehicle
1μM CX-5461
500μJ UV

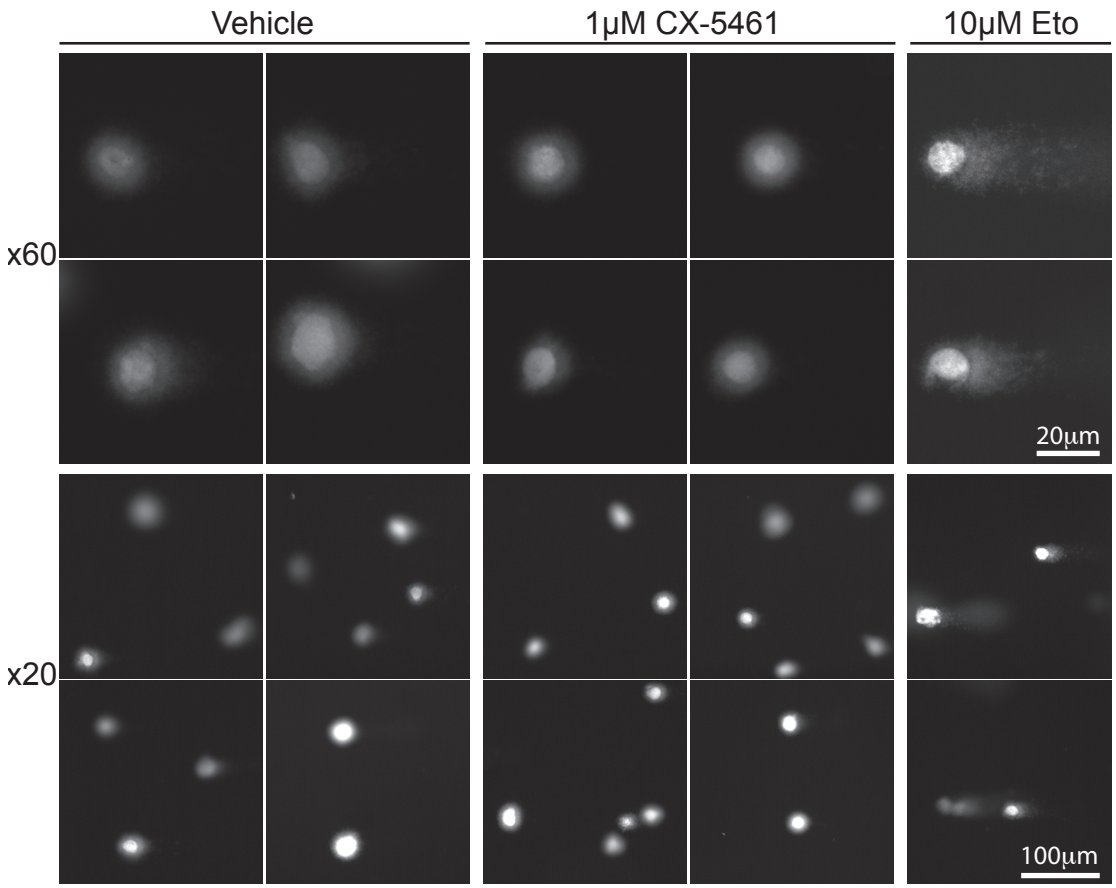
Vehicle
1μM CX-5461
10μM Eto
x60
x20
20μm
100μm

FIGURE 22. ATM and ATR signaling pathways mediate the p53-independent S and G2 phase cell cycle checkpoints following inhibition of Pol I transcription by 1μM CX-5461 in BJ-T cells. A) Cell cycle analysis and survival analysis of BJ-T cells following 24hr treatment with NaH_2PO_4 vehicle control or 1μM CX-5461, +/- treatment with 5μM KU-55933 (ATMi) and/or 1μM VE-821 (ATRi). Cells were incubated with BrdU for 30min in culture immediately prior to collection. Cells were stained for BrdU incorporation for DNA replication (S-phase), and PI for DNA content (G1 and G2/M). i) Representative cell cycle profiles of n=3 experiments. ii) Quantitation of cell cycle populations in live cells using Modfit 3.0 software (representative populations of n=3 experiments). iii) Quantitation of cell death determined by Sub-G1 DNA content analysis following PI staining for DNA content (left panel; n=3 mean±sem), and Annexin V staining following PI exclusion analysis of live cells (right panel; n=3 mean ±sem) using FCS express software. **B)** Cell cycle analysis and survival analysis of BJ-Tp53shRNA cells following 24hr treatment with NaH_2PO_4 vehicle control or 1μM CX-5461, +/- treatment with 5μM KU-55933 (ATMi) and/or 1μM VE-821 (ATRi). Cells were incubated with BrdU for 30min in culture immediately prior to collection. Cells were stained for BrdU incorporation for DNA replication (S-phase), and PI for DNA content (G1 and G2/M). i) Representative cell cycle profiles of n=3 experiments. ii) Quantitation of cell cycle populations in live cells using Modfit 3.0 software (n=3 mean±sem ***p<0.0001, **p<0.005, and *p<0.05 relative to DMSO/vehicle treated population (black) or CX-5461/vehicle treated population (red)). iii) Quantitation of cell death determined by Sub-G1 DNA content analysis following PI staining for DNA content (left panel; n=3 mean±sem *p=0.0432 relative to DMSO/vehicle treated population (black) or CX-5461/vehicle treated population (red)), and Annexin V staining following PI exclusion analysis in live cells (right panel; n=3 mean±sem) using FCS express software. **C)** Cell cycle analysis of BJ-T p53shRNA cells following 3, 6, 12, 24, and 96hr treatment with 1μM CX-5461, +/- treatment with 10μM KU-55933 (ATMi) and/or 10μM VE-821 (ATRi). Cells were incubated with BrdU for 30min in culture immediately prior to collection. Cells were stained for BrdU incorporation for DNA replication (S-phase), PI for DNA content (G1 and G2/M) (n=1). **D)** Phos-H3 analysis for mitosis of BJ-T p53shRNA cells following 12hr treatment with 1μM CX-5461, +/- treatment with 10μM KU-55933 (ATMi) and/or 10μM VE-821 (ATRi) Left: cell cycle profiles. Right: quantitation of phos-H3 positive cells (n=1).

FIGURE 22
A)
i)

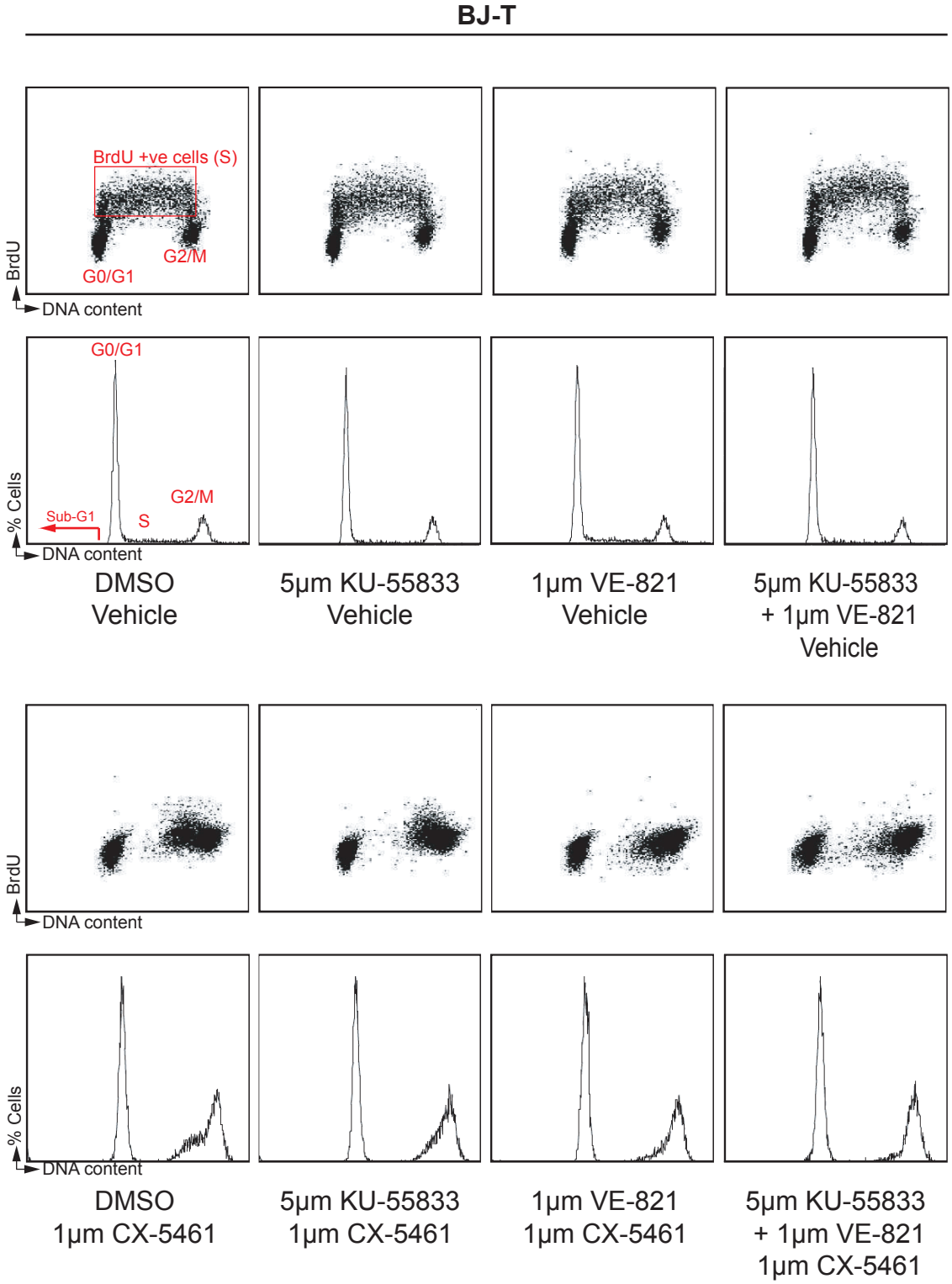
BJ-T
BrdU +ve cells (S)
G0/G1
G2/M
BrdU
DNA content
G0/G1
G2/M
Sub-G1
S
% Cells
DNA content
DMSO
Vehicle
5μm KU-55833
Vehicle
1μm VE-821
Vehicle
5μm KU-55833
+ 1μm VE-821
Vehicle
BrdU
DNA content
% Cells
DNA content
DMSO
1μm CX-5461
5μm KU-55833
1μm CX-5461
1μm VE-821
1μm CX-5461
5μm KU-55833
+ 1μm VE-821
1μm CX-5461

ii)

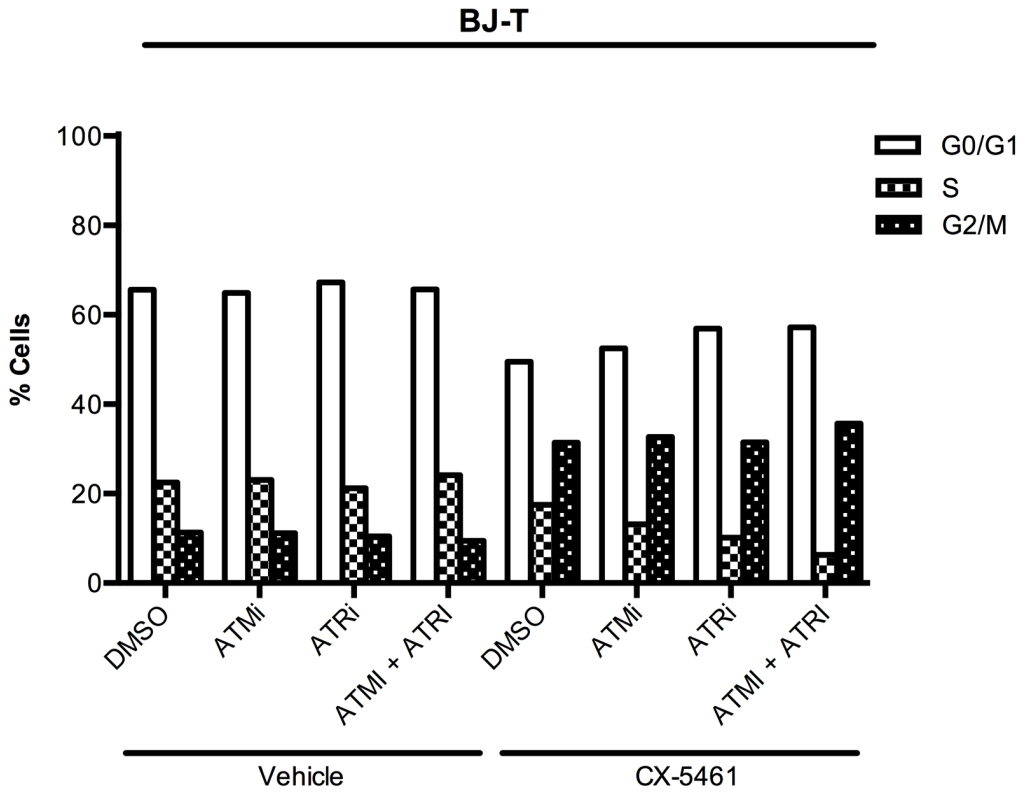
BJ-T
100
80
60
40
20
0
% Cells
G0/G1
S
G2/M
DMSO
ATMi
ATRi
ATMI + ATRI
DMSO
ATMi
ATRi
ATMI + ATRI
Vehicle
CX-5461

iii)

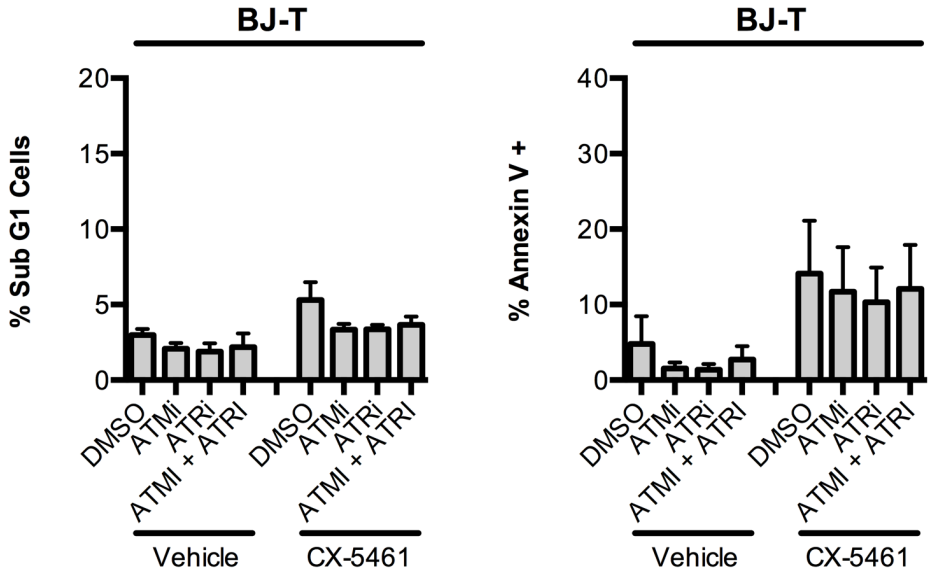
BJ-T
% Sub G1 Cells
20
15
10
5
0
DMSO
ATMi
ATRi
ATMI + ATRI
DMSO
ATMi
ATRi
ATMI + ATRI
Vehicle
CX-5461
BJ-T
% Annexin V +
40
30
20
10
0
DMSO
ATMi
ATRi
ATMI + ATRI
DMSO
ATMi
ATRi
ATMI + ATRI
Vehicle
CX-5461

B)
i)

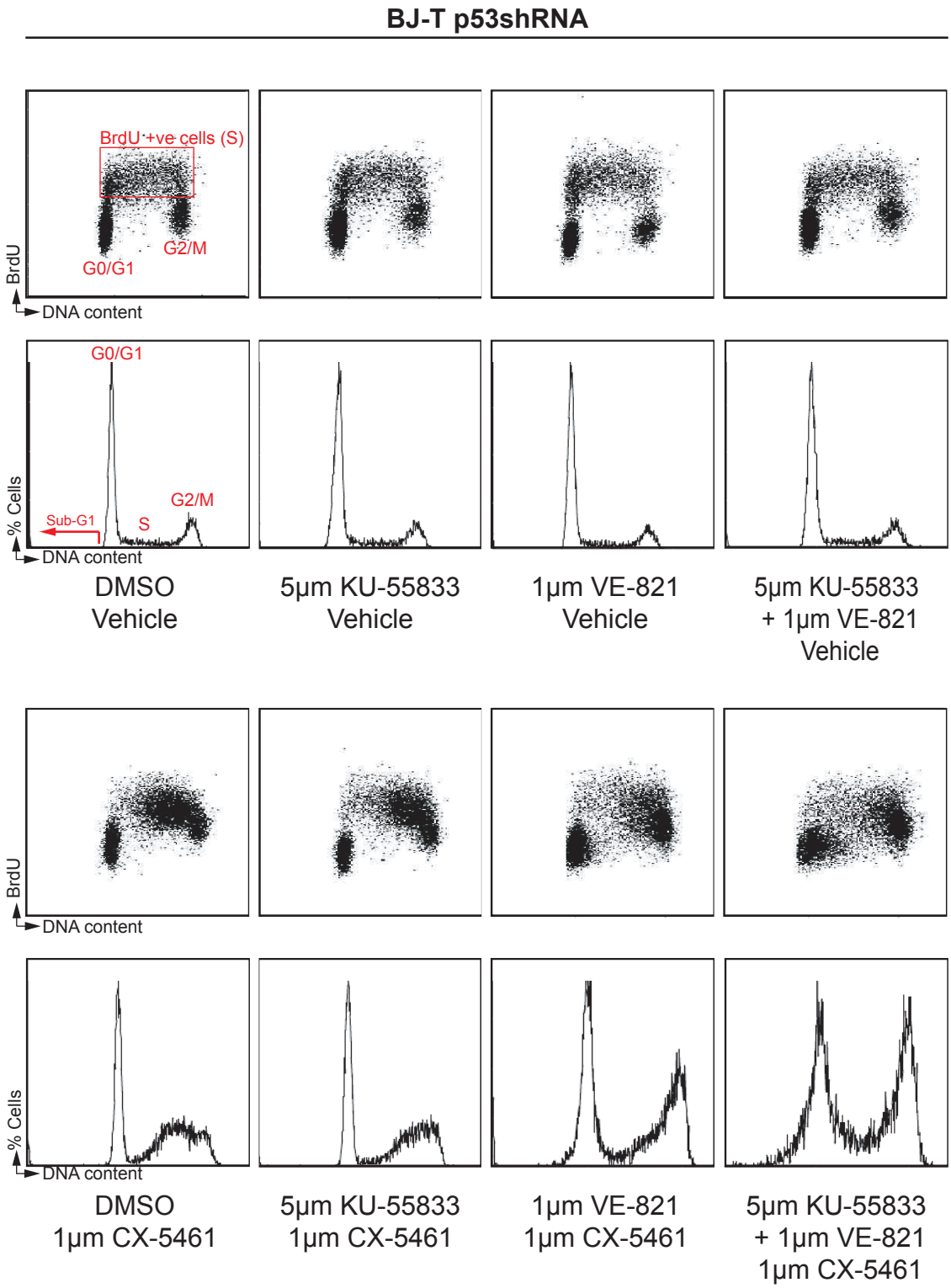
BJ-T p53shRNA
BrdU +ve cells (S)
G0/G1
G2/M
BrdU
DNA content
G0/G1
G2/M
Sub-G1
S
% Cells
DNA content
DMSO
Vehicle
5μm KU-55833
Vehicle
1μm VE-821
Vehicle
5μm KU-55833
+ 1μm VE-821
Vehicle
BrdU
DNA content
% Cells
DNA content
DMSO
1μm CX-5461
5μm KU-55833
1μm CX-5461
1μm VE-821
1μm CX-5461
5μm KU-55833
+ 1μm VE-821
1μm CX-5461

ii)

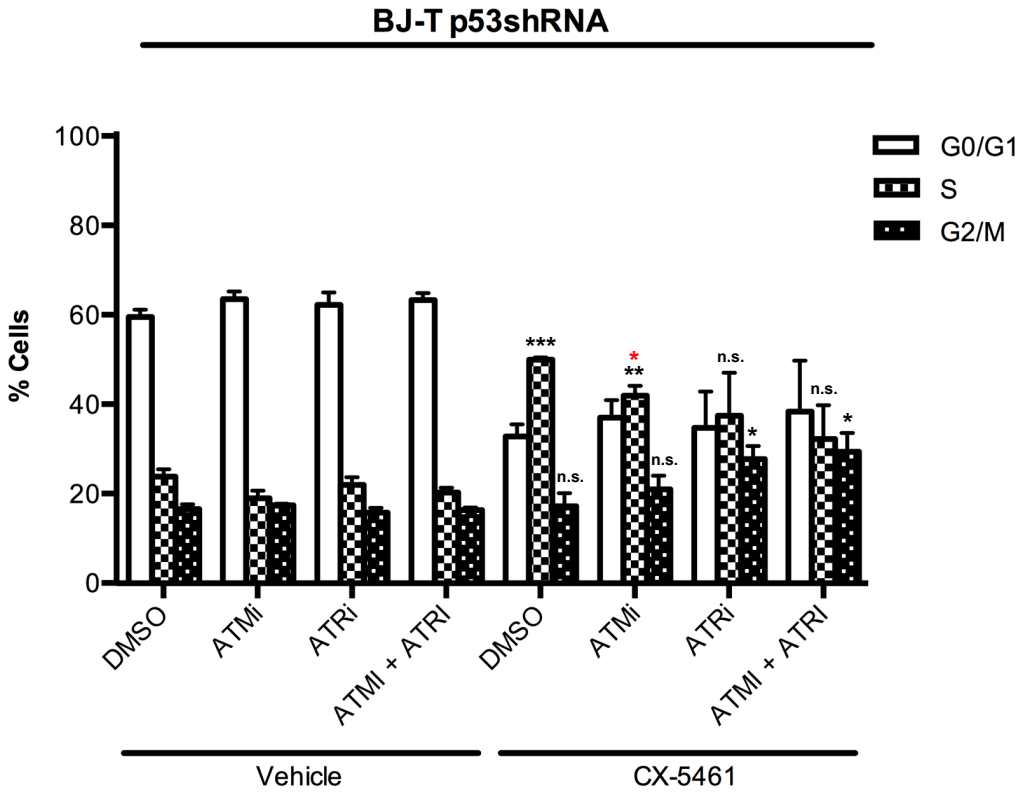
BJ-T p53shRNA
% Cells
100
80
60
40
20
0
G0/G1
S
G2/M
***
*
**
n.s.
n.s.
n.s.
*
n.s.
*
DMSO
ATMi
ATRi
ATMI + ATRI
DMSO
ATMi
ATRi
ATMI + ATRI
Vehicle
CX-5461

iii)

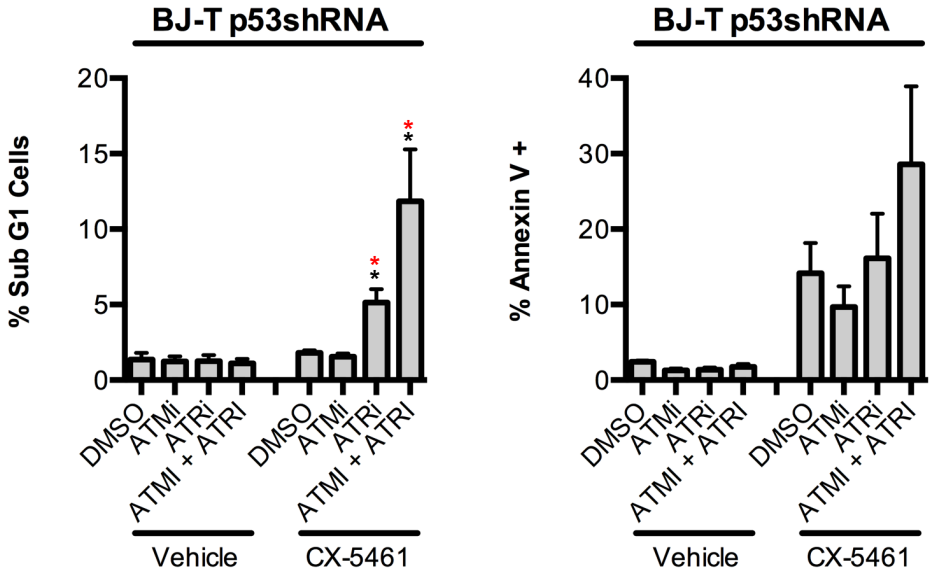
BJ-T p53shRNA
% Sub G1 Cells
20
15
10
5
0
*
**
*
**
DMSO
ATMi
ATRi
ATMI + ATRI
DMSO
ATMi
ATRi
ATMI + ATRI
Vehicle
CX-5461
BJ-T p53shRNA
% Annexin V +
40
30
20
10
0
DMSO
ATMi
ATRi
ATMI + ATRI
DMSO
ATMi
ATRi
ATMI + ATRI
Vehicle
CX-5461

C)

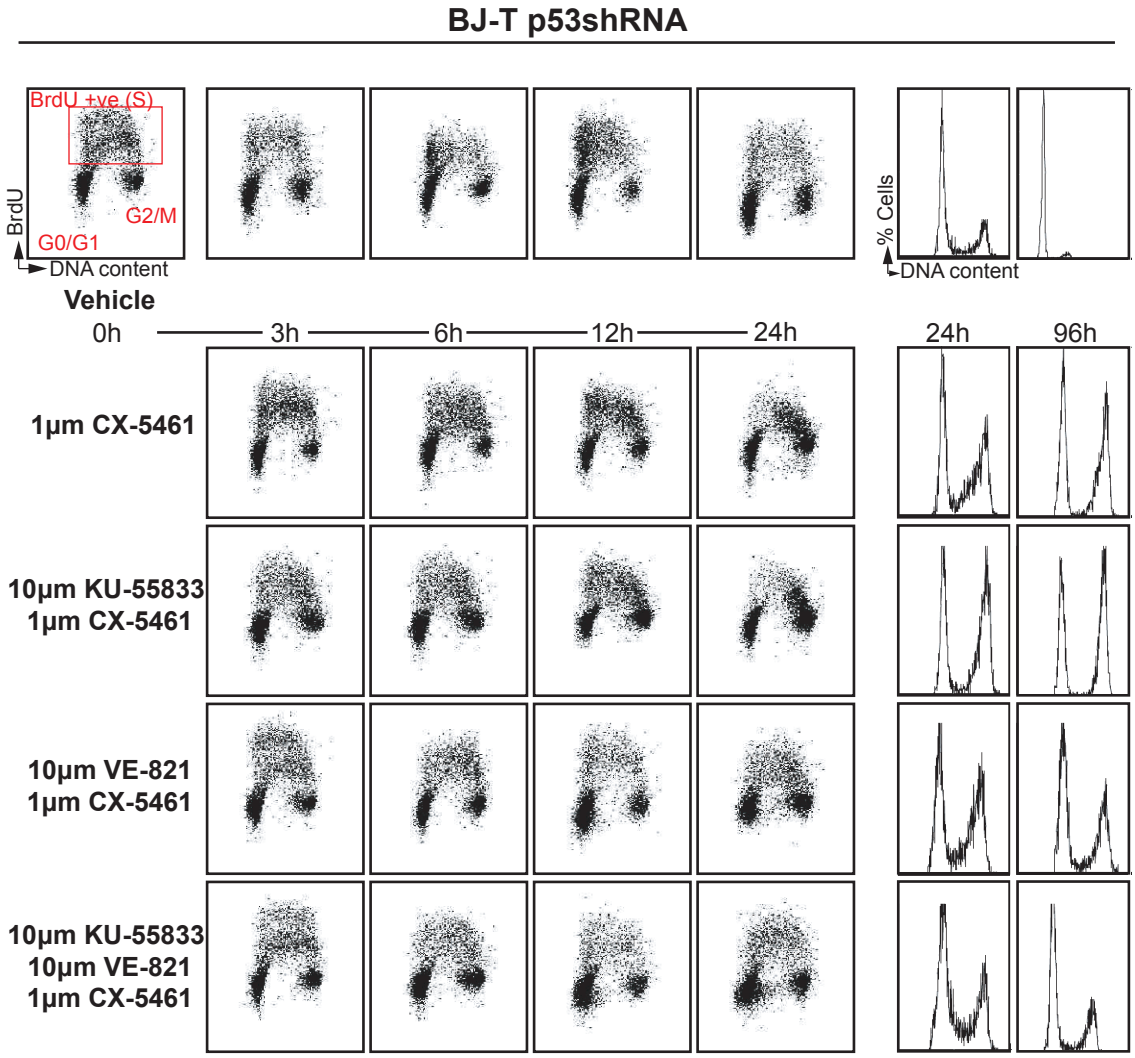
BJ-T p53shRNA
BrdU +ve (S)
G2/M
G0/G1
BrdU
DNA content
% Cells
DNA content
Vehicle
0h
3h
6h
12h
24h
24h
96h
1µm CX-5461
10µm KU-55833
1µm CX-5461
10µm VE-821
1µm CX-5461
10µm KU-55833
10µm VE-821
1µm CX-5461

D)

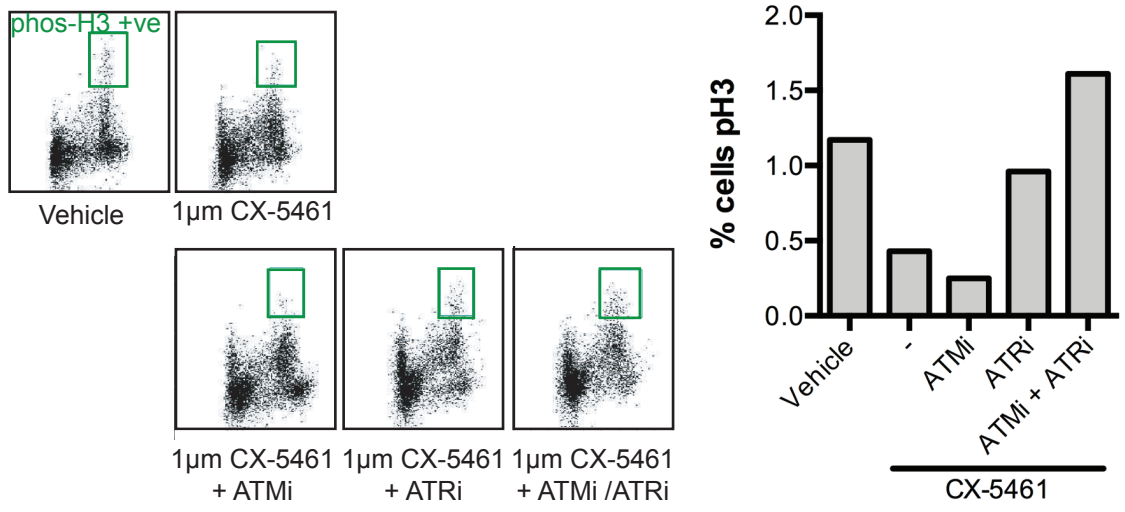
BJ-T p53shRNA
phos-H3 +ve
Vehicle
1µm CX-5461
1µm CX-5461
+ ATMi
1µm CX-5461
+ ATRi
1µm CX-5461
+ ATMi /ATRi
% cells pH3
2.0
1.5
1.0
0.5
0.0
Vehicle
-
ATMi
ATRi
ATMi + ATRi
CX-5461

FIGURE 23. Inhibition of ATM and ATR signaling pathways in combination with inhibition of Pol I transcription by 100nM CX-5461 induces cell death in the absence of p53. Proliferation analysis of BJ cells over a time course of 0-120hr as determined by % cell confluency on IncuCyte ZOOM. Cells were treated with NaH_2PO_4 vehicle control or 1μM CX-5461, +/- treatment with 5μM KU-55933 (ATMi) and/or 1μM VE-821 (ATRi), or 50nM AZD-7762 (CHK1/CHK2i) (n=1 representative experiments of n=3, mean±sem of technical replicates, normalized to % confluency at 0hr). For **A)** BJ-T cells, **B)** BJ-T p53shRNA cells, and **C)** BJ-LSTR cells. (****p<0.0001, ***p<0.0005, **p<0.005, and *p<0.05 shown for cell viability at 120hr for n=3 experiments relative to vehicle control (red) or 1μM CX-5461 (black)).

FIGURE 23
A)

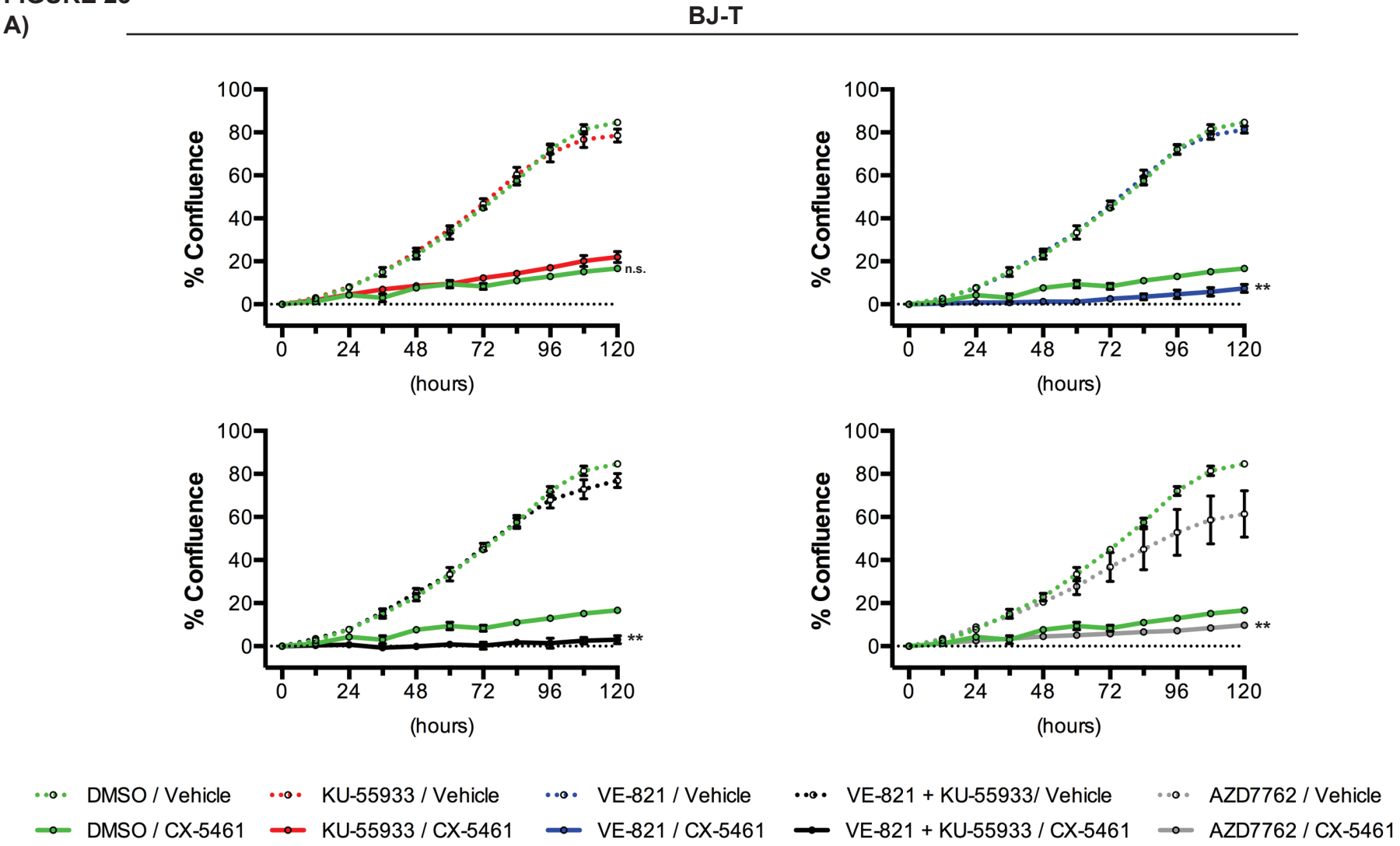
BJ-T
% Confluence
100
80
60
40
20
0
0
24
48
72
96
120
(hours)
n.s.
**
**
**
DMSO / Vehicle
DMSO / CX-5461
KU-55933 / Vehicle
KU-55933 / CX-5461
VE-821 / Vehicle
VE-821 / CX-5461
VE-821 + KU-55933/ Vehicle
VE-821 + KU-55933 / CX-5461
AZD7762 / Vehicle
AZD7762 / CX-5461

B)

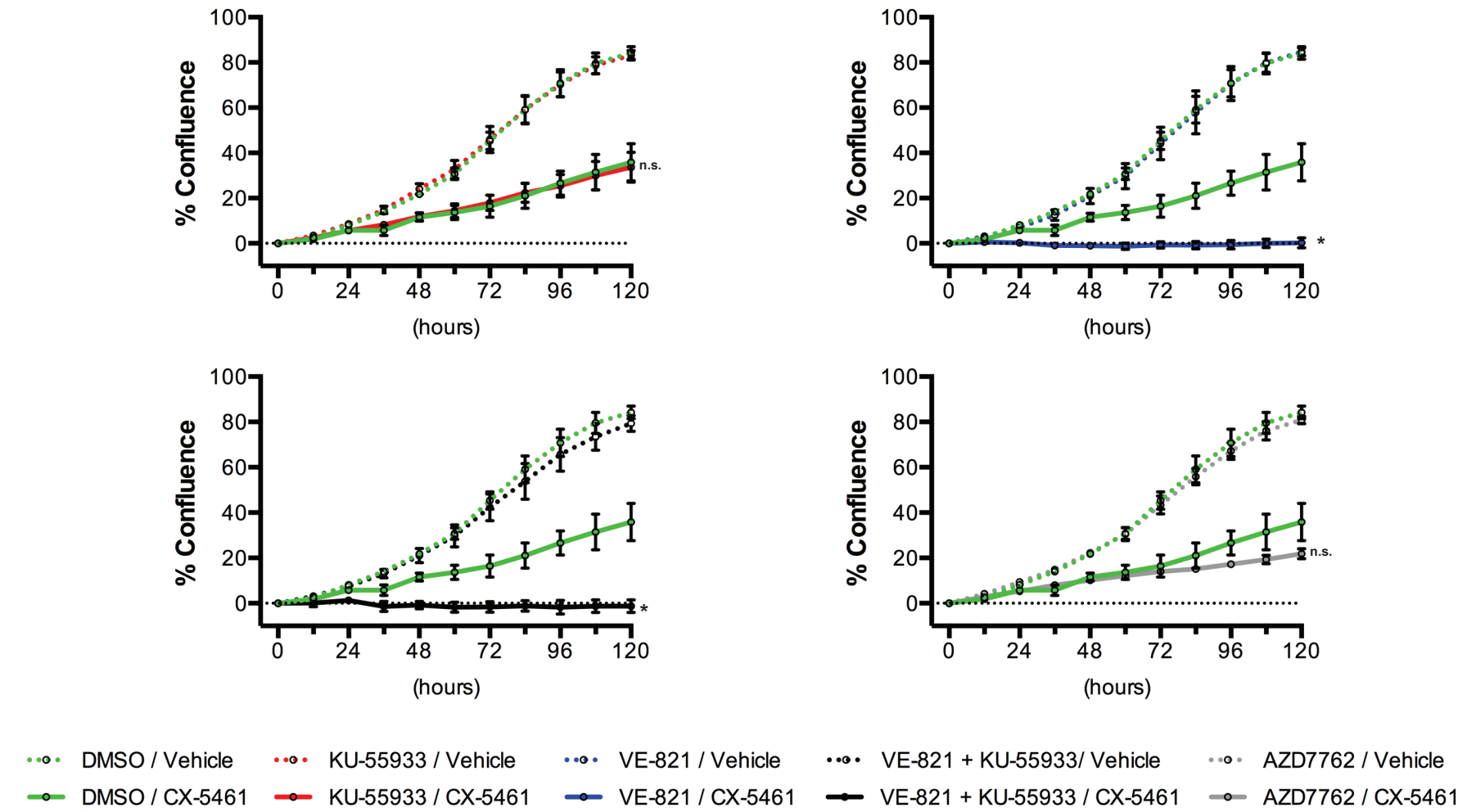
BJ-T p53shRNA
% Confluence
(hours)
0
24
48
72
96
120
n.s.
*
DMSO / Vehicle
DMSO / CX-5461
KU-55933 / Vehicle
KU-55933 / CX-5461
VE-821 / Vehicle
VE-821 / CX-5461
VE-821 + KU-55933/ Vehicle
VE-821 + KU-55933 / CX-5461
AZD7762 / Vehicle
AZD7762 / CX-5461

C)

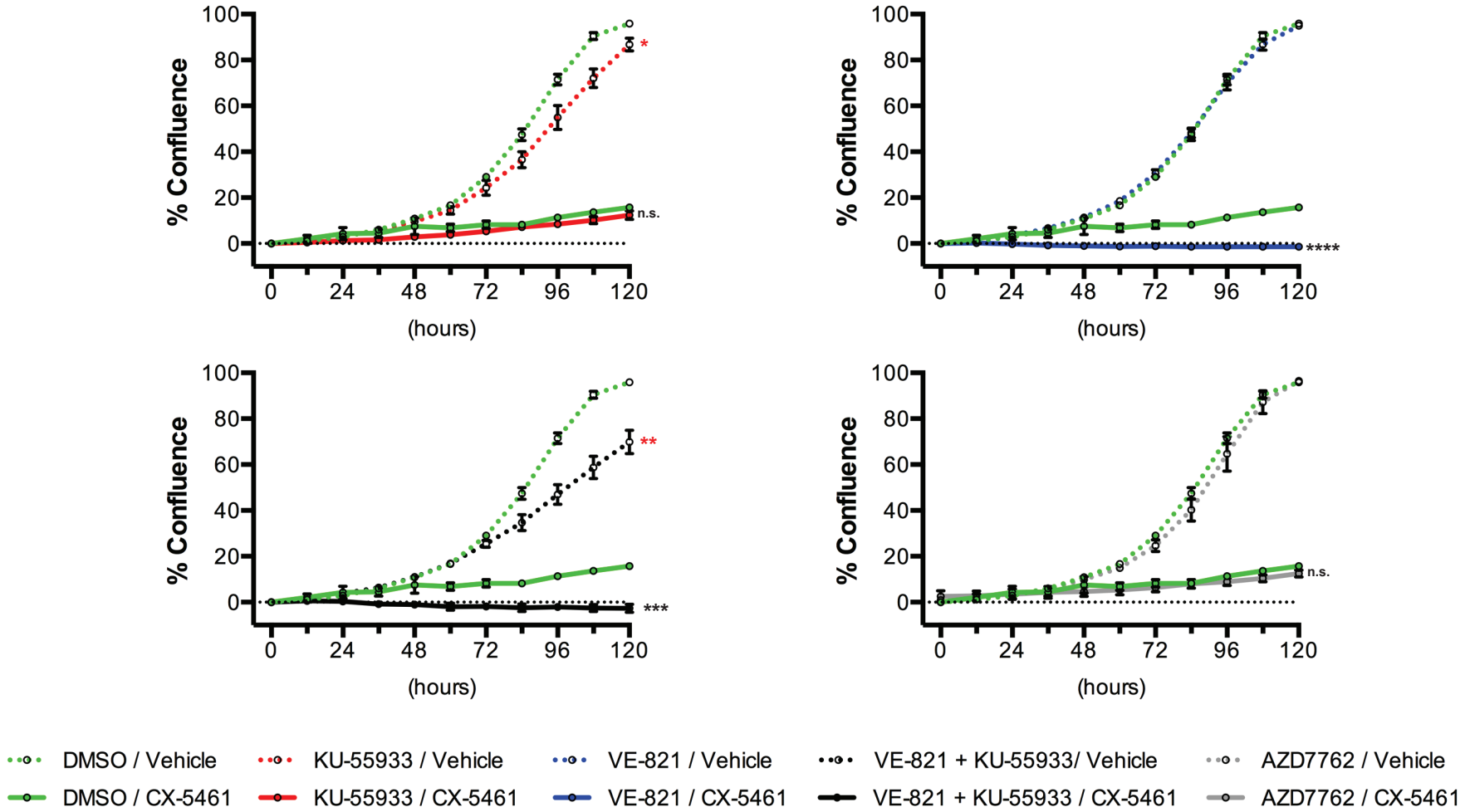
BJ-LSTR
% Confluence
(hours)
0
24
48
72
96
120
0
20
40
60
80
100
*
n.s.
****
**
***
n.s.
DMSO / Vehicle
DMSO / CX-5461
KU-55933 / Vehicle
KU-55933 / CX-5461
VE-821 / Vehicle
VE-821 / CX-5461
VE-821 + KU-55933/ Vehicle
VE-821 + KU-55933 / CX-5461
AZD7762 / Vehicle
AZD7762 / CX-5461

FIGURE 24. Model of p53 and ATM/ATR signaling pathways mediating the cell cycle checkpoint responses to inhibition of Pol I transcription by CX-5461.

FIGURE 24

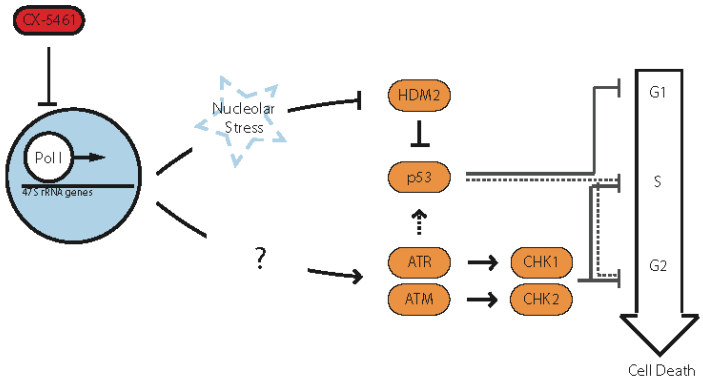
CX-5461
Pol I
47S rRNA genes
Nucleolar Stress
?
HDM2
p53
ATR
ATM
CHK1
CHK2
G1
S
G2
Cell Death

CHAPTER 6. INHIBITION OF POL I TRANSCRIPTION INITITATION BY CX-5461 ACTIVATES ATM/ATR SIGNALING AT THE NUCLEOLI, AND IMPAIRS DNA DAMAGE RESPONSE.

6.1 Introduction.

We have shown that inhibition of Pol I transcription by CX-5461 activates ATM/ATR signaling pathways in the absence of global DNA damage. The canonical ATM and ATR pathways are activated by DSBs and ssDNA, respectively. Therefore, inhibition of Pol I transcription by CX-5461 activates these pathways by an unknown novel mechanism.

The activation of ATM and ATR in the absence of DNA damage has been reported under some conditions (Reviewed in (Shiloh and Ziv, 2013; Burgess and Misteli, 2015)). For example, during the mitotic spindle checkpoint ATM is activated at low levels by Aurora B kinase, leading to ATM-mediated activation of kinetochore protein BUB1 (Yang et al., 2011). ATM can also be activated by ATMIN (ATM interacting protein), for example in response to hypotonic conditions or treatment with chloroquine, by a mechanism distinct from ATM pathway activation by DSBs (Kanu and Behrens, 2007; Zhang et al., 2012). Under conditions of oxidative stress, direct oxidation of Cys residues result in disulphide crosslinked ATM dimers and activation of ATM in a manner independent of DSBs (Guo et al., 2010). Both ATM and ATR can be activated under conditions of hypoxia, which leads to replication stress but not DNA damage (Hammond et al., 2007; Bencokova et al., 2009; Olcina et al., 2010). ATR can be activated by p14ARF, in a manner that is independent of DNA damage and results in targeting of a set of proteins distinct from that following UV irradiation (Rocha et al., 2005). It is also possible that ATM and ATR are targeted by their canonical activation pathways even without DNA damage. For example, some studies have concluded that ATM may be activated by either tethering to chromatin or by chromatin conformational changes associated with DSBs (You et al., 2007; Jazayeri et al., 2008; Soutoglou and Misteli, 2008)). Alternatively, Pol II transcriptional stress has been shown to activate p53 in an ATR dependent manner. The authors propose that as the elongating Pol II acts as a sensor of DNA damage, transcription blockage alone may be sufficient to trigger DDR signaling (Derheimer et al., 2007). Thus, ATM and ATR can be activated by several different mechanisms, and their kinase activity may be broadly utilised in the response to diverse stimuli. Therefore, we hypothesise that defects in Pol I

transcription and/or rDNA chromatin are sufficient to activate ATM and ATR signaling in the absence of DSBs.

Furthermore, it is plausible that the deregulation of nucleolar integrity resulting from inhibition of Pol I transcription can lead to a DNA damage response. Indeed, a functional relationship between the nucleoli and DNA damage response has recently begun to emerge. As discussed earlier (Section 1.2.2.3), DNA damage results in the rapid inhibition of Pol I transcription by ATM, ATR and/or DNA-PK pathways, and the reorganisation of nucleolar structure (Kruhlak et al., 2007; Gilder et al., 2011; Moore et al., 2011; Calkins et al., 2013; Jin et al., 2014; Larsen et al., 2014; Lin et al., 2014; Sokka et al., 2015)(Reviewed in (van Sluis and McStay, 2015; Larsen and Stucki, 2016)). A number of proteins involved in DDR localise to the nucleoli, and many have been shown to translocate between the nucleoli and the nucleoplasm in response to specific types of DNA damage (Cohen et al., 2008; Boisvert et al., 2010; Boisvert and Lamond, 2010; Moore et al., 2011). Thus, the nucleoli may mediate the function of these proteins in DNA damage response through nucleolar sequestration and release (See TABLE 1). For example, hCDC14B is phosphorylated by CHK1 and released from the nucleoli following DNA damage, leading to hCDC14B-induced activation of APC/C^{Cdh1}, and consequently the degradation of PLK1 (polo-like kinase 1) mitotic kinase resulting in G2 cell cycle arrest (Bassermann et al., 2008; Peddibhotla et al., 2011). In the case of p53 activation in response to DNA damage, the role of nucleolar stress signaling is well established (See Section 1.2.1). The importance of the nucleoli in mediating p53-dependent DDR is underscored by the observation that induction of nucleolplasmic DNA damage, without causing DNA damage at the rDNA and nucleolar disruption, does not activate p53 (Rubbi and Milner, 2003). Therefore, the nucleoli may act as a sensor for DNA damage response, undergoing changes following DNA damage, and activating appropriate DDR pathways.

These findings suggest it is possible that ATM/ATR signaling pathways can be activated by a mechanism related to the function of the nucleoli, extending its proposed role as a ‘hub’ for stress signaling responses. However, the acute activation of ATM/ATR by inhibition of Pol I transcription and/or nucleolar disruption had not previously been described. Therefore, we investigated the mechanisms by which inhibition of Pol I transcription by CX-5461 could activate the ATM/ATR signaling pathways.

6.2 ATM/ATR signaling is activated by small molecule inhibitors of Pol I transcription initiation, CX-5461 and CX-5488, but not Actinomycin D.

6.2.1. Introduction

CX-5461 is highly selective for inhibition of Pol I pre-initiation complex (PIC) formation. We have previously shown that CX-5461 does not directly inhibit Pol II transcription, DNA replication, or protein synthesis at the doses used for inhibition of transcription of the 47S pre-rRNA (Drygin et al., 2011). Further, the RNA-sequencing data presented above specifically shows that Pol II transcription is not inhibited by CX-5461 under conditions sufficient to activate ATM/ATR signaling. In fact, ATM/ATR signaling is activated following 30min 1μM CX-5461 treatment, at which time there is approximately 75% reduction in rRNA synthesis, but very few changes in Pol II gene expression (See Section 4.2).

ActD selectively inhibits Pol I transcription of the rRNA genes by intercalating GC-rich sequences, preventing progression of Pol I through the GC-rich rDNA and elongation of the 47S rRNA transcript (Reviewed in (Koba and Konopa, 2005)). However, treatment of BJT p53shRNA cells with this commonly used inhibitor of Pol I transcription did not result in G2 cell cycle arrest (See FIGURE 16). Furthermore, differential expression of genes associated with DDR was specific to CX-5461 treatment as opposed to ActD treatment in our RNA-sequencing analysis. This suggests that inhibition of Pol I transcription by ActD may not be sufficient to activate ATM/ATR signaling and G2 checkpoint arrest.

Therefore, in order to address whether ATM/ATR pathway activation by CX-5461 arises as a result of inhibition of the Pol I pre-initiation complex formation, rather than any as yet unidentified non-specific effects, we examined the activity of additional inhibitors of Pol I transcription. We utilized both ActD, and two additional small molecules related to CX-5461, CX-5447 and CX-5488.

6.2.2. Results

First, we examined ATM/ATR pathway activation following inhibition of Pol I transcription elongation by ActD. We treated BJ-T p53shRNA cells with 5nM ActD, for 30min and 3hr, or 1μM CX-5461, for 30min, 1hr and 3hr, as described for FIGURE 16, and performed Western analysis of phos-CHK2(T68). Cells treated with 1μM CX-5461 showed increased levels of phos-CHK2(T68) by 30min, as we had previously

observed (See FIGURE 20). However, cells treated with 5nM ActD did not show any increase in phos-CHK2(T68), even after 3h (FIGURE 25 A). This confirms that that the ATM/ATR pathway is not activated by ActD, consistent with the lack of G2 arrest in ActD treated BJ-T p53shRNA cells.

Therefore, to further examine whether ATM/ATR pathway activation is a result of inhibition of Pol I transcription initiation, we examined the activity of two additional small molecules related to CX-5461. CX-5447 has an almost identical structure to CX-5461 (FIGURE 25 B), but has no effect on the stability of the Pol I/SL1 complex or activity towards Pol I transcription (Drygin et al., 2011). CX-5488 is a newly developed small molecule inhibitor of Pol I transcription, chosen for its divergent structure to CX-5461 (personal communication, D.Drygin) (FIGURE 25 B).

CX-5447 was shown to have no activity towards Pol I transcription following 3h treatment in BJ-T cells at doses up to 10μM (FIGURE 25 C). Correspondingly, it did not induce either p53 or ATM/ATR signaling pathways (FIGURE 25 D), nor affect BJ-T proliferation and cell cycle progression (FIGURE 25 E). CX-5488 inhibited Pol I transcription at similar levels to CX-5461; following 3h of 1μM treatment in BJ-T cells, Pol I transcription was reduced to levels approximately 20% of that in vehicle control cells for both drugs (1μM CX-5461 Mean = 21.74% ****$p<0.0001$ relative to vehicle control; 1μM CX-5488 Mean = 20.09%****$p<0.0001$ relative to vehicle control) (FIGURE 25 C). Consistent with results observed for CX-5461, 1μM CX-5488 treatment resulted in a proliferation defect associated with G1 arrest, S-phase delay and G2 arrest in BJ-T cells, and this proliferation defect was p53-independent (approximate doubling times: BJT+vehicle=20hr, BJ-T+CX-5488=50hr, BJTp53shRNA+vehicle=20hr, BJ-Tp53shRNA+CX-5488=53hr, for n=1 experiment) (FIGURE 15 E and F). Importantly, inhibition of Pol I transcription by 1μM CX-5488 induced phos-CHK2(T68) and phos-p53(S15) (FIGURE 15 D). These results indicate that it is unlikely ATM/ATR signaling pathway activation arises as a result of non-specific effects of these small molecules - CX-5447 is structurally very similar to CX-5461 and does not cause pathway activation, while CX-5488 has a more divergent structure and the ATM/ATR signaling pathway is activated following inhibition of Pol I transcription initiation by this small molecule.

6.2.3. Conclusions

These results support that the activation of ATM/ATR signaling by CX-5461 is due to inhibition of Pol I transcription initiation, rather than unknown off target effects. CX-

5447 (an inactive isomer with almost identical structure to CX-5461) did not activate these pathways, while CX-5488 (which inhibits Pol I transcription initiation similarly to CX-5461 but has a divergent structure) can activate ATM/ATR signaling. However, the absence of ATM/ATR signaling activation following ActD treatment suggests that inhibition of Pol I transcription at different steps such as initiation or elongation can elicit different responses.

6.3 CX-5461, but not Actinomycin D, displaces Pol I from 'open' rDNA repeats.

6.3.1. Introduction

As inhibitors of initiation of Pol I transcription (CX-5461 and CX-5488), but not elongation of Pol I transcription (ActD), activate the ATM/ATR signaling pathway, we reasoned that the stimuli of ATM/ATR pathway activation may be related to the differences between these approaches.

We have previously shown that CX-5461 inhibits rDNA transcription by preventing association of SL1 with the rDNA promoters thus blocking PIC assembly. Cell free transcription 'order of addition' assays show that CX-5461 inhibits Pol I transcription prior to PIC formation, but only minimally effects Pol I transcription after this stage. ChIP analysis in a number of transformed cell lines show that occupancy of Pol I, UBF, and most significantly SL1 are reduced at the rDNA promoter. Electromobility shift assay (EMSA) of human SL1 and DNA fragments corresponding to the rDNA promoter shows CX-5461 disrupts the SL1/rDNA complex (Drygin et al., 2011). In contrast, ActD does not prevent PIC assembly at the rDNA or initiation of Pol I transcription (Fetherston et al., 1984; Sollnerwebb and Tower, 1986).

Based on our knowledge of the activity of both ActD and CX-5461, we hypothesised that ActD and CX-5461 will have different effects on Pol I association with rDNA. We therefore examined Pol I binding to rRNA gene promoters and transcribed region by ChIP following treatment with ActD and CX-5461.

6.3.2. Results

To examine Pol I binding at the rDNA following inhibition of Pol I transcription with either ActD or CX-5461, we performed ChIP analysis for a number of regions across the canonical rDNA sequences (Shown in FIGURE 26 A). First, in BJ-T cells, Pol I was enriched across the rDNA in vehicle treated cells, relative to the –ve antibody

(sera only) control. Following 3hr treatment with 1μM CX-5461, Pol I was no longer enriched at the rDNA (with over a 5-fold reduction in Pol I compared to vehicle treated cells at all rDNA regions tested. n.s. for n=3 experiments) (FIGURE 26 B). We then extended this analysis in BJ-T p53shRNA cells. Pol I is enriched at the promoter and across the entire transcribed region of the rDNA, but not across the untranscribed region (IGS), in vehicle treated cells. Following 3hr treatment with 1μM CX-5461, levels of Pol I association with the rDNA were significantly reduced, with enrichment of Pol I no longer detected at the promoter or transcribed regions of the rDNA (with an approximately 4-fold reduction at Promoter *$p<0.05$, 8-fold reduction at ETS2 *$p<0.05$, and over 10-fold reduction at subsequent transcribed regions from 18S to Terminator **$p<0.005$). Following 3hr treatment with 5nM ActD, levels of Pol I association with the rDNA were unchanged at the promoter, but reduced across the transcribed region of the rDNA (with over 4-fold reduction at transcribed regions from 18S to Terminator *$p<0.05$) (FIGURE 26 B). Therefore, consistent with the known mechanisms of inhibition of Pol I transcription by these drugs, Pol I remained at the rDNA promoter following ActD treatment, and was displaced from the rDNA promoter following CX-5461 treatment. As predicted, Pol I was also absent across the entire transcribed rDNA sequence following CX-5461 treatment. While, following ActD treatment, Pol I remained associated with the rDNA, but at levels that were reduced in the direction of Pol I transcription.

Copies of the rRNA genes typically exist in two different states (See Section 1.1.2): active genes are associated with the cytoarchitectural transcription factor UBF, resulting in an 'open' chromatin conformation, while inactive genes are not associated with UBF and have a 'closed' chromatin conformation (Sanij et al., 2008)(Reviewed in (Sanij and Hannan, 2009; Grummt and Langst, 2013)). Active rRNA genes can achieve very high rates of transcription by Pol I, accounting for over 30% of transcriptional activity in an exponentially growing cell, and typically have dense Pol I loading across the transcribed region (Warner, 1999; Warner et al., 2001)(Reviewed in (Moss et al., 2007)). Therefore, we examined whether CX-5461 treatment and consequent displacement of Pol I from the rDNA alter the euchromatic state of rRNA genes and/or affect the proportion of active 'open' rRNA genes.

First, we performed ChIP analysis for UBF in BJ-T cells. UBF was enriched across the rDNA in vehicle treated cells, relative to the –ve control (rabbit sera). Following 3hr treatment with 1μM CX-5461, UBF was enriched at the rDNA at similar levels,

although it appears slightly reduced specifically at the promoter region (with approximately 3-fold reduction for Promoter, n.s. for n=3 experiments) (FIGURE 26 B). We then extended this analysis in BJ-T p53shRNA cells. Following 3hr treatment with either 5nM ActD or 1μM CX-5461, UBF is enriched at the enhancer, promoter, and across the entire transcribed region of the rDNA, at similar levels to those observed in vehicle treated cells (FIGURE 26 B). Therefore, treatment with CX-5461 and displacement of Pol I from the rDNA did not result in changes in levels of UBF associated with the rDNA. As UBF is responsible for maintaining the euchromatic 'open' chromatin structure of rRNA genes (Sanij et al., 2008), our data suggest that CX-5461 treatment does not influence UBF binding to rDNA or its role in establishing 'open' rDNA chromatin.

To further examine the effect of inhibition of initiation of Pol I transcription by CX-5461 on the proportion of active 'open' rRNA genes, we performed psoralen crosslinking Southern blotting analysis. Active 'open' rDNA copies are accessible to psoralen, while inactive 'closed' rDNA copies are inaccessible to psoralen due to their silenced heterochomatic configuration. rDNA copies that have been crosslinked with psoralen can be distinguished by Southern blotting due to their differing rates of migration - active 'open' rDNA migrate more slowly due to their association with psoralen, and are therefore apparent as a separate band (FIGURE 26 C). We treated BJ-T cells with 1μM CX-5461 for 3hr, 12hr, 24hr, and 48hr. In vehicle treated cells, approximately 25% of rDNA copies were in an active 'open' chromatin conformation. There was no change in the proportion of active 'open' rDNA copies following 3h treatment with 1μM CX-5461, consistent with the absence of any changes in UBF loading at rDNA (FIGURE 26 B and C). Following 12h treatment with 1μM CX-5461, there was still no change in the proportion of active 'open' rDNA genes. However, after 24 and 48hr treatment, the proportion of active 'open' rDNA copies appeared to increase (to approximately 40% and 45% of rDNA copies, respectively. n.s for n=3 experiments) (FIGURE 26 C). Therefore, CX-5461 treatment and consequent displacement of Pol I from the rDNA did not result in reduced active 'open' rDNA copies.

6.3.3. Conclusions

Inhibition of Pol I transcription initiation by CX-5461 results in rDNA repeats that are devoid of Pol I, but maintain an 'open' chromatin conformation. Therefore, the 'open' subset of rDNA repeats, which were formerly associated with Pol I and undergoing transcription, have a novel 'exposed' chromatin state following CX-5461 treatment. In

contrast, inhibition of Pol I transcription elongation by ActD results in rDNA repeats that remain associated with Pol I at reduced levels. These changes in Pol I loading at the rDNA are observed at early timepoints, corresponding to the activation of the ATM/ATR signaling pathway in CX-5461, but not ActD, treated cells. This suggests that inhibition of Pol I recruitment to the rDNA and the subsequent 'exposed' chromatin state of rDNA, rather than inhibition of Pol I transcription *per se*, is responsible for activation of the ATM/ATR signaling pathways.

6.4 Hypotheses addressing the direct mechanism by which inhibition of Pol I transcription initiation by CX-5461 activates ATM/ATR signaling.

Inhibition of Pol I transcription by CX-5461 rapidly reduces levels of 47S rRNA transcription, prevents Pol I transcription initiation at the rDNA promoter, and displaces Pol I from the rDNA repeats. We considered how this might result in activation of the ATM/ATR signaling pathways. Three distinct hypotheses were chosen for investigation.

Broadly, they are as follows:

1) ATM and ATR are locally activated at the rDNA due to displacement of Pol I across the rDNA repeats following CX-5461 treatment.
2) A defect in replication arises specifically at the rDNA due to displacement of Pol I across the rDNA repeats following CX-5461 treatment.
3) DDR proteins that localise to the nucleoli activate DDR signaling pathways following inhibition of Pol I transcription by CX-5461 due to distinct changes in nucleolar structure.

Each of these hypotheses are explained in more detail in the corresponding sections below.

6.4.1 Hypothesis 1. ATM substrate NBS1 (phos-S345) is specifically activated at the nucleoli during S/G2 following CX-5461 treatment.

6.4.1.1 Introduction

The canonical ATM/ATR signaling pathways are activated as a result of DNA damage, as described in detail in Section 5.1. However, a number of publications have reported the activation of ATM and ATR by additional mechanisms. Particularly, we considered whether ATM/ATR could be locally activated at the rDNA following CX-5461 treatment,

as a result of changes in active 'open' rDNA copies to an 'exposed' chromatin state. ATM activation may result from changes in chromatin structure. Conditions that alter chromatin structure, such as hypotonic conditions, treatment with chloroquine, or treatment with HDAC inhibitors, can induce rapid and diffuse activation of ATM (Bakkenist and Kastan, 2003). On the other hand, the stable association of ATM with chromatin, by expression of ATM-lacR fusion protein in cells with stably integrated lacO sequence repeats, was sufficient to activate ATM (Soutoglou and Misteli, 2008). ATR can also be locally activated specifically at the rDNA. A crucial activator of ATR response, TOPBP1, preferentially localises to the rDNA when overexpressed and induces ATR dependent responses distinct from its canonical role in DNA replication (Sokka et al., 2015). Therefore, we hypothesised that following inhibition of Pol I initiation by CX-5461, rDNA copies become more available for association with ATM/ATR and their mediator proteins, and that this is sufficient for activation of ATM/ATR signaling.

6.4.1.2 Results.

Initially we performed IF and ChIP analysis in BJ-T p53shRNA cell lines for both ATM, and replication protein A (RPA), which binds ssDNA and recruits ATR (Reviewed in (Cimprich and Cortez, 2008)). We could not detect enrichment of ATM or RPA at the rDNA in cells treated for 3hr with either vehicle or 1μM CX-5461, by either IF (with co-staining for UBF as a marker for active rDNA) or ChIP assays (Results not shown). However, we could not conclude that ATM and ATR proteins were absent from the rDNA, as we did not have a positive control suitable to detect their binding at the rDNA in these cells. Therefore, we once again utilised the U2TR I-*Ppo*I-dd cell line, in which DNA damage can be induced at a defined site in the rDNA (Described in Section 5.3 above). As the site of the DSBs are known, it is possible to both directly assess the level of DNA damage using a primer set that spans the I-*Ppo*I cut site, and identify bound proteins by ChIP using a primer set directly adjacent to the I-*Ppo*I cut site (FIGURE 27 A). I-*Ppo*I activity was induced in U2TR I-*Ppo*I-dd cells, and the onset of DNA damage confirmed by real-time PCR amplification of the 28S rDNA endonuclease target site, as described above (See FIGURE 21). We performed ChIP analysis for ATM in cells treated for 2hr with either vehicle or 1μM CX-5461, as well as 3hr I-*Ppo*I induced cells as a positive control. As expected, in I-*Ppo*I induced cells ATM was significantly enriched at the I-*Ppo*I endonuclease rDNA cut site (approximately 10-fold over negative antibody IgG control, ***$p<0.0005$). However, no enrichment was

observed for ATM following vehicle or CX-5461 treatment either at the rDNA promoter or at the I-*Ppo*I endonuclease rDNA cut site (FIGURE 27 B).

The recruitment of ATM to chromatin is mediated by the MRE11/RAD50/NBS1 (MRN) complex. The stable association of both MRE11 and NBS1 with chromatin, by expression of lacR fusion proteins in cells with stably integrated lacO sequence repeats, results in ATM activation and G2 cell cycle arrest (Soutoglou and Misteli, 2008). Therefore, we next performed IF analysis for the MRN complex at the rDNA. Specifically, for Nijmegen Breakage Syndrome 1 (NBS1) phosphorylation at S345, which was selected as it is a substrate for ATM kinase activity. As the ATM/ATR signaling pathways are activated specifically in S-phase and G2, we utilized BJ-T p53shRNA cells transfected with fluorescent ubiquitinylation cell cycle indicator (FUCCI). These cells are transfected with pCSII-EF-mCherry-hCdt1(30-120) and pCSII-EF-mVenus-hGeminin(1-110), resulting in Cherry (red) signal during G1 phase prior to the onset of DNA replication, due to expression of the DNA replication licensing factor Cdt1, and Venus (green) signal during S and G2 phase, due to expression of the Cdt1 inhibitor Geminin (Sakaue-Sawano et al., 2008). Cells express both proteins (yellow) specifically during the late G1 - S phase transition. We performed co-immunofluoresence analysis of NBS1 (phos-S345) and the nucleolar protein NPM in this BJ-T p53shRNA FUCCI cell line. Following 1hr treatment with 1μM CX-5461, a small but significant increase in levels of NBS1 (phos-S345) could be detected specifically in the nucleoli of S/G2 cells (1.2 fold, **p<0.005) (FIGURE 27 C). Consistent with our previous results, we did not detect increased levels of γH2A.X in the nucleus or the nucleoli in these populations (γH2A.X was reduced 1.1 fold in the nucleus (**p<0.005) and nucleolus (****p<0.0001) in S/G2 cells following CX-5461 treatment) (FIGURE 27 D). Therefore, the MRN complex component can localize to the nucleoli independent of DNA damage, and following inhibition of Pol I transcription initiation by CX-5461 is associated with ATM activation in the nucleoli specifically during S/G2. These experiments were performed in collaboration with Dr Keefe Chan and Dr Elaine Sanij.

6.4.1.3 Conclusions.

We did not detect significantly increased levels of ATM associated with 28S rDNA chromatin following inhibition of Pol I transcription initiation with CX-5461 in exponentially growing cell populations. However, when we specifically examined S/G2 cell cycle populations, in which activation of ATM/ATR signaling is observed following

CX-5461 treatment, we observed increased levels of the ATM substrate NBS1 (phos-S345) in the nucleoli. NBS1 is part of the MRN complex, which recruits ATM to chromatin. Therefore, our results suggest that following changes in Pol I occupancy at the rDNA due to inhibition of Pol I transcription initiation by CX-5461, ATM can be transiently recruited to rDNA chromatin and activated, in the absence of DNA damage.

6.4.2 Hypothesis 2. Delay in DNA replication occurs rapidly following CX-5461 treatment and occurs in both early and late S-phase.

6.4.2.1. Introduction.

The rDNA repeats pose challenges to replication, due to their highly transcribed and highly repetitive nature. Studies in *S. cerevisiae* have illustrated unique mechanisms used at the rDNA to ensure correct replication and prevent instability. These include replication occurring in the same direction as transcription, as a result of a Replication Fork Blocking (RFB) site 3' of the rDNA transcribed region, which stalls replication forks moving 5' to the rRNA genes and thus prevents collision with transcription apparatus. In mammals, the regulation of rDNA replication and stability is less well defined, but it appears to share similarities with yeast. RFBs have been described close to the 3' end of the rDNA transcriptional unit in mice, where they are reported to colocalise with Pol I transcriptional terminator elements (Lopez-Estrano et al., 1998), and in humans, where they are reported to be bi-polar, arresting forks traveling in both directions (Little et al., 1993; Akamatsu and Kobayashi, 2015). Pol I transcription may be required for efficient replication: Active rRNA genes replicate in early S, and inactive rDNA genes replicate in late S (Li et al., 2005); while at pseudo-NORs, which have an open chromatin state but lack Pol I transcription, replication starts early in S-phase, but is delayed and continues into late S-phase (Smirnov et al., 2011). These features at the rDNA have implications for the relationship between transcription and replication. The unidirectional progression of replication forks prevents the presence of elongating Pol I from interfering with replication, as would occur at other loci due to the collision of replication and transcription apparatus. In fact, the presence of Pol I may facilitate replication at the rDNA - proteins involved in DNA replication are reported to be associated with transcriptionally competent Pol I, suggesting Pol I is recruited to the rDNA promoter as part of a complex that coordinates both rRNA synthesis as well as DNA replication (Hannan et al., 1999)(Reviewed in (Drygin et al., 2010)). On the other hand, the absence of Pol I from the active rDNA genes could result in unusual chromatin structures, as a result of the 'exposed' state of these copies, presenting a challenge for DNA replication.

Therefore, as ATM/ATR signaling is activated predominantly in S-phase following CX-5461 treatment, we investigated whether activation of ATM/ATR signaling arises due to a replication defect at the rDNA genes following inhibition of Pol I transcription. As inhibition of Pol I transcription initiation by CX-5461 specifically targets only active, early-replicating rRNA genes, we hypothesised that this scenario would result in a replication defect arising during early but not late S-phase.

6.4.2.2. Results.

The efficiency of replication of rDNA genes in early and late S-phase was determined by IP analysis of BrdU incorporation at newly synthesized rDNA in BJ-Tp53shRNA cells. Asynchronously growing cells were treated with vehicle control or 1μM CX-5461 for 3h, and pulse labeled with BrdU for the final 2h of treatment. Fixed cells were then sorted into G1, early S-phase, and late S-phase populations, on the basis of DNA content by FACs (See FIGURE 28 A). BrdU-IP was performed on these populations and the relative enrichment at genomic regions determined by real-time PCR.

First, to ensure specificity of the BrdU antibody, enrichment relative to an IgG negative control was determined, for populations cultured in the presence or absence of BrdU for 24h that had been mock sorted by FACS (n=1). The percentage of total DNA (ETS-1 rDNA) associated with α-BrdU in treated populations was over 200-fold higher than for untreated populations (FIGURE 28 B). During experimental optimisation 2h BrdU incorporation was found to be the shortest time that resulted in levels of BrdU sufficient to detect enrichment.

As total amounts of genomic DNA vary between early and late S-phase populations, it is inappropriate to calculate BrdU incorporation in sorted populations as a percentage of total DNA. Therefore, enrichment was determined relative to mitochondrial DNA - mitochondrial DNA replicates throughout the cell cycle, and is equally represented in early and late S-phase (Reviewed in (Mishra and Chan, 2014)). G1 sorted populations were used as the negative control – since no replication of genomic DNA occurs in G1, this population controls for both BrdU enrichment at sites other than nascent DNA, and the accuracy of FACs sorting of cell cycle populations.

In control cells, BrdU incorporation was observed at the rDNA at equal levels in both early and late S-phase (with a ratio of 1 in early S-phase to 0.8 in late S-phase, n.s for n=4 experiments) (FIGURE 28 C), indicating that in human cells the rDNA is replicated during both phases of the cell cycle, as has been previously reported in mice (Li et al.,

2005). BrdU incorporation was also observed for a known early replicating gene (MMP15, (Ryba et al., 2011)) in early S-phase (with a ratio of 1 in early S-phase to 0.4 in late S-phase, **p<0.005) and a known late replicating gene (HBB, (Ryba et al., 2011)) in late S-phase (with a ratio of 0.3 in early S-phase to 1 in late S-phase, ****p<0.0001). However, in both cases some BrdU incorporation was also observed for the alternative S-phase population. This may be a result of the 2h BrdU incorporation period – BJ-Tp53shRNA cells take approximately 6h to complete S phase (See FIGURE 11), so some early S-phase cells may have sufficient time to move into the late S-phase population while BrdU is being incorporated. Following CX-5461 treatment, significant reduction in BrdU incorporation was observed for rDNA replicating in both early and late S-phase (with a ratio of 1 in early S-phase control treated cells to 0.3 in early S-phase (**p<0.005) and 0.3 in late S-phase (*p<0.05) CX-5461 treated cells) (FIGURE 28 C), indicating that replication at the rDNA is delayed at both stages of S-phase. Significantly reduced incorporation of BrdU was also observed for MMP15 (with a ratio of 1 in control treated to 0.2 in CX-5461 treated early S-phase cells, **p<0.005) and HBB (with a ratio of 1 in control treated to 0.3 in CX-5461 treated late S-phase cells, ****p<0.0001), indicating that there is a genome wide delay in replication. In the case of early replicating MMP15, BrdU incorporation was no longer increased in early S-phase compared to late S-phase, suggesting replication timing was delayed and continued into late S-phase.

6.4.2.3. Conclusions.

These results show that the observed S-phase defect does not preferentially affect cells in early S-phase. Note that this assay is unable to determine whether there is a replication defect at the rDNA in general: while replication of rDNA repeats is delayed when cells are treated with CX-5461 in both early and late S-phase, acute checkpoint activation in S-phase by other mechanisms would result in a genome wide delay in S-phase progression at both the rDNA and other loci. However, as we observe a delay in replication in cells that are in late-S phase when treated with CX-5461, we can exclude the scenario that early replicating active rDNA repeats specifically experience a replication defect following CX-5461 treatment.

6.4.3 Hypothesis 3. CX-5461 treatment results in disruption of nucleolar structure, and altered localisation of DNA damage response proteins, in a manner distinct from DNA damage.

6.4.3.1. Introduction.

A number of DDR proteins localise to the nucleoli, as shown by proteomic analysis. In

response to genotoxic insults, a distinct population of proteins translocate between the nucleoli and the nucleoplasm (Cohen et al., 2008; Boisvert et al., 2010; Boisvert and Lamond, 2010; Moore et al., 2011). In addition to systematic analysis, the nucleolar regulation of some DDR proteins is beginning to be characterised in greater detail. For example, DNA repair factors RNF8 (ring finger protein 8) and BRCA1 localise to the nucleoli, where they interact with ribosomal protein RPSA, and translocate to DDR foci in the nucleus following γIR (Guerra-Rebollo et al., 2012). RecQ helicase WRN (Werner syndrome protein) is localised to the nucleoli, but translocates to the nucleoplasm after DNA damage in a manner that appears to be regulated by p300/CBP-mediated acetylation and SIRT1-mediated deacetylation (Kahyo et al., 2008; Muftuoglu et al., 2008; Lee et al., 2015). NCL interacts with a number of proteins involved in DDR (including WRN (Indig et al., 2012), PCNA, (Yang et al., 2009), RAD51 (De et al., 2006), RPA (Daniely et al., 2002), and TopoI (Bharti et al., 1996; Edwards et al., 2000)), and translocates from the nucleoli to the nucleoplasm following DNA damage, where it can accumulate at γIR induced DSB sites (Kobayashi et al., 2012). NPM regulates the nucleolar localisation of several base excision repair (BER) proteins, and both NPM and BER proteins relocalise from the nucleoli to the nucleoplasm following DNA damage induced by cisplatin (Moore et al., 2013; Poletto et al., 2014b). Conversely, both p21 and RAD9B migrate to a compartment within the nucleoli in response to DNA damage induced by adriamycin (Abella et al., 2010; Perez-Castro and Freire, 2012), while transcription factor E2F1 is sequestered in the nucleoli by p14ARF as an early ATM-dependent response to DNA damage (Jin et al., 2014). These and other examples begin to paint a picture in which the nucleolus has a key functional role in regulating DDR through the sequestration and release of DDR proteins (Reviewed in (Nalabothula et al., 2010; Antoniali et al., 2014)).

Consistent with a role for the nucleoli in mediating DDR, DNA damage generally results in the inhibition of Pol I transcription and the reorganisation of nucleolar structure (Reviewed in (Boulon et al., 2010b)). In fact, both ATM and ATR have been shown to inhibit Pol I transcription: In response to DNA DSBs, Pol I initiation is inhibited in an ATM-dependent manner, specifically at those nucleoli where DNA damage is induced (Kruhlak et al., 2007; Jin et al., 2014)(Reviewed in(Larsen and Stucki, 2016)); while ATR can be locally activated at the rDNA by association of its activator TOPBP1 with the rDNA repeats, leading to inhibition of Pol I transcription in an ATR-dependent manner (Sokka et al., 2015). There is some variation in the nucleolar response to DNA damage, with different DNA damaging agents such as UV, IR, or drugs (for example topoisomerase II inhibitors) reported to result in Pol I

inhibition and nucleolar reorganisation of different degrees (Rubbi and Milner, 2003; Al-Baker et al., 2004; Kruhlak et al., 2007; Moore et al., 2011)(Reviewed in (Boulon et al., 2010b)). However, the commonly described nucleolar structure following DNA damage is that of 'nucleolar segregation', where condensation of the nucleoli, separation of the granular and fibrillar components, and the formation of 'nucleolar caps' containing distinct nucleolar proteins surrounding a central body are observed (Shav-Tal et al., 2005)(Reviewed in (Hernandez-Verdun et al., 2010)). Similar changes occur following treatment with low dose ActD, suggesting that it is the inhibition of Pol I transcription following DNA damage that affects the reorganisation of nucleolar structure (Shav-Tal et al., 2005; Perez-Castro and Freire, 2012)(Reviewed in (Boulon et al., 2010b; Hernandez-Verdun et al., 2010)) Therefore - considering that first, DNA damage leads to inhibition of Pol I transcription and reorganisation of the nucleoli, and second, multiple DDR proteins translocate from the nucleoli in a regulated manner following DNA damage - we hypothesise that inhibition of Pol I transcription by CX-5461 may result in the translocation of DDR proteins from the nucleoli and this may be sufficient to activate DDR signaling.

The activation of DDR following inhibition of Pol I transcription by CX-5461, but not ActD, could be explained by the absence of Pol I transcription complex at the rDNA following CX-5461 treatment resulting in more significant changes in nucleolar structure. The mechanisms that control protein targeting the nucleoli are not well defined, as discussed earlier (Section 1.1.1), any high affinity interactions for nucleolar components can impart nucleolar localization (Reviewed in (Emmott and Hiscox, 2009)). The role of the Pol I transcription complex itself, independent of rates of rRNA transcription, in the formation of nucleoli is not clear. McStay *et. al.* have shown that pseudo-NORs that recruit Pol I transcription complex components but are transcriptionally inactive, are able to adopt some but not all of the morphological characteristics of the nucleoli (Reviewed in (Prieto and McStay, 2008)). Studies by Grummt *et. al*. in mice addressed the role of the Pol I transcription complex more specifically, by deleting the Pol I transcription factor RRN3/TIF-1A. This resulted in nucleolar changes different from those induced by inhibition of Pol I transcription by ActD, with the complete disappearance of nucleolar structures (Yuan et al., 2005)(Reviewed in(Hernandez-Verdun et al., 2010)). While these studies still do not satisfactorily define the role of Pol I occupancy alone in establishing nucleolar structure, they suggest that it could play a role independent of rRNA transcription. It is possible that, as the Pol I transcription complex interacts directly with the rDNA as well as with numerous other nucleolar proteins, its displacement following CX-5461

treatment may result in a reduced scaffold on which the network of interactions responsible for nucleolar localisation can take place. Therefore CX-5461 treatment may have unique consequences for nucleolar structure, that differs to changes induced by signals or inhibitors that reduce rates of Pol I transcription (such as low dose ActD).

6.4.3.2. Results.

To examine nucleolar structure following treatment with CX-5461, we performed immunofluorescence (IF) and fluorescence in-situ hybridisation (FISH) analysis. Initially experiments were performed in BJ-T cells, as disruption of the nucleoli is known to result in activation of p53 (See Section 1.2.1), and therefore we could compare the timecourse of any changes in nucleolar structure to activation of both p53 (as a control) and the DDR proteins CHK1/CHK2.

First, to initially establish whether CX-5461 induced changes in nucleolar structure, we performed FISH analysis with a probe targeting the intergenic spacer of the rDNA repeat (rDNA-FISH). To ensure specificity of the probe, co-IF was performed for UBF, which binds across the entire transcribed region of open rDNA repeats. In control cells, rDNA repeats were observed both in large nucleoli, with an open conformation associated with UBF, and in condensed foci, corresponding to inactive NORs devoid of UBF. Following 48hr treatment with 1μM CX-5461, the rDNA repeats were organised in condensed structures, even those associated with UBF (FIGURE 29 A). We then examined whether the reorganisation of the rDNA into condensed structures occurs at early timepoints. Following 1hr treatment with 1μM CX-5461, rDNA repeats had already begun to coalesce, with rDNA-FISH showing a more condensed localisation in 1hr CX-5461 treated cells than control cells, though not yet to the same degree as for 48hr CX-5461 treated cells above (FIGURE 29 B). Thus, nucleolar structure is altered following CX-5461 treatment, with open rDNA reorganising into condensed nucleoli.

Next, to establish the timecourse of nucleolar reorganisation, we performed IF analysis of nucleolar proteins that localise to each of the tripartite nucleolar components - the FC, DFC, and GC (See Section 1.1.1). UBF localises to the FCs, as this is where the rDNA and Pol I transcription machinery are concentrated. The DFCs can be identified by the localisation of early pre-RNA processing factors, such as the snoRNP component Fibrillarin (FBL). The GCs are identified by the localisation of factors

involved in ribosome maturation, assembly and transport, such as nucleophosmin (NPM). Following 1μM CX-5461 treatment, we observed nucleolar structure at 30min, 1hr, 3hr, 12hr and 24hr. Control cells showed typical structures of active nucleoli with multiple UBF and FBL foci, corresponding to FC and GFC components respectively, interspersed within a single NPM structure, corresponding to the surrounding GC. After CX-5461 treatment both UBF and FBL foci compact, and NPM forms a single ring at the periphery of the nucleoli. There is also an increased proportion of NPM in the nucleoplasm (FIGURE 20 C). Changes in nucleolar structure had begun by 30min, and by 3hr nucleoli appear to have completed reorganisation, with UBF, FBL and NPM structures appearing the same at 3hr as for later 12hr (not shown) and 24hr timepoints. Therefore, CX-5461 results in changes in nucleolar structure as early as 30min following treatment, which is consistent with the activation of p53 and CHK1/CHK2 observed at these timepoints (See FIGURE 20 B).

However, the changes in nucleolar structure following inhibition of Pol I transcription initiation by CX-5461 treatment may not correspond to changes in nucleolar structure that occur following DNA damage. The changes observed here following CX-5461 treatment were markedly different from those that were observed following DNA damage induced by I-*PpoI* endonuclease, where UBF relocalised to one or two foci at the periphery of a condensed nucleoli (see FIGURE 20 F). To further compare nucleolar reorganisation following inhibition of Pol I transcription initiation by CX-5461 to nucleolar reorganisation following DNA damage, we performed IF following CX-5461 treatment, UV-irradiation, or γ-irradiation, for NPM and WRN. WRN is a RecQ helicase with roles in DNA replication, repair, transcription and telomere maintenance (Reviewed in (Brosh and Bohr, 2002)). WRN is localised to the nucleoli under normal conditions, but following DNA damage translocates to the nucleoplasm where it can interact with certain other DDR proteins and repair foci (Gray et al., 1998; Marciniak et al., 1998; Sakamoto et al., 2001; Suzuki et al., 2001; Karmakar and Bohr, 2005; Lee et al., 2015). In this case, experiments were performed in BJ-T p53shRNA cells, as the translocation of some nucleolar proteins may be dependent upon p53 status (Boisvert and Lamond, 2010). We examined the localisation of NPM and WRN 1hr following 1μM CX-5461 treatment, 100μJ UV-irradiation, or 10Gy γ-irradiation (FIGURE 29 D). In control cells, WRN was predominantly localised to the nucleoli. After CX-5461 treatment, WRN was excluded from the nucleoli, and diffused throughout the nucleoplasm. For both control and CX-5461 treatment, a background number of cells (approximately one quarter) also displayed WRN foci in the nucleus. Following DNA

damage by both UV and γ-IR, the majority of cells displayed numerous WRN foci in the nucleus. In these cells, WRN was not predominantly nucleolar, but largely distributed through the nucleoplasm. However, in contrast to CX-5461 treatment, WRN was not entirely excluded from the nucleoli - instead, cells had a sub-population of WRN that remained within the nucleoli. Further, UV and γ-IR cells did not undergo reorganisation of the nucleoli as observed for CX-5461 above – rather, the localisation of NPM reflected a similar nucleolar structure to control cells. Therefore, there are marked differences in the reorganisation of the nucleolus and translocation of nucleolar DDR proteins following inhibition of Pol I transcription initiation by CX-5461 compared to those following DNA damage.

6.4.3.3. Conclusions.

These results show that nucleolar structure is reorganised within 3hr following CX-5461 treatment, which corresponds to the timeline of activation of p53 and ATM/ATR signaling. DDR proteins specifically can also relocalise following CX-5461 treatment, as shown here for WRN. However, these changes to not appear to correspond to changes in nucleolar structure following treatment with DNA damaging agents. Nor do these changes seem consistent with the apparently precisely regulated translocation of DDR proteins to and from the nucleoli in response to specific DNA damage, as discussed above. Therefore, it is unclear whether changes in nucleolar structure following inhibition of Pol I transcription by CX-5461 could be involved in activation of DDR signaling pathways.

6.5 DNA damage repair is compromised following inhibition of Pol I transcription initiation by CX-5461

6.5.1 Introduction.

A link between the nucleoli and DDR signaling pathways has been drawn by a wide range of reports, as discussed above (see Section 6.4.3.1). Now, we have additionally shown that treatment with an inhibitor of Pol I transcription initiation, CX-5461, is sufficient to activate the ATM/ATR key DDR signaling pathways. However, to our knowledge, the impact of changes in nucleolar structure and function upon the DNA damage response as a whole has not been comprehensively investigated.

It has been proposed that as the rDNA repeats are particularly vulnerable to DNA damage and instability, due to their repetitive nature and high rates of transcription, the

nucleoli may be utilised to activate DDR in a highly sensitive manner, performing a protective function for the genome as a whole (Stults et al., 2008)(Reviewed in (Kobayashi, 2011)). In fact, in the case of p53 activation, Rubbi and Millner demonstrated in their landmark study that DNA damage at the nucleoli, but not at nucleoplasmic DNA, is necessary and sufficient to activate p53. This activation of p53 can be achieved by the inhibition of Pol I transcription, even in the absence of DNA damage (Rubbi and Milner, 2003). Conversely, upregulated rRNA synthesis can result in decreased p53 response to cytotoxic stress (Donati et al., 2011a). These studies indicate that p53 activation in response to DNA damage is directly related to nucleolar structure and function. However, less is known about how perturbations at the nucleoli impact upon other DDR pathways, and the overall sensitivity to DNA damage.

For some DDR proteins, conditions that alter their nucleolar localisation have in fact been reported to impact upon their function in response to DNA damage. For example, PARP1, which regulates multiple cellular processes, is enriched in the nucleoli where it is involved in regulation of Pol I transcription through maintenance of repressive epigenetic state (Guetg et al., 2012). Upon DNA damage PARP1 translocates to the nucleoplasm, where it is activated by binding to DNA breaks, and is involved in DNA repair and induction of cell death (Rancourt and Satoh, 2009; Moore et al., 2011). Notably, delocalization of PARP1 from the nucleoli and its enrichment in the nucleoplasm sensitises cells to DNA-damage induced cell death (Rancourt and Satoh, 2009). NPM also translocates from the nucleoli following DNA damage, as described above, and it can localise to DNA DSBs in the nucleoplasm (Koike et al., 2010). Inhibition of NPM association with γH2A.X sensitises cells to IR (Sekhar et al., 2011). BER protein APE1 (apurinic/apyrimidinic endonuclease 1), whose nucleolar localisation is modulated by NPM, translocates to the nucleoplasm following cisplatin treatment. Cells expressing mutant APE1, which does not relocalise after cisplatin treatment, showed significantly increased sensitivity to the drug (Poletto et al.). Conversely, tumor suppressor ING1 (inhibitor of growth protein 1) accumulates in the nucleoli after UV-irradtiation and stabilises CSIG, which activates downstream effectors to promote apoptosis. Mutant ING1 proteins that are not targeted to the nucleoli are unable to promote apoptosis following DNA damage (Scott et al., 2001; Li et al., 2012). Therefore, it is possible that the relocalisation of DDR proteins following changes in rates of Pol I transcription has consequences for sensitivity to DNA damage.

These findings suggest it is possible that DDR is altered when nucleolar structure and function is disrupted by inhibition of Pol I transcription by CX-5461. However, it is difficult to predict whether cells will be rendered less sensitive to DNA damage, for example due to the early activation of DDR pathways, or more sensitive to DNA damage, for example due to misregulation of DDR. Therefore, we considered two alternative hypotheses, that a) CX-5461 treatment protects cells from DNA damage, or conversely b) CX-5461 treatment sensitises cells to DNA damage.

6.5.2 Results.

To determine whether the repair of DNA damage is affected by the cellular response to CX-5461, we first performed alkaline comet assays to determine levels of DNA damage following UV irradiation in the presence of CX-5461. We utilised BJ-T cells, with wild-type p53, as we wished to establish the overall consequences of nucleolar disruption on DDR, rather than signaling through any specific DDR pathway. BJ-T cells were pre-treated with vehicle or 1μM CX-5461 for 10min, then irradiated with 250J/m^2 UV and incubated for 20min (FIGURE 30 A). Following 30min treatment with CX-5461 alone, no difference was observed in comet tail moment compared to vehicle treated cells (difference between means -20.66±16.34, n.s. for n=2 experiments), as we had previously shown (see Section 5.3). Following 20min after 250J/m^2 UV irradiation, increased comet tail moment was observed compared to vehicle treated cells, as expected following DNA damage (from 163 ETM in vehicle treated cells, to 510 ETM in UV treated cells ****$p<0.0001$). Strikingly, cells that were UV irradiated in the presence of CX-5461 showed increased levels of DNA damage, with significantly increase tail moment compared to UV alone (from 510 ETM in vehicle treated cells, to 653 ETM in UV treated cells ****$p<0.0001$). This indicates that cellular response to CX-5461 is associated with attenuated repair of DNA damage. These experiments were performed in collaboration with Dr. Amit Khot and Dr. Elaine Sanij.

To extend this analysis, we performed IF analysis for γH2A.X in BJ-T cells following γIR in the presence of CX-5461. BJ-T cells were pre-treated with vehicle or 1μM CX-5461 for 10min, then irradiated with 10Gy γIR and incubated for 30min, 1hr, 3hr or 6hr (FIGURE 30 B). Following 1μM CX-5461 alone, there was no increase in γH2A.X foci compared to vehicle treated cells, as we have shown previously (See Section 5.3). Following γIR alone, increased γH2A.X foci were observed, as expected following DNA damage. The maximum number of foci were observed at 30min following irradiation, with reduced foci at later time points, likely due to the DNA repair of DSBs.

Interestingly, cells that were exposed to γIR in the presence of CX-5461 displayed increased γH2A.X foci compared to vehicle treated cells at all time points, but displayed reduced number and intensity of γH2A.X foci compared to γIR alone at 30min following irradiation. In these cells, γH2A.X foci were not reduced at later time points, but were sustained at low levels. This suggests that DDR proteins are recruited to sites of DNA damage at reduced levels following CX-5461 treatment delaying DNA repair.

Next, we examined whether the cellular response to CX-5461 is associated with attenuated repair of DNA damage at the rDNA, specifically. There is recent evidence that repair of DNA damage at the rDNA occurs by mechanisms that differ to those at other sites (Stimpson et al., 2014; van Sluis and McStay, 2015)(Reviewed in (Larsen and Stucki, 2016)). Rates of Pol I transcription could conceivably influence DNA repair at the rDNA, however it is unclear whether this is the case. On one hand, the association of a number of DDR proteins with Pol I has led others to propose that DNA repair is coordinated with rRNA synthesis (Reviewed in (Drygin et al., 2010)). On the other hand, increased rates of Pol I transcription can result in increased levels of DNA damage and instability at the rDNA (Guetg et al., 2010; Ide et al., 2010; Wang et al., 2013). Further, the increased activation of DDR proteins specifically in the nucleoli following CX-5461 treatment, as we have shown for NBS1 above, may be protective for the rDNA loci. Therefore, conditions that influence repair of genome outside of the nucleous may not extend to the rDNA.

To determine whether the cellular response to CX-5461 prevents DNA repair at the rDNA, we utilised the U2TR-I-*Ppo*I-dd system described above to examine levels of DNA damage at the 28S I-*Ppo*I target site (See Section 5.3). As I-*Ppo*I continues to cleave DNA while earlier lesions are undergoing DNA repair, the relative levels of DNA damage detected reflect the balance between these two processes. I-*Ppo*I activity was induced in U2TR I-*Ppo*I-dd cells as described above, and cells were treated with either vehicle or 1μM CX-5461 for the final two hours of endonuclease activation (FIGURE 30 C). Cells treated with 1μM CX-5461 during I-*Ppo*I activation showed a significant increase in 28S DNA damage, compared to I-*Ppo*I induction alone (corresponding to a 1.5-fold reduction in amplification of the of the target site, *$p<0.05$). Interestingly a slight increase in levels of 28S DNA damage was also observed in the presence of CX-5461 treatment alone (corresponding to a 1.1-fold reduction in amplification of the of the target site, n.s. for n=3 experiments). This may have arisen as a result of

reduced DNA repair of background I-*Ppo*I endonuclease activity, as described above. These results indicate that DNA repair is compromised at the rDNA following CX-5461 treatment.

We also used this system to examine whether CX-5461 treatment affects the recruitment of DDR proteins to DSBs at the rDNA. ChIP analysis was performed for ATM at rDNA adjacent to the I-*Ppo*I endonuclease target site, for the conditions described above. ATM was recruited to the rDNA at similar levels following both I-*Ppo*I induction alone, and CX-5461 treatment during I-*Ppo*I activation (% total DNA I-*Ppo*I induction alone =0.088, I-*Ppo*I induction +CX-5461 =0.091, difference between means 0.0025±0.0013, n.s. for n=3 experiments) (FIGURE 30 C). However, as there was significantly more DNA damage in these cells (see FIGURE 30 C), this suggests there are reduced levels of ATM per DNA damage site. This was also observed for NBS1, where enrichment at the I-*Ppo*I endonuclease target site was reduced by approximately half in the presence of CX-5461 (n.s. for n=1 experiment). Therefore, DDR proteins can be recruited to DNA damage sites at the rDNA in the presence of CX-5461, however this may be at reduced levels.

6.5.3 Conclusions.

These results suggest that DNA damage repair is attenuated following treatment with CX-5461. While CX-5461 alone does not induce DNA damage at early time points, when DNA damage arises from other sources (for example UV or γ-IR), increased levels of DNA damage are observed in the presence of CX-5461. DNA damage repair appeared to be attenuated at both the rDNA, and at sites across the entire genome. However, we have not investigated the mechanisms by which this occurs in depth.

6.6 Discussion.

We investigated the mechanism by which CX-5461 activates the ATM/ATR signaling pathway independently of DNA damage. While a small number of publications have shown that activation of ATM and ATR can occur in the absence of DNA DSBs and/or ssDNA, none of the currently known mechanism of activation are linked to nucleolar function.

6.6.1 Unique characteristics of inhibition of Pol I transcription by CX-5461.

First, we established whether ATM/ATR signaling pathway activation was a result of inhibition of Pol I transcription specifically, rather than any as yet unidentified effects of

CX-5461. This was of particular interest as treatment with ActD, a commonly used inhibitor of Pol I transcription elongation, did not result in ATM/ATR signaling pathway activation or G2 cell cycle arrest in BJ-T p53shRNA cells. Treatment with a small molecule with almost identical structure to CX-5461, which did not inhibit Pol I transcription (CX-5447), did not activate the ATM/ATR signaling pathway. This gives us confidence that this class of small molecules does not result in non-specific activation of ATM/ATR. Treatment with another small molecule inhibitor of Pol I transcription, with a more divergent structure to CX-5461 (CX-5488), did activate the ATM/ATR signaling pathway (FIGURE 25). This indicates that ATM/ATR activation arises as a result of inhibition of Pol I transcription initiation, specifically. Interestingly, a recent publication by Ma and Pederson (Ma and Pederson, 2013) found that HeLa cells treated with ActD do undergo S phase delay and G2 cell cycle arrest. This is also associated with the activation of ATR, independently of DNA damage. In their experiments, specific conditions of ActD treatment were required to activate the ATR-mediated G2 cell cycle checkpoint: 30min treatment with ActD resulted in inhibition of Pol I transcription to undetectable levels, but transcription recovered and there was no significant change in cell cycle profile; However, 2hr treatment with ActD resulted in inhibition of Pol I transcription that was sustained for up to 20hr, when cell cycle arrest was observed. Therefore, these results may be consistent with our hypothesis that ATM/ATR activation arises as a result of certain conditions of Pol I occupancy at the rDNA, rather than inhibition of Pol I transcription *per se*.

As CX-5461, but not ActD, acutely activates the ATM/ATR signaling pathways, we reasoned that the mechanism of ATM/ATR activation is related to the difference between these inhibitors. Based on our knowledge of the mechanism of Pol I transcription inhibition by ActD (which prevents Pol I transcription elongation) and CX-5461 (which inhibits PIC assembly and Pol I transcription initiation), we expected that a key difference between these treatments would be the level of Pol I occupancy at the rDNA, and we demonstrated that this was the case. Following 2hr ActD treatment, Pol I remained associated with the rDNA promoter and across the transcribed region, while following 2hr CX-5461 treatment, Pol I is displaced from the rDNA promoter and across the entire rDNA repeat (FIGURE 26).

Interestingly, different signaling pathways mediate Pol I transcription at different stages, including PIC formation, initiation of transcription, and transcriptional elongation (See Section 1.1.3). For DNA damage signaling pathways specifically, in the few cases where the mechanism of inhibition Pol I transcription has been

elucidated, it has been found that the association of SL1 at the rDNA and/or PIC assembly is targeted. For example, p53 binds directly to SL1 preventing its interaction with UBF and PIC assembly (Zhai and Comai, 2000), induction of DSBs results in ATM activation and interferes with Pol I initiation complex assembly (Kruhlak et al., 2007), and DNA-PK auto-phosphorylation promotes displacement of SL1 from the rDNA (Michaelidis and Grummt, 2002). Therefore, targeting of SL1 and inhibition of PIC assembly by CX-5461 may resemble the nucleolar response to DNA damage.

These results would be strengthened by additional controls that inhibit either Pol I transcription initiation or Pol I transcription elongation. We attempted to target Pol I transcription initiation by siRNA depletion of POLR1A and RRN3. However, we were unable to achieve sufficient reduction of Pol I transcription - rates of Pol I transcription were reduced by approximately 50% after 48hr. This may be due to the fact that less than 10% of Pol I is utilised for transcription at any time, so even a small amount remaining after knockdown enables effective rates of 47S pre-rRNA transcription (See FIGURE 11 F). Under these conditions of inhibition, we could not detect activation of ATM/ATR signaling. We expect this is due to the differences in rapid inhibition of over 80% of Pol I transcription by CX-5461 within 1 hour of treatment, compared to relatively delayed and less efficient inhibition of Pol I transcription by RNAi, as the lack of correlation between small molecule inhibition and RNAi phenotypes is an established phenomenon (Weiss et al., 2007).

The displacement of Pol I from active ‘open’ rDNA repeats following CX-5461 treatment creates unusual ‘exposed’ rDNA repeats (FIGURE 26). Typically, Pol I is present at very high levels on active ‘open’ rDNA repeats - studies in yeast have shown that Pol I is 10-100x more dense than Pol II per open reading frame, with frequent contact between adjacent polymerases and continuous tracks of Pol I (French et al., 2003; Albert et al., 2011). The ‘exposed’ rDNA repeats are characterised by an ‘open’ chromatin conformation, with association of UBF across the length of the transcribed region and accessibility to psoralen, but the complete absence of Pol I. This is an unusual state, as even during the complete shut down of Pol I transcription and disassembly of the nucleoli during mitosis, Pol I remains associated with the open rDNA repeats (Reviewed in (Dimario, 2004)). During differentiation, when rates of rDNA transcription are reduced, the proportion of active ‘open’ rDNA repeats are also reduced, suggesting rDNA transcription is concentrated at fewer genes in order to maintain the mean number of polymerases per gene (Reviewed in (Sanij and Hannan, 2009)). Therefore it is possible that ‘exposed’ rDNA repeats have functional

consequences for the cell.

An interesting observation is that following long term CX-5461 (24hr or 48hr), there was an increased proportion of rDNA repeats in an 'open' conformation accessible to psoralen (FIGURE 26 C). As this arose well after the activation of the ATM/ATR signaling pathways, we did not pursue it in depth. However, this could conceivably occur due to either a) a change in the conformation of rDNA repeats from open to closed, or a change in the total number of rDNA repeats, with either b) an increased number of open rDNA repeats, or c) a decreased number of closed rDNA repeats. We speculated that it could be due to preferential replication of active rDNA repeats associated with the S-phase defect in these cells - active rDNA repeats are replicated in early S-phase while inactive rDNA repeats are replicated in late S-phase (ie. scenario 'b') (Li et al., 2005) (Dimitrova, 2011). However, BrdU-IP experiments determining rates of rDNA replication in early and late S-phase showed that this was not the case (FIGURE 28). Another possibility is that CX-5461 treatment prevents Pol I transcription of the pRNA component of the nucleolar remodelling complex (NoRC), which is required for the epigenetic silencing of rDNA repeats (ie. scenario 'a'). The pRNA is transcribed by Pol I from transcriptionally competent rRNA genes during mid S-phase, acting in trans with NoRC to inherit repression of late replicating silent rDNA copies. Strikingly, depletion of another NoRC component, TIP5, has been shown to result in a reduction in rDNA copy number, specifically of late-replicating inactive rDNA (ie. scenario 'c') (Li et al., 2005; Guetg et al., 2010; Santoro et al., 2010). Thus, it would be interesting to pursue whether CX-5461 also inhibits Pol I transcription of pRNA, as based on these results we predict this may result in abrogation of NoRC-dependent rDNA silencing and drive rDNA instability.

6.6.2 Addressing the mechanisms of ATM/ATR pathway activation by CX-5461.

Having ascertained that there are distinct differences between the inhibition of Pol I transcription by CX-5461 and ActD - namely that following CX-5461 treatment Pol I is absent the rDNA promoter, which remains in an 'open' configuration - we developed hypotheses relating to how the ATM/ATR signaling pathway could be activated by inhibition of Pol I transcription initiation, rather than inhibition of Pol I transcription *per se.* A review of the current literature suggested a surprisingly diverse number mechanism by which this could occur. Broadly, they fell into three different groups. The first was that ATM/ATR could be locally activated at the rDNA, due to the interaction of ATM/ATR or their mediator proteins with 'exposed' rDNA chromatin. The second was that the specialised mechanisms that regulate rDNA replication could be

compromised by the absence of Pol I from the active rDNA repeats. The third was that DDR proteins that localise to the nucleoli could be released due to changes in nucleolar structure, and act in DDR signaling pathways. Therefore, we chose to address each of these general scenarios individually, in order to begin to narrow down the potential mechanisms by which CX-5461 treatment can activate the ATM/ATR signaling pathway.

The first hypothesis received the most support from our results. ATM and ATR can be activated in the absence of DNA damage by a number of mechanisms, which include among others activation by chromatin conformation changes and/or association of certain ATM/ATR pathway proteins with chromatin (Soutoglou and Misteli, 2008; Sokka et al., 2015). As active rDNA repeats become 'exposed' following CX-5461 treatment, we considered they could be more available to ATM, ATR, or their associated proteins, resulting in local activation of ATM/ATR across these genes. Our results show that following 1hr CX-5461 treatment, there is a significant increase in levels of NBS1 phos-S345 in the nucleolus (FIGURE 27). NBS1 is part of the MRN complex that mediates the recruitment of ATM to chromatin, and NBS1 phosphorylation at S345 is a substrate for ATM, suggesting that ATM is recruited to rDNA chromatin and activated following CX-5461 treatment. We detected this increased level of nucleolar NBS1 phos-S345 specifically in S/G2, the cell cycle phase in which ATM/ATR signaling is predominantly activated following CX-5461 treatment. It has been previously established by Soutoglou and Mistelli (Soutoglou and Misteli, 2008) that tethering of either ATM or NBS1 to chromatin is sufficient to result in ATM activation and G2 cell cycle arrest in NIH3T3 cells the absence of DNA damage. In their experiments, tethering of NBS1 to chromatin resulted in recruitment of other MRN components, as well as NBS1-S345 and ATM-S1987 activating phosphorylations, however the recruitment of ATM at the chromatin was not detected. Similarly, we did not detect ATM binding at the rDNA by CHIP analysis (FIGURE 27), suggesting that it is transiently activated at this site. Therefore, we propose that following inhibition of Pol I transcription initiation by CX-5461, MRN components are recruited to the rDNA chromatin, and this is sufficient to activate ATM signaling in the absence of DNA damage. A similar mechanism could conceivably be involved in ATR activation, for example TopBP1 can bind to the rDNA repeat and locally activate ATR in the absence of DNA damage (Sokka et al., 2015). However, we have not demonstrated the direct recruitment of NBS1 or other ATM/ATR pathway proteins to rDNA following CX-5461 treatment. Our ChIP assays may have had insufficient sensitivity as they were performed in asynchronous cell cycle populations (in which we expect <25% to be in

S-phase), or because the enrichment of ATM/ATR pathway proteins at any certain position across the 13.3 kb transcribed region of the rDNA repeat is relatively small. Alternatively, we cannot rule out that the observed association of NBS1 with the nucleoli and activation of ATM following inhibition of Pol I transcription initiation by CX-5461 occurs via indirect association with rDNA chromatin.

The second hypothesis is not supported by our results. Replication of the rDNA involves specialised mechanisms that enable coordinated Pol I transcription and replication. As such, we considered inhibition of Pol I transcription initiation by CX-5461 could affect rDNA replication specifically at active 'open' rDNA copies. For example, the absence of Pol I may prevent the recruitment of factors required for efficient replication of rDNA repeats, such as TTF1, which is recruited to the RFB and required for fork arrest specifically at transcriptionally competent rDNA (Akamatsu and Kobayashi, 2015). Also, due to the repetitive nature and high GC content of the rDNA, 'exposed' rDNA repeats could be prone to the formation of DNA secondary structures or DNA:RNA hybrids, which would pose a challenge to DNA replication (Maizels and Gray, 2013) (Chan et al., 2014). However, a defect in replication would be expected to give rise to ssDNA associated with RPA in order to activate ATR, and DSBs associated with γH2A.X in order to activate ATM, neither of which were observed following short-term CX-5461 treatment (FIGURE 21). We investigated a potential replication defect at the rDNA regardless of this for two reasons: first, as there are specialised mechanisms of replication and repair at the rDNA, we considered there was a slight possibility that a replication defect may not be recognised by these canonical pathways; second, while we had appropriate controls for detection of DSBs and ATM association with the rDNA, this was not the case for ssDNA and ATR. We were able to address the question of whether inhibition of Pol I transcription initiation by CX-5461 affects replication specifically at the active 'open' rDNA by determining if a defect in replication arises when cell are treated with CX-5461 either in early S-phase (when active rDNA repeats are replicated), or late S-phase (when inactive rDNA is replicated) (Li et al., 2005). We showed that both active and inactive rDNA repeats, as well as early and late replicating genes at other loci, display a delay in replication directly following 2 hours of CX-5461 treatment; this indicates that the delay in replication arises as a result of activation of a general S-phase checkpoint, rather than a defect in replication specifically at active rDNA repeats from which Pol I has been displaced.

For the third hypothesis, our results are less conclusive. We considered whether activation of ATM/ATR signaling occurs is a diffuse manner, as a result of signaling by DDR pathway proteins, whose activity can be modulated by the nucleoli. This hypothesis is supported by two key ideas: first, that numerous proteins associated with DDR localise to the nucleoli; second, that activation of DDR response following DNA damage is associated with inhibition of Pol I transcription and reorganisation of nucleolar structure. The activation of ATM/ATR via changes in nucleolar structure is supported more directly by a number of publications. For example, ATM can be activated by Aurora B, which is present in the nucleoli (Andersen et al., 2005; Yang et al., 2011). ATR can be activated by nucleolar protein p14ARF, resulting in its relocalisation to the nucleoli (Rocha et al., 2005). MDM2 can bind Nbs1, and this interaction occurs at a site overlapping that of RPL5 binding to MDM2, suggesting Nbs1 is released under conditions of nucleolar stress (Alt et al., 2005). NCL relocalises from the nucleoli to the DSBs following DNA damage, and knockdown of NCL results in reduced ATM activation (Kobayashi et al., 2012). Our results showed that inhibition of Pol I transcription by CX-5461 resulted in significant changes in nucleolar structure. These changes occurred early and corresponded with the onset of ATM/ATR signaling pathway activation (FIGURE 20 and FIGURE 29). Following inhibition of Pol I transcription initiation by CX-5461 for as little as 30min, rDNA repeats coalesce, the FC, DFC, and GC condense around them, and some nucleolar components disperse into the nucleoplasm. Therefore, it is likely proteins that act in DDR do translocate from the nucleoli following inhibition of Pol I transcription inititation by CX-5461, such as we observed for WRN (FIGURE 29). However, the reorganization of nucleolar structure following CX-5461 treatment appears to be different from the reorganization of nucleolar structure that occurs during DNA damage response. For example, following DNA damage induced by I-*PpoI* endonuclease in the U2TR-I-*Ppo*I-dd cell lines, UBF relocalised to one or two foci at the periphery of a condensed nucleoli (FIGURE 21). We do not believe this prohibits the scenario that DDR pathway proteins have functional consequences when relocated from the nucleolus in response to CX-5461. However, we did not pursue whether this was the case. As we have shown that NBS1 activation occurs within the nucleoli (FIGURE 27), our data therefore strongly suggest that ATM/ATR pathway activation occurs at the rDNA, rather than due to diffuse signaling outside of the nucleolus.

6.6.3 The nucleoli as mediators of DNA damage response.

There are several lines of evidence that the nucleoli are involved in DDR, including that inhibition of Pol I transcription and reorganisation of nucleolar structure following

DNA damage is associated with translocation of DDR proteins to and from the nucleoli. Further, p53 activation following DNA damage only occurs when damage occurs within the nucleoli (Rubbi and Milner, 2003; Moore et al., 2011). This has led others to propose that the nucleoli play a key role in mediating DDR as a whole, however to our knowledge this has never been directly established. On the one hand, it has been suggested that rDNA is particularly prone to DNA damage, and the nucleoli may be utilised to activate DDR in a highly sensitive manner to protect the genome as a whole (Reviewed in (Boisvert et al., 2010; Kobayashi, 2011)). On the other hand, the correct localisation of DDR proteins to the nucleoli may be required for their function in DDR (Rancourt and Satoh, 2009; Li et al., 2012; Poletto et al., 2014a). We considered how the cellular response to CX-5461 might affect DNA damage response: could CX-5461 prime cells to rapidly respond to DNA damage due to an abundance of pre-activated ATM/ATR kinases, or conversely, prevent the cells from responding to DNA damage by engaging the available ATM/ATR kinases in a separate pathway? For example, oxidation mediated activation of ATM prevents further activation of ATM by the MRN pathway, and is suggested to direct ATM kinase activity to a different set of targets (Guo et al., 2010). Therefore, we investigated whether CX-5461 results in altered response to DNA damage.

We have shown that the repair of DNA damage in general is impaired following treatment with CX-5461 (FIGURE 30). At the rDNA, we were able to utilize I-*Ppo*I endonuclease induced DNA DSBs to observe that rates of repair at these loci are reduced following CX-5461 treatment, and that the recruitment of DDR proteins to a specific DSB is also relatively reduced (FIGURE 30). In addition, IF analysis of DNA damage repair foci in BJ-T and BJ-T p53shRNA cells (E.Sanij and K. Chan, personal communication) have yielded similar results, suggesting that the observed phenotype arises at least in part through p53-independent DDR pathways. The compromised DNA repair following treatment with CX-5461 was associated with a number of observations that may relate to DDR pathway function. First, RNA sequencing results indicate that there is not an overall decrease in rates of transcription across the genome following inhibition of Pol I transcription initiation by CX-5461. This is also supported by our previously published microarray results in transformed cell lines (Drygin et al., 2011). This suggest that DNA damage repair is not compromised as a consequence of reduced recognition of DNA lesions by transcribing polymerases. Second, the localisation of DDR proteins in the nucleoli is altered following CX-5461 treatment, and this differs to the changes in localisation observed following DNA damage alone. This suggests that the regulation of DDR proteins by the nucleoli may

be altered following inhibition of Pol I transcription initiation. For example, regulatory modifications of DDR factors that occur in the nucleoli may be compromised (Kahyo et al., 2008; Muftuoglu et al., 2008; Lee et al., 2015), or proteins that are accumulated in the nucleoli in order to buffer their activity may be inappropriately released to interact with their targets and/or undergo proteasomal degradation (Jin et al., 2014). Third, the association of DDR proteins with DNA damage foci appears to be reduced following CX-5461 treatment (for example ATM, NBS1, γH2A.X). This could be due to either compromised recruitment of DDR proteins to DNA damage sites, or reduced levels of DDR proteins. Strikingly, our RNA sequencing results showed that the expression of a number of DDR proteins was down regulated at early timepoints following CX-5461 treatment (FIGURE 18). Also, a recent publication from our laboratory has shown that Pol I transcription factor UBF is also associated with a number of highly expressed Pol II transcribed genes, including genes involved in the regulation of cell cycle checkpoints and DDR (Sanij et al., 2015). This indicates nucleolar transcription factors may be utilised to coordinate Pol I transcription with distinct Pol II transcription programs, such as DDR and other stress responses. Overall, we have been able to utilise the acute and specific inhibition of Pol I transcription initiation by CX-5461 to begin to directly address the recent speculation that the nucleoli can mediate DDR. Our results suggest that targeting the nucleoli by inhibition of Pol I transcription initiation by CX-5461 can attenuate DNA damage repair.

6.6.4 Conclusions.

Altogether, we have shown that inhibition of Pol I transcription initiation by CX-5461, which results in displacement of Pol I from active rDNA repeats, is associated with activating the ATM/ATR signaling pathways. The mechanism by which the pathway is activated is not clearly defined, but we have shown that there are increased levels of the ATM substrate NBS1 (phos-S345) specifically in the nucleoli during S/G2, corresponding to ATM/ATR pathway activation following CX-5461 treatment. This leads us to propose a model where ATM and ATR are locally activated at the nucleoli due to association with exposed rDNA chromatin. However, there may be different pathways involved in regulation of ATM/ATR signaling at the nucleoli. For instance, nucleolar regulation of p53 alone has been shown to be a precise and multifaceted process (See Section 1.2.1). Therefore, the regulation of other stress signaling may be just as complex. Intriguingly, inhibition of Pol I transcription initiation by CX-5461 appears to attenuate the repair of DNA damage. This may simply be a result of disruption of nucleolar structure and function, leading to ineffective nucleolar regulation of DDR pathways. Alternatively, it is possible that it mimics a physiologically relevant

function of the nucleoli, related to its role in coordinating cellular stress response. In support of this, the altered localisation of some proteins from the nucleoli to the nucleoplasm can sensitise cells to DNA damage (Rancourt and Satoh, 2009; Poletto et al., 2014a). Therefore, under sub-optimal growth conditions that inhibit Pol I transcription, or in response to defects in rDNA chromatin, the nucleoli may mediate a switch in DDR, preventing DNA repair and subsequent cell cycle progression, and promoting senescence or cell death pathways. This extends the model of the nucleoli as a central 'hub' that collates the numerous cell growth and stress signaling pathways, and then in turn coordinates appropriate cell growth or stress response.

FIGURE 25. ATM/ATR signaling is activated by small molecule inhibitors of Pol I transcription initiation, CX-5461 and CX-5488, but not Actinomycin D. A) Western blot analysis of phos-CHK2(T68) in BJ-T p53shRNA cells following treatment with NaH_2PO_4 vehicle control (30min), 5nM ActD (30min, 3hr) or 1μM CX-5461 (30min, 1hr, 3hr) (representative of n=3) **B)** Structure of small molecules CX-5461, CX-5447 and CX-5488. **C)** qRT-PCR analysis of expression of 47S pre-rRNA following 10nM-10μM dose curve treatment with CX-5461, CX-5447 or CX-5488. Fold change relative to vehicle control (n=3±sem. ****p<0.0001; 1μM CX-5461 mean = 21.74%; 1μM CX-5488 mean = 20.09%). **D)** Western blot analysis of BJ-T cells treated with 10nM-1μM dose curve of CX-5461, CX-5447 or CX-5488 (representative of n=3). **E)** Cell cycle analysis with PI staining for DNA content of BJ-T cells following 48hr treatment with vehicle control, 1μM CX-5447 or 1μM CX-5488 (representative of n=3). **F)** Dose-response cell proliferation assays for BJ-T (solid line) and BJ-T p53shRNA (dashed line) cells treated with vehicle control or 1μM CX-5461 from 0hr to 96hr. Cell proliferation is determined by % confluency of live cells in culture measured using an IncuCyte Zoom (Essen Biosciences) (n=1, mean±SD of technical replicates).

FIGURE 25

A)

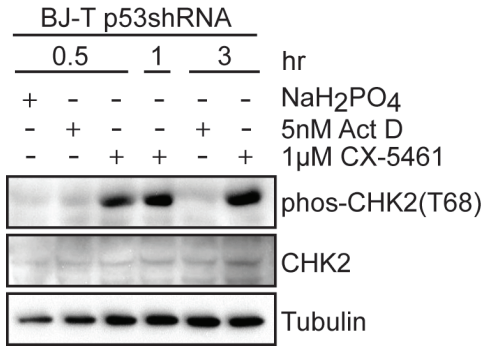
BJ-T p53shRNA
0.5
1
3
hr
+ - - - - - NaH2PO4
- + - - + - 5nM Act D
- - + + - + 1μM CX-5461
phos-CHK2(T68)
CHK2
Tubulin

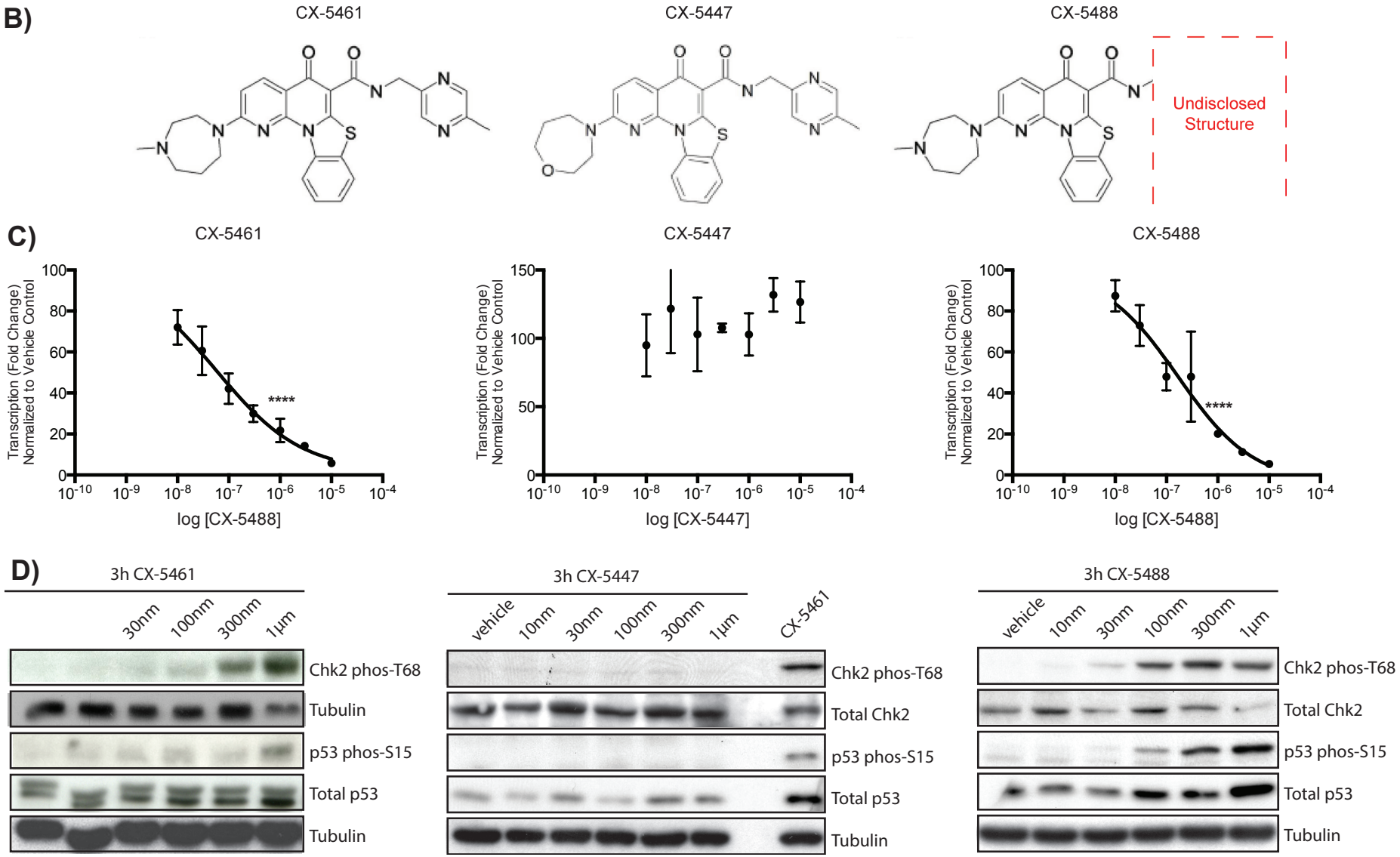
B)
CX-5461
CX-5447
CX-5488
Undisclosed Structure
C)
CX-5461
CX-5447
CX-5488
Transcription (Fold Change) Normalized to Vehicle Control
log [CX-5488]
log [CX-5447]
****
D)
3h CX-5461
3h CX-5447
3h CX-5488
30nm
100nm
300nm
1µm
vehicle
10nm
CX-5461
Chk2 phos-T68
Tubulin
p53 phos-S15
Total p53
Total Chk2

E)

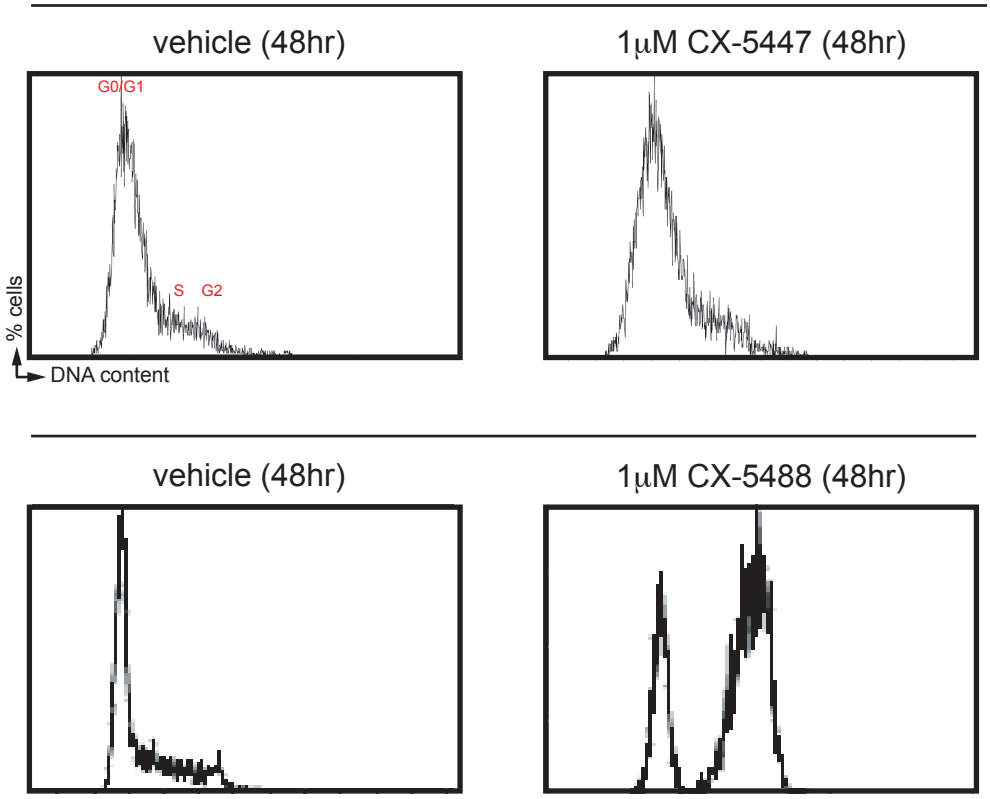
vehicle (48hr)
1μM CX-5447 (48hr)
G0/G1
S
G2
% cells
DNA content
vehicle (48hr)
1μM CX-5488 (48hr)

F)

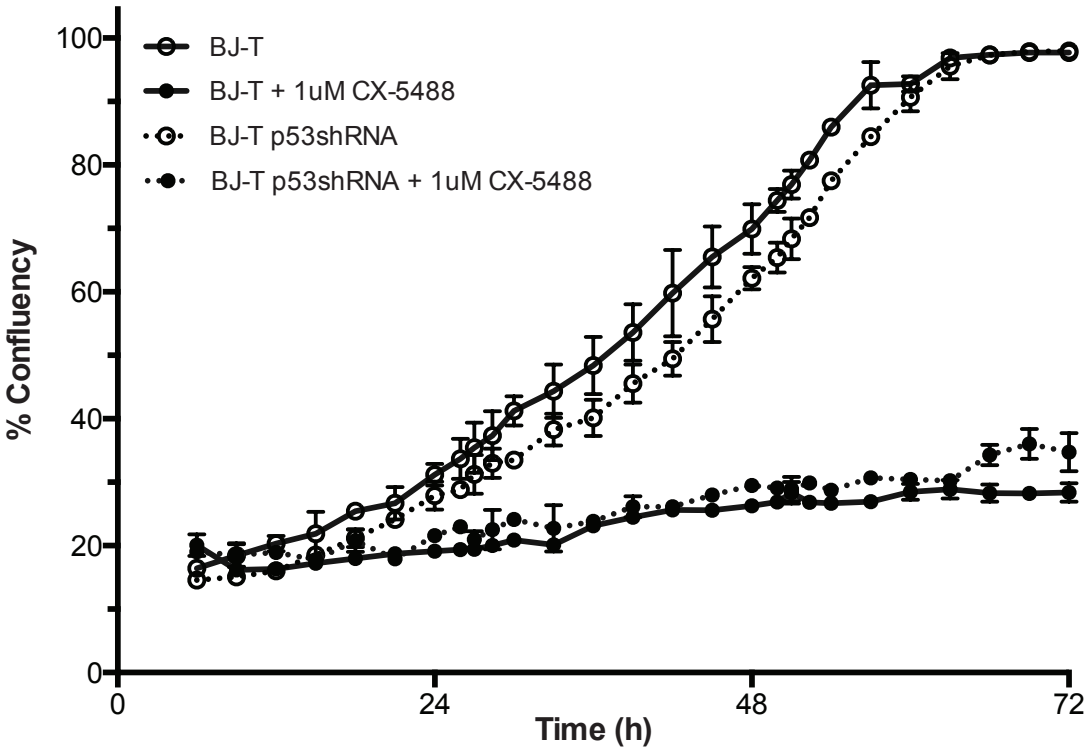
BJ-T
BJ-T + 1uM CX-5488
BJ-T p53shRNA
BJ-T p53shRNA + 1uM CX-5488
% Confluency
Time (h)
0
20
40
60
80
100
0
24
48
72

FIGURE 26. CX-5461, but not Actinomycin D, displaces Pol I from 'open' rDNA repeats. A) Schematic of human rDNA repeats and the position of pRT-PCR amplicons (ENH, enhancer; ETS, external transcribed spacer; ITS, internal transcribed spacer; T, terminator; RFB, replication fork barrier; IGS, intergenic spacer), as well as the position of the amplicon used to generate a probe for Sal I digested rDNA used in psoralen crosslinked Southern blotting analysis. **B)** ChIP analysis of Pol I (POLR1A) and UBF binding to rDNA in BJ-T (n=3) and BJ-T p53shRNA (n=3(UBF) / n=4(POLR1A)) cells treated with vehicle control, 5nM ActD, or 1μM CX-5461 (mean±sem. *p<0.05, **p<0.005, relative to vehicle control sample). **C)** Analysis of rDNA chromatin conformation in BJ-T cells treated with 1μM CX-5461 for 3hr-48hr. (Left panel) Southern blotting of rDNA isolated from psoralen crosslinked nuclei (representative image of n=3). (Right panel) Quantitation of the proportion of open versus closed rDNA using Phosphoimager Imagequant software (n=3, mean ± s.e.m).

FIGURE 26

A)

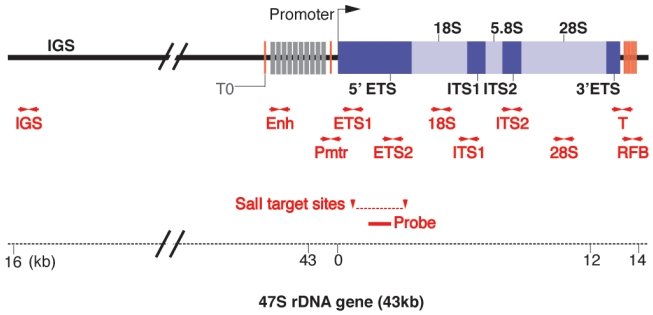

B)

BJ-T

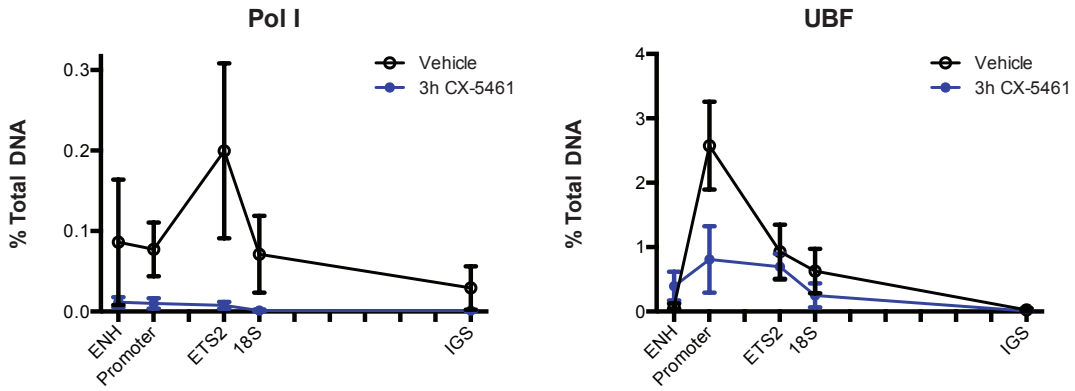

BJ-T p53shRNA

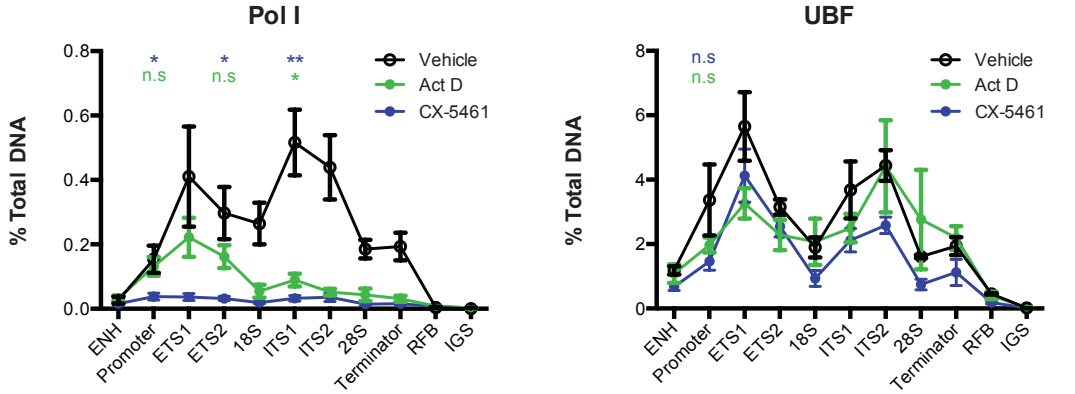

C)

Psoralen Crosslinking Southern Blot

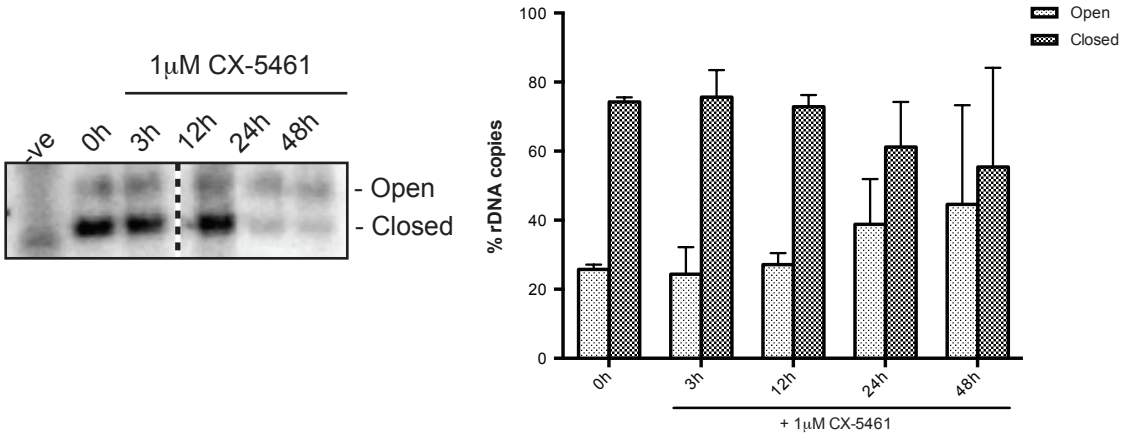

FIGURE 27. ATM substrate NBS1 (phos-S345) is specifically activated at the nucleoli during S/G2 following CX-5461 treatment. A) Schematic of human rDNA repeats and the position of the I-*Ppo*I endonuclease target site within 28S, as well as the qRT-PCR amplicons across (Primer Set 1) and adjacent (Primer Set 2) to the cut sites. **B)** ChIP analysis of ATM binding at the 28S I-*Ppo*I endonuclease target site (left) and the rDNA promoter (right) in U2TR I-*Ppo*I-dd cells following 2hr treatment with 1μM CX-5461 or 3hr stabilization of I-*Ppo*I endonuclease in U2TR I-*Ppo*I-dd cells (n=3, mean±SD, ***p<0.005 relative to IgG control). **C&D)** Co-immunofluorescence analysis of nucleolar protein NPM1 with NBS1 phos-S343 (C) and γH2A.X (D) in BJT p53shRNA cells expressing FUCCI mCherry-hCdt1 (red; G1) and mVenus-hGemini (green; S/G2/M), 1hr following treatment with vehicle control, 1μM CX-5461, or 10Gy γIR. Upper panels: Quantitation of mean nuclear and mean nucleolar (co-localised with NPM1) signal intensity of γH2A.X (C) and NBS1 phos-S343 (D) in S/G2 populations. S/G2 is defined as Cherry/Venus signal ratio <1.2. (n=2 experiments with >200 nuclei per condition, mean ± SD, normalized to average signal intensity of vehicle control. **p<0.005 ****p<0.0001). Lower panel: representative images for each treatment.

FIGURE 27

A)

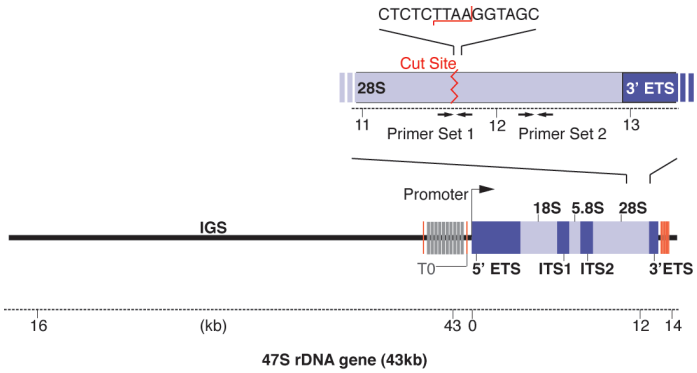
CTCTCTTAAGGTAGC
Cut Site
28S
3' ETS
11
Primer Set 1
12
Primer Set 2
13
Promoter
18S
5.8S
28S
IGS
T0
5' ETS
ITS1
ITS2
3'ETS
16
(kb)
43 0
12
14
47S rDNA gene (43kb)

B)

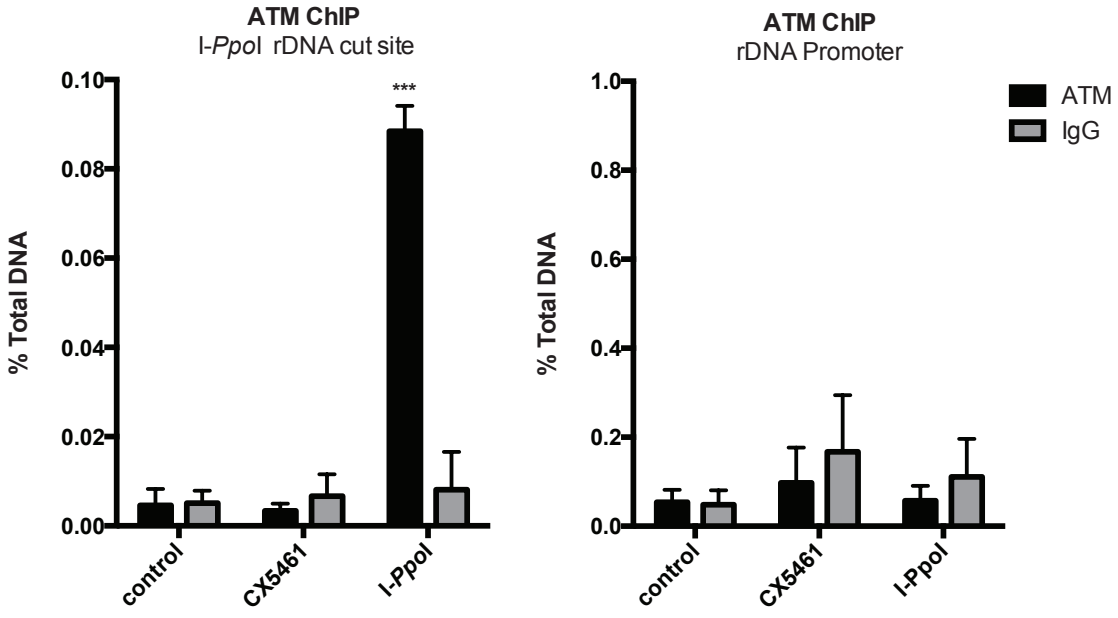
ATM ChIP
I-PpoI rDNA cut site
% Total DNA
0.10
0.08
0.06
0.04
0.02
0.00
***
control
CX5461
I-PpoI
ATM ChIP
rDNA Promoter
% Total DNA
1.0
0.8
0.6
0.4
0.2
0.0
control
CX5461
I-PpoI
ATM
IgG

C)

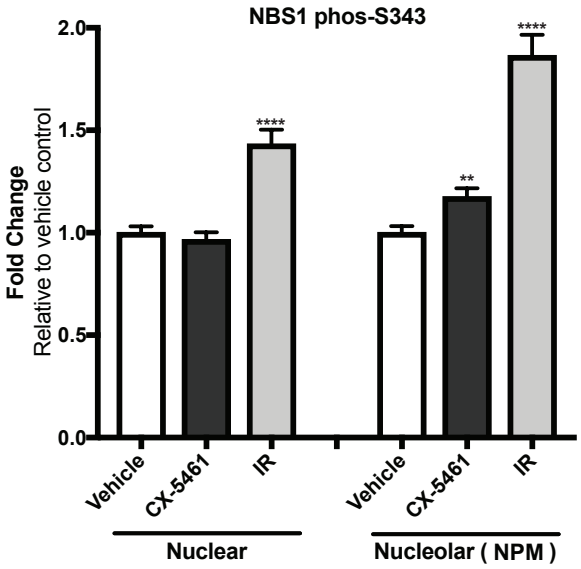
NBS1 phos-S343
Fold Change
Relative to vehicle control
2.0
1.5
1.0
0.5
0.0
****
**
****
Vehicle
CX-5461
IR
Vehicle
CX-5461
IR
Nuclear
Nucleolar (NPM)

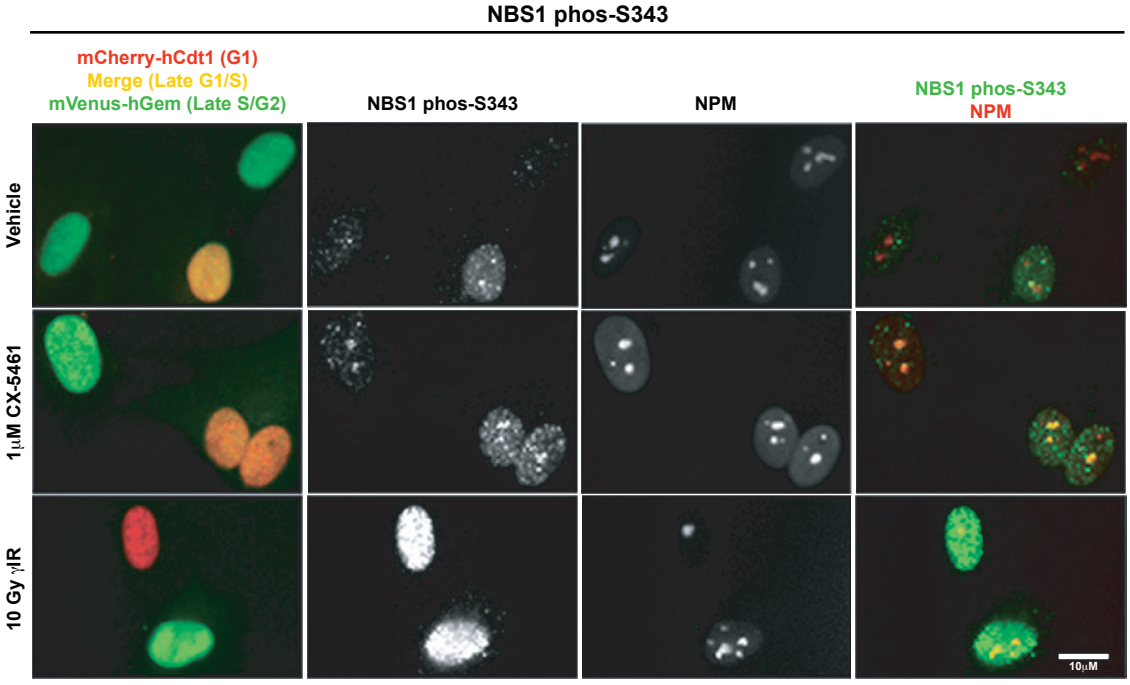
NBS1 phos-S343
mCherry-hCdt1 (G1)
Merge (Late G1/S)
mVenus-hGem (Late S/G2)
NBS1 phos-S343
NPM
NBS1 phos-S343
NPM
Vehicle
1μM CX-5461
10 Gy γIR
10μM

D)

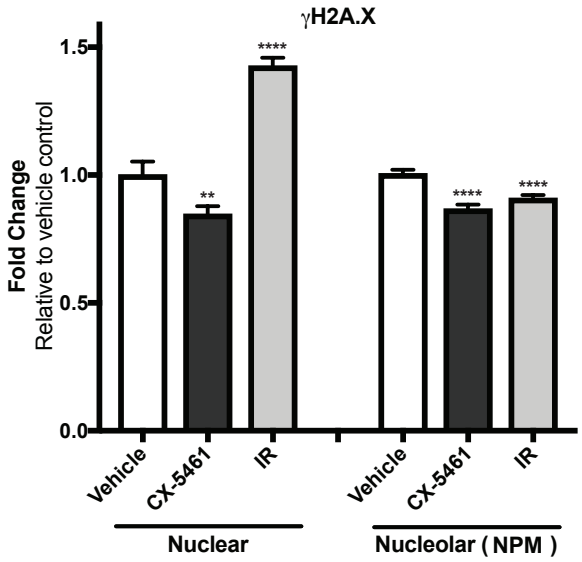
γH2A.X
Fold Change
Relative to vehicle control
1.5
1.0
0.5
0.0
**
****
****
****
Vehicle
CX-5461
IR
Vehicle
CX-5461
IR
Nuclear
Nucleolar (NPM)

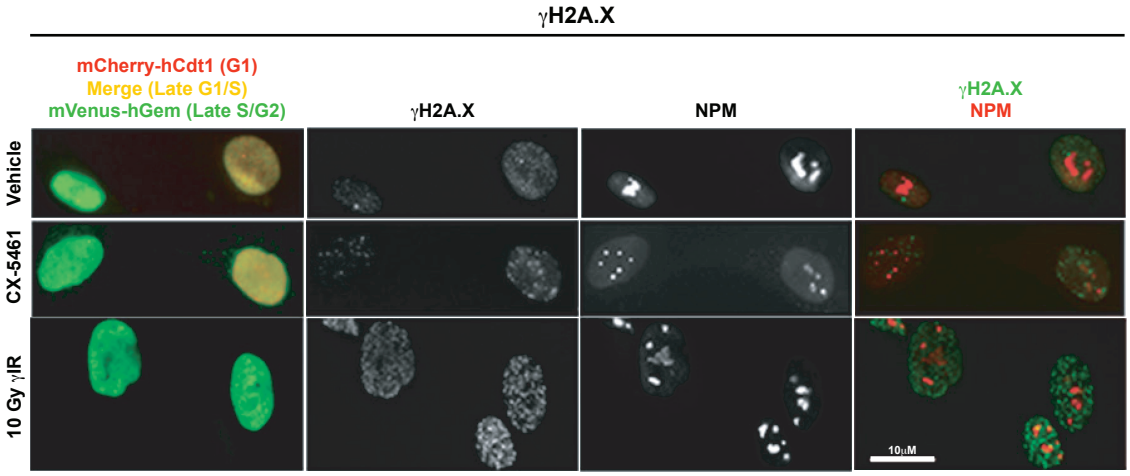
γH2A.X
mCherry-hCdt1 (G1)
Merge (Late G1/S)
mVenus-hGem (Late S/G2)
γH2A.X
NPM
γH2A.X
NPM
Vehicle
CX-5461
10 Gy γIR
10μM

FIGURE 28. Delay in DNA replication occurs rapidly following CX-5461 treatment and occurs in both early and late S-phase. A) Representative image of classification of cell cycle populations on the basis of DNA content for FACS. **B)** IP analysis of BrdU enrichment (BrdU-IP) at the rDNA (ETS-1) in asynchronous BJ-T cells following 2hr incubation in the presence or absence of BrdU (n=1). **C)** BrdU-IP analysis of G1, early S-phase and late S-phase BJ-T cell populations following 2hr BrdU incubation in the presence of absence of 1μM CX-5461. BrdU enrichment was determined for rDNA (ETS-1), early replicating gene MMP15 and late replicating gene HBB, relative to mitochondrial DNA (n=4, mean±sem. *p<0.05, **p<0.005, ****p<0.0001 relative to equivalent cell cycle population in untreated cells).

FIGURE 28

A)

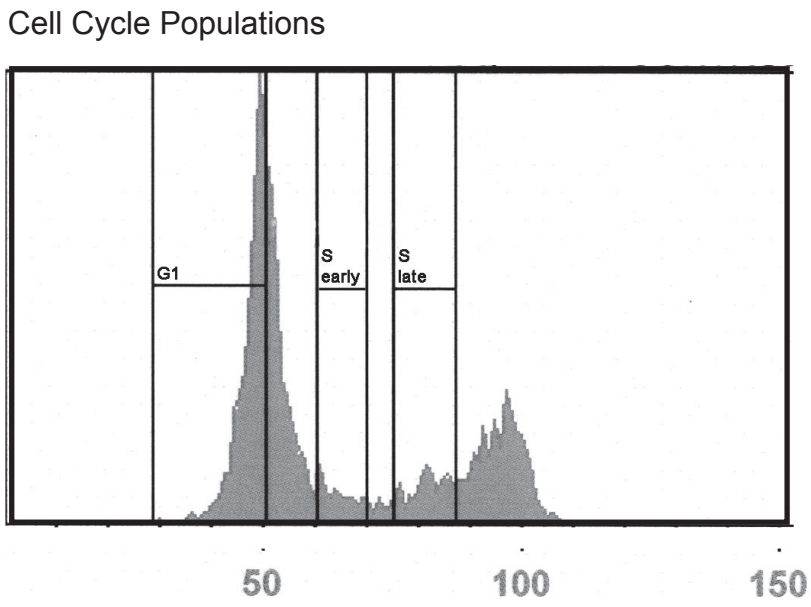
Cell Cycle Populations
G1
S early
S late
50
100
150

B)

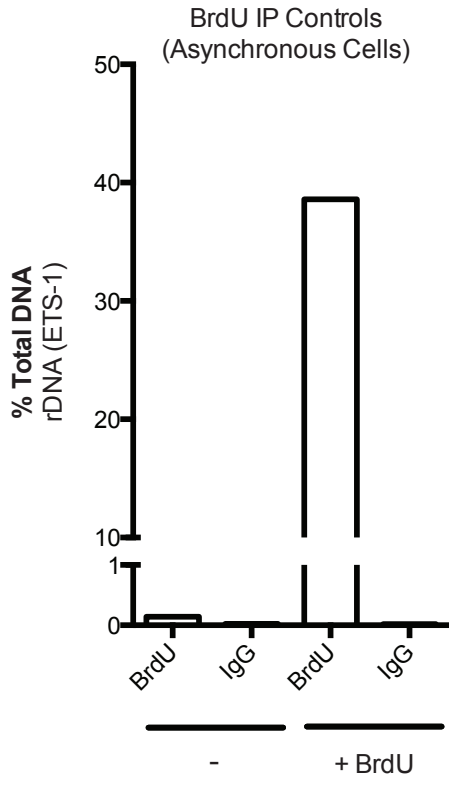
BrdU IP Controls
(Asynchronous Cells)
% Total DNA
rDNA (ETS-1)
50
40
30
20
10
1
0
BrdU
IgG
BrdU
IgG
-
+ BrdU

C)

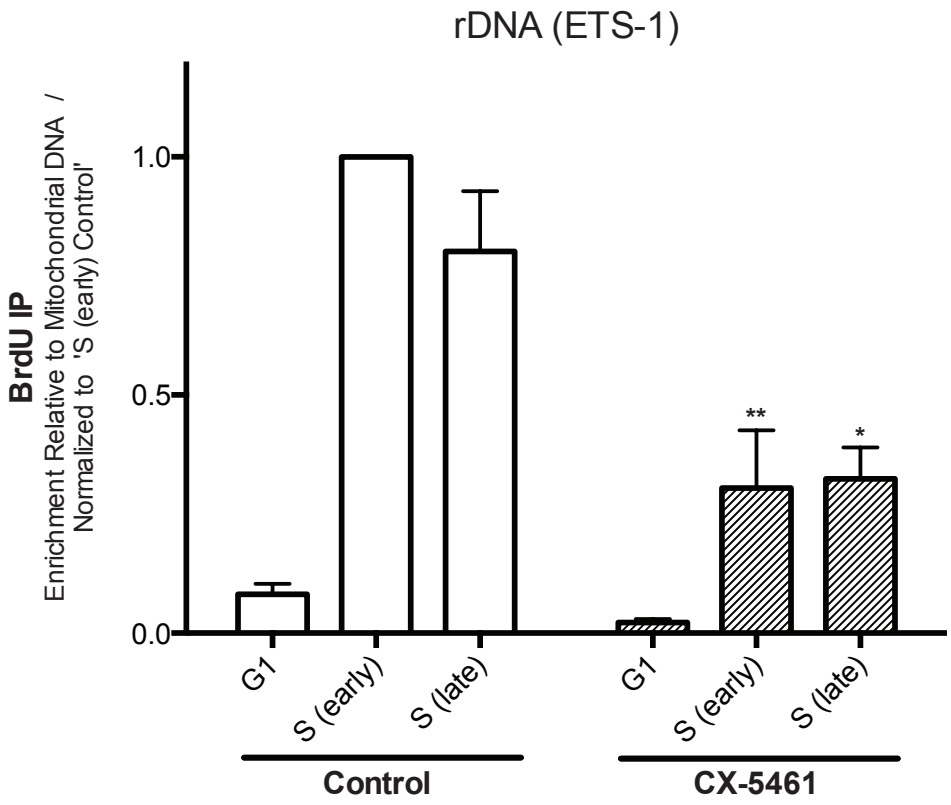
rDNA (ETS-1)
BrdU IP
Enrichment Relative to Mitochondrial DNA / Normalized to 'S (early) Control'
1.0
0.5
0.0
**
*
G1
S (early)
S (late)
G1
S (early)
S (late)
Control
CX-5461

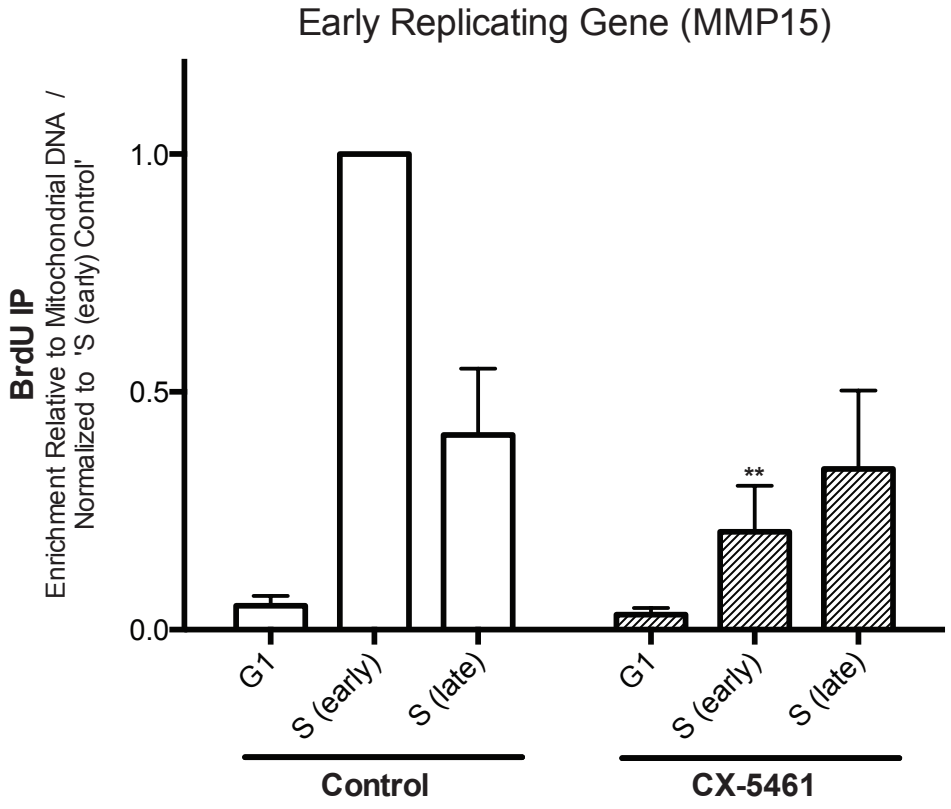
Early Replicating Gene (MMP15)
BrdU IP
Enrichment Relative to Mitochondrial DNA / Normalized to 'S (early) Control'
1.0
0.5
0.0
**
G1
S (early)
S (late)
G1
S (early)
S (late)
Control
CX-5461

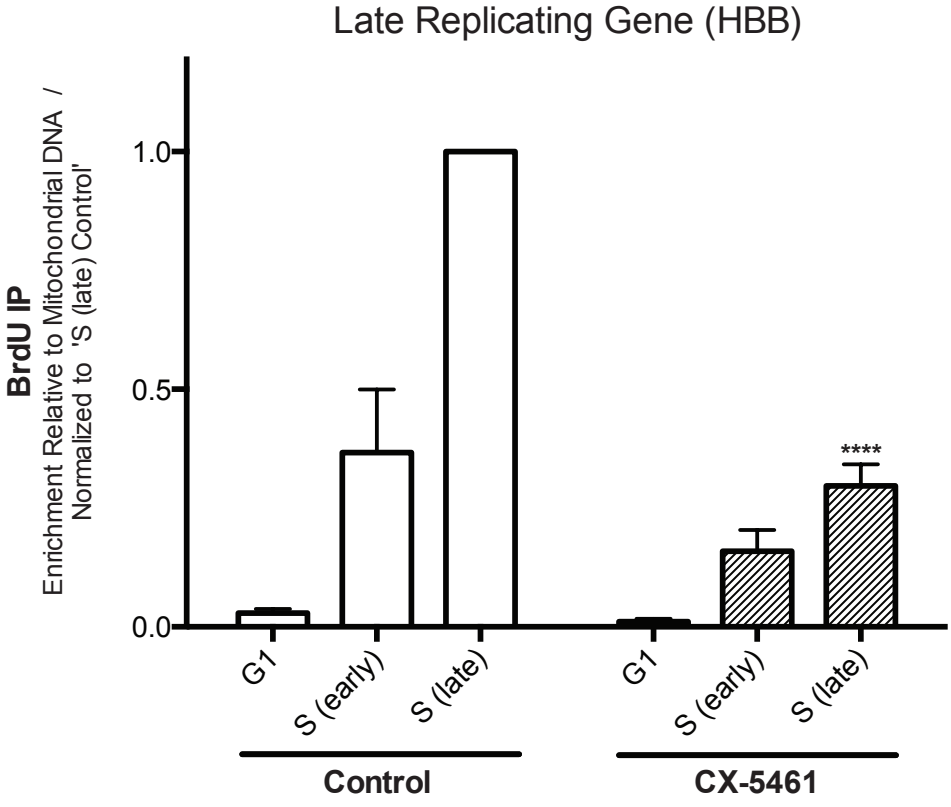
Late Replicating Gene (HBB)
BrdU IP
Enrichment Relative to Mitochondrial DNA / Normalized to 'S (late) Control'
1.0
0.5
0.0
****
G1
S (early)
S (late)
G1
S (early)
S (late)
Control
CX-5461

FIGURE 29. CX-5461 treatment results in disruption of nucleolar structure, and altered localisation of DNA damage response proteins, in a manner distinct from DNA damage. A) Combined IF (for UBF; red) and FISH (for rDNA; green) analysis of untreated control or 48hr 1μM CX-5461 BJ-T cells (representative images for n=1 experiment). rDNA FISH identifies both open rDNA repeats (co-stained with UBF) and inactive NORs (devoid of UBF; see example indicated by white arrow). **B)** FISH analysis of rDNA (green) with DAPI counterstain (blue) of untreated control or 1hr 1μM CX-5461 BJ-T cells (representative images for n=1 experiment. Upper panel: single cell images. Lower panel: whole field images). **C**) IF analysis of UBF, FIB and NPM in BJ-T cells following treatment with 1μM CX-5461 for 0hr (30min untreated control), 30min, 1hr, 3hr and 24hr. (Representative images of n=2/3 experiments). **D)** IF analysis of WRN (red) and NPM (green) with DAPI counterstain (blue) in BJ-T p53shNA cells 1hr following 1μM CX-5461 treatment, 100μJ/m^2 UV, or 10Gy γIR (representative images for n=1 experiment).

FIGURE 29

A)

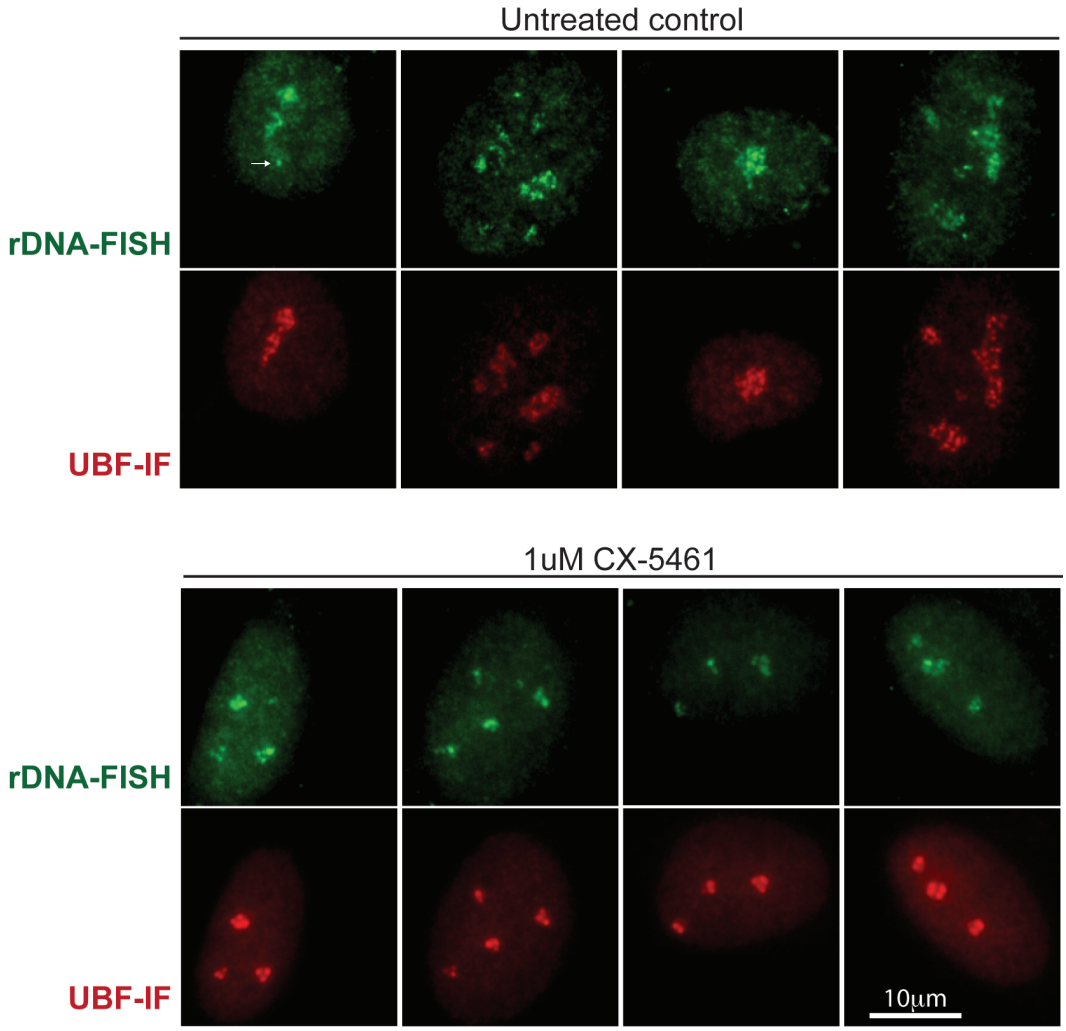
Untreated control
rDNA-FISH
UBF-IF
1uM CX-5461
rDNA-FISH
UBF-IF
10µm

B)

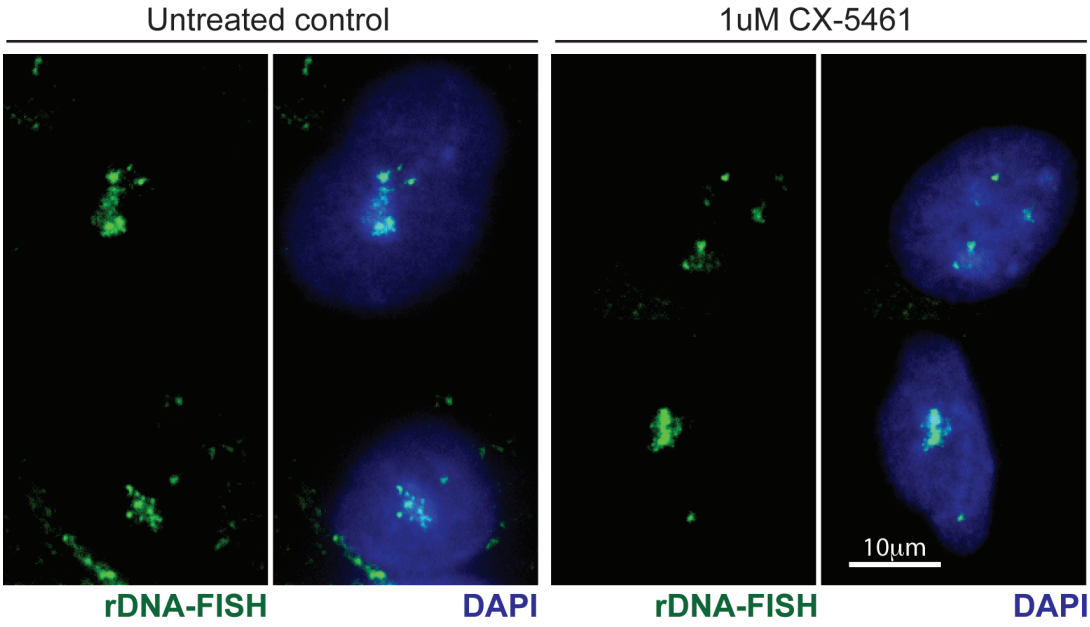
Untreated control
1uM CX-5461
10μm
rDNA-FISH
DAPI
rDNA-FISH
DAPI

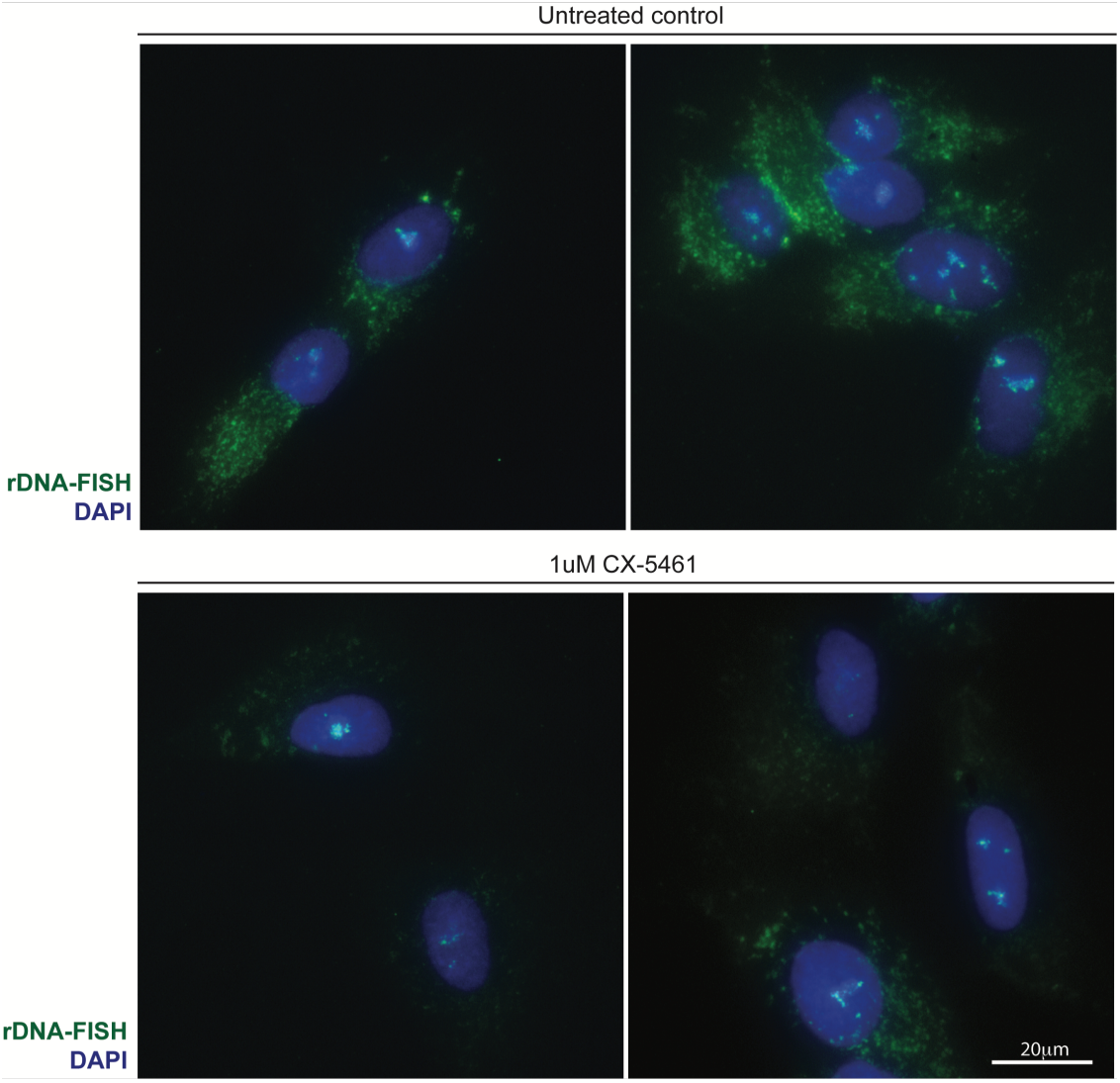
Untreated control
rDNA-FISH
DAPI
1uM CX-5461
rDNA-FISH
DAPI
20µm

C)

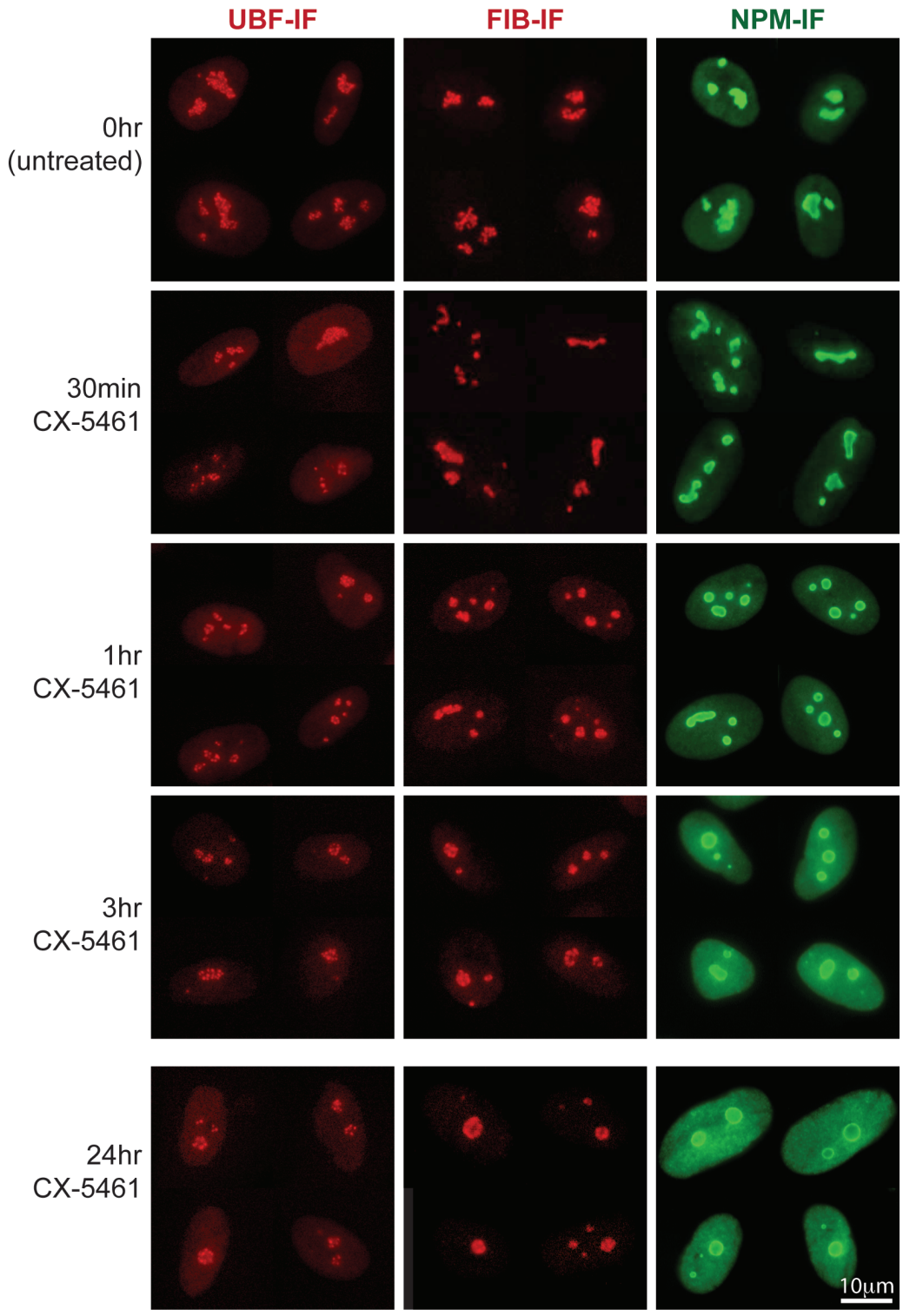
UBF-IF
FIB-IF
NPM-IF
0hr
(untreated)
30min
CX-5461
1hr
CX-5461
3hr
CX-5461
24hr
CX-5461
10μm

D)

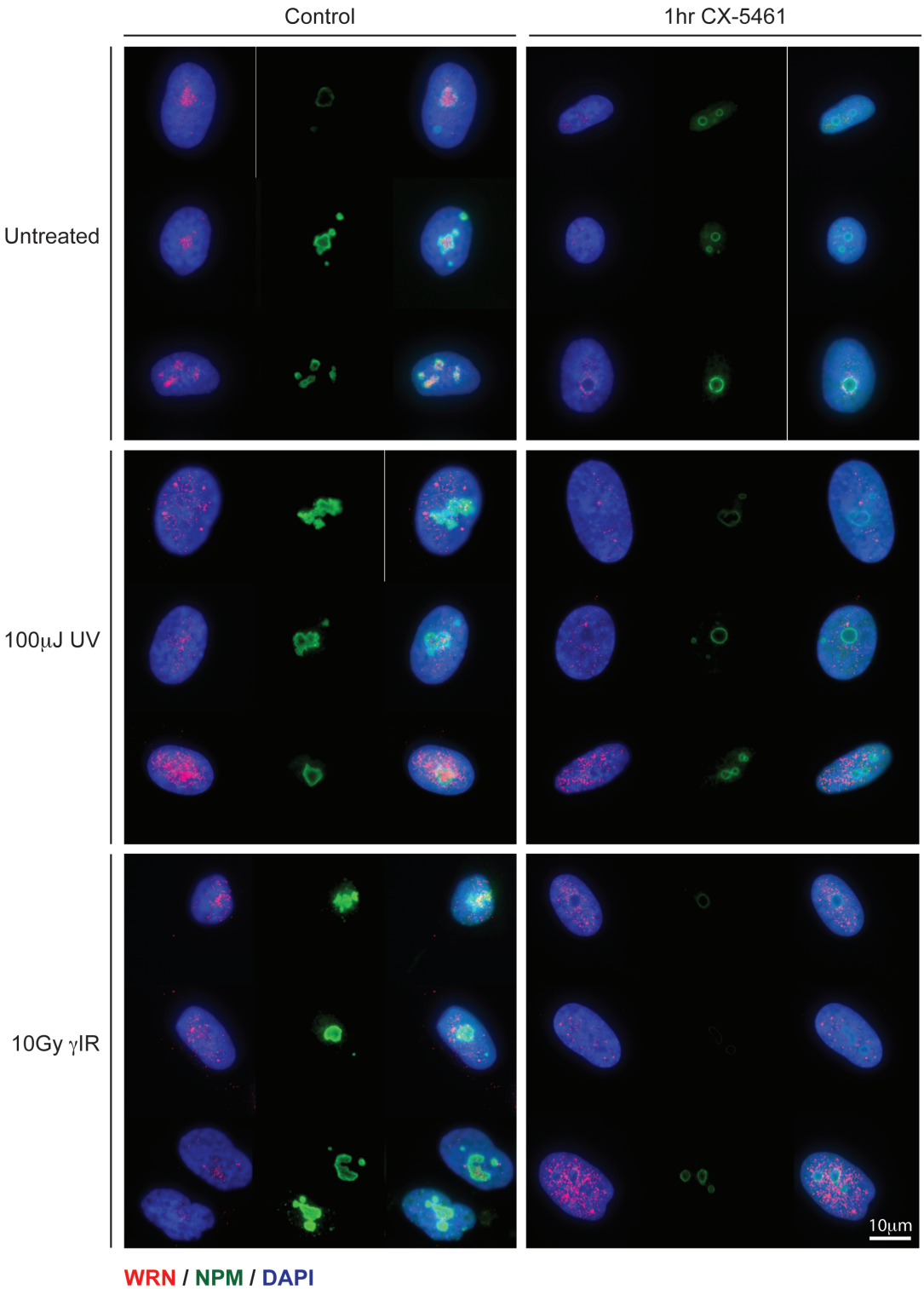
Control
1hr CX-5461
Untreated
100μJ UV
10Gy γIR
10μm
WRN / NPM / DAPI

FIGURE 30. DNA damage repair is compromised following inhibition of Pol I transcription initiation by CX-5461. A) Alkaline comet assay for DNA damage in BJ-T cells following 30min treatment with NaH_2PO_4 vehicle control or 1μM CX-5461, ± 250J/m^2 UV at t=10min treatment. Upper panel: representative images of n=2 experiments. Lower panel: quantitation of extent tail moment (Extent tail moment = Tail Length x Tail % DNA, calculated using MetaMorph MetaImaging Software) (n=2, mean±sem ****p<0.0001 relative to corresponding vehicle treated sample). **B)** Immunofluorescence analysis of γH2A.X (red) with DAPI counterstain (blue) in BJ-T cells at 30min and 3hr timepoints following 1μM CX-5461 treatment from t=0hr and/or 250J/m^2 UV at t=10min (representative images of n=2 experiments**). C)** qRT-PCR analysis of DNA damage induced at the I-*Ppo*I restriction sequence in 28S rDNA following 3hr stabilization of I-*Ppo*I endonuclease in U2TR I-*Ppo*I-dd cells ± 2hr 1μM CX-5461 treatment. Relative amplification across the 28S rDNA cut site in I-*Ppo*I induced compared to vehicle treated cells, normalized to amplification of the rDNA promoter to control for rDNA copy number (n=3, mean ±sem. *p<0.05). **D)** ChIP analysis of ATM (n=3, mean±SD) and NBS1-phosS343 (n=1) at the 28S I-*Ppo*I endonuclease target site in U2TR I-*Ppo*I-dd cells treated with vehicle control, 3hr stabilization of I-*Ppo*I endonuclease and/or 2hr 1μM CX-5461 treatment.

FIGURE 30
A)

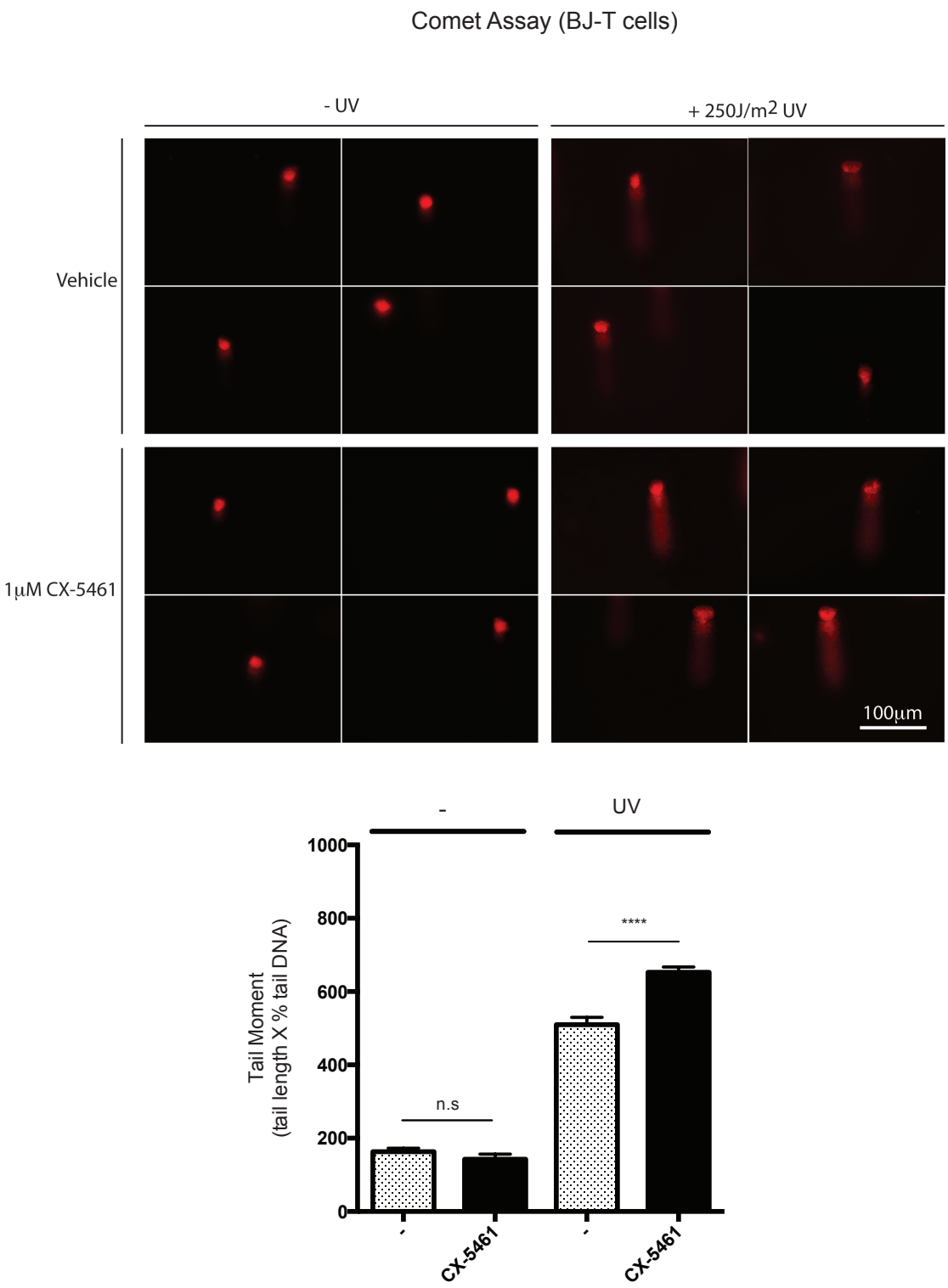
Comet Assay (BJ-T cells)
- UV
+ 250J/m2 UV
Vehicle
1μM CX-5461
100μm
-
UV
Tail Moment
(tail length X % tail DNA)
1000
800
600
400
200
0
n.s
****
-
CX-5461
-
CX-5461

B) γH2A.X IF (BJ-T cells)

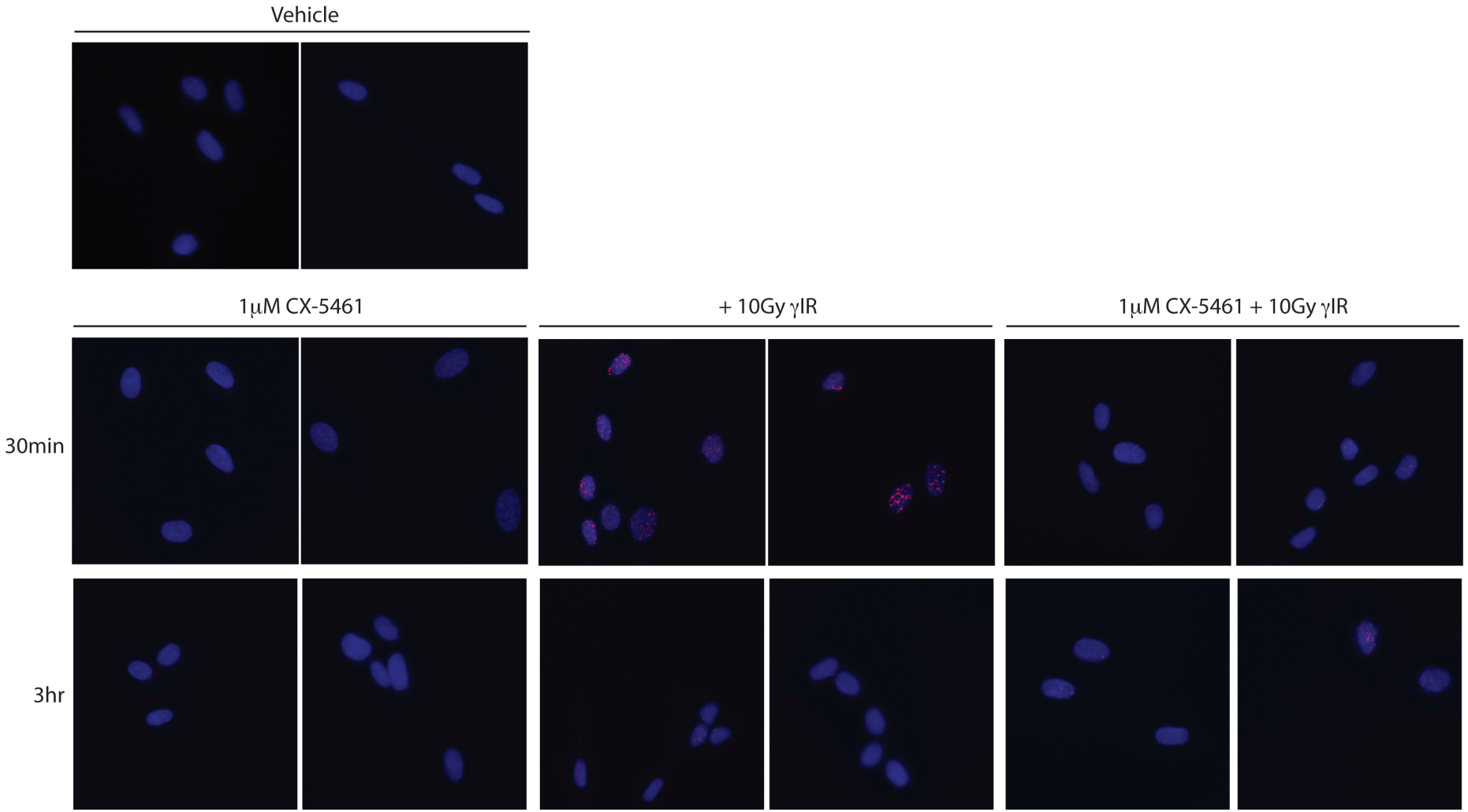

C)

Induction of DSBs at 28S region of rDNA (U2TR-I-*Ppo*I-dd cells)

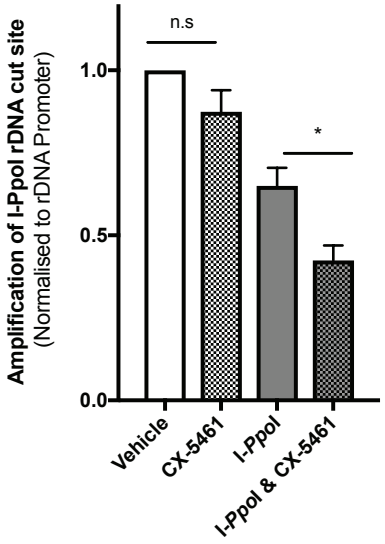

D)

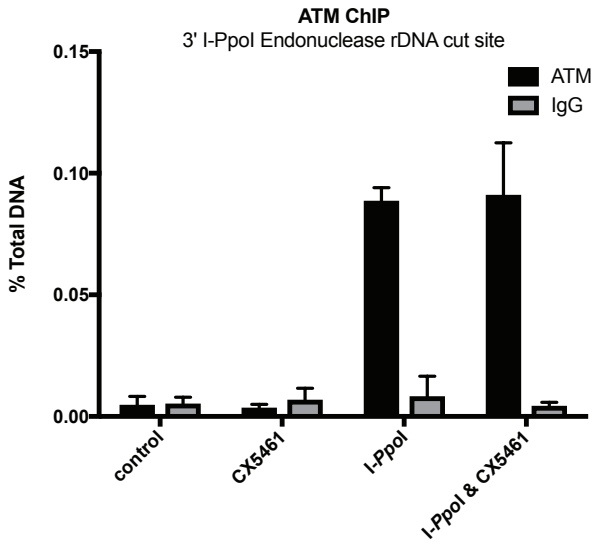

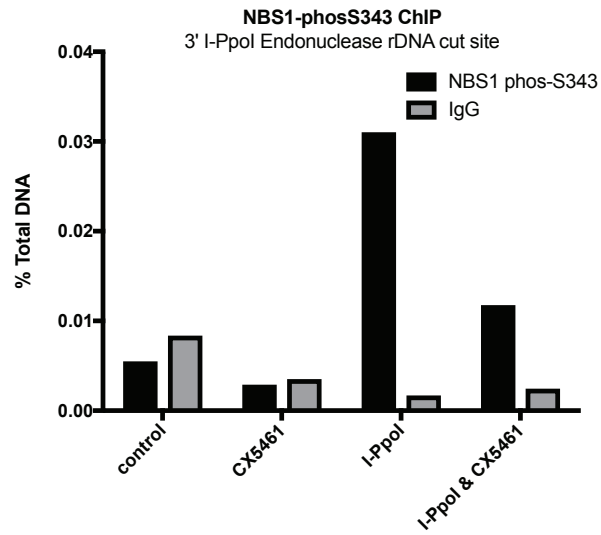

CHAPTER 7: GENERAL DISCUSSION.

7.1 Summary

At the commencement of this research project, we hypothesised that selective inhibition of Pol I transcription can offer a novel strategy for cancer therapy. Increased rates of Pol I transcription and dysregulated nucleoli are prevalent in cancer cells, and there is an emerging understanding of how nucleolar functions (such as the activation of p53 by the nuclear stress pathway) might be related to the hallmarks of cancer. This led us to investigate whether there is therapeutic window in which inhibition of Pol I transcription can selectively target cancer cells. Specifically, the aims of this research project were to utilise CX-5461, the newly developed specific inhibitor of Pol I transcription to: 1) investigate the cellular responses of isogenic cell lines at defined stages of transformation to inhibition of Pol I transcription initiation; and 2&3) investigate the phenotypic responses to inhibition of Pol I transcription, and the molecular pathways that mediate these responses, in normal untransformed cells.

The results presented here demonstrate that in the BJ fibroblast series of isogenic cells lines, normal minimally immortalised cells undergo less cell death following inhibition of Pol I transcription initiation by CX-5461 than tumorigenic cells. This is consistent with our hypothesis that there is a therapeutic window in which inhibition of Pol I transcription can specifically target and kill cancer cells without prohibitively detrimental effects on normal untransformed cells. In this model, the sensitivity of tumorigenic cells to undergo cell death following CX-5461 treatment is a consequence of the evasion of growth and proliferation checkpoints, a typical hallmark acquired during the process of transformation. We have shown that normal minimally immortalised cells undergo cell cycle arrest at G1, S and G2, following inhibition of Pol I transcription initiation. These cell cycle checkpoints are mediated by both the p53 nucleolar stress pathway, and a novel p53-independent ATM/ATR signaling pathways. Inactivation of both these pathways results in escape from cell cycle checkpoints, and increased rates of cell death, following inhibition of Pol I transcription initiation by CX-5461.

7.2 Implications for the utility of CX-5461 in cancer therapy

These findings highlight the importance of understanding the different pathways by which cells respond to inhibitors of Pol I transcription to facilitate the advancement of

this novel class of cancer therapeutics toward clinical use. Our research group has assessed the utility and efficacy of CX-5461 in pre-clinical cancer models. We reported that in the murine model of Eμ-*Myc* lymphoma CX-5461 selectively induces apoptosis in malignant B-cells *in vivo* without affecting the wild-type B-cell compartment. Further, the sensitivity of Eμ-*Myc* lymphoma cells to CX-5461 is dependent upon p53 activation by the nucleolar stress pathway (Bywater et al., 2012). However, we have now shown CX-5461 can also activate the ATM/ATR pathway and induce a G2/M checkpoint in this model, and that in p53 -/- Eμ-*Myc* lymphoma, combination therapy with CX-5461 and a dual inhibitor of CHK1/CHK2 can confer a significantly improved survival benefit, compared to a modest survival benefit conferred by CX-5461 treatment alone (Quin et al., 2016). Therefore, the identification of pathways activated in response to CX-5461 can enable us to target therapy to specific cancer types based on the integrity of these pathways, and/or identify rational combination therapies that function in p53 mutant cancers.

Our research group has also extended these findings to acute myeloid leukemia (AML), in mouse models of AML subtypes driven by mixed-linage leukemia (MLL) or AML/ETO fusion proteins, as well as patient derived xenograft models (Hein et al., 2017). Consistent with the results presented above, inhibition of Pol I transcription by CX-5461 in both murine and human AML can induce p53-dependent apoptotic cell death, as well as activation of CHK1/CHK2 kinases and a G2/M cell cycle defect in both p53 null and p53 wild-type AML tumor cell population (Hein et al., 2017). CX-5461 displayed potent single agent efficacy, including towards the highly aggressive MLL AML subtype. Interestingly, in this model inhibition of Pol I transcription initiation by CX-5461 also impacts AML tumor cell differentiation, with induction of myeloid differentiation of leukemic blasts, and the reduction of leukemia initiating cell populations. In this case, Pol I transcription appears to be required for the maintenance of self-renewal capacity. This is consistent with recent reports that rates of rRNA transcription and the nucleoli may play a regulatory role in the control of pluripotency and differentiation (Zhang et al., 2014; Woolnough et al., 2016), and that and inhibition of Pol I transcription can induce differentiation (Hayashi et al., 2014; Savic et al., 2014) (See Section 1.2.2.6). The suppression of clonogenic capacity in AML is proposed to be responsible for the potent efficacy and lasting therapeutic benefit of CX-5461 treatment in this tumor type.

Therefore, in different cell and tumor types, diverse pathways may mediate the response to inhibition of Pol I transcription initiation, and define the predominant mechanism that determines the therapeutic efficacy of CX-5461 treatment. For example, in some models, the selectivity of CX-5461 for targeting tumor cells depends upon the non-genotoxic activation of p53 by the nucleolar stress pathway (eg. Eμ-*Myc* lymphoma; (Bywater et al., 2012; Devlin et al., 2016)), while in most other tumor cells sensitivity to CX-5461 is independent of p53 status (Drygin et al., 2011; Hein et al., 2017). The nucleolus is proposed to act as a 'hub' for coordinating cellular growth and proliferation, and cellular stress response. The well described p53 nucleolar stress response serves as a paradigm – it is a complex and nuanced process, with multiple layers of regulation targeting p53 transcription, translation, localization, stability, and activity as a transcription factor (Reviewed in (Russo and Russo, 2017)). The ability of CX-5461 to selectively activate p53 and induce apoptosis specifically in tumor cells is proposed to arise as a result of 'addiction' to high rates of ribosome biogenesis. In this model, in tumor types that have hyperactive Pol I transcription (such as those that are driven by the oncogene MYC), the nucleoli are no longer responsive to cellular stress signals, therefore the nucleolar stress response is not activated and cells escape activation of p53 and its tumor suppressor functions; direct inhibition of Pol I transcription immediately restores the nucleolar stress response in these tumor types, resulting in the abrupt activation of p53 (Reviewed in (Hannan et al., 2013b)). There is now strong evidence that the nucleoli can coordinate multiple other pathways, including cell cycle regulation, DNA damage response, or differentiation (Reviewed in (Tsai and Pederson, 2014; Woolnough et al., 2016; Tsekrekou et al., 2017)). We predict that nucleolar regulation of these additional responses will be found to be similarly as multifaceted as for p53. Importantly, we have demonstrated that knowledge of these pathways can be exploited to more effectively utilise inhibition of Pol I transcription in cancer therapy.

Early studies have indeed shown promise for improved efficacy of CX-5461 based target and/or rational combination therapies. In our research group, Devlin *et. al.* (Devlin et al., 2016) demonstrated that in the same murine model of Eμ-*Myc* lymphoma discussed above, targeting ribosome biogenesis and translation at multiple steps by combining CX-5461 with and the mTORC1 inhibitor everolimus, thereby inhibiting PI3K–AKT–mTORC1-dependent ribosome biogenesis and protein synthesis, resulted in significantly improved survival of tumor bearing mice. Similarly, in the Hi-MYC mouse model of prostate cancer, combination of CX-5461 with an inhibitor of PIM kinases - which increases MYC stability and transcriptional activity, and are

frequently overexpressed with MYC in prostate cancer – leads to reduced proliferation and invasion, and reversion of tumors (Rebello et al., 2016). Interestingly, in chemotherapy-resistant and –sensitive models of ovarian cancer cell lines, chemoresistant cells had both increased Pol I occupancy and rRNA synthesis, and enhanced sensitivity to treatment with CX-5461, which was associated with DNA damage checkpoint activation and G2 arrest through mitotic catastrophe (Cornelison et al., 2017). These results were consistent with patient derived xenografts of ovarian cancer, which showed increased Pol I activity after chemotherapy, and had a variable response to CX-5461, in which one model showed complete response (Cornelison et al., 2017). Therefore, CX-5461 may be a novel therapeutic strategy for targeting chemoresistant cancers.

An intriguing model is that the prevalence of upregulation of Pol I transcription in cancer cells exists, not because of an advantage conferred by increased ribosome biogenesis and protein synthesis, but rather because it is necessary to enable cancer cells to escape nucleolar regulation of cellular stress response pathways. In support of this, work from our laboratory has shown that a 35% reduction in rDNA transcription following Rrn3 knockdown in Eu-*Myc*-Bcl2+ cells confers no proliferative disadvantage for up to 4 days, when Bcl2 was overexpressed to prevent the activation of apoptosis by the nucleolar stress pathway (Bywater et al., 2012). This suggests that increased Pol I transcription is in excess of that required to sustain growth and proliferation in cancer cells. Proto-oncogenes may have evolved to coordinately upregulate Pol I transcription alongside promoting growth and proliferation, not simply to provide sufficient ribosomes, but instead to prevent the activation of cellular stress response pathways by the nucleoli. For example, the *C-MYC* oncogene drives cell growth through transcriptional regulation by MYC of a cohort of genes that comprise around 15% of the genome, including upregulation ribosomal protein genes and 5S rRNA genes. Therefore, the direct upregulation of Pol I transcription by MYC may in part be to ensure that L5/L11/5S rRNA are incorporated into new ribosomes, rather than available to interact with HDM2 and activate the p53 via the nucleolar stress pathway. (Zeller et al., 2001; Schlosser et al., 2003; Poortinga et al., 2004; Arabi et al., 2005; Grandori et al., 2005; Grewal et al., 2005; Gomez-Roman et al., 2006; Shiue et al., 2009; Poortinga et al., 2011b)(Reviewed in (Patel et al., 2004; Dang et al., 2006; Ruggero, 2009)). This may make cancers driven by oncogenes such as *C-MYC* particularly vulnerable CX-5461, as nucleolar stress response signaling would be amplified upon inhibition of Pol I transcription.

7.3 Investigating the mechanisms of ATM/ATR pathway activation by CX-5461.

We have extended our initial aims to begin to investigate the mechanisms by which the ATM/ATR pathway may be regulated by inhibition of Pol I transcription initiation by CX-5461. We have not yet developed a comprehensive understanding of how both ATM and ATR signaling pathways are activated independently of DNA damage by CX-5461. However, we have established that inhibition of Pol I transcription initiation by CX-5461 results in the displacement of Pol I at 'open' rDNA chromatin, the reorganisation of nucleolar structure, and the nucleolar activation of NBS1, which recruits ATM to chromatin, at its ATM target site (NBS1 phos-S343). This supports a model in which 'exposed' rDNA arises from the displacement of Pol I at active rRNA genes, making rDNA chromatin available to associate with ATM/ATR pathway proteins, which is sufficient for the activation of ATM and ATR independently of DNA damage (Soutoglou and Misteli, 2008; Sokka et al., 2015).

Further experiments addressing the mechanisms of ATM/ATR pathway activation by CX-5461 would benefit from additional controls for its specificity for inhibition Pol I transcription initiation. We could not recapitulate ATM/ATR pathway activation following inhibition of Pol I transcription initiation by siRNA knock-down of POLR1A and RRN3, likely due to the relatively delayed and less efficient inhibition of Pol I transcription by this method. We were able to recapitulate ATM/ATR pathway activation using CX-5488, a small molecule inhibitor of Pol I transcription related to CX-5461 but with divergent structure. However, we cannot exclude the possibility that members of this class of molecule share off target effects unrelated to inhibition of Pol I transcription initiation. Therefore, a different approach would more comprehensively test our model that inhibition of Pol I transcription initiation is the mechanism responsible for activation of ATM/ATR pathway following CX-5461 treatment. For example, inducible knock-out of Pol I complex components or transcription factors may achieve more rapid and specific inhibition of Pol I transcription (for example, utilising CRISPR/Cas systems (Cong et al., 2013; Mali et al., 2013)). Alternatively, as interest in inhibition of Pol I transcription as a therapeutic approach for cancer grows, other appropriate inhibitors of Pol I transcription initiation may become available. Another approach to more comprehensively address the specificity of CX-5461 for inhibition of Pol I transcription would be to specifically measure changes in nascent RNA following CX-5461 treatment, for example utilising global run-on sequencing (GRO-seq). RNA-sequencing measures the steady state level of RNAs, which is a product of the rates

of transcription as well as the post-transcriptional processing, stability and degradation of a given RNA. Techniques such as GRO-seq, which measure levels of nascent RNA, provide a more specific assay of rates of transcription (Core et al., 2008). Utilising GRO-seq at acute timepoints would therefore allow us to more sensitively determine whether CX-5461 is inhibiting transcription at certain other loci, as well as more accurately detect the acute downstream transcriptional regulatory pathway responses to CX-5461 treatment. A complementary approach would be to perform genome-wide analysis of CX-5461 target sites, for example using Chem-seq (chemical affinity capture and massively parallel DNA sequencing) (Reviewed in (Rodriguez and Miller, 2014)). A combination of GRO-seq and Chem-Seq experimental approaches would enable us to precisely identify the direct genomic targets of CX-5461. These would strengthen our data indicating it is the rapid and specific inhibition of Pol I transcription initiation that drives activation of the ATM/ATR pathway by CX-5461.

A key observation is that the activation of the ATM/ATR pathway occurs in S-phase and G2 following CX-5461 treatment. For example, CHK1/CHK2 activation is predominantly observed during S-phase of the cell cycle (FIGURE 20 C), BJ-T p53shRNA cells arrest in G2 following CX-5461 treatment after they have progressed through S-phase in the presence of the drug (FIGURE 14 B), and nucleolar activation of NBS1 at its ATM target site is increased specifically in S/G2 cell populations (FIGURE 27 C). We initially considered whether this was due to inhibition of Pol I transcription directly causing a defect in rDNA replication. However, this is not supported by our data. Following CX-5461 treatment, activation of the S-phase delay occurs in early S-phase, when active rDNA copies are replicated, but also in late S-phase when inactive rDNA copies, that we do not expect to be affected by inhibition of Pol I transcription, are replicated (FIGURE 28 C). Another more comprehensive replication assay to consider would be a DNA fibre assay, which visualizes the progression of individual replication forks. This would give additional information such as origin usage, speed, stalling, and termination of replication forks, and can be combined with FISH to analyse the rDNA specifically (Nieminuszczy et al., 2016). Considering that the proportion of cells in S-phase is only approximately 30% in exponentially growing BJ-T cells, and that the proportion of cells in S-phase can vary considerably at different time points following CX-5461 treatment, it is important that future studies addressing the mechanisms of ATM/ATR pathway activation take into account the cell cycle phase in order to sensitively detect changes that occur specifically in S-phase.

Currently, we do not have a clear understanding of how the activation of ATM/ATR in S-phase and G2 relates to our model presented above, where changes in rDNA chromatin state following inhibition of Pol I transcription initiation make it more available to associate with and activate ATM/ATR pathway proteins. One possibility is that 'exposed' rRNA gene copies enable increased R-loop formation at the rDNA. R-loops are three-stranded structures formed by a DNA:RNA hybrid and a displaced ssDNA strand identical with sequence identical to the RNA molecule (Reviewed in (Santos-Pereira and Aguilera, 2015)) . The rDNA is particularly prone to R-loop formation, likely with RNA acting in *trans*, and G-rich sequences such as those downstream of the rDNA promoter increase the stability of R-loop structures (Nadel et al., 2015). Interestingly, the displacement of G-rich ssDNA in the formation of R-loops results in G4 DNA structures (see further discussion below). Altered DNA accessibility can meditate the formation of R-loops independently of changes in transcription; for example, in Drosophila depletion of linker H1 results in increased accumulation of R-loops in heterochromatic regions (Bayona-Feliu et al., 2017). R-loops stall replication fork progression, which if unresolved can result in DSBs and genomic instability, and BRCA1 and BRCA2 are key processing enzymes implicated in the resolution of these structures and the removal of R-loops (Bhatia et al., 2014; Hatchi et al., 2015)(Reviewed in (Stirling and Hieter, 2017)). Therefore, ATM/ATR signaling may be activated at R-loops during DNA replication in S-phase. It would be interesting to pursue whether increased DNA damage can be detected at the rDNA following CX-5461 treatment specifically in cell types deficient in the homologous recombination (HR) DNA repair pathway, in which BRCA1 and/or BRCA2 are frequently mutated, due to unresolved R-loops (Xu et al., 2017)(Reviewed in (Prakash et al., 2015)). Another possibility is that inhibition of Pol I transcription prevents the establishment of silent chromatin states at newly replicated rDNA in S-phase, resulting in more exposed rDNA copies available to associate with ATM/ATR pathway proteins. The pRNA component of the nucleolar remodelling complex (NoRC) is transcribed by Pol I from the rDNA promoter, and is required for epigenetic silencing of newly replicated rDNA repeats. Depletion of another NoRC component, TIP5, has been shown to result in a reduction in inactive rDNA copies (Li et al., 2005; Guetg et al., 2010; Santoro et al., 2010). We have also reported here that following 24hr CX-5461 treatment there is an increased proportion of rDNA repeats in an 'open' conformation accessible to psoralen (FIGURE 26 C). Therefore, it would be interesting to pursue whether CX-5461 also inhibits Pol I transcription of pRNA and thus epigenetic silencing of rDNA repeats.

Alternatively, we could commit the resources to pursue unbiased analysis and develop a screen (for example RNAi knock-down or CRISPR/Cas knock-out) to identify genes that mediate the p53-independent anti-proliferative response to CX-5461 treatment. While this would be a significant undertaking, it could conceivably both a) identify genes required for the activation of the ATM/ATR signaling pathway in response to CX-5461, and downstream transmitters and effectors of the ATM/ATR signaling pathway in response to CX-5461, but also b) identify additional novel pathways that mediated the p53-independent responses to inhibition of Pol I transcription by CX-5461, and c) identify targets whose inhibition synergises with CX-5461 to induce cell death, and could be exploited to enhance the therapeutic efficacy of this treatment approach.

Another interesting observation is that CX-5461 treatment can attenuate the repair of DNA damage. While no increase in DNA damage is detected at early time points following CX-5461 treatment alone, DNA damage introduced from other sources (for example irradiation, or induction of a targeted endonuclease) is less efficiently repaired following CX-5461 treatment (FIGURE 30). At present, we can only speculate the mechanism underlying this. For example, it is possible that perturbation of nucleolar structure affects the regulation of DDR proteins by nucleolar localisation (Reviewed in (Tsekrekou et al., 2017)). Alternatively, the engagement of the ATM/ATR kinases in a separate nucleolar pathway may prevent them from being available for global DNA damage response (Guo et al., 2010). Regardless, this phenomenon may also have implications for the selective targeting of cancer cells by inhibition of Pol I transcription by CX-5461. Genomic instability is a common characteristic that underlies the acquisition of mutations that result in the hallmarks of cancer. Therefore, many tumor types have defects in DDR and high baseline DNA damage as a feature of their tumorigenic phenotype. This has motivated the strategy of developing DDR inhibitors for cancer therapeutics (Reviewed in (Gavande et al., 2016)). Similarly, CX-5461 could potentially be utilised to exacerbate DNA damage in tumorigenic cells, specifically inducing toxicity in these cells while sparing normal undamaged cells. Therefore, investigating the efficacy of inhibition of Pol I transcription initiation by CX-5461 in cancers with defects in specific DNA damage repair pathways, or in combination with traditional DNA damage inducing therapeutics, may be a promising avenue for targeted therapy.

7.4 G4 stabilisation following CX-5461 treatment

Recently, Samual Aparicio's research group reported that CX-5461 acts as a DNA G-quadruplex stabiliser (Xu et al., 2017). Single stranded G-rich DNA sequences can fold into stable four stranded DNA structures called G-quadruplexes (G4s). In normal cells, G4s are detected at approximately 1% of the over 700,000 predicted G4 forming sequences (Reviewed in (Hansel-Hertsch et al., 2017)). The determinants of G4 formation are not fully understood. Most G4s form at transcriptionally active chromatin. Transcription of G-rich templates such as the rDNA can be accompanied by the formation of G4 DNA structures in the non-template strand (Duquette et al., 2004). G4 DNA structures are enriched in gene regulatory regions that include promoters, 5′ untranslated regions and splicing sites (Chambers et al., 2015). G4 targeting ligands and/or mutations in G4-resolving helicases can alter the regulation of genes with promoters that are enriched in predicted G4 motifs, suggesting a link between G4s and transcription regulation (Siddiqui-Jain et al., 2002; Cogoi and Xodo, 2006; Johnson et al., 2010; Tang et al., 2016). G4 DNA increases in S-phase, suggesting that when the DNA strands are transiently separated at the replication fork, it allows the single strands to fold into G4 structures (Biffi et al., 2013). Also, replication origins are predicted to contain G4 motifs, and the ORC complex can bind to G4 DNA sequences in vitro, suggesting G4 structures may be involved in initiation of replication (Besnard et al., 2012; Hoshina et al., 2013). In the absence of helicases that resolve G4 structures in DNA, stable G4 structures can impede the progression of DNA polymerases and lead to replication stalling, DNA damage and genomic instability. Ligands that stabilise G4 structures can induce DNA breakage in human cells (Rodriguez et al., 2012).

The rDNA is G-rich and therefore prone to forming G4 structures (Hanakahi et al., 1999; Drygin et al., 2009). Another agent that inhibits Pol I transcription identified by Cylene Pharmaceuticals is the fluroquinine derivative quarfloxin (CX-3543). Unlike CX-5461, CX-3543 does not directly target formation of the Pol I transcription complex. Rather, CX-3543 accumulates specifically in the nucleoli, disrupts the interaction of nucleolin with rDNA G4 structures, and inhibits Pol I transcription at the elongation stage (Drygin et al., 2009). During development by Cylene Pharmaceuticals, CX-5461 did not show the same affinity for targeting for rDNA G4 structures as quarfloxin (Denis Drygin, personal communication). However, Xu *et. al.* report that CX-5461 is able to bind and stabilise G4 forming sequences *in vitro* in a similar manner to quarfloxin. In HCT-116 colorectal carcinoma cells, 24hr treatment with 100nM CX-5461 resulted in

increased G4 detection by IF analysis with an antibody specific to G4 DNA structures (BG4, (Biffi et al., 2013)), and increased detection of DNA damage foci across the entire genome by IF analysis. Increased DNA damage could be detected by alkaline comet assay following just 30min treatment with 100nM CX-5461. DNA damage was detected predominantly during DNA replication in S-phase, leading the authors to propose it arises as a result of CX-5461 binding to DNA and impeding replication forks, and that non-resolved forks give rise to DNA breaks. After 30min treatment with 1μM CX-5461, replication fork rate was not significantly reduced in WT HCT-116 cells, but was significantly reduced in HCT-116 cells deficient in homolgous recompination (HR) repair factor BRCA2, which is involved in repairing G4 associated DNA damage (Zimmer et al., 2016). Accordingly, cell viability assays demonstrated that the IC50 of CX-5461 was roughly 10-fold lower in BRCA2 deficient than WT HCT-116 cells (Xu et al., 2017).

The stabilisation of G4s by CX-5461 is therefore consistent with an S-phase delay and G2 cell cycle arrest, and activation of ATM/ATR signaling, as a result of unresolved G4s leading to stalled replication forks and consequently DNA damage. However, if stabilisation of G4s were the mechanisms responsible for the activation of ATM/ATR signaling in BJ-T cells, we would also expect increased levels of DNA damage at early time points corresponding to activation of this pathway. This does not occur: we observed activation of the ATM/ATR pathway by 30min following CX-5461 treatment (FIGURE 19), at which time neither alkaline comet analysis of DNA damage (FIGURE 21), nor Western blot and IF analysis of γH2A.X DNA damage foci (FIGURE 21), showed increased levels in DNA damage. To more directly address whether stabilisation of G4 structures by CX-5461 drives the activation of ATM/ATR signaling in BJ-T cells, we performed analysis of G4 levels by immunofluorescent microscopy analysis with an antibody specific to G4 DNA structures (1H6, (Henderson et al., 2014)). Following 1h treatment with 1μM CX-5461, we could not detect any increase in signal for G4 DNA structures compared to that observed in untreated control cells (Supplementary FIGURE 31 A). Therefore, in BJ-T cells, activation of ATM/ATR signaling at the rDNA in BJ-T cells following CX-5461 treatment is independent of G4 stabilisation.

Currently we can only speculate what determines the sensitivity of specific cell lines but not others to stabilisation of G4 DNA by CX-5461. A common property of transformed cells is genomic instability, and DNA secondary structures such as G4s

can cause a threat to genomic stability if they are not resolved. It is possible that transformed cells are more prone to defects in G4 resolution. In support of this, a number of publications have reported a higher prevalence of G4 structures in some cancer cell lines than normal cells (Hansel-Hertsch et al., 2017). Alternatively, a number of abundant nucleolar proteins have high affinity for G4 structures, for example NCL (Hanakahi et al., 1999). As inhibition of Pol I transcription by CX-5461 results in the relocalisation of nucleolar proteins, it is possible that they additionally act to stabilise G4 structures, and thus in transformed cell lines that are 'addicted' to high rates of Pol I transcription and ribosome biogenesis, such effects are amplified. In support of this, while quarfloxin accumulates in the nucleoli (Drygin et al., 2009), increased G4s were detected across the entire genome following quarfloxin treatment (Xu et al., 2017).

Our research group has been able corroborate the results of Xu *et. al.* and observe stabilisation of G4 structures following CX-5461 treatment in ovarian cancer cell lines (Experiments performed by Dr. Elaine Sanij). For example, we have examined the effects of acute CX-5461 treatment on the formation of G4s using immunofluorescence analysis with the 1H6 antibody. While 1hr treatment with 1μM CX-5461 induced G4 stabilisation at similar kinetics to a bona fide G4 stabiliser (TMPyP4) in the OV90 malignant papillary serous adenocarcinoma cell line, CX-5461 did not induce G4 stabilisation in the OVCAR4 high grade ovarian serous adenocarcinoma cell line (Supplementary FIGURE 1 B). Notably, activation of ATM phos-S1981, CHK1 phos-S345 and CHK2 phos-T68 were detected in both cell lines following 1hr treatment with 1μM CX-5461 CX-5461, irrespective of G4 stabilisation. In contrast, TMPyP4 did not activate CHK1 phos-S345 and CHK2 phos-T68. Moreover, unpublished studies from our research group deomonstrate that doses of CX-5461 that induce cell death in AML cell lines are significantly lower than doses of CX-5461 required for G4 stabilisation in this model. This strongly demonstrates that activation of ATM/ATR signaling by CX-5461 is independent of its role in G4 stabilisation.

The report by Xu *et. al.* presents another valuable avenue for targeted therapy by CX-5461, in cells deficient in BRCA1/2-mediated HR DNA damage repair. Xu *et. al.* measured the anti-proliferative effect of CX-5461 across a panel of 50 breast cancer cell lines, and found that triple negative breast cancer (TBNC) cell lines deficient in HR pathway components (BRCA1, BRCA2 or RAD51) are more sensitive to CX-5461. In xenograft models of HCT-116 cell line pairs WT or deficient for BRCA2, CX-5461 treatment significantly inhibited growth rate only of tumors from BRCA2 deficient cell

lines. While in three TNBC patient derived xenografts, tumor growth inhibition was greater in two containing BRCA1 and BRCA2 mutations than BRCA WT. This has motivated the phase I/II clinical trials of CX-5461 in ovarian and prostate cancer by our research group (Peter MacCallum Cancer Centre) and in TNBC (Canadian trial, NCT02719977), for the treatment of patients with HR deficient tumors.

7.5 Conclusion

The advantages of CX-5461 as a novel class of cancer therapy compared to traditional cancer therapeutics appears have two facets. First, in specific cancers it appears that 'addiction' to high rates of Pol I transcription is responsible for attenuating the activation of p53 tumor suppressor functions, and therefore in these tumor types CX-5461 can restore nucleolar stress signaling to rapidly and non-genotoxically activate p53 (Bywater et al., 2012). Second, CX-5461 also has therapeutic efficacy in cancer types without functional p53. As p53 is reported to be mutated in approximately half of all human tumors, and this is associated with more aggressive disease and therapy resistance, therapies targeting tumors without functional p53 are of particular value (Petitjean et al., 2007a). In fact, our results suggest that the absence of functional p53 and/or DNA damage repair pathways results in escape from normal cell cycle checkpoints, rendering cancer cells more vulnerable to CX-5461 treatment.

Over the course of this project, the concept of inhibiting Pol I transcription as an approach for cancer therapy has progressed from theory, to the use of Pol I inhibitors for the treatment of patients in phase I clinical trials. Utilising the first-in-class CX-5461 small molecule specific inhibitor of Pol I transcription, we began by simply establishing that inhibition of Pol I transcription can selectively target transformed cell lines, such as in the isogenic BJ fibroblast panel of cells at defined staged of transformation (Drygin et al., 2011). Since then, a number of publications from our research group have demonstrated the efficacy of CX-5461 in the treatment of different *in vivo* cancer models (Bywater et al., 2012; Devlin et al., 2016; Quin et al., 2016; Hein et al., 2017). The seminal publication by Bywater *et. al.* (Bywater et al., 2012) described that in the murine model of Eμ-*Myc* lymphoma, CX-5461 can selectively induce cell death in malignant B-cells while leaving normal B-cells unaffected, and that the sensitivity of this tumor type to CX-5461 is dependent upon p53 activation by the well characterised nucleolar stress pathway. Employing CX-5461 in minimally immortalized BJ-T cells, we were able to identify an additional pathway of response to inhibition of Pol I transcription initiation - p53-independent ATM/ATR pathway activation of cell cycle

checkpoints in the absence of global DNA damage (Quin et al., 2016). Following this, we demonstrated that this pathway is activated during the therapeutic response to CX-5461 *in vivo* in murine models of Eμ-*Myc* lymphoma (Quin et al., 2016) and AML (Hein et al., 2017), and that combination therapy with ATM/ATR pathway inhibitors can improve the efficacy of CX-5461 in p53 null cancers (Quin et al., 2016). Clinical trials have now been initiated for phase I / II studies of CX-5461 in patients with haematological malignancies (Peter MacCallum Cancer Centre, ACTRN12613001061729) and solid cancers (Canadian Cancer Trials Group, NCT02719977). Promisingly, initial results in haematological malignancies report durable periods of partial response or stable disease in heavily pretreated chemorefractory patients (Amit Khot, 2017). Going forward, our understanding of the mechanisms that mediate the response to inhibition of Pol I transcription initiation and subsequent defects in rDNA chromatin will inform rational clinical applications of this emerging and promising approach to therapeutics in a range of cancer types.

FIGURE 31. (Supplementary). A) Co-IF analysis of G4 (1H6; green) and UBF (red) with costaining for DAPI in BJT cell line following 1hr treatment with vehicle control or 1μM CX-5461 (n=1). **B)** Co-IF analysis of G4 (1H6; green) and UBF (red) with costaining for DAPI in OVCAR4 (high grade ovarian serous adenocarcinoma) and OV90 (malignant papillary serous adenocarcinoma) cell lines following 1hr treatment with vehicle control, 1μM CX-5461, or 10μM TMPyP4 (Experiments performed by Dr. Elaine Sanij). **C)** Western blot analysis. (Left panel) ATM phos-S1981 and total ATM levels in OVCAR4 cell lines following 1hr and 3hr treatment with vehicle control, 100nM CX-5461 or 1μM CX-5461. (Right panel) CHK1 phos-S345 and CHK2 phos-T68 levels in OVCAR4 and OV90 cell lines following 1hr and 3hr treatment with 1μM CX-5461 or 10μM TMPyP4 (Experiments performed by Dr. Elaine Sanij).

FIGURE 31 (Supplementary)

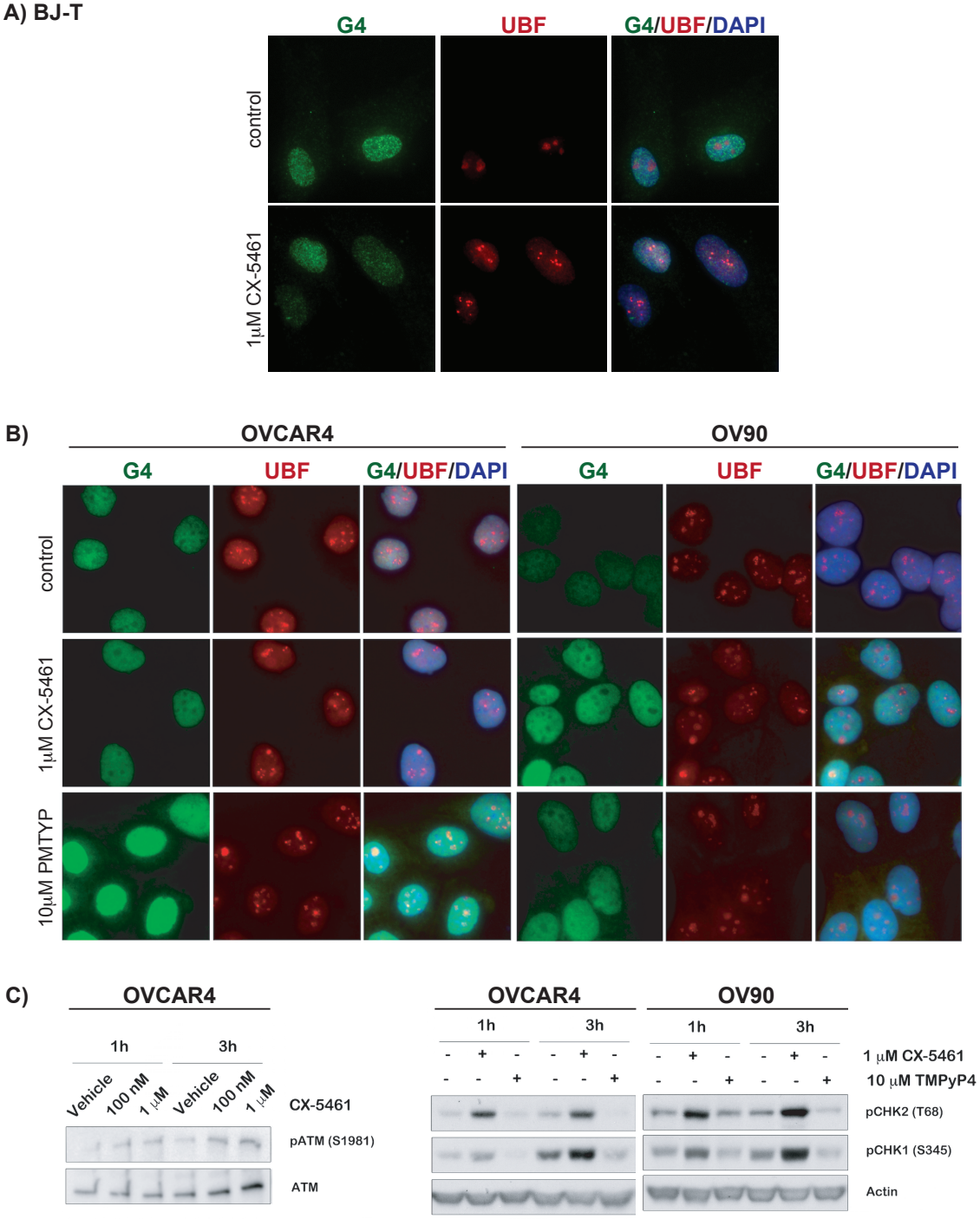

BIBLIOGRAPHY.

Abbas, T., and Dutta, A. (2009a). p21 in cancer: intricate networks and multiple activities. Nature reviews Cancer *9*, 400-414.

Abbas, T., and Dutta, A. (2009b). p21 in cancer: intricate networks and multiple activities. Nat Rev Cancer *9*, 400-414.

Abella, N., Brun, S., Calvo, M., Tapia, O., Weber, J.D., Berciano, M.T., Lafarga, M., Bachs, O., and Agell, N. (2010). Nucleolar disruption ensures nuclear accumulation of p21 upon DNA damage. Traffic *11*, 743-755.

Acosta, J.C., Banito, A., Wuestefeld, T., Georgilis, A., Janich, P., Morton, J.P., Athineos, D., Kang, T.W., Lasitschka, F., Andrulis, M.*, et al.* (2013). A complex secretory program orchestrated by the inflammasome controls paracrine senescence. Nat Cell Biol *15*, 978-990.

Adams, J.M., Harris, A.W., Pinkert, C.A., Corcoran, L.M., Alexander, W.S., Cory, S., Palmiter, R.D., and Brinster, R.L. (1985). The c-myc oncogene driven by immunoglobulin enhancers induces lymphoid malignancy in transgenic mice. Nature *318*, 533-538.

Ahuja, D., Sáenz-Robles, M.T., and Pipas, J.M. (2005). SV40 large T antigen targets multiple cellular pathways to elicit cellular transformation. Oncogene *24*, 7729.

Akamatsu, Y., and Kobayashi, T. (2015). The Human RNA Polymerase I Transcription Terminator Complex Acts as a Replication Fork Barrier That Coordinates the Progress of Replication with rRNA Transcription Activity. Mol Cell Biol *35*, 1871-1881.

Akhmanova, A., Verkerk, T., Langeveld, A., Grosveld, F., and Galjart, N. (2000). Characterisation of transcriptionally active and inactive chromatin domains in neurons. J Cell Sci *113 Pt 24*, 4463-4474.

Akhurst, R.J., and Hata, A. (2012). Targeting the TGFbeta signalling pathway in disease. Nat Rev Drug Discov *11*, 790-811.

Al-Baker, E.A., Boyle, J., Harry, R., and Kill, I.R. (2004). A p53-independent pathway regulates nucleolar segregation and antigen translocation in response to DNA damage induced by UV irradiation. Exp Cell Res *292*, 179-186.

Albert, B., Leger-Silvestre, I., Normand, C., Ostermaier, M.K., Perez-Fernandez, J., Panov, K.I., Zomerdijk, J.C., Schultz, P., and Gadal, O. (2011). RNA polymerase I-specific subunits promote polymerase clustering to enhance the rRNA gene transcription cycle. J Cell Biol *192*, 277-293.

Alt, J.R., Bouska, A., Fernandez, M.R., Cerny, R.L., Xiao, H., and Eischen, C.M. (2005). Mdm2 binds to Nbs1 at sites of DNA damage and regulates double strand break repair. J Biol Chem *280*, 18771-18781.

Amit Khot, N.B., Donald P Cameron, Gretchen Poortinga, Elaine Sanij, John Lim, John Soong, Nadine Hein, Emma Link, Richard B Pearson, Ross Hannan, Grant A. McArthur, and Simon J. Harrison (2017). RNA Polymerase I Transcription Inhibitor CX-5461 in Patients with Advanced Hematologic Malignancies: Results of a Phase I First in Human Study. In American Society of Hematology 59th Annual Meeting & Exposition (Atlanta GA).

Anders, S., and Huber, W. (2010). Differential expression analysis for sequence count data. Genome Biol *11*, R106.

Anders, S., Pyl, P.T., and Huber, W. (2015). HTSeq—a Python framework to work with high-throughput sequencing data. Bioinformatics *31*, 166-169.

Andersen, J.S., Lam, Y.W., Leung, A.K.L., Ong, S.E., Lyon, C.E., Lamond, A.I., and Mann, M. (2005). Nucleolar proteome dynamics. Nature *433*, 77-83.

Andersen, J.S., Lyon, C.E., Fox, A.H., Leung, A.K.L., Lam, Y.W., Steen, H., Mann, M., and Lamond, A.I. (2002). Directed proteomic analysis of the human nucleolus. Curr Biol *12*, 1-+.

Andrews, W.J., Panova, T., Normand, C., Gadal, O., Tikhonova, I.G., and Panov, K.I. (2013). Old drug, new target: ellipticines selectively inhibit RNA polymerase I transcription. J Biol Chem *288*, 4567-4582.

Andrique, L., Fauvin, D., El Maassarani, M., Colasson, H., Vannier, B., and Seite, P. (2012). ErbB3(80) (kDa), a nuclear variant of the ErbB3 receptor, binds to the Cyclin D1 promoter to activate cell proliferation but is negatively controlled by p14(ARF). Cell Signal *24*, 1074-1085.

Angus, S.P., Solomon, D.A., Kuschel, L., Hennigan, R.F., and Knudsen, E.S. (2003). Retinoblastoma tumor suppressor: Analyses of dynamic behavior in living cells reveal multiple modes of regulation. Molecular and Cellular Biology *23*, 8172-8188.

Antoniali, G., Lirussi, L., Poletto, M., and Tell, G. (2014). Emerging roles of the nucleolus in regulating the DNA damage response: the noncanonical DNA repair enzyme APE1/Ref-1 as a paradigmatical example. Antioxid Redox Signal *20*, 621-639.

Arabi, A., Wu, S.Q., Ridderstrale, K., Bierhoff, H., Shiue, C., Fatyol, K., Fahlen, S., Hydbring, P., Soderberg, O., Grummt, I.*, et al.* (2005). c-Myc associates with ribosomal DNA and activates RNA polymerase I transcription. Nat Cell Biol *7*, 303-310.

Arenzana-Seisdedos, F., Turpin, P., Rodriguez, M., Thomas, D., Hay, R.T., Virelizier, J.L., and Dargemont, C. (1997). Nuclear localization of I kappa B alpha promotes active transport of NF-kappa B from the nucleus to the cytoplasm. J Cell Sci *110 (Pt 3)*, 369-378.

Asghar, U., Witkiewicz, A.K., Turner, N.C., and Knudsen, E.S. (2015). The history and future of targeting cyclin-dependent kinases in cancer therapy. Nat Rev Drug Discov *14*, 130-146.

Audas, T.E., Jacob, M.D., and Lee, S. (2012). Immobilization of Proteins in the Nucleolus by Ribosomal Intergenic Spacer Noncoding RNA. Molecular Cell *45*, 147-157.

Avraham, R., Sas-Chen, A., Manor, O., Steinfeld, I., Shalgi, R., Tarcic, G., Bossel, N., Zeisel, A., Amit, I., Zwang, Y.*, et al.* (2010). EGF Decreases the Abundance of MicroRNAs That Restrain Oncogenic Transcription Factors. Sci Signal *3*, ra43.

Ayer, D.E., Kretzner, L., and Eisenman, R.N. (1993). Mad: a heterodimeric partner for Max that antagonizes Myc transcriptional activity. Cell *72*, 211-222.

Ayrault, O., Andrique, L., Fauvin, D., Eymin, B., Gazzeri, S., and Seite, P. (2006). Human tumor suppressor p14(ARF) negatively regulates rRNA transcription and inhibits UBF1 transcription factor phosphorylation. Oncogene *25*, 7577-7586.

Ayrault, O., Andrique, L., Larsen, C.J., and Seite, P. (2004). Human Arf tumor suppressor specifically interacts with chromatin containing the promoter of rRNA genes. Oncogene *23*, 8097-8104.

Bahrami, S., and Drablos, F. (2016). Gene regulation in the immediate-early response process. Adv Biol Regul *62*, 37-49.

Bai, B., Liu, H., and Laiho, M. (2014). Small RNA expression and deep sequencing analyses of the nucleolus reveal the presence of nucleolus-associated microRNAs. FEBS Open Bio *4*, 441-449.

Bakkenist, C.J., and Kastan, M.B. (2003). DNA damage activates ATM through intermolecular autophosphorylation and dimer dissociation. Nature *421*, 499-506.

Banaszynski, L.A., Chen, L.C., Maynard-Smith, L.A., Ooi, A.G.L., and Wandless, T.J. (2006). A rapid, reversible, and tunable method to regulate protein function in living cells using synthetic small molecules. Cell *126*, 995-1004.

Bassermann, F., Frescas, D., Guardavaccaro, D., Busino, L., Peschiaroli, A., and Pagano, M. (2008). The Cdc14B-Cdh1-Plk1 axis controls the G2 DNA-damage-response checkpoint. Cell *134*, 256-267.

Bayona-Feliu, A., Casas-Lamesa, A., Reina, O., Bernues, J., and Azorin, F. (2017). Linker histone H1 prevents R-loop accumulation and genome instability in heterochromatin. Nat Commun *8*, 283.

Beckerman, R., Donner, A.J., Mattia, M., Peart, M.J., Manley, J.L., Espinosa, J.M., and Prives, C. (2009). A role for Chk1 in blocking transcriptional elongation of p21 RNA during the S-phase checkpoint. Genes Dev *23*, 1364-1377.

Bell, S.P., Learned, R.M., Jantzen, H.M., and Tjian, R. (1988). FUNCTIONAL COOPERATIVITY BETWEEN TRANSCRIPTION FACTOR-UBF1 AND FACTOR-SL1 MEDIATES HUMAN RIBOSOMAL-RNA SYNTHESIS. Science *241*, 1192-1197.

Bellodi, C., Krasnykh, O., Haynes, N., Theodoropoulou, M., Peng, G.A., Montanaro, L., and Ruggero, D. (2010). Loss of Function of the Tumor Suppressor DKC1 Perturbs p27 Translation Control and Contributes to Pituitary Tumorigenesis. Cancer Res *70*, 6026-6035.

Bencokova, Z., Kaufmann, M.R., Pires, I.M., Lecane, P.S., Giaccia, A.J., and Hammond, E.M. (2009). ATM Activation and Signaling under Hypoxic Conditions. Molecular and Cellular Biology *29*, 526-537.

Berkovich, E., Monnat, R.J., and Kastan, M.B. (2007). Roles of ATM and NBS1 in chromatin structure modulation and DNA double-strand break repair. Nat Cell Biol *9*, 683-U137.

Berkovich, E., Monnat, R.J., and Kastan, M.B. (2008). Assessment of protein dynamics and DNA repair following generation of DNA double-strand breaks at defined genomic sites. Nat Protoc *3*, 915-922.

Bertrand, E., Houser-Scott, F., Kendall, A., Singer, R.H., and Engelke, D.R. (1998). Nucleolar localization of early tRNA processing. Genes & Development *12*, 2463-2468.

Besnard, E., Babled, A., Lapasset, L., Milhavet, O., Parrinello, H., Dantec, C., Marin, J.M., and Lemaitre, J.M. (2012). Unraveling cell type-specific and reprogrammable human replication origin signatures associated with G-quadruplex consensus motifs. Nat Struct Mol Biol *19*, 837-844.

Bharti, A.K., Olson, M.O., Kufe, D.W., and Rubin, E.H. (1996). Identification of a nucleolin binding site in human topoisomerase I. J Biol Chem *271*, 1993-1997.

Bhaskaran, N., van Drogen, F., Ng, H.F., Kumar, R., Ekholm-Reed, S., Peter, M., Sangfelt, O., and Reed, S.I. (2013). Fbw7alpha and Fbw7gamma collaborate to shuttle cyclin E1 into the nucleolus for multiubiquitylation. Mol Cell Biol *33*, 85-97.

Bhat, K.P., Itahana, K., Jin, A.W., and Zhang, Y.P. (2004). Essential role of ribosomal protein L11 in mediating growth inhibition-induced p53 activation. Embo Journal *23*, 2402-2412.

Bhatia, V., Barroso, S.I., Garcia-Rubio, M.L., Tumini, E., Herrera-Moyano, E., and Aguilera, A. (2014). BRCA2 prevents R-loop accumulation and associates with TREX-2 mRNA export factor PCID2. Nature *511*, 362-365.

Bhatt, P., d'Avout, C., Kane, N.S., Borowiec, J.A., and Saxena, A. (2012). Specific domains of nucleolin interact with Hdm2 and antagonize Hdm2-mediated p53 ubiquitination. The FEBS journal *279*, 370-383.

Bierhoff, H., Dammert, M.A., Brocks, D., Dambacher, S., Schotta, G., and Grummt, I. (2014). Quiescence-induced LncRNAs trigger H4K20 trimethylation and transcriptional silencing. Mol Cell *54*, 675-682.

Bierhoff, H., Schmitz, K., Maass, F., Ye, J., and Grummt, I. (2010). Noncoding transcripts in sense and antisense orientation regulate the epigenetic state of ribosomal RNA genes. Cold Spring Harb Symp Quant Biol *75*, 357-364.

Biffi, G., Tannahill, D., McCafferty, J., and Balasubramanian, S. (2013). Quantitative visualization of DNA G-quadruplex structures in human cells. Nat Chem *5*, 182-186.

Billin, A.N., Eilers, A.L., Queva, C., and Ayer, D.E. (1999). Mlx, a novel Max-like BHLHZip protein that interacts with the Max network of transcription factors. J Biol Chem *274*, 36344-36350.

Boddapati, N., Anbarasu, K., Suryaraja, R., Tendulkar, A.V., and Mahalingam, S. (2012). Subcellular distribution of the human putative nucleolar GTPase GNL1 is regulated by a novel arginine/lysine-rich domain and a GTP binding domain in a cell cycle-dependent manner. J Mol Biol *416*, 346-366.

Boisvert, F.M., Lam, Y.W., Lamont, D., and Lamond, A.I. (2010). A quantitative proteomics analysis of subcellular proteome localization and changes induced by DNA damage. Mol Cell Proteomics *9*, 457-470.

Boisvert, F.M., and Lamond, A.I. (2010). p53-Dependent subcellular proteome localization following DNA damage. Proteomics *10*, 4087-4097.

Bonev, B., and Cavalli, G. (2016). Organization and function of the 3D genome. Nat Rev Genet *17*, 772.

Bonizzi, G., and Karin, M. (2004). The two NF-kappaB activation pathways and their role in innate and adaptive immunity. Trends in immunology *25*, 280-288.

Bootsma, D., Budke, L., and Vos, O. (1964). Studies on Synchronous Division of Tissue Culture Cells Initiated by Excess Thymidine. Exp Cell Res *33*, 301-309.

Boulon, S., Westman, B.J., Hutten, S., Boisvert, F.M., and Lamond, A.I. (2010a). The Nucleolus under Stress. Molecular Cell *40*, 216-227.

Boulon, S., Westman, B.J., Hutten, S., Boisvert, F.M., and Lamond, A.I. (2010b). The nucleolus under stress. Mol Cell *40*, 216-227.

Boutros, T., Chevet, E., and Metrakos, P. (2008). Mitogen-Activated Protein (MAP) Kinase/MAP Kinase Phosphatase Regulation: Roles in Cell Growth, Death, and Cancer. Pharmacological Reviews *60*, 261-310.

Boyd, M.T., Vlatkovic, N., and Rubbi, C.P. (2011). The nucleolus directly regulates p53 export and degradation. J Cell Biol *194*, 689-703.

Bradsher, J., Auriol, J., de Santis, L.P., Iben, S., Vonesch, J.L., Grummt, I., and Egly, J.M. (2002). CSB is a component of RNA pol I transcription. Molecular Cell *10*, 819-829.

Brocke-Heidrich, K., Ge, B., Cvijic, H., Pfeifer, G., Loffler, D., Henze, C., McKeithan, T.W., and Horn, F. (2006). BCL3 is induced by IL-6 via Stat3 binding to intronic enhancer HS4 and represses its own transcription. Oncogene *25*, 7297-7304.

Brosh, R.M., Jr., and Bohr, V.A. (2002). Roles of the Werner syndrome protein in pathways required for maintenance of genome stability. Exp Gerontol *37*, 491-506.

Brown, K., Park, S., Kanno, T., Franzoso, G., and Siebenlist, U. (1993). Mutual regulation of the transcriptional activator NF-kappa B and its inhibitor, I kappa B-alpha. Proceedings of the National Academy of Sciences *90*, 2532-2536.

Brummelkamp, T.R., Bernards, R., and Agami, R. (2002). A system for stable expression of short interfering RNAs in mammalian cells. Science *296*, 550-553.

Bruno, P.M., Liu, Y., Park, G.Y., Murai, J., Koch, C.E., Eisen, T.J., Pritchard, J.R., Pommier, Y., Lippard, S.J., and Hemann, M.T. (2017). A subset of platinum-containing chemotherapeutic agents kills cells by inducing ribosome biogenesis stress. Nat Med *23*, 461-471.

Bunz, F., Dutriaux, A., Lengauer, C., Waldman, T., Zhou, S., Brown, J.P., Sedivy, J.M., Kinzler, K.W., and Vogelstein, B. (1998). Requirement for p53 and p21 to sustain G2 arrest after DNA damage. Science *282*, 1497-1501.

Burger, K., Muhl, B., Harasim, T., Rohrmoser, M., Malamoussi, A., Orban, M., Kellner, M., Gruber-Eber, A., Kremmer, E., Holzel, M.*, et al.* (2010). Chemotherapeutic drugs inhibit ribosome biogenesis at various levels. J Biol Chem *285*, 12416-12425.

Burgess, R.C., and Misteli, T. (2015). Not All DDRs Are Created Equal: Non-Canonical DNA Damage Responses. Cell *162*, 944-947.

Bursac, S., Brdovcak, M.C., Pfannkuchen, M., Orsolic, I., Golomb, L., Zhu, Y., Katz, C., Daftuar, L., Grabusic, K., Vukelic, I.*, et al.* (2012). Mutual protection of ribosomal proteins L5 and L11 from

degradation is essential for p53 activation upon ribosomal biogenesis stress. Proc Natl Acad Sci U S A *109*, 20467-20472.

Burton, D.G., and Krizhanovsky, V. (2014). Physiological and pathological consequences of cellular senescence. Cell Mol Life Sci *71*, 4373-4386.

Bywater, M.J., Poortinga, G., Sanij, E., Hein, N., Peck, A., Cullinane, C., Wall, M., Cluse, L., Drygin, D., Anderes, K.*, et al.* (2012). Inhibition of RNA Polymerase I as a Therapeutic Strategy to Promote Cancer-Specific Activation of p53. Cancer Cell *22*, 51-65.

Caburet, S., Conti, C., Schurra, C., Lebofsky, R., Edelstein, S.J., and Bensimon, A. (2005). Human ribosomal RNA gene arrays display a broad range of palindromic structures. Genome Res *15*, 1079-1085.

Calkins, A.S., Iglehart, J.D., and Lazaro, J.B. (2013). DNA damage-induced inhibition of rRNA synthesis by DNA-PK and PARP-1. Nucleic Acids Research *41*, 7378-7386.

Calle, E., Berciano, M.T., Fernandez, R., and Lafarga, M. (1999). Activation of the autophagy, c-FOS and ubiquitin expression, and nucleolar alterations in Schwann cells precede demyelination in tellurium-induced neuropathy. Acta Neuropathol *97*, 143-155.

Campisi, J., and di Fagagna, F.D. (2007). Cellular senescence: when bad things happen to good cells. Nat Rev Mol Cell Biol *8*, 729-740.

Carmo-Fonseca, M., Mendes-Soares, L., and Campos, I. (2000). To be or not to be in the nucleolus. Nat Cell Biol *2*, E107-112.

Caudron-Herger, M., Pankert, T., Seiler, J., Nemeth, A., Voit, R., Grummt, I., and Rippe, K. (2015). Alu element-containing RNAs maintain nucleolar structure and function. Embo j *34*, 2758-2774.

Caunt, C.J., Sale, M.J., Smith, P.D., and Cook, S.J. (2015). MEK1 and MEK2 inhibitors and cancer therapy: the long and winding road. Nat Rev Cancer *15*, 577-592.

Cavanaugh, A.H., Hempel, W.M., Taylor, L.J., Rogalsky, V., Todorov, G., and Rothblum, L.I. (1995). ACTIVITY OF RNA-POLYMERASE-I TRANSCRIPTION FACTOR UBF BLOCKED BY RB GENE-PRODUCT. Nature *374*, 177-180.

Chambers, V.S., Marsico, G., Boutell, J.M., Di Antonio, M., Smith, G.P., and Balasubramanian, S. (2015). High-throughput sequencing of DNA G-quadruplex structures in the human genome. Nat Biotechnol *33*, 877-881.

Chan, J.C., Hannan, K.M., Riddell, K., Ng, P.Y., Peck, A., Lee, R.S., Hung, S., Astle, M.V., Bywater, M., Wall, M.*, et al.* (2011). AKT promotes rRNA synthesis and cooperates with c-MYC to stimulate ribosome biogenesis in cancer. Sci Signal *4*, ra56.

Chan, J.C., Hannan, K.M., Riddell, K., Pui Yee, N., Peck, A., Lee, R.S., Hung, S., Astle, M.V., Bywater, M., Wall, M.*, et al.* AKT Promotes rRNA Synthesis and Cooperates with c-MYC to Stimulate Ribosome Biogenesis in Cancer. Sci Signal *4*.

Chan, Y.A., Aristizabal, M.J., Lu, P.Y., Luo, Z., Hamza, A., Kobor, M.S., Stirling, P.C., and Hieter, P. (2014). Genome-wide profiling of yeast DNA:RNA hybrid prone sites with DRIP-chip. PLoS Genet *10*, e1004288.

Chao, J.C., Wan, X.S., Engelsberg, B.N., Rothblum, L.I., and Billings, P.C. (1996). Intracellular distribution of HMG1, HMG2 and UBF change following treatment with cisplatin. Biochimica Et Biophysica Acta-Gene Structure and Expression *1307*, 213-219.

Charles, C.H., Simske, J.S., O'Brien, T.P., and Lau, L.F. (1990). Pip92: a short-lived, growth factor-inducible protein in BALB/c 3T3 and PC12 cells. Molecular and Cellular Biology *10*, 6769-6774.

Chen, D., Belmont, A.S., Huang, S., and Lorand, L. (2004). Upstream Binding Factor Association Induces Large-Scale Chromatin Decondensation. Proceedings of the National Academy of Sciences of the United States of America *101*, 15106-15111.

Chen, D., Zhang, Z., Li, M., Wang, W., Li, Y., Rayburn, E.R., Hill, D.L., Wang, H., and Zhang, R. (2007). Ribosomal protein S7 as a novel modulator of p53-MDM2 interaction: binding to MDM2, stabilization of p53 protein, and activation of p53 function. Oncogene *26*, 5029-5037.

Chen, H., Duo, Y., Hu, B., Wang, Z., Zhang, F., Tsai, H., Zhang, J., Zhou, L., Wang, L., Wang, X.*, et al.* (2016a). PICT-1 triggers a pro-death autophagy through inhibiting rRNA transcription and AKT/mTOR/p70S6K signaling pathway. Oncotarget.

Chen, H., Duo, Y., Hu, B., Wang, Z., Zhang, F., Tsai, H., Zhang, J., Zhou, L., Wang, L., Wang, X.*, et al.* (2016b). PICT-1 triggers a pro-death autophagy through inhibiting rRNA transcription and AKT/mTOR/p70S6K signaling pathway. Oncotarget *7*, 78747-78763.

Chen, L., Ma, S., Li, B., Fink, T., Zachar, V., Takahashi, M., Cuttichia, J., Tsui, L.-C., Ebbesen, P., and Liu, X. (2003). Transcriptional activation of immediate‚Äìearly gene ETR101 by human T-cell leukaemia virus type I Tax. Journal of General Virology *84*, 3203-3214.

Chen, W.X., Hu, Q., Qiu, M.T., Zhong, S.L., Xu, J.J., Tang, J.H., and Zhao, J.H. (2013). miR-221/222: promising biomarkers for breast cancer. Tumor Biology *34*, 1361-1370.

Chiou, H.-Y., Liu, S.-Y., Lin, C.-H., and Lee, E. (2014). Hes-1 SUMOylation by protein inhibitor of activated STAT1 enhances the suppressing effect of Hes-1 on GADD45alpha expression to increase cell survival. J Biomed Sci *21*, 53.

Cho, H.J., Park, S.M., Hwang, E.M., Baek, K.E., Kim, I.K., Nam, I.K., Im, M.J., Park, S.H., Bae, S., Park, J.Y.*, et al.* (2010). Gadd45b mediates Fas-induced apoptosis by enhancing the interaction between p38 and retinoblastoma tumor suppressor. J Biol Chem *285*, 25500-25505.

Chomczynski, P., and Sacchi, N. (2006). The single-step method of RNA isolation by acid guanidinium thiocyanate-phenol-chloroform extraction: twenty-something years on. Nat Protoc *1*, 581-585.

Chung, K.C., Gomes, I., Wang, D.H., Lau, L.F., and Rosner, M.R. (1998). Raf and fibroblast growth factor phosphorylate Elk1 and activate the serum response element of the immediate early gene pip92 by mitogen-activated protein kinase-independent as well as -dependent signaling pathways. Molecular and Cellular Biology *18*, 2272-2281.

Chung, K.C., Kim, S.M., Rhang, S.G., Lau, L.F., Gomes, I., and Ahn, Y.S. (2000a). Expression of immediate early gene pip92 during anisomycin-induced cell death is mediated by the JNK- and p38-dependent activation of Elk1. European Journal of Biochemistry *267*, 4676-4684.

Chung, K.C., Shin, S.W., Yoo, M., Lee, M.Y., Lee, H.W., Choe, B.K., and Ahn, Y.S. (2000b). A systemic administration of NMDA induces immediate early gene pip92 in the hippocampus. J Neurochem *75*, 9-17.

Ciganda, M., and Williams, N. (2011). Eukaryotic 5S rRNA biogenesis. Wiley Interdiscip Rev RNA *2*, 523-533.

Cimprich, K.A., and Cortez, D. (2008). ATR: an essential regulator of genome integrity. Nat Rev Mol Cell Biol *9*, 616-627.

Cmejla, R., Cmejlova, J., Handrkova, H., Petrak, J., and Pospisilova, D. (2007). Ribosomal protein S17 gene (RPS17) is mutated in Diamond-Blackfan anemia. Hum Mutat *28*, 1178-1182.

Cogoi, S., and Xodo, L.E. (2006). G-quadruplex formation within the promoter of the KRAS proto-oncogene and its effect on transcription. Nucleic Acids Res *34*, 2536-2549.

Cogswell, P.C., Guttridge, D.C., Funkhouser, W.K., and Baldwin, A.S., Jr. (2000). Selective activation of NF-kappa B subunits in human breast cancer: potential roles for NF-kappa B2/p52 and for Bcl-3. Oncogene *19*, 1123-1131.

Cohen, A.A., Geva-Zatorsky, N., Eden, E., Frenkel-Morgenstern, M., Issaeva, I., Sigal, A., Milo, R., Cohen-Saidon, C., Liron, Y., Kam, Z.*, et al.* (2008). Dynamic Proteomics of Individual Cancer Cells in Response to a Drug. Science *322*, 1511-1516.

Coleclough, C., Kuhn, L., and Lefkovits, I. (1990). REGULATION OF MESSENGER-RNA ABUNDANCE IN ACTIVATED LYMPHOCYTE-T - IDENTIFICATION OF MESSENGER-RNA SPECIES AFFECTED BY THE INHIBITION OF PROTEIN-SYNTHESIS. Proceedings of the National Academy of Sciences of the United States of America *87*, 1753-1757.

Collins, A.R. (2002). The comet assay. Principles, applications, and limitations. Methods Mol Biol *203*, 163-177.

Comings, D.E. (1980). ARRANGEMENT OF CHROMATIN IN THE NUCLEUS. Human Genetics *53*, 131-143.

Cong, L., Ran, F.A., Cox, D., Lin, S., Barretto, R., Habib, N., Hsu, P.D., Wu, X., Jiang, W., Marraffini, L.A.*, et al.* (2013). Multiplex genome engineering using CRISPR/Cas systems. Science *339*, 819-823.

Cong, R., Das, S., Ugrinova, I., Kumar, S., Mongelard, F., Wong, J., and Bouvet, P. (2012). Interaction of nucleolin with ribosomal RNA genes and its role in RNA polymerase I transcription. Nucleic Acids Res *40*, 9441-9454.

Coppe, J.P., Desprez, P.Y., Krtolica, A., and Campisi, J. (2010). The senescence-associated secretory phenotype: the dark side of tumor suppression. Annu Rev Pathol *5*, 99-118.

Coppe, J.P., Kauser, K., Campisi, J., and Beausejour, C.M. (2006). Secretion of vascular endothelial growth factor by primary human fibroblasts at senescence. J Biol Chem *281*, 29568-29574.

Core, L.J., Waterfall, J.J., and Lis, J.T. (2008). Nascent RNA sequencing reveals widespread pausing and divergent initiation at human promoters. Science *322*, 1845-1848.

Cornelison, R., Dobbin, Z.C., Katre, A.A., Jeong, D.H., Zhang, Y., Chen, D., Petrova, Y., Llaneza, D.C., Steg, A.D., Parsons, L.*, et al.* (2017). Targeting RNA-Polymerase I in Both Chemosensitive and Chemoresistant Populations in Epithelial Ovarian Cancer. Clin Cancer Res.

Coute, Y., Burgess, J.A., Diaz, J.J., Chichester, C., Lisacek, F., Greco, A., and Sanchez, J.C. (2006). Deciphering the human nucleolar proteome. Mass Spectrom Rev *25*, 215-234.

Curry, C.L., Reed, L.L., Nickoloff, B.J., Miele, L., and Foreman, K.E. (2006). Notch-independent regulation of Hes-1 expression by c-Jun N-terminal kinase signaling in human endothelial cells. Lab Invest *86*, 842-852.

Daftuar, L., Zhu, Y., Jacq, X., and Prives, C. (2013). Ribosomal proteins RPL37, RPS15 and RPS20 regulate the Mdm2-p53-MdmX network. PLoS One *8*, e68667.

Dai, M.S., and Lu, H. (2004). Inhibition of MDM2-mediated p53 ubiquitination and degradation by ribosomal protein L5. Journal of Biological Chemistry *279*, 44475-44482.

Dai, M.S., Shi, D.D., Jin, Y.T., Sun, X.X., Zhang, Y.P., Grossman, S.R., and Lu, H. (2006). Regulation of the MDM2-p53 pathway by ribosomal protein L11 involves a post-ubiquitination mechanism. Journal of Biological Chemistry *281*, 24304-24313.

Dai, M.S., Sun, X.X., and Lu, H. (2008). Aberrant expression of nucleostemin activates p53 and induces cell cycle arrest via inhibition of MDM2. Molecular and Cellular Biology *28*, 4365-4376.

Dang, C.V. (2012). MYC on the path to cancer. Cell *149*, 22-35.

Dang, C.V., O'Donnell, K.A., Zeller, K.I., Nguyen, T., Osthus, R.C., and Li, F. (2006). The c-Myc target gene network. Semin Cancer Biol *16*, 253-264.

Daniely, Y., Dimitrova, D.D., and Borowiec, J.A. (2002). Stress-dependent nucleolin mobilization mediated by p53-nucleolin complex formation. Molecular and Cellular Biology *22*, 6014-6022.

De, A.Y., Donahue, S.L., Tabah, A., Castro, N.E., Mraz, N., Cruise, J.L., and Campbell, C. (2006). A novel interation of nucleolin with Rad51. Biochemical and Biophysical Research Communications *344*, 206-213.

De Keersmaecker, K., Atak, Z.K., Li, N., Vicente, C., Patchett, S., Girardi, T., Gianfelici, V., Geerdens, E., Clappier, E., Porcu, M.*, et al.* (2013). Exome sequencing identifies mutation in CNOT3 and ribosomal genes RPL5 and RPL10 in T-cell acute lymphoblastic leukemia. Nature Genetics *45*, 186-190.

De Smaele, E., Zazzeroni, F., Papa, S., Nguyen, D.U., Jin, R., Jones, J., Cong, R., and Franzoso, G. (2001). Induction of gadd45beta by NF-kappaB downregulates pro-apoptotic JNK signalling. Nature *414*, 308-313.

Debacq-Chainiaux, F., Erusalimsky, J.D., Campisi, J., and Toussaint, O. (2009). Protocols to detect senescence-associated beta-galactosidase (SA-beta gal) activity, a biomarker of senescent cells in culture and in vivo. Nat Protoc *4*, 1798-1806.

Dentelli, P., Rosso, A., Orso, F., Olgasi, C., Taverna, D., and Brizzi, M.F. (2010). microRNA-222 controls neovascularization by regulating signal transducer and activator of transcription 5A expression. Arterioscler Thromb Vasc Biol *30*, 1562-1568.

Derenzini, M., Montanaro, L., and Trere, D. (2009). What the nucleolus says to a tumour pathologist. Histopathology *54*, 753-762.

Derenzini, M., Trere, D., Pession, A., Govoni, M., Sirri, V., and Chieco, P. (2000). Nucleolar size indicates the rapidity of cell proliferation in cancer tissues. J Pathol *191*, 181-186.

Derenzini, M., Trere, D., Pession, A., Montanaro, L., Sirri, V., and Ochs, R.L. (1998). Nucleolar function and size in cancer cells. American Journal of Pathology *152*, 1291-1297.

Derheimer, F.A., O'Hagan, H.M., Krueger, H.M., Hanasoge, S., Paulsen, M.T., and Ljungman, M. (2007). RPA and ATR link transcriptional stress to p53. Proceedings of the National Academy of Sciences of the United States of America *104*, 12778-12783.

Devlin, J.R., Hannan, K.M., Hein, N., Cullinane, C., Kusnadi, E., Ng, P.Y., George, A.J., Shortt, J., Bywater, M.J., Poortinga, G.*, et al.* (2016). Combination Therapy Targeting Ribosome Biogenesis and mRNA Translation Synergistically Extends Survival in MYC-Driven Lymphoma. Cancer Discov *6*, 59-70.

Di Leva, G., Gasparini, P., Piovan, C., Ngankeu, A., Garofalo, M., Taccioli, C., Iorio, M.V., Li, M., Volinia, S., Alder, H.*, et al.* (2010). MicroRNA cluster 221-222 and estrogen receptor alpha interactions in breast cancer. Journal of the National Cancer Institute *102*, 706-721.

Dianzani, I., Garelli, E., and Ramenghi, U. (2000). Diamond-Blackfan Anaemia: an overview. Paediatr Drugs *2*, 345-355.

Diesch, J., Hannan, R.D., and Sanij, E. (2014). Perturbations at the ribosomal genes loci are at the centre of cellular dysfunction and human disease. Cell Biosci *4*, 43.

Diesch, J., Hannan, R.D., and Sanij, E. (2015). Genome wide mapping of UBF binding-sites in mouse and human cell lines. Genomics Data *3*, 103-105.

Diller, L., Kassel, J., Nelson, C.E., Gryka, M.A., Litwak, G., Gebhardt, M., Bressac, B., Ozturk, M., Baker, S.J., Vogelstein, B.*, et al.* (1990). p53 functions as a cell cycle control protein in osteosarcomas. Mol Cell Biol *10*, 5772-5781.

Dimario, P.J. (2004). Cell and molecular biology of nucleolar assembly and disassembly. Int Rev Cytol *239*, 99-178.

Dimitrova, D.S. (2011). DNA replication initiation patterns and spatial dynamics of the human ribosomal RNA gene loci. J Cell Sci *124*, 2743-2752.

Dimri, G.P., Lee, X., Basile, G., Acosta, M., Scott, G., Roskelley, C., Medrano, E.E., Linskens, M., Rubelj, I., Pereira-Smith, O.*, et al.* (1995). A biomarker that identifies senescent human cells in culture and in aging skin in vivo. Proc Natl Acad Sci U S A *92*, 9363-9367.

Donati, G., Bertoni, S., Brighenti, E., Vici, M., Trere, D., Volarevic, S., Montanaro, L., and Derenzini, M. (2011a). The balance between rRNA and ribosomal protein synthesis up- and downregulates the tumour suppressor p53 in mammalian cells. Oncogene *30*, 3274-3288.

Donati, G., Brighenti, E., Vici, M., Mazzini, G., Trere, D., Montanaro, L., and Derenzini, M. (2011b). Selective inhibition of rRNA transcription downregulates E2F-1: a new p53-independent mechanism linking cell growth to cell proliferation. J Cell Sci *124*, 3017-3028.

Donati, G., Brighenti, E., Vici, M., Mazzini, G., Trere, D., Montanaro, L., and Derenzini, M. (2011c). Selective inhibition of rRNA transcription downregulates E2F-1: a new p53-independent mechanism linking cell growth to cell proliferation. J Cell Sci *124*, 3017-3028.

Dong, X.Y., Guo, P., Boyd, J., Sun, X.D., Li, Q.N., Zhou, W., and Dong, J.T. (2009). Implication of snoRNA U50 in human breast cancer. Journal of Genetics and Genomics *36*, 447-454.

Dong, X.Y., Rodriguez, C., Guo, P., Sun, X.D., Talbot, J.T., Zhou, W., Petros, J., Li, Q., Vessella, R.L., Kibel, A.S.*, et al.* (2008). SnoRNA U50 is a candidate tumor-suppressor gene at 6q14.3 with a mutation associated with clinically significant prostate cancer. Hum Mol Genet *17*, 1031-1042.

Donzelli, M., and Draetta, G.F. (2003). Regulating mammalian checkpoints through Cdc25 inactivation. EMBO Rep *4*, 671-677.

Drakas, R., Tu, X., and Baserga, R. (2004). Control of cell size through phosphorylation of upstream binding factor 1 by nuclear phosphatidylinositol 3-kinase. Proc Natl Acad Sci U S A *101*, 9272-9276.

Draptchinskaia, N., Gustavsson, P., Andersson, B., Pettersson, M., Willig, T.N., Dianzani, I., Ball, S., Tchernia, G., Klar, J., Matsson, H.*, et al.* (1999). The gene encoding ribosomal protein S19 is mutated in Diamond-Blackfan anaemia. Nature Genetics *21*, 169-175.

Drygin, D., Lin, A., Bliesath, J., Ho, C.B., O'Brien, S.E., Proffitt, C., Omori, M., Haddach, M., Schwaebe, M.K., Siddiqui-Jain, A.*, et al.* (2011). Targeting RNA Polymerase I with an Oral Small Molecule CX-5461 Inhibits Ribosomal RNA Synthesis and Solid Tumor Growth. Cancer Res *71*, 1418-1430.

Drygin, D., Rice, W.G., and Grummt, I. (2010). The RNA Polymerase I Transcription Machinery: An Emerging Target for the Treatment of Cancer. Annu Rev Pharmacol Toxicol *50*, 131-156.

Drygin, D., Siddiqui-Jain, A., O'Brien, S., Schwaebe, M., Lin, A., Bliesath, J., Ho, C.B., Proffitt, C., Trent, K., Whitten, J.P.*, et al.* (2009). Anticancer Activity of CX-3543: A Direct Inhibitor of rRNA Biogenesis. Cancer Res *69*, 7653-7661.

Duquette, M.L., Handa, P., Vincent, J.A., Taylor, A.F., and Maizels, N. (2004). Intracellular transcription of G-rich DNAs induces formation of G-loops, novel structures containing G4 DNA. Genes Dev *18*, 1618-1629.

Dutt, S., Narla, A., Lin, K., Mullally, A., Abayasekara, N., Megerdichian, C., Wilson, F.H., Currie, T., Khanna-Gupta, A., Berliner, N.*, et al.* (2011). Haploinsufficiency for ribosomal protein genes causes selective activation of p53 in human erythroid progenitor cells. Blood *117*, 2567-2576.

Ebert, B.L. (2010). Genetic deletions in AML and MDS. Best Pract Res Clin Haematol *23*, 457-461.

Ebert, B.L., Pretz, J., Bosco, J., Chang, C.Y., Tamayo, P., Galili, N., Raza, A., Root, D.E., Attar, E., Ellis, S.R.*, et al.* (2008). Identification of RPS14 as a 5q- syndrome gene by RNA interference screen. Nature *451*, 335-339.

Ebina, M., Tsuruta, F., Katoh, M.C., Kigoshi, Y., Someya, A., and Chiba, T. (2013). Myeloma Overexpressed 2 (Myeov2) Regulates L11 Subnuclear Localization through Nedd8 Modification. PLoS One *8*.

Edwards, T.K., Saleem, A., Shaman, J.A., Dennis, T., Gerigk, C., Oliveros, E., Gartenberg, M.R., and Rubin, E.H. (2000). Role for nucleolin/Nsr1 in the cellular localization of topoisomerase I. Journal of Biological Chemistry *275*, 36181-36188.

el-Deiry, W.S., Tokino, T., Velculescu, V.E., Levy, D.B., Parsons, R., Trent, J.M., Lin, D., Mercer, W.E., Kinzler, K.W., and Vogelstein, B. (1993). WAF1, a potential mediator of p53 tumor suppression. Cell *75*, 817-825.

Emmott, E., and Hiscox, J.A. (2009). Nucleolar targeting: the hub of the matter. EMBO Rep *10*, 231-238.

Eschelbach, A., Hunziker, A., and Klimaschewski, L. (1998). Differential display PCR reveals induction of immediate early genes by vasoactive intestinal peptide in PC12 cells. In Vip, Pacap, and Related Peptides: Third International Symposium (New York: New York Acad Sciences), pp. 181-188.

Esposito, D., Crescenzi, E., Sagar, V., Loreni, F., Russo, A., and Russo, G. (2014). Human rpL3 plays a crucial role in cell response to nucleolar stress induced by 5-FU and L-OHP. Oncotarget *5*, 11737-11751.

Etheridge, K.T., Banik, S.S., Armbruster, B.N., Zhu, Y., Terns, R.M., Terns, M.P., and Counter, C.M. (2002). The nucleolar localization domain of the catalytic subunit of human telomerase. J Biol Chem *277*, 24764-24770.

Eymin, B., Karayan, L., Seite, P., Brambilla, C., Brambilla, E., Larsen, C.J., and Gazzeri, S. (2001). Human ARF binds E2F1 and inhibits its transcriptional activity. Oncogene *20*, 1033-1041.

Farrar, J.E., Nater, M., Caywood, E., McDevitt, M.A., Kowalski, J., Takemoto, C.M., Talbot, C.C., Jr., Meltzer, P., Esposito, D., Beggs, A.H.*, et al.* (2008). Abnormalities of the large ribosomal subunit protein, Rpl35a, in Diamond-Blackfan anemia. Blood *112*, 1582-1592.

Fatyol, K., and Szalay, A.A. (2001). The p14ARF tumor suppressor protein facilitates nucleolar sequestration of hypoxia-inducible factor-1alpha (HIF-1alpha) and inhibits HIF-1-mediated transcription. J Biol Chem *276*, 28421-28429.

Fedoriw, A.M., Starmer, J., Yee, D., and Magnuson, T. (2012). Nucleolar association and transcriptional inhibition through 5S rDNA in mammals. PLoS Genet *8*, e1002468.

Felle, M., Exler, J.H., Merkl, R., Dachauer, K., Brehm, A., Grummt, I., and Langst, G. (2010). DNA sequence encoded repression of rRNA gene transcription in chromatin. Nucleic Acids Res *38*, 5304-5314.

Fetherston, J., Werner, E., and Patterson, R. (1984). PROCESSING OF THE EXTERNAL TRANSCRIBED SPACER OF MURINE RIBOSOMAL-RNA AND SITE OF ACTION OF ACTINOMYCIN-D. Nucleic Acids Research *12*, 7187-7198.

Fischer, A., and Gessler, M. (2007). Delta-Notch--and then? Protein interactions and proposed modes of repression by Hes and Hey bHLH factors. Nucleic Acids Res *35*, 4583-4596.

Flick, K.E., Jurica, M.S., Monnat, R.J., and Stoddard, B.L. (1998). DNA binding and cleavage by the nuclear intron-encoded homing endonuclease I-PpoI. Nature *394*, 96-101.

Floutsakou, I., Agrawal, S., Nguyen, T.T., Seoighe, C., Ganley, A.R., and McStay, B. (2013). The shared genomic architecture of human nucleolar organizer regions. Genome Res *23*, 2003-2012.

Fornari, F., Milazzo, M., Galassi, M., Callegari, E., Veronese, A., Miyaaki, H., Sabbioni, S., Mantovani, V., Marasco, E., Chieco, P.*, et al.* (2014). p53/mdm2 feedback loop sustains miR-221 expression and dictates the response to anticancer treatments in hepatocellular carcinoma. Mol Cancer Res *12*, 203-216.

Fowler, T., Sen, R., and Roy, Ananda L. (2011). Regulation of Primary Response Genes. Molecular Cell *44*, 348-360.

Freeman, J.A., and Espinosa, J.M. (2013). The impact of post-transcriptional regulation in the p53 network. Briefings in Functional Genomics *12*, 46-57.

French, S.L., Osheim, Y.N., Cioci, F., Nomura, M., and Beyer, A.L. (2003). In exponentially growing Saccharomyces cerevisiae cells, rRNA synthesis is determined by the summed RNA polymerase I loading rate rather than by the number of active genes. Mol Cell Biol *23*, 1558-1568.

Freund, A., Orjalo, A.V., Desprez, P.Y., and Campisi, J. (2010). Inflammatory networks during cellular senescence: causes and consequences. Trends Mol Med *16*, 238-246.

Friedrich, J.K., Panov, K.I., Cabart, P., Russell, J., and Zomerdijk, J. (2005). TBP-TAF complex SL1 directs RNA polymerase I pre-initiation complex formation and stabilizes upstream binding factor at the rDNA promoter. Journal of Biological Chemistry *280*, 29551-29558.

Fumagalli, S., Di Cara, A., Neb-Gulati, A., Natt, F., Schwemberger, S., Hall, J., Babcock, G.F., Bernardi, R., Pandolfi, P.P., and Thomas, G. (2009). Absence of nucleolar disruption after impairment of 40s ribosome biogenesis reveals an rpL11-translation-dependent mechanism of p53 induction. Nat Cell Biol *11*, 501-U350.

Fumagalli, S., Ivanenkov, V.V., Teng, T., and Thomas, G. (2012). Suprainduction of p53 by disruption of 40S and 60S ribosome biogenesis leads to the activation of a novel G2/M checkpoint. Genes Dev *26*, 1028-1040.

Galardi, S., Mercatelli, N., Farace, M.G., and Ciafre, S.A. (2011). NF-kB and c-Jun induce the expression of the oncogenic miR-221 and miR-222 in prostate carcinoma and glioblastoma cells. Nucleic Acids Res *39*, 3892-3902.

Galbraith, M.D., and Espinosa, J.M. (2011). Lessons on transcriptional control from the serum response network. Current Opinion in Genetics & Development *21*, 160-166.

Ganley, A.R.D., Ide, S., Saka, K., and Kobayashi, T. (2009). The Effect of Replication Initiation on Gene Amplification in the rDNA and Its Relationship to Aging. Molecular Cell *35*, 683-693.

Garofalo, M., Quintavalle, C., Romano, G., Croce, C.M., and Condorelli, G. (2012). miR221/222 in cancer: their role in tumor progression and response to therapy. Curr Mol Med *12*, 27-33.

Gately, D.P., Hittle, J.C., Chan, G.K., and Yen, T.J. (1998). Characterization of ATM expression, localization, and associated DNA-dependent protein kinase activity. Mol Biol Cell *9*, 2361-2374.

Gavande, N.S., VanderVere-Carozza, P.S., Hinshaw, H.D., Jalal, S.I., Sears, C.R., Pawelczak, K.S., and Turchi, J.J. (2016). DNA repair targeted therapy: The past or future of cancer treatment? Pharmacol Ther *160*, 65-83.

Gazda, H.T., Grabowska, A., Merida-Long, L.B., Latawiec, E., Schneider, H.E., Lipton, J.M., Vlachos, A., Atsidaftos, E., Ball, S.E., Orfali, K.A.*, et al.* (2006). Ribosomal protein S24 gene is mutated in Diamond-Blackfan anemia. Am J Hum Genet *79*, 1110-1118.

Gerbi, S.A., Borovjagin, A.V., and Lange, T.S. (2003). The nucleolus: a site of ribonucleoprotein maturation. Curr Opin Cell Biol *15*, 318-325.

Gerbi, S.A., and Lange, T.S. (2002). All Small Nuclear RNAs (snRNAs) of the [U4/U6.U5] Tri-snRNP Localize to Nucleoli; Identification of the Nucleolar Localization Element of U6 snRNA. Molecular Biology of the Cell *13*, 3123-3137.

Gibbons, J.G., Branco, A.T., Godinho, S.A., Yu, S., and Lemos, B. (2015). Concerted copy number variation balances ribosomal DNA dosage in human and mouse genomes. Proc Natl Acad Sci U S A *112*, 2485-2490.

Gibcus, J.H., and Dekker, J. (2013). The hierarchy of the 3D genome. Mol Cell *49*, 773-782.

Giglia-Mari, G., Zotter, A., and Vermeulen, W. (2011a). DNA Damage Response. Cold Spring Harbor Perspect Biol *3*.

Giglia-Mari, G., Zotter, A., and Vermeulen, W. (2011b). DNA damage response. Cold Spring Harb Perspect Biol *3*, a000745.

Gilder, A.S., Do, P.M., Carrero, Z.I., Cosman, A.M., Broome, H.J., Velma, V., Martinez, L.A., and Hebert, M.D. (2011). Coilin participates in the suppression of RNA polymerase I in response to cisplatin-induced DNA damage. Mol Biol Cell *22*, 1070-1079.

Giono, L.E., and Manfredi, J.J. (2006). The p53 tumor suppressor participates in multiple cell cycle checkpoints. J Cell Physiol *209*, 13-20.

Gobet, C., and Naef, F. (2017). Ribosome profiling and dynamic regulation of translation in mammals. Current Opinion in Genetics & Development *43*, 120-127.

Gomard, T., Jariel-Encontre, I., Basbous, J., Bossis, G., Moquet-Torcy, G., and Piechaczyk, M. (2008). Fos family protein degradation by the proteasome. Biochem Soc Trans *36*, 858-863.

Gomez-Roman, N., Felton-Edkins, Z.A., Kenneth, N.S., Goodfellow, S.J., Athineos, D., Zhang, J.X., Ramsbottom, B.A., Innes, F., Kantidakis, T., Kerr, E.R.*, et al.* (2006). Activation by c-Myc of transcription by RNA polymerases I, II and III. In Transcription, pp. 141-154.

Goodfellow, S.J., and Zomerdijk, J.C.B.M. (2012). Basic Mechanisms in RNA Polymerase I Transcription of the Ribosomal RNA Genes. Sub-cellular biochemistry *61*, 10.1007/1978-1094-1007-4525-1004_1010.

Gorlich, D., and Mattaj, I.W. (1996). Nucleocytoplasmic transport. Science *271*, 1513-1518.

Grandori, C., Cowley, S.M., James, L.P., and Eisenman, R.N. (2000). THE MYC/MAX/MAD NETWORK AND THE TRANSCRIPTIONAL CONTROL OF CELL BEHAVIOR. Annual Review of Cell and Developmental Biology *16*, 653-699.

Grandori, C., Gomez-Roman, N., Felton-Edkins, Z.A., Ngouenet, C., Galloway, D.A., Eisenman, R.N., and White, R.J. (2005). c-Myc binds to human ribosomal DNA and stimulates transcription of rRNA genes by RNA polymerase I. Nat Cell Biol *7*, 311-U121.

Gray, M.D., Wang, L., Youssoufian, H., Martin, G.M., and Oshima, J. (1998). Werner helicase is localized to transcriptionally active nucleoli of cycling cells. Exp Cell Res *242*, 487-494.

Grewal, S.S., Li, L., Orian, A., Eisenman, R.N., and Edgar, B.A. (2005). Myc-dependent regulation of ribosomal RNA synthesis during Drosophila development. Nat Cell Biol *7*, 295-302.

Grinstein, E., Shan, Y., Karawajew, L., Snijders, P.J.F., Meijer, C., Royer, H.D., and Wernet, P. (2006). Cell cycle-controlled interaction of nucleolin with the retinoblastoma protein and cancerous cell transformation. Journal of Biological Chemistry *281*, 22223-22235.

Grob, A., Colleran, C., and McStay, B. (2014a). Construction of synthetic nucleoli in human cells reveals how a major functional nuclear domain is formed and propagated through cell division. Genes & Development *28*, 220-230.

Grob, A., Colleran, C., and McStay, B. (2014b). Construction of synthetic nucleoli in human cells reveals how a major functional nuclear domain is formed and propagated through cell division. Genes Dev *28*, 220-230.

Grummt, I., and Langst, G. (2013). Epigenetic control of RNA polymerase I transcription in mammalian cells. Biochim Biophys Acta *1829*, 393-404.

Grummt, I., and Pikaard, C.S. (2003). Epigenetic silencing of RNA polymerase I transcription. Nat Rev Mol Cell Biol *4*, 641-649.

Guerra-Rebollo, M., Mateo, F., Franke, K., Huen, M.S., Lopitz-Otsoa, F., Rodriguez, M.S., Plans, V., and Thomson, T.M. (2012). Nucleolar exit of RNF8 and BRCA1 in response to DNA damage. Exp Cell Res *318*, 2365-2376.

Guetg, C., Lienemann, P., Sirri, V., Grummt, I., Hernandez-Verdun, D., Hottiger, M.O., Fussenegger, M., and Santoro, R. (2010). The NoRC complex mediates the heterochromatin formation and stability of silent rRNA genes and centromeric repeats. EMBO J *29*, 2135-2146.

Guetg, C., and Santoro, R. (2012). Formation of nuclear heterochromatin: the nucleolar point of view. Epigenetics *7*, 811-814.

Guetg, C., Scheifele, F., Rosenthal, F., Hottiger, M.O., and Santoro, R. (2012). Inheritance of silent rDNA chromatin is mediated by PARP1 via noncoding RNA. Mol Cell *45*, 790-800.

Guo, Z., Kozlov, S., Lavin, M.F., Person, M.D., and Paull, T.T. (2010). ATM activation by oxidative stress. Science *330*, 517-521.

Haddach, M., Schwaebe, M.K., Michaux, J., Nagasawa, J., O'Brien, S.E., Whitten, J.P., Pierre, F., Kerdoncuff, P., Darjania, L., Stansfield, R.*, et al.* (2012). Discovery of CX-5461, the First Direct and Selective Inhibitor of RNA Polymerase I, for Cancer Therapeutics. ACS Medicinal Chemistry Letters *3*, 602-606.

Haeusler, R.A., and Engelke, D.R. (2006). Spatial organization of transcription by RNA polymerase III. Nucleic Acids Res *34*, 4826-4836.

Hahn, W.C., Counter, C.M., Lundberg, A.S., Beijersbergen, R.L., Brooks, M.W., and Weinberg, R.A. (1999). Creation of human tumour cells with defined genetic elements. Nature *400*, 464-468.

Hammond, E.M., Kaufmann, M.R., and Giaccia, A.J. (2007). Oxygen sensing and the DNA-damage response. Curr Opin Cell Biol *19*, 680-684.

Hamperl, S., Wittner, M., Babl, V., Perez-Fernandez, J., Tschochner, H., and Griesenbeck, J. (2013). Chromatin states at ribosomal DNA loci. Biochimica et Biophysica Acta (BBA) - Gene Regulatory Mechanisms *1829*, 405-417.

Hanahan, D., and Weinberg, R.A. (2000). The hallmarks of cancer. Cell *100*, 57-70.

Hanahan, D., and Weinberg, R.A. (2011a). Hallmarks of Cancer: The Next Generation. Cell *144*, 646-674.

Hanahan, D., and Weinberg, R.A. (2011b). Hallmarks of cancer: the next generation. Cell *144*, 646-674.

Hanakahi, L.A., Sun, H., and Maizels, N. (1999). High affinity interactions of nucleolin with G-G-paired rDNA. J Biol Chem *274*, 15908-15912.

Hannan, K.M., Brandenburger, Y., Jenkins, A., Sharkey, K., Cavanaugh, A., Rothblum, L., Moss, T., Poortinga, G., McArthur, G.A., Pearson, R.B.*, et al.* (2003). mTOR-Dependent regulation of ribosomal gene transcription requires S6K1 and is mediated by phosphorylation of the carboxy-terminal activation domain of the nucleolar transcription factor UBF. Molecular and Cellular Biology *23*, 8862-8877.

Hannan, K.M., Hannan, R.D., Smith, S.D., Jefferson, L.S., Lun, M.Y., and Rothblum, L.I. (2000a). Rb and p130 regulate RNA polymerase I transcription: Rb disrupts the interaction between UBF and SL-1. Oncogene *19*, 4988-4999.

Hannan, K.M., Kennedy, B.K., Cavanaugh, A.H., Hannan, R.D., Hirschler-Laszkiewicz, I., Jefferson, L.S., and Rothblum, L.I. (2000b). RNA polymerase I transcription in confluent cells: Rb downregulates rDNA transcription during confluence-induced cell cycle arrest. Oncogene *19*, 3487-3497.

Hannan, K.M., Sanij, E., Rothblum, L.I., Hannan, R.D., and Pearson, R.B. (2013a). Dysregulation of RNA polymerase I transcription during disease. Biochim Biophys Acta *1829*, 342-360.

Hannan, R.D., Cavanaugh, A., Hempel, W.M., Moss, T., and Rothblum, L. (1999). Identification of a mammalian RNA polymerase I holoenzyme containing components of the DNA repair/replication system. Nucleic Acids Research *27*, 3720-3727.

Hannan, R.D., Drygin, D., and Pearson, R.B. (2013b). Targeting RNA polymerase I transcription and the nucleolus for cancer therapy. Expert Opinion on Therapeutic Targets *17*, 873-878.

Hansel-Hertsch, R., Di Antonio, M., and Balasubramanian, S. (2017). DNA G-quadruplexes in the human genome: detection, functions and therapeutic potential. Nat Rev Mol Cell Biol *18*, 279-284.

Harper, J.V. (2005). Synchronization of cell populations in G1/S and G2/M phases of the cell cycle. Methods Mol Biol *296*, 157-166.

Hatchi, E., Skourti-Stathaki, K., Ventz, S., Pinello, L., Yen, A., Kamieniarz-Gdula, K., Dimitrov, S., Pathania, S., McKinney, K.M., Eaton, M.L.*, et al.* (2015). BRCA1 recruitment to transcriptional pause sites is required for R-loop-driven DNA damage repair. Mol Cell *57*, 636-647.

Hayashi, Y., Kuroda, T., Kishimoto, H., Wang, C., Iwama, A., and Kimura, K. (2014). Downregulation of rRNA transcription triggers cell differentiation. PLoS One *9*, e98586.

Heerboth, S., Housman, G., Leary, M., Longacre, M., Byler, S., Lapinska, K., Willbanks, A., and Sarkar, S. (2015). EMT and tumor metastasis. Clin Transl Med *4*, 6.

Hein, N., Cameron, D.P., Hannan, K.M., Nguyen, N.N., Fong, C.Y., Sornkom, J., Wall, M., Pavy, M., Cullinane, C., Diesch, J.*, et al.* (2017). Inhibition of Pol I transcription treats murine and human AML by targeting the leukemia-initiating cell population. Blood *129*, 2882-2895.

Hein, N., Jiang, K., Cornelissen, C., and Luscher, B. (2011). TGFbeta1 enhances MAD1 expression and stimulates promoter-bound Pol II phosphorylation: basic functions of C/EBP, SP and SMAD3 transcription factors. BMC Mol Biol *12*, 9.

Hein, N.E.S., Jaclyn Quin, Katherine M. Hannan, Austen Ganley and Ross D. Hannan (2012). The Nucleolus and Ribosomal Genes in Aging and Senescence.

Heiss, N.S., Knight, S.W., Vulliamy, T.J., Klauck, S.M., Wiemann, S., Mason, P.J., Poustka, A., and Dokal, I. (1998). X-linked dyskeratosis congenita is caused by mutations in a highly conserved gene with putative nucleolar functions. Nat Genet *19*, 32-38.

Heix, J., Vente, A., Voit, R., Budde, A., Michaelidis, T.M., and Grummt, I. (1998). Mitotic silencing of human rRNA synthesis: inactivation of the promoter selectivity factor SL1 by cdc2 cyclin B-mediated phosphorylation. Embo Journal *17*, 7373-7381.

Heliot, L., Kaplan, H., Lucas, L., Klein, C., Beorchia, A., Doco-Fenzy, M., Menager, M., Thiry, M., O'Donohue, M.F., and Ploton, D. (1997). Electron tomography of metaphase nucleolar organizer regions: evidence for a twisted-loop organization. Mol Biol Cell *8*, 2199-2216.

Hempel, W.M., Cavanaugh, A.H., Hannan, R.D., Taylor, L., and Rothblum, L.I. (1996). The species-specific RNA polymerase I transcription factor SL-1 binds to upstream binding factor. Mol Cell Biol *16*, 557-563.

Henderson, A., Wu, Y., Huang, Y.C., Chavez, E.A., Platt, J., Johnson, F.B., Brosh, R.M., Jr., Sen, D., and Lansdorp, P.M. (2014). Detection of G-quadruplex DNA in mammalian cells. Nucleic Acids Res *42*, 860-869.

Henderson, A.S., Warburton, D., and Atwood, K.C. (1972). Location of ribosomal DNA in the human chromosome complement. Proc Natl Acad Sci U S A *69*, 3394-3398.

Hendzel, M.J., Wei, Y., Mancini, M.A., Van Hooser, A., Ranalli, T., Brinkley, B.R., Bazett-Jones, D.P., and Allis, C.D. (1997). Mitosis-specific phosphorylation of histone H3 initiates primarily within pericentromeric heterochromatin during G2 and spreads in an ordered fashion coincident with mitotic chromosome condensation. Chromosoma *106*, 348-360.

Henras, A.K., Soudet, J., Gerus, M., Lebaron, S., Caizergues-Ferrer, M., Mougin, A., and Henry, Y. (2008). The post-transcriptional steps of eukaryotic ribosome biogenesis. Cell Mol Life Sci *65*, 2334-2359.

Her, J., and Chung, I.K. (2012). The AAA-ATPase NVL2 is a telomerase component essential for holoenzyme assembly. Biochem Biophys Res Commun *417*, 1086-1092.

Hernandez-Verdun, D., Roussel, P., Thiry, M., Sirri, V., and Lafontaine, D.L. (2010). The nucleolus: structure/function relationship in RNA metabolism. Wiley Interdiscip Rev RNA *1*, 415-431.

Hershey, J.W.B., Sonenberg, N., and Mathews, M.B. (2012). Principles of Translational Control: An Overview. Cold Spring Harbor Perspect Biol *4*.

Hickson, I., Zhao, Y., Richardson, C.J., Green, S.J., Martin, N.M.B., Orr, A.I., Reaper, P.M., Jackson, S.P., Curtin, N.J., and Smith, G.C.M. (2004). Identification and Characterization of a Novel and Specific Inhibitor of the Ataxia-Telangiectasia Mutated Kinase ATM. Cancer Res *64*, 9152-9159.

Hientz, K., Mohr, A., Bhakta-Guha, D., and Efferth, T. (2017). The role of p53 in cancer drug resistance and targeted chemotherapy. Oncotarget *8*, 8921-8946.

Hirota, T., Lipp, J.J., Toh, B.H., and Peters, J.M. (2005). Histone H3 serine 10 phosphorylation by Aurora B causes HP1 dissociation from heterochromatin. Nature *438*, 1176-1180.

Ho, J.S.L., Ma, W.L., Mao, D.Y.L., and Benchimol, S. (2005). p53-dependent transcriptional repression of c-myc is required for G(1) cell cycle arrest. Molecular and Cellular Biology *25*, 7423-7431.

Holmberg Olausson, K., Nister, M., and Lindstrom, M.S. (2012). p53 -Dependent and -Independent Nucleolar Stress Responses. Cells *1*, 774-798.

Hong, S.W., Kim, C.J., Park, W.S., Shin, J.S., Lee, S.D., Ko, S.G., Jung, S.I., Park, I.C., An, S.K., Lee, W.K.*, et al.* (2009). p34SEI-1 inhibits apoptosis through the stabilization of the X-linked inhibitor of apoptosis protein: p34SEI-1 as a novel target for anti-breast cancer strategies. Cancer Res *69*, 741-746.

Hong, S.W., Moon, J.H., Kim, J.S., Shin, J.S., Jung, K.A., Lee, W.K., Jeong, S.Y., Hwang, J.J., Lee, S.J., Suh, Y.A.*, et al.* (2014). p34 is a novel regulator of the oncogenic behavior of NEDD4-1 and PTEN. Cell Death and Differentiation *21*, 146-160.

Hong, S.W., Shin, J.S., Lee, Y.M., Kim, D.G., Lee, S.Y., Yoon, D.H., Jung, S.Y., Hwang, J.J., Lee, S.J., Cho, D.H.*, et al.* (2011). p34 (SEI-1) inhibits ROS-induced cell death through suppression of ASK1. Cancer Biol Ther *12*, 421-426.

Hoppe, S., Bierhoff, H., Cado, I., Weber, A., Tiebe, M., Grummt, I., and Voit, R. (2009). AMP-activated protein kinase adapts rRNA synthesis to cellular energy supply. Proc Natl Acad Sci U S A *106*, 17781-17786.

Horn, H.F., and Vousden, K.H. (2008). Cooperation between the ribosomal proteins L5 and L11 in the p53 pathway. Oncogene *27*, 5774-5784.

Hoshina, S., Yura, K., Teranishi, H., Kiyasu, N., Tominaga, A., Kadoma, H., Nakatsuka, A., Kunichika, T., Obuse, C., and Waga, S. (2013). Human origin recognition complex binds preferentially to G-quadruplex-preferable RNA and single-stranded DNA. J Biol Chem *288*, 30161-30171.

Hsu, S.I., Yang, C.M., Sim, K.G., Hentschel, D.M., O'Leary, E., and Bonventre, J.V. (2001). TRIP-Br: a novel family of PHD zinc finger- and bromodomain-interacting proteins that regulate the transcriptional activity of E2F-1/DP-1. EMBO J *20*, 2273-2285.

Huang, S., Deerinck, T.J., Ellisman, M.H., and Spector, D.L. (1997). The dynamic organization of the perinucleolar compartment in the cell nucleus. Journal of Cell Biology *137*, 965-974.

Huang, S., Rothblum, L.I., and Chen, D. (2006). Ribosomal chromatin organization. Biochem Cell Biol *84*, 444-449.

Hubackova, S., Krejcikova, K., Bartek, J., and Hodny, Z. (2012). IL1- and TGFbeta-Nox4 signaling, oxidative stress and DNA damage response are shared features of replicative, oncogene-induced, and drug-induced paracrine 'bystander senescence'. Aging (Albany NY) *4*, 932-951.

Hung, S.S., Lesmana, A., Peck, A., Lee, R., Tchoubrieva, E., Hannan, K.M., Lin, J., Sheppard, K.E., Jastrzebski, K., Quinn, L.M.*, et al.* (2017). Cell cycle and growth stimuli regulate different steps of RNA polymerase I transcription. Gene *612*, 36-48.

Hurlin, P.J., and Huang, J. (2006). The MAX-interacting transcription factor network. Semin Cancer Biol *16*, 265-274.

Huttenhofer, A., Brosius, J., and Bachellerie, J.P. (2002). RNomics: identification and function of small, non-messenger RNAs. Curr Opin Chem Biol *6*, 835-843.

Iadevaia, V., Caldarola, S., Biondini, L., Gismondi, A., Karlsson, S., Dianzani, I., and Loreni, F. (2010). PIM1 kinase is destabilized by ribosomal stress causing inhibition of cell cycle progression. Oncogene *29*, 5490-5499.

Iadevaia, V., Zhang, Z., Jan, E., and Proud, C.G. (2012). mTOR signaling regulates the processing of pre-rRNA in human cells. Nucleic Acids Res *40*, 2527-2539.

Ide, S., Miyazaki, T., Maki, H., and Kobayashi, T. (2010). Abundance of ribosomal RNA gene copies maintains genome integrity. Science *327*, 693-696.

Indig, F.E., Rybanska, I., Karmakar, P., Devulapalli, C., Fu, H., Carrier, F., and Bohr, V.A. (2012). Nucleolin inhibits G4 oligonucleotide unwinding by Werner helicase. PLoS One *7*, e35229.

Ingram, W.J., McCue, K.I., Tran, T.H., Hallahan, A.R., and Wainwright, B.J. (2008). Sonic Hedgehog regulates Hes1 through a novel mechanism that is independent of canonical Notch pathway signalling. Oncogene *27*, 1489-1500.

Itahana, K., Bhat, K.P., Jin, A.W., Itahana, Y., Hawke, D., Kobayashi, R., and Zhang, Y.P. (2003). Tumor suppressor ARF degrades B23, a nucleolar protein involved in ribosome biogenesis and cell proliferation. Molecular Cell *12*, 1151-1164.

Jackman, J., and O'Connor, P.M. (2001). Methods for Synchronizing Cells at Specific Stages of the Cell Cycle. In Current Protocols in Cell Biology (John Wiley & Sons, Inc.).

Jacob, M.D., Audas, T.E., Uniacke, J., Trinkle-Mulcahy, L., and Lee, S. (2013). Environmental cues induce a long noncoding RNA-dependent remodeling of the nucleolus. Mol Biol Cell *24*, 2943-2953.

Jacobson, M.R., and Pederson, T. (1998). Localization of signal recognition particle RNA in the nucleolus of mammalian cells. Proc Natl Acad Sci U S A *95*, 7981-7986.

James, A., Wang, Y., Raje, H., Rosby, R., and DiMario, P. (2014). Nucleolar stress with and without p53. Nucleus *5*, 402-426.

Jantzen, H.M., Chow, A.M., King, D.S., and Tjian, R. (1992). MULTIPLE DOMAINS OF THE RNA POLYMERASE-I ACTIVATOR HUBF INTERACT WITH THE TATA-BINDING PROTEIN COMPLEX HSL1 TO MEDIATE TRANSCRIPTION. Genes & Development *6*, 1950-1963.

Jarrous, N., Wolenski, J.S., Wesolowski, D., Lee, C., and Altman, S. (1999). Localization in the nucleolus and coiled bodies of protein subunits of the ribonucleoprotein ribonuclease P. J Cell Biol *146*, 559-572.

Jastrzebski, K., Hannan, K.M., Tchoubrieva, E.B., Hannan, R.D., and Pearson, R.B. (2007). Coordinate regulation of ribosome biogenesis and function by the ribosomal protein S6 kinase, a key mediator of mTOR function. Growth Factors *25*, 209-226.

Jazayeri, A., Balestrini, A., Garner, E., Haber, J.E., and Costanzo, V. (2008). Mre11-Rad50-Nbs1-dependent processing of DNA breaks generates oligonucleotides that stimulate ATM activity. Embo Journal *27*, 1953-1962.

Jiang, K., Hein, N., Eckert, K., Luscher-Firzlaff, J., and Luscher, B. (2008). Regulation of the MAD1 promoter by G-CSF. Nucleic Acids Res *36*, 1517-1531.

Jin, A., Itahana, K., O'Keefe, K., and Zhang, Y. (2004). Inhibition of HDM2 and activation of p53 by ribosomal protein L23. Molecular and Cellular Biology *24*, 7669-7680.

Jin, R., De Smaele, E., Zazzeroni, F., Nguyen, D.U., Papa, S., Jones, J., Cox, C., Gelinas, C., and Franzoso, G. (2002). Regulation of the gadd45beta promoter by NF-kappaB. DNA Cell Biol *21*, 491-503.

Jin, Y.Q., An, G.S., Ni, J.H., Li, S.Y., and Jia, H.T. (2014). ATM-dependent E2F1 accumulation in the nucleolus is an indicator of ribosomal stress in early response to DNA damage. Cell Cycle *13*, 1627-1638.

Johnson, J.E., Cao, K., Ryvkin, P., Wang, L.S., and Johnson, F.B. (2010). Altered gene expression in the Werner and Bloom syndromes is associated with sequences having G-quadruplex forming potential. Nucleic Acids Res *38*, 1114-1122.

Jordan, P., and Carmo-Fonseca, M. (1998). Cisplatin inhibits synthesis of ribosomal RNA in vivo. Nucleic Acids Research *26*, 2831-2836.

Jordan, P., Mannervik, M., Tora, L., and Carmo-Fonseca, M. (1996). In vivo evidence that TATA-binding protein/SL1 colocalizes with UBF and RNA polymerase I when rRNA synthesis is either active or inactive. J Cell Biol *133*, 225-234.

Jun, J.I., and Lau, L.F. (2011). Taking aim at the extracellular matrix: CCN proteins as emerging therapeutic targets. Nat Rev Drug Discov *10*, 945-963.

Jung, S., Li, C., Jeong, D., Lee, S., Ohk, J., Park, M., Han, S., Duan, J., Kim, C., Yang, Y.*, et al.* (2013). Oncogenic function of p34SEI-1 via NEDD41mediated PTEN ubiquitination/degradation and activation of the PI3K/AKT pathway. Int J Oncol *43*, 1587-1595.

Jung, Y.S., Qian, Y., and Chen, X. (2010). Examination of the expanding pathways for the regulation of p21 expression and activity. Cell Signal *22*, 1003-1012.

Kahyo, T., Mostoslavsky, R., Goto, M., and Setou, M. (2008). Sirtuin-mediated deacetylation pathway stabilizes Werner syndrome protein. FEBS Lett *582*, 2479-2483.

Kang, H.-J., and Park, H.-J. (2009). Novel Molecular Mechanism for Actinomycin D Activity as an Oncogenic Promoter G-Quadruplex Binder. Biochemistry *48*, 7392-7398.

Kang, J., Kusnadi, E.P., Ogden, A.J., Hicks, R.J., Bammert, L., Kutay, U., Hung, S., Sanij, E., Hannan, R.D., Hannan, K.M.*, et al.* (2016). Amino acid-dependent signaling via S6K1 and MYC is essential for regulation of rDNA transcription. Oncotarget *7*, 48887-48904.

Kannan, S., Fang, W., Song, G., Mullighan, C.G., Hammitt, R., McMurray, J., and Zweidler-McKay, P.A. (2011). Notch/HES1-mediated PARP1 activation: a cell type-specific mechanism for tumor suppression. Blood *117*, 2891-2900.

Kanu, N., and Behrens, A. (2007). ATMIN defines an NBS1-independent pathway of ATM signalling. EMBO J *26*, 2933-2941.

Kar, B., Liu, B., Zhou, Z., and Lam, Y.W. (2011). Quantitative nucleolar proteomics reveals nuclear re-organization during stress- induced senescence in mouse fibroblast. BMC Cell Biol *12*, 33.

Karin, M. (1995). The regulation of AP-1 activity by mitogen-activated protein kinases. J Biol Chem *270*, 16483-16486.

Karmakar, P., and Bohr, V.A. (2005). Cellular dynamics and modulation of WRN protein is DNA damage specific. Mechanisms of Ageing and Development *126*, 1146-1158.

Kashatus, D., Cogswell, P., and Baldwin, A.S. (2006). Expression of the Bcl-3 proto-oncogene suppresses p53 activation. Genes & Development *20*, 225-235.

Katagiri, N., Kuroda, T., Kishimoto, H., Hayashi, Y., Kumazawa, T., and Kimura, K. (2015). The nucleolar protein nucleophosmin is essential for autophagy induced by inhibiting Pol I transcription. Sci Rep *5*.

Khuu, C., Utheim, T.P., and Sehic, A. (2016). The Three Paralogous MicroRNA Clusters in Development and Disease, miR-17-92, miR-106a-363, and miR-106b-25. Scientifica *2016*, 1379643.

Kind, J., Pagie, L., Ortabozkoyun, H., Boyle, S., de Vries, Sandra S., Janssen, H., Amendola, M., Nolen, Leisha D., Bickmore, Wendy A., and van Steensel, B. (2013). Single-Cell Dynamics of Genome-Nuclear Lamina Interactions. Cell *153*, 178-192.

Kinross, K.M., Brown, D.V., Kleinschmidt, M., Jackson, S., Christensen, J., Cullinane, C., Hicks, R.J., Johnstone, R.W., and McArthur, G.A. (2011). In vivo activity of combined PI3K/mTOR and MEK inhibition in a Kras(G12D);Pten deletion mouse model of ovarian cancer. Mol Cancer Ther *10*, 1440-1449.

Klein, J., and Grummt, I. (1999). Cell cycle-dependent regulation of RNA polymerase I transcription: the nucleolar transcription factor UBF is inactive in mitosis and early G1. Proc Natl Acad Sci U S A *96*, 6096-6101.

Klibanov, S.A., O'Hagan, H.M., and Ljungman, M. (2001). Accumulation of soluble and nucleolar-associated p53 proteins following cellular stress. J Cell Sci *114*, 1867-1873.

Koba, M., and Konopa, J. (2005). [Actinomycin D and its mechanisms of action]. Postepy Hig Med Dosw (Online) *59*, 290-298.

Kobayashi, J., Fujimoto, H., Sato, J., Hayashi, I., Burma, S., Matsuura, S., Chen, D.J., and Komatsu, K. (2012). Nucleolin participates in DNA double-strand break-induced damage response through MDC1-dependent pathway. PLoS One *7*, e49245.

Kobayashi, T. (2011). Regulation of ribosomal RNA gene copy number and its role in modulating genome integrity and evolutionary adaptability in yeast. Cell Mol Life Sci *68*, 1395-1403.

Koberna, K., Malinsky, J., Pliss, A., Masata, M., Vecerova, J., Fialova, M., Bednar, J., and Raska, I. (2002). Ribosomal genes in focus: new transcripts label the dense fibrillar components and form clusters indicative of "Christmas trees" in situ. J Cell Biol *157*, 743-748.

Koike, A., Nishikawa, H., Wu, W., Okada, Y., Venkitaraman, A.R., and Ohta, T. (2010). Recruitment of phosphorylated NPM1 to sites of DNA damage through RNF8-dependent ubiquitin conjugates. Cancer Res *70*, 6746-6756.

Korhonen, R., and Moilanen, E. (2014). Mitogen-Activated Protein Kinase Phosphatase 1 as an Inflammatory Factor and Drug Target. Basic & Clinical Pharmacology & Toxicology *114*, 24-36.

Kreiner, G., Bierhoff, H., Armentano, M., Rodriguez-Parkitna, J., Sowodniok, K., Naranjo, J.R., Bonfanti, L., Liss, B., Schutz, G., Grummt, I.*, et al.* (2013). A neuroprotective phase precedes striatal degeneration upon nucleolar stress. Cell Death Differ *20*, 1455-1464.

Kressler, D., Hurt, E., and Bassler, J. (2017). A Puzzle of Life: Crafting Ribosomal Subunits. Trends Biochem Sci *42*, 640-654.

Kruhlak, M., Crouch, E.E., Orlov, M., Montano, C., Gorski, S.A., Nussenzweig, A., Misteli, T., Phair, R.D., and Casellas, R. (2007). The ATM repair pathway inhibits RNA polymerase I transcription in response to chromosome breaks. Nature *447*, 730-U716.

Kruse, J.P., and Gu, W. (2009). MSL2 promotes Mdm2-independent cytoplasmic localization of p53. J Biol Chem *284*, 3250-3263.

Kuhn, A., Vente, A., Doree, M., and Grummt, I. (1998). Mitotic phosphorylation of the TBP-containing factor SL1 represses ribosomal gene transcription. J Mol Biol *284*, 1-5.

Kumazawa, T., Nishimura, K., Katagiri, N., Hashimoto, S., Hayashi, Y., and Kimura, K. (2015). Gradual reduction in rRNA transcription triggers p53 acetylation and apoptosis via MYBBP1A. Scientific Reports *5*, 10854.

Kumazawa, T., Nishimura, K., Kuroda, T., Ono, W., Yamaguchi, C., Katagiri, N., Tsuchiya, M., Masumoto, H., Nakajima, Y., Murayama, A.*, et al.* (2011). Novel nucleolar pathway connecting intracellular energy status with p53 activation. J Biol Chem *286*, 20861-20869.

Kurki, S., Peltonen, K., Latonen, L., Kiviharju, T.M., Ojala, P.M., Meek, D., and Laiho, M. (2004). Nucleolar protein NPM interacts with HDM2 and protects tumor suppressor protein p53 from HDM2-mediated degradation. Cancer Cell *5*, 465-475.

Kuroda, T., Murayama, A., Katagiri, N., Ohta, Y.M., Fujita, E., Masumoto, H., Ema, M., Takahashi, S., Kimura, K., and Yanagisawa, J. (2011). RNA content in the nucleolus alters p53 acetylation via MYBBP1A. EMBO J *30*, 1054-1066.

Lam, Y.W., Lamond, A.I., Mann, M., and Andersen, J.S. (2007). Analysis of nucleolar protein dynamics reveals the nuclear degradation of ribosomal proteins. Curr Biol *17*, 749-760.

Lange, T.S., and Gerbi, S.A. (2000). Transient Nucleolar Localization Of U6 Small Nuclear RNA In Xenopus Laevis Oocytes. Molecular Biology of the Cell *11*, 2419-2428.

Langmead, B., Trapnell, C., Pop, M., and Salzberg, S.L. (2009). Ultrafast and memory-efficient alignment of short DNA sequences to the human genome. Genome Biol *10*, R25.

Langst, G., Blank, T.A., Becker, P.B., and Grummt, I. (1997). RNA polymerase I transcription on nucleosomal templates: the transcription termination factor TTF-I induces chromatin remodeling and relieves transcriptional repression. EMBO J *16*, 760-768.

Larsen, D.H., Hari, F., Clapperton, J.A., Gwerder, M., Gutsche, K., Altmeyer, M., Jungmichel, S., Toledo, L.I., Fink, D., Rask, M.B.*, et al.* (2014). The NBS1-Treacle complex controls ribosomal RNA transcription in response to DNA damage. Nat Cell Biol *16*, 792-803.

Larsen, D.H., and Stucki, M. (2016). Nucleolar responses to DNA double-strand breaks. Nucleic Acids Res *44*, 538-544.

Lau, L.F. (2011). CCN1/CYR61: the very model of a modern matricellular protein. Cell Mol Life Sci *68*, 3149-3163.

Lau, L.F., and Nathans, D. (1985). IDENTIFICATION OF A SET OF GENES EXPRESSED DURING THE G0/G1 TRANSITION OF CULTURED MOUSE CELLS. Embo Journal *4*, 3145-3151.

Lau, L.F., and Nathans, D. (1987). Expression of a set of growth-related immediate early genes in BALB/c 3T3 cells: coordinate regulation with c-fos or c-myc. Proc Natl Acad Sci U S A *84*, 1182-1186.

Lauschke, V.M., Vorrink, S.U., Moro, S.M.L., Rezayee, F., Nordling, A., Hendriks, D.F.G., Bell, C.C., Sison-Young, R., Park, B.K., Goldring, C.E.*, et al.* (2016). Massive rearrangements of cellular MicroRNA signatures are key drivers of hepatocyte dedifferentiation. Hepatology *64*, 1743-1756.

Learned, R.M., Cordes, S., and Tjian, R. (1985). Purification and characterization of a transcription factor that confers promoter specificity to human RNA polymerase I. Mol Cell Biol *5*, 1358-1369.

Learned, R.M., Learned, T.K., Haltiner, M.M., and Tjian, R.T. (1986). HUMAN RIBOSOMAL-RNA TRANSCRIPTION IS MODULATED BY THE COORDINATE BINDING OF 2-FACTORS TO AN UPSTREAM CONTROL ELEMENT. Cell *45*, 847-857.

Lee, B., Matera, A.G., Ward, D.C., and Craft, J. (1996). Association of RNase mitochondrial RNA processing enzyme with ribonuclease P in higher ordered structures in the nucleolus: a possible coordinate role in ribosome biogenesis. Proc Natl Acad Sci U S A *93*, 11471-11476.

Lee, J.T., and Gu, W. (2010). The multiple levels of regulation by p53 ubiquitination. Cell Death Differ *17*, 86-92.

Lee, S.L., Hong, S.W., Shin, J.S., Kim, J.S., Ko, S.G., Hong, N.J., Kim, D.J., Lee, W.J., Jin, D.H., and Lee, M.S. (2009). p34SEI-1 inhibits doxorubicin-induced senescence through a pathway mediated by protein kinase C-delta and c-Jun-NH2-kinase 1 activation in human breast cancer MCF7 cells. Mol Cancer Res *7*, 1845-1853.

Lee, S.Y., Lee, H., Kim, E.S., Park, S., Lee, J., and Ahn, B. (2015). WRN translocation from nucleolus to nucleoplasm is regulated by SIRT1 and required for DNA repair and the development of chemoresistance. Mutat Res *774*, 40-48.

Leger, I., Guillaud, M., Krief, B., and Brugal, G. (1994). INTERACTIVE COMPUTER-ASSISTED ANALYSIS OF CHROMOSOME-1 COLOCALIZATION WITH NUCLEOLI. Cytometry *16*, 313-323.

Lessard, F., Morin, F., Ivanchuk, S., Langlois, F., Stefanovsky, V., Rutka, J., and Moss, T. (2010). The ARF tumor suppressor controls ribosome biogenesis by regulating the RNA polymerase I transcription factor TTF-I. Mol Cell *38*, 539-550.

Leung, A.K.L., Gerlich, D., Miller, G., Lyon, C., Lam, Y.W., Lleres, D., Daigle, N., Zomerdijk, J., Ellenherg, J., and Lamond, A.I. (2004). Quantitative kinetic analysis of nucleolar breakdown and reassembly during mitosis in live human cells. Journal of Cell Biology *166*, 787-800.

Leung, A.K.L., Trinkle-Mulcahy, L., Lam, Y.W., Andersen, J.S., Mann, M., and Lamond, A.I. (2006). NOPdb: nucleolar proteome database. Nucleic Acids Research *34*, D218-D220.

Li, J., Längst, G., and Grummt, I. (2006). NoRC-dependent nucleosome positioning silences rRNA genes. The EMBO Journal *25*, 5735-5741.

Li, J., Melvin, W.S., Tsai, M.D., and Muscarella, P. (2004). The nuclear protein p34SEI-1 regulates the kinase activity of cyclin-dependent kinase 4 in a concentration-dependent manner. Biochemistry *43*, 4394-4399.

Li, J.W., Santoro, R., Koberna, K., and Grummt, I. (2005). The chromatin remodeling complex NoRC controls replication timing of rRNA genes. Embo Journal *24*, 120-127.

Li, N., Zhao, G., Chen, T., Xue, L., Ma, L., Niu, J., and Tong, T. (2012). Nucleolar protein CSIG is required for p33ING1 function in UV-induced apoptosis. Cell Death Dis *3*, e283.

Li, W., Guo, F., Wang, P., Hong, S., and Zhang, C. (2014). miR-221/222 Confers Radioresistance in Glioblastoma Cells Through Activating Akt Independent of PTEN Status. Curr Mol Med *14*, 185-195.

Li, Y., and Yang, D.Q. (2010). The ATM inhibitor KU-55933 suppresses cell proliferation and induces apoptosis by blocking Akt in cancer cells with overactivated Akt. Mol Cancer Ther *9*, 113-125.

Li, Z.F., Liang, Y.M., Lau, P.N., Shen, W., Wang, D.K., Cheung, W.T., Xue, C.J., Poon, L.M., and Lam, Y.W. (2013). Dynamic localisation of mature microRNAs in Human nucleoli is influenced by exogenous genetic materials. PLoS One *8*, e70869.

Lian, C.Y., Robinson, H., and Wang, A.H.J. (1996). Structure of actinomycin D bound with (GAAGCTTC)(2) and (GATGCTTC)(2) and its binding to the (CAG)(n):(CTG)(n) triplet sequence as determined by NMR analysis. J Am Chem Soc *118*, 8791-8801.

Lin, C.H., and Lee, E.H. (2012). JNK1 inhibits GluR1 expression and GluR1-mediated calcium influx through phosphorylation and stabilization of Hes-1. J Neurosci *32*, 1826-1846.

Lin, T., Meng, L., Lin, T.C., Wu, L.J., Pederson, T., and Tsai, R.Y. (2014). Nucleostemin and GNL3L exercise distinct functions in genome protection and ribosome synthesis, respectively. J Cell Sci *127*, 2302-2312.

Little, R.D., Platt, T.H.K., and Schildkraut, C.L. (1993). INITIATION AND TERMINATION OF DNA-REPLICATION IN HUMAN RIBOSOMAL-RNA GENES. Molecular and Cellular Biology *13*, 6600-6613.

Liu, H., Herrmann, C.H., Chiang, K., Sung, T.L., Moon, S.H., Donehower, L.A., and Rice, A.P. (2010). 55K isoform of CDK9 associates with Ku70 and is involved in DNA repair. Biochem Biophys Res Commun *397*, 245-250.

Liu, S., Sun, X., Wang, M., Hou, Y., Zhan, Y., Jiang, Y., Liu, Z., Cao, X., Chen, P., Liu, Z.*, et al.* (2014). A microRNA 221- and 222-mediated feedback loop maintains constitutive activation of NFkappaB and STAT3 in colorectal cancer cells. Gastroenterology *147*, 847-859 e811.

Liu, Z., Jiang, Y., Hou, Y., Hu, Y., Cao, X., Tao, Y., Xu, C., Liu, S., Wang, S., Wang, L.*, et al.* (2013). The IkappaB family member Bcl-3 stabilizes c-Myc in colorectal cancer. J Mol Cell Biol *5*, 280-282.

Lohrum, M.A.E., Ludwig, R.L., Kubbutat, M.H.G., Hanlon, M., and Vousden, K.H. (2003). Regulation of HDM2 activity by the ribosomal protein L11. Cancer Cell *3*, 577-587.

Lopez-Estrano, C., Schvartzman, J.B., Krimer, D.B., and Hernandez, P. (1998). Co-localization of polar replication fork barriers and rRNA transcription terminators in mouse rDNA. J Mol Biol *277*, 249-256.

Lowe, S.W., Cepero, E., and Evan, G. (2004). Intrinsic tumour suppression. Nature *432*, 307-315.

Lu, B., Ferrandino, A.F., and Flavell, R.A. (2004). Gadd45beta is important for perpetuating cognate and inflammatory signals in T cells. Nat Immunol *5*, 38-44.

Lupini, L., Bassi, C., Ferracin, M., Bartonicek, N., D'Abundo, L., Zagatti, B., Callegari, E., Musa, G., Moshiri, F., Gramantieri, L.*, et al.* (2013). miR-221 affects multiple cancer pathways by modulating the level of hundreds messenger RNAs. Front Genet *4*, 64.

Luscher, B. (2012). MAD1 and its life as a MYC antagonist: an update. Eur J Cell Biol *91*, 506-514.

Ma, H., and Pederson, T. (2013). The nucleolus stress response is coupled to an ATR-Chk1-mediated G2 arrest. Mol Biol Cell *24*, 1334-1342.

Ma, N., Matsunaga, S., Takata, H., Ono-Maniwa, R., Uchiyama, S., and Fukui, K. (2007). Nucleolin functions in nucleolus formation and chromosome congression. J Cell Sci *120*, 2091-2105.

MacCarty, W.C. (1936). The value of the macronucleolus in the cancer problem. Amer Jour Cancer *26*, 529-532.

MacDonald, B.T., Tamai, K., and He, X. (2009a). Wnt/beta-catenin signaling: components, mechanisms, and diseases. Dev Cell *17*, 9-26.

MacDonald, B.T., Tamai, K., and He, X. (2009b). Wnt/Œ≤-catenin signaling: components, mechanisms, and diseases. Developmental Cell *17*, 9-26.

Machwe, A., Orren, D.K., and Bohr, V.A. (2000). Accelerated methylation of ribosomal RNA genes during the cellular senescence of Werner syndrome fibroblasts. FASEB J *14*, 1715-1724.

Macias, E., Jin, A., Deisenroth, C., Bhat, K., Mao, H., Lindstrom, M.S., and Zhang, Y. (2010). An ARF-independent c-MYC-activated tumor suppression pathway mediated by ribosomal protein-Mdm2 Interaction. Cancer Cell *18*, 231-243.

Maggi, L.B., Winkeler, C.L., Miceli, A.P., Apicelli, A.J., Brady, S.N., Kuchenreuther, M.J., and Weber, J.D. (2014). ARF tumor suppression in the nucleouls. Biochim Biophys Acta-Mol Basis Dis *1842*, 831-839.

Mahajan, P.B. (1994). Modulation of transcription of rRNA genes by rapamycin. Int J Immunopharmacol *16*, 711-721.

Mahata, B., Sundqvist, A., and Xirodimas, D.P. (2012a). Recruitment of RPL11 at promoter sites of p53-regulated genes upon nucleolar stress through NEDD8 and in an Mdm2-dependent manner. Oncogene *31*, 3060-3071.

Mahata, B., Sundqvist, A., and Xirodimas, D.P. (2012b). Recruitment of RPL11 at promoter sites of p53-regulated genes upon nucleolar stress through NEDD8 and in an Mdm2-dependent manner. Oncogene *31*, 3060-3071.

Mais, C., Wright, J.E., Prieto, J.L., Raggett, S.L., and McStay, B. (2005). UBF-binding site arrays form pseudo-NORs and sequester the RNA polymerase I transcription machinery. Genes & Development *19*, 50-64.

Maizels, N., and Gray, L.T. (2013). The G4 genome. PLoS Genet *9*, e1003468.

Maldonado, V., and Melendez-Zajgla, J. (2011). Role of Bcl-3 in solid tumors. Molecular Cancer *10*, 152-152.

Mali, P., Yang, L., Esvelt, K.M., Aach, J., Guell, M., DiCarlo, J.E., Norville, J.E., and Church, G.M. (2013). RNA-guided human genome engineering via Cas9. Science *339*, 823-826.

Marciniak, R.A., Lombard, D.B., Johnson, F.B., and Guarente, L. (1998). Nucleolar localization of the Werner syndrome protein in human cells. Proc Natl Acad Sci U S A *95*, 6887-6892.

Martinez, P., and Blasco, M.A. (2011). Telomeric and extra-telomeric roles for telomerase and the telomere-binding proteins. Nat Rev Cancer *11*, 161-176.

Matera, A.G., Frey, M.R., Margelot, K., and Wolin, S.L. (1995). A perinucleolar compartment contains several RNA polymerase III transcripts as well as the polypyrimidine tract-binding protein, hnRNP I. J Cell Biol *129*, 1181-1193.

Matheson, T.D., and Kaufman, P.D. (2016). Grabbing the genome by the NADs. Chromosoma *125*, 361-371.

Matsuoka, S., Ballif, B.A., Smogorzewska, A., McDonald, E.R., 3rd, Hurov, K.E., Luo, J., Bakalarski, C.E., Zhao, Z., Solimini, N., Lerenthal, Y.*, et al.* (2007). ATM and ATR substrate analysis reveals extensive protein networks responsive to DNA damage. Science *316*, 1160-1166.

Mayer, C., Bierhoff, H., and Grummt, I. (2005). The nucleolus as a stress sensor: JNK2 inactivates the transcription factor TIF-IA and down-regulates rRNA synthesis. Genes & Development *19*, 933-941.

Mayer, C., Schmitz, K.M., Li, J., Grummt, I., and Santoro, R. (2006). Intergenic transcripts regulate the epigenetic state of rRNA genes. Mol Cell *22*, 351-361.

Mayer, C., Zhao, J., Yuan, X.J., and Grummt, I. (2004). mTOR-dependent activation of the transcription factor TIMA links rRNA synthesis to nutrient availability. Genes & Development *18*, 423-434.

McKay, M.M., and Morrison, D.K. (2007). Integrating signals from RTKs to ERK/MAPK. Oncogene *26*, 3113-3121.

McStay, B., and Grummt, I. (2008). The Epigenetics of rRNA Genes: From Molecular to Chromosome Biology. Annual Review of Cell and Developmental Biology *24*, 131-157.

Mekhail, K., Gunaratnam, L., Bonicalzi, M.E., and Lee, S. (2004). HIF activation by pH-dependent nucleolar sequestration of VHL. Nat Cell Biol *6*, 642-647.

Mekhail, K., Khacho, M., Carrigan, A., Hache, R.R.J., Gunaratnam, L., and Lee, S. (2005). Regulation of ubiquitin ligase dynamics by the nucleolus. Journal of Cell Biology *170*, 733-744.

Meng, L.-h., and Zheng, X.F.S. (2015). Toward rapamycin analog (rapalog)-based precision cancer therapy. Acta Pharmacologica Sinica *36*, 1163-1169.

Meng, L.J., Lin, T., and Tsai, R.Y.L. (2008). Nucleoplasmic mobilization of nucleostemin stabilizes MDM2 and promotes G2-M progression and cell survival. J Cell Sci *121*, 4037-4046.

Meraner, J., Lechner, M., Loidl, A., Goralik-Schramel, M., Voit, R., Grummt, I., and Loidl, P. (2006). Acetylation of UBF changes during the cell cycle and regulates the interaction of UBF with RNA polymerase I. Nucleic Acids Research *34*, 1798-1806.

Meroni, G., Cairo, S., Merla, G., Messali, S., Brent, R., Ballabio, A., and Reymond, A. (2000). Mlx, a new Max-like bHLHZip family member: the center stage of a novel transcription factors regulatory pathway? Oncogene *19*, 3266-3277.

Michaelidis, T.M., and Grummt, I. (2002). Mechanism of inhibition of RNA polymerase I transcription by DNA-dependent protein kinase. Biol Chem *383*, 1683-1690.

Miller, G., Panov, K.I., Friedrich, J.K., Trinkle-Mulcahy, L., Lamond, A.I., and Zomerdijk, J. (2001). hRRN3 is essential in the SL1-mediated recruitment of RNA polymerase I to rRNA gene promoters. Embo Journal *20*, 1373-1382.

Miller, O.L., and Bakken, A.H. (1972). MORPHOLOGICAL STUDIES OF TRANSCRIPTION. Acta Endocrinol, 155-&.

Mills, K.D. (2013). Tumor suppression: putting p53 in context. Cell Cycle *12*, 3461-3462.

Mishra, P., and Chan, D.C. (2014). Mitochondrial dynamics and inheritance during cell division, development and disease. Nat Rev Mol Cell Biol *15*, 634-646.

Mita, H., Tsutsui, J., Takekawa, M., Witten, E.A., and Saito, H. (2002). Regulation of MTK1/MEKK4 kinase activity by its N-terminal autoinhibitory domain and GADD45 binding. Mol Cell Biol *22*, 4544-4555.

Mochizuki, Y., He, J., Kulkarni, S., Bessler, M., and Mason, P.J. (2004). Mouse dyskerin mutations affect accumulation of telomerase RNA and small nucleolar RNA, telomerase activity, and ribosomal RNA processing. Proc Natl Acad Sci U S A *101*, 10756-10761.

Mohammad, F., Pandey, R.R., Nagano, T., Chakalova, L., Mondal, T., Fraser, P., and Kanduri, C. (2008). Kcnq1ot1/Lit1 noncoding RNA mediates transcriptional silencing by targeting to the perinucleolar region. Molecular and Cellular Biology *28*, 3713-3728.

Moir, R.D., and Willis, I.M. (2013). Regulation of pol III transcription by nutrient and stress signaling pathways. Biochim Biophys Acta *1829*, 361-375.

Monnat Jr, R.J., Hackmann, A.F.M., and Cantrell, M.A. (1999). Generation of Highly Site-Specific DNA Double-Strand Breaks in Human Cells by the Homing Endonucleases I-PpoI and I-CreI. Biochemical and Biophysical Research Communications *255*, 88-93.

Montanaro, L., Brigotti, M., Clohessy, J., Barbieri, S., Ceccarelli, C., Santini, D., Taffurelli, M., Calienni, M., Teruya-Feldstein, J., Trere, D.*, et al.* (2006). Dyskerin expression influences the level of ribosomal RNA pseudo-uridylation and telomerase RNA component in human breast cancer. J Pathol *210*, 10-18.

Montanaro, L., Calienni, M., Bertoni, S., Rocchi, L., Sansone, P., Storci, G., Santini, D., Ceccarelli, C., Taffurelli, M., Carnicelli, D.*, et al.* (2010). Novel dyskerin-mediated mechanism of p53 inactivation through defective mRNA translation. Cancer Res *70*, 4767-4777.

Moore, H.M., Bai, B., Boisvert, F.M., Latonen, L., Rantanen, V., Simpson, J.C., Pepperkok, R., Lamond, A.I., and Laiho, M. (2011). Quantitative proteomics and dynamic imaging of the nucleolus reveal distinct responses to UV and ionizing radiation. Mol Cell Proteomics *10*, M111 009241.

Moore, H.M., Bai, B., Matilainen, O., Colis, L., Peltonen, K., and Laiho, M. (2013). Proteasome Activity Influences UV-Mediated Subnuclear Localization Changes of NPM. PLoS One *8*, e59096.

Moss, T. (2004). At the crossroads of growth control; making ribosomal RNA. Current Opinion in Genetics & Development *14*, 210-217.

Moss, T., Langlois, F., Gagnon-Kugler, T., and Stefanovsky, V. (2007). A housekeeper with power of attorney: the rRNA genes in ribosome biogenesis. Cellular and Molecular Life Sciences *64*, 29-49.

Muftuoglu, M., Kusumoto, R., Speina, E., Beck, G., Cheng, W.H., and Bohr, V.A. (2008). Acetylation regulates WRN catalytic activities and affects base excision DNA repair. PLoS One *3*, e1918.

Murayama, A., Ohmori, K., Fujimura, A., Minami, H., Yasuzawa-Tanaka, K., Kuroda, T., Oie, S., Daitoku, H., Okuwaki, M., Nagata, K.*, et al.* (2008). Epigenetic control of rDNA loci in response to intracellular energy status. Cell *133*, 627-639.

Muscarella, D.E., Ellison, E.L., Ruoff, B.M., and Vogt, V.M. (1990). CHARACTERIZATION OF I-PPO, AN INTRON-ENCODED ENDONUCLEASE THAT MEDIATES HOMING OF A GROUP-I INTRON IN THE RIBOSOMAL DNA OF PHYSARUM-POLYCEPHALUM. Molecular and Cellular Biology *10*, 3386-3396.

Muth, V., Nadaud, S., Grummt, I., and Voit, R. (2001). Acetylation of TAF(I)68, a subunit of TIF-IB/SL1, activates RNA polymerase I transcription. Embo Journal *20*, 1353-1362.

Nadel, J., Athanasiadou, R., Lemetre, C., Wijetunga, N.A., P, O.B., Sato, H., Zhang, Z., Jeddeloh, J., Montagna, C., Golden, A.*, et al.* (2015). RNA:DNA hybrids in the human genome have distinctive nucleotide characteristics, chromatin composition, and transcriptional relationships. Epigenetics Chromatin *8*, 46.

Nalabothula, N., Indig, F.E., and Carrier, F. (2010). The Nucleolus Takes Control of Protein Trafficking Under Cellular Stress. Mol Cell Pharmacol *2*, 203-212.

Narayanan, A., Lukowiak, A., Jady, B.E., Dragon, F., Kiss, T., Terns, R.M., and Terns, M.P. (1999). Nucleolar localization signals of box H/ACA small nucleolar RNAs. EMBO J *18*, 5120-5130.

Neeb, A., Wallbaum, S., Novac, N., Dukovic-Schulze, S., Scholl, I., Schreiber, C., Schlag, P., Moll, J., Stein, U., and Sleeman, J.P. (2012). The immediate early gene Ier2 promotes tumor cell motility and metastasis, and predicts poor survival of colorectal cancer patients. Oncogene *31*, 3796-3806.

Negi, S.S., and Brown, P. (2015a). rRNA synthesis inhibitor, CX-5461, activates ATM/ATR pathway in acute lymphoblastic leukemia, arrests cells in G2 phase and induces apoptosis. Oncotarget *6*, 18094-18104.

Negi, S.S., and Brown, P. (2015b). Transient rRNA synthesis inhibition with CX-5461 is sufficient to elicit growth arrest and cell death in acute lymphoblastic leukemia cells. Oncotarget *6*, 34846-34858.

Nemeth, A., Conesa, A., Santoyo-Lopez, J., Medina, I., Montaner, D., Peterfia, B., Solovei, I., Cremer, T., Dopazo, J., and Langst, G. (2010). Initial genomics of the human nucleolus. PLoS Genet *6*, e1000889.

Nemeth, A., Strohner, R., Grummt, I., and Langst, G. (2004). The chromatin remodeling complex NoRC and TTF-I cooperate in the regulation of the mammalian rRNA genes in vivo. Nucleic Acids Research *32*, 4091-4099.

Nesbit, C.E., Tersak, J.M., and Prochownik, E.V. (1999). MYC oncogenes and human neoplastic disease. Oncogene *18*, 3004-3016.

Nieminuszczy, J., Schwab, R.A., and Niedzwiedz, W. (2016). The DNA fibre technique - tracking helicases at work. Methods *108*, 92-98.

Nishimura, K., Kumazawa, T., Kuroda, T., Katagiri, N., Tsuchiya, M., Goto, N., Furumai, R., Murayama, A., Yanagisawa, J., and Kimura, K. (2015). Perturbation of ribosome biogenesis drives cells into senescence through 5S RNP-mediated p53 activation. Cell Rep *10*, 1310-1323.

Nolan, G.P., Fujita, T., Bhatia, K., Huppi, C., Liou, H.C., Scott, M.L., and Baltimore, D. (1993). The bcl-3 proto-oncogene encodes a nuclear I kappa B-like molecule that preferentially interacts with NF-kappa B p50 and p52 in a phosphorylation-dependent manner. Mol Cell Biol *13*, 3557-3566.

O'Sullivan, A.C., Sullivan, G.J., and McStay, B. (2002). UBF binding in vivo is not restricted to regulatory sequences within the vertebrate ribosomal DNA repeat. Molecular and Cellular Biology *22*, 657-668.

Ofir-Rosenfeld, Y., Boggs, K., Michael, D., Kastan, M.B., and Oren, M. (2008). Mdm2 Regulates p53 mRNA Translation through Inhibitory Interactions with Ribosomal Protein L26. Molecular Cell *32*, 180-189.

Ohtsuka, T., Ishibashi, M., Gradwohl, G., Nakanishi, S., Guillemot, F., and Kageyama, R. (1999). Hes1 and Hes5 as Notch effectors in mammalian neuronal differentiation. The EMBO Journal *18*, 2196-2207.

Okuda, M., Horn, H.F., Tarapore, P., Tokuyama, Y., Smulian, A.G., Chan, P.K., Knudsen, E.S., Hofmann, I.A., Snyder, J.D., Bove, K.E*., et al.* (2000). Nucleophosmin/B23 is a target of CDK2/Cyclin E in centrosome duplication. Cell *103*, 127-140.

Olcina, M., Lecane, P.S., and Hammond, E.M. (2010). Targeting hypoxic cells through the DNA damage response. Clin Cancer Res *16*, 5624-5629.

Ono, W., Akaogi, K., Waku, T., Kuroda, T., Yokoyama, W., Hayashi, Y., Kimura, K., Kishimoto, H., and Yanagisawa, J. (2013). Nucleolar protein, Myb-binding protein 1A, specifically binds to nonacetylated p53 and efficiently promotes transcriptional activation. Biochem Biophys Res Commun *434*, 659-663.

Osborne, J.K., Zaganjor, E., and Cobb, M.H. (2012). Signal control through Raf: in sickness and in health. Cell Res *22*, 14-22.

Östlund Farrants, A.K. (2017). Chapter 10 - Epigenetic Regulation of Nucleolar Functions A2 - Göndör, Anita. In Chromatin Regulation and Dynamics (Boston: Academic Press), pp. 235-274.

Pallares, J., Martinez-Guitarte, J.L., Dolcet, X., Llobet, D., Rue, M., Palacios, J., Prat, J., and Matias-Guiu, X. (2004). Abnormalities in the NF-kappaB family and related proteins in endometrial carcinoma. The Journal of pathology *204*, 569-577.

Pandey, R.R., Mondal, T., Mohammad, F., Enroth, S., Redrup, L., and Komorowski, J. (2008). Kcnq1ot1 antisense noncoding RNA mediates lineage-specific transcriptional silencing through chromatin-level regulation. Mol Cell *32*.

Panse, V.G., and Johnson, A.W. (2010). Maturation of eukaryotic ribosomes: acquisition of functionality. Trends Biochem Sci *35*, 260-266.

Papa, S., Monti, S.M., Vitale, R.M., Bubici, C., Jayawardena, S., Alvarez, K., De Smaele, E., Dathan, N., Pedone, C., Ruvo, M.*, et al.* (2007). Insights into the structural basis of the GADD45beta-mediated inactivation of the JNK kinase, MKK7/JNKK2. J Biol Chem *282*, 19029-19041.

Papa, S., Zazzeroni, F., Bubici, C., Jayawardena, S., Alvarez, K., Matsuda, S., Nguyen, D.U., Pham, C.G., Nelsbach, A.H., Melis, T.*, et al.* (2004). Gadd45 beta mediates the NF-kappa B suppression of JNK signalling by targeting MKK7/JNKK2. Nat Cell Biol *6*, 146-153.

Paredes, S., Branco, A.T., Hartl, D.L., Maggert, K.A., and Lemos, B. (2011). Ribosomal DNA deletions modulate genome-wide gene expression: "rDNA-sensitive" genes and natural variation. PLoS Genet *7*, e1001376.

Paredes, S., and Maggert, K.A. (2009). Ribosomal DNA contributes to global chromatin regulation. Proceedings of the National Academy of Sciences of the United States of America *106*, 17829-17834.

Park, S.G., Chung, C., Kang, H., Kim, J.Y., and Jung, G. (2006). Up-regulation of cyclin D1 by HBx is mediated by NF-kappaB2/BCL3 complex through kappaB site of cyclin D1 promoter. J Biol Chem *281*, 31770-31777.

Parrinello, S., Coppe, J.P., Krtolica, A., and Campisi, J. (2005). Stromal-epithelial interactions in aging and cancer: senescent fibroblasts alter epithelial cell differentiation. J Cell Sci *118*, 485-496.

Patel, J.H., Loboda, A.P., Showe, M.K., Showe, L.C., and McMahon, S.B. (2004). Opinion - Analysis of genomic targets reveals complex functions of MYC. Nat Rev Cancer *4*, 562-568.

Paulsen, M.T., Veloso, A., Prasad, J., Bedi, K., Ljungman, E.A., Tsan, Y.C., Chang, C.W., Tarrier, B., Washburn, J.G., Lyons, R.*, et al.* (2013). Coordinated regulation of synthesis and stability of RNA during the acute TNF-induced proinflammatory response. Proc Natl Acad Sci U S A *110*, 2240-2245.

Peddibhotla, S., Wei, Z.B., Papineni, R., Lam, M.H., Rosen, J.M., and Zhang, P.M. (2011). The DNA damage effector Chk1 kinase regulates Cdc14B nucleolar shuttling during cell cycle progression. Cell Cycle *10*, 671-679.

Pederson, T. (1998). The plurifunctional nucleolus. Nucleic Acids Research *26*, 3871-3876.

Pederson, T. (2011). The nucleolus. Cold Spring Harb Perspect Biol *3*.

Pederson, T., and Politz, J.C. (2000). The Nucleolus and the Four Ribonucleoproteins of Translation. The Journal of Cell Biology *148*, 1091-1096.

Pederson, T., and Tsai, R.Y.L. (2009). In search of nonribosomal nucleolar protein function and regulation. Journal of Cell Biology *184*, 771-776.

Peng, Y., Zhao, S.M., Song, L.Y., Wang, M.Y., and Jiao, K. (2013). Sertad1 encodes a novel transcriptional co-activator of SMAD1 in mouse embryonic hearts. Biochemical and Biophysical Research Communications *441*, 751-756.

Perez-Castro, A.J., and Freire, R. (2012). Rad9B responds to nucleolar stress through ATR and JNK signalling, and delays the G1-S transition. J Cell Sci *125*, 1152-1164.

Perez-Mancera, P.A., Young, A.R., and Narita, M. (2014). Inside and out: the activities of senescence in cancer. Nat Rev Cancer *14*, 547-558.

Perry, R.P. (1963). SELECTIVE EFFECTS OF ACTINOMYCIN D ON INTRACELLULAR DISTRIBUTION OF RNA SYNTHESIS IN TISSUE CULTURE CELLS. Exp Cell Res *29*, 400-&.

Perry, R.P., and Kelley, D.E. (1970). INHIBITION OF RNA SYNTHESIS BY ACTINOMYCIN-D - CHARACTERISTIC DOSE-RESPONSE OF DIFFERENT RNA SPECIES. J Cell Physiol *76*, 127-&.

Petitjean, A., Achatz, M.I., Borresen-Dale, A.L., Hainaut, P., and Olivier, M. (2007a). TP53 mutations in human cancers: functional selection and impact on cancer prognosis and outcomes. Oncogene *26*, 2157-2165.

Petitjean, A., Mathe, E., Kato, S., Ishioka, C., Tavtigian, S.V., Hainaut, P., and Olivier, M. (2007b). Impact of mutant p53 functional properties on TP53 mutation patterns and tumor phenotype: Lessons from recent developments in the IARC TP53 database. Human Mutation *28*, 622-629.

Phair, R.D., and Misteli, T. (2000). High mobility of proteins in the mammalian cell nucleus. Nature *404*, 604-609.

Pianese, G. (1896). Beitrag zur Histologie und Aetiologie der Carcinoma. Histologische und experimentelle
Untersuchungen. . Beitr Pathol Anat Allgem Pathol *142*, 1-193.

Pichiorri, F., Palmieri, D., De Luca, L., Consiglio, J., You, J., Rocci, A., Talabere, T., Piovan, C., Lagana, A., Cascione, L.*, et al.* (2013). In vivo NCL targeting affects breast cancer aggressiveness through miRNA regulation. J Exp Med *210*, 951-968.

Pickering, B.F., Yu, D., and Van Dyke, M.W. (2011). Nucleolin protein interacts with microprocessor complex to affect biogenesis of microRNAs 15a and 16. J Biol Chem *286*, 44095-44103.

Pietrzak, M., Rempala, G., Nelson, P.T., Zheng, J.J., and Hetman, M. (2011). Epigenetic silencing of nucleolar rRNA genes in Alzheimer's disease. PLoS One *6*, e22585.

Poletto, M., Lirussi, L., Wilson, D.M., 3rd, and Tell, G. (2014a). Nucleophosmin modulates stability, activity, and nucleolar accumulation of base excision repair proteins. Mol Biol Cell *25*, 1641-1652.

Poletto, M., Lirussi, L., Wilson, D.M., and Tell, G. (2014b). Nucleophosmin modulates stability, activity, and nucleolar accumulation of base excision repair proteins. Molecular Biology of the Cell *25*, 1641-1652.

Politz, J.C., Hogan, E.M., and Pederson, T. (2009). MicroRNAs with a nucleolar location. RNA *15*, 1705-1715.

Politz, J.C., Lewandowski, L.B., and Pederson, T. (2002). Signal recognition particle RNA localization within the nucleolus differs from the classical sites of ribosome synthesis. J Cell Biol *159*, 411-418.

Politz, J.C., Yarovoi, S., Kilroy, S.M., Gowda, K., Zwieb, C., and Pederson, T. (2000). Signal recognition particle components in the nucleolus. Proceedings of the National Academy of Sciences of the United States of America *97*, 55-60.

Politz, J.C., Zhang, F., and Pederson, T. (2006). MicroRNA-206 colocalizes with ribosome-rich regions in both the nucleolus and cytoplasm of rat myogenic cells. Proc Natl Acad Sci U S A *103*, 18957-18962.

Pollock, C., and Huang, S. (2010). The perinucleolar compartment. Cold Spring Harb Perspect Biol *2*, a000679.

Pondarre, C., Strumberg, D., Fujimori, A., Torres-Leon, R., and Pommier, Y. (1997). In vivo sequencing of camptothecin-induced topoisomerase I cleavage sites in human colon carcinoma cells. Nucleic Acids Res *25*, 4111-4116.

Ponten, J., and Saksela, E. (1967). Two established in vitro cell lines from human mesenchymal tumours. Int J Cancer *2*, 434-447.

Poortinga, G., Hannan, K.M., Snelling, H., Walkley, C.R., Jenkins, A., Sharkey, K., Wall, M., Brandenburger, Y., Palatsides, M., Pearson, R.B.*, et al.* (2004). MAD1 and c-MYC regulate UBF and rDNA transcription during granulocyte differentiation. Embo Journal *23*, 3325-3335.

Poortinga, G., Wall, M., Sanij, E., Siwicki, K., Ellul, J., Brown, D., Holloway, T.P., Hannan, R.D., and McArthur, G.A. (2011a). c-MYC coordinately regulates ribosomal gene chromatin remodeling and Pol I availability during granulocyte differentiation. Nucleic Acids Research *39*, 3267-3281.

Poortinga, G., Wall, M., Sanij, E., Siwicki, K., Ellul, J., Brown, D., Holloway, T.P., Hannan, R.D., and McArthur, G.A. (2011b). c-MYC coordinately regulates ribosomal gene chromatin remodeling and Pol I availability during granulocyte differentiation. Nucleic Acids Res *39*, 3267-3281.

Powell, M.A., Mutch, D.G., Rader, J.S., Herzog, T.J., Huang, T.H.M., and Goodfellow, P.J. (2002). Ribosomal DNA methylation in patients with endometrial carcinoma - An independent prognostic marker. Cancer *94*, 2941-2952.

Prakash, R., Zhang, Y., Feng, W., and Jasin, M. (2015). Homologous recombination and human health: the roles of BRCA1, BRCA2, and associated proteins. Cold Spring Harb Perspect Biol *7*, a016600.

Prieto, J.L., and McStay, B. (2007). Recruitment of factors linking transcription and processing of pre-rRNA to NOR chromatin is UBF-dependent and occurs independent of transcription in human cells. Genes & Development *21*, 2041-2054.

Prieto, J.L., and McStay, B. (2008). Pseudo-NORs: A novel model for studying nucleoli. Biochimica Et Biophysica Acta-Molecular Cell Research *1783*, 2116-2123.

Puvion-Dutilleul, F., Bachellerie, J.P., and Puvion, E. (1991). Nucleolar organization of HeLa cells as studied by in situ hybridization. Chromosoma *100*, 395-409.

Pylayeva-Gupta, Y., Grabocka, E., and Bar-Sagi, D. (2011). RAS oncogenes: weaving a tumorigenic web. Nat Rev Cancer *11*, 761-774.

Quin, J., Chan, K.T., Devlin, J.R., Cameron, D.P., Diesch, J., Cullinane, C., Ahern, J., Khot, A., Hein, N., George, A.J.*, et al.* (2016). Inhibition of RNA polymerase I transcription initiation by CX-5461 activates non-canonical ATM/ATR signaling. Oncotarget *7*, 49800-49818.

Rancourt, A., and Satoh, M.S. (2009). Delocalization of nucleolar poly(ADP-ribose) polymerase-1 to the nucleoplasm and its novel link to cellular sensitivity to DNA damage. DNA Repair *8*, 286-297.

Rawlins, D.J., and Shaw, P.J. (1990). LOCALIZATION OF RIBOSOMAL AND TELOMERIC DNA-SEQUENCES IN INTACT PLANT NUCLEI BY INSITU HYBRIDIZATION AND 3-DIMENSIONAL OPTICAL MICROSCOPY. Journal of Microscopy-Oxford *157*, 83-89.

Reaper, P.M., Griffiths, M.R., Long, J.M., Charrier, J.D., Maccormick, S., Charlton, P.A., Golec, J.M., and Pollard, J.R. (2011). Selective killing of ATM- or p53-deficient cancer cells through inhibition of ATR. Nat Chem Biol *7*, 428-430.

Rebello, R.J., Kusnadi, E., Cameron, D.P., Pearson, H.B., Lesmana, A., Devlin, J.R., Drygin, D., Clark, A.K., Porter, L., Pedersen, J.*, et al.* (2016). The Dual Inhibition of RNA Pol I Transcription and PIM Kinase as a New Therapeutic Approach to Treat Advanced Prostate Cancer. Clin Cancer Res *22*, 5539-5552.

Rebollo, A., Dumoutier, L., Renauld, J.C., Zaballos, A., Ayllon, V., and Martinez, A.C. (2000). Bcl-3 expression promotes cell survival following interleukin-4 deprivation and is controlled by AP1 and AP1-like transcription factors. Mol Cell Biol *20*, 3407-3416.

Revollo, J.R., Oakley, R.H., Lu, N.Z., Kadmiel, M., Gandhavadi, M., and Cidlowski, J.A. (2013). HES1 is a master regulator of glucocorticoid receptor-dependent gene expression. Sci Signal *6*, ra103.

Reyes-Gutierrez, P., Ritland Politz, J.C., and Pederson, T. (2014). A mRNA and cognate microRNAs localize in the nucleolus. Nucleus *5*, 636-642.

Richard, M., Louahed, J., Demoulin, J.B., and Renauld, J.C. (1999). Interleukin-9 regulates NF-kappaB activity through BCL3 gene induction. Blood *93*, 4318-4327.

Ridanpaa, M., van Eenennaam, H., Pelin, K., Chadwick, R., Johnson, C., Yuan, B., vanVenrooij, W., Pruijn, G., Salmela, R., Rockas, S*., et al.* (2001). Mutations in the RNA component of RNase MRP cause a pleiotropic human disease, cartilage-hair hypoplasia. Cell *104*, 195-203.

Rill, R.L., and Hecker, K.H. (1996). Sequence-specific actinomycin D binding to single-stranded DNA inhibits HIV reverse transcriptase and other polymerases. Biochemistry *35*, 3525-3533.

Robledo, S., Idol, R.A., Crimmins, D.L., Ladenson, J.H., Mason, P.J., and Bessler, M. (2008). The role of human ribosomal proteins in the maturation of rRNA and ribosome production. RNA *14*, 1918-1929.

Rocha, S., Garrett, M.D., Campbell, K.J., Schumm, K., and Perkins, N.D. (2005). Regulation of NF-kappaB and p53 through activation of ATR and Chk1 by the ARF tumour suppressor. EMBO J *24*, 1157-1169.

Rodier, F., and Campisi, J. (2011). Four faces of cellular senescence. The Journal of Cell Biology *192*, 547-556.

Rodier, F., Coppe, J.P., Patil, C.K., Hoeijmakers, W.A., Munoz, D.P., Raza, S.R., Freund, A., Campeau, E., Davalos, A.R., and Campisi, J. (2009). Persistent DNA damage signalling triggers senescence-associated inflammatory cytokine secretion. Nat Cell Biol *11*, 973-979.

Rodier, F., Munoz, D.P., Teachenor, R., Chu, V., Le, O., Bhaumik, D., Coppe, J.P., Campeau, E., Beausejour, C.M., Kim, S.H*., et al.* (2011). DNA-SCARS: distinct nuclear structures that sustain damage-induced senescence growth arrest and inflammatory cytokine secretion. J Cell Sci *124*, 68-81.

Rodriguez, R., and Miller, K.M. (2014). Unravelling the genomic targets of small molecules using high-throughput sequencing. Nat Rev Genet *15*, 783-796.

Rodriguez, R., Miller, K.M., Forment, J.V., Bradshaw, C.R., Nikan, M., Britton, S., Oelschlaegel, T., Xhemalce, B., Balasubramanian, S., and Jackson, S.P. (2012). Small-molecule-induced DNA damage identifies alternative DNA structures in human genes. Nat Chem Biol *8*, 301-310.

Roussel, P., Andre, C., Comai, L., and HernandezVerdun, D. (1996). The rDNA transcription machinery is assembled during mitosis in active NORs and absent in inactive NORs. Journal of Cell Biology *133*, 235-246.

Roussel, P., Andre, C., Masson, C., Geraud, G., and Hernandez-Verdun, D. (1993). Localization of the RNA polymerase I transcription factor hUBF during the cell cycle. J Cell Sci *104 (Pt 2)*, 327-337.

Rubbi, C.P., and Milner, J. (2003). Disruption of the nucleolus mediates stabilization of p53 in response to DNA damage and other stresses. Embo Journal *22*, 6068-6077.

Ruggero, D. (2009). The Role of Myc-Induced Protein Synthesis in Cancer. Cancer Res *69*, 8839-8843.

Ruggero, D., Grisendi, S., Piazza, F., Rego, E., Mari, F., Rao, P.H., Cordon-Cardo, C., and Pandolfi, P.P. (2003). Dyskeratosis congenita and cancer in mice deficient in ribosomal RNA modification. Science *299*, 259-262.

Russell, J., and Zomerdijk, J. (2005). RNA-polymerase-I-directed rDNA transcription, life and works. Trends in Biochemical Sciences *30*, 87-96.

Russo, A., Esposito, D., Catillo, M., Pietropaolo, C., Crescenzi, E., and Russo, G. (2013). Human rpL3 induces G(1)/S arrest or apoptosis by modulating p21 (waf1/cip1) levels in a p53-independent manner. Cell Cycle *12*, 76-87.

Russo, A., Pagliara, V., Albano, F., Esposito, D., Sagar, V., Loreni, F., Irace, C., Santamaria, R., and Russo, G. (2016). Regulatory role of rpL3 in cell response to nucleolar stress induced by Act D in tumor cells lacking functional p53. Cell Cycle *15*, 41-51.

Russo, A., and Russo, G. (2017). Ribosomal Proteins Control or Bypass p53 during Nucleolar Stress. Int J Mol Sci *18*.

Ryba, T., Battaglia, D., Pope, B.D., Hiratani, I., and Gilbert, D.M. (2011). Genome-Scale Analysis of Replication Timing: from Bench to Bioinformatics. Nat Protoc *6*, 870-895.

Sakai, K., Ohta, T., Minoshima, S., Kudoh, J., Wang, Y., de Jong, P.J., and Shimizu, N. (1995). Human ribosomal RNA gene cluster: identification of the proximal end containing a novel tandem repeat sequence. Genomics *26*, 521-526.

Sakamoto, S., Nishikawa, K., Heo, S.J., Goto, M., Furuichi, Y., and Shimamoto, A. (2001). Werner helicase relocates into nuclear foci in response to DNA damaging agents and co-localizes with RPA and Rad51. Genes Cells *6*, 421-430.

Sakaue-Sawano, A., Kurokawa, H., Morimura, T., Hanyu, A., Hama, H., Osawa, H., Kashiwagi, S., Fukami, K., Miyata, T., Miyoshi, H.*, et al.* (2008). Visualizing spatiotemporal dynamics of multicellular cell-cycle progression. Cell *132*, 487-498.

Salama, R., Sadaie, M., Hoare, M., and Narita, M. (2014). Cellular senescence and its effector programs. Genes Dev *28*, 99-114.

Salminen, A., Kauppinen, A., and Kaarniranta, K. (2012). Emerging role of NF-kappaB signaling in the induction of senescence-associated secretory phenotype (SASP). Cell Signal *24*, 835-845.

Samuels, Y., Wang, Z., Bardelli, A., Silliman, N., Ptak, J., Szabo, S., Yan, H., Gazdar, A., Powell, S.M., Riggins, G.J.*, et al.* (2004). High Frequency of Mutations of the PIK3CA Gene in Human Cancers. Science *304*, 554.

Sang, L.Y., Roberts, J.M., and Coller, H.A. (2010). Hijacking HES1: how tumors co-opt the anti-differentiation strategies of quiescent cells. Trends Mol Med *16*, 17-26.

Sanij, E., Diesch, J., Lesmana, A., Poortinga, G., Hein, N., Lidgerwood, G., Cameron, D.P., Ellul, J., Goodall, G.J., Wong, L.H.*, et al.* (2015). A novel role for the Pol I transcription factor UBTF in maintaining genome stability through the regulation of highly transcribed Pol II genes. Genome Res *25*, 201-212.

Sanij, E., and Hannan, R.D. (2009). The role of UBF in regulating the structure and dynamics of transcriptionally active rDNA chromatin. Epigenetics *4*, 274-281.

Sanij, E., Poortinga, G., Sharkey, K., Hung, S., Holloway, T.P., Quin, J., Robb, E., Wong, L.H., Thomas, W.G., Stefanovsky, V.*, et al.* (2008). UBF levels determine the number of active ribosomal RNA genes in mammals. J Cell Biol *183*, 1259-1274.

Santoro, R., and Grummt, I. (2005). Epigenetic mechanism of rRNA gene silencing: Temporal order of NoRC-mediated histone modification, chromatin remodeling, and DNA methylation. Molecular and Cellular Biology *25*, 2539-2546.

Santoro, R., Li, J.W., and Grummt, I. (2002). The nucleolar remodeling complex NoRC mediates heterochromatin formation and silencing of ribosomal gene transcription. Nature Genetics *32*, 393-396.

Santoro, R., Schmitz, K.M., Sandoval, J., and Grummt, I. (2010). Intergenic transcripts originating from a subclass of ribosomal DNA repeats silence ribosomal RNA genes in trans. EMBO Rep *11*, 52-58.

Santos-Pereira, J.M., and Aguilera, A. (2015). R loops: new modulators of genome dynamics and function. Nat Rev Genet *16*, 583-597.

Saporita, A.J., Chang, H.C., Winkeler, C.L., Apicelli, A.J., Kladney, R.D., Wang, J., Townsend, R.R., Michel, L.S., and Weber, J.D. (2011). RNA helicase DDX5 is a p53-independent target of ARF that participates in ribosome biogenesis. Cancer Res *71*, 6708-6717.

Sartorelli, A., Johns, D., and Goldberg, I. (1975). Actinomycin D. In Antineoplastic and Immunosuppressive Agents (Springer Berlin Heidelberg), pp. 582-592.

Sasaki, M., Kawahara, K., Nishio, M., Mimori, K., Kogo, R., Hamada, K., Itoh, B., Wang, J., Komatsu, Y., Yang, Y.R.*, et al.* (2011). Regulation of the MDM2-P53 pathway and tumor growth by PICT1 via nucleolar RPL11. Nat Med *17*, 944-U153.

Savic, N., Bar, D., Leone, S., Frommel, S.C., Weber, F.A., Vollenweider, E., Ferrari, E., Ziegler, U., Kaech, A., Shakhova, O.*, et al.* (2014). lncRNA maturation to initiate heterochromatin formation in the nucleolus is required for exit from pluripotency in ESCs. Cell Stem Cell *15*, 720-734.

Saxena, A., Rorie, C.J., Dimitrov, D., Daniely, Y., and Borowiec, J.A. (2006). Nucleolin inhibits Hdm2 by multiple pathways leading to p53 stabilization. Oncogene *25*, 7274-7288.

Scheer, U., and Rose, K.M. (1984). Localization of RNA polymerase I in interphase cells and mitotic chromosomes by light and electron microscopic immunocytochemistry. Proc Natl Acad Sci U S A *81*, 1431-1435.

Scherl, A., Coute, Y., Deon, C., Calle, A., Kindbeiter, K., Sanchez, J.-C., Greco, A., Hochstrasser, D., and Diaz, J.-J. (2002). Functional Proteomic Analysis of Human Nucleolus. Mol Biol Cell *13*, 4100-4109.

Schlosser, I., Holzel, M., Murnseer, M., Burtscher, H., Weidle, U.H., and Eick, D. (2003). A role for c-Myc in the regulation of ribosomal RNA processing. Nucleic Acids Research *31*, 6148-6156.

Schmidt, E.V. (1999). The role of c-myc in cellular growth control. Oncogene *18*, 2988-2996.

Schmitz, K.M., Mayer, C., Postepska, A., and Grummt, I. (2010). Interaction of noncoding RNA with the rDNA promoter mediates recruitment of DNMT3b and silencing of rRNA genes. Genes Dev *24*, 2264-2269.

Schneider, A., Fischer, A., Weber, D., von Ahsen, O., Scheek, S., Kruger, C., Rossner, M., Klaussner, B., Faucheron, N., Kammandel, B.*, et al.* (2004). Restriction-mediated differential display (RMDD) identifies pip92 as a pro-apoptotic gene product induced during focal cerebral ischemia. J Cereb Blood Flow Metab *24*, 224-236.

Scott, J.L., Dunn, S.M., Zeng, T., Baker, E., Sutherland, G.R., and Burns, G.F. (1994). PHORBOL ESTER-INDUCED TRANSCRIPTION OF AN IMMEDIATE-EARLY RESPONSE GENE BY HUMAN T-CELLS IS INHIBITED BY CO-TREATMENT WITH CALCIUM IONOPHORE. J Cell Biochem *54*, 135-144.

Scott, M., Boisvert, F.M., Vieyra, D., Johnston, R.N., Bazett-Jones, D.P., and Riabowol, K. (2001). UV induces nucleolar translocation of ING1 through two distinct nucleolar targeting sequences. Nucleic Acids Research *29*, 2052-2058.

Scott, M.L., Fujita, T., Liou, H.C., Nolan, G.P., and Baltimore, D. (1993). The p65 subunit of NF-kappa B regulates I kappa B by two distinct mechanisms. Genes & Development *7*, 1266-1276.

Sears, R., Leone, G., DeGregori, J., and Nevins, J.R. (1999). Ras enhances Myc protein stability. Molecular Cell *3*, 169-179.

Sekhar, K.R., Reddy, Y.T., Reddy, P.N., Crooks, P.A., Venkateswaran, A., McDonald, W.H., Geng, L., Sasi, S., Van Der Waal, R.P., Roti, J.L.*, et al.* (2011). The novel chemical entity YTR107 inhibits recruitment of nucleophosmin to sites of DNA damage, suppressing repair of DNA double-strand breaks and enhancing radiosensitization. Clin Cancer Res *17*, 6490-6499.

Sharpless, N.E. (2005). INK4a/ARF: A multifunctional tumor suppressor locus. Mutat Res-Fundam Mol Mech Mutagen *576*, 22-38.

Shaulian, E. (2010). AP-1--The Jun proteins: Oncogenes or tumor suppressors in disguise? Cell Signal *22*, 894-899.

Shav-Tal, Y., Blechman, J., Darzacq, X., Montagna, C., Dye, B.T., Patton, J.G., Singer, R.H., and Zipori, D. (2005). Dynamic sorting of nuclear components into distinct nucleolar caps during transcriptional inhibition. Molecular Biology of the Cell *16*, 2395-2413.

Shelton, D.N., Chang, E., Whittier, P.S., Choi, D., and Funk, W.D. (1999). Microarray analysis of replicative senescence. Curr Biol *9*, 939-945.

Shen, M., Zhou, T., Xie, W., Ling, T., Zhu, Q., Zong, L., Lyu, G., Gao, Q., Zhang, F., and Tao, W. (2013). The chromatin remodeling factor CSB recruits histone acetyltransferase PCAF to rRNA gene promoters in active state for transcription initiation. PLoS One *8*, e62668.

Sheppard, K., Kinross, K.M., Solomon, B., Pearson, R.B., and Phillips, W.A. (2012a). Targeting PI3 kinase/AKT/mTOR signaling in cancer. Crit Rev Oncog *17*, 69-95.

Sheppard, K.E., Kinross, K.M., Solomon, B., Pearson, R.B., and Phillips, W.A. (2012b). Targeting PI3 Kinase/AKT/mTOR Signaling in Cancer. Critical Reviews in Oncogenesis *17*, 69-95.

Sherr, C.J. (2006). Divorcing ARF and p53: an unsettled case. Nat Rev Cancer *6*, 663-673.

Sherr, C.J., and McCormick, F. (2002). The RB and p53 pathways in cancer. Cancer Cell *2*, 103-112.

Shi, Z., and Barna, M. (2015). Translating the genome in time and space: specialized ribosomes, RNA regulons, and RNA-binding proteins. Annu Rev Cell Dev Biol *31*, 31-54.

Shiao, Y.H., Leighty, R.M., Wang, C., Ge, X., Crawford, E.B., Spurrier, J.M., McCann, S.D., Fields, J.R., Fornwald, L., Riffle, L.*, et al.* (2011). Ontogeny-driven rDNA rearrangement, methylation, and transcription, and paternal influence. PLoS One *6*, e22266.

Shiloh, Y., and Ziv, Y. (2013). The ATM protein kinase: regulating the cellular response to genotoxic stress, and more. Nat Rev Mol Cell Biol *14*, 197-210.

Shimizu, N., Ohta, M., Fujiwara, C., Sagara, J., Mochizuki, N., Oda, T., and Utiyama, H. (1991). Expression of a novel immediate early gene during 12-O-tetradecanoylphorbol-13-acetate-induced macrophagic differentiation of HL-60 cells. Journal of Biological Chemistry *266*, 12157-12161.

Shiohama, A., Sasaki, T., Noda, S., Minoshima, S., and Shimizu, N. (2007). Nucleolar localization of DGCR8 and identification of eleven DGCR8-associated proteins. Exp Cell Res *313*, 4196-4207.

Shiue, C.N., Berkson, R.G., and Wright, A.P. (2009). c-Myc induces changes in higher order rDNA structure on stimulation of quiescent cells. Oncogene.

Siddiqui-Jain, A., Grand, C.L., Bearss, D.J., and Hurley, L.H. (2002). Direct evidence for a G-quadruplex in a promoter region and its targeting with a small molecule to repress c-MYC transcription. Proc Natl Acad Sci U S A *99*, 11593-11598.

Sirri, V., Hernandez-Verdun, D., and Roussel, P. (2002). Cyclin-dependent kinases govern formation and maintenance of the nucleolus. Journal of Cell Biology *156*, 969-981.

Sirri, V., Roussel, P., and Hernandez-Verdun, D. (1999). The mitotically phosphorylated form of the transcription termination factor TTF-1 is associated with the repressed rDNA transcription machinery. J Cell Sci *112*, 3259-3268.

Sloan, Katherine E., Bohnsack, Markus T., and Watkins, Nicholas J. (2013). The 5S RNP Couples p53 Homeostasis to Ribosome Biogenesis and Nucleolar Stress. Cell Reports *5*, 237-247.

Smirnov, E., Cmarko, D., Kovacik, L., Hagen, G.M., Popov, A., Raska, O., Prieto, J.L., Ryabchenko, B., Amim, F., McStay, B.*, et al.* (2011). Replication timing of pseudo-NORs. J Struct Biol *173*, 213-218.

Smirnov, E., Cmarko, D., Mazel, T., Hornáček, M., and Raška, I. (2016). Nucleolar DNA: the host and the guests. Histochem Cell Biol *145*, 359-372.

Smith, J., Tho, L.M., Xu, N., and Gillespie, D.A. (2010). The ATM-Chk2 and ATR-Chk1 pathways in DNA damage signaling and cancer. Adv Cancer Res *108*, 73-112.

Sobell, H.M. (1985). ACTINOMYCIN AND DNA-TRANSCRIPTION. Proceedings of the National Academy of Sciences of the United States of America *82*, 5328-5331.

Sokka, M., Rilla, K., Miinalainen, I., Pospiech, H., and Syvaoja, J.E. (2015). High levels of TopBP1 induce ATR-dependent shut-down of rRNA transcription and nucleolar segregation. Nucleic Acids Res *43*, 4975-4989.

Sollnerwebb, B., and Tower, J. (1986). TRANSCRIPTION OF CLONED EUKARYOTIC RIBOSOMAL-RNA GENES. Annu Rev Biochem *55*, 801-830.

Song, M.J., Yoo, E.H., Lee, K.O., Kim, G.N., Kim, H.J., Kim, S.Y., and Kim, S.H. (2010). A novel initiation codon mutation in the ribosomal protein S17 gene (RPS17) in a patient with Diamond-Blackfan anemia. Pediatr Blood Cancer *54*, 629-631.

Song, T.J., Yang, L.X., Kabra, N., Chen, L.H., Koomen, J., Haura, E.B., and Chen, J.D. (2013). The NAD(+) Synthesis Enzyme Nicotinamide Mononucleotide Adenylyltransferase (NMNAT1) Regulates Ribosomal RNA Transcription. Journal of Biological Chemistry *288*, 20908-20917.

Sorensen, P.D., and Frederiksen, S. (1991). Characterization of human 5S rRNA genes. Nucleic Acids Res *19*, 4147-4151.

Soutoglou, E., and Misteli, T. (2008). Activation of the cellular DNA damage response in the absence of DNA lesions. Science *320*, 1507-1510.

Stahl, A., Hartung, M., Vagnercapodano, A.M., and Fouet, C. (1976). CHROMOSOMAL CONSTITUTION OF NUCLEOLUS-ASSOCIATED CHROMATIN IN MAN. Human Genetics *35*, 27-34.

Staley, J.P., and Woolford, J.L., Jr. (2009). Assembly of ribosomes and spliceosomes: complex ribonucleoprotein machines. Curr Opin Cell Biol *21*, 109-118.

Stefanovsky, V., Langlois, F., Gagnon-Kugler, T., Rothblum, L.I., and Moss, T. (2006a). Growth factor signaling regulates elongation of RNA polymerase I transcription in mammals via UBF phosphorylation and r-chromatin remodeling. Molecular Cell *21*, 629-639.

Stefanovsky, V., and Moss, T. (2006). Regulation of rRNA synthesis in human and mouse cells is not determined by changes in active gene count. Cell Cycle *5*, 735-739.

Stefanovsky, V.Y., Langlois, F., Bazett-Jones, D., Pelletier, G., and Moss, T. (2006b). ERK modulates DNA bending and enhancesome structure by phosphorylating HMG1-boxes 1 and 2 of the RNA polymerase I transeniption factor UBF. Biochemistry *45*, 3626-3634.

Stefanovsky, V.Y., Pelletier, G., Bazett-Jones, D.P., Crane-Robinson, C., and Moss, T. (2001a). DNA looping in the RNA polymerase I enhancesome is the result of non-cooperative in-phase bending by two UBF molecules. Nucleic Acids Research *29*, 3241-3247.

Stefanovsky, V.Y., Pelletier, G., Hannan, R., Gagnon-Kugler, T., Rothblum, L.I., and Moss, T. (2001b). An immediate response of ribosomal transcription to growth factor stimulation in mammals is mediated by ERK phosphorylation of UBF. Molecular Cell *8*, 1063-1073.

Stimpson, K.M., Sullivan, L.L., Kuo, M.E., and Sullivan, B.A. (2014). Nucleolar organization, ribosomal DNA array stability, and acrocentric chromosome integrity are linked to telomere function. PLoS One *9*, e92432.

Stirling, P.C., and Hieter, P. (2017). Canonical DNA Repair Pathways Influence R-Loop-Driven Genome Instability. J Mol Biol *429*, 3132-3138.

Stockhausen, M.T., Sjolund, J., and Axelson, H. (2005). Regulation of the Notch target gene Hes-1 by TGFalpha induced Ras/MAPK signaling in human neuroblastoma cells. Exp Cell Res *310*, 218-228.

Stott, F.J., Bates, S., James, M.C., McConnell, B.B., Starborg, M., Brookes, S., Palmero, I., Ryan, K., Hara, E., Vousden, K.H.*, et al.* (1998). The alternative product from the human CDKN2A locus, p14(ARF), participates in a regulatory feedback loop with p53 and MDM2. EMBO J *17*, 5001-5014.

Stults, D.M., Killen, M.W., Pierce, H.H., and Pierce, A.J. (2008). Genomic architecture and inheritance of human ribosomal RNA gene clusters. Genome Res *18*, 13-18.

Sugimoto, M., Nakamura, T., Ohtani, N., Hampson, L., Hampson, I.N., Shimamoto, A., Furuichi, Y., Okumura, K., Niwa, S., Taya, Y.*, et al.* (1999). Regulation of CDK4 activity by a novel CDK4-binding protein, p34(SEI-1). Genes Dev *13*, 3027-3033.

Sullivan, G.J., Bridger, J.M., Cuthbert, A.P., Newbold, R.F., Bickmore, W.A., and McStay, B. (2001). Human acrocentric chromosomes with transcriptionally silent nucleolar organizer regions associate with nucleoli. The EMBO Journal *20*, 2867-2877.

Sullivan, K.D., Gallant-Behm, C.L., Henry, R.E., Fraikin, J.L., and Espinosa, J.M. (2012). The p53 circuit board. Biochim Biophys Acta *1825*, 229-244.

Sun, S.C., Ganchi, P.A., Ballard, D.W., and Greene, W.C. (1993). NF-kappa B controls expression of inhibitor I kappa B alpha: evidence for an inducible autoregulatory pathway. Science *259*, 1912-1915.

Sundqvist, A., Liu, G., Mirsaliotis, A., and Xirodimas, D.P. (2009). Regulation of nucleolar signalling to p53 through NEDDylation of L11. EMBO Rep *10*, 1132-1139.

Suzuki, A., Kogo, R., Kawahara, K., Sasaki, M., Nishio, M., Maehama, T., Sasaki, T., Mimori, K., and Mori, M. (2012). A new PICTure of nucleolar stress. Cancer Sci *103*, 632-637.

Suzuki, T., Shiratori, M., Furuichi, Y., and Matsumoto, T. (2001). Diverged nuclear localization of Werner helicase in human and mouse cells. Oncogene *20*, 2551-2558.

Takagi, M., Absalon, M.J., McLure, K.G., and Kastan, M.B. (2005). Regulation of p53 translation and induction after DNA damage by ribosomal protein L26 and nucleolin. Cell *123*, 49-63.

Takaya, T., Kasatani, K., Noguchi, S., and Nikawa, J. (2009). Functional Analyses of Immediate Early Gene ETR101 Expressed in Yeast. Biosci Biotechnol Biochem *73*, 1653-1660.

Takekawa, M., and Saito, H. (1998). A family of stress-inducible GADD45-like proteins mediate activation of the stress-responsive MTK1/MEKK4 MAPKKK. Cell *95*, 521-530.

Takekawa, M., Tatebayashi, K., Itoh, F., Adachi, M., Imai, K., and Saito, H. (2002). Smad-dependent GADD45beta expression mediates delayed activation of p38 MAP kinase by TGF-beta. EMBO J *21*, 6473-6482.

Takemura, M., Ohoka, F., Perpelescu, M., Ogawa, M., Matsushita, H., Takaba, T., Akiyama, T., Umekawa, H., Furuichi, Y., Cook, P.R.*, et al.* (2002). Phosphorylation-dependent migration of retinoblastoma protein into the nucleolus triggered by binding to nucleophosmin/B23. Exp Cell Res *276*, 233-241.

Tamura, R.E., de Vasconcellos, J.F., Sarkar, D., Libermann, T.A., Fisher, P.B., and Zerbini, L.F. (2012). GADD45 proteins: central players in tumorigenesis. Curr Mol Med *12*, 634-651.

Tan, S.B., Li, J., Chen, X., Zhang, W., Zhang, D., Zhang, C., Li, D., and Zhang, Y. (2014). Small molecule inhibitor of myogenic microRNAs leads to a discovery of miR-221/222-myoD-myomiRs regulatory pathway. Chem Biol *21*, 1265-1270.

Tanaka, R., Satoh, H., Moriyama, M., Satoh, K., Morishita, Y., Yoshida, S., Watanabe, T., Nakamura, Y., and Mori, S. (2000). Intronic U50 small-nucleolar-RNA (snoRNA) host gene of no protein-coding potential is mapped at the chromosome breakpoint t(3;6)(q27;q15) of human B-cell lymphoma. Genes to Cells *5*, 277-287.

Tanaka, Y., Okamoto, K., Teye, K., Umata, T., Yamagiwa, N., Suto, Y., Zhang, Y., and Tsuneoka, M. (2010). JmjC enzyme KDM2A is a regulator of rRNA transcription in response to starvation. EMBO J *29*, 1510-1522.

Tang, W., Robles, A.I., Beyer, R.P., Gray, L.T., Nguyen, G.H., Oshima, J., Maizels, N., Harris, C.C., and Monnat, R.J., Jr. (2016). The Werner syndrome RECQ helicase targets G4 DNA in human cells to modulate transcription. Hum Mol Genet *25*, 2060-2069.

Tao, W.K., and Levine, A.J. (1999a). Nucleocytoplasmic shuttling of oncoprotein Hdm2 is required for Hdm2-mediated degradation of p53. Proceedings of the National Academy of Sciences of the United States of America *96*, 3077-3080.

Tao, W.K., and Levine, A.J. (1999b). P19(ARF) stabilizes p53 by blocking nucleo-cytoplasmic shuttling of Mdm2. Proceedings of the National Academy of Sciences of the United States of America *96*, 6937-6941.

Terasawa, K., Ichimura, A., Sato, F., Shimizu, K., and Tsujimoto, G. (2009). Sustained activation of ERK1/2 by NGF induces microRNA-221 and 222 in PC12 cells. The FEBS journal *276*, 3269-3276.

Thomas, D.B., and Lingwood, C.A. (1975). A model of cell cycle control: effects of thymidine on synchronous cell cultures. Cell *5*, 37-42.

Thomas, G. (2000). An encore for ribosome biogenesis in the control of cell proliferation. Nat Cell Biol *2*, E71-72.

Thompson, M., Haeusler, R.A., Good, P.D., and Engelke, D.R. (2003). Nucleolar clustering of dispersed tRNA genes. Science *302*, 1399-1401.

Thomson, E., Ferreira-Cerca, S., and Hurt, E. (2013). Eukaryotic ribosome biogenesis at a glance. J Cell Sci *126*, 4815.

Thornburg, N.J., Pathmanathan, R., and Raab-Traub, N. (2003). Activation of nuclear factor-kappaB p50 homodimer/Bcl-3 complexes in nasopharyngeal carcinoma. Cancer Res *63*, 8293-8301.

Tomlinson, R.L., Ziegler, T.D., Supakorndej, T., Terns, R.M., and Terns, M.P. (2006). Cell cycle-regulated trafficking of human telomerase to telomeres. Molecular Biology of the Cell *17*, 955-965.

Trask, D.K., and Muller, M.T. (1988). STABILIZATION OF TYPE-I TOPOISOMERASE DNA COVALENT COMPLEXES BY ACTINOMYCIN-D. Proceedings of the National Academy of Sciences of the United States of America *85*, 1417-1421.

Treiber, D.K., Zhai, X.Q., Jantzen, H.M., and Essigmann, J.M. (1994). CISPLATIN-DNA ADDUCTS ARE MOLECULAR DECOYS FOR THE RIBOSOMAL-RNA TRANSCRIPTION FACTOR HUBF (HUMAN UPSTREAM BINDING-FACTOR). Proceedings of the National Academy of Sciences of the United States of America *91*, 5672-5676.

Tremblay, C.d.S., Huard, C.C., Huang, F.-F., Habi, O., Bourdages, V.r., L√©vesque, G., and Carreau, M. (2009). The Fanconi Anemia Core Complex Acts as a Transcriptional Co-regulator in Hairy Enhancer of Split 1 Signaling. Journal of Biological Chemistry *284*, 13384-13395.

Tremblay, C.S., Huang, F.F., Habi, O., Huard, C.C., Godin, C., Levesque, G., and Carreau, M. (2008). HES1 is a novel interactor of the Fanconi anemia core complex. Blood *112*, 2062-2070.

Tsai, R.Y., and Pederson, T. (2014). Connecting the nucleolus to the cell cycle and human disease. FASEB J *28*, 3290-3296.

Tsai, R.Y.L. (2009). Nucleolar modulation of TRF1 A dynamic way to regulate telomere and cell cycle by nucleostemin and GNL3L. Cell Cycle *8*, 2912-2916.

Tsekrekou, M., Stratigi, K., and Chatzinikolaou, G. (2017). The Nucleolus: In Genome Maintenance and Repair. Int J Mol Sci *18*.

Tu, K., Liu, Z., Yao, B., Xue, Y., Xu, M., Dou, C., Yin, G., and Wang, J. (2016). BCL-3 promotes the tumor growth of hepatocellular carcinoma by regulating cell proliferation and the cell cycle through cyclin D1. Oncol Rep *35*, 2382-2390.

Tuan, J.C., Zhai, W.G., and Comai, L. (1999). Recruitment of TATA-binding protein-TAF, complex SL1 to the human ribosomal DNA promoter is mediated by the carboxy-terminal activation domain of upstream binding factor (UBF) and is regulated by UBF phosphorylation. Molecular and Cellular Biology *19*, 2872-2879.

Tumurbaatar, I., Cizmecioglu, O., Hoffmann, I., Grummt, I., and Voit, R. (2011). Human Cdc14B promotes progression through mitosis by dephosphorylating Cdc25 and regulating Cdk1/cyclin B activity. PLoS One *6*, e14711.

Uemura, M., Zheng, Q., Koh, C.M., Nelson, W.G., Yegnasubramanian, S., and De Marzo, A.M. (2012). Overexpression of ribosomal RNA in prostate cancer is common but not linked to rDNA promoter hypomethylation. Oncogene *31*, 1254-1263.

Ugrinova, I., Monier, K., Ivaldi, C., Thiry, M., Storck, S., Mongelard, F., and Bouvet, P. (2007). Inactivation of nucleolin leads to nucleolar disruption, cell cycle arrest and defects in centrosome duplication. Bmc Molecular Biology *8*.

Vairapandi, M., Balliet, A.G., Fornace, A.J., Jr., Hoffman, B., and Liebermann, D.A. (1996). The differentiation primary response gene MyD118, related to GADD45, encodes for a nuclear protein which interacts with PCNA and p21WAF1/CIP1. Oncogene *12*, 2579-2594.

Vairapandi, M., Balliet, A.G., Hoffman, B., and Liebermann, D.A. (2002). GADD45b and GADD45g are cdc2/cyclinB1 kinase inhibitors with a role in S and G2/M cell cycle checkpoints induced by genotoxic stress. J Cell Physiol *192*, 327-338.

Valin, A., Ouyang, J., and Gill, G. (2013). Transcription factor Sp3 represses expression of p21CIP(1) via inhibition of productive elongation by RNA polymerase II. Mol Cell Biol *33*, 1582-1593.

van Koningsbruggen, S., Gierlinski, M., Schofield, P., Martin, D., Barton, G.J., Ariyurek, Y., den Dunnen, J.T., and Lamond, A.I. (2010). High-resolution whole-genome sequencing reveals that specific chromatin domains from most human chromosomes associate with nucleoli. Mol Biol Cell *21*, 3735-3748.

van Riggelen, J., Yetil, A., and Felsher, D.W. (2010). MYC as a regulator of ribosome biogenesis and protein synthesis. Nat Rev Cancer *10*, 301-309.

van Sluis, M., and McStay, B. (2015). A localized nucleolar DNA damage response facilitates recruitment of the homology-directed repair machinery independent of cell cycle stage. Genes Dev *29*, 1151-1163.

Venkata Narayanan, I., Paulsen, M.T., Bedi, K., Berg, N., Ljungman, E.A., Francia, S., Veloso, A., Magnuson, B., di Fagagna, F.d.A., Wilson, T.E.*, et al.* (2017). Transcriptional and post-transcriptional regulation of the ionizing radiation response by ATM and p53. Scientific Reports *7*, 43598.

Vintermist, A., Bohm, S., Sadeghifar, F., Louvet, E., Mansen, A., Percipalle, P., and Ostlund Farrants, A.K. (2011). The chromatin remodelling complex B-WICH changes the chromatin structure and recruits histone acetyl-transferases to active rRNA genes. PLoS One *6*, e19184.

Vlachos, A., Rosenberg, P.S., Atsidaftos, E., Alter, B.P., and Lipton, J.M. (2012). Incidence of neoplasia in Diamond Blackfan anemia: a report from the Diamond Blackfan Anemia Registry. Blood *119*, 3815-3819.

Voit, R., and Grummt, I. (2001). Phosphorylation of UBF at serine 388 is required for interaction with RNA polymerase I and activation of rDNA transcription. Proceedings of the National Academy of Sciences of the United States of America *98*, 13631-13636.

Voit, R., Hoffmann, M., and Grummt, I. (1999). Phosphorylation by G(1)-specific cdk-cyclin complexes activates the nucleolar transcription factor UBF. Embo Journal *18*, 1891-1899.

Voit, R., Schafer, K., and Grummt, I. (1997). Mechanism of repression of RNA polymerase I transcription by the retinoblastoma protein. Molecular and Cellular Biology *17*, 4230-4237.

Voit, R., Seiler, J., and Grummt, I. (2015). Cooperative Action of Cdk1/cyclin B and SIRT1 Is Required for Mitotic Repression of rRNA Synthesis. PLoS Genet *11*, e1005246.

Vousden, K.H., and Lane, D.P. (2007). p53 in health and disease. Nat Rev Mol Cell Biol *8*, 275-283.

Waldman, T., Kinzler, K.W., and Vogelstein, B. (1995). p21 is necessary for the p53-mediated G1 arrest in human cancer cells. Cancer Res *55*, 5187-5190.

Wall, D.S., Mears, A.J., McNeill, B., Mazerolle, C., Thurig, S., Wang, Y., Kageyama, R., and Wallace, V.A. (2009). Progenitor cell proliferation in the retina is dependent on Notch-independent Sonic hedgehog/Hes1 activity. J Cell Biol *184*, 101-112.

Wang, J., Leung, J.W., Gong, Z., Feng, L., Shi, X., and Chen, J. (2013). PHF6 regulates cell cycle progression by suppressing ribosomal RNA synthesis. J Biol Chem *288*, 3174-3183.

Wang, J., Liu, S., Sun, G.P., Wang, F., Zou, Y.F., Jiao, Y., Ning, J., and Xu, J. (2014). Prognostic significance of microRNA-221/222 expression in cancers: evidence from 1,204 subjects. Int J Biol Markers *29*, e129-141.

Wang, Y.Z., Guan, J., Wang, H.Y., Wang, Y., Leeper, D., and Iliakis, G. (2001). Regulation of DNA replication after heat shock by replication protein A-nucleolin interactions. Journal of Biological Chemistry *276*, 20579-20588.

Warmerdam, D.O., and Kanaar, R. (2010). Dealing with DNA damage: relationships between checkpoint and repair pathways. Mutat Res *704*, 2-11.

Warner, J.R. (1999). The economics of ribosome biosynthesis in yeast. Trends in Biochemical Sciences *24*, 437-440.

Warner, J.R., Vilardell, J., and Sohn, J.H. (2001). Economics of ribosome biosynthesis. Cold Spring Harb Symp Quant Biol *66*, 567-574.

Watanabe-Fukunaga, R., Iida, S., Shimizu, Y., Nagata, S., and Fukunaga, R. (2005). SEI family of nuclear factors regulates p53-dependent transcriptional activation. Genes Cells *10*, 851-860.

Weisenberger, D., and Scheer, U. (1995). A possible mechanism for the inhibition of ribosomal RNA gene transcription during mitosis. J Cell Biol *129*, 561-575.

Weiss, W.A., Taylor, S.S., and Shokat, K.M. (2007). Recognizing and exploiting differences between RNAi and small-molecule inhibitors. Nat Chem Biol *3*, 739-744.

Welting, T.J., van Venrooij, W.J., and Pruijn, G.J. (2004). Mutual interactions between subunits of the human RNase MRP ribonucleoprotein complex. Nucleic Acids Res *32*, 2138-2146.

White, R.J. (2005). RNA polymerases I and III, growth control and cancer. Nat Rev Mol Cell Biol *6*, 69-78.

Williams, G.T., and Farzaneh, F. (2012). Are snoRNAs and snoRNA host genes new players in cancer? Nat Rev Cancer *12*, 84-88.

Williamson, D., Lu, Y.J., Fang, C., Pritchard-Jones, K., and Shipley, J. (2006). Nascent pre-rRNA overexpression correlates with an adverse prognosis in alveolar rhabdomyosarcoma. Gene Chromosomes Cancer *45*, 839-845.

Wong, C.C., Traynor, D., Basse, N., Kay, R.R., and Warren, A.J. (2011). Defective ribosome assembly in Shwachman-Diamond syndrome. Blood *118*, 4305-4312.

Wong, J.M.Y., Kusdra, L., and Collins, K. (2002). Subnuclear shuttling of human telomerase induced by transformation and DNA damage. Nat Cell Biol *4*, 731-U735.

Wong, L.H., Brettingham-Moore, K.H., Chan, L., Quach, J.M., Anderson, M.A., Northrop, E.L., Hannan, R., Saffery, R., Shaw, M.L., Williams, E.*, et al.* (2007). Centromere RNA is a key component for the assembly of nucleoproteins at the nucleolus and centromere. Genome Res *17*, 1146-1160.

Woolnough, J.L., Atwood, B.L., Liu, Z., Zhao, R., and Giles, K.E. (2016). The Regulation of rRNA Gene Transcription during Directed Differentiation of Human Embryonic Stem Cells. PLoS One *11*, e0157276.

Wu, A., Tu, X., Prisco, M., and Baserga, R. (2005). Regulation of upstream binding factor 1 activity by insulin-like growth factor I receptor signaling. J Biol Chem *280*, 2863-2872.

Xie, N., Ma, L., Zhu, F., Zhao, W., Tian, F., Yuan, F., Fu, J., Huang, D., Lv, C., and Tong, T. (2016). Regulation of the MDM2-p53 pathway by the nucleolar protein CSIG in response to nucleolar stress. Sci Rep *6*, 36171.

Xie, W., Ling, T., Zhou, Y., Feng, W., Zhu, Q., Stunnenberg, H.G., Grummt, I., and Tao, W. (2012). The chromatin remodeling complex NuRD establishes the poised state of rRNA genes characterized by bivalent histone modifications and altered nucleosome positions. Proc Natl Acad Sci U S A *109*, 8161-8166.

Xu, H., Di Antonio, M., McKinney, S., Mathew, V., Ho, B., O'Neil, N.J., Santos, N.D., Silvester, J., Wei, V., Garcia, J.*, et al.* (2017). CX-5461 is a DNA G-quadruplex stabilizer with selective lethality in BRCA1/2 deficient tumours. Nat Commun *8*, 14432.

Yadavilli, S., Mayo, L.D., Higgins, M., Lain, S., Hegde, V., and Deutsch, W.A. (2009). Ribosomal protein S3: A multi-functional protein that interacts with both p53 and MDM2 through its KH domain. DNA Repair *8*, 1215-1224.

Yamada, K., Ono, M., Perkins, N.D., Rocha, S., and Lamond, A.I. (2013). Identification and functional characterization of FMN2, a regulator of the cyclin-dependent kinase inhibitor p21. Mol Cell *49*, 922-933.

Yan, S., Frank, D., Son, J., Hannan, K.M., Hannan, R.D., Chan, K.T., Pearson, R.B., and Sanij, E. (2017). The Potential of Targeting Ribosome Biogenesis in High-Grade Serous Ovarian Cancer. Int J Mol Sci *18*.

Yang, C., Kim, M.S., Chakravarty, D., Indig, F.E., and Carrier, F. (2009). Nucleolin Binds to the Proliferating Cell Nuclear Antigen and Inhibits Nucleotide Excision Repair. Mol Cell Pharmacol *1*, 130-137.

Yang, C., Tang, X., Guo, X., Niikura, Y., Kitagawa, K., Cui, K., Wong, S.T., Fu, L., and Xu, B. (2011). Aurora-B mediated ATM serine 1403 phosphorylation is required for mitotic ATM activation and the spindle checkpoint. Mol Cell *44*, 597-608.

Yang, F., Deng, X., Ma, W., Berletch, J.B., Rabaia, N., Wei, G., Moore, J.M., Filippova, G.N., Xu, J., Liu, Y.*, et al.* (2015). The lncRNA Firre anchors the inactive X chromosome to the nucleolus by binding CTCF and maintains H3K27me3 methylation. Genome Biology *16*, 52.

Yang, L., Song, T., Chen, L., Kabra, N., Zheng, H., Koomen, J., Seto, E., and Chen, J. (2013a). Regulation of SirT1-Nucleomethylin Binding by rRNA Coordinates Ribosome Biogenesis with Nutrient Availability. Molecular and Cellular Biology *33*, 3835-3848.

Yang, Q.E., Racicot, K.E., Kaucher, A.V., Oatley, M.J., and Oatley, J.M. (2013b). MicroRNAs 221 and 222 regulate the undifferentiated state in mammalian male germ cells. Development *140*, 280-290.

Ye, X., Zerlanko, B., Kennedy, A., Banumathy, G., Zhang, R., and Adams, P.D. (2007). Downregulation of Wnt signaling is a trigger for formation of facultative heterochromatin and onset of cell senescence in primary human cells. Mol Cell *27*, 183-196.

Yoo, J., Ghiassi, M., Jirmanova, L., Balliet, A.G., Hoffman, B., Fornace, A.J., Jr., Liebermann, D.A., Bottinger, E.P., and Roberts, A.B. (2003). Transforming growth factor-beta-induced apoptosis is mediated by Smad-dependent expression of GADD45b through p38 activation. J Biol Chem *278*, 43001-43007.

You, Z., Bailis, J.M., Johnson, S.A., Dilworth, S.M., and Hunter, T. (2007). Rapid activation of ATM on DNA flanking double-strand breaks. Nat Cell Biol *9*, 1311-1318.

Yu, Y.T., Shu, M.D., Narayanan, A., Terns, R.M., Terns, M.P., and Steitz, J.A. (2001). Internal modification of U2 small nuclear (sn)RNA occurs in nucleoli of Xenopus oocytes. J Cell Biol *152*, 1279-1288.

Yuan, X., Feng, W., Imhof, A., Grummt, I., and Zhou, Y. (2007). Activation of RNA polymerase I transcription by Cockayne syndrome group B protein and histone methyltransferase G9a. Molecular Cell *27*, 585-595.

Yuan, X.J., Zhou, Y.G., Casanova, E., Chai, M.Q., Kiss, E., Grone, H.J., Schutz, G., and Grummt, I. (2005). Genetic inactivation of the transcription factor TIF-IA leads to nucleolar disruption, cell cycle arrest, and p53-mediated apoptosis. Molecular Cell *19*, 77-87.

Zabludoff, S.D., Deng, C., Grondine, M.R., Sheehy, A.M., Ashwell, S., Caleb, B.L., Green, S., Haye, H.R., Horn, C.L., Janetka, J.W.*, et al.* (2008). AZD7762, a novel checkpoint kinase inhibitor, drives checkpoint abrogation and potentiates DNA-targeted therapies. Molecular Cancer Therapeutics *7*, 2955.

Zeller, K.I., Haggerty, T.J., Barrett, J.F., Guo, Q.B., Wonsey, D.R., and Dang, C.V. (2001). Characterization of nucleophosmin (B23) as a Myc target by scanning chromatin immunoprecipitation. Journal of Biological Chemistry *276*, 48285-48291.

Zhai, W.G., and Comai, L. (2000). Repression of RNA polymerase I transcription by the tumor suppressor p53. Molecular and Cellular Biology *20*, 5930-5938.

Zhang, C., Comai, L., and Johnson, D.L. (2005). PTEN represses RNA polymerase I transcription by disrupting the SL1 complex. Molecular and Cellular Biology *25*, 6899-6911.

Zhang, L.F., Huynh, K.D., and Lee, J.T. (2007a). Perinucleolar targeting of the inactive X during S phase: Evidence for a role in the maintenance of silencing. Cell *129*, 693-706.

Zhang, L.F., Huynh, K.D., and Lee, J.T. (2007b). Perinucleolar targeting of the inactive X during S phase: evidence for a role in the maintenance of silencing. Cell *129*.

Zhang, Q., Shalaby, N.A., and Buszczak, M. (2014). Changes in rRNA transcription influence proliferation and cell fate within a stem cell lineage. Science *343*, 298-301.

Zhang, S., and Yu, D. (2010). PI(3)king apart PTEN's role in cancer. Clin Cancer Res *16*, 4325-4330.

Zhang, T., Penicud, K., Bruhn, C., Loizou, J.I., Kanu, N., Wang, Z.Q., and Behrens, A. (2012). Competition between NBS1 and ATMIN controls ATM signaling pathway choice. Cell Rep *2*, 1498-1504.

Zhang, Y., Wang, J., Yuan, Y., Zhang, W., Guan, W., Wu, Z., Jin, C., Chen, H., Zhang, L., Yang, X.*, et al.* (2010). Negative regulation of HDM2 to attenuate p53 degradation by ribosomal protein L26. Nucleic Acids Res *38*, 6544-6554.

Zhang, Y.P., Wolf, G.W., Bhat, K., Jin, A., Allio, T., Burkhart, W.A., and Xiong, Y. (2003). Ribosomal protein L11 negatively regulates oncoprotein MDM2 and mediates a p53-dependent ribosomal-stress checkpoint pathway. Molecular and Cellular Biology *23*, 8902-8912.

Zhang, Y.P., Xiong, Y., and Yarbrough, W.G. (1998). ARF promotes MDM2 degradation and stabilizes p53: ARF-INK4a locus deletion impairs both the Rb and p53 tumor suppression pathways. Cell *92*, 725-734.

Zhao, J., Yuan, X.J., Frodin, M., and Grummt, I. (2003). ERK-dependent phosphorylation of the transcription initiation factor TIF-IA is required for RNA polymerase I transcription and cell growth. Molecular Cell *11*, 405-413.

Zhao, J.J., Roberts, T.M., and Hahn, W.C. (2004). Functional genetics and experimental models of human cancer. Trends Mol Med *10*, 344-350.

Zhou, Y., Schmitz, K.-M., Mayer, C., Yuan, X., Akhtar, A., and Grummt, I. (2009). Reversible acetylation of the chromatin remodelling complex NoRC is required for non-coding RNA-dependent silencing. Nat Cell Biol *11*, 1010-1016.

Zhou, Y.G., Santoro, R., and Grummt, I. (2002). The chromatin remodeling complex NoRC targets HDAC1 to the ribosomal gene promoter and represses RNA polymerase I transcription. Embo Journal *21*, 4632-4640.

Zhu, Q., Meng, L., Hsu, J.K., Lin, T., Teishima, J., and Tsai, R.Y. (2009a). GNL3L stabilizes the TRF1 complex and promotes mitotic transition. J Cell Biol *185*, 827-839.

Zhu, Q., Yasumoto, H., and Tsai, R.Y. (2006). Nucleostemin delays cellular senescence and negatively regulates TRF1 protein stability. Mol Cell Biol *26*, 9279-9290.

Zhu, Q.Y., Liu, Q., Chen, J.X., Lan, K., and Ge, B.X. (2010). MicroRNA-101 targets MAPK phosphatase-1 to regulate the activation of MAPKs in macrophages. J Immunol *185*, 7435-7442.

Zhu, Y., Poyurovsky, M.V., Li, Y.C., Biderman, L., Stahl, J., Jacq, X., and Prives, C. (2009b). Ribosomal Protein S7 Is Both a Regulator and a Substrate of MDM2. Molecular Cell *35*, 316-326.

Zieve, G.W., Turnbull, D., Mullins, J.M., and McIntosh, J.R. (1980). Production of large numbers of mitotic mammalian cells by use of the reversible microtubule inhibitor nocodazole. Nocodazole accumulated mitotic cells. Exp Cell Res *126*, 397-405.

Zillner, K., Komatsu, J., Filarsky, K., Kalepu, R., Bensimon, A., and Nemeth, A. (2015). Active human nucleolar organizer regions are interspersed with inactive rDNA repeats in normal and tumor cells. Epigenomics *7*, 363-378.

Zimmer, J., Tacconi, E.M.C., Folio, C., Badie, S., Porru, M., Klare, K., Tumiati, M., Markkanen, E., Halder, S., Ryan, A.*, et al.* (2016). Targeting BRCA1 and BRCA2 Deficiencies with G-Quadruplex-Interacting Compounds. Mol Cell *61*, 449-460.

Zumbrun, S.D., Hoffman, B., and Liebermann, D.A. (2009). Distinct mechanisms are utilized to induce stress sensor gadd45b by different stress stimuli. J Cell Biochem *108*, 1220-1231.